

Copyright

by

Zhi Ren

2016

The Dissertation Committee for Zhi Ren
Certifies that this is the approved version of the following dissertation:

Palladium-Catalyzed Carbon-Hydrogen Bond Functionalization
Utilizing an *Exo*-Directing Strategy

APPROVED BY
SUPERVISING COMMITTEE:

Supervisor:

Guangbin Dong, Supervisor

Michael J. Krische

Eric V. Anslyn

Michael J. Rose

Hung-wen (Ben) Liu

**Palladium-Catalyzed Carbon-Hydrogen Bond Functionalization
Utilizing an *Exo*-Directing Strategy**

by

Zhi Ren, B.S.; M.S.

Dissertation

Presented to the Faculty of the Graduate School of

The University of Texas at Austin

in Partial Fulfillment

of the Requirements

for the Degree of

Doctor of Philosophy

The University of Texas at Austin

May 2016

Dedication

To my family and friends

Acknowledgements

First of all, I would like to thank my supporting advisor, Prof. Guangbin Dong, for your mentorship and guidance over the last five years. Your wisdom and kindness will be appreciated for the rest of my life.

Next, I would like to send my appreciation to my Dong group colleagues for their support and friendship. I must thank Fanyang, Yan, Guobing, Jonathan, and Jianchun, who I have worked with, and especially my roommate/coworker Zhe. I highly appreciate the linguistic advice from Rachel, John, Brandon, Nik, Alpay, Mike, and Marshall. I also learned much knowledge from Tao, Haye Min, Zhiqian, Xuan, Hee Nam, Rong, and Ying. I will cherish the friendship with other group members: Zhongxing, Penghao, Ki-young, Lin, Tatsuhiko, Jiaxin, Chengpeng, Danny, Saiyong, and Dong. I would like to thank all my friends outside of Dong group: Andrew, Changxia, Di, Xin, and Ryan.

Finally, I need to thank my parents and other members of my family for giving me the chance to fulfill my ambition in science.

Thank all from whom I gained strengths or learned lessons.

Abstract

Palladium-Catalyzed Carbon-Hydrogen Bond Functionalization Utilizing an *Exo*-Directing Strategy

Zhi Ren, Ph.D

The University of Texas at Austin, 2016

Supervisor: Guangbin Dong

Transition metal catalyzed functionalization of carbon-hydrogen bonds (C–H bonds) has become an exponentially growing field. Particularly, Pd-catalyzed methods with various directing groups (DGs) have been developed for site selectivity. In addition, the use of an oxime as a DG proved to be an efficient and removable DG. However, alcohol-based directing strategies are still rare and underdeveloped. The research and development in this dissertation mainly focused on the utilization of masked alcohols as DGs for late stage diversification. With an *exo*-directing strategy, the syntheses of chemically differentiated vicinal diols and 2-hydroxyalkylphenol derivatives were achieved. Through a series of studies on cyclopalladation of methine groups, the first direct C–H activation complex was prepared and characterized. Additionally, a comprehensive introduction of TM-catalyzed alkylation of aromatic C–H bonds with simple olefins was illustrated.

Table of Contents

List of Tables	x
List of Figures.....	xii
List of Schemes	xiii
CHAPTER 1: PALLADIUM-CATALYZED C–H FUNCTIONALIZATION OF OXIMES	1
1.1 Introduction.....	1
1.2 Pd-Catalyzed C–H Functionalization via an <i>Endo</i> -Directing Strategy	4
1.2.1 Functionalization of SP^3 C–H bonds	4
1.2.2 Functionalization of SP^2 C–H bonds	9
1.3 Pd-Catalyzed C–H Functionalization via an <i>Endo</i> -Directing Strategy	14
1.3.1 Functionalization of SP^3 C–H bonds	14
1.3.2 Functionalization of SP^2 C–H bonds	18
1.4 Other Pd-Catalyzed Functionalization of Oximes C–H Bonds	21
1.5 Conclusion	24
CHAPTER 2: PALLADIUM-CATALYZED FUNCTIONALIZATION OF UNACTIVATED ALIPHATIC C–H BONDS OF MASKED ALCOHOLS VIA <i>exo</i>-DIRECTING GROUPS	25
2.1 Introduction.....	25
2.2 Background.....	26
2.3 Reaction Development and Scope	28
2.4 Conclusion	36
2.5 Experiment Results	36
2.5.1 General considerations.....	36
2.5.2 General procedure and characterization.....	37

CHAPTER 3: PALLADIUM-CATALYZED <i>ORTHO</i>-ACETOXYLATION OF MASKED BENZYL ALCOHOLS VIA AN <i>EXO</i>-DIRECTING MODE	148
3.1 Introduction.....	148
3.2 Background.....	149
3.3 Reaction development and scope.....	150
3.4. Conclusion	158
3.5. Experiment Results	158
3.5.1 General consideration	158
3.5.2 General procedure and characterization.....	160
CHAPTER 4: PRELIMINARY MECHANISTIC STUDIES ON PALLADIUM CATALYZED C–H BOND ACTIVATION WITH <i>EXO</i>-DIRECTING GROUPS	280
4.1 Introduction.....	280
4.2 Background.....	281
4.3 Reaction Design and Discussion.....	283
4.4 Conclusion	288
4.5 Experiment results	289
4.5.1 General considerations.....	289
4.5.2 General procedure and characterization.....	290
CHAPTER 5: TRANSITION-METALS CATALYZED ALKYLATION OF AROMATIC C–H BONDS WITH SIMPLE OLEFINS	368
5.1 Introduction.....	368
5.2 Background.....	371
5.3 TM-Catalyzed Alkylation of Aromatic C–H Bonds.....	371
5.3.1 Ruthenium catalysis.....	371
5.3.1.1 Chelation controlled.....	371
5.3.1.2 Non-chelation control	384

5.3.1.3 Application of Ruthenium-Catalyzed Arene C–H Bond Alkylation	388
5.3.2 Rhodium catalysis	391
5.3.2.1 Electron-Rich Benzene Rings and Heterocycles	391
5.3.2.2 Application of Rhodium-Catalyzed Arene C–H Bond Alkylation	415
REFERENCES.....	419
Chapter 1 References.....	419
Chapter 2 References.....	421
Chapter 3 References.....	423
Chapter 4 References.....	424
Chapter 5 References.....	426

List of Tables

Table 2.1. Selected optimization of reaction conditions.	29
Table 2.2. Summary of the substrate scope.....	32
Table 2.2. Summary of the substrate scope (continued).	33
Table 2.3. The scale of the reaction.	35
Table 2.4. Crystal data and structure refinement for 2.9b	93
Table 2.5. Crystal data and structure refinement for 2.13	95
Table 2.6. Crystal data and structure refinement for 2.14	97
Table 3.1. Selected Optimization of Reaction Conditions.	152
Table 4.1.2. Atomic coordinates and equivalent isotropic displacement parameters for Pd complex 4.5	302
Table 4.1.3. Bond lengths [Å] and angles [°] for Pd complex 4.5	303
Table 4.1.4. Anisotropic displacement parameters for Pd complex 4.5	307
Table 4.1.5. H coordinates and isotropic displacement parameters for Pd complex 4.5	308
Table 4.1.6. Torsion angles [°] for Pd complex 4.5	309
Table 4.2.1. Crystal data and structure refinement for Pd complex 4.7	312
Table 4.2.2. Atomic coordinates and equivalent isotropic displacement parameters for 4.7	313
Table 4.2.3. Bond lengths [Å] and angles [°] for 4.7	315
Table 4.2.4. Anisotropic displacement parameters for 4.7	322
Table 4.2.5. H coordinates and isotropic displacement parameters for 4.7	324
Table 4.2.6. Torsion angles [°] for 4.7	326
Table 4.3.1. Crystal data and structure refinement for Pd complex 4.8	329

Table 4.3.2. Atomic coordinates and equivalent isotropic displacement parameters for 4.8.....	331
Table 4.3.3. Bond lengths [Å] and angles [°] for 4.8.	332
Table 4.3.4. Anisotropic displacement parameters for 4.8.....	336
Table 4.3.5. H coordinates and isotropic displacement parameters for 4.8.	338
Table 4.3.6. Torsion angles [°] for 4.8.	339
Table 4.4.1. Crystal data and structure refinement for Pd complex 4.10.....	342
Table 4.4.2. Atomic coordinates and equivalent isotropic displacement parameters for 4.10.....	343
Table 4.4.3. Bond lengths [Å] and angles [°] for 4.10.	345
Table 4.4.4. Anisotropic displacement parameters for 4.10.....	352
Table 4.4.5. H coordinates and isotropic displacement parameters for 4.10.	354
Table 4.4.6. Torsion angles [°] for 4.10.	357

List of Figures

Figure 1.1. Pd-catalyzed sp^3 C–H oxidative rearrangement.	16
Figure 1.2. One example using oxime DG in aromatic C–H oxidation.....	18
Figure 2.1. Representing natural products containing 1,2-diol moieties.	27
Figure 2.2. <i>endo</i> -Directing vs. <i>exo</i> -directing.	27
Figure 2.3. <i>exo</i> -Directing strategy with Pd catalysis.	28
Figure 2.4. The intermolecular KIE result.	35
Figure 3.1. Isolation of Palladacycle 3.19c	156
Figure 4.1. The mechanism for C–H activation at tertiary carbon center.	281
Figure 4.2. Pd-catalyzed C–H functionalization of norbornyl substrate.	282
Figure 4.3. Pd-mediated elimination of aldoxime to give 2,6-dimethoxynitrile.	285

List of Schemes

Scheme 1.1.1. First cyclopalladation with aromatic oximes.	1
Scheme 1.1.2. <i>endo</i> -Directing vs. <i>exo</i> -directing strategy.	2
Scheme 1.1.3. Three types of C–H functionalization of oximes.	3
Scheme 1.2.1. Pd-catalyzed sp^3 C–H acetoxylation.....	4
Scheme 1.2.2. Pd-catalyzed sp^3 C–H oxidation with transformable DG.	5
Scheme 1.2.3. NaNO ₃ as catalytic co-oxidant in aerobic C–H oxygenation.	5
Scheme 1.2.4. Pd-catalyzed sp^3 C–H amidation with nitrene.	6
Scheme 1.2.5. Pd-catalyzed arylation with diaryliodonium salts.....	6
Scheme 1.2.7. Total synthesis of natural products with catalytic Pd.	9
Scheme 1.2.8. Pd-catalyzed sp^2 C–H acetoxylation and methoxylation.....	10
Scheme 1.2.9. Application in acetoxylation of [2.2]paracyclophane oximes with Pd catalysis.	10
Scheme 1.2.10. Pd-catalyzed sp^2 C–H hydroxylation and application in Zaltoprofen synthesis.	11
Scheme 1.2.11. Pd-catalyzed sp^2 C–H amidation.	12
Scheme 1.2.12. Pd-catalyzed sp^2 C–H ethoxycarbonylation.	13
Scheme 1.2.13. Pd-catalyzed sp^2 C–H arylation.	14
Scheme 1.3.1. Pd-catalyzed sp^3 C–H acetoxylation for 1,2-diol synthesis.....	15
Scheme 1.3.2. Pd-catalyzed sp^3 C–H sulfonyloxylation for diverse functionalization.	16
Scheme 1.3.3. Pd-catalyzed sp^3 C–H for the synthesis of the cyclic ether.	17
Scheme 1.3.4. Pd-catalyzed sp^2 C–H acetoxylation.....	19
Scheme 1.3.5. Pd-catalyzed sp^2 C–H olefination with acrylate derivatives.	20

Scheme 1.3.6. Pd-catalyzed sp^2 C–H arylation with aryl boronic acid pinacol esters.	20
Scheme 1.4.1. Pd-catalyzed synthesis of heterocycles via Heck-type cyclization of oxime ethers.	22
Scheme 1.4.2. Pd-catalyzed cyclization for the synthesis of heterocyclic oximes with tethered vinyl iodide.	22
Scheme 1.4.3. Pd-catalyzed synthesis of fluorenone via dual C–H functionalization.	23
Scheme 2.1. Pd-catalyzed C–H functionalization of ketone oximes.	25
Scheme 2.2. Alcohol or masked-alcohol directed C–H bond functionalization. ..	26
Scheme 2.3. <i>endo</i> -Effect using oxazoline as a DG.	28
Scheme 2.4. Two-pot preparation of oxime substrates.	30
Scheme 2.5. A Pd-triggered oxidative rearrangement.....	34
Scheme 2.6. Orthogonal protecting groups.	36
Scheme 3.1. Different directing modes in aromatic palladation.	148
Scheme 3.2. Alcohol or masked alcohol-directed arene C–H oxidation.	149
Scheme 3.3. The scope with primary alcohol-derived substrates.	153
Scheme 3.4. The scope with secondary alcohol-derived substrates.	154
Scheme 3.5. Reaction TON test and mono-oxidation.	156
Scheme 3.6. Cleavage of the Directing Group	157
Scheme 4.1. Pd-Catalyzed C–H oxidation with <i>exo</i> -directing strategy.	280
Scheme 4.2. Representative Pd-catalyzed methine C–H functionalization.	282
Scheme 4.3. Representative tertiary alkyl Pd complexes.....	283
Scheme 4.4. Pd-catalyzed oxidation of bridgehead C–H bonds via an <i>exo</i> -DG.	284
Scheme 4.5. Preparation of Pd complex 4.5	285

Scheme 4.6. Preparation of Pd complex 4.7	286
Scheme 4.7. C–H cyclopalladation at tertiary sp^3 positions with substrate 4.6 ..	287
Scheme 4.8. C–H cyclopalladation at tertiary sp^3 positions with substrate 4.9 ..	288
Scheme 5.1. Two representative alkylation reactions.	368
Scheme 5.2. Three pathways for the alkylation of aromatic C–H bonds.....	370
Scheme 5.3. Ru-catalyzed <i>ortho</i> -selective C–H alkylation of phenols with ethylene.	372
Scheme 5.4. Ru-catalyzed C–H alkylation of phenols with styrene.	372
Scheme 5.5. Ru-catalyzed <i>ortho</i> -alkylation of aromatic ketones with olefins....	373
Scheme 5.6. Proposed mechanism for Ru-catalyzed <i>ortho</i> -alkylation of aromatic ketones.	374
Scheme 5.7. The deuterium scrambling experiment for Ru alkylation.	374
Scheme 5.8. Ru-catalyzed alkylation of heterocycles with silylated olefins.	375
Scheme 5.9. Ru-catalyzed alkylation of aromatic ketones containing 9-ferrocenyl groups.....	376
Scheme 5.10. Ru-catalyzed <i>ortho</i> -alkylation of aromatic imines with simple olefins.	376
Scheme 5.11. Ru-catalyzed chemoselective alkylations with simple olefins.	377
Scheme 5.12. Room temperature alkylation with an <i>in situ</i> generated Ru catalyst.	377
Scheme 5.13. Room temperature alkylation with a fully characterized Ru catalyst.	378
Scheme 5.14. A versatile Ru catalyst for alkylations of both aromatic ketones and imines.....	378
Scheme 5.15. Mechanistic study of formate salt in Ru-catalyzed alkylation.....	379
Scheme 5.16. Ru-catalyzed alkylation with isopropanol to lower the temperature.	380

Scheme 5.17. Ru-catalyzed room temperature C–H alkylation of aromatic ketones.	380
Scheme 5.18. Reactivity in alkylation with new Ru catalysts.....	381
Scheme 5.19. Ru-catalyzed alkylation with various functional groups.	381
Scheme 5.20. Ru-catalyzed alkylation of 2-phenylpyridine derivatives.	382
Scheme 5.21. Ru-catalyzed alkylation using heterocycles as the directing groups.	383
Scheme 5.22. Ru-catalyzed alkylation/tautomerization reaction of allylic and homoallylic alcohols.	383
Scheme 5.23. One example on Ru-catalyzed alkylation of <i>N</i> -methyl aniline.....	384
Scheme 5.24. Ru-catalyzed C–H alkylation of simple benzene.	385
Scheme 5.25. Proposed mechanism for Ru-catalyzed C–H alkylation of simple benzene.	385
Scheme 5.26. Ru-catalyzed C–H alkylation of simple benzene with 1-hexene..	386
Scheme 5.27. Ru-catalyzed alkylation of heteroaromatic substrates.	387
Scheme 5.28. Mechanistic study on Ru-catalyzed alkylation of simple arenes. .	387
Scheme 5.29. Ru-catalyzed alkylation of simple arenes with high TON.....	388
Scheme 5.30. Ru-catalyzed step-growth copolymerization with acetophenone. .	389
Scheme 5.31. Ru-catalyzed copolymerization with <i>in situ</i> generated catalyst....	389
Scheme 5.32. Ru-catalyzed a post-functionalization with a silicon-based polymer.	390
Scheme 5.33. Ru-catalyzed derivatization of diterpenoid natural products.	390
Scheme 5.34. Rh-catalyzed hydroarylation of norbornene with aniline or diphenylamine.....	391
Scheme 5.35. Rh-catalyzed multi-alkylation of aryl boronic acids.....	392
Scheme 5.36. Deuterium labeling in Rh-catalyzed multi-alkylation.	392
Scheme 5.37. Proposed mechanism for Rh-catalyzed multi-alkylation.....	393

Scheme 5.38. Rh-catalyzed <i>ortho</i> -alkylation of phenols and anilines.	394
Scheme 5.39. Rh-catalyzed alkylation of aromatic ketones with new Rh catalyst.	394
Scheme 5.41. Rh-catalyzed <i>ipso</i> - and <i>ortho</i> -dialkylation of benzaldehydes.....	396
Scheme 5.42. Rh-catalyzed alkylation of aromatic ketimines with internal olefins.	396
Scheme 5.43. The proposed mechanism of Rh-catalyzed alkylation of aromatic ketimines.	397
Scheme 5.44. Rh-catalyzed alkylation of aromatic ketones with catalytic benzylamine.	398
Scheme 5.45. Rh catalysis using recyclable self-assembly-supported (SAS) system.	399
Scheme 5.46. Rh-catalyzed alkylation of aromatic aldimines and ketimines with olefins.....	400
Scheme 5.47. Rh-catalyzed alkylation of terephthaldimine with olefins.	401
Scheme 5.48. Rh-catalyzed alkylation of aromatic ketones with diynes and enynes.	402
Scheme 5.49. Rh-catalyzed alkylation of 2-phenylpyridines with olefins.	403
Scheme 5.50. Rh-catalyzed alkylation of 2-phenylpyridines with styrene.	403
Scheme 5.51. Rh-catalyzed atroposelective alkylation with pyridine DG.	404
Scheme 5.52. Rh-catalyzed intramolecular C–H alkylation of heteroarenes.	404
Scheme 5.53. Mechanistic study of the intramolecular alkylation of heterocycles.	405
Scheme 5.54. Rh-catalyzed intermolecular C–H alkylation of heteroarenes.	405
Scheme 5.55. Proposed mechanism for intermolecular alkylation of heterocycles.	406
Scheme 5.56. Rh-catalyzed alkylation of 4,4-dimethyl-2-oxazolines with olefins.	407
Scheme 5.57. Rh-catalyzed alkylation of 3,4-dihydroquinazoline with simple olefins.	408

Scheme 5.58. DFT calculations on Rh-catalyzed alkylation of 3,4-dihydroquinazoline.	409
Scheme 5.59. Rh-catalyzed alkylation of quinolines and pyridines with olefins.	409
Scheme 5.60. Rh-catalyzed annulation of aromatic imines using Wilkinson's catalyst.	410
Scheme 5.61. Rh-catalyzed enantioselective alkylation using chiral ligands.	411
Scheme 5.62. Rh-catalyzed asymmetric alkylation using chiral aromatic imines.	412
Scheme 5.63. Rh-catalyzed alkylation of 2,2'-bipyridines and 2,2'-bisquinolines.	413
Scheme 5.64. The proposed mechanism of Rh-catalyzed alkylation of 2,2'-bipyridines.	413
Scheme 5.65. Rh-catalyzed intramolecular alkylation of 2-aryl-3-vinylpyridines.	414
Scheme 5.66. Rh-catalyzed synthesis of a tricyclic mescaline analog.	415
Scheme 5.68. Rh-catalyzed enantioselective synthesis of a protein kinase C inhibitor.	416
Scheme 5.69. Rh-catalyzed a concise synthesis of potent bicyclic bisaryl imidazoles.	417
Scheme 5.70. Rh-catalyzed alkylation of aromatic ketimines with polybutadiene.	418

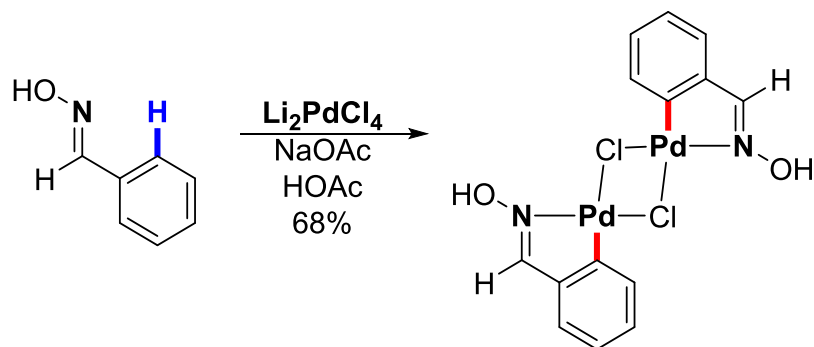
CHAPTER 1: PALLADIUM-CATALYZED C–H FUNCTIONALIZATION OF OXIMES

1.1 Introduction

Transition metals catalyzed carbon-hydrogen bond functionalization (C–H functionalization) represents the one of the challenging yet fruitful fields.¹ In particular, many novel transformations using palladium catalysis have been developed.² To achieve the high site-selectivity, directing groups (DGs) was introduced and applied as a strategy to overcome the wide existence of C–H bonds in organic molecules.³ Among various DGs, such as pyridine and oxazoline, using oxime groups as DGs are demonstrated to possess synthetic advantages, as oxime DGs can be removed or transformed into other function groups.⁴

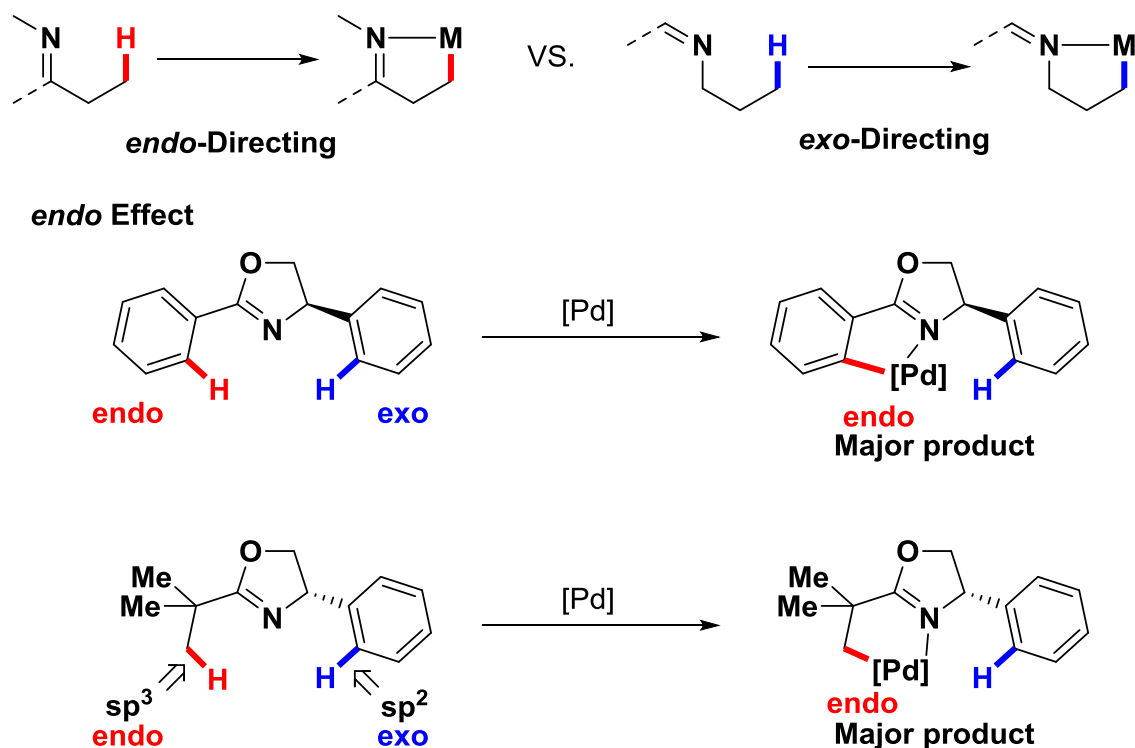
The first C–H cyclopalladation with oximes was documented in 1970 (Scheme 1.1.1).⁵ Using Li_2PdCl_4 with NaOAc in acetic acid at room temperature, the *ortho* aromatic C–H bonds was successfully activated to give a 5-membered palladacycle. The NaOAc was found to be crucial for the C–H activation step to occur, which could be explained by the mechanism that was now known as the concerted metalation-deprotonation (CMD) pathway.

Scheme 1.1.1. First cyclopalladation with aromatic oximes.



In general, the sp^2 nitrogen-centered ligands are known to form two types of metalation: an *endo*-directing mode in which the C=N double bond is inside of the palladacycle, and *exo*-directing mode in which C=N double bond is outside of the palladacycle (Scheme 1.1.2).⁶ The *endo*-directing mode is favored over *exo*-directing mode when both activation modes are possible, and even the sp^2 -*exo* C-H bond is less competitive than sp^3 -*endo* C-H bond, which has been known as *endo* effect.⁷

Scheme 1.1.2. *endo*-Directing vs. *exo*-directing strategy.

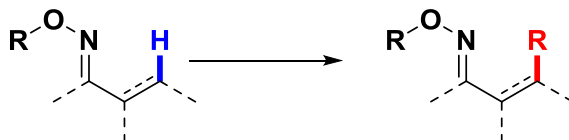


Using oximes as DGs in C-H functionalization, three different types of C-H bonds can be activated: 1) the C-H bond on the nitrogen side, 2) the C-H bond on the oxygen side, and 3) the sp^2 C-H bond on the carbon-nitrogen double bond. Therefore, in this review, the transformations are divided into the three corresponding parts: *endo*-mode, *exo*-mode, and the other types of reactions as shown in corresponding **Type A**, **B**,

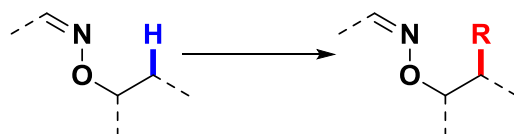
or C in Scheme 1.1.2. The reactions involving *in situ* cleavage of N–O bond of oximes for heterocycle synthesis are not reviewed in this chapter.⁸

Scheme 1.1.3. Three types of C–H functionalization of oximes.

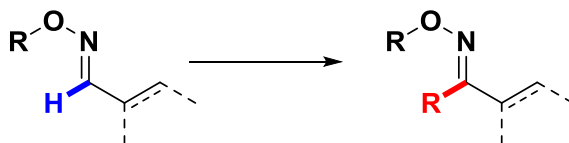
Type A: *endo*-Directing Mode



Type B: *exo*-Directing Mode



Type C: Other Reactions

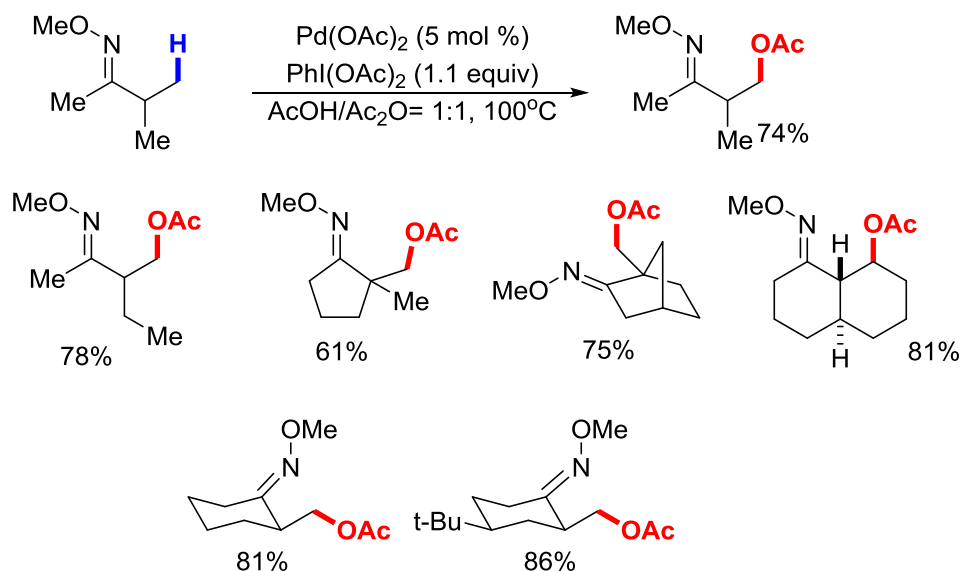


1.2 Pd-Catalyzed C–H Functionalization via an *Endo*-Directing Strategy

1.2.1 FUNCTIONALIZATION OF sp^3 C–H BONDS

The first seminal work in Pd-catalyzed sp^3 C–H acetoxylation with *endo* oxime DG (**Type A**) was developed by Sanford and co-workers in 2004 (Scheme 1.2.1).⁹ The oxime substrates are prepared by condensation between parent ketones and *O*-methylhydroxylamine. In the help of the oxime sp^2 nitrogen, Pd catalyst can selectively activate the C–H bond at the β -position of the parent ketones to give the five-membered palladacycle, which could be further oxidized by the oxidant, $\text{PhI}(\text{OAc})_2$, to give acetoxylation product in good yield. The C–H bonds at both methyl and cyclic methylene group were successfully oxidized under the optimal condition. When cyclic methylene substrate was applied (e.g. trans-decline *O*-methyl oxime), the C–H oxidation occurred diastereoselectively at the equatorial position.

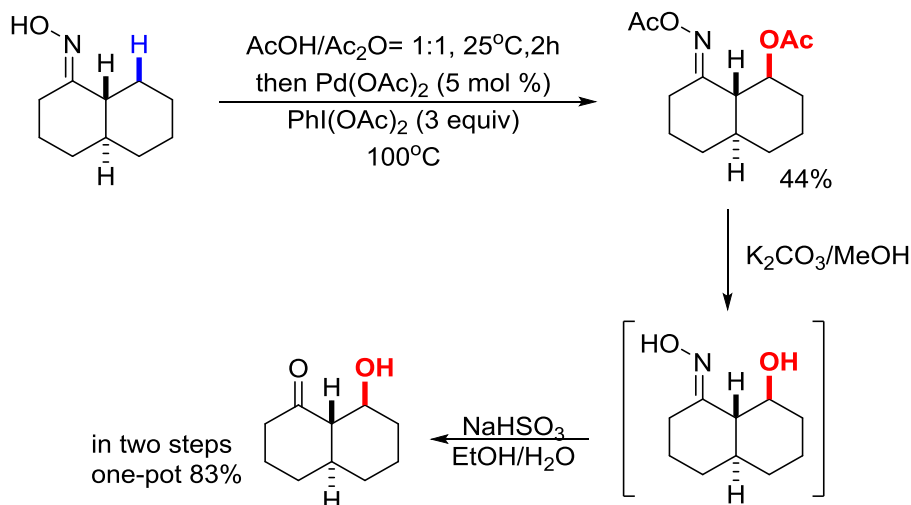
Scheme 1.2.1. Pd-catalyzed sp^3 C–H acetoxylation.



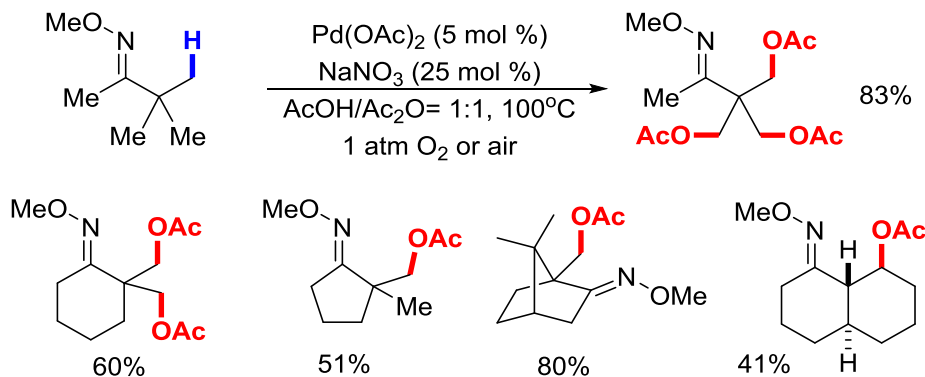
However, the further transformations for the C–H functionalization products with *O*-methyl oxime DG were found to be problematic, as the β -hydroxyl ketone derivatives

tend to give elimination products under strong acidic conditions. In 2010, Sanford and co-worker developed a transformable DG, which can be removed within two steps in one-pot to solve this problem (Scheme 1.2.2).¹⁰

Scheme 1.2.2. Pd-catalyzed sp^3 C–H oxidation with transformable DG.



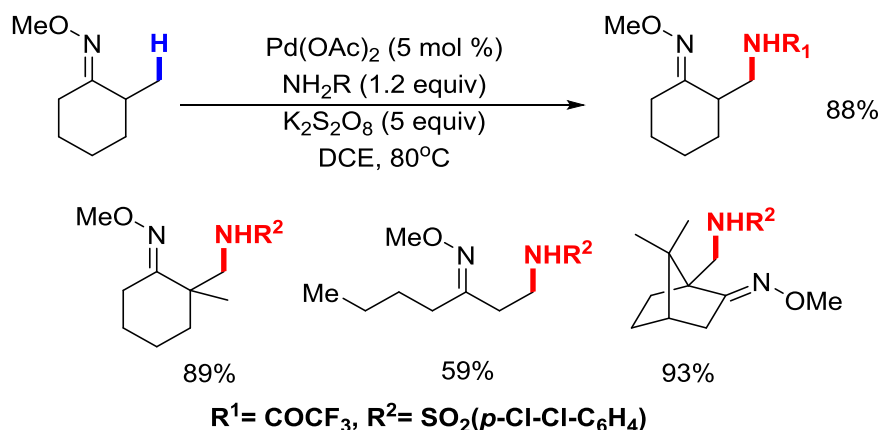
Scheme 1.2.3. NaNO_3 as catalytic co-oxidant in aerobic C–H oxygenation.



In 2012, the further studies by Sanford group led to the discovery of NaNO_3 or NaNO_2 , as catalytic co-oxidant, which enabled the aerobic C–H oxygenation (Scheme 1.2.3).¹¹ According to the preliminary mechanistic studies, NO was proposed to be the key intermediate in this NO_x redox co-catalyst system, in which NO could be oxidized to NO_2 by oxygen, and NO_2 could oxidize $\text{Pd}(\text{II})$ to $\text{Pd}(\text{III})$.

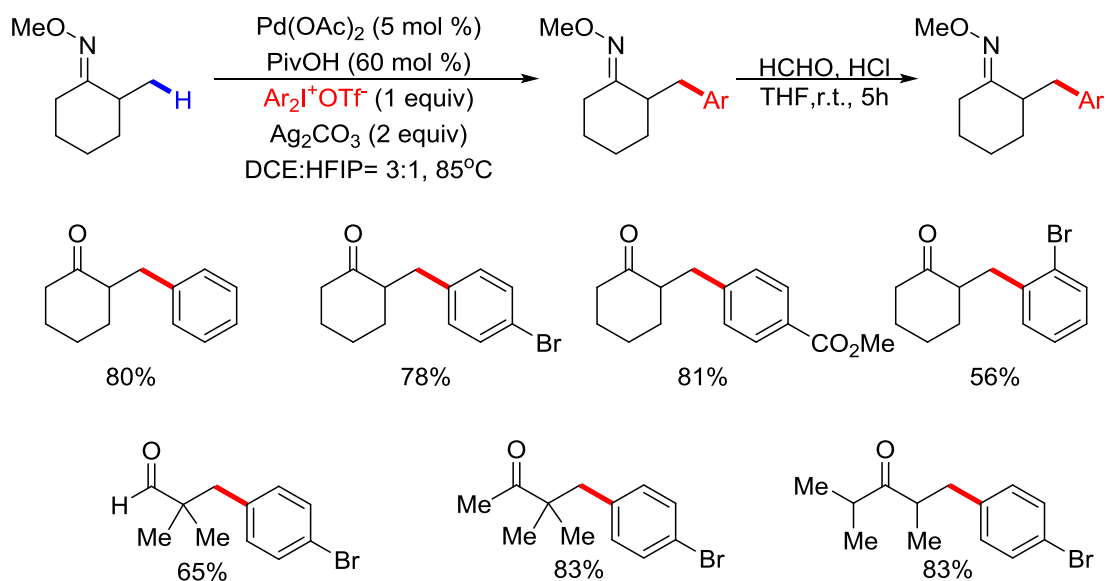
In 2006, Che and Yu co-team developed the Pd-catalyzed C–H amidation of oximes with nitrene insertion (Scheme 1.2.4).¹² The sp^3 C–H functionalization selectively occurs at β -position of parent oxime to give amidation products in good to excellent yields. The nitrene was demonstrated to be generated *in situ* by reacting the primary amides or sulfonamides with $K_2S_2O_8$. However, the nature of the reactive nitrene species that inserted into the palladacycle during the reaction is still uncertain. The similar transformation with Ir catalysis and TsN_3 as nitrene precursor was achieved by Chang's group in 2014.¹³

Scheme 1.2.4. Pd-catalyzed sp^3 C–H amidation with nitrene.



In 2016, Chen's group demonstrated the arylation of *O*-methyl oxime substrates with diaryliodonium salts (Scheme 1.2.5).¹⁴ The optimized condition requires a super-stoichiometric amount of silver salt to give the desired products in good to excellent yields with various diaryliodonium salts. The counterion of diaryliodonium salts was also found to be critical, and the OTf salt gave the best result. The proposed palladation intermediate was isolated and offered the desired product under the standard condition.

Scheme 1.2.5. Pd-catalyzed arylation with diaryliodonium salts.

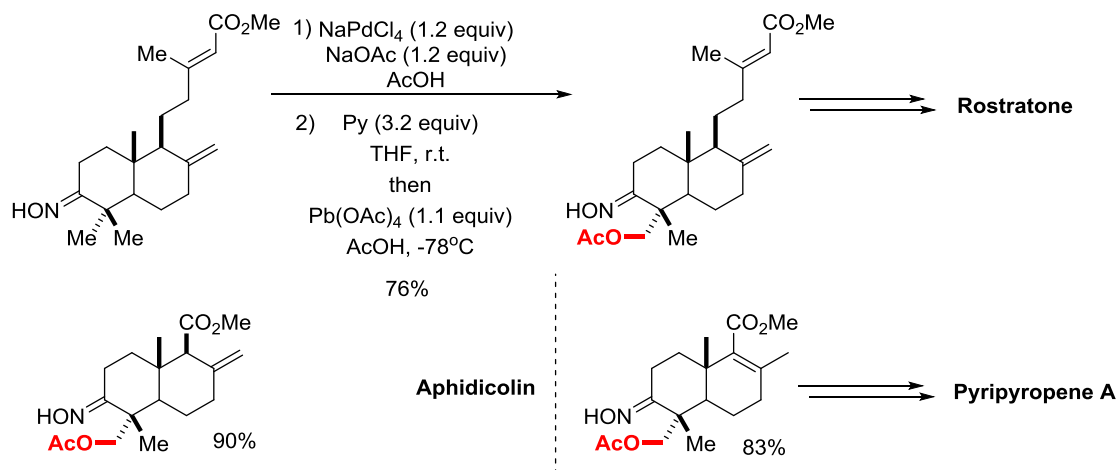


Before the transformable DG was introduced, the *O*-methyl oxime DG cannot be easily removed. Therefore, the applications need to use stoichiometric Pd in total synthesis with oxime as DG (Scheme 1.2.6). In 2005, the Oltra and Cueva team applied the β -oxygenation in the total synthesis of Rostratone, and toward Aphidicolin and Pyripyropene A with $\text{Pb}(\text{OAc})_4$ as an oxidant in two separate steps.¹⁵ In 2007, the Parra and co-workers followed the stoichiometric Pd C–H oxidation in the partial synthesis of hyptatic acid A.¹⁶

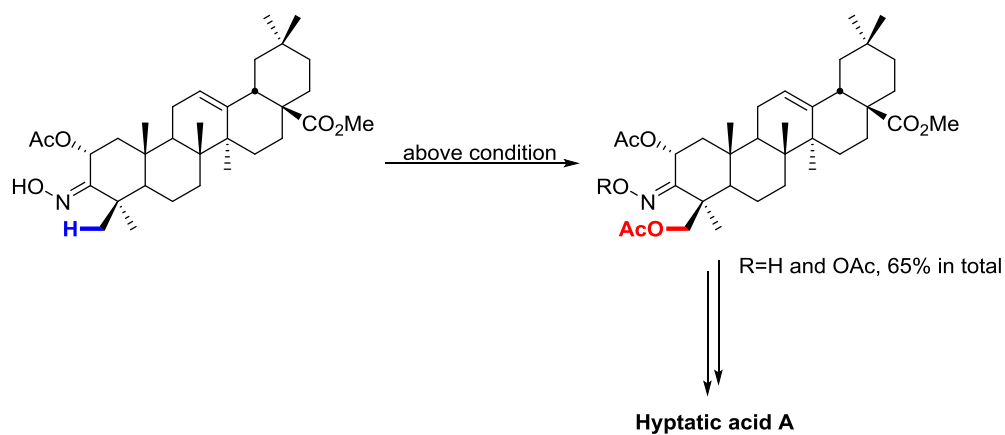
The development of removable DG for C–H functionalization enables the applications of catalytic Pd in the total synthesis of natural products (Scheme 1.2.7). In 2004, Sorensen and co-workers synthesize Jiadifenolide with the transformable DG.¹⁷ Later in 2015, Johnson and co-worker prepared the intermediated for the synthesis of Paspaline¹⁸, and Trotta group and Li group applied *O*-methyl oxime DG in the preparation of Oridamycin B¹⁹.

Scheme 1.2.6. Total synthesis of natural products with stoichiometric Pd.

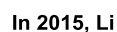
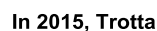
In 2005, Oltra and Cuerva team



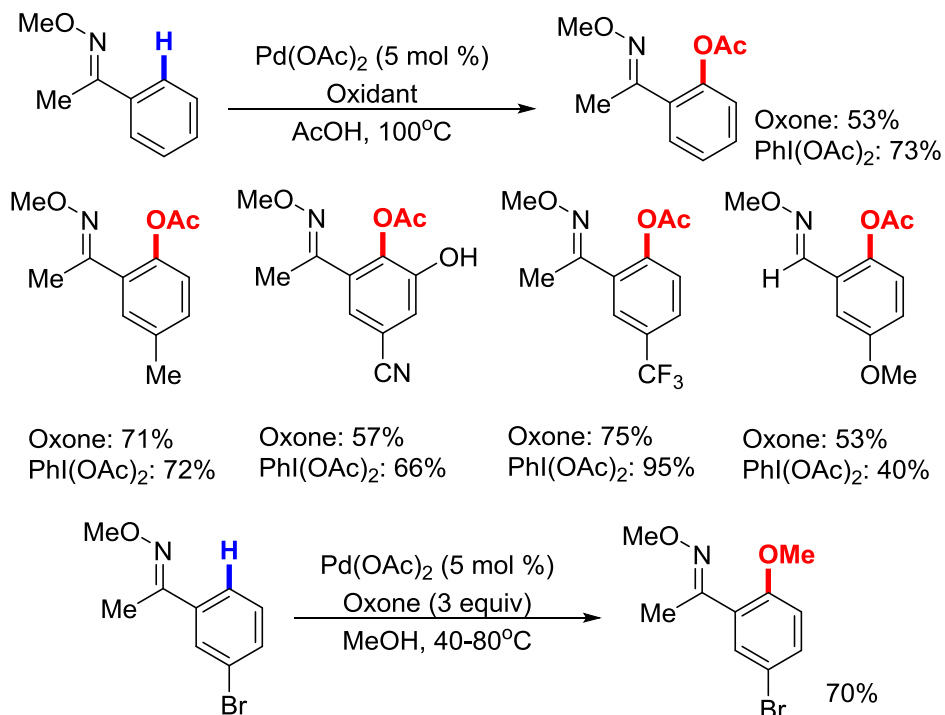
In 2007, Parra and co-workers



In 2014, Sorensen and co-workers

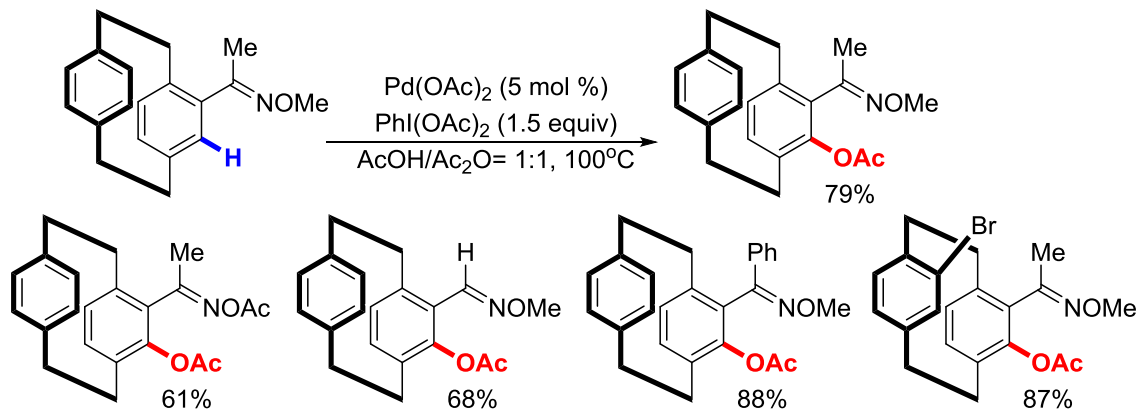


Scheme 1.2.8. Pd-catalyzed sp^2 C–H acetoxylation and methoxylation.



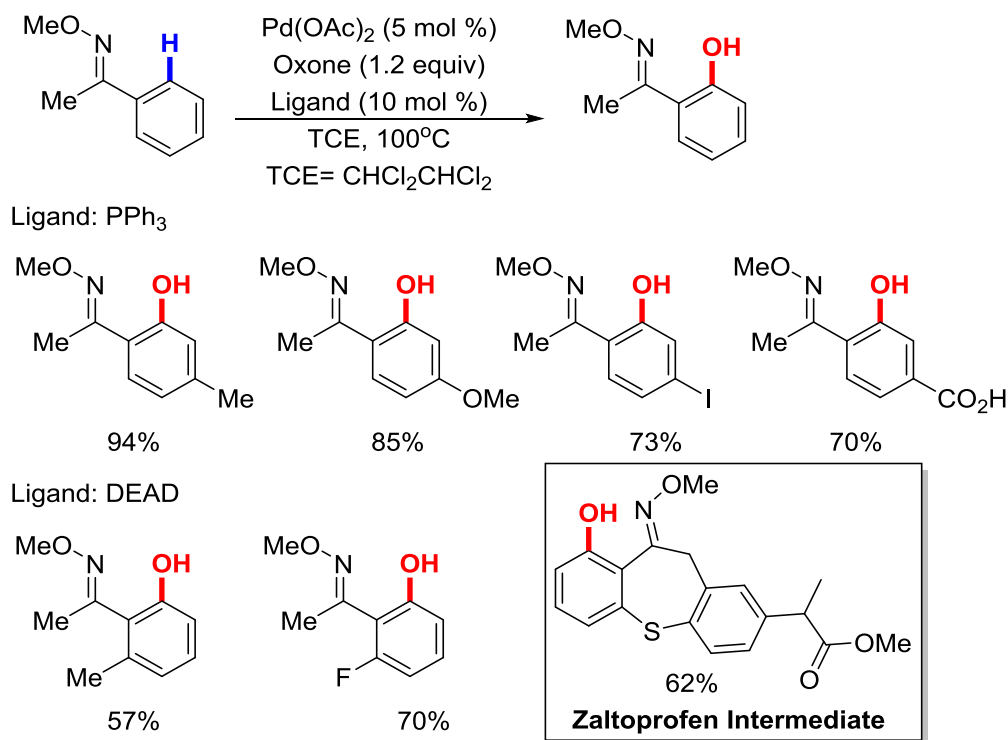
In 2012, Bolm and co-workers applied the Pd-catalyzed C–H functionalization to the oxidation of *ortho*-aromatic C–H bond in [2.2]paracyclophane oxime derivatives (Scheme 1.2.9).²¹ The [2.2]paracyclophane and its derivatives have significant applications in the material science and asymmetric synthesis as ligands or catalysts.

Scheme 1.2.9. Application in acetoxylation of [2.2]paracyclophane oximes with Pd catalysis.



In 2015, Jiao's group developed the Pd-catalyzed C–H hydroxylation of aromatic C–H bonds using *O*-methyl oxime as a DG (Scheme 1.2.10).²² With PPh₃ or DEAD as ligand and Oxone as the oxidant, the *ortho* selective C–H hydroxylation offers the phenol products in good to excellent yields. Through oxygen isotope labeling experiments, the incoming oxygen atom of the hydroxyl group was proposed to be transferred from the Oxone. The key intermediate for Zaltoprofen synthesis was prepared to demonstrate the application potential of this method.

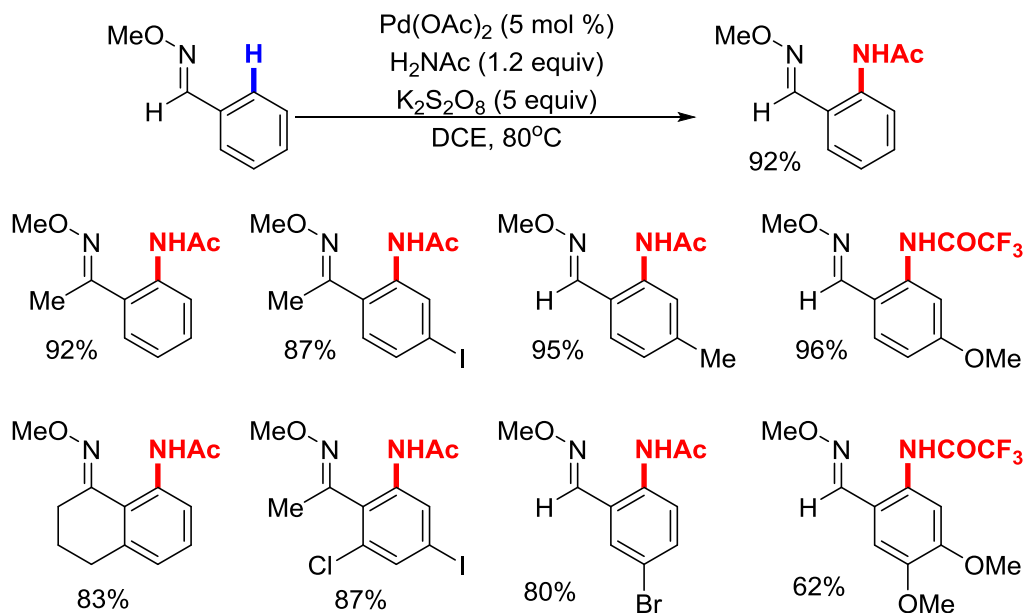
Scheme 1.2.10. Pd-catalyzed sp^2 C–H hydroxylation and application in Zaltoprofen synthesis.



In 2006, the Che and Yu co-team developed the Pd-catalyzed amidation reaction of aromatic C–H bonds using oxime DGs (1.2.11).¹² Comparing to the sp^3 C–H functionalization, the aromatic C–H amidation can undergo with the less acidic primary amides, such as acetamide, to provide the acetylaniline derivatives in good to excellent

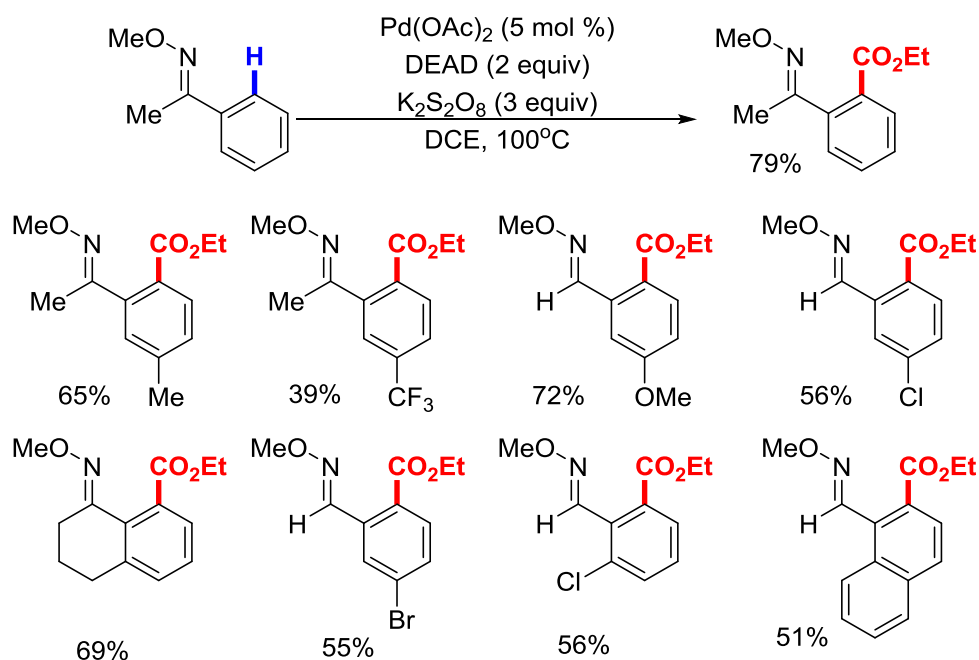
yields. The pathway for this reaction was proposed to give the palladation first and then nitrene insertion to give the final product. To clarify the nature of the nitrene species during the insertion step, the further mechanistic studies are still in demand.

Scheme 1.2.11. Pd-catalyzed sp^2 C–H amidation.



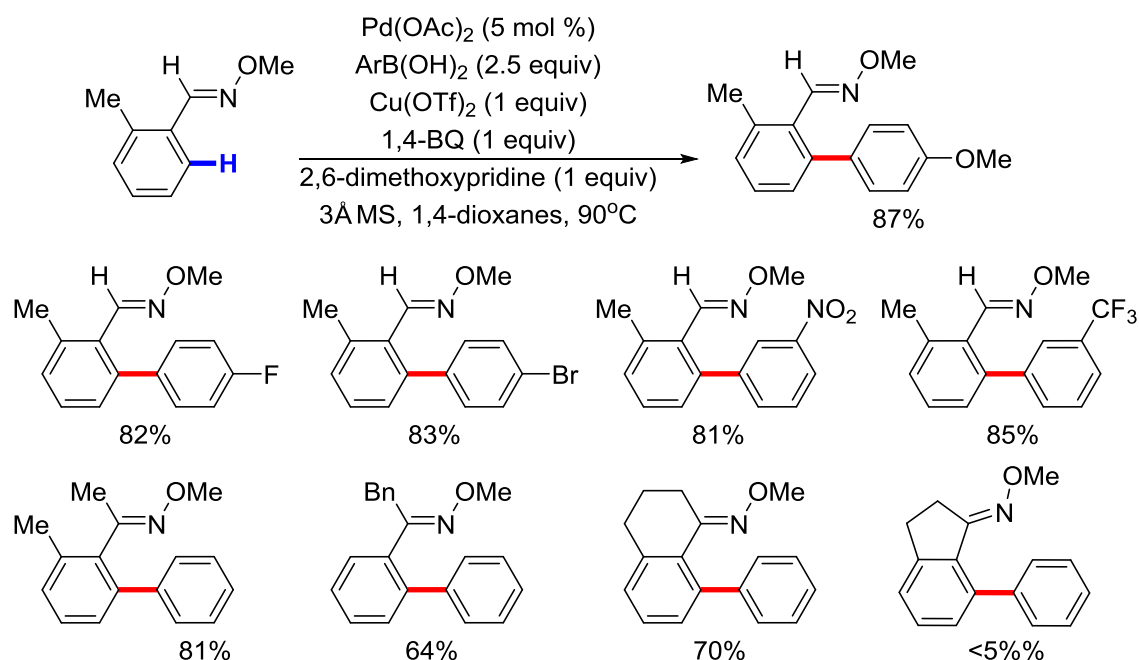
In 2008, Yu's group demonstrated the Pd-catalyzed ethoxycarbonylation of aromatic C–H bonds (Scheme 1.2.12).²³ Using DEAD as the source of the acyl group and $\text{K}_2\text{S}_2\text{O}_8$ as the oxidant, the aromatic ethyl esters were obtained in acceptable to moderate yields. The mechanistic studies suggest that this reaction may involve a radical pathway as the DEAD can thermally decompose to ethoxycarbonyl radical, and the addition of the radical scavenger dramatically decreases the yield. However, the detailed mechanism for the radical insertion into the palladacycle requires more comprehensive examination. Since the reaction is conducted under the strong oxidative condition, the Pd(IV) pathway could be an alternative pathway for the formation of C–C bond.

Scheme 1.2.12. Pd-catalyzed sp^2 C–H ethoxycarbonylation.



In 2010, the Shi's group demonstrated the arylation of oximes with aryl boronic acids (Scheme 1.2.13).²⁴ In the help of copper salt, 1,4-benzoquinone, 2,6-methoxypyridine, and 3 Å molecular sieves, the Pd-catalyzed *ortho*-arylation reaction give the biaryl products in moderate to good yields. Under the arylation condition, the 1-tetralone oxime gave the product in good yield, while the more strained 1-indanone oxime did not offer the desired biaryl product. The role of the copper salt was proposed to be the terminal oxidant for regenerating Pd(II) from Pd(0) with the assistance of 1,4-benzoquinone. The base, 2,6-methoxypyridine, is used to neutralize the strong acid, HOTf, generated through the reaction to avoid the acid mediated cyclization to give the fluorenone derivatives.

Scheme 1.2.13. Pd-catalyzed sp^2 C–H arylation.



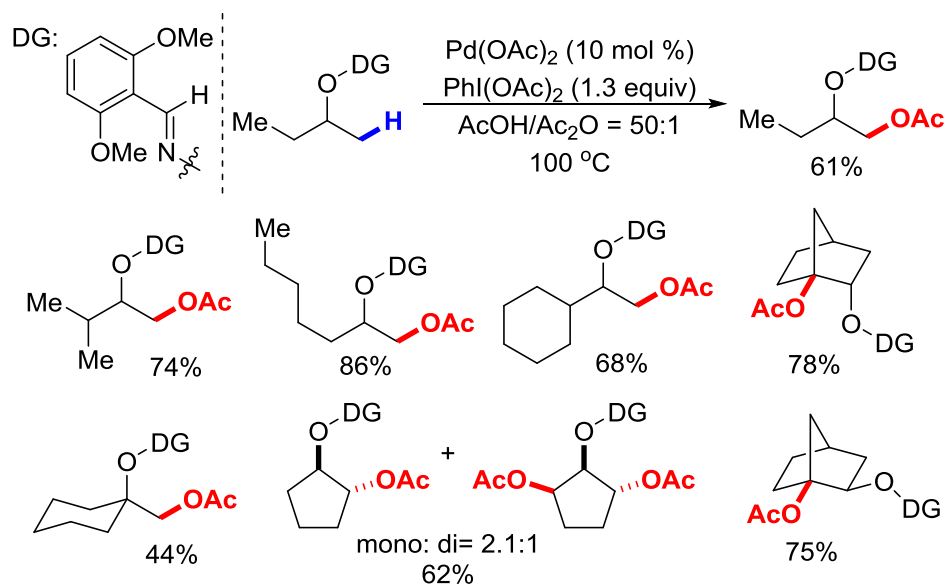
1.3 Pd-Catalyzed C–H Functionalization via an *Endo*-Directing Strategy

1.3.1 FUNCTIONALIZATION OF SP^3 C–H BONDS

As demonstrated in the previous sections, the traditional *endo*-DGs played a significant role in Pd-catalyzed C–H functionalization. However, it is difficult to rationalize the application of such strategy in free alcohols or masked alcohols functionalization. On the other hand, the prevalence of hydroxyl groups in natural products and bioactive compounds demands methodologies to functionalize the β -position preferably in late stage. Therefore, the development of a new directing strategy is required to solve this scientific problem, and will have a significant impact on the synthesis of bioactive compounds for pharmaceutical studies. As demonstrated in this section, the *exo*-directing strategy (**Type B**) exhibits an exclusive advantage in the functionalization of masked alcohols.

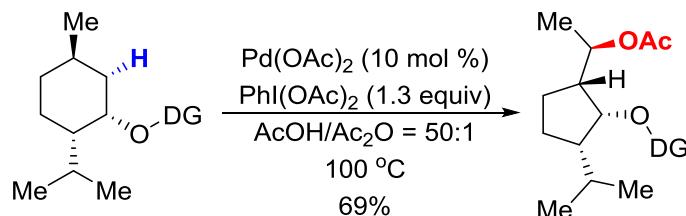
In 2012, Dong and co-workers first utilized the *exo*-directing strategy (**Type B**) in Pd-catalyzed C–H functionalization of the oxime masked alcohols to synthesize chemically differentiated 1,2-diols (Scheme 1.3.1).²⁵ Through the appropriate design of the DG, the palladation occurred selectively at the β -position of the original hydroxyl group via an *exo*-directing mode, and after the oxidation to give the acetate protected 1,2-diols. Under the reaction condition, not only the regular methyl and cyclic methylene C–H bonds, but also the bridgehead methine C–H bonds were oxidized in good to excellent yields. The DG and acetate group can be removed under orthogonal conditions to give a chemically differentiated 1,2-diols, which could work as valuable building blocks for pharmaceutical industrial and academic research.

Scheme 1.3.1. Pd-catalyzed sp^3 C–H acetoxylation for 1,2-diol synthesis.

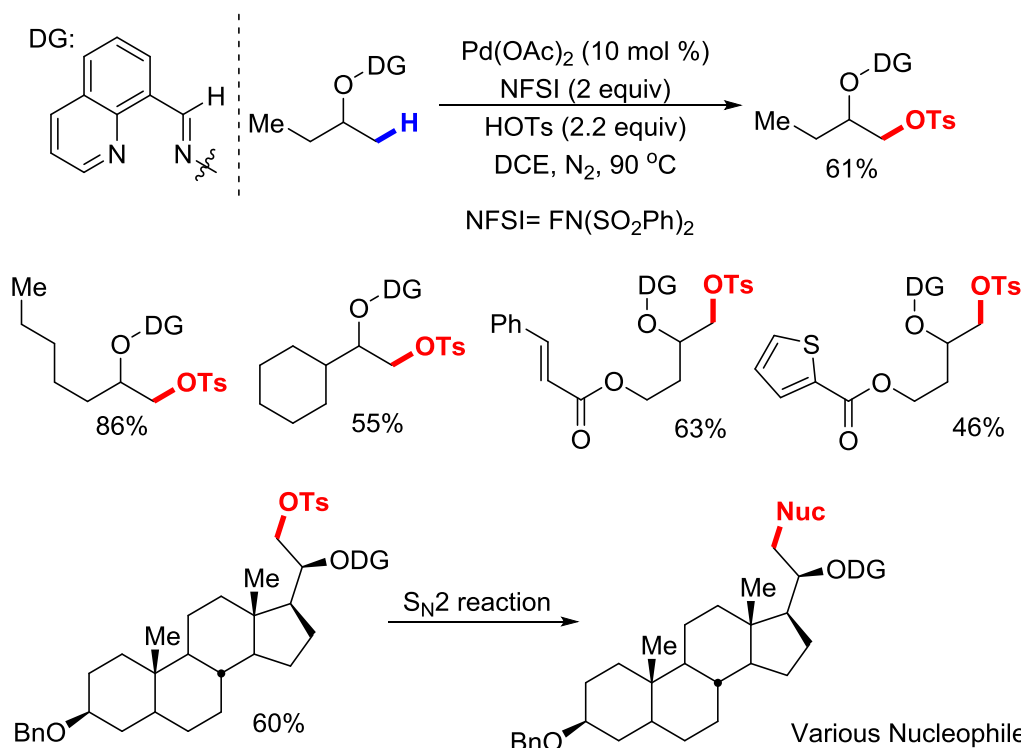


Surprisingly, when the menthol derived oxime substrate was submitted to the Pd-catalyzed condition, an oxidative rearrangement product was obtained as a single diastereomer (Figure 1.1). The structure of the product is a 1,3-diol derivative containing a 5-membered ring, which was confirmed by X-ray crystallography.

Figure 1.1. Pd-catalyzed sp^3 C–H oxidative rearrangement.



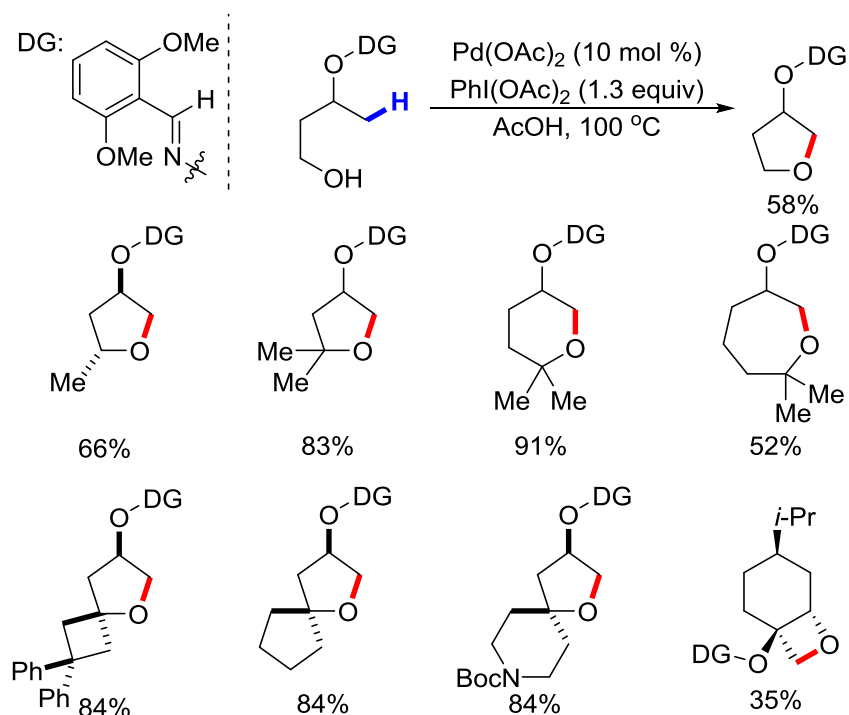
Scheme 1.3.2. Pd-catalyzed sp^3 C–H sulfonyloxylation for diverse functionalization.



In 2015, the same group developed the Pd-catalyzed C–H sulfonyloxylation at the β -position of alcohols (Scheme 1.3.2).²⁶ In general, the OTs group is considered as an excellent leaving group while a terrible nucleophile under most conditions. Therefore, enabling HOTs as a nucleophile has a great advantage to introduce a good leaving group for the rapid diversification of drug molecules in late stage. The optimal condition involves an electrophilic fluorination reagent, NFSI, as the oxidant, and HOTs as a nucleophile to give the products in good to excellent yields. Many interesting functional

groups including olefins, amines, arenes and heterocycles were tolerated. The steroid intermediate, 2H-pregnanediol oxime, was used to demonstrate the late-stage diversification of the product through S_N2 reaction with various nucleophiles including nucleophiles based on carbon, oxygen, sulfur, phosphine, and halogens. When menthol derived oxime substrate was used, the fluorinated product was obtained.

Scheme 1.3.3. Pd-catalyzed *sp*³ C–H for the synthesis of the cyclic ether.



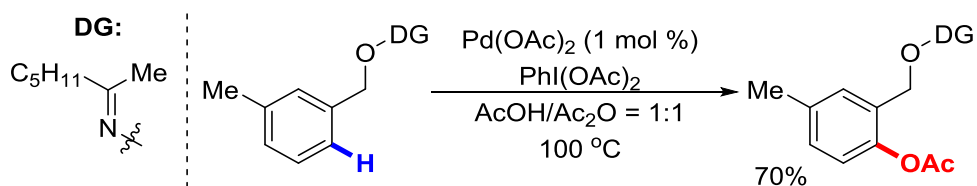
In the same year, Dong's group demonstrated a Pd-catalyzed dehydrogenative cyclization for the synthesis of cyclic ether (Scheme 1.3.3).²⁷ The primary, secondary, and tertiary free alcohols all worked under the optimized condition to give the cyclic ethers in good to excellent yields. The oxidative cyclization occurs through the tethered free hydroxyl group attacking the C–Pd bond via S_N2 reaction to form four- to seven-membered rings. The fused four- and six-membered oxetane product demonstrates the

potential application in the bioactive compound syntheses, e.g. paclitaxel. Many types of functional groups are tolerated, including amides, carbamates, cyclobutane, and arenes.

1.3.2 FUNCTIONALIZATION OF sp^2 C–H BONDS

Comparing to the functionalization of sp^3 C–H bonds, sp^2 C–H functionalization with *exo*-directing strategy goes through a six-membered *exo*-palladacycle. Differed from the C=N double bond in the *endo*-directing mode, the C–O single bond in *exo*-DGs can freely rotate. This unique feature allows the multiple C–H bonds functionalization under Pd-catalyzed conditions, which is another consideration when applying these methods.

Figure 1.2. One example using oxime DG in aromatic C–H oxidation.

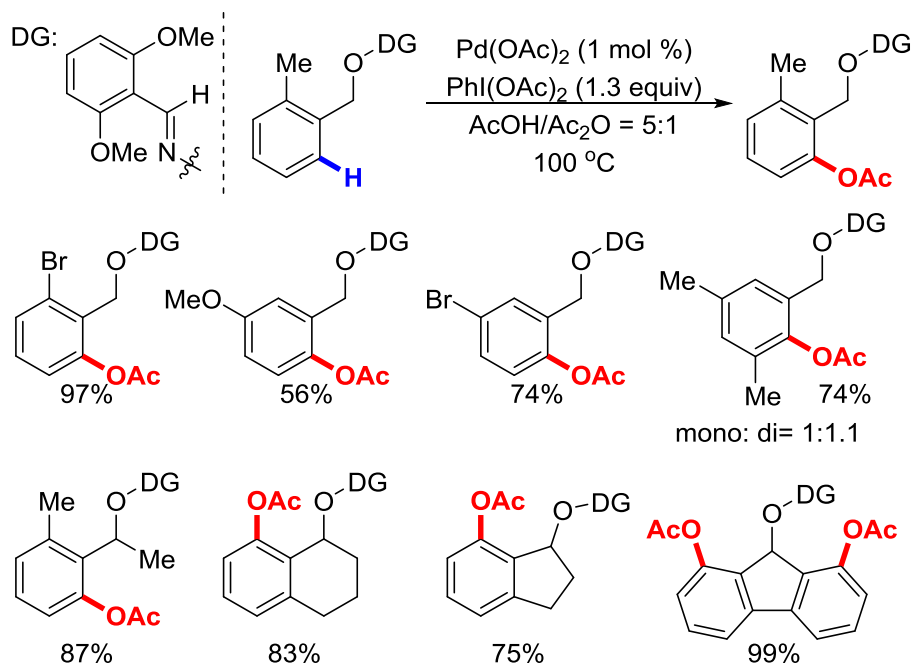


In 2008, Sanford group conducted a series of experiments to compare the directing ability among various functional groups and reported a single example using oxime in directed aromatic C–H oxidation (Figure 1.2).²⁸ This seminal work provides moderate yield, due to the relatively low efficiency of the DG. Therefore, a better DG is still needed for higher reactivity and turnover numbers.

The Pd-catalyzed oxygenation of aromatic C–H bonds was developed by Dong group in 2015 (Scheme 1.3.4).²⁹ As the wide existence of 2-hydroxyalkylphenol derivatives in the natural products and drugs, the rapid and straightforward synthetic methods are required. For practical purpose, high catalyst turnover numbers are favored for the application. By adopting the 2,6-dimethoxyoxime as DG, 1700 TON was achieved for each oxidation with 0.1 mol % Pd(OAc)₂, attribute to the extra stability provided by the weak coordination of methoxy groups. To take the advantage of benzylic

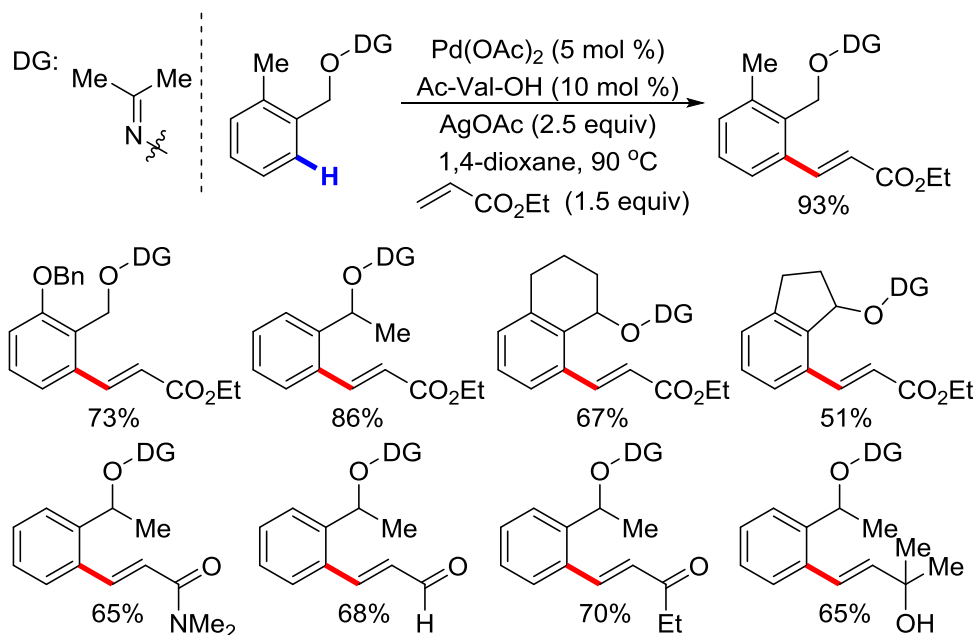
oximes, the DG can be removed through either C–O or N–O cleavage to offer versatility for different synthetic purposes.

Scheme 1.3.4. Pd-catalyzed sp^2 C–H acetoxylation.

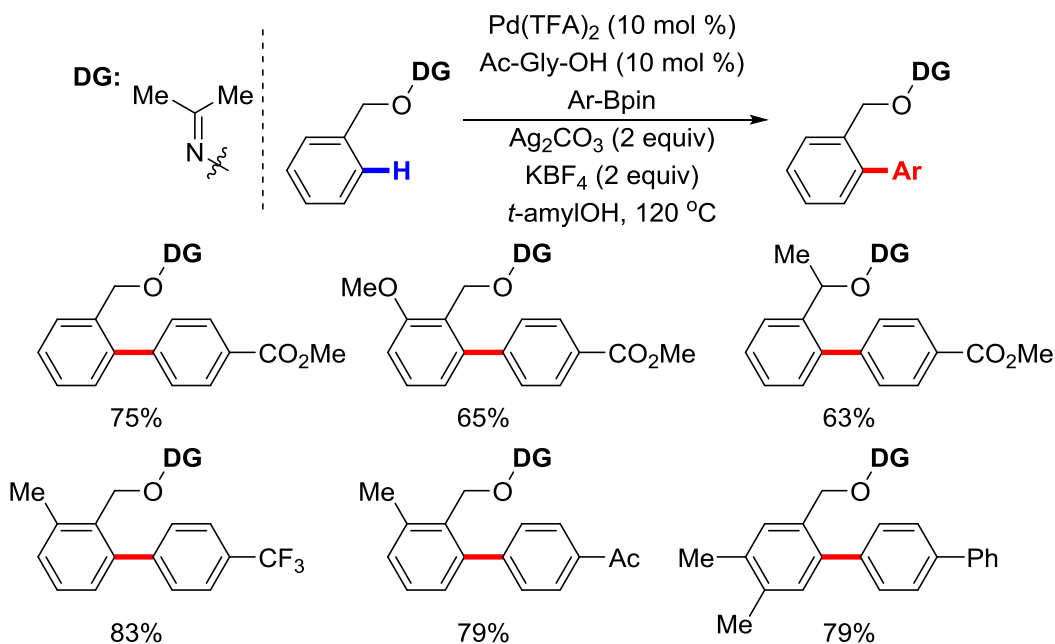


In 2015, Zhao's group demonstrated the *ortho*-olefination of aromatic C–H bond via oxidative Heck reaction (Scheme 1.3.5).³⁰ As the lack of additional coordination from the DG, an extra amino acid was required to facilitate the C–H activation step.³¹ In the presence of stoichiometric silver acetate, the olefination products were obtained in moderate to good yields. As demonstrated by the application in the total synthesis of 3-deoxyisoochacinic acid, the DG was removed using the expensive and superstoichiometric reagent, $\text{Mo}(\text{CO})_6$, because the newly generated alkenes cannot be tolerated under the reductive condition.

Scheme 1.3.5. Pd-catalyzed sp^2 C–H olefination with acrylate derivatives.



Scheme 1.3.6. Pd-catalyzed sp^2 C–H arylation with aryl boronic acid pinacol esters.



In the same year, Zhao and co-workers developed a C–H arylation reaction with aryl boronic acid pinacol esters as coupling partners (Scheme 1.3.6).³² By using the

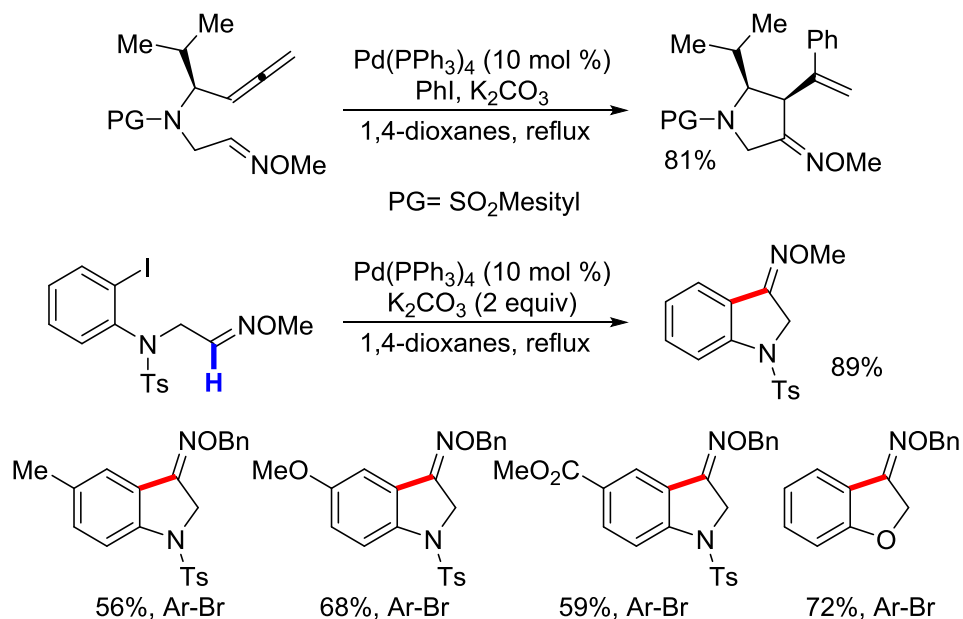
similar combination of amino acid ligand, Ag_2CO_3 , and KBF_4 , the C–H arylation gives *ortho*-arylation products in good yields. The scope of the substrate for this transformation is demonstrated by various substituted aromatic oximes with aryl boronic acid pinacol esters with different electronic properties. The amino acid ligand was known to promote the C–H activation while the Ag_2CO_3 was proposed to be the oxidant to regenerate the Pd(II) catalyst. However, the detailed role of KBF_4 salt is still unclear.

1.4 Other Pd-Catalyzed Functionalization of Oximes C–H Bonds

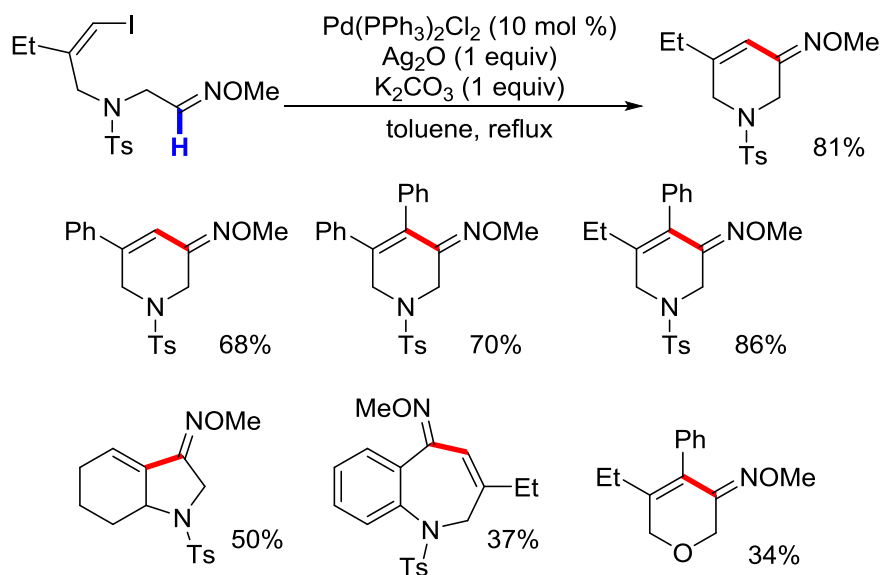
Pd-catalyzed functionalization of the imine C–H bond at aldoxime undergoes a different mechanistic pathway, which is known as insertion/elimination pathway. Unlike the Type A and Type B reactions (*endo/exo*-directed C–H functionalization), Type C reaction did not go through C–H activation of the imine hydrogen. Instead, the imine hydrogen was removed by β -hydride elimination to regenerate the Pd catalysis. These methods were applied to prepare heterocycles and fluorenone.

In 2007, Tanaka, Ohno, and co-workers developed a Pd-catalyzed synthesis of heterocycles via Heck-type cyclization of oxime ethers (Scheme 1.4.1).³³ The reaction was discovered during the investigations toward the cyclization of allene with additional double bonds. An unexpected Pd-catalyzed C–H functionalization of aldoxime with iodobenzene occurred and gave the pyrrolidine derivative. This reaction was further extended into the intramolecular fashion to prepare 3-indolinone or 3-benzofuranone oxime analogs in moderate to good yields. The inconsistency of E/Z ratio in starting materials and products suggests an insertion/elimination mechanism for cyclization reaction.

Scheme 1.4.1. Pd-catalyzed synthesis of heterocycles via Heck-type cyclization of oxime ethers.

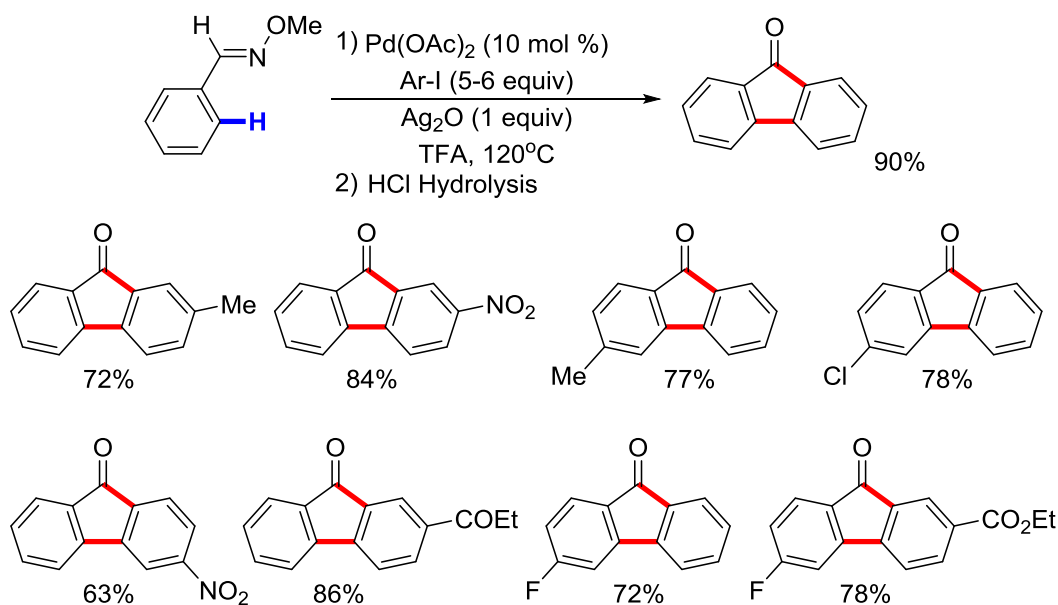


Scheme 1.4.2. Pd-catalyzed cyclization for the synthesis of heterocyclic oximes with tethered vinyl iodide.



In 2011, Tong' group extended the Pd-catalyzed cyclization for heterocyclic oximes synthesis with tethered vinyl iodide moiety (Scheme 1.4.2).³⁴ With PPh₃ as ligand and stoichiometric silver salt, the Heck-type cyclization with different tether length to give heterocyclic products in moderate yields. Since the desired product can be obtained with catalyst turnover by solely using K₂CO₃, the role of silver was suggested as a base.

Scheme 1.4.3. Pd-catalyzed synthesis of fluorenone via dual C–H functionalization.



In 2008, Cheng's group demonstrated a Pd-catalyzed synthesis of 9-fluorenone through dual C–H functionalization of *O*-methyl oximes with aryl iodides (Scheme 1.4.3).³⁵ The reaction proceeded through the *ortho* C–H arylation at the aldoximes, and the Heck-type cyclization to form the 5-membered ring and through acid prompted hydrolysis to give 9-fluorenone derivatives in good yields. The process was supported by using the biaryl intermediate under the reaction condition to give the desired product in good yields. Silver salt was proposed to contribute as the halides scavenger to facilitate the reductive elimination and the oxidant to regenerate Pd(II) from Pd(0).

1.5 Conclusion

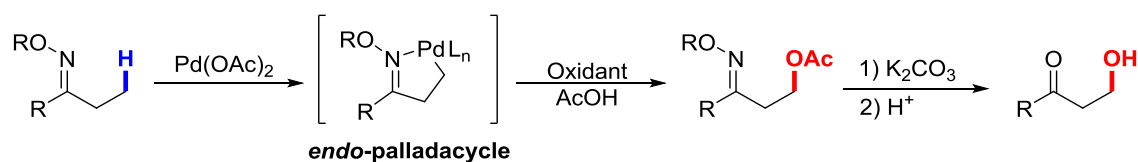
The directing strategy is still widely deployed in the field of C–H functionalization for site selectivity. Utilizing oxime group as DG in different modes has been proven to provide novel and efficient transformations in Pd-catalyzed C–H functionalization. Up to date, the methods using C–H functionalization to form C–O, C–N, C–C bonds have been developed and described. For the development of the DG point of view, the removability becomes an important concern in the perspective of the application. As the weakness of the N–O bond in oxime substrates, there are many ways has been demonstrated to achieve the cleavage of the oxime DG.

CHAPTER 2: PALLADIUM-CATALYZED FUNCTIONALIZATION OF UNACTIVATED ALIPHATIC C–H BONDS OF MASKED ALCOHOLS VIA *EXO*-DIRECTING GROUPS

2.1 Introduction

Transition metal catalyzed C–H functionalization has been rapid growth in the past two decades.¹ Many novel transformations have been realized to provide building blocks and applied to natural products.² Since the chemo- and site-selectivity is one of the challenges for developing the predictable and reliable transformations, different groups have solved this problem in their ways. For the metal carbenoid insertion reaction, both the substrate and catalyst-controlled C–H functionalization reactions have been developed by Davies' group.³ The Hartwig group demonstrated to utilize the sterical effect of substrates to control the chemo- and regioselectivity in borylation and silylation of arenes and alkanes.⁴ Besides the substrate or ligand-controlled examples, Sanford,⁵ Daugulis⁶ and Yu⁷ have developed various types of directing groups (DGs) for the C–H functionalization.

Scheme 2.1. Pd-catalyzed C–H functionalization of ketone oximes.



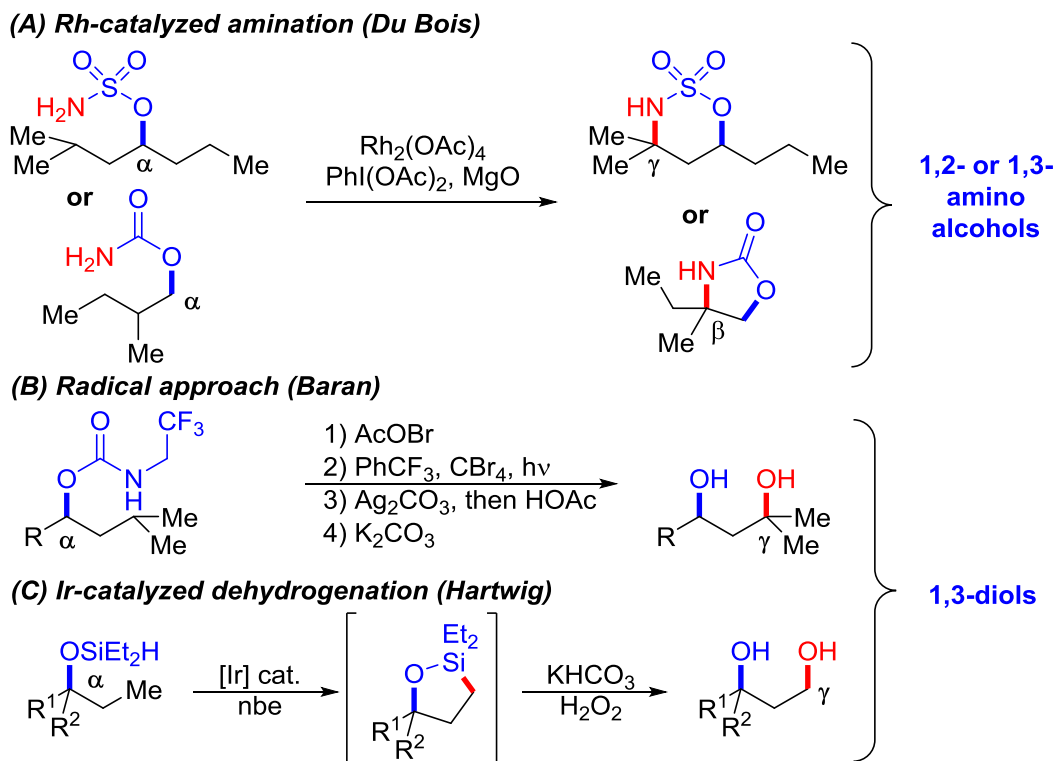
Pd-catalyzed C–H functionalization and carbon-heteroatom bond formation have been demonstrated as an efficient method to change the oxidation state of organic molecules.⁸ To achieve high site selectivity, the oxime as *endo*-DGs was established and studied by Sanford's group.⁹ However, the functionalization of alcohols or masked alcohols to synthesis 1,2-diols has not been realized before.¹⁰ Our group has utilized an

exo-directing strategy to achieve the C–H functionalization for C–O bonds formation to synthesize 1,2-diols.

2.2 Background

There are only a few methods have been developed for the unactivated sp^3 C–H functionalization of alcohols or masked alcohols.¹¹ In 2010, Du Bois and co-workers realized the Rh-catalyzed 1,2- or 1,3- amino alcohols synthesis through carbamate- or sulfamate-tethered nitrene insertion.¹² In 2008, Baran's group developed a four-step one-pot radical process to prepare 1,3-diols inspired by Hofmann-Löffler type reaction.¹³ In 2012, Hartwig's work on 1,3-diols synthesis from mono alcohols using Ir-catalyst with silicon as a temporary functional group.¹⁴ However, there is no 1,2-diols synthesis via C–H functionalization has been demonstrated before.

Scheme 2.2. Alcohol or masked-alcohol directed C–H bond functionalization.



As demonstrated in chapter 1, there are many examples of using oximes as *endo*-DGs for sp^3 C–H oxygenation of parent ketones. However, it is difficult to rationalize the *endo*-directing strategy in the functionalization of alcohols or masked alcohols. Therefore, a new strategy is demanded the synthesis of 1,2-diol moieties, which is common in natural products, such as Taxol, Picato, and Bryostatin 7 (Figure 2.1).¹⁵

Figure 2.1. Representing natural products containing 1,2-diol moieties.

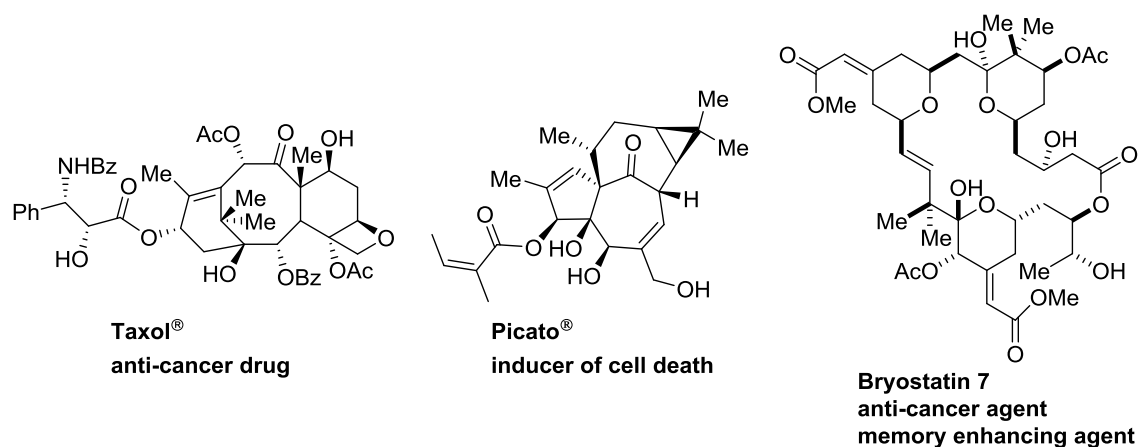
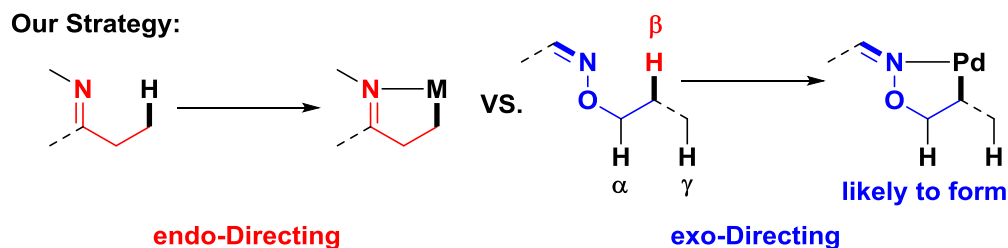


Figure 2.2. *endo*-Directing vs. *exo*-directing.



Considering C–H bonds that at the β -position of alcohol is more electron-poor than the ones at α -position, because of the inductive effect of the oxygen atom. This electron distribution makes the transition metal-oxo species prefer to insertion of the C–H bonds at the α -position.¹⁶ Another consideration is the removability of DGs after the reaction to recover the free hydroxyl group. We hypothesize that with appropriate oxime

as DG, the C–H functionalization of β -position of masked alcohols could be realized by new *exo*-directing strategy (Figure 2.2).

2.3 Reaction Development and Scope

The design of *exo*-DG encounters the problem that the formation of *endo*-metallacycle is much favored compared to *exo*-metallacycle.¹⁷ This *endo*-effect suggests that all the possible *endo* C–H activation sites need to be blocked on the new DG for the *exo*-metallation.¹⁸ Therefore, we decided to employ 2,6-dimethoxyaldehyde oxime as DG for the formation of a 5-membered *exo*-metallacycle.

Scheme 2.3. *endo*-Effect using oxazoline as a DG.

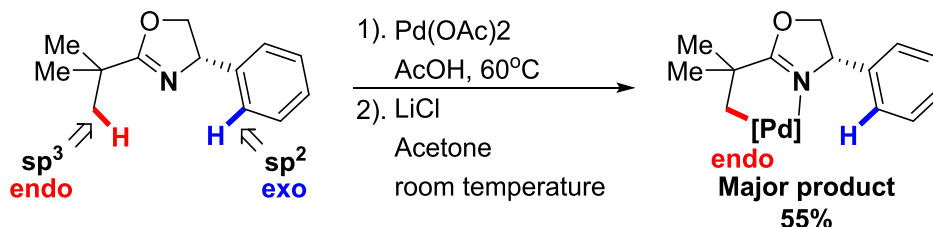
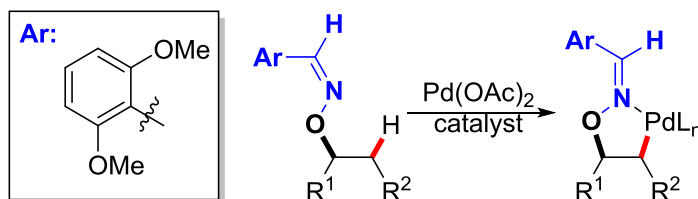


Figure 2.3. *exo*-Directing strategy with Pd catalysis.



To test this hypothesis, oxime masked 2-butanol was prepared and applied to the reaction as the standard substrate. With the optimized the reaction conditions, the desired 1,2-diol product was prepared in 67% yield without observation of γ -C–H oxidation.

Table 2.1. Selected optimization of reaction conditions.

entry	variation from the "standard conditions"	yield ^{b,d}
1	none	67%(61% ^c)
2	no Pd(OAc) ₂	0%
3	5 mol % Pd(OAc) ₂	50%
4	no PhI(OAc) ₂	0%
5	no Ac ₂ O	61%
6	H ₂ O instead of Ac ₂ O	50%
7	chlorobenzene instead of HOAc	7%
8	toluene instead of HOAc	7%
9	1,2-dichloroethane instead of HOAc	10%
10	K ₂ S ₂ O ₈ instead of PhI(OAc) ₂	24%
11	add 0.1 equiv of LiOAc	67%
12	0.25 mL of HOAc	53%
13	1 mL of HOAc	52%
14	use "DG A"	0%
15	use "DG B"	31%

DG A:

DG B:

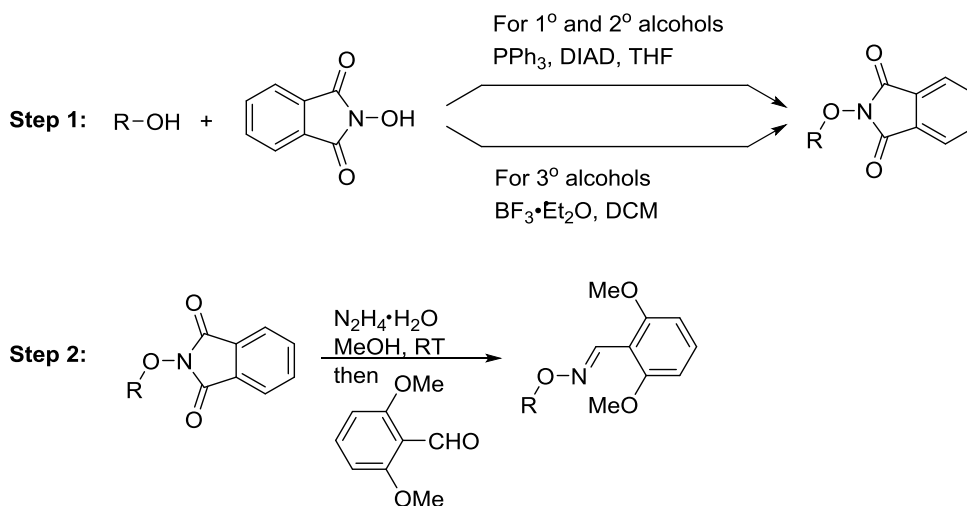
^aReaction conditions: all the reactions were run on a 0.1 mmol scale with 0.5 mL of solvents in 2 h. ^bNMR yield determined using 1,1,2,2-tetrachloroethane as internal standard. ^cIsolated yield. ^dProduct consisted of a mixture of oxime E/Z stereoisomers.

A series of control reactions was conducted to obtain some detailed insights of this aliphatic C–H oxidation reaction (Table 2.1). Without the Pd(OAc)₂ or PhI(OAc)₂, no desired product was detected, while less catalyst loading gave lower yield due to low conversion (entry 2 and 4). In the absence of water scavenger, Ac₂O, the yield was slightly decreased (entry 3). However, the addition of a small amount of water gave significant lower yield, implying that water could interfere this reaction (entry 6).¹⁹ The representing solvents gave the product in lower yield as shown from entry 7 to 9. Using K₂S₂O₈ as the oxidant led to low yield with a large amount of 2,6-dimethoxybenzonitrile which is the side product from elimination (entry 10). Additive, such as LiOAc, did not change the yield of the reaction (entry 11). Neither high nor lower concentration from the optimal condition gave lower yield (entry 11 and 12). Two other DGs were tested, and

with pyridine based DG no product was observed (entry 14), due to the pyridine could chelate to Pd too strong to give any catalyst turnover. On the contrary, the chloride in the DG B has a much weaker ability to bound the Pd resulted in lower yield (entry 15).²⁰

The substrates were prepared by a two-pot three steps procedure (Scheme 2.4). According to the nature of the parent alcohols, the *N*-alkoxy phthalimides were installed by either Mitsunobu reaction for 1° and 2° alcohols, or S_N1-type reaction for 3° ones. Followed by sequential one-pot deprotection/condensation to give the corresponding oxime masked alcohols. This preparation procedure is easy to operate, but the corresponding stereocenter of the parent alcohols is inverted. Therefore, a short DG installation method with the retention of the stereocenter is still needed.

Scheme 2.4. Two-pot preparation of oxime substrates.



To our delight, all the oxime masked primary, secondary and tertiary alcohol substrates underwent smoothly under the optimized condition, and the 1,2-diols were isolated in good yields (entry 1-9). As expected, the aliphatic C–H bonds at the β -position of the parent alcohols were selectively oxidized, and the C–H bond at methyl group is found to be more reactive than the one at non-methyl alkyl group (entry 3-7). As

shown in entry 5-7, the substrates with different steric hindrance were submitted to the optimal reaction condition, and the results suggest the alcohols with more hindered group on one side tend to give better yields. Compared to the tertiary substrates, the masked secondary alcohol substrates demonstrated to give higher yield attributing to higher conversion.

Other than methyl C-H bonds, the cyclic methylene C-H oxidation also has been demonstrated by oxime masked cyclopentanol substrate (entry 10). In that case, both mono- and bis-oxidized products were isolated. Notably, the first oxidation occurs at the opposite side of the DG to give a *trans*-diol **2.10b**, whereas the second oxidation happens on the same side of the DG to generate a *cis/trans*-triol **2.10c**. The observation can be explained by the conformational analysis of the preferential transition states of this substrate.

To our surprise, when masked either *endo*- or *exo*-norbornyl alcohol substrates were used, the selective oxidative C-H functionalization occurred at the methine C-H bonds at β -position in the presence of the less hindered cyclic β -methylene C-H bonds (entry 11 and 12). The conformational structure of the products (**2.11b** and **2.12b**) were confirmed by removal of both protecting groups and DG to compare with the known 1,2-diols.²¹ There is only one special example in literature that demonstrates the nonselective functionalization tertiary C-H bonds at strained cyclopropane ring.²² As demonstrated by our further studies (Scheme 1.3.2 and Scheme 1.3.3), the functional groups, such as ether, ester, oxime, and aryl groups should be tolerated in this reaction.

Table 2.2. Summary of the substrate scope.

$ \begin{array}{c} \text{DG} \\ \\ \text{O} \\ \\ \text{R}^1\text{---}\text{C}^*\text{---}\text{C}^*\text{---}\text{H} \\ \quad \\ \text{R}^2 \quad \text{R}^3 \end{array} \xrightarrow[\text{AcOH/Ac}_2\text{O (50:1 v/v), 0.2M, 100 }^\circ\text{C}]{10 \text{ mol\% Pd(OAc)}_2, 1.3 \text{ equiv. PhI(OAc)}_2} \begin{array}{c} \text{DG} \\ \\ \text{O} \\ \\ \text{R}^1\text{---}\text{C}^*\text{---}\text{C}^*\text{---}\text{OAc} \\ \quad \\ \text{R}^2 \quad \text{R}^3 \end{array} $			
Entry	Substrate	Product	Yield ^a
1	 2.1a	 2.1b	61% ^{b,c}
2	 2.2a	 2.2b	65% ^c
3	 2.3a	 2.3b + 2.3c	79% ^b 2.3b:2.3c=2.6:1
4	 2.4a	 2.4b	86% ^b
5	 2.5a	 2.5b	72% ^b
6	 2.6a	 2.6b	74% ^b
7	 2.7a	 2.7b	68% ^b

^aIsolated yields. ^bProduct consisted of a mixture of oxime E/Z stereoisomers. ^cStarting material and product consisted of a mixture of oxime E/Z. ^d1 equiv of PhI(OAc)₂ was used. ^e3 equiv of PhI(OAc)₂ were used.

Table 2.2. Summary of the substrate scope (continued).

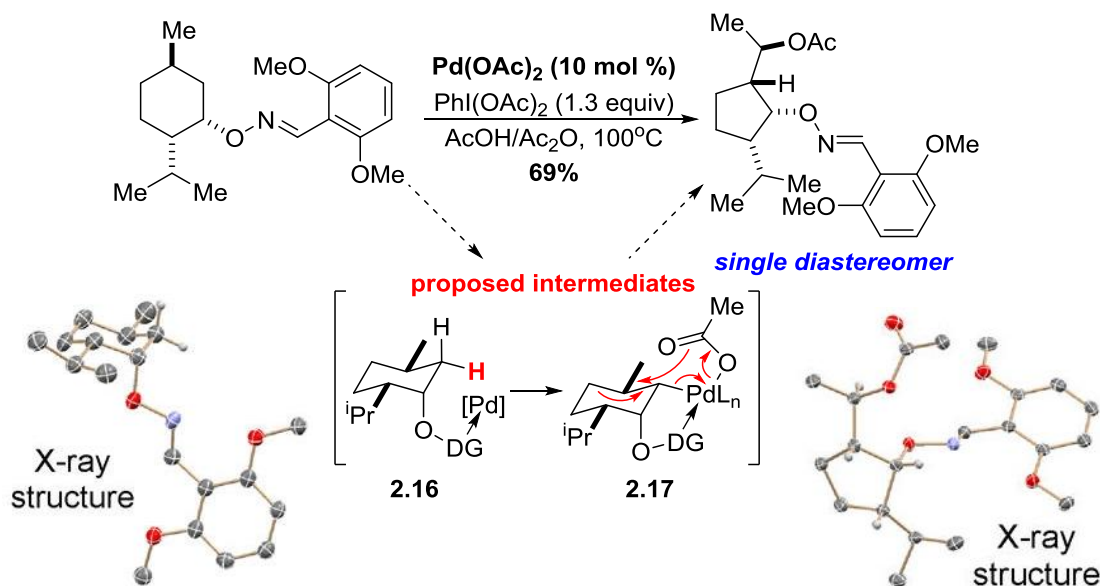
<div style="display: flex; align-items: center; justify-content: center;"> <div style="text-align: center;"> </div> <div style="margin: 0 20px;"> DG: </div> </div>			
Entry	Substrate	Product	Yield ^a
8	 2.8a	 2.8b	50% ^{b,d} 2.8b:2.8c=1.4:1
9	 2.9a	 2.9b	44% ^{b,c} (79% brsm)
10	 2.10a	 2.10b	62% ^e 2.10b:2.10c=2.1:1
11	 2.11a	 2.11b	78% ^b
12	 2.12a	 2.12b	75% ^b

^aIsolated yields. ^bProduct consisted of a mixture of oxime E/Z stereoisomers. ^cStarting material and product consisted of a mixture of oxime E/Z. ^d1 equiv of PhI(OAc)₂ was used. ^e3 equiv of PhI(OAc)₂ were used.

When the oxime masked menthol substrate was used, an interesting ring contraction rearrangement to give a five-membered ring product was discovered (Scheme 2.5).²³ The starting material and product were confirmed by X-ray crystallography, and the product was obtained as a single diastereomer with 1,3-diol moieties in good yield.

The detailed mechanism is still unclear, but presumably through palladation to give an intermediate similar to **2.16**, and the sequential oxidation to offer the palladium III or IV species **2.17**, which underwent a Pd-triggered oxidative rearrangement to give the final product.

Scheme 2.5. A Pd-triggered oxidative rearrangement.



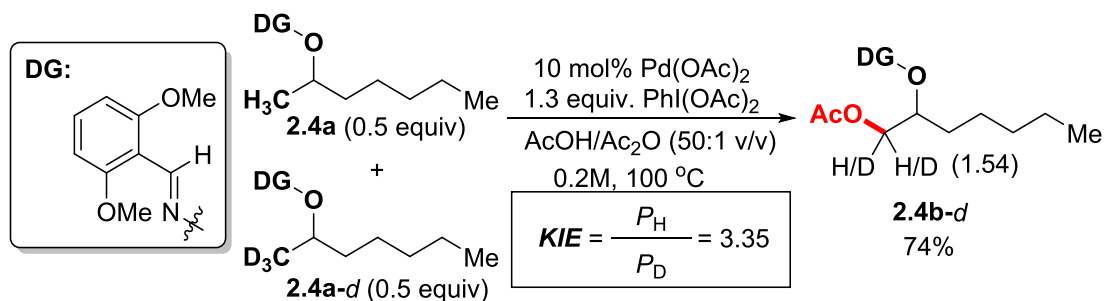
The reaction scales were also examined by conducting oxidation with substrate **2.1a** in Table 2.3. Interestingly, the reactions on larger scale exhibited a higher catalyst turnover to give higher yield. For examples in entry 3, on a 2 mmol scale, the yield was increased to 74% from 61% with an even lower catalyst loading of $\text{Pd}(\text{OAc})_2$ (2 mol %). As shown in entry 4, on a 5 mmol scale, the yield increased to 80%. The results demonstrate that the large-scale reaction is less sensitive to the impurities, and the lower surface area ratio could prevent the Pd black to aggregate.

Table 2.3. The scale of the reaction.

Entry	Scale	Isolated yields
1	0.1 mmol	61%
2	0.3 mmol	68%
3	2 mmol (2 mol % catalyst)	74%
4	5 mmol (Gram Scale)	80%

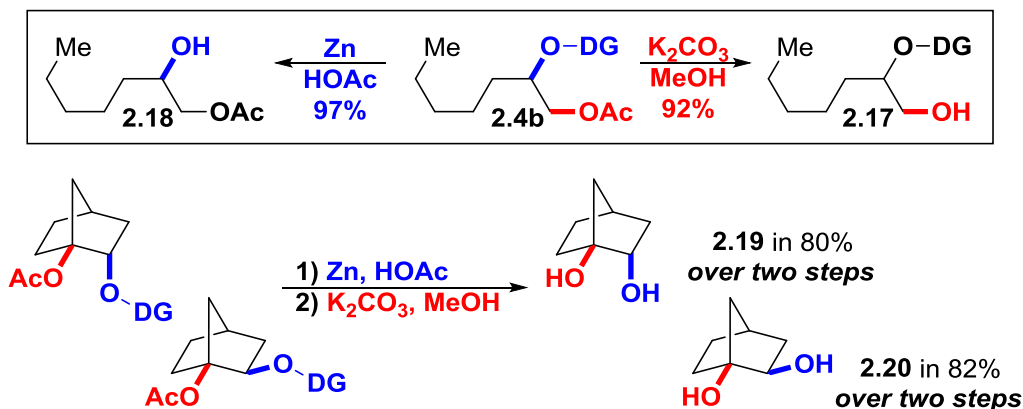
An intermolecular experiment of kinetic isotope effect (KIE) was conducted to investigate the reaction mechanism (Figure 2.4). The observed intermolecular KIE result ($k_{H/D} = 3.35$) suggests the C–H cleavage step could be the rate-determining step.

Figure 2.4. The intermolecular KIE result.



The DG and Ac group were removed in excellent yields using orthogonal chemical methods to demonstrate the two hydroxyl groups in the product are chemically differentiated (Scheme 2.6). This feature shows a great potential for the application of this synthetic method.

Scheme 2.6. Orthogonal protecting groups.



2.4 Conclusion

In summary, a new strategy for the Pd-catalyzed site-selective functionalization of unactivated aliphatic C–H bonds to access the chemically differentiated 1,2-diols from oxime masked mono alcohols. The oxime group served as both the DG and protection of alcohol for this oxidative reaction. The *exo*-DGs in C–H activation, as demonstrated by this work, have opened doors for the discovery of new transformations and new removable DGs.

2.5 Experiment Results

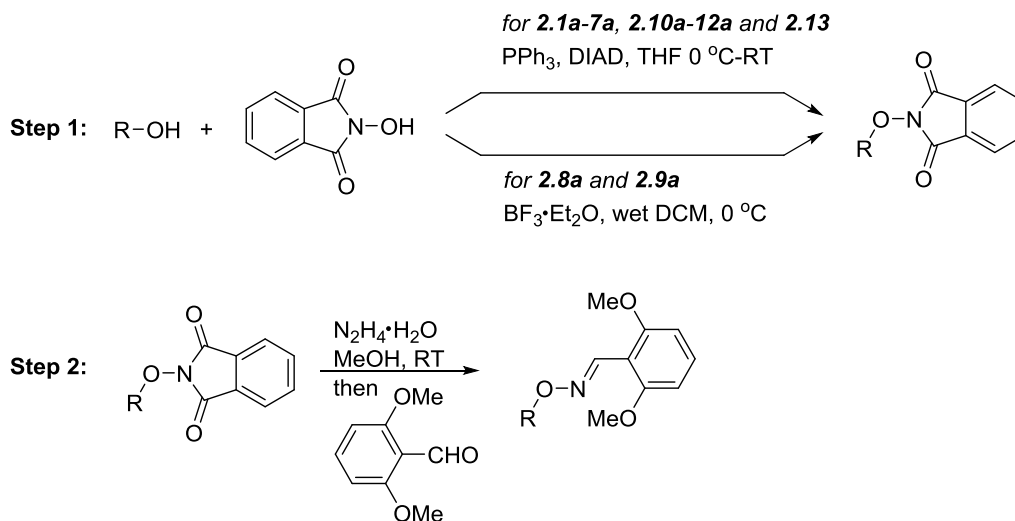
2.5.1 GENERAL CONSIDERATIONS

Unless otherwise noted, all experiments were carried out under air atmosphere. 1,2-Dichloroethane (DCE) was distilled over CaH_2 . Toluene and tetrahydrofuran (THF) were distilled over sodium. The other reagents and solvents were directly used from the supplier without further purification unless noted. Analytical thin-layer chromatography (TLC) was carried out using 0.2 mm commercial silica gel plates (silica gel 60, F254, EMD chemical). The vials (1 dram, 15×45 mm with PTFE-lined cap attached) were purchased from Qorpak and dried in an oven overnight and cooled in air. Infrared spectra

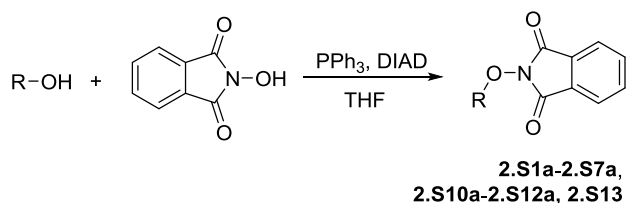
were recorded on a Nicolet 380 FTIR using neat thin film technique. High-resolution mass spectra (HRMS) were obtained on a Karatos MS9 and are reported as m/z (relative intensity). Accurate masses are reported for the molecular ion $[M+Na]^+$ or $[M+H]^+$. Nuclear magnetic resonance spectra (1H NMR and ^{13}C NMR) were recorded with Varian Gemini (400 MHz, 1H at 400 MHz, ^{13}C at 100 MHz) or Varian Unity+ (300 MHz, 1H at 300 MHz, ^{13}C at 75 MHz). For $CDCl_3$ solutions, the chemical shifts are reported as parts per million (ppm) referenced to residual protium or carbon of the solvents; $CHCl_3$ δ H (7.26 ppm) and $CDCl_3$ δ C (77.00 ppm). Coupling constants are reported in Hertz (Hz). Data for 1H NMR spectra are reported as follows: chemical shift (ppm, referenced to protium; s = singlet, d = doublet, t = triplet, q = quartet, p = pentet (quintet), dd = doublet of doublets, td = triplet of doublets, ddd = doublet of doublet of doublets, m = multiplet, coupling constant (Hz), and integration).

2.5.2 GENERAL PROCEDURE AND CHARACTERIZATION

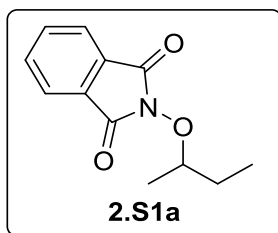
General survey of all substrates syntheses



General procedure: Mitsunobu reaction for syntheses of 2.S1a-2.S7a, 2.S10a-2.S12a and 2.S13:



To a solution of alcohol (5 mmol, 1.0 equiv), N-Hydroxyphthalimide (978 mg, 6 mmol, 1.2 equiv) and PPh₃ (1.572 g, 6 mmol, 1.2 equiv) in 20 mL THF was added diisopropyl azodicarboxylate (1.2 mL, 6 mmol, 1.2 equiv) dropwise at 0 °C. Then the reaction was allowed to room temperature. The reaction was monitored by TLC. Upon done, the solvent was removed under reduced pressure. The residue was purified by flash column chromatography on silica gel to give the title compounds. **All the yields are not optimized.**



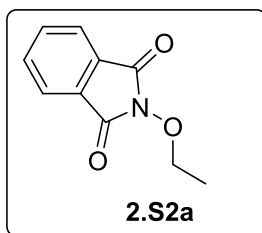
2-(*sec*-Butoxy)isoindoline-1,3-dione (2.S1a)

White solid. Yield 85%. R_f = 0.3 (Hex/EA=15:1).

^1H NMR (400 MHz, CDCl_3) δ 7.83-7.78 (m, 2H), 7.74-7.70 (m, 2H), 4.34-4.26 (m, 1H), 1.86-1.75 (m, 1H), 1.68-1.57 (m, 1H), 1.31 (d, J = 6.3 Hz, 3H), 1.02 (t, J = 7.5 Hz, 3H).

^{13}C NMR (100 MHz, CDCl_3) δ 164.34, 134.35, 128.97, 123.39, 85.61, 27.70, 18.18, 9.53.

Match cited literature²⁴.

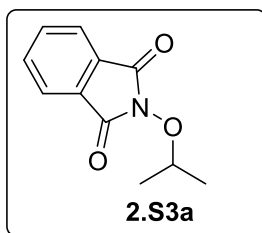


2-Ethoxyisoindoline-1,3-dione (2.S2a)

White solid. Yield 90%. R_f = 0.4 (Hex/EA=5:1).

^1H NMR (400 MHz, CDCl_3) δ 7.84-7.81 (m, 2H), 7.74-7.73 (m, 2H), 4.27 (q, J = 7.1 Hz, 2H), 1.40 (t, J = 7.1 Hz, 3H).

^{13}C NMR (100 MHz, CDCl_3) δ 163.74, 134.45, 128.89, 123.49, 74.10, 13.64. Match cited literature²⁵.

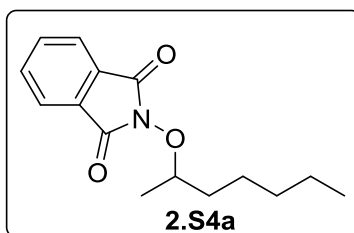


2-Isopropoxyisoindoline-1,3-dione (2.S3a)

White solid. Yield 97%. R_f = 0.4 (Hex/EA=5:1).

^1H NMR (400 MHz, CDCl_3) δ 7.84-7.80 (m, 2H), 7.75-7.71 (m, 2H), 4.53 (hept, J = 6.2 Hz, 1H), 1.36 (d, J = 6.2 Hz, 6H).

^{13}C NMR (100 MHz, CDCl_3) δ 164.33, 134.40, 128.92, 123.44, 80.65, 20.78. Match cited literature²⁵.



2-(Heptan-2-yloxy)isoindoline-1,3-dione (2.S4a)

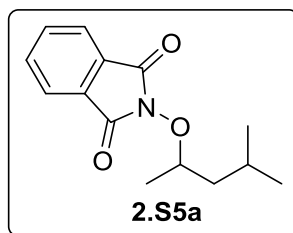
Colorless oil. Yield 61%. R_f = 0.3 (Hex/EA=15:1).

IR (KBr) 2927, 2856, 1790, 1733, 1467, 1377, 1188, 1119, 977 cm^{-1} .

^1H NMR (400 MHz, CDCl_3) δ 7.82 (td, J = 5.3, 2.1 Hz, 2H), 7.75 (td, J = 5.3, 2.1 Hz, 2H), 4.37 (dd, J = 12.5, 6.3 Hz, 1H), 1.88-1.72 (m, 1H), 1.68-1.52(m, 2H), 1.52-1.39(m, 3H), 1.39-1.28 (m, 6H), 0.89 (t, J = 7.1 Hz, 3H).

^{13}C NMR (100 MHz, CDCl_3) δ 164.50, 134.50, 129.13, 123.54, 84.64, 34.97, 31.91, 29.83, 25.08, 22.68, 18.94, 14.16.

HRMS calcd. for $\text{C}_{15}\text{H}_{19}\text{NO}_3\text{Na}^+$ $[\text{M}+\text{Na}]^+$: 284.12571. Found: 284.12612.



2-((4-Methylpentan-2-yl)oxy)isoindoline-1,3-dione (2.S5a)

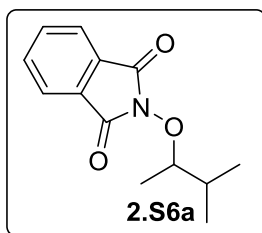
White solid. Yield 77%. Mp. 60-62 °C. R_f = 0.3 (Hex/EA=15:1).

IR (KBr) 2957, 1790, 1733, 1379, 1188, 976, 878, 713, 519 cm^{-1} .

^1H NMR (400 MHz, CDCl_3) δ 7.86-7.82 (m, 2H), 7.77-7.73 (m, 2H), 4.51-4.43 (m, 1H), 1.99-1.88 (m, 1H), 1.77 (ddd, J = 14.1, 7.6, 6.6 Hz, 1H), 1.41 (ddd, J = 14.0, 7.6, 5.7 Hz, 1H), 1.32 (d, J = 6.2 Hz, 3H), 1.03 (d, J = 6.6 Hz, 3H), 0.93 (d, J = 6.6 Hz, 3H).

^{13}C NMR (100 MHz, CDCl_3) δ 164.38, 134.35, 128.96, 123.38, 82.79, 44.15, 24.74, 22.72, 22.57, 19.40.

HRMS: calcd. $\text{C}_{14}\text{H}_{17}\text{NO}_3\text{Na}^+$ $[\text{M}+\text{Na}]^+$: 270.11061. Found: 270.10999.



2-((3-Methylbutan-2-yl)oxy)isoindoline-1,3-dione (2.S6a)

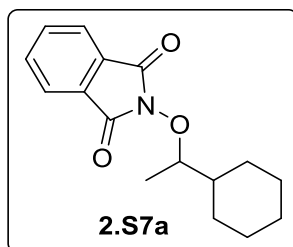
Colorless oil. Yield 51%. R_f = 0.3 (Hex/EA=15:1).

IR (KBr) 2962, 2875, 1733, 1657, 1652, 1448, 1386, 1294, 1129 cm^{-1} .

^1H NMR (400 MHz, CDCl_3) δ 7.86-7.79 (m, 2H), 7.77-7.71 (m, 2H), 4.24-4.15 (m, 1H), 2.03 (tt, J = 12.1, 3.4 Hz, 1H), 1.26 (d, J = 6.4 Hz, 3H), 1.05 (t, J = 6.6 Hz, 6H).

^{13}C NMR (100 MHz, CDCl_3) δ 164.50, 134.48, 129.16, 123.51, 88.82, 31.78, 18.79, 17.22, 14.79.

HRMS calcd. for $\text{C}_{13}\text{H}_{15}\text{NO}_3\text{Na}^+$ $[\text{M}+\text{Na}]^+$: 256.09441. Found: 256.09444.



2-(1-Cyclohexylethoxy)isoindoline-1,3-dione (2.S7a)

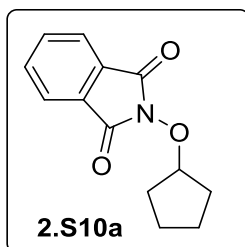
Colorless oil. Yield 50%. R_f = 0.3 (Hex/EA=15:1).

IR (KBr) 2926, 2853, 1790, 1733, 1376, 1188, 975, 878, 701 cm^{-1} .

^1H NMR (400 MHz, CDCl_3) δ 7.83-7.79 (m, 2H), 7.74-7.69 (m, 2H), 4.19-4.13 (m, 1H), 1.92-1.88 (m, 2H), 1.79-1.73 (m, 2H), 1.71-1.63 (m, 2H), 1.31-1.09 (m, 8H).

^{13}C NMR (100 MHz, CDCl_3) δ 164.37, 134.30, 129.01, 123.34, 88.19, 77.31, 76.99, 76.67, 41.73, 28.95, 27.64, 26.44, 26.10, 26.04, 15.41.

HRMS: calcd. $\text{C}_{16}\text{H}_{19}\text{NO}_3\text{Na}^+$ $[\text{M}+\text{Na}]^+$: 296.12626. Found: 296.12570.



2-(Cyclopentyloxy)isoindoline-1,3-dione (2.S10a)

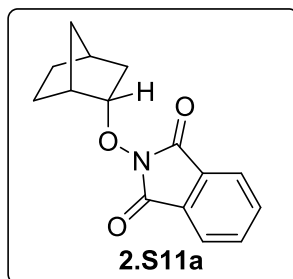
White solid. Yield 82%. Mp. 70-73 °C. R_f = 0.4 (Hex/EA=15:1).

IR (KBr) 2954, 2872, 1731, 1654, 1649, 1294, 1275, 1129, 1084 cm^{-1} .

^1H NMR (400 MHz, CDCl_3) δ 7.87-7.80 (m, 2H), 7.78-7.71 (m, 2H), 4.87-4.81 (m, 1H), 2.09-1.88 (m, 4H), 1.84-1.69 (m, 2H), 1.69-1.56 (m, 2H).

^{13}C NMR (100 MHz, CDCl_3) δ 164.49, 134.52, 129.15, 123.58, 90.51, 31.67, 23.68.

HRMS calcd. for $\text{C}_{13}\text{H}_{13}\text{NO}_3\text{Na}^+$ $[\text{M}+\text{Na}]^+$: 254.07876. Found: 254.07868.



Endo-2-((bicyclo[2.2.1]heptan-2-yl)oxy)isoindoline-1,3-dione (2.S11a)

Starting from *exo*-norborneol, the reaction was carried out at -78 °C, then slowly allowed to room temperature. *Endo/exo* 11:1.

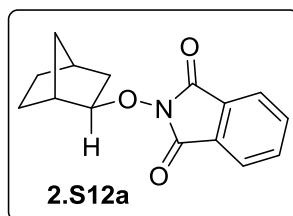
White solid. Yield 23%. R_f = 0.5 (Hex/EA=5:1). Mp. 79-81 °C.

IR (KBr) 2956, 2872, 1789, 1730, 1376, 1187, 877, 700 cm^{-1} .

^1H NMR (400 MHz, CDCl_3) δ 7.83-7.78 (m, 2H), 7.74-7.70 (m, 2H), 4.75-4.70 (m, 1H), 2.49 (t, J = 4.2 Hz, 1H), 2.40-2.33 (m, 1H), 2.24 (t, J = 4.7 Hz, 1H), 1.98-1.90 (m, 1H), 1.68-1.57 (m, 1H), 1.52-1.40 (m, 2H), 1.36-1.33 (m, 3H).

^{13}C NMR (100 MHz, CDCl_3) δ 163.97, 134.34, 128.95, 123.38, 89.45, 40.37, 37.50, 36.75, 35.13, 29.58, 20.32.

HRMS: calcd. $\text{C}_{15}\text{H}_{15}\text{NO}_3\text{Na}^+$ $[\text{M}+\text{Na}]^+$: 280.09496. Found: 280.09423.



Exo-2-((bicyclo[2.2.1]heptan-2-yl)oxy)isoindoline-1,3-dione (2.S12a)

Starting from *endo*-norborneol, the reaction was carried out at room temperature and gave single *exo* isomer.

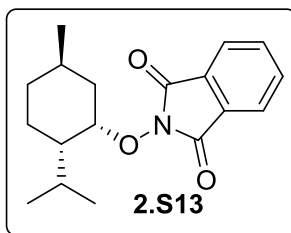
White solid. Yield 56%. R_f = 0.5 (Hex/EA=5:1). Mp. 105-107 °C.

IR (KBr) 2960, 2872, 1789, 1731, 1375, 1186, 978, 878, 701 cm^{-1} .

^1H NMR (400 MHz, CDCl_3) δ 7.84-7.79 (m, 2H), 7.74-7.71 (m, 2H), 4.37-4.34 (m, 1H), 2.42 (d, J = 4.8 Hz, 1H), 2.33 (s, 1H), 1.91-1.87 (m, 1H), 1.72-1.63 (m, 2H), 1.55-1.39 (m, 2H), 1.22-1.18 (m, 1H), 1.08-1.02 (m, 1H), 0.97-0.91 (m, 1H).

^{13}C NMR (100 MHz, CDCl_3) δ 164.22, 134.35, 128.98, 123.41, 90.43, 40.46, 37.36, 35.18, 34.70, 28.28, 23.67.

HRMS: calcd. $\text{C}_{15}\text{H}_{15}\text{NO}_3\text{Na}^+$ $[\text{M}+\text{Na}]^+$: 280.09496. Found: 280.09427.



2-(((1S,2S,5R)-2-Isopropyl-5-methylcyclohexyl)oxy)isoindoline-1,3-dione (2.S13)

White solid. Yield 20%. Mp. 98-100 °C. $[\alpha]_D^{20} = +57^\circ$. $R_f = 0.2$ (Hex/EA=15:1).

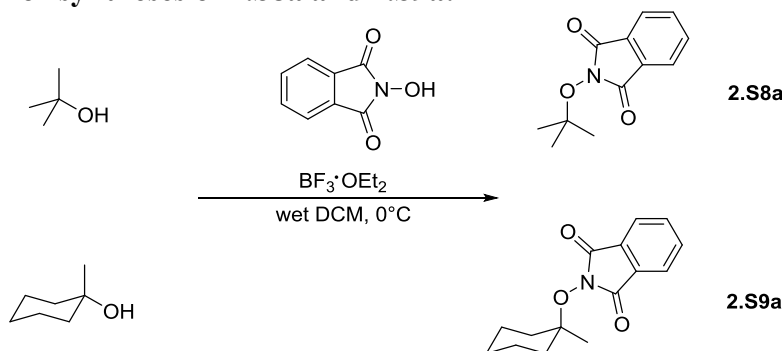
IR (KBr) 2943, 2863, 1729, 1468, 1370, 1131, 882, 698 cm^{-1} .

^1H NMR (400 MHz, CDCl_3) δ 7.84-7.79 (m, 2H), 7.76-7.71 (m, 2H), 4.66 (d, $J = 2.4$ Hz, 1H), 2.40-2.27 (m, 1H), 2.02-1.90 (m, 2H), 1.87-1.81 (m, 1H), 1.76-1.70 (m, 1H), 1.61-1.50 (m, 1H), 1.19 (d, $J = 6.6$ Hz, 3H), 1.14-1.07 (m, 1H), 1.01-0.92 (m, 5H), 0.88 (d, $J = 6.6$ Hz, 3H).

^{13}C NMR (100 MHz, CDCl_3) δ 164.45, 134.28, 129.09, 123.25, 83.82, 47.96, 37.92, 34.94, 28.90, 25.85, 24.27, 22.20, 21.20, 21.07.

HRMS: calcd. $\text{C}_{18}\text{H}_{23}\text{NO}_3\text{Na}^+$ $[\text{M}+\text{Na}]^+$: 324.15756. Found: 324.15707.

S_N1 reactions for syntheses of 2.S8a and 2.S9a:



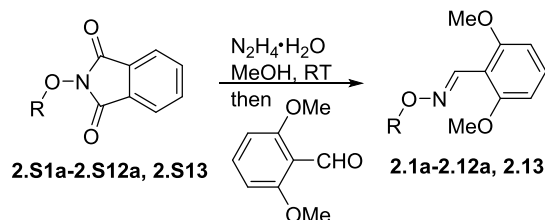
To a slurry of *N*-hydroxy phthalimide (54 mmol, 2 equiv), tertiary alcohol (27 mmol, 1 equiv) in 90 mL wet DCM, $\text{BF}_3 \cdot \text{OEt}_2$ (8.0 mL, 30 mmol, 1.1 equiv) was added dropwise over 10 mins at 0°C . The reaction mixture was stirred for over 1 hour at room temperature. When the reaction was finished, 30 mL 5% K_2CO_3 was added. The aqueous layer was extracted with DCM (30 mL \times 3), the combined organic layers were combined and dried over MgSO_4 . The residue was purified by flash column chromatography on silica gel (Hex/EA=5:1) to give titled compounds. **2.S8a**, yield 46%, white solid.

^1H NMR (400 MHz, CDCl_3) δ 7.85-7.81 (m, 2H), 7.76-7.74 (m, 2H), 1.42 (s, 9H). **2.S9a**, yield 44%, white solid.

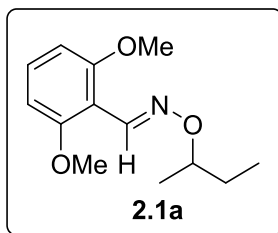
^1H NMR (400 MHz, CDCl_3) δ 7.87-7.81 (m, 2H), 7.78-7.72 (m, 2H), 1.94-1.80 (m, 4H), 1.72-1.63 (m, 2H), 1.51-1.38 (m, 4H), 1.36 (s, 3H).

Both **2.S8a** and **2.S9a** match cited literature²⁶.

The general procedure for preparing compound 2.1a-2.12a, 2.1a DG A, 2.1a DG B and 2.13:



To a solution of N-Alkoxyphthalimide (1.0 equiv) in MeOH (5 mL/mmol) was added hydrazine monohydrate (1.0 equiv) at room temperature. The reaction was monitored by TLC and usually completed in 0.5 h. Then 2,6-dimethoxybenzaldehyde (1.0 equiv) was added. The reaction was monitored by TLC. After 0.5 h the mixture was filtered to remove precipitate if formed and then the solvent was removed under reduced pressure. The residue was purified by flash column chromatography on silica gel to give the title compounds. **All the yields are not optimized.**



(E)-2,6-dimethoxybenzaldehyde O-(sec-butyl) oxime (2.1a)

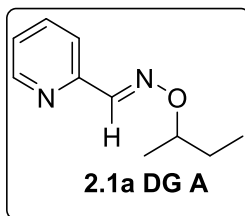
Colorless oil. Yield 94%. R_f = 0.3 (Hex/EA=15:1).

IR (KBr) 2966, 2935, 2838, 1595, 1470, 1432, 1256, 1207, 1114 cm^{-1} .

^1H NMR (400 MHz, CDCl_3) δ 8.39 (s, 1H), 7.24 (t, J = 8.4 Hz, 2H), 6.56 (d, J = 8.4 Hz, 2H), 4.34-4.24 (m, 1H), 3.84 (s, 6H), 1.85-1.70 (m, 1H), 1.63-1.51 (m, 1H), 1.29 (d, J = 6.3 Hz, 3H), 0.97 (t, J = 7.5 Hz, 3H).

^{13}C NMR (100 MHz, CDCl_3) δ 159.07, 143.33, 130.58, 110.14, 104.27, 80.26, 56.25, 28.72, 19.36, 9.89.

HRMS calcd. for $\text{C}_{13}\text{H}_{20}\text{NO}_3^+$ $[\text{M}+\text{H}]^+$: 238.14377. Found: 238.14356.



(E)-Picolinaldehyde O-(sec-butyl) oxime (2.1a DG A)

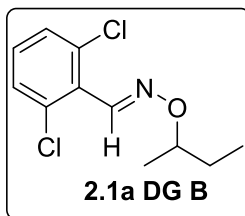
2,6-Dimethoxybenzaldehyde was replaced by pyridine-2-carbaldehyde to give a colorless oil. Yield 41%. $R_f = 0.3$ (Hex/EA=5:1).

IR (KBr) 2966, 2925, 2853, 1738, 1585, 1468, 1434, 1375, 1329, 1112 cm^{-1} .

^1H NMR (400 MHz, CDCl_3) δ 8.61 (ddd, $J = 4.9, 1.8, 1.0$ Hz, 1H), 8.15 (s, 1H), 7.80 (dt, $J = 8.0, 1.1$ Hz, 1H), 7.68 (tdd, $J = 8.0, 1.8, 0.5$ Hz, 1H), 7.24 (ddd, $J = 7.5, 4.9, 1.2$ Hz, 1H), 4.30 (dd, $J = 12.6, 6.3$ Hz, 1H), 1.84-1.70 (m, 1H), 1.66-1.53 (m, 1H), 1.30 (d, $J = 6.3$ Hz, 3H), 0.96 (t, $J = 7.5$ Hz, 3H).

^{13}C NMR (100 MHz, CDCl_3) δ 152.35, 149.75, 148.60, 136.47, 123.80, 120.97, 81.67, 28.60, 19.38, 9.86.

HRMS calcd. for $\text{C}_{10}\text{H}_{15}\text{N}_2\text{O}^+$ $[\text{M}+\text{H}]^+$: 179.11789. Found: 179.11779.



(E)-2,6-dichlorobenzaldehyde O-(sec-butyl) oxime (2.1a DG B)

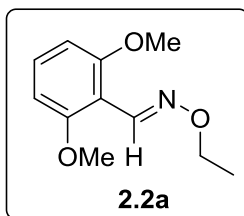
2,6-dimethoxybenzaldehyde was replaced by 2,6-dichlorobenzaldehyde to give a colorless oil. Yield 63%. R_f = 0.4 (Hex/EA=15:1).

IR (KBr) 2967, 2924, 2851, 1556, 1441, 1427, 1373, 1188 cm^{-1} .

^1H NMR (400 MHz, CDCl_3) δ 8.28 (s, 1H), 7.34 (d, J = 8.0 Hz, 2H), 7.22-7.16 (m, 1H), 4.29 (h, J = 6.3 Hz, 1H), 1.85-1.73 (m, 1H), 1.67-1.54 (m, 1H), 1.31 (d, J = 6.3 Hz, 3H), 0.98 (t, J = 7.5 Hz, 3H).

^{13}C NMR (100 MHz, CDCl_3) δ 143.69, 135.19, 130.04, 129.56, 128.81, 81.43, 28.58, 19.33, 9.79.

HRMS calcd. for $\text{C}_{11}\text{H}_{14}\text{Cl}_2\text{NO}^+$ $[\text{M}+\text{H}]^+$: 246.04470. Found: 246.04487.



(E)-2,6-dimethoxybenzaldehyde O-ethyl oxime (2a)

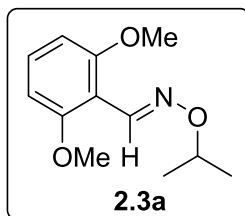
Colorless oil. Yield 96%. R_f = 0.5 (Hex/EA=5:1).

IR (KBr) 2973, 2936, 2838, 1595, 1576, 1559, 1472, 1433, 1257, 1208, 1113, 1053 cm^{-1} .

^1H NMR (400 MHz, CDCl_3) δ 8.43 (s, 1H), 7.25 (t, J = 8.4 Hz, 1H), 6.56 (d, J = 8.4 Hz, 2H), 4.25 (q, J = 7.1 Hz, 2H), 3.83 (s, 6H), 1.33 (t, J = 7.1 Hz, 3H).

^{13}C NMR (100 MHz, CDCl_3) δ 159.07, 144.03, 130.82, 109.61, 104.13, 69.46, 56.18, 14.71.

HRMS calcd. for $\text{C}_{11}\text{H}_{16}\text{NO}_3^+$ $[\text{M}+\text{H}]^+$: 210.11247. Found: 210.11248.



(E)-2,6-dimethoxybenzaldehyde O-isopropyl oxime (2.3a)

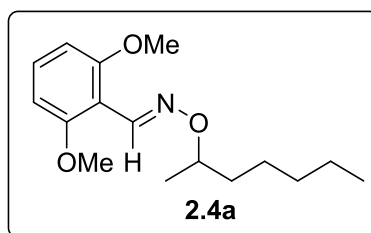
White solid. Yield 99%. Mp. 41-44 °C. R_f = 0.6 (Hex/EA=5:1).

IR (KBr) 2972, 2938, 2838, 1595, 1577, 1471, 1433, 1256, 1207, 1149, 1113 cm^{-1} .

^1H NMR (400 MHz, CDCl_3) δ 8.38 (s, 1H), 7.25 (t, J = 8.4 Hz, 1H), 6.56 (d, J = 8.4 Hz, 2H), 4.54-4.46 (m, 1H), 3.84 (s, 6H), 1.31 (d, J = 6.2 Hz, 6H).

^{13}C NMR (100 MHz, CDCl_3) δ 158.91, 143.28, 130.49, 109.88, 104.09, 75.09, 56.05, 21.76.

HRMS calcd. for $\text{C}_{12}\text{H}_{18}\text{NO}_3^+$ $[\text{M}+\text{H}]^+$: 224.12812. Found: 224.12814.



(E)-2,6-dimethoxybenzaldehyde O-heptan-2-yl oxime (2.4a)

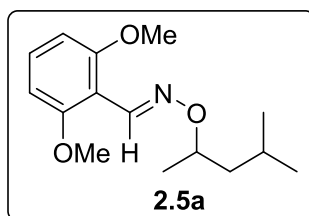
Colorless oil. Yield 84%. R_f = 0.3 (Hex/EA=15:1).

IR (KBr) 2932, 2857, 1595, 1469, 1431, 1256, 1206, 1114, 1035 cm^{-1} .

^1H NMR (400 MHz, CDCl_3) δ 8.38 (s, 1H), 7.23 (d, J = 8.4 Hz, 1H), 6.56 (d, J = 8.4 Hz, 2H), 4.34 (dd, J = 12.5, 6.2 Hz, 1H), 3.84 (d, J = 3.7 Hz, 6H), 1.82-1.69 (m, 1H), 1.56-1.37 (m, 3H), 1.37-1.27 (m, 8H), 0.89 (dd, J = 8.8, 5.1 Hz, 3H).

^{13}C NMR (100 MHz, CDCl_3) δ 159.04, 143.24, 130.55, 110.12, 104.23, 79.15, 56.18, 35.92, 32.14, 25.27, 22.77, 19.96, 14.22.

HRMS calcd. for $\text{C}_{16}\text{H}_{25}\text{NO}_3\text{Na}^+$ $[\text{M}+\text{Na}]^+$: 302.17266. Found: 302.17226.



(E)-2,6-dimethoxybenzaldehyde O-(4-methylpentan-2-yl) oxime (2.5a)

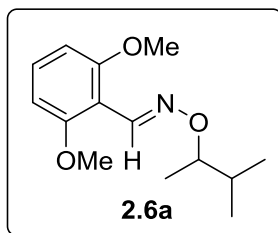
Colorless oil. Yield 91%. R_f = 0.25 (Hex/EA=15:1).

IR (KBr) 2956, 1595, 1470, 1432, 1256, 1114, 947, 777 cm^{-1} .

^1H NMR (400 MHz, CDCl_3) δ 8.35 (s, 1H), 7.22 (t, J = 8.4 Hz, 1H), 6.54 (d, J = 8.4 Hz, 2H), 4.45-4.37 (m, 1H), 3.82 (s, 6H), 1.86-1.76 (m, 1H), 1.65 (ddd, J = 14.1, 7.5, 6.7 Hz, 1H), 1.31-1.26 (m, 4H), 0.94 (d, J = 6.6 Hz, 3H), 0.91 (d, J = 6.6 Hz, 3H).

^{13}C NMR (100 MHz, CDCl_3) δ 158.88, 142.97, 130.37, 109.99, 104.09, 77.38, 56.02, 45.11, 24.72, 22.97, 22.83, 20.47.

HRMS: calcd. $\text{C}_{15}\text{H}_{24}\text{NO}_3^+$ $[\text{M}+\text{H}]^+$: 266.17562. Found: 266.17502.



(E)-2,6-dimethoxybenzaldehyde O-(3-methylbutan-2-yl) oxime (2.6a)

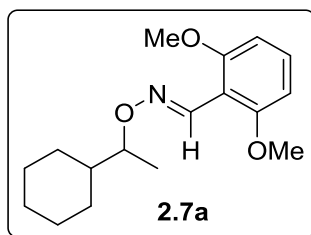
Colorless oil. Yield 86%. R_f = 0.3 (Hex/EA=15:1).

IR (KBr) 2961, 2837, 1595, 1470, 1432, 1384, 1256, 1207, 1114, 1055 cm^{-1} .

^1H NMR (400 MHz, CDCl_3) δ 8.39 (s, 1H), 7.23 (t, J = 8.4 Hz, 1H), 6.56 (d, J = 8.4 Hz, 2H), 4.22-4.12 (m, 1H), 3.84 (s, 6H), 2.05-1.94 (m, 1H), 1.23 (d, J = 6.4 Hz, 3H), 0.96 (dd, J = 13.2, 6.9 Hz, 6H).

^{13}C NMR (75 MHz, CDCl_3) δ 158.98, 143.05, 130.47, 110.10, 104.20, 83.40, 56.12, 32.21, 18.83, 17.40, 15.83.

HRMS calcd. for $\text{C}_{14}\text{H}_{22}\text{NO}_3^+$ $[\text{M}+\text{H}]^+$: 252.15942. Found: 252.15921.



(E)-2,6-dimethoxybenzaldehyde O-(1-cyclohexylethyl) oxime (2.7a)

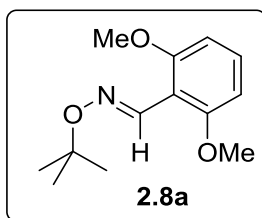
Colorless oil. Yield 83%. $R_f = 0.25$ (Hex/EA=15:1).

IR (KBr) 2924, 1595, 1470, 1432, 1256, 1114, 948, 777 cm^{-1} .

^1H NMR (400 MHz, CDCl_3) δ 8.35 (s, 1H), 7.22 (t, $J = 8.4$ Hz, 1H), 6.54 (d, $J = 8.4$ Hz, 2H), 4.17-4.10 (m, 1H), 3.82 (s, 6H), 1.87-1.84 (m, 1H), 1.76-1.72 (m, 3H), 1.67-1.59 (m, 2H), 1.29-1.19 (m, 5H), 1.16-0.98 (m, 3H).

^{13}C NMR (100 MHz, CDCl_3) δ 158.89, 142.85, 130.34, 110.08, 104.12, 82.90, 56.06, 42.39, 29.17, 27.96, 26.71, 26.37, 26.34, 16.55.

HRMS: calcd. $\text{C}_{17}\text{H}_{26}\text{NO}_3^+$ $[\text{M}+\text{H}]^+$: 292.19127. Found: 292.19058.



(E)-2,6-dimethoxybenzaldehyde O-(tert-butyl) oxime (2.8a)

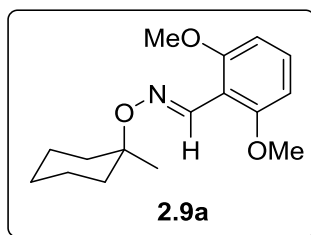
White Solid. Yield 86%. Mp. 77-81 °C. R_f = 0.5 (Hex/EA=5:1).

IR (KBr) 2975, 1593, 1577, 1469, 1359, 1255, 1205, 1192, 1111, 939 cm^{-1} .

^1H NMR (400 MHz, CDCl_3) δ 8.36 (s, 1H), 7.23 (t, J = 8.4 Hz, 1H), 6.56 (d, J = 8.4 Hz, 2H), 3.83 (s, 6H), 1.37 (s, 9 H).

^{13}C NMR (100 MHz, CDCl_3) δ 159.06, 142.50, 130.29, 110.75, 104.51, 78.49, 56.21, 27.79.

HRMS calcd. for $\text{C}_{13}\text{H}_{20}\text{NO}_3^+$ $[\text{M}+\text{H}]^+$: 238.14377. Found: 238.14370.



(E)-2,6-dimethoxybenzaldehyde O-(1-methylcyclohexyl) oxime (2.9a)

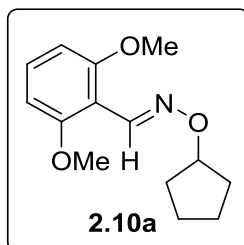
Colorless oil. Yield 99%. *E/Z* = 6.6:1. R_f = 0.5 (Hex/EA=5:1).

IR (KBr) 2932, 2859, 2838, 1594, 1470, 1432, 1255, 1206, 1166, 1115 cm^{-1} .

^1H NMR (400 MHz, CDCl_3) δ 8.40 (s, 1H), 7.22 (t, J = 8.4 Hz, 1H), 6.56 (d, J = 8.4 Hz, 2H), 3.83 (s, 6H), 2.00-1.89 (m, 2H), 1.72-1.59 (m, 2H), 1.59-1.40 (m, 6H), 1.34 (s, 3H).

^{13}C NMR (100 MHz, CDCl_3) δ 159.08, 142.53, 130.21, 110.95, 104.59, 79.23, 56.26, 36.39, 25.99, 25.90, 22.42.

HRMS calcd. for $\text{C}_{16}\text{H}_{24}\text{NO}_3^+$ $[\text{M}+\text{H}]^+$: 278.17507. Found: 278.17483.



(E)-2,6-dimethoxybenzaldehyde O-cyclopentyl oxime (2.10a)

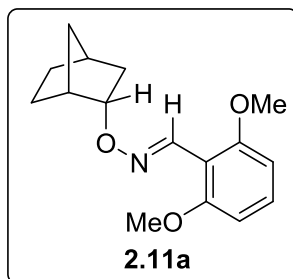
Colorless oil. Yield 96%. $R_f = 0.3$ (Hex/EA=15:1).

IR (KBr) 2959, 2838, 1595, 1470, 1432, 1340, 1306, 1256, 1207, 1181, 1113 cm^{-1} .

^1H NMR (400 MHz, CDCl_3) δ 8.35 (s, 1H), 7.25 (t, $J = 8.4$ Hz, 1H), 6.56 (d, $J = 8.4$ Hz, 2H), 4.88-4.79 (m, 1H), 3.84 (s, 6H), 1.97-1.68 (m, 6H), 1.65-1.51 (m, 2H).

^{13}C NMR (100 MHz, CDCl_3) δ 159.03, 143.73, 130.63, 110.01, 104.20, 84.95, 56.19, 32.30, 24.02.

HRMS calcd. for $\text{C}_{14}\text{H}_{20}\text{NO}_3^+$ $[\text{M}+\text{H}]^+$: 250.14377. Found: 250.14374.



(E)-2,6-dimethoxybenzaldehyde O-((endo)-bicyclo[2.2.1]heptan-2-yl) oxime (2.11a)

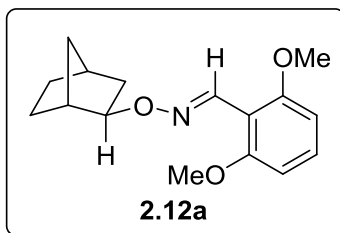
White solid. Yield 99%. Mp. 50-51 °C. R_f = 0.3 (Hex/EA=10:1).

IR (KBr) 2952, 2869, 1595, 1470, 1257, 1114, 1031, 947 cm^{-1} .

^1H NMR (400 MHz, CDCl_3) δ 8.41 (s, 1H), 7.23 (t, J = 8.4 Hz, 1H), 6.54 (d, J = 8.4 Hz, 2H), 4.73 (dtd, J = 10.4, 4.0, 1.4 Hz, 1H), 3.82 (s, 6H), 2.57 (t, J = 3.3 Hz, 1H), 2.19 (t, J = 4.3 Hz, 1H), 1.95 (dddd, J = 13.4, 10.5, 4.7, 3.1 Hz, 1H), 1.90-1.83 (m, 1H), 1.66-1.49 (m, 1H), 1.42-1.27 (m, 4H), 1.10 (dt, J = 13.1, 3.6 Hz, 1H).

^{13}C NMR (100 MHz, CDCl_3) δ 158.95, 143.91, 130.54, 109.81, 104.13, 83.38, 56.08, 40.81, 37.31, 36.71, 35.98, 29.74, 20.61.

HRMS: calcd. $\text{C}_{16}\text{H}_{22}\text{NO}_3^+$ $[\text{M}+\text{H}]^+$: 276.15997. Found: 276.15936.



(E)-2,6-dimethoxybenzaldehyde O-((exo)-bicyclo[2.2.1]heptan-2-yl) oxime (2.12a)

2.12a:

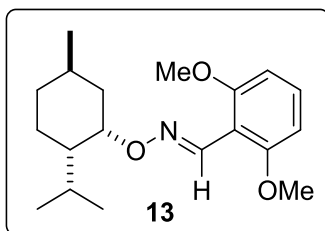
Colorless oil. Yield 99%. $R_f = 0.3$ (Hex/EA=10:1).

IR (KBr) 2956, 1595, 1470, 1432, 1257, 1113, 1001, 944 cm^{-1} .

^1H NMR (400 MHz, CDCl_3) δ 8.33 (s, 1H), 7.23 (t, $J = 8.4$ Hz, 1H), 6.54 (d, $J = 8.4$ Hz, 2H), 4.31-4.28 (m, 1H), 3.82 (s, 6H), 2.52 (d, $J = 4.2$ Hz, 1H), 2.25 (t, $J = 3.4$ Hz, 1H), 1.68-1.61 (m, 2H), 1.58-1.38 (m, 4H), 1.14-1.04 (m, 2H).

^{13}C NMR (100 MHz, CDCl_3) δ 158.87, 143.67, 130.50, 109.78, 104.01, 85.40, 56.03, 41.02, 38.17, 35.39, 34.65, 28.63, 24.24.

HRMS: calcd. $\text{C}_{16}\text{H}_{22}\text{NO}_3^+$ $[\text{M}+\text{H}]^+$: 276.15997. Found: 276.15955.



(E)-2,6-dimethoxybenzaldehyde O-((1S,2S,5R)-2-isopropyl-5-methylcyclohexyl) oxime (2.13)

White solid. Yield 93%. Mp. 72-74 °C. $[\alpha]_D^{20} = -56^\circ$. $R_f = 0.25$ (Hex/EA=15:1).

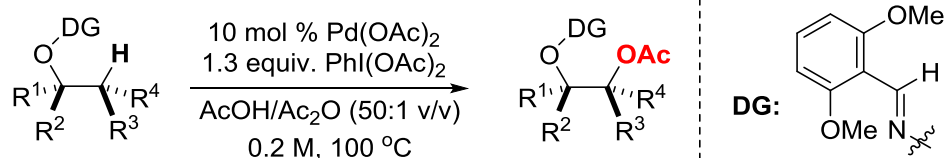
IR (KBr) 3018, 2952, 2840, 1602, 1471, 1258, 1115, 967, 777, 636 cm^{-1} .

^1H NMR (400 MHz, CDCl_3) δ 8.35 (s, 1H), 7.21 (t, $J = 8.4$ Hz, 1H), 6.54 (d, $J = 8.4$ Hz, 2H), 4.60 (d, $J = 2.5$ Hz, 1H), 3.82 (s, 6H), 2.24 (ddd, $J = 13.7, 6.0, 3.5$ Hz, 1H), 1.75-1.66 (m, 4H), 1.44-1.33 (m, 1H), 1.02-0.95 (m, 5H), 0.94-0.88 (m, 4H), 0.85 (d, $J = 6.4$ Hz, 3H).

^{13}C NMR (100 MHz, CDCl_3) δ 158.86, 142.50, 130.20, 110.23, 104.13, 78.58, 56.01, 47.48, 39.60, 35.19, 29.07, 26.05, 25.21, 22.54, 21.26, 21.01.

HRMS: calcd. $\text{C}_{19}\text{H}_{30}\text{NO}_3^+ [\text{M}+\text{H}]^+$: 320.22257. Found: 320.22204.

General procedure for Pd-catalyzed β -oxidation of oximes:



$\text{Pd}(\text{OAc})_2$ (2.2 mg, 0.01 mmol, 10 mol %), iodosobenzene diacetate (42 mg, 0.13 mmol, 1.3 equiv) and oxime (0.1 mmol, 1 equiv) were charged in a scintillation vial, followed by 0.5 mL AcOH , 10 μL Ac_2O . The vial was tightly capped and stirred at 100 °C. The reaction was monitored by TLC and observation of Pd black. Upon done, the mixture was directly purified by flash column chromatography on silica gel (Hex/EA= about 15:1 in most cases) to give the title compounds.

Procedure for large scale reaction for preparation of compound 2.1b:

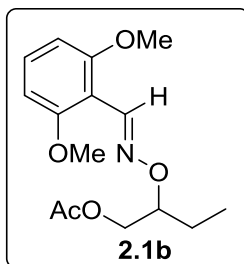
Pd(OAc)₂ (10 mol %), iodosobenzene diacetate (1.3 equiv) and **2.1a** (1 equiv) were charged in a scintillation vial, followed by AcOH and Ac₂O to make a 0.2 M solution. The vial was tightly capped and stirred at 100 °C. The reaction was monitored by both TLC and observation of Pd black. Upon done, the mixture was diluted with Ethyl Acetate. The solvent was removed under reduced pressure. The residue was purified by flash column chromatography on silica gel (Hex/EA=15:1) to give **2.1b**.

On 0.3 mmol scale: Obtained **2.1b** as yellow oil 53 mg, yield 68%, *E/Z* = 3.6:1.

On 5 mmol scale: Obtained **2.1b** as yellow oil 1.18 g, yield 80%, *E/Z* = 3.0:1.

On 2 mmol scale with 2 mol % Pd(OAc)₂ (9 mg): Obtained **2.1b** as yellow oil 0.436 g, yield 74%, *E/Z* = 4.6:1.

Note: NMR assignments of the minor *Z*-isomer are provided for all the compounds when *E/Z* ratio is less than 5:1.



(E)-2-(((2,6-dimethoxybenzylidene)amino)oxy)butyl acetate (2.1b)

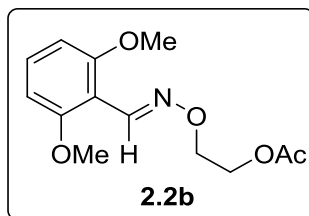
Yellow oil. Yield 61%. *E/Z* = 10.7:1. R_f = 0.4 (Hex/EA=15:1).

IR (KBr) 2966, 2940, 2839, 1739, 1595, 1471, 1433, 1368, 1305, 1256, 1208, 1113 cm^{-1} .

^1H NMR (400 MHz, CDCl_3) δ 8.44 (s, 1H), 7.24 (t, J = 8.4 Hz, 1H), 6.54 (d, J = 8.4 Hz, 2H), 4.36-4.30 (m, 1H), 4.30-4.27 (m, 2H), 3.82 (s, 6H), 2.09-2.02 (s, 3H), 1.83-1.58 (m, 2H), 1.00 (t, J = 7.5 Hz, 3H).

^{13}C NMR (100 MHz, CDCl_3) δ 171.31, 159.14, 144.42, 130.91, 109.65, 104.23, 81.67, 65.14, 56.19, 23.89, 21.13, 9.92.

HRMS calcd. for $\text{C}_{15}\text{H}_{21}\text{NO}_5\text{Na}^+$ $[\text{M}+\text{Na}]^+$: 318.13119. Found: 318.13114.



(E)-2-(((2,6-dimethoxybenzylidene)amino)oxy)ethyl acetate (2.2b)

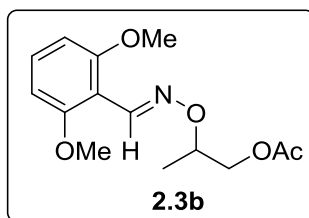
Used 1.0 equiv oxidant. Colorless oil. Yield 65%. $R_f = 0.4$ (Hex/EA=5:1).

IR (KBr) 2941, 2840, 1738, 1595, 1472, 1433, 1372, 1305, 1257, 1209, 1113 cm^{-1} .

^1H NMR (400 MHz, CDCl_3) δ 8.49 (s, 1H), 7.28 (t, $J = 8.4$ Hz, 1H), 6.57 (d, $J = 8.4$ Hz, 2H), 4.39 (s, 4H), 3.85 (s, 6H), 2.10 (s, 3H).

^{13}C NMR (100 MHz, CDCl_3) δ 171.26, 159.15, 145.24, 131.18, 109.17, 104.14, 71.69, 63.24, 56.19, 21.13.

HRMS calcd. for $\text{C}_{13}\text{H}_{17}\text{NNaO}_5^+$ $[\text{M}+\text{Na}]^+$: 290.09989. Found: 290.09973.



(E)-2-(((2,6-dimethoxybenzylidene)amino)oxy)propyl acetate (2.3b)

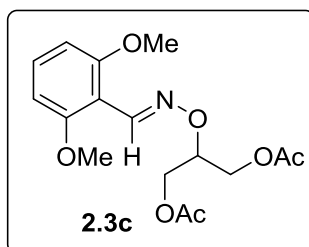
Used 1.0 equiv oxidant. Colorless oil. Yield 57%. *E/Z* = 6.3:1. *R_f* = 0.4 (Hex/EA=15:1).

IR (KBr) 2919, 2848, 1737, 1595, 1481, 1472, 1433, 1371, 1304, 1257, 1208, 1113 cm⁻¹.

¹H NMR (400 MHz, CDCl₃) δ 8.44 (s, 1H), 7.44 (t, *J* = 8.5 Hz, 1H), 6.59-6.55 (m, 2H), 4.62-4.52 (m, 1H), 4.26 (dd, *J* = 4.8, 2.0 Hz, 2H), 3.84 (s, 6H), 2.09 (s, 3H), 1.34 (d, *J* = 6.6 Hz, 3H).

¹³C NMR (100 MHz, CDCl₃) δ 171.09, 158.98, 144.41, 130.80, 109.42, 104.05, 76.36, 66.41, 56.03, 20.94, 16.47.

HRMS: calcd. for C₁₄H₁₉NO₅Na⁺ [*M*+Na]⁺: 304.11554. Found: 304.11552.



(E)-2-(((2,6-dimethoxybenzylidene)amino)oxy)propane-1,3-diyl diacetate (2.3c)

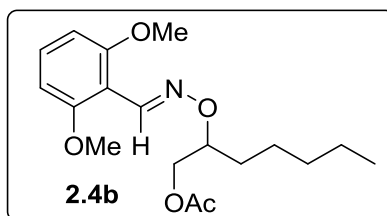
Used 1.0 equiv oxidant. Colorless oil. Yield 22%. *E/Z* = 7.7:1. *R_f* = 0.2 (Hex/EA=5:1).

IR (KBr) 2940, 2840, 1740, 1595, 1472, 1433, 1368, 1306, 1257, 1229, 1113 cm⁻¹.

¹H NMR (400 MHz, CDCl₃) δ 8.49 (s, 1H), 7.27 (t, *J* = 8.4 Hz, 1H), 6.56 (d, *J* = 8.4 Hz, 2H), 4.65 (p, *J* = 5.2 Hz, 1H), 4.36 (d, *J* = 5.2 Hz, 4H), 3.84 (s, 6H), 2.09 (s, 6H).

¹³C NMR (75 MHz, CDCl₃) δ 170.97, 159.23, 145.65, 131.31, 109.12, 104.18, 78.06, 62.87, 56.18, 21.02.

HRMS: calcd. for C₁₆H₂₁NO₇Na⁺ [*M*+Na]⁺: 362.12102. Found: 362.12119.



(E)-2-(((2,6-dimethoxybenzylidene)amino)oxy)heptyl acetate (2.4b)

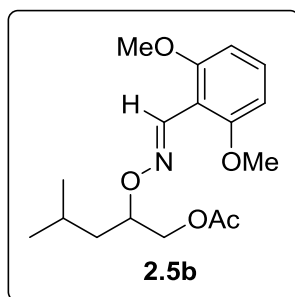
Colorless oil. Yield 86%. *E/Z* = 5.6:1. R_f = 0.4 (Hex/EA=5:1).

IR (KBr) 2933, 2858, 1740, 1595, 1471, 1433, 1367, 1256, 1208, 1114, 1036 cm^{-1} .

^1H NMR (400 MHz, CDCl_3) δ 8.44 (s, 1H), 7.25 (t, J = 8.4 Hz, 1H), 6.55 (d, J = 8.4 Hz, 2H), 4.43-4.36 (m, 1H), 4.29 (dd, J = 4.7, 1.5 Hz, 2H), 3.83 (s, 6H), 2.08 (s, 3H), 1.81-1.69 (m, 1H), 1.67-1.56 (m, 2H), 1.56-1.36 (m, 1H), 1.35-1.24 (m, 4H), 0.89 (t, J = 7.1 Hz, 3H).

^{13}C NMR (100 MHz, CDCl_3) δ 171.31, 159.13, 144.34, 130.89, 109.67, 104.21, 80.50, 65.52, 56.17, 32.00, 30.81, 25.16, 22.68, 21.13, 14.19.

HRMS: calcd. for $\text{C}_{18}\text{H}_{27}\text{NO}_5\text{Na}^+$ $[\text{M}+\text{Na}]^+$: 361.18144. Found: 361.18022.



(E)-2-(((2,6-dimethoxybenzylidene)amino)oxy)-4-methylpentyl acetate (2.5b)

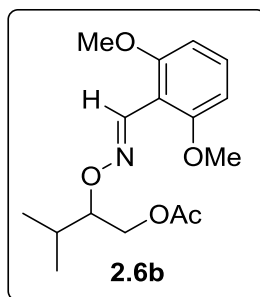
Colorless oil. Yield 72%. *E/Z* = 5:1. R_f = 0.4 (Hex/EA=5:1).

IR (KBr) 2962, 1740, 1595, 1471, 1306, 1256, 1114, 1065, 939, 778 cm^{-1} .

^1H NMR (400 MHz, CDCl_3) δ 8.41 (s, 1H), 7.23 (t, J = 8.4 Hz, 1H), 6.54 (d, J = 8.4 Hz, 2H), 4.47 (td, J = 9.0, 4.9 Hz, 1H), 4.27-4.26 (m, 2H), 3.81 (s, 6H), 2.06 (s, 3H), 1.90-1.79 (m, 1H), 1.72-1.65 (m, 1H), 1.39-1.32 (m, 1H), 0.95 (d, J = 1.9 Hz, 3H), 0.94 (d, J = 2.0 Hz, 3H).

^{13}C NMR (100 MHz, CDCl_3) δ 171.15, 158.96, 144.05, 130.72, 109.50, 104.05, 78.67, 65.76, 55.99, 39.69, 24.47, 23.24, 22.35, 20.96.

HRMS: calcd. $\text{C}_{17}\text{H}_{26}\text{NO}_5$ $[\text{M}+\text{H}]^+$: 324.18110. Found: 324.18039.



(E)-2-(((2,6-dimethoxybenzylidene)amino)oxy)-3-methylbutyl acetate (2.6b)

Colorless oil. Yield 74%. *E/Z* = 4.3:1. R_f = 0.4 (Hex/EA=5:1).

IR (KBr, mixed isomer) 2962, 1740, 1595, 1471, 1306, 1256, 1114, 1065, 939, 778 cm^{-1} .

Major isomer:

^1H NMR (400 MHz, CDCl_3) δ 8.43 (s, 1H), 7.23 (t, J = 8.4 Hz, 1H), 6.54 (d, J = 8.4 Hz, 2H), 4.36-4.32 (m, 1H), 4.29-4.25 (m, 1H), 4.19-4.09 (m, 2H), 3.81 (s, 6H), 2.05 (s, 3H), 1.03 (d, J = 6.8 Hz, 3H), 0.98 (d, J = 6.9 Hz, 3H).

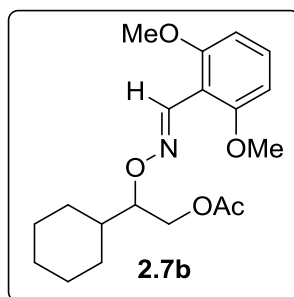
^{13}C NMR (100 MHz, CDCl_3) δ 171.18, 158.95, 143.96, 130.68, 109.54, 104.06, 85.03, 63.78, 56.00, 29.15, 20.98, 18.44.

Minor isomer (distinct resonances):

^1H NMR (400 MHz, CDCl_3) δ 7.37 (s, 1H), 3.77 (s, 6H), 2.01 (s, 3H), 0.90 (d, J = 6.9 Hz, 3H), 0.87 (d, J = 6.9 Hz, 3H).

^{13}C NMR (100 MHz, CDCl_3) δ 171.02, 157.71, 141.31, 130.33, 103.42, 85.30, 63.99, 55.60, 29.28, 20.91, 17.80.

HRMS (mixed isomers): calcd. $\text{C}_{16}\text{H}_{24}\text{NO}_5^+$ $[\text{M}+\text{H}]^+$: 310.16545. Found: 310.16485.



(E)-2-cyclohexyl-2-(((2,6-dimethoxybenzylidene)amino)oxy)ethyl acetate (2.7b)

Colorless oil. Yield 68%. *E/Z* = 3.7:1. R_f = 0.4 (Hex/EA=5:1).

IR (KBr, mixed isomers) 2926, 2851, 1738, 1595, 1471, 1256, 1114, 1046, 939, 778 cm^{-1} .

Major isomer:

^1H NMR (400 MHz, CDCl_3) δ 8.41 (s, 1H), 7.23 (t, J = 8.4 Hz, 1H), 6.54 (d, J = 8.4 Hz, 2H), 4.38-4.34 (m, 1H), 4.29-4.25 (m, 1H), 4.20-4.11 (m, 2H), 3.81 (s, 6H), 2.05 (s, 3H), 1.80-1.69 (m, 5H), 1.19-1.05 (m, 5H).

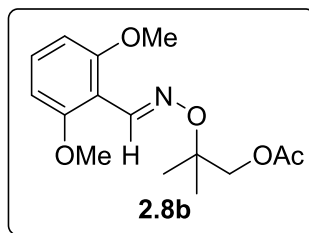
^{13}C NMR (100 MHz, CDCl_3) δ 171.20, 158.94, 143.84, 130.66, 109.59, 104.07, 84.44, 63.76, 56.00, 38.84, 28.81, 28.74, 26.45, 26.22, 26.10, 21.01.

Minor isomer (distinct resonances):

^1H NMR (400 MHz, CDCl_3) δ 7.36 (s, 1H), 3.77 (s, 6H), 2.01 (s, 3H).

^{13}C NMR (100 MHz, CDCl_3) δ 171.04, 157.71, 141.20, 130.33, 109.62, 103.45, 84.91, 63.96, 55.61, 39.04, 28.72, 28.22, 26.17, 26.07, 20.93.

HRMS (mixed isomers): calcd. $\text{C}_{19}\text{H}_{28}\text{NO}_5^+$ $[\text{M}+\text{H}]^+$: 350.19675. Found: 350.19603.



(E)-2-(((2,6-dimethoxybenzylidene)amino)oxy)-2-methylpropyl acetate (2.8b)

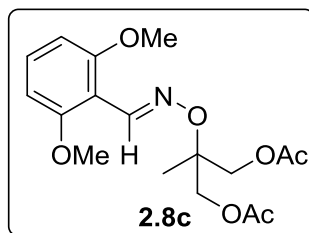
Used 1.0 equiv oxidant. Colorless oil. Yield 29%. R_f = 0.4 (Hex/EA=5:1).

IR (KBr) 2933, 2839, 1740, 1595, 1472, 1433, 1387, 1374, 1256, 1239, 1206, 1177, 1114 cm^{-1} .

^1H NMR (400 MHz, CDCl_3) δ 8.41 (s, 1H), 7.24 (t, J = 8.4 Hz, 1H), 6.56 (d, J = 8.4 Hz, 2H), 4.23 (s, 2H), 3.83 (s, 6H), 2.09 (s, 3H), 1.37 (s, 6H).

^{13}C NMR (100 MHz, CDCl_3) δ 171.30, 159.17, 143.60, 130.65, 110.25, 104.38, 78.78, 69.12, 56.19, 23.29, 21.16.

HRMS calcd. for $\text{C}_{15}\text{H}_{21}\text{NO}_5\text{Na}^+$ $[\text{M}+\text{Na}]^+$: 318.13119. Found: 318.13138.



(E)-2-(((2,6-dimethoxybenzylidene)amino)oxy)-2-methylpropane-1,3-diyl diacetate (2.8c)

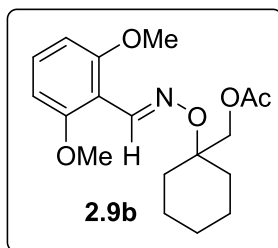
Used 1.0 equiv oxidant. Colorless oil. Yield 21%. *E/Z* = 5.6:1. *R_f* = 0.2 (Hex/EA=5:1).

IR (KBr) 2924, 2853, 1740, 1595, 1471, 1433, 1377, 1256, 1113, 1045 cm⁻¹.

¹H NMR (400 MHz, CDCl₃) δ 8.44 (s, 1H), 7.25 (t, *J* = 8.4 Hz, 1H), 6.55 (d, *J* = 8.4 Hz, 2H), 4.31 (q, *J* = 11.4 Hz, 4H), 3.83 (s, 6H), 2.09 (s, 6H), 1.40 (s, 3H).

¹³C NMR (100 MHz, CDCl₃) δ 170.99, 159.23, 144.59, 130.98, 109.73, 104.25, 79.45, 66.06, 56.16, 21.09, 18.93.

HRMS: calcd. for C₁₇H₂₃NO₇Na⁺ [*M*+Na]⁺: 376.13667. Found: 376.13656.



(E)-1-(((2,6-dimethoxybenzylidene)amino)oxy)cyclohexyl)methyl acetate (2.9b)

White solid. Yield 44%. *E/Z* = 3.9:1. *R_f* = 0.4 (Hex/EA=5:1). Mp. 82-85 °C.

IR (KBr, mixed isomers) 2935, 2860, 1740, 1594, 1472, 1432, 1380, 1304, 1255, 1207, 1114, 1043 cm⁻¹.

Major isomer:

¹H NMR (400 MHz, CDCl₃) δ 8.44 (s, 1H), 7.22 (t, *J* = 8.4 Hz, 1H), 6.54 (d, *J* = 8.4 Hz, 2H), 4.25 (s, 2H), 3.81 (s, 6H), 2.06 (s, 3H), 2.00-1.82 (m, 2H), 1.70-1.55 (m, 2H), 1.53-1.22 (m, 6H).

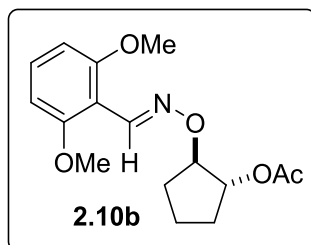
¹³C NMR (100 MHz, CDCl₃) δ 171.27, 159.01, 143.43, 130.40, 110.23, 104.26, 79.08, 68.08, 56.03, 31.24, 25.64, 21.25, 21.02.

Minor isomer (distinct resonances):

¹H NMR (400 MHz, CDCl₃) δ 7.40 (s, 1H), 4.16 (s, 2H), 3.79 (s, 6H), 2.01 (s, 3H).

¹³C NMR (100 MHz, CDCl₃) δ 171.15, 158.02, 140.96, 130.27, 110.29, 103.68, 79.09, 68.53, 55.74, 31.27, 21.14, 21.06.

HRMS (mixed isomers): calcd. for C₁₈H₂₅NO₅Na⁺ [M+Na]⁺: 358.16249. Found: 358.16282.



Trans-2-(((E)-2,6-dimethoxybenzylidene)amino)oxy)cyclopentyl acetate (2.10b)

Used 3.0 equiv oxidant. Colorless oil. Yield 42%. $R_f = 0.4$ (Hex/EA=5:1).

IR (KBr) 2924, 2851, 1735, 1595, 1470, 1433, 1374, 1256, 1208, 1113, 1036 cm^{-1} .

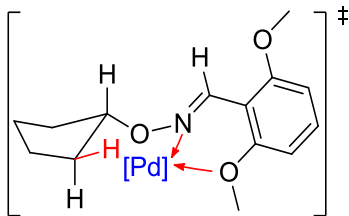
^1H NMR (400 MHz, CDCl_3) δ 8.37 (s, 1H), 7.27 (t, $J = 8.4$ Hz, 1H), 6.55 (d, $J = 8.4$ Hz, 2H), 5.44-4.96 (m, 1H), 4.92-4.55 (m, 1H), 3.84 (s, 6H), 2.21-2.05 (m, 2H), 2.04 (s, 3H), 1.93-1.58 (m, 4H).

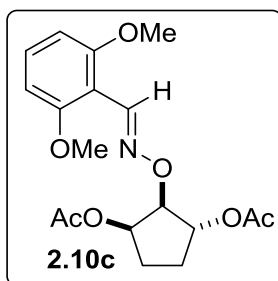
^{13}C NMR (100 MHz, CDCl_3) δ 170.52, 159.14, 144.77, 130.97, 109.57, 104.17, 87.33, 79.32, 56.18, 30.86, 29.93, 22.08, 21.47.

HRMS calcd. for $\text{C}_{16}\text{H}_{21}\text{NO}_5\text{Na}^+$ $[\text{M}+\text{Na}]^+$: 330.13119. Found: 330.13092.

This *trans* stereochemistry is assigned based on 1D nOe and a fact that cleavage of the DG to give a known mono-protected-diol²⁷.

Possible transition state of the first *trans*-activation:





Cis/trans-2-(((E)-2,6-dimethoxybenzylidene)amino)oxy)cyclopentane-1,3-diyl diacetate (2.10c)

Used 3.0 equiv oxidant. Colorless oil. Yield 20%. $R_f = 0.3$ (Hex/EA=5:1).

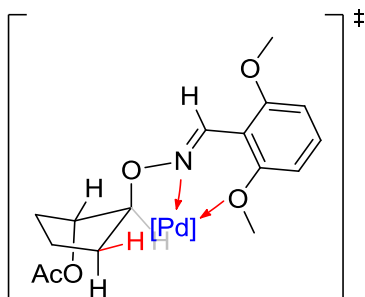
IR (KBr) 2938, 2848, 1742, 1689, 1595, 1475, 1435, 1373, 1305, 1257, 1114 cm^{-1} .

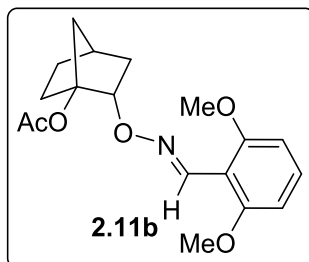
^1H NMR (400 MHz, CDCl_3) δ 8.40 (s, 1H), 7.26 (t, $J = 8.4$ Hz, 1H), 6.56 (d, $J = 8.4$ Hz, 2H), 5.44-5.34 (m, 2H), 4.85-4.78 (m, 1H), 3.84 (s, 6H), 2.37-2.14 (m, 2H), 2.07 (s, 3H), 2.04 (s, 3H), 1.92-1.75 (m, 2H).

^{13}C NMR (100 MHz, CDCl_3) δ 170.23, 169.95, 159.01, 145.05, 130.92, 109.23, 103.98, 84.40, 76.74, 73.11, 55.99, 27.18, 26.43, 20.94, 20.84.

HRMS calcd. for $\text{C}_{18}\text{H}_{23}\text{NO}_7\text{Na}^+$ $[\text{M}+\text{Na}]^+$: 388.13667. Found: 388.13638.

Possible transition state of the second *cis*-activation:





Endo-2-((((E)-2,6-dimethoxybenzylidene)amino)oxy)bicyclo[2.2.1]heptan-1-yl acetate (2.11b)

Colorless oil. Yield 78%. *E/Z* = 4.2:1. R_f = 0.4 (Hex/EA=5:1).

IR (KBr, mixed isomers) 2961, 2838, 1738, 1595, 1471, 1257, 1114, 937, 779 cm^{-1} .

Major isomer:

^1H NMR (400 MHz, CDCl_3) δ 8.51 (s, 1H), 7.23 (t, J = 8.4 Hz, 1H), 6.54 (d, J = 8.4 Hz, 2H), 5.19-5.16 (m, 1H), 3.82 (s, 6H), 2.28-2.10 (m, 4H), 2.00 (s, 3H), 1.89-1.66 (m, 4H), 1.38 (dt, J = 13.3, 3.6 Hz, 1H).

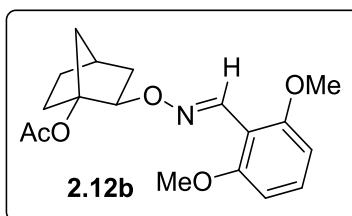
^{13}C NMR (100 MHz, CDCl_3) δ 170.56, 159.03, 144.53, 130.51, 109.52, 104.20, 90.07, 80.88, 56.09, 39.43, 36.29, 33.27, 28.63, 24.39, 22.12.

Minor isomer (distinct resonances):

^1H NMR (400 MHz, CDCl_3) δ 7.41 (s, 1H), 5.08-5.04 (m, 1H), 3.79 (s, 6H), 2.01 (s, 3H).

^{13}C NMR (100 MHz, CDCl_3) δ 157.77, 141.70, 103.49, 90.07, 80.88, 55.74.

HRMS (mixed isomers): calcd. $\text{C}_{18}\text{H}_{24}\text{NO}_5^+$ $[\text{M}+\text{H}]^+$: 334.16545. Found: 334.16481.



**Exo-2-((((E)-2,6-dimethoxybenzylidene)amino)oxy)bicyclo[2.2.1]heptan-1-yl acetate
(2.12b)**

Colorless oil. Yield 75%. *E/Z* = 4.3:1. *R_f* = 0.4 (Hex/EA=5:1).

IR (KBr, mixed isomers) 2965, 1742, 1594, 1471, 1257, 1114, 943, 778 cm⁻¹.

Major isomer:

¹H NMR (400 MHz, CDCl₃) δ 8.47 (s, 1H), 7.22 (t, *J* = 8.4 Hz, 1H), 6.53 (d, *J* = 8.4 Hz, 2H), 4.87-4.85 (m, 1H), 3.83 (s, 6H), 2.16-2.06 (m, 2H), 2.03-1.93 (m, 2H), 1.90 (s, 3H), 1.81-1.64 (m, 3H), 1.59-1.55 (m, 1H), 1.38-1.29 (m, 1H).

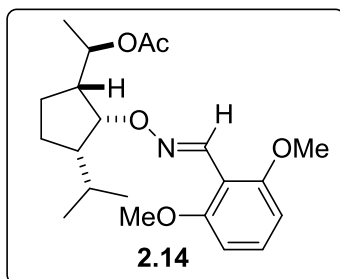
¹³C NMR (100 MHz, CDCl₃) δ 170.41, 159.00, 143.92, 130.57, 109.40, 103.85, 88.65, 80.30, 55.83, 38.60, 38.39, 30.39, 29.97, 28.28, 21.41.

Minor isomer (distinct resonances):

¹H NMR (400 MHz, CDCl₃) δ 7.34 (s, 1H), 6.51 (d, *J* = 8.4 Hz, 2H), 4.77-4.74 (m, 1H), 3.77 (s, 6H), 1.92 (s, 3H).

¹³C NMR (100 MHz, CDCl₃) δ 170.41, 157.78, 140.99, 130.21, 103.37, 88.51, 80.92, 55.60, 38.26, 38.13, 30.41, 29.93, 28.12, 21.36.

HRMS (mixed isomers): calcd. C₁₈H₂₄NO₅⁺ [*M*+H]⁺: 334.16545. Found: 334.16435.



(R)-1-((1R,2R,3S)-2-((((E)-2,6-dimethoxybenzylidene)amino)oxy)-3-isopropylcyclopentyl)ethyl acetate (2.14)

White solid. Yield 69%. *E/Z* = 4.3:1. Mp. 73-75 °C. $[\alpha]_D^{20} = +7^\circ$. $R_f = 0.4$ (Hex/EA=5:1).

IR (KBr, mixed isomers) 2956, 1734, 1595, 1472, 1256, 1115, 951, 778 cm^{-1} .

Major isomer:

^1H NMR (400 MHz, CDCl_3) δ 8.28 (s, 1H), 7.19 (t, $J = 8.4$ Hz, 1H), 6.51 (d, $J = 8.4$ Hz, 2H), 4.93 (dq, $J = 10.1, 6.2$ Hz, 1H), 4.78-4.76 (m, 1H), 3.79 (s, 6H), 1.90 (s, 3H), 1.78-1.69 (m, 3H), 1.59-1.44 (m, 4H), 1.19 (d, $J = 6.2$ Hz, 3H), 1.04 (d, $J = 6.4$ Hz, 3H), 0.86 (d, $J = 6.7$ Hz, 3H).

^{13}C NMR (100 MHz, CDCl_3) δ 170.43, 158.93, 142.22, 130.09, 110.07, 104.06, 84.75, 71.14, 55.84, 53.70, 50.03, 28.27, 27.58, 25.39, 22.14, 21.92, 21.26, 19.08.

Minor isomer (distinct resonances):

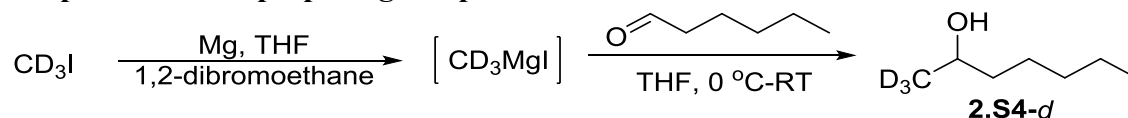
^1H NMR (400 MHz, CDCl_3) δ 7.24 (s, 1H), 6.48 (d, $J = 8.4$ Hz, 1H), 3.76 (s, 6H), 2.02 (s, 3H), 1.12 (d, $J = 6.2$ Hz, 3H), 0.95 (d, $J = 6.4$ Hz, 3H), 0.78 (d, $J = 6.6$ Hz, 3H).

^{13}C NMR (100 MHz, CDCl_3) δ 170.24, 157.61, 140.25, 129.89, 109.89, 103.06, 85.02, 55.47, 52.95, 50.41, 28.01, 27.40, 25.03, 21.99, 21.78, 21.42, 19.02.

HRMS (mixed isomers): calcd. $\text{C}_{21}\text{H}_{32}\text{NO}_5^+ [\text{M}+\text{H}]^+$: 378.22805. Found: 378.22734.

Isotope materials syntheses and kinetic isotope effect experiment

The procedure for preparing compound 2.4a-d:



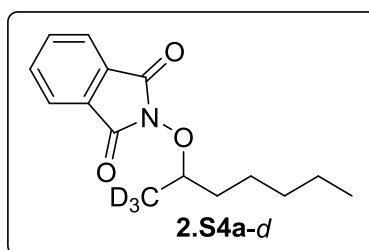
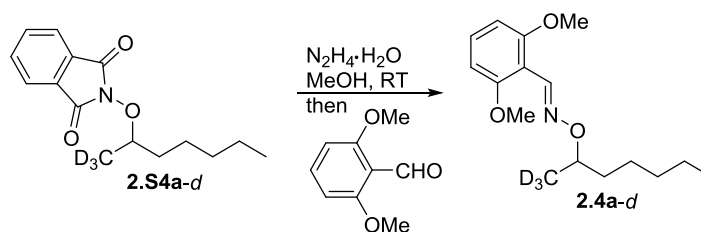
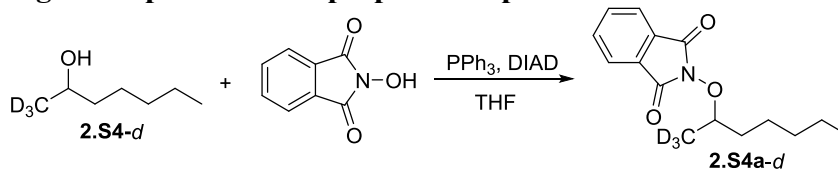
Magnesium (1.200 g, 50 mmol) was charged in a 2-necked round bottom flask equipped with a condenser and a septum, followed by 20 mL dry THF. To this mixture was added 1,2-dibromoethane (564 mg, 3 mmol) at 60 °C. The reaction started to bubble and ceased in about 15 min. Then a solution of deuterated methyl iodide (725 mg, 5 mmol) in 10 mL THF was added dropwise over 10 min. The reaction was allowed at this temperature for additional 0.5 h and cooled down to 0 °C. The above Grignard solution was injected into a solution of hexanal (500 mg, 5 mmol) in 10 mL dry THF via syringe at 0 °C. After additional 1 h at this temperature, the reaction was quenched by 20 mL NH_4Cl saturated aqueous solution, extracted with EA (10 mL \times 3), combined organic layers were dried over Na_2SO_4 . The solvent was removed under reduced pressure, and the residue was purified by flash column chromatography on silica gel (Hex/EA= 10:1) to give 246 mg 2.S4-d as a colorless oil, 41% yield. R_f = 0.2 (Hex/EA = 10:1).

IR (KBr) 3440, 2956, 2931, 2860, 1732, 1467, 1177 cm^{-1} .

^1H NMR (400 MHz, CDCl_3) δ 3.77 (s, 1H), 1.61-1.27 (m, 9H), 0.87 (t, J = 6.8 Hz, 3H).

^{13}C NMR (100 MHz, CDCl_3) δ 68.03, 39.24, 31.82, 25.41, 22.61, 14.01.

Followed the general procedure to prepare compound **2.4a-d**:



2.S4a-d: Colorless oil. Yield 65%. $R_f = 0.3$ (Hex/EA=10:1).

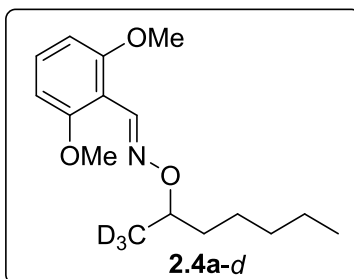
IR (KBr) 2930, 2860, 1789, 1734, 1467, 1376, 1188, 1122, 1082, 977, 878, 700, 519 cm^{-1} .

¹H NMR.

¹H NMR (400 MHz, CDCl_3) δ 7.86-7.82 (m, 2H), 7.77-7.72 (m, 2H), 4.37 (t, $J = 6.3$ Hz, 1H), 1.85-1.76 (m, 1H), 1.64-1.55 (m, 1H), 1.52-1.44 (m, 2H), 1.38-1.25 (m, 4H), 0.92-0.88 (m, 3H).

¹³C NMR (100 MHz, CDCl_3) 164.35, 134.46, 128.97, 123.50, 84.33, 34.74, 31.76, 24.91, 22.52, 14.07.

HRMS: calcd. $\text{C}_{15}\text{H}_{16}\text{D}_3\text{NO}_3\text{Na}^+ [\text{M}+\text{Na}]^+$: 287.14509. Found: 287.14421.



2.4a-d: Colorless oil. Yield 84%. R_f = 0.5 (Hex/EA=5:1).

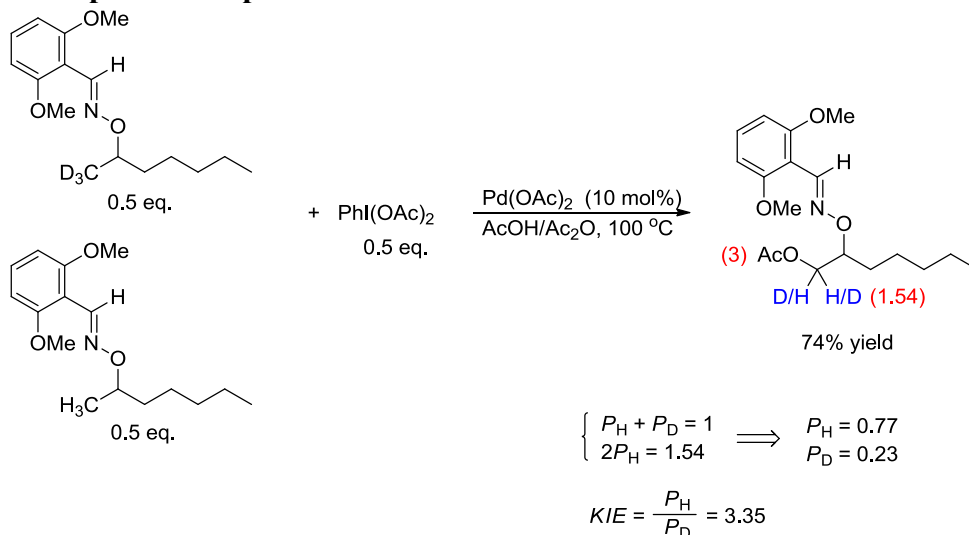
IR (KBr) 2931, 2858, 1595, 1470, 1432, 1256, 1114, 941 cm^{-1} .

^1H NMR (400 MHz, CDCl_3) δ 8.36 (s, 1H), 7.22 (t, J = 8.4 Hz, 1H), 6.54 (d, J = 8.4 Hz, 2H), 4.31 (t, J = 6.1 Hz, 1H), 3.82 (s, 6H), 1.77-1.69 (m, 1H), 1.54-1.27 (m, 7H), 0.88 (t, J = 7.0 Hz, 3H).

^{13}C NMR (100 MHz, CDCl_3) δ 158.89, 143.08, 130.41, 109.98, 104.03, 78.87, 56.10, 35.70, 31.99, 25.10, 22.61, 14.09.

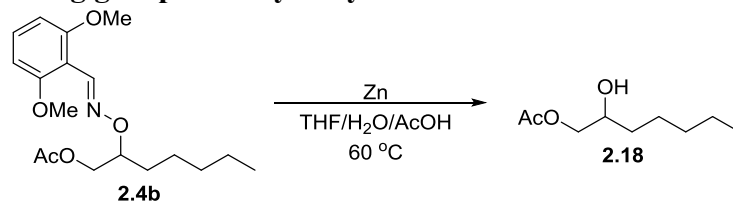
HRMS: calcd. $\text{C}_{16}\text{H}_{23}\text{D}_3\text{NO}_3^+$ $[\text{M}+\text{H}]^+$: 283.21010. Found: 283.20950.

Kinetic isotope effect experiment:



$\text{Pd}(\text{OAc})_2$ (4.4 mg, 0.02 mmol, 10 mol %), iodosobenzene diacetate (32 mg, 0.1 mmol, 0.5 equiv) were charged in a 2 mL scintillation vial, followed by **2.4a** (28 mg, 0.1 mmol, 0.5 equiv), **2.4a-d** (28 mg, 0.1 mmol, 0.5 equiv), 1 mL AcOH and 20 μL Ac_2O . The vial was tightly capped and stirred at $100\text{ }^\circ\text{C}$ for 1 h. The mixture was directly purified by flash column chromatography on silica gel (Hex/EA= 15:1). A broad range around the product was collected to give 25 mg product as yellow oil. ^1H NMR analysis of this crude showed that when the integral of OAc group (2.06 ppm) was set to 3, the adjacent CH_2 (4.32-4.22 ppm) integral was 1.54. Thus, the KIE number is determined as 3.35.

Removal of directing groups and hydrolysis of acetic esters.



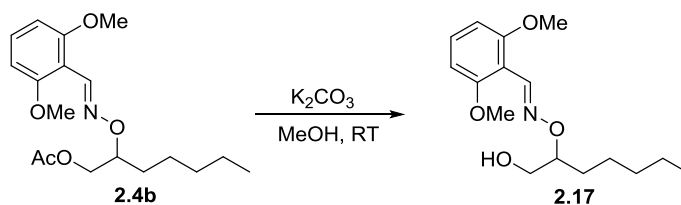
To a solution of **2.4b** (220 mg, 0.65 mmol, 1 equiv) in 7.5 mL AcOH-THF-Water (3:1:1), Zinc powder (390 mg, 6 mmol, 9.2 equiv) was added in portion at room temperature. Then the mixture was stirred at 60 °C. The reaction was monitored by TLC. After 2 h, the mixture was quenched with 20 mL water and extracted with EA (20 mL×3), dried over Na₂SO₄, the solvent was removed under reduced pressure. The residue was purified by flash column chromatography on silica gel (Hex/EA 5:1 to 4:1) to give 110 mg compound **2.18** as a yellow oil, yield 97%.

IR (KBr) 3435, 2956, 2932, 2860, 1741, 1371, 1240, 1040 cm⁻¹.

¹H NMR (400 MHz, CDCl₃) δ 4.12 (dd, *J* = 11.4, 3.0 Hz, 1H), 3.94 (dd, *J* = 11.4, 7.4 Hz, 1H), 3.86-3.80 (m, 1H), 2.08 (s, 3H), 2.07 (s, 1H), 1.49-1.40 (m, 3H), 1.34-1.23 (m, 5H), 0.87 (t, *J* = 6.8 Hz, 3H).

¹³C NMR (100 MHz, CDCl₃) 171.38, 69.93, 68.68, 33.19, 31.69, 24.99, 22.50, 20.87, 13.97.

HRMS: calcd. C₉H₁₈O₃Na⁺ [M+H]⁺: 197.11536. Found: 197.11474. Match cited literature²⁸.



To a solution of **2.4b** (100 mg, 0.29 mmol, 1 equiv) in 2 mL MeOH, K₂CO₃ (138 mg, 1 mmol, 3.4 equiv) was added. The reaction was stirred at room temperature, monitored by TLC. After 1 h, the solvent was removed under reduced pressure, and the residue was purified by flash column chromatography on silica gel (Hex/EA= 5:1) to give 80 mg compound **2.17** as white solid, yield 92%. *E/Z* = 2.7:1.

IR (KBr, mixed isomers) 3430, 2936, 2858, 1596, 1481, 1434, 1259, 1114, 778 cm⁻¹.

Major Isomer:

¹H NMR (400 MHz, CDCl₃) δ 8.45 (s, 1H), 7.24 (t, *J* = 8.4 Hz, 1H), 6.53 (d, *J* = 8.4 Hz, 2H), 4.72 (s, 1H), 4.30-4.24 (m, 1H), 3.81 (s, 8H), 1.66-1.56 (s, 1H), 1.52-1.22 (m, 7H), 0.86 (t, *J* = 7.0 Hz, 3H).

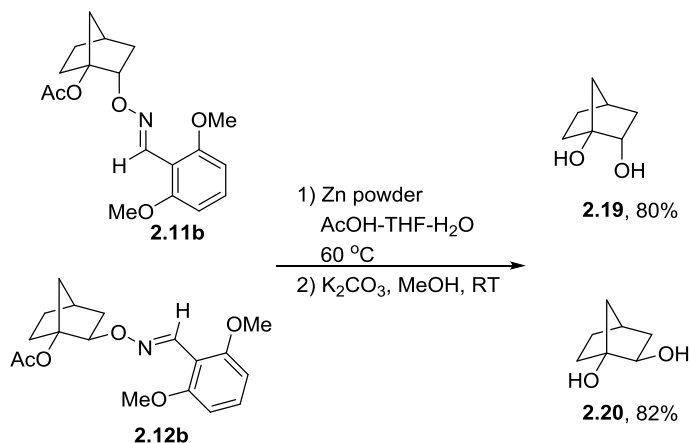
¹³C NMR (100 MHz, CDCl₃) δ 158.95, 143.57, 131.07, 108.73, 103.85, 83.19, 68.23, 55.77, 31.80, 30.13, 25.36, 22.52, 14.02.

Minor isomer (distinct resonances):

¹H NMR (400 MHz, CDCl₃) δ 7.40 (t, *J* = 8.5 Hz, 1H), 3.87 (s, 6H).

¹³C NMR (100 MHz, CDCl₃) δ 162.63, 134.64, 103.37, 56.15.

HRMS (mixed isomers): calcd. C₁₆H₂₆NO₄⁺ [M+H]⁺: 296.18618. Found: 296.18582.



To a solution of **2.11b** (198 mg, 0.59 mmol) in 10 mL AcOH-THF-Water (3:1:1), Zinc powder (390 mg, 6 mmol) was added in a portion at room temperature. Then the mixture was stirred at 60 °C. The reaction was monitored by TLC. After 4 h, the mixture was quenched with 20 mL water and extracted with EA (20 mL×3), dried over Na₂SO₄. The solvent was removed under reduced pressure, and the residue was directly used in the next step without further purification. To above residue in 1 mL MeOH was added K₂CO₃ (83 mg, 0.6 mmol). The reaction was stirred at room temperature, monitored by TLC. After 2 h, the solvent was removed under reduced pressure, and the residue was purified by flash column chromatography on silica gel (Hex/EA 2:1 to 1:1) to give 30 mg compound **2.19** as white solid, yield 80%. Mp. 213-215 °C. *R_f* = 0.1 (Hex/EA=1:1).

IR (KBr) 3325, 2951, 2870, 1451, 1235, 1137, 1076, 1047, 970, 732, 606 cm⁻¹.

¹H NMR (400 MHz, CDCl₃) δ 4.06 (ddd, *J* = 10.7, 3.3, 2.4 Hz, 1H), 3.20 (d, *J* = 22.9 Hz, 2H), 2.21-2.10 (m, 2H), 2.00 (t, *J* = 4.6 Hz, 1H), 1.85-1.76 (m, 1H), 1.55-1.46 (m, 3H), 1.37 (tdd, *J* = 12.5, 4.3, 2.2 Hz, 1H), 1.13 (dt, *J* = 13.2, 3.2 Hz, 1H).

^{13}C NMR (100 MHz, CDCl_3) δ 84.97, 75.09, 42.37, 38.70, 33.68, 30.32, 25.94.

HRMS: calcd. $\text{C}_7\text{H}_{12}\text{O}_2\text{Na}^+$ $[\text{M}+\text{Na}]^+$: 151.07350. Found: 151.07277.

2.12b was obtained by following the two-step procedure to give compound **2.20** as white solid in 82% yield. Mp. 164-166 °C.

IR (KBr) 3370, 2957, 2872, 1307, 1224, 1170, 11121, 1079, 1045 cm^{-1} .

^1H NMR (400 MHz, CDCl_3) δ 3.57 (d, J = 6.8 Hz, 1H), 2.54 (b, 2H), 2.04-2.02 (m, 1H), 1.87 (ddd, J = 13.4, 6.9, 2.3 Hz, 1H), 1.81-1.59 (m, 3H), 1.54-1.49 (m, 1H), 1.31-1.22 (m, 3H).

^{13}C NMR (100 MHz, CDCl_3) δ 83.30, 73.96, 41.51, 38.79, 32.16, 30.41, 29.72.

HRMS: calcd. $\text{C}_7\text{H}_{12}\text{O}_2\text{Na}^+$ $[\text{M}+\text{Na}]^+$: 151.07350. Found: 151.07288.

Both **2.12a** and **2.12b** match cited literature²¹.

X-Ray data for compound 2.9b, 2.13 and 2.14.

X-ray structure of compound **2.9b**:

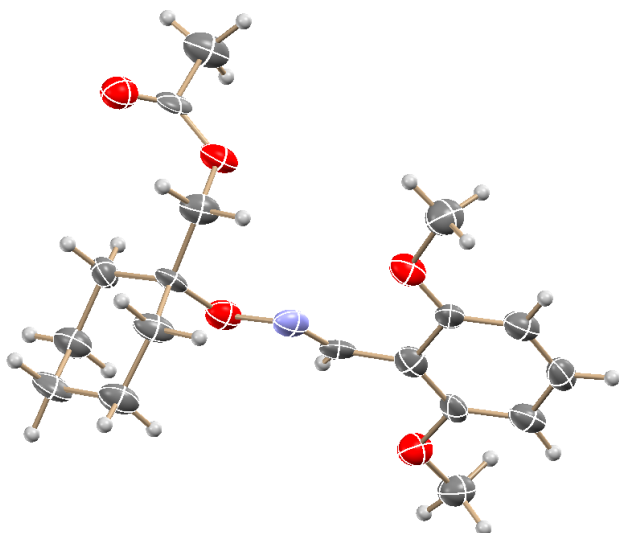


Table 2.4. Crystal data and structure refinement for **2.9b**.

Empirical formula	C18 H25 N O5	
Formula weight	335.39	
Temperature	100(2) K	
Wavelength	0.71075 Å	
Crystal system	Orthorhombic	
Space group	Pca21	
Unit cell dimensions	a = 29.976(4) Å	= 90°.
	b = 7.7137(11) Å	= 90°.
	c = 7.5088(10) Å	= 90°.
Volume	1736.2(4) Å ³	
Z	4	

Density (calculated)	1.283 Mg/m ³
Absorption coefficient	0.093 mm ⁻¹
F(000)	720
Crystal size	0.21 x 0.19 x 0.01 mm ³
Theta range for data collection	3.03 to 25.00°.
Index ranges	-35 ≤ h ≤ 35, -9 ≤ k ≤ 8, -7 ≤ l ≤ 8
Reflections collected	10288
Independent reflections	1620 [R(int) = 0.1600]
Completeness to theta = 25.00°	98.0 %
Absorption correction	Semi-empirical from equivalents
Max. and min. transmission	1.00 and 0.310
Refinement method	Full-matrix least-squares on F ²
Data / restraints / parameters	1620 / 1 / 220
Goodness-of-fit on F ²	1.190
Final R indices [I > 2σ(I)]	R1 = 0.0970, wR2 = 0.2167
R indices (all data)	R1 = 0.1412, wR2 = 0.2449
Largest diff. peak and hole	0.375 and -0.349 e.Å ⁻³

X-ray structure of compound **2.13**:

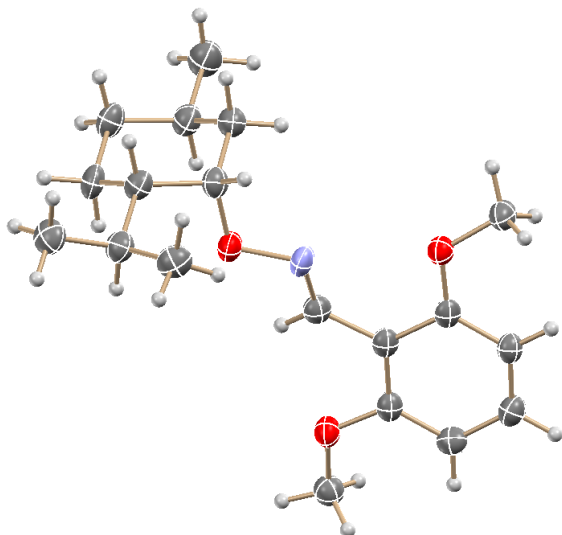


Table 2.5. Crystal data and structure refinement for **2.13**.

Empirical formula	C ₁₉ H ₂₉ N O ₃	
Formula weight	319.43	
Temperature	100(2) K	
Wavelength	0.71075 Å	
Crystal system	Monoclinic	
Space group	P2 ₁	
Unit cell dimensions	a = 6.8937(12) Å	= 90°.
	b = 15.987(3) Å	= 101.917(4)°.
	c = 16.978(3) Å	= 90°.
Volume	1830.8(6) Å ³	
Z	4	
Density (calculated)	1.159 Mg/m ³	
Absorption coefficient	0.077 mm ⁻¹	

F(000)	696
Crystal size	0.30 x 0.10 x 0.02 mm
Theta range for data collection	3.02 to 27.50°.
Index ranges	-8<=h<=8, -20<=k<=20, -21<=l<=22
Reflections collected	33914
Independent reflections	4324 [R(int) = 0.1207]
Completeness to theta = 27.50°	99.6 %
Absorption correction	Semi-empirical from equivalents
Max. and min. transmission	1.00 and 0.390
Refinement method	Full-matrix least-squares on F2
Data / restraints / parameters	4324 / 1 / 425
Goodness-of-fit on F2	1.107
Final R indices [I>2sigma(I)]	R1 = 0.0669, wR2 = 0.1347
R indices (all data)	R1 = 0.0940, wR2 = 0.1472
Largest diff. peak and hole	0.247 and -0.247 e.Å ⁻³

X-ray structure of compound **2.14**:

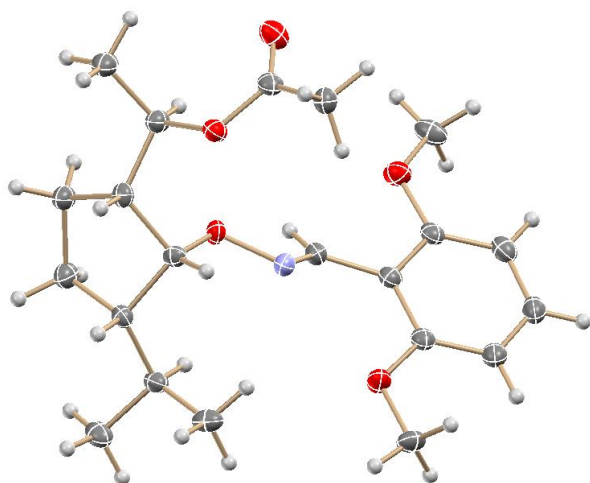
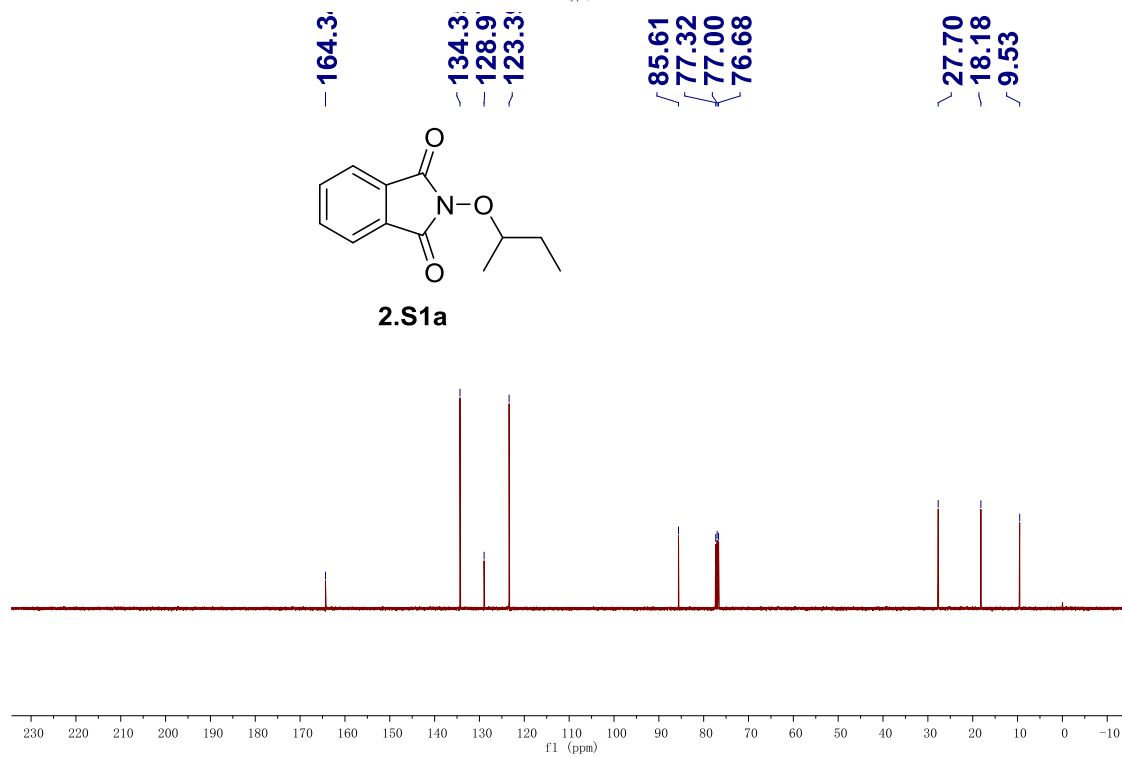
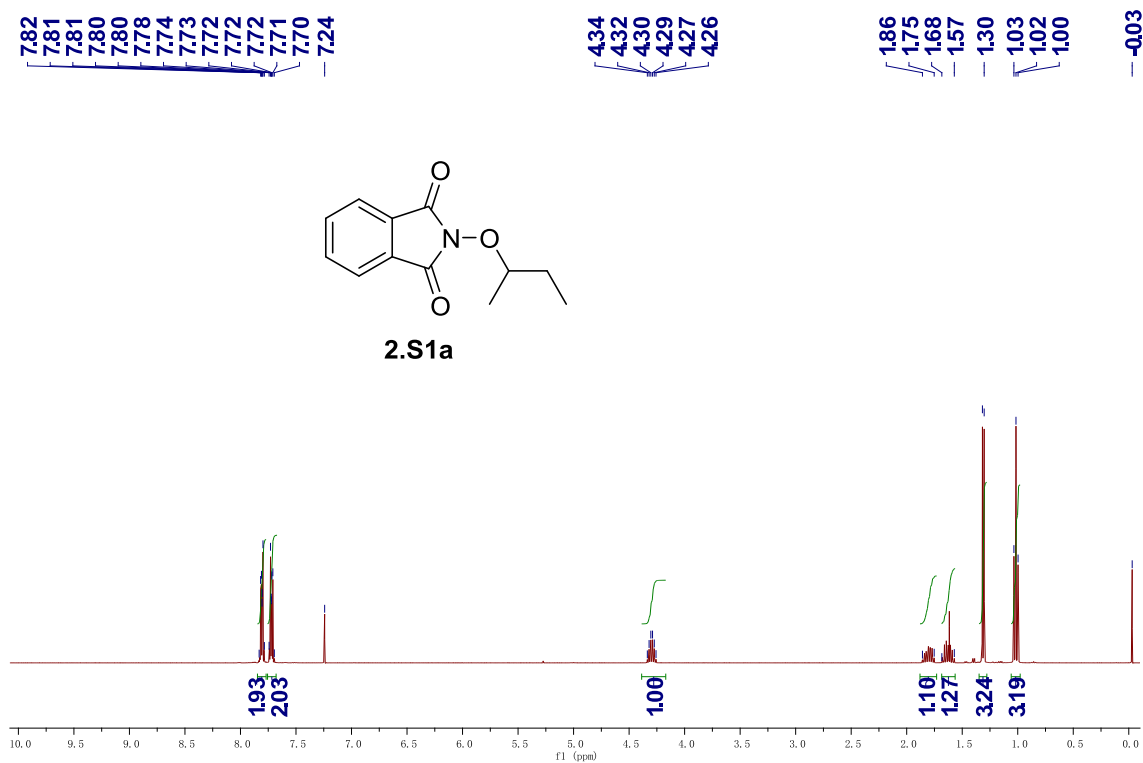
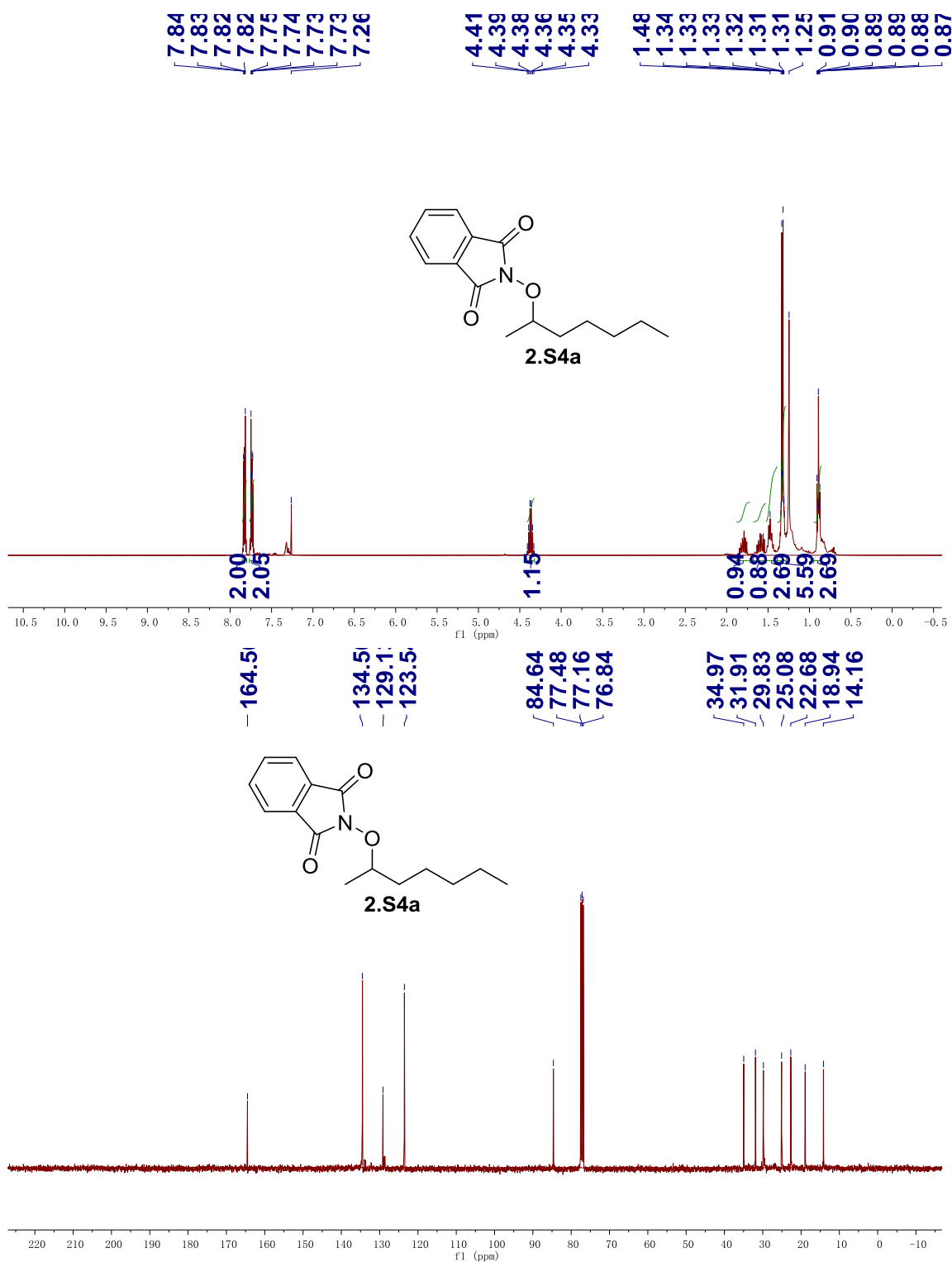


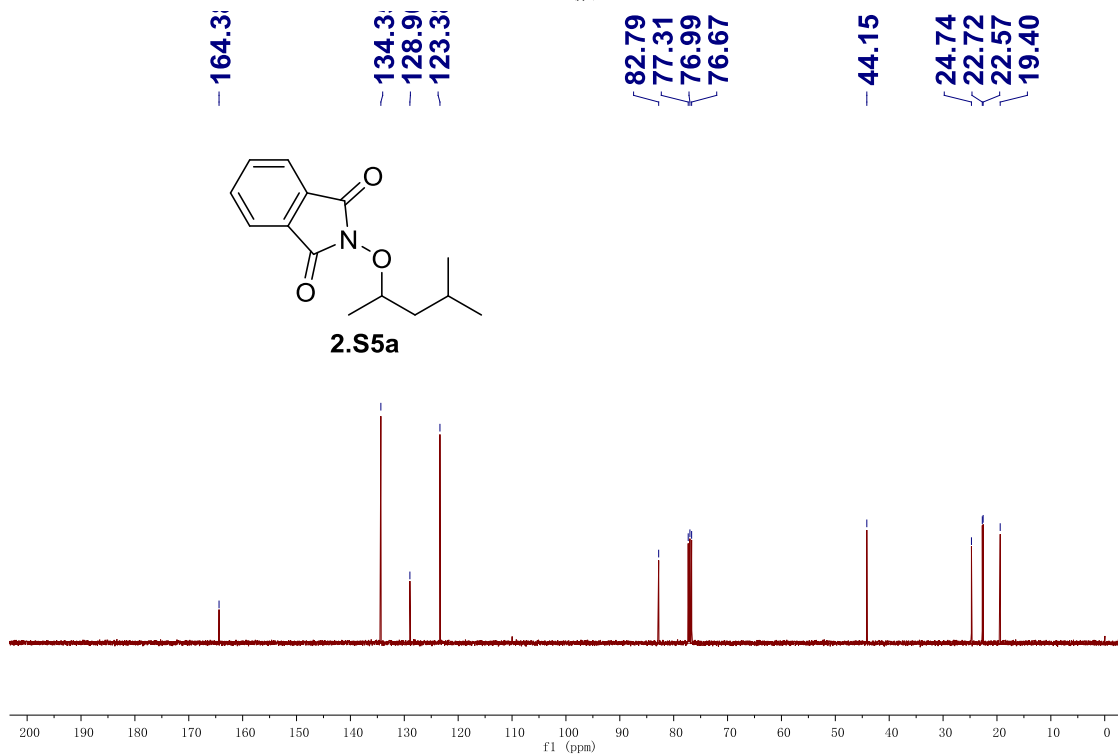
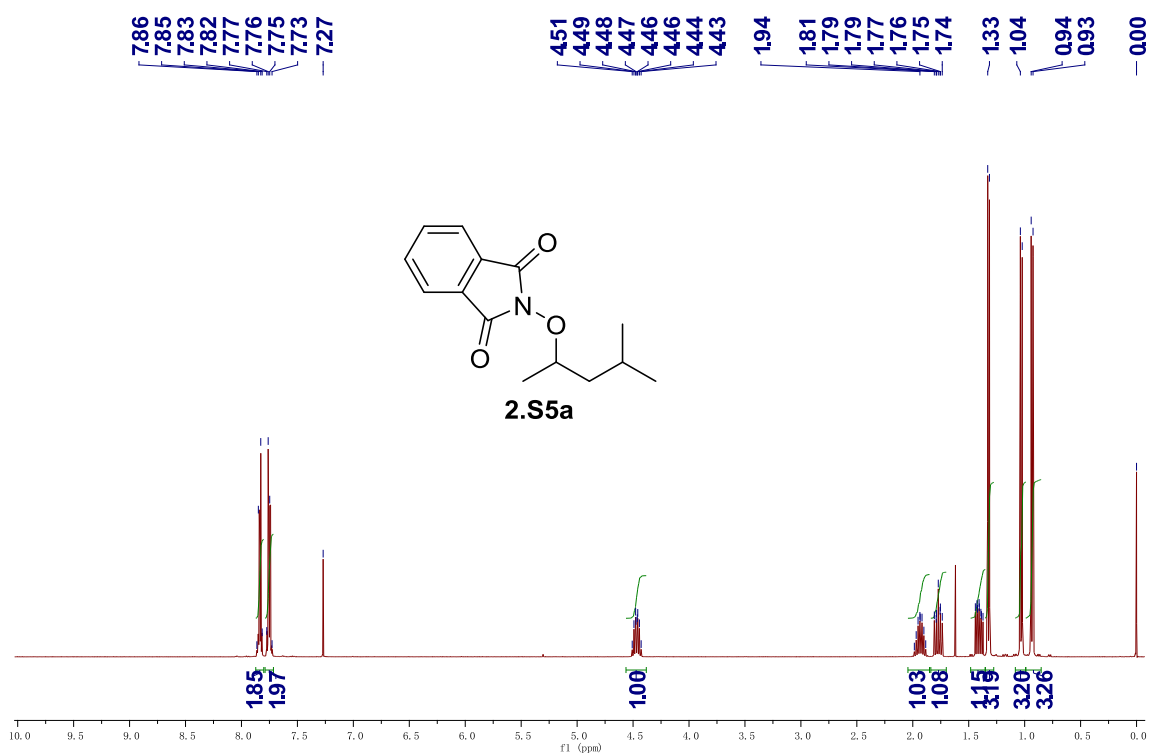
Table 2.6. Crystal data and structure refinement for **2.14**.

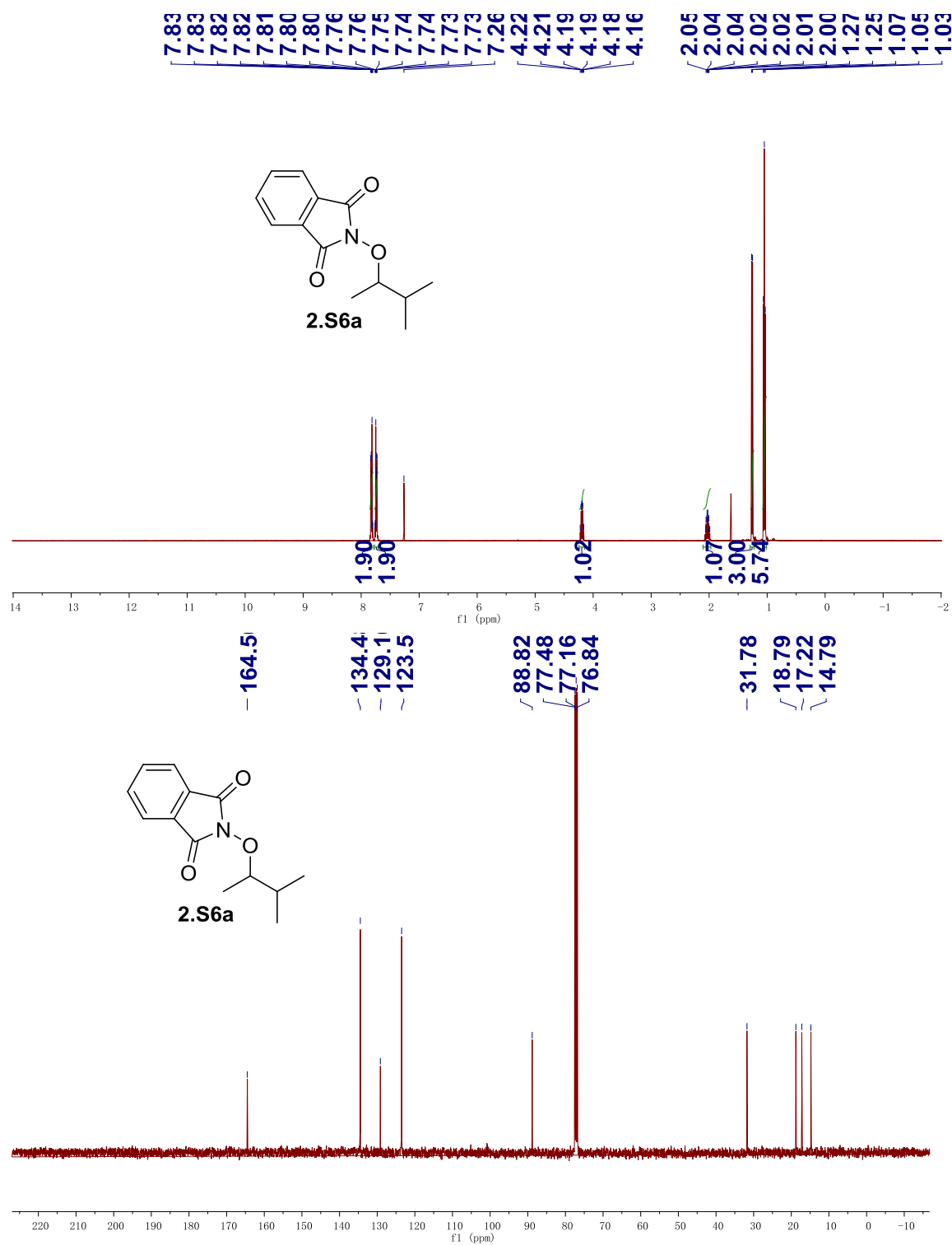
Empirical formula	C ₂₁ H ₃₁ N O ₅
Formula weight	377.47
Temperature	100(2) K
Wavelength	0.71075 Å
Crystal system	Monoclinic
Space group	P21
Unit cell dimensions	$a = 13.5787(15) \text{ Å}$ $= 90^\circ$. $b = 5.2656(8) \text{ Å}$ $= 91.579(4)^\circ$. $c = 14.435(2) \text{ Å}$ $= 90^\circ$.
Volume	1031.7(2) Å ³
Z	2
Density (calculated)	1.215 Mg/m ³
Absorption coefficient	0.086 mm ⁻¹
F(000)	408

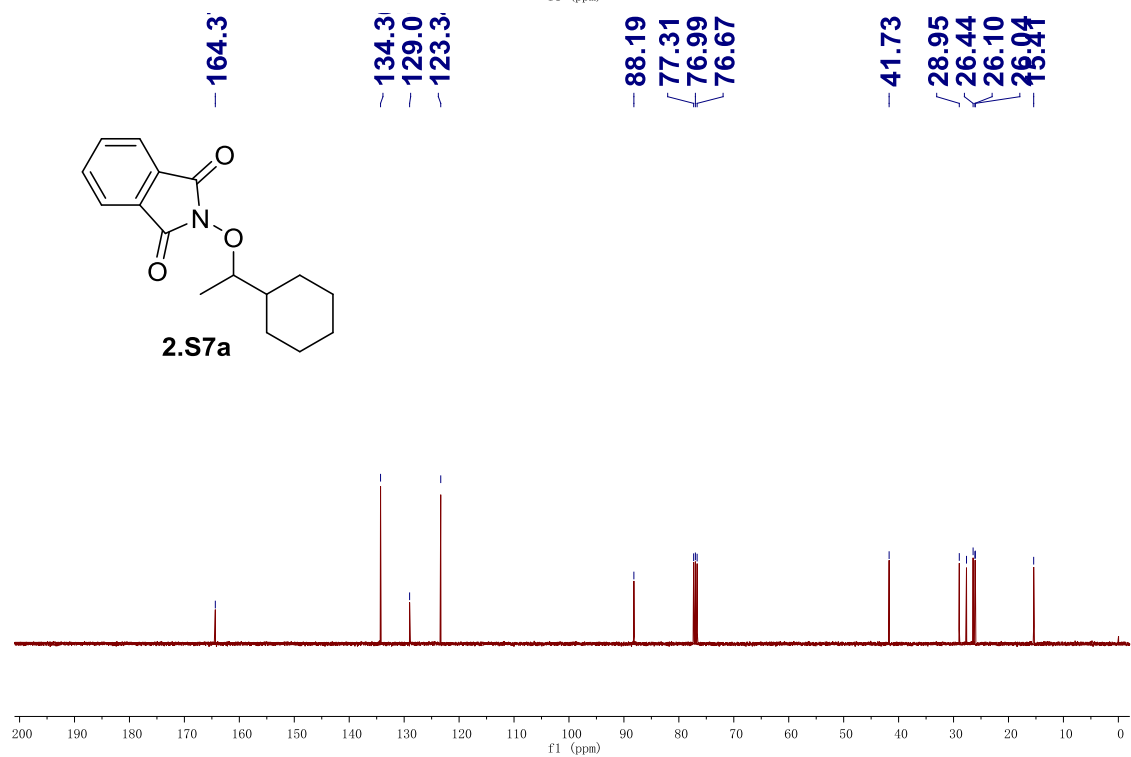
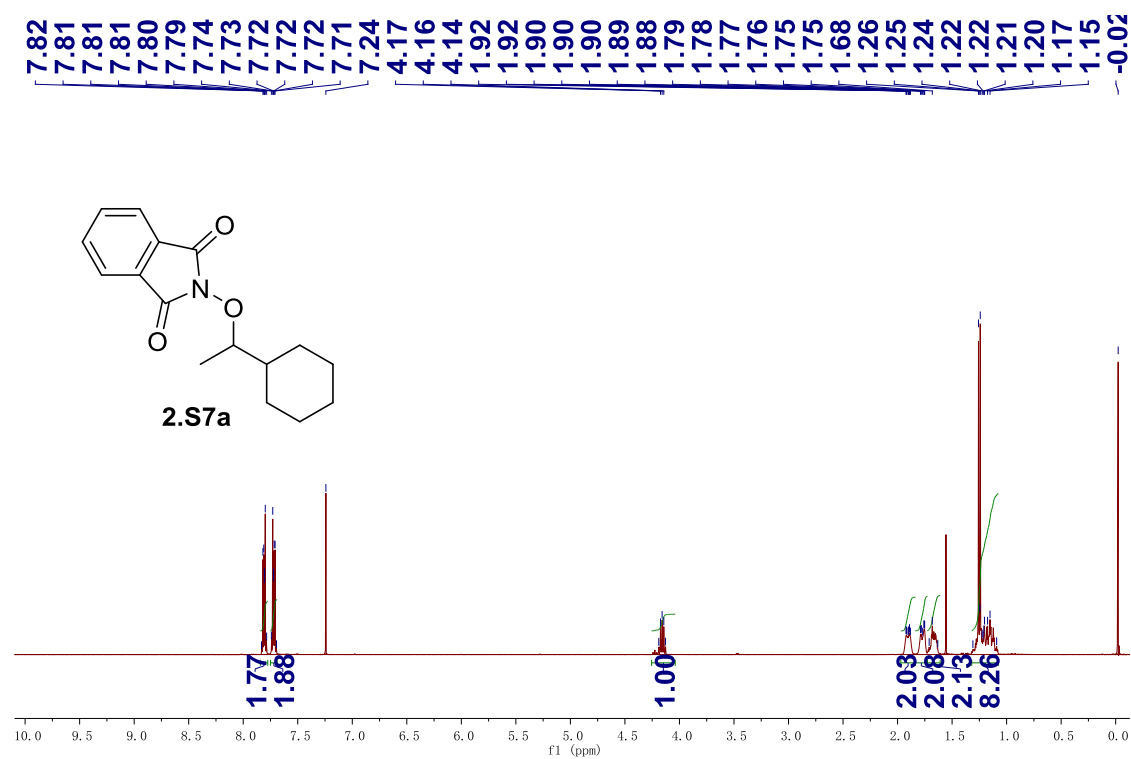
Crystal size	0.26 x 0.07 x 0.04 mm
Theta range for data collection	3.00 to 27.48°.
Index ranges	-17<=h<=17, -6<=k<=6, -18<=l<=18
Reflections collected	19263
Independent reflections	2610 [R(int) = 0.0644]
Completeness to theta = 27.48°	99.8 %
Absorption correction	Semi-empirical from equivalents
Max. and min. transmission	1.00 and 0.729
Refinement method	Full-matrix least-squares on F2
Data / restraints / parameters	2610 / 1 / 250
Goodness-of-fit on F2	1.107
Final R indices [I>2sigma(I)]	R1 = 0.0484, wR2 = 0.1113
R indices (all data)	R1 = 0.0568, wR2 = 0.1151
Largest diff. peak and hole	0.214 and -0.272 e.Å ⁻³

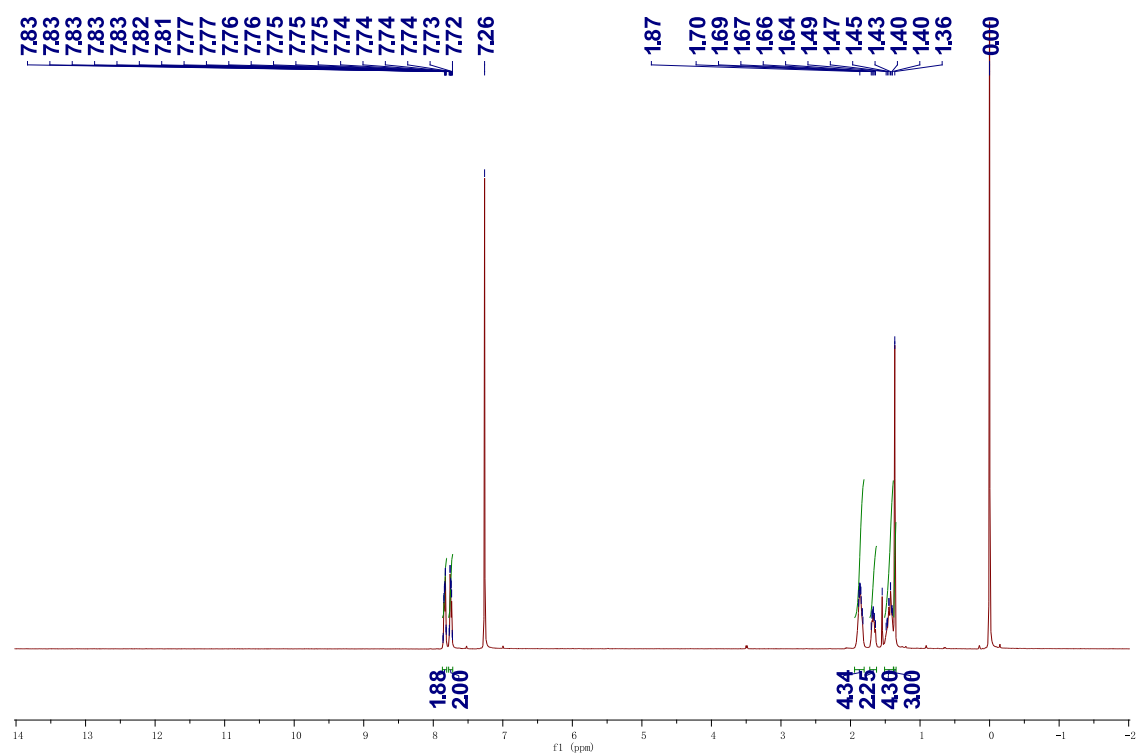


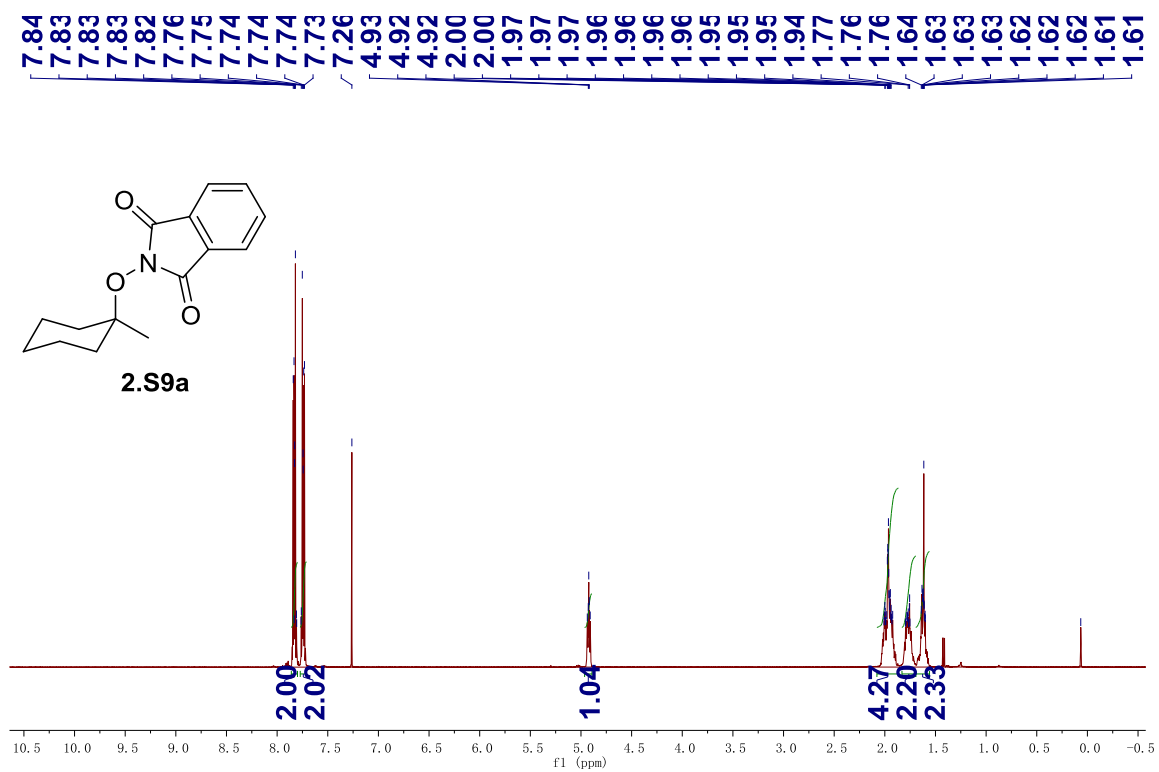


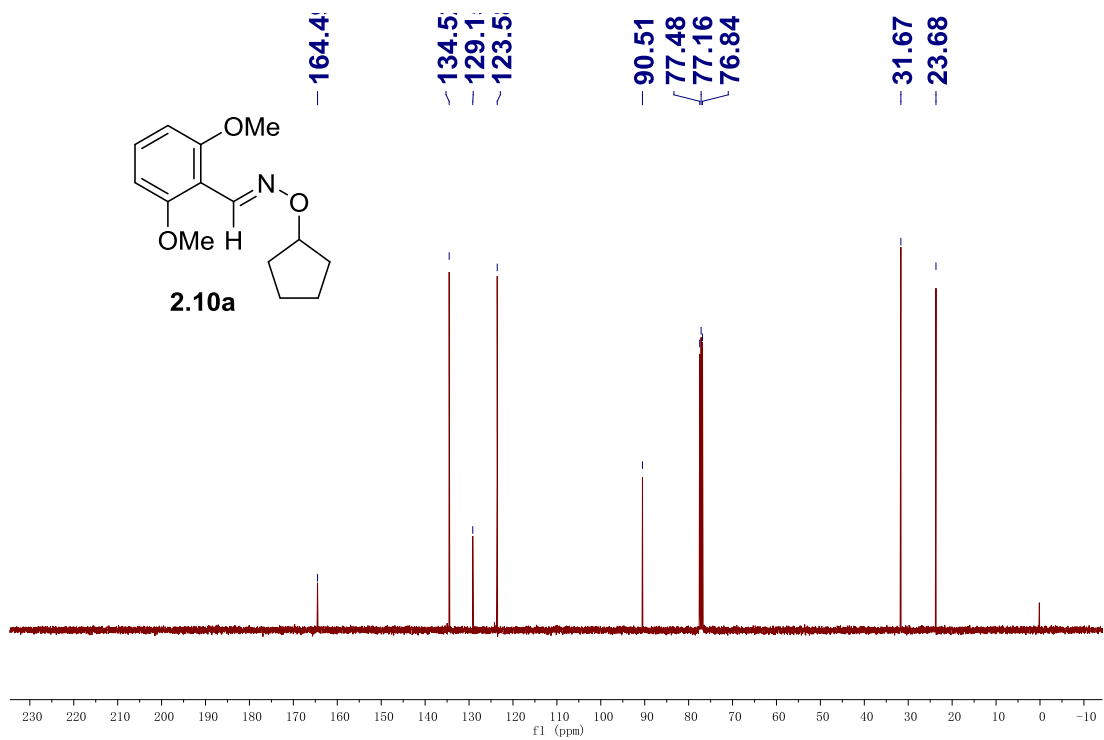
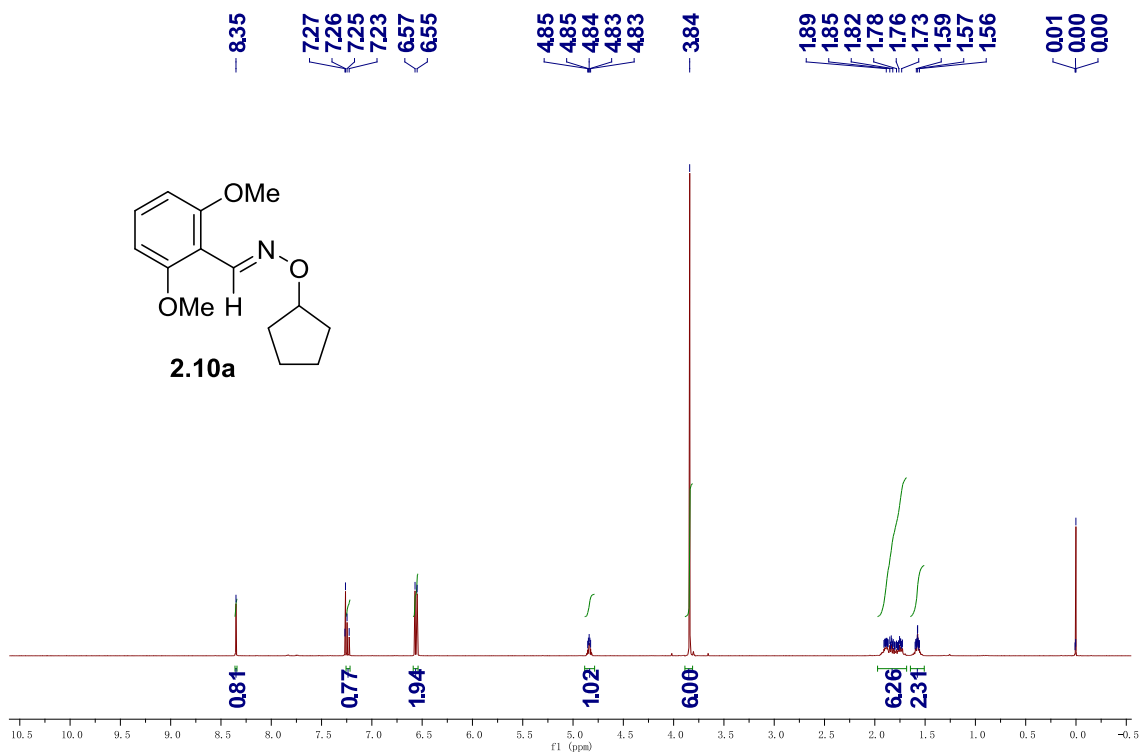


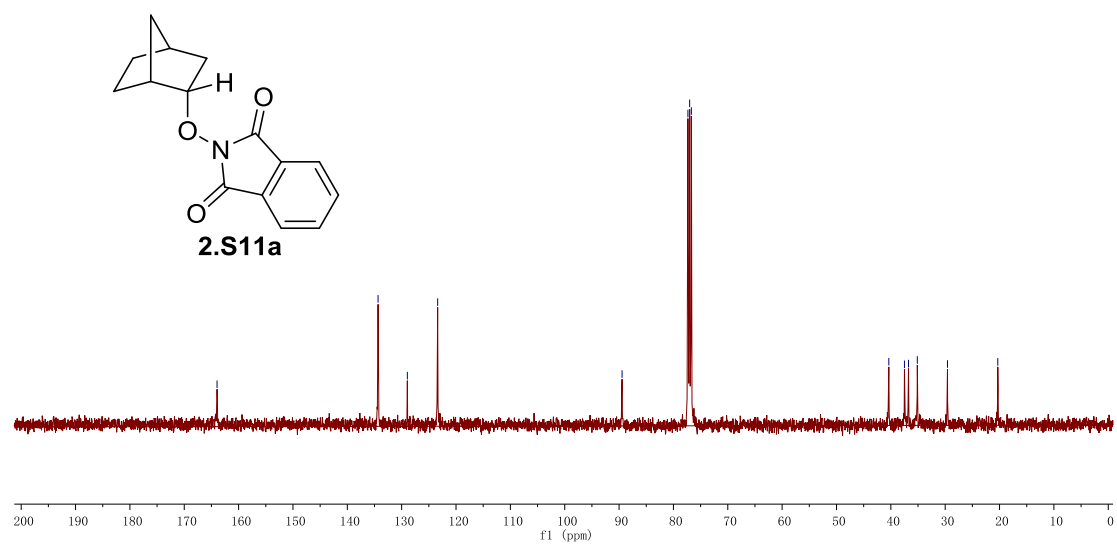
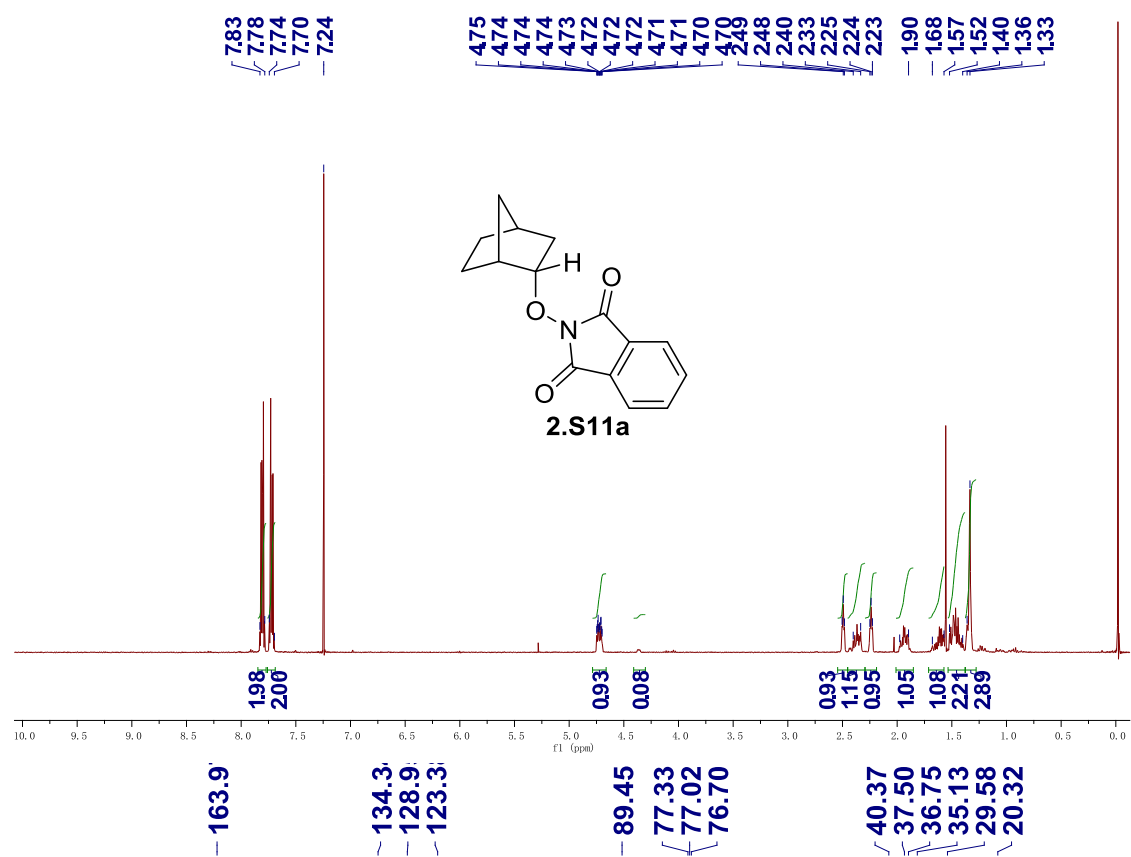


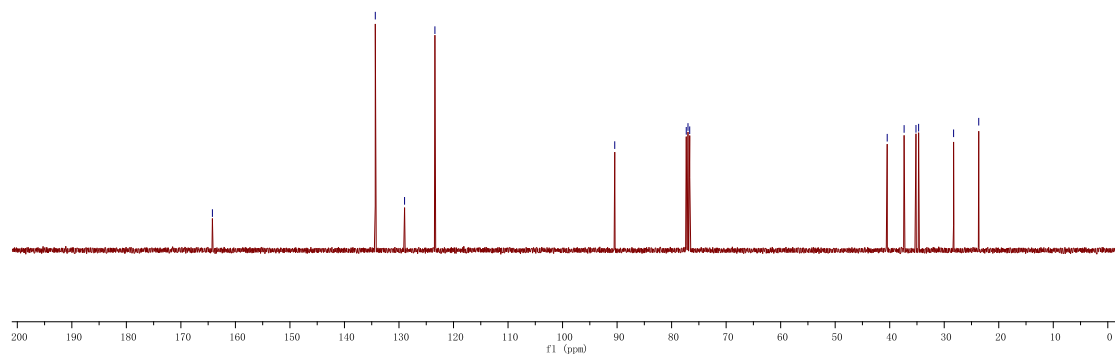
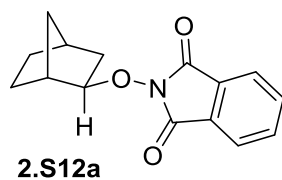
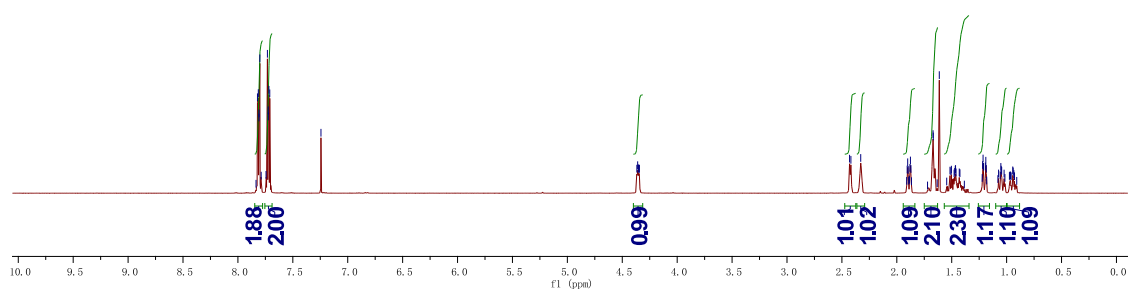
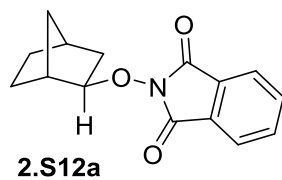


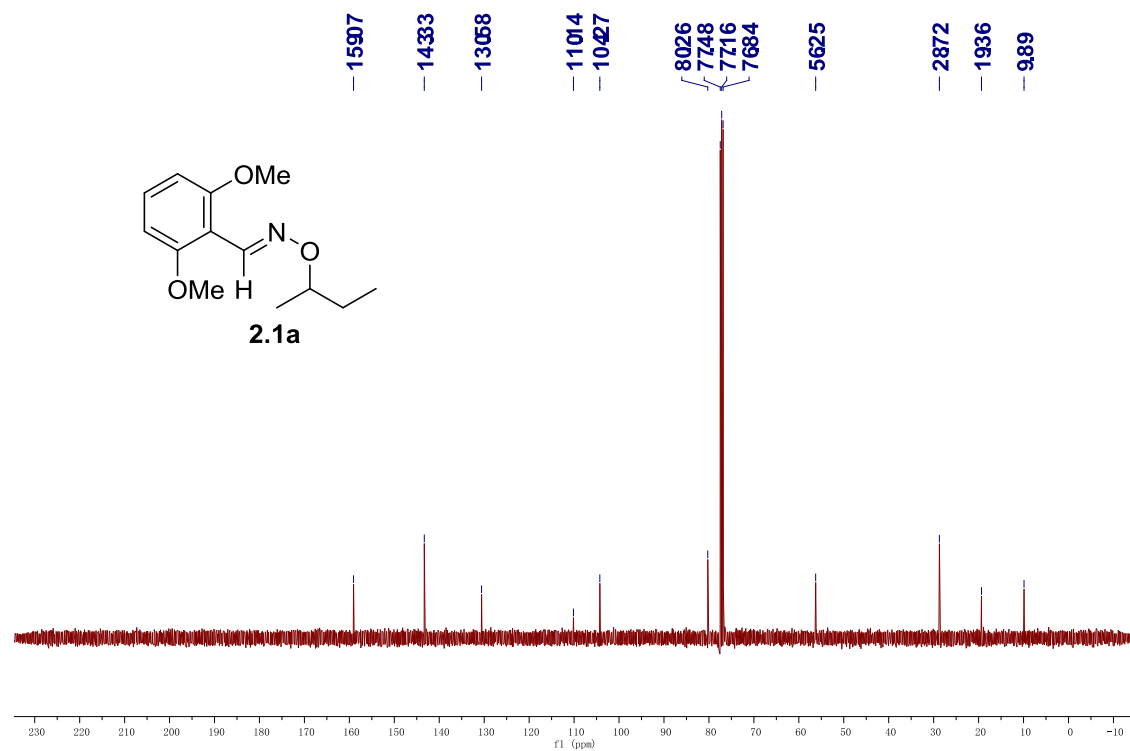
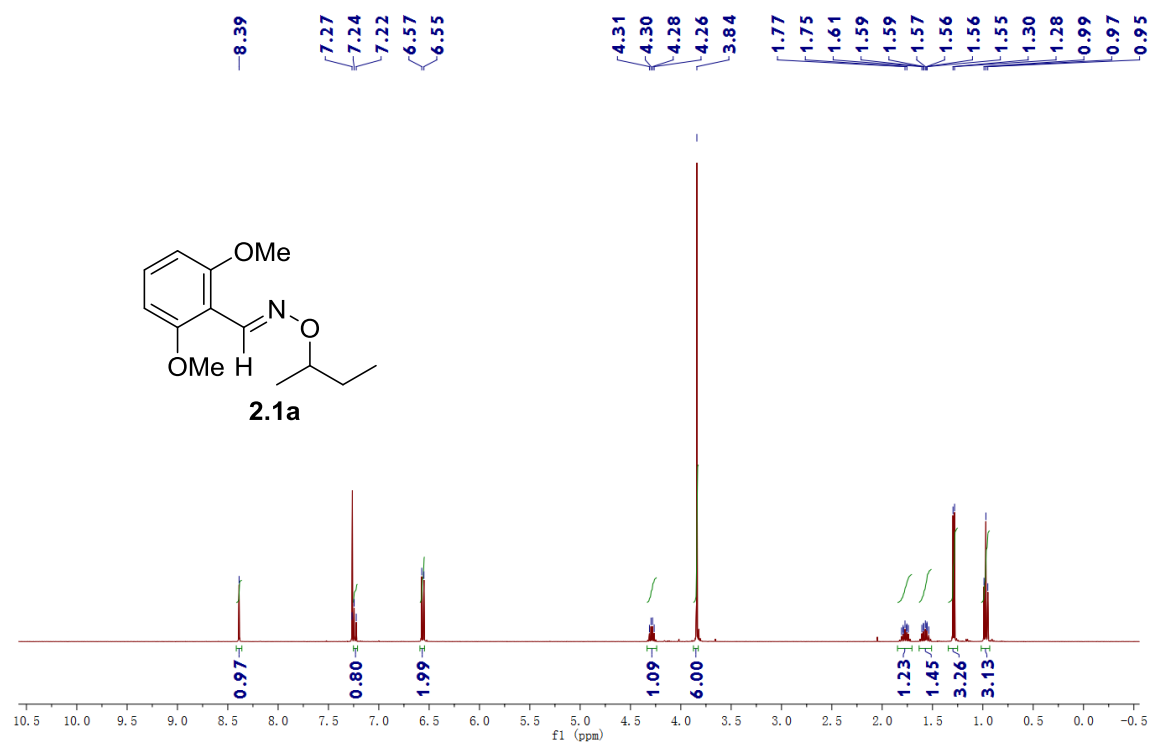


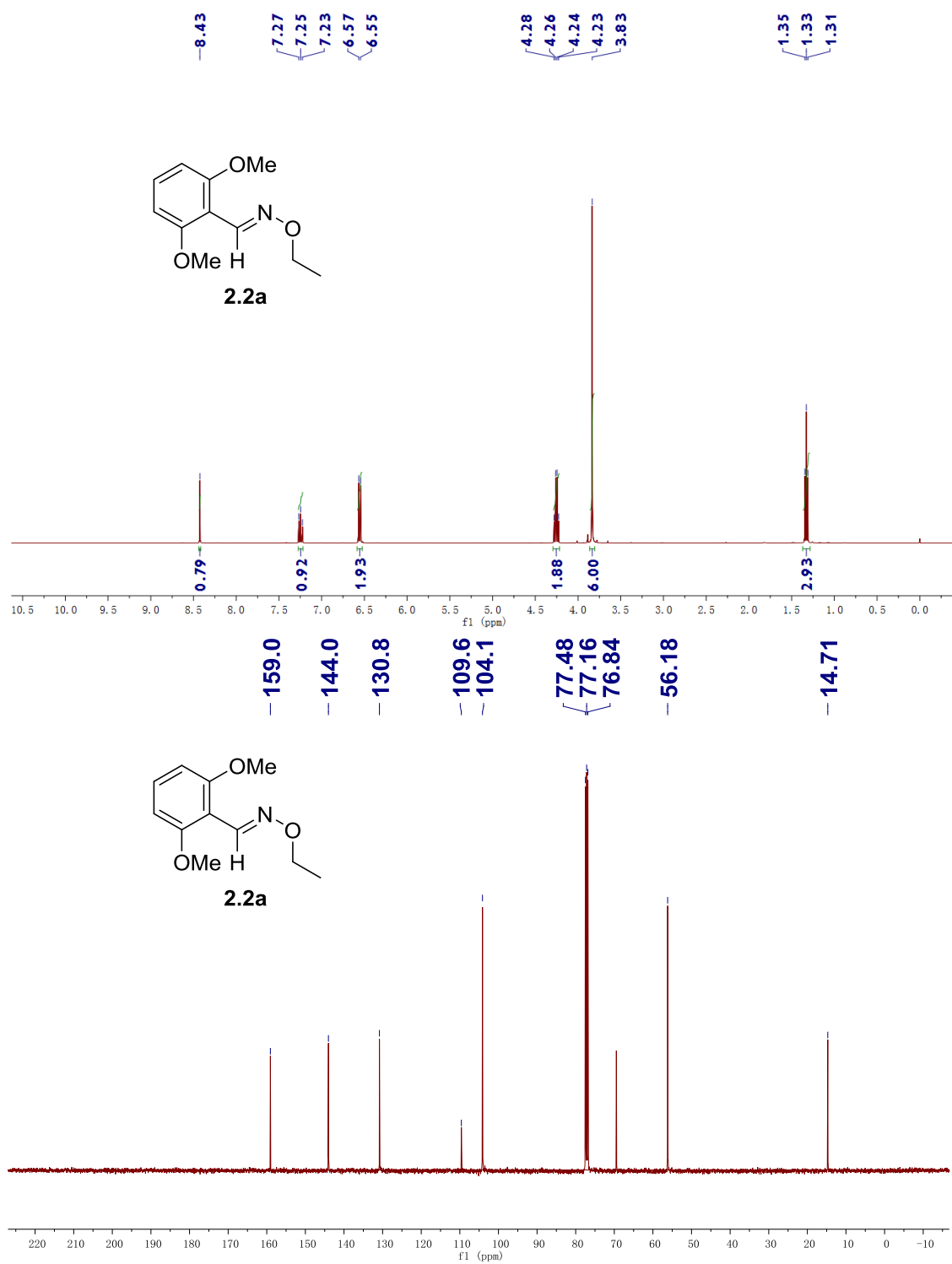


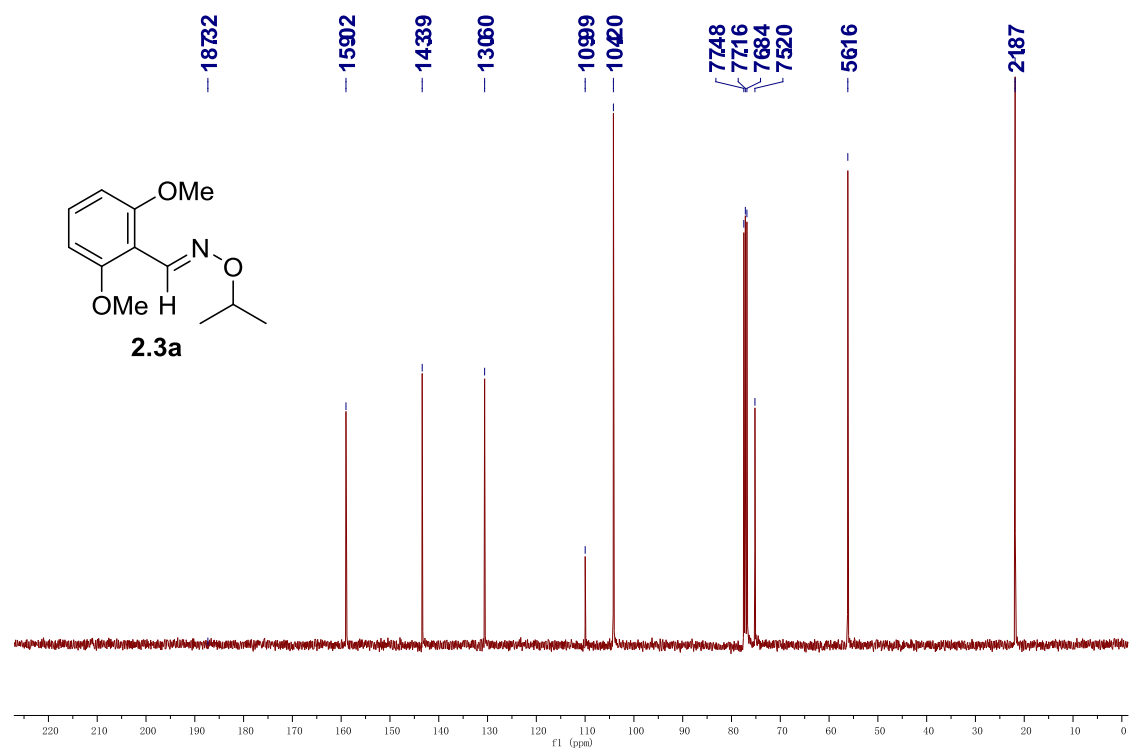
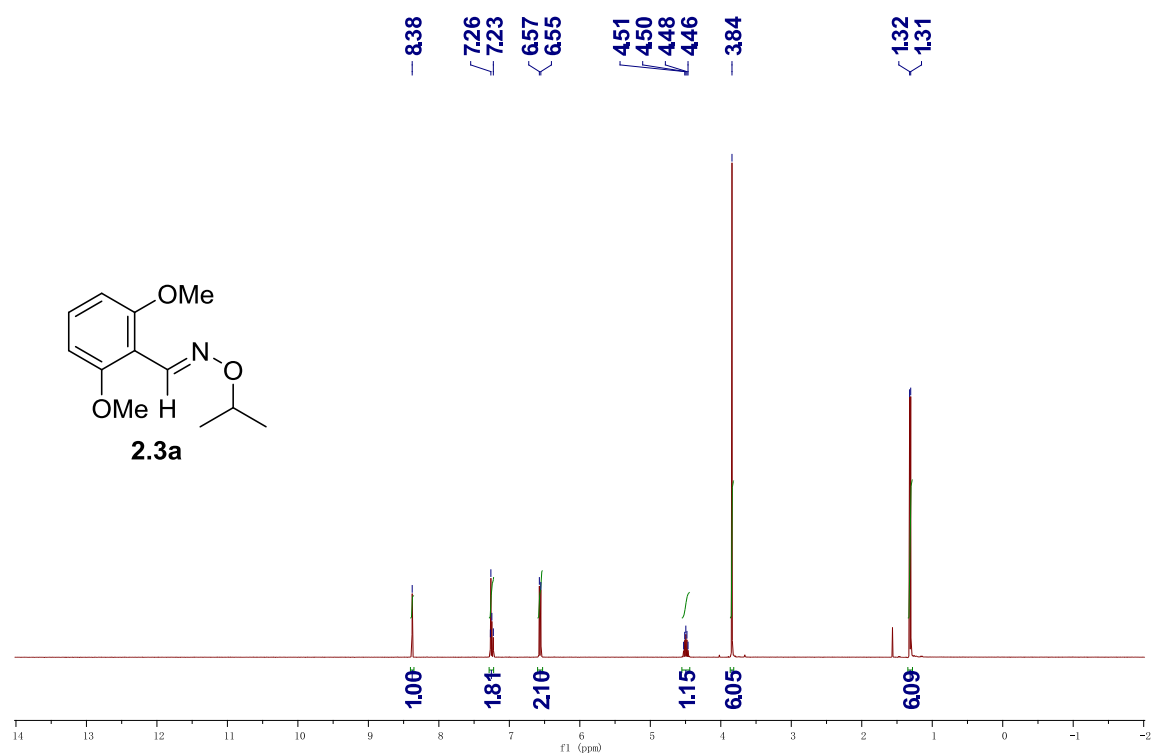


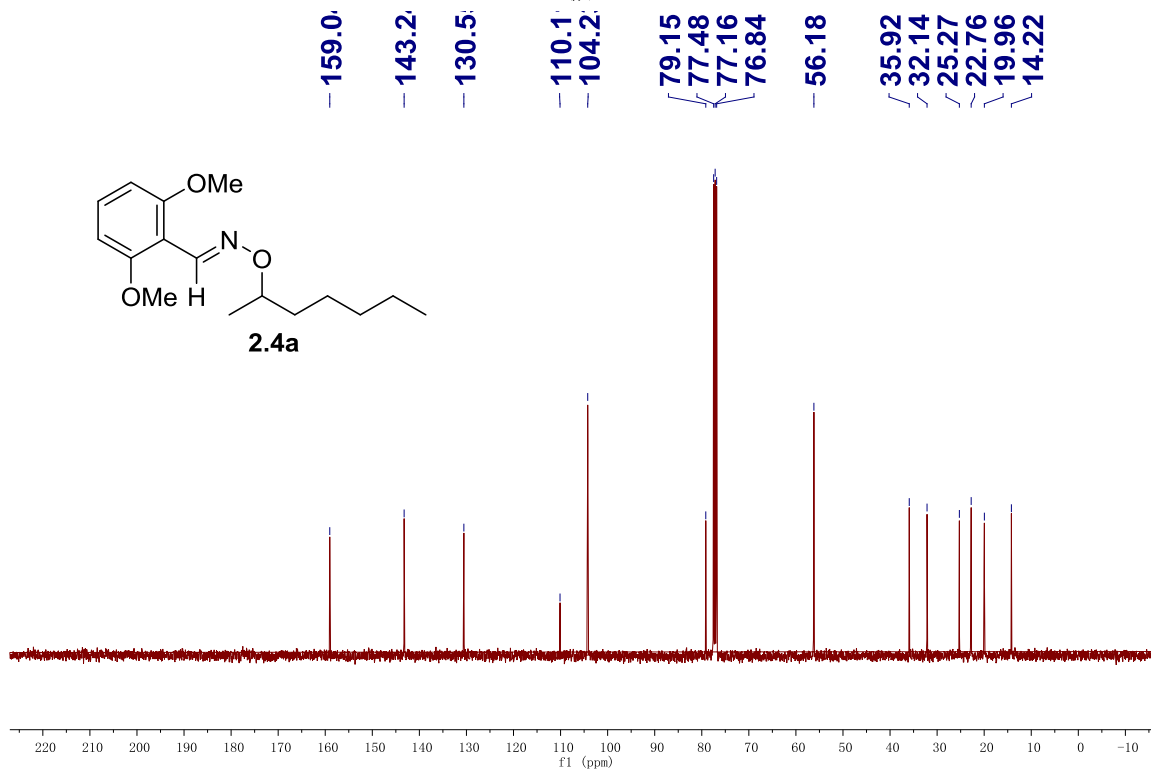
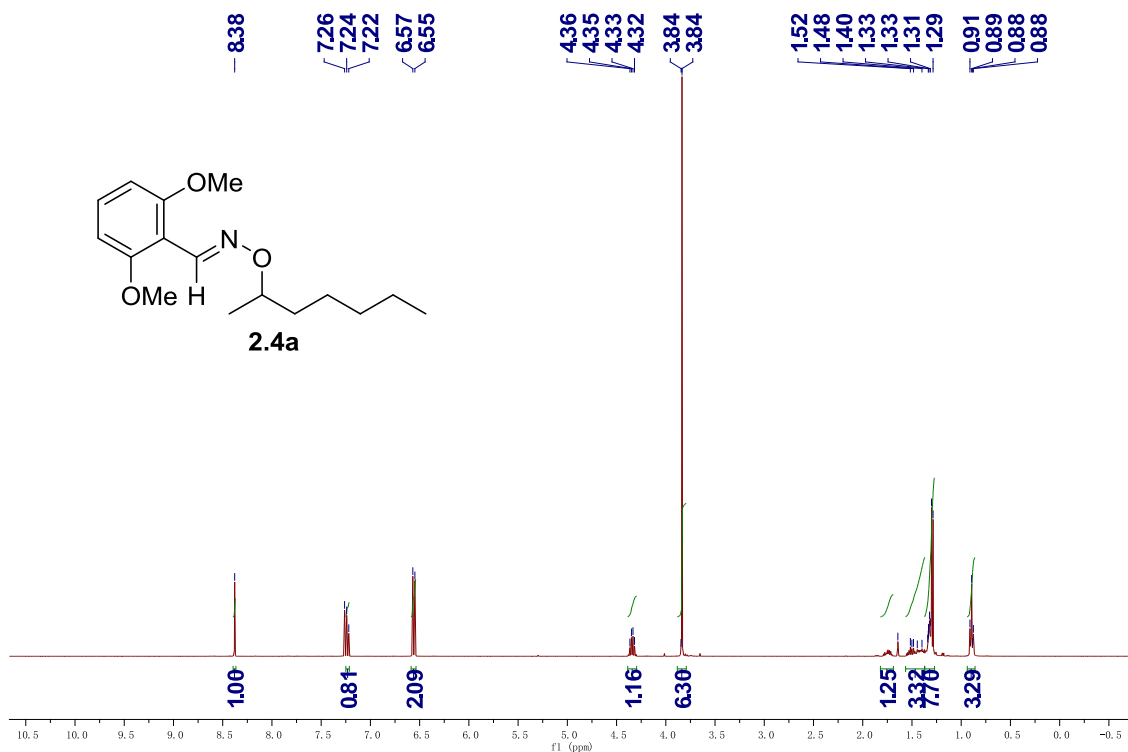


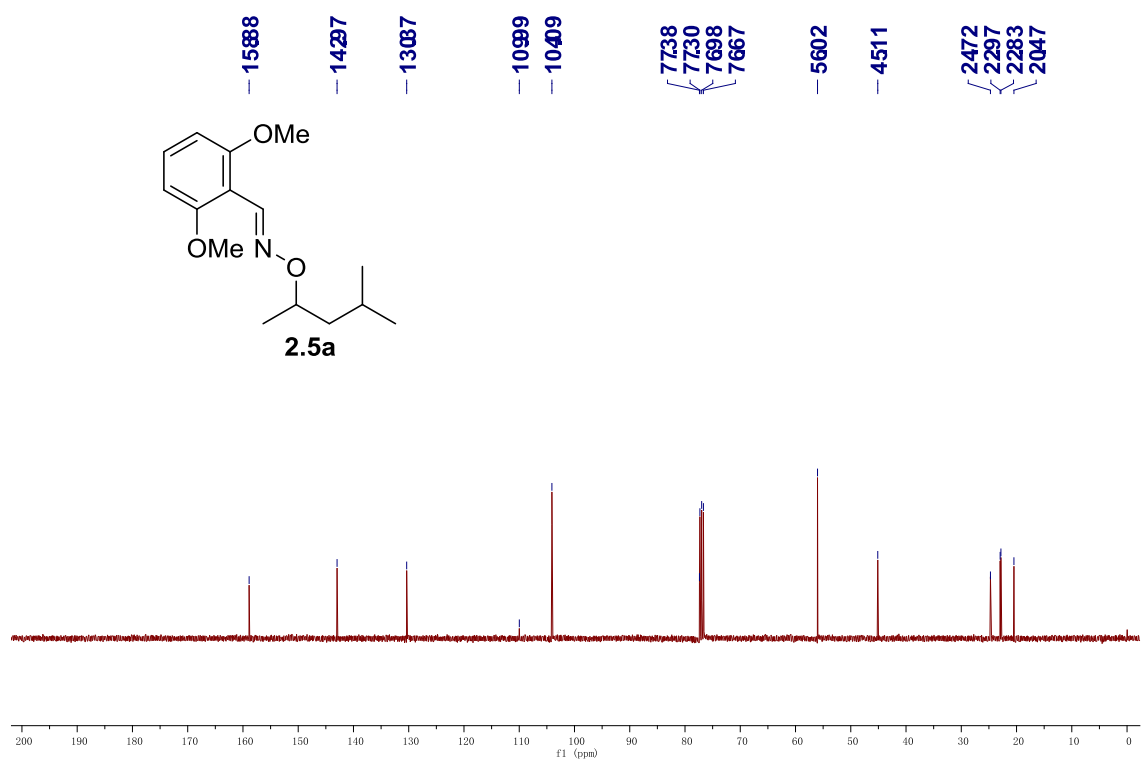
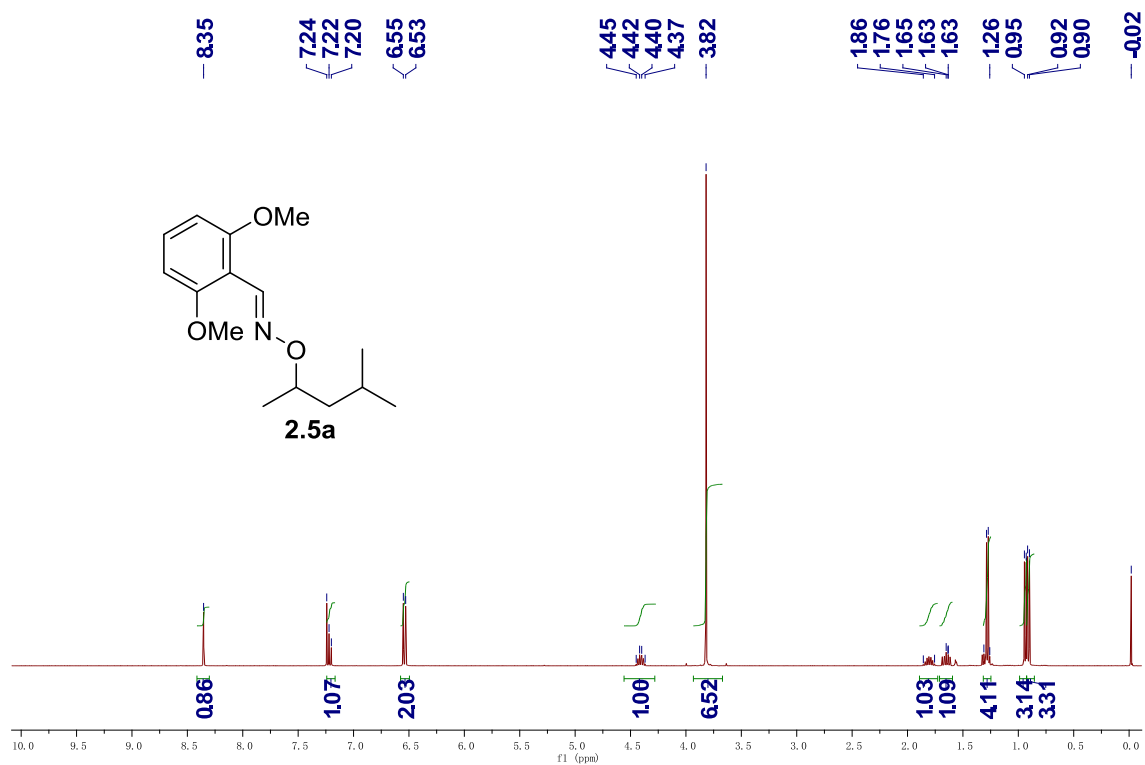


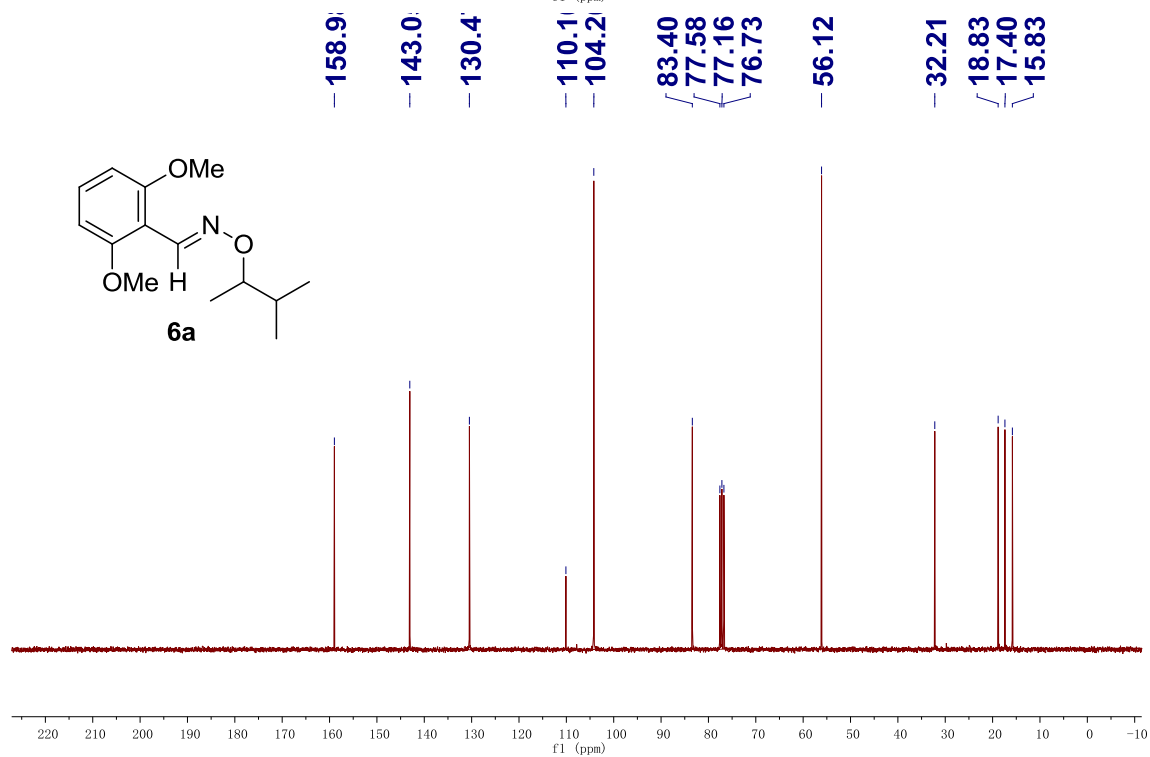
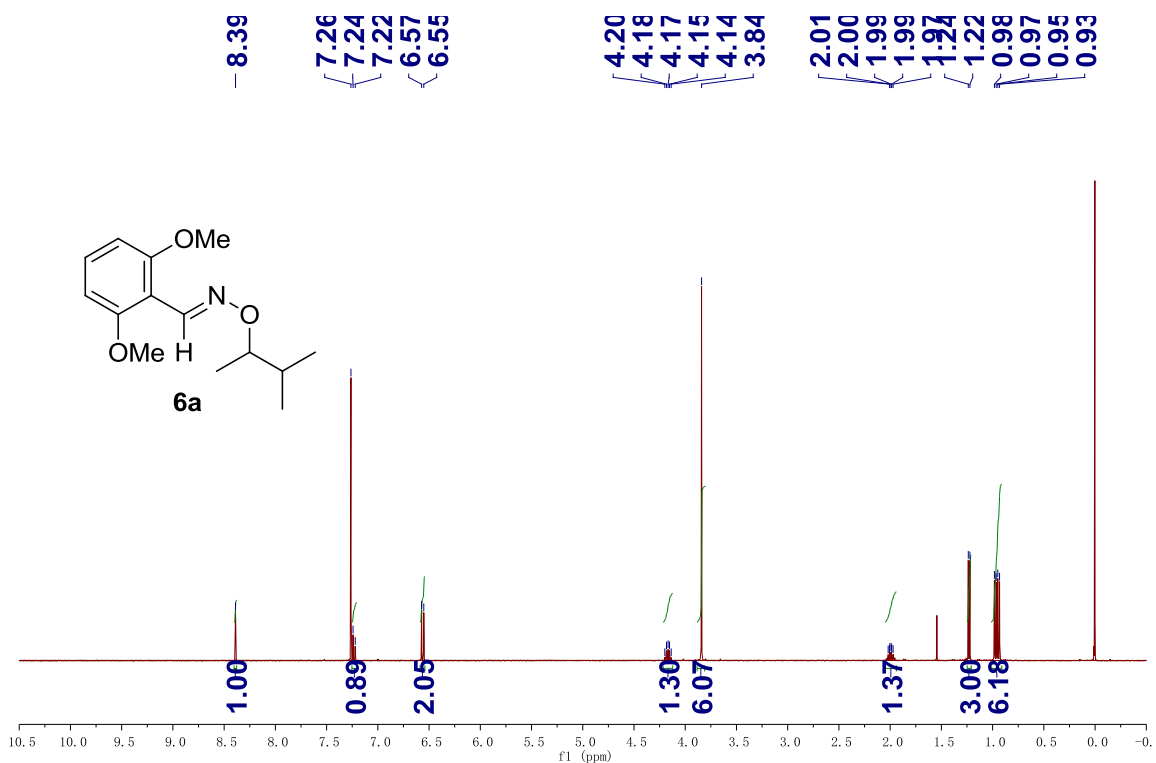


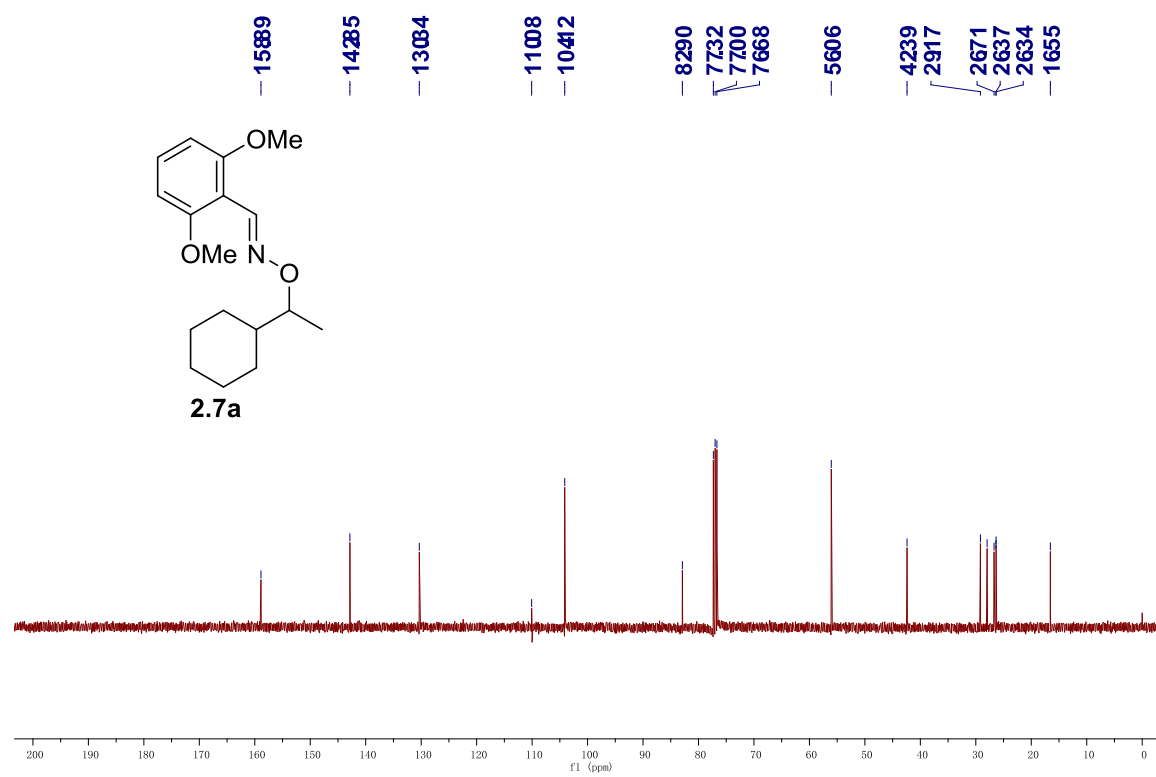
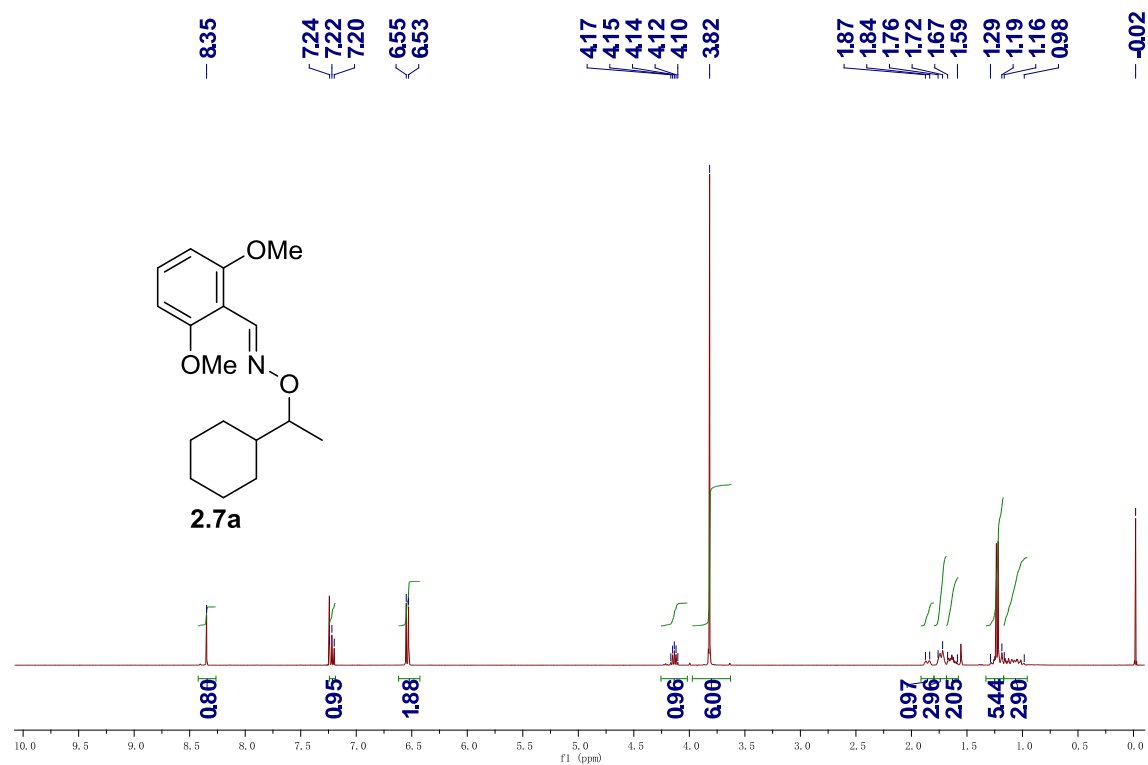


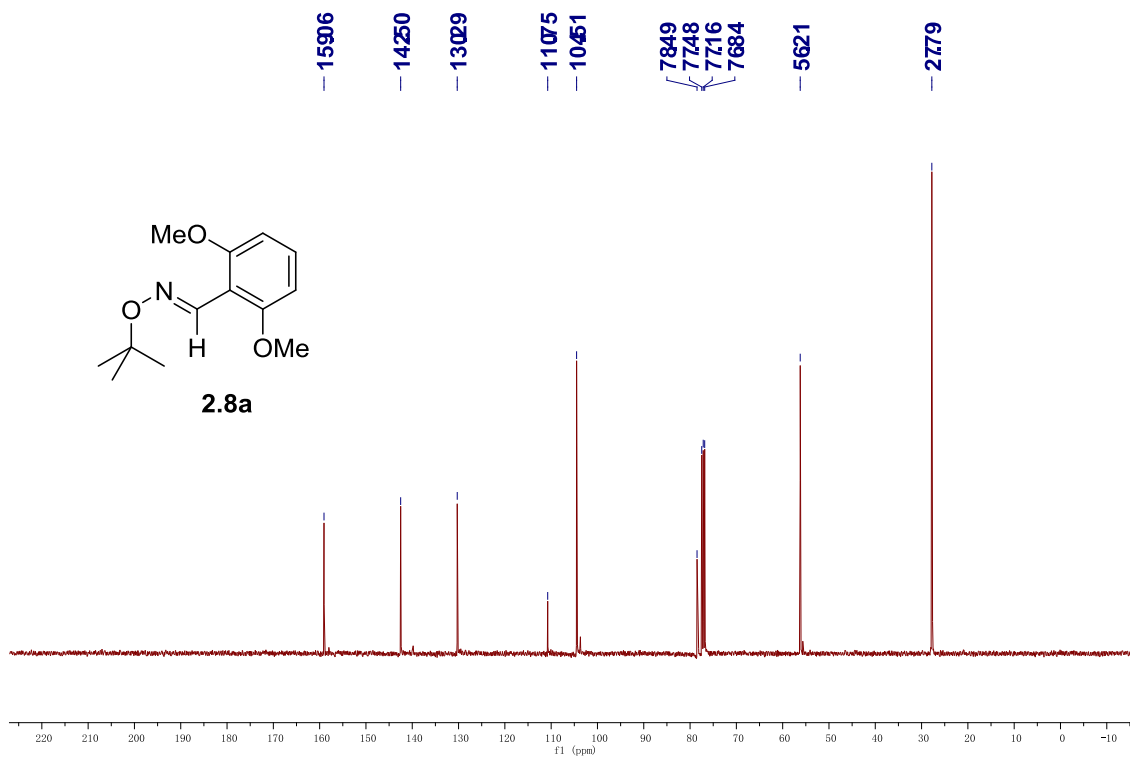
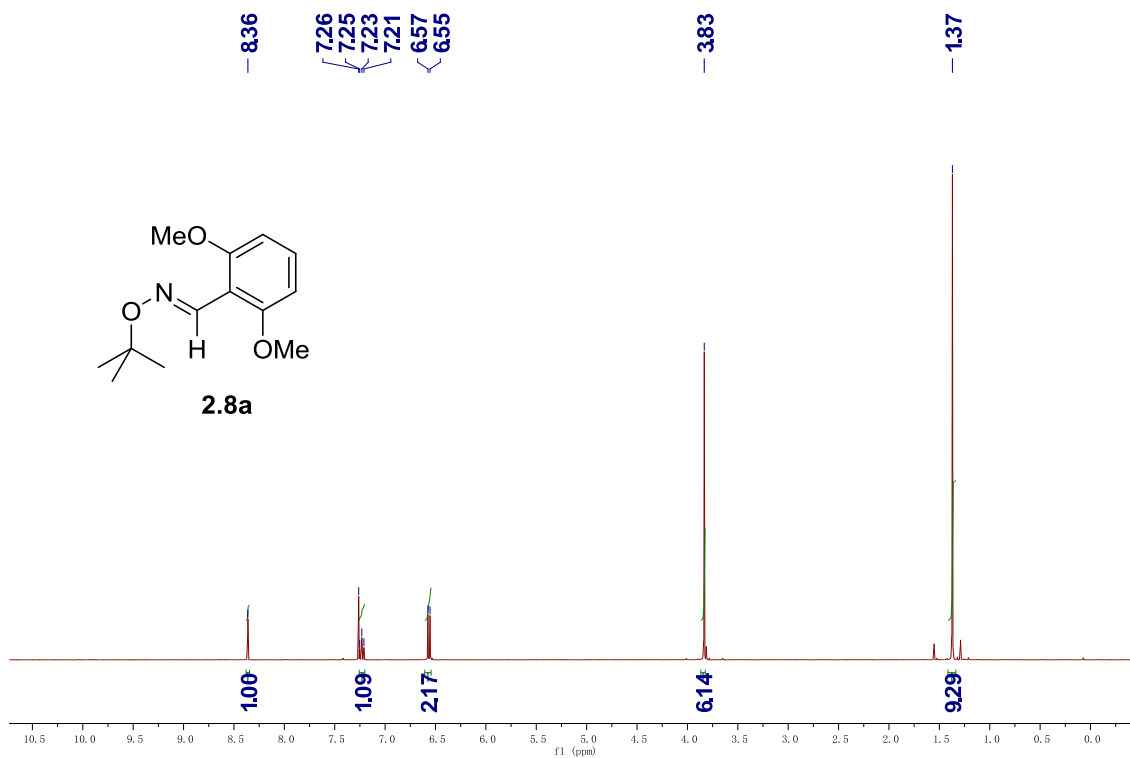


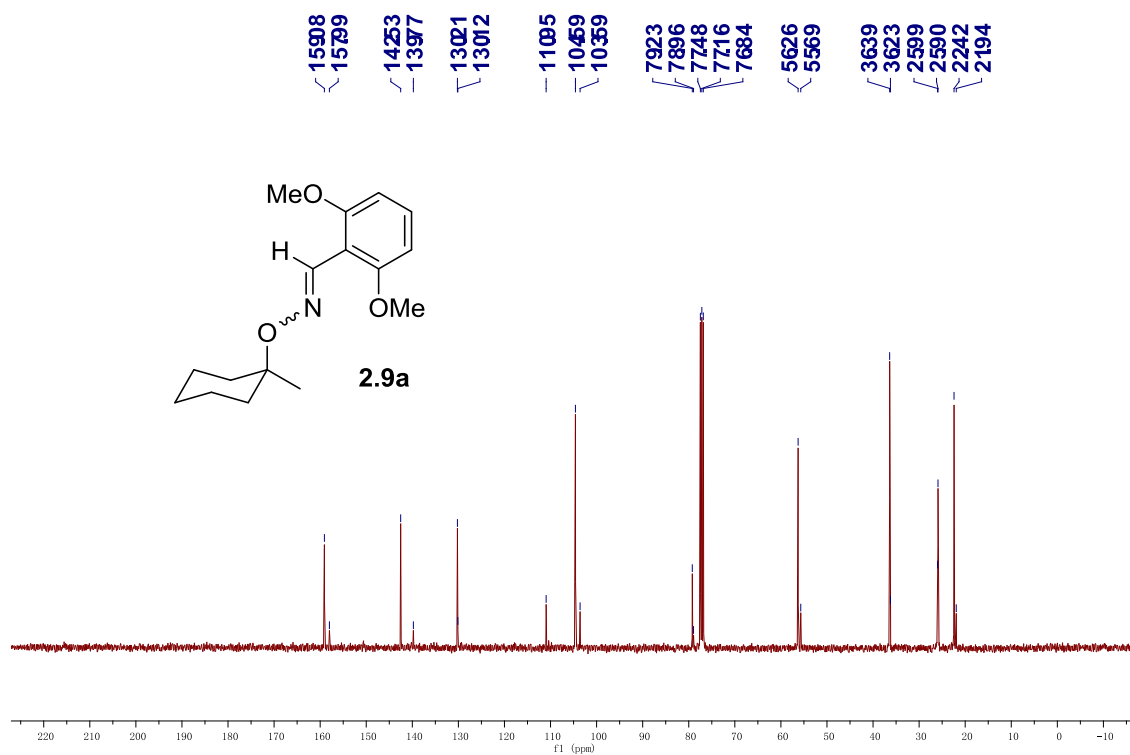
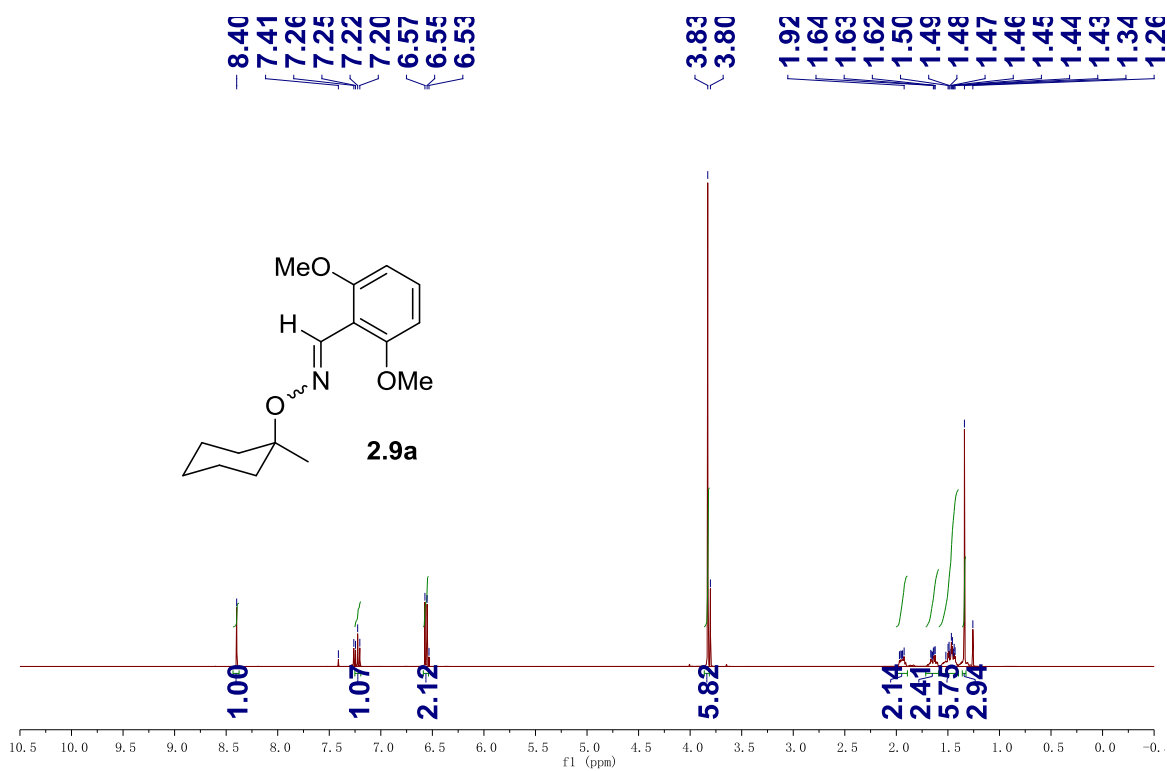


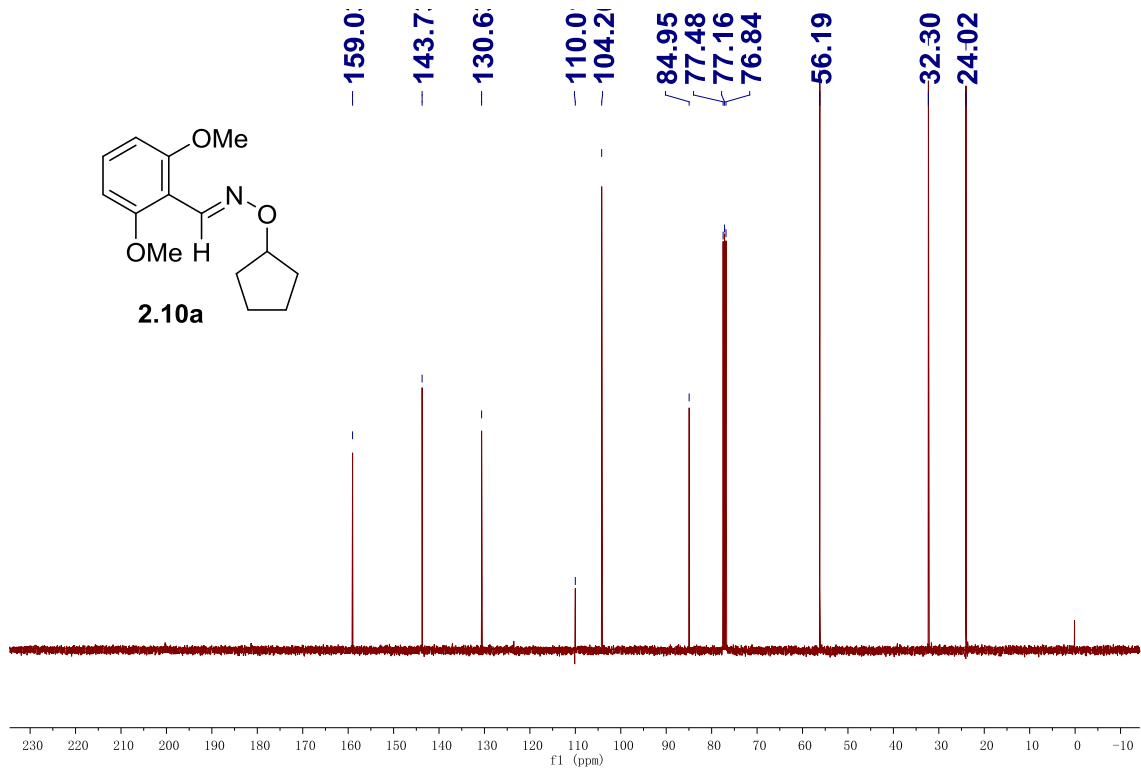
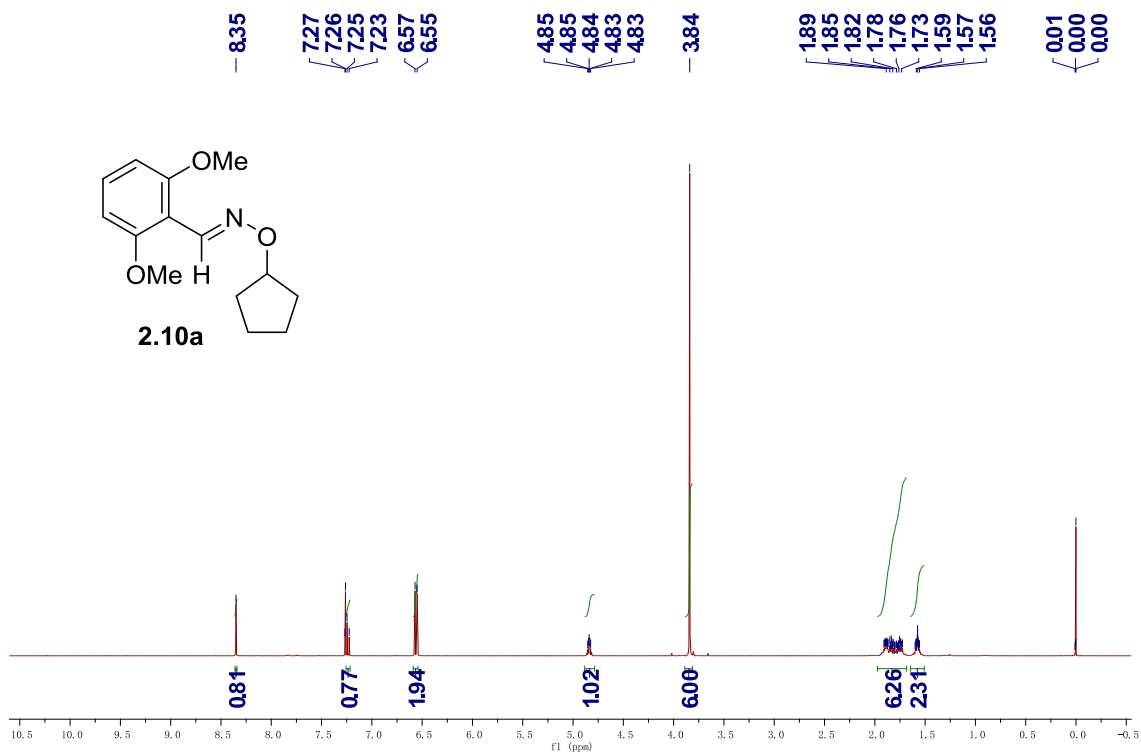


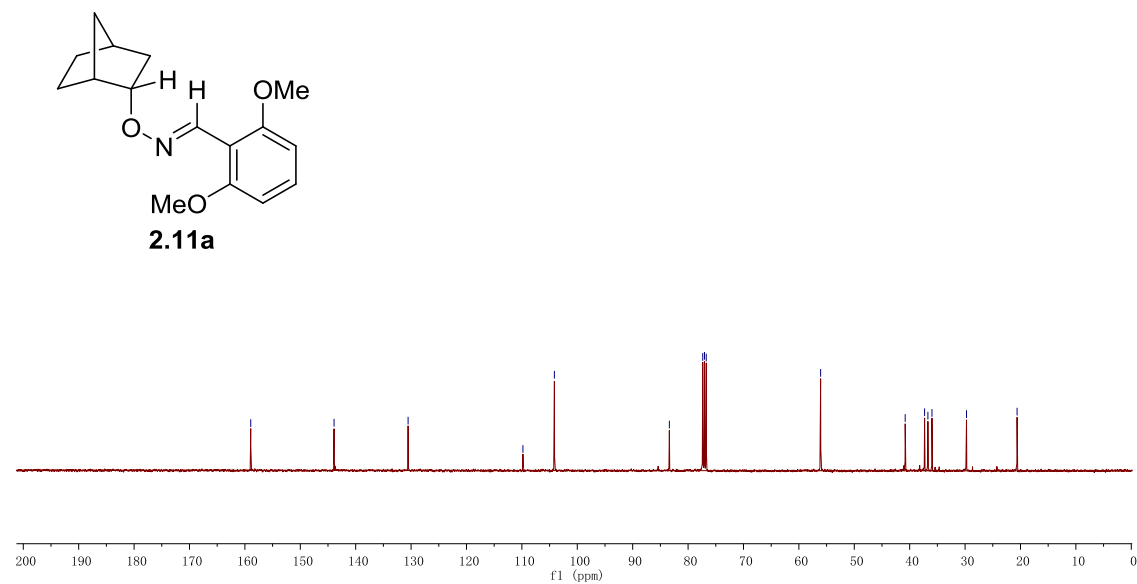
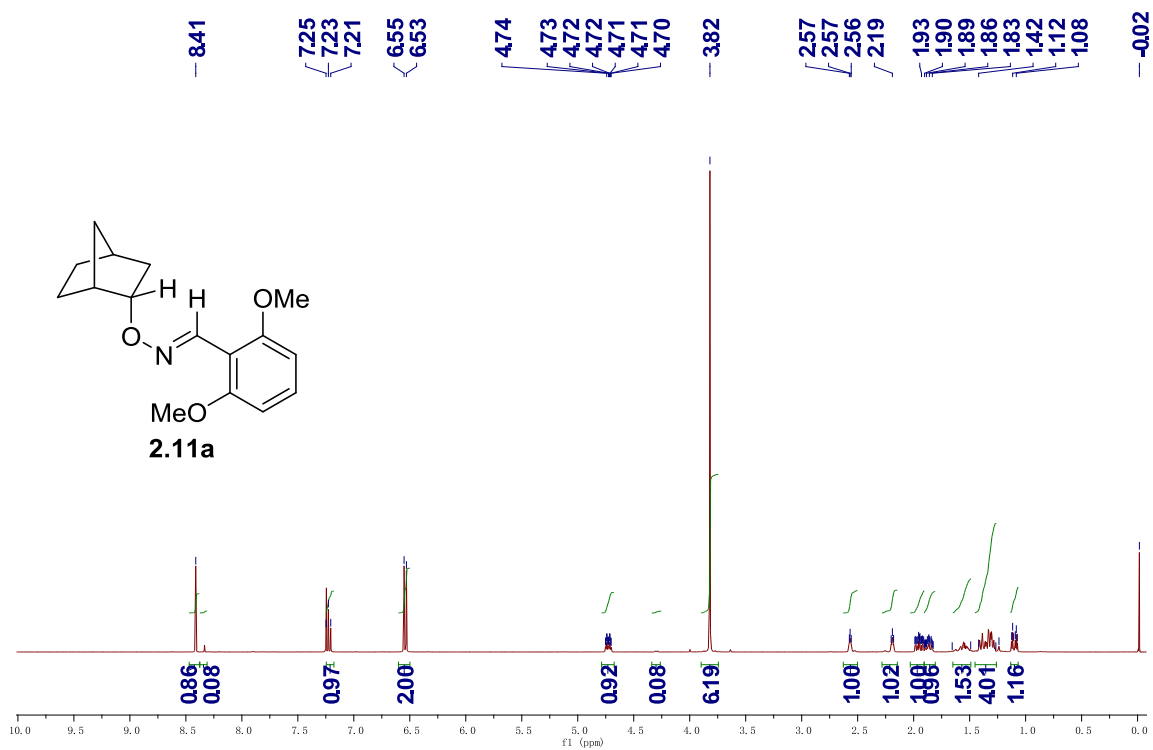


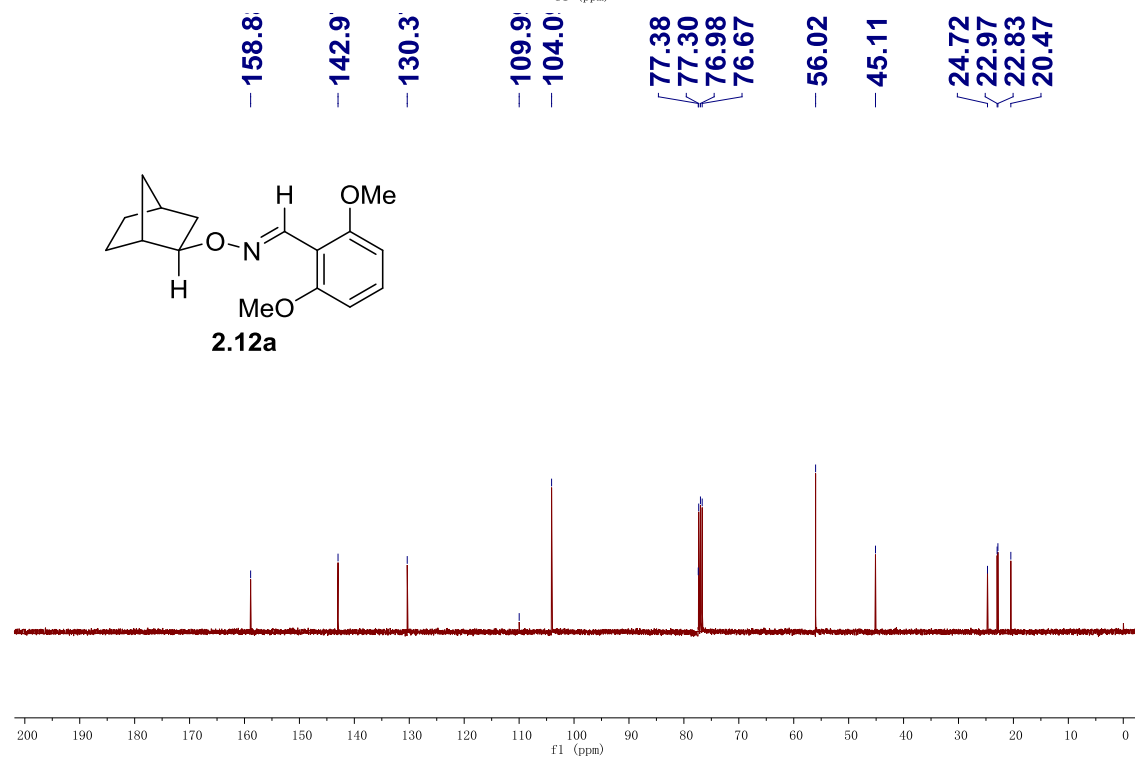
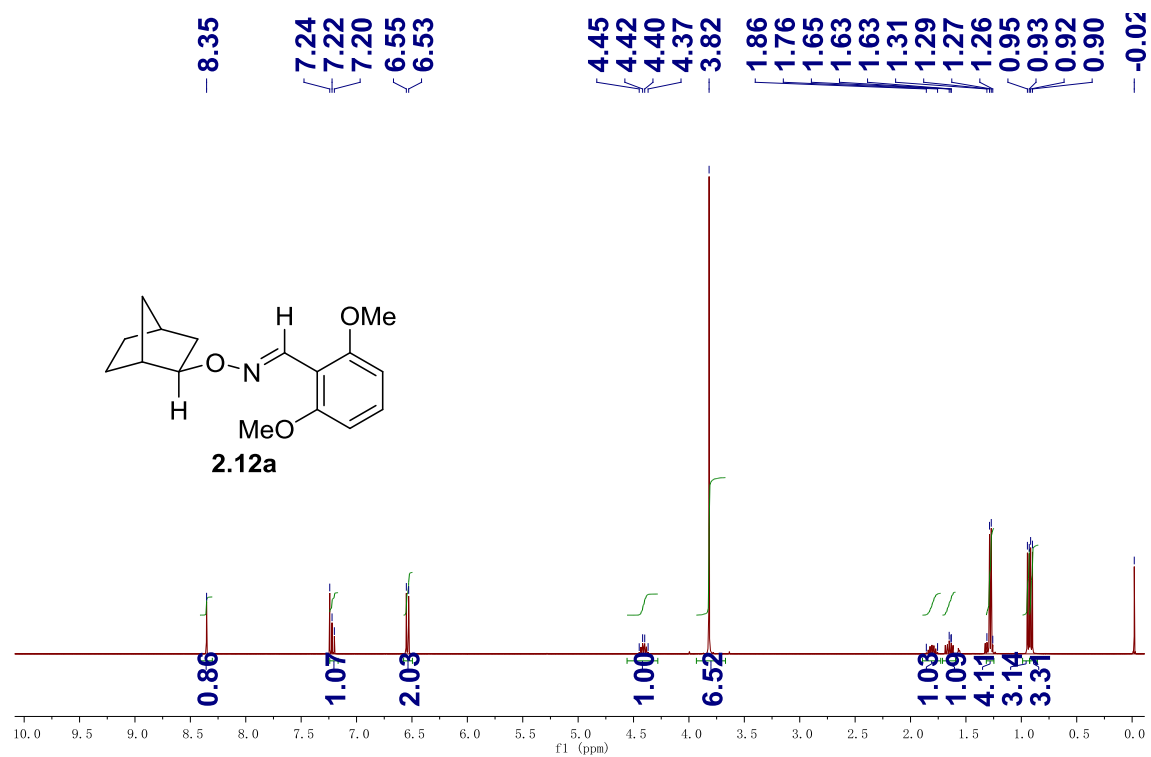


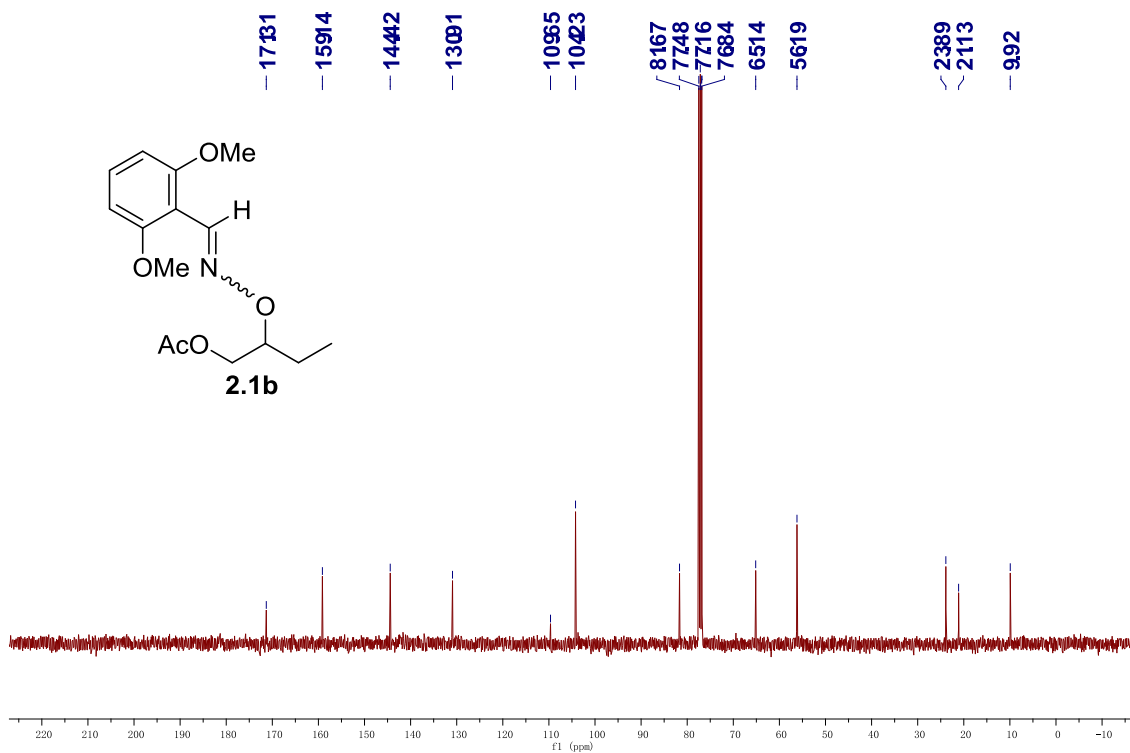
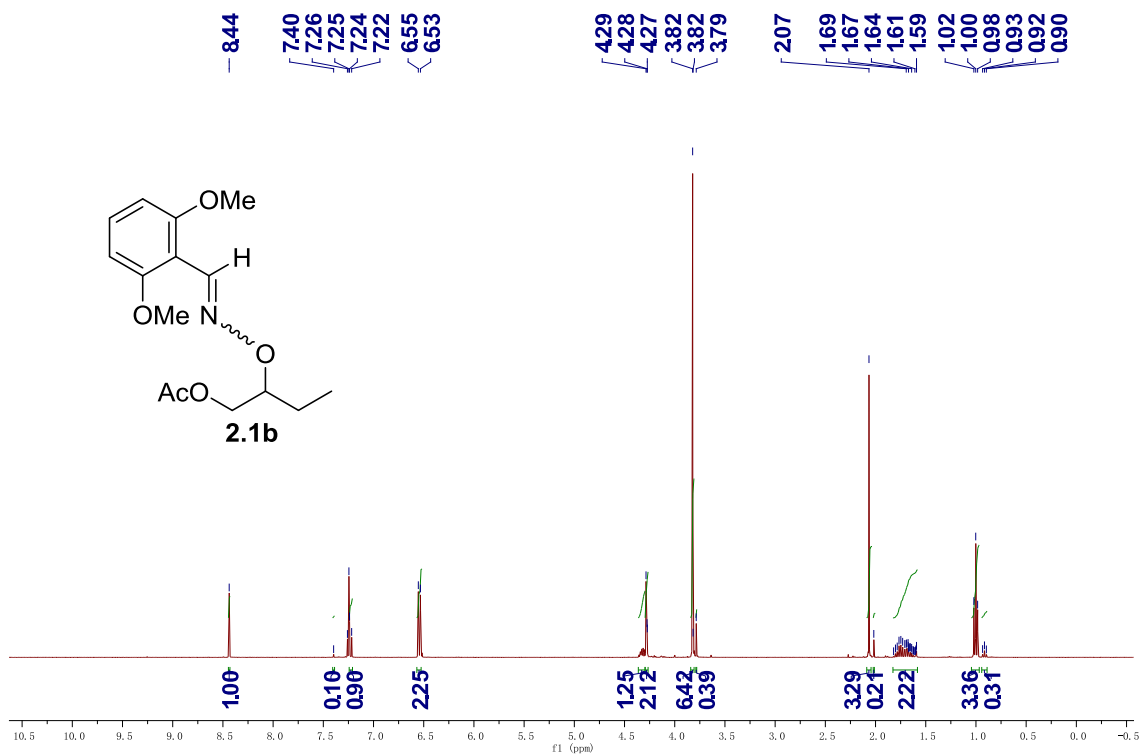


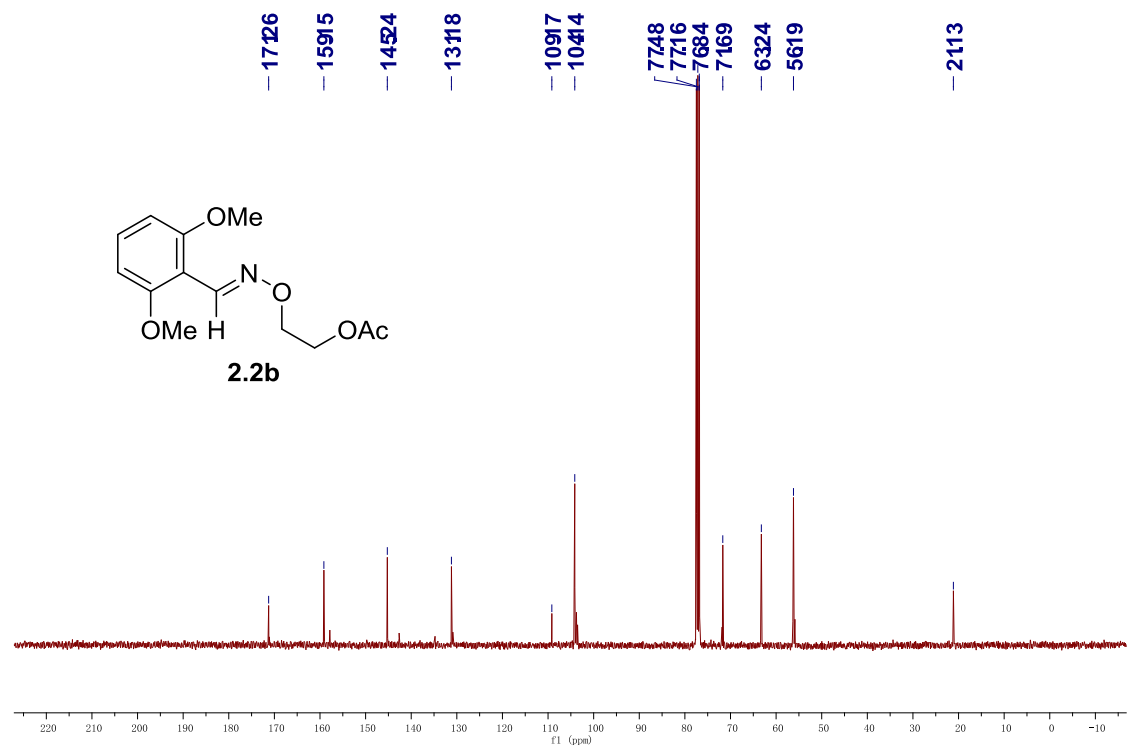
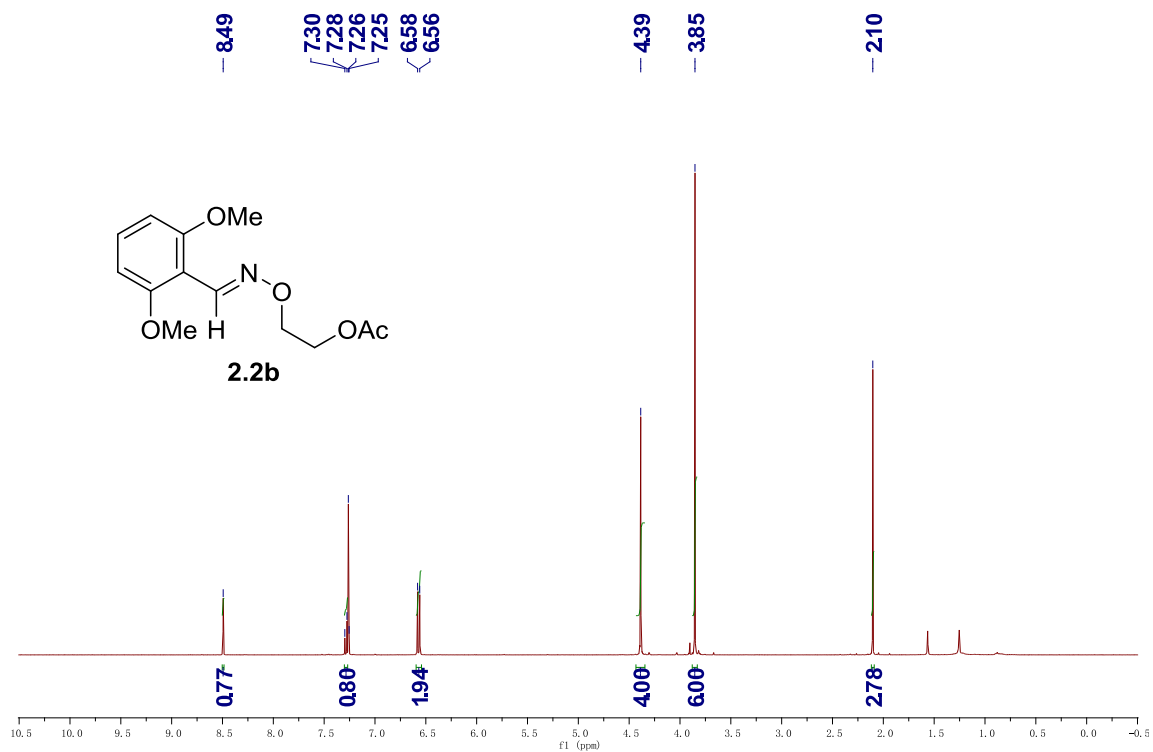


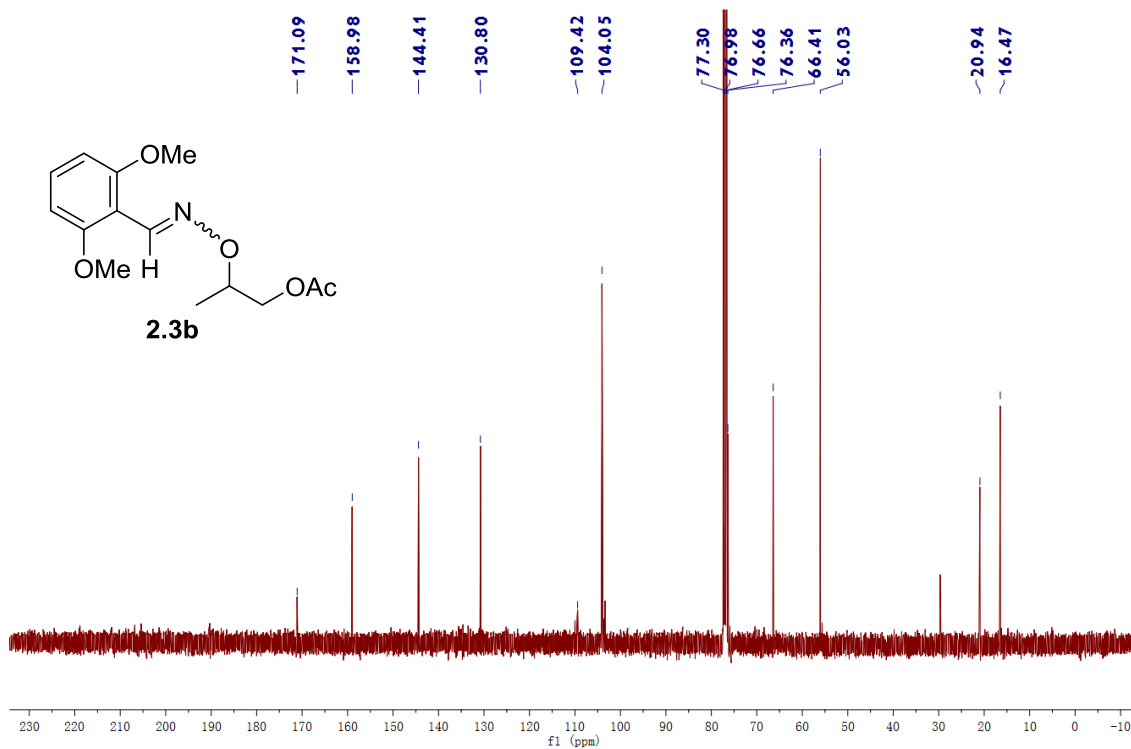
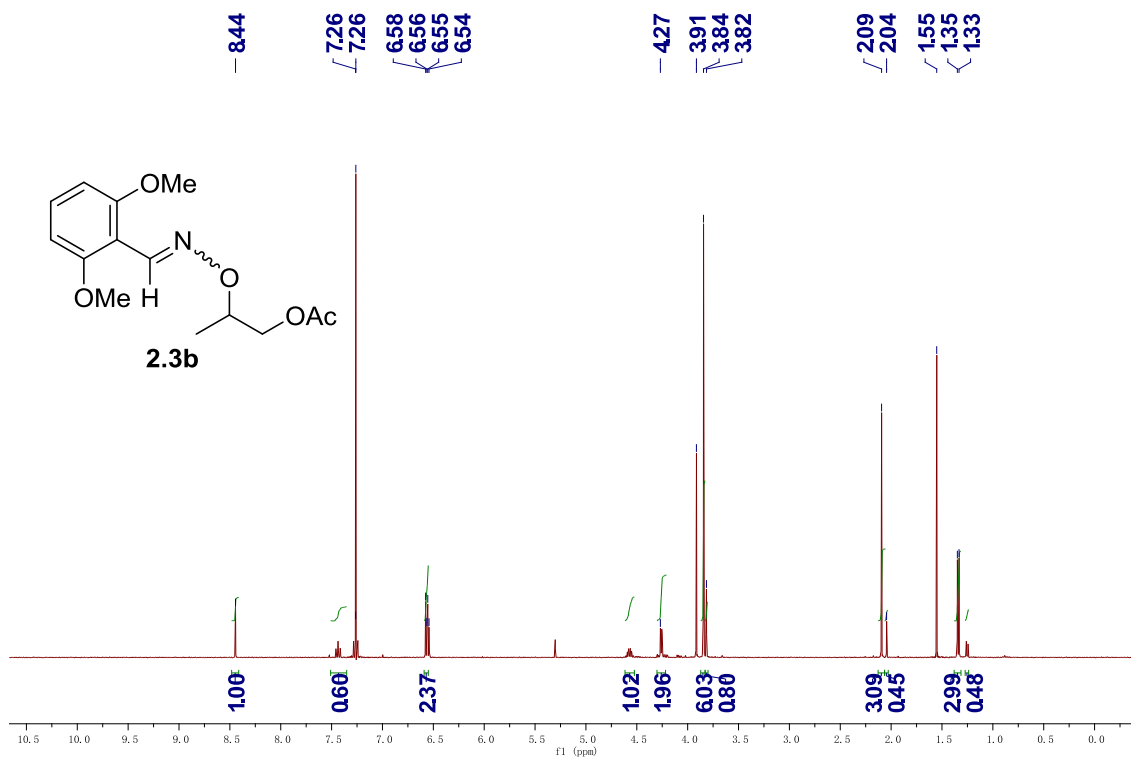


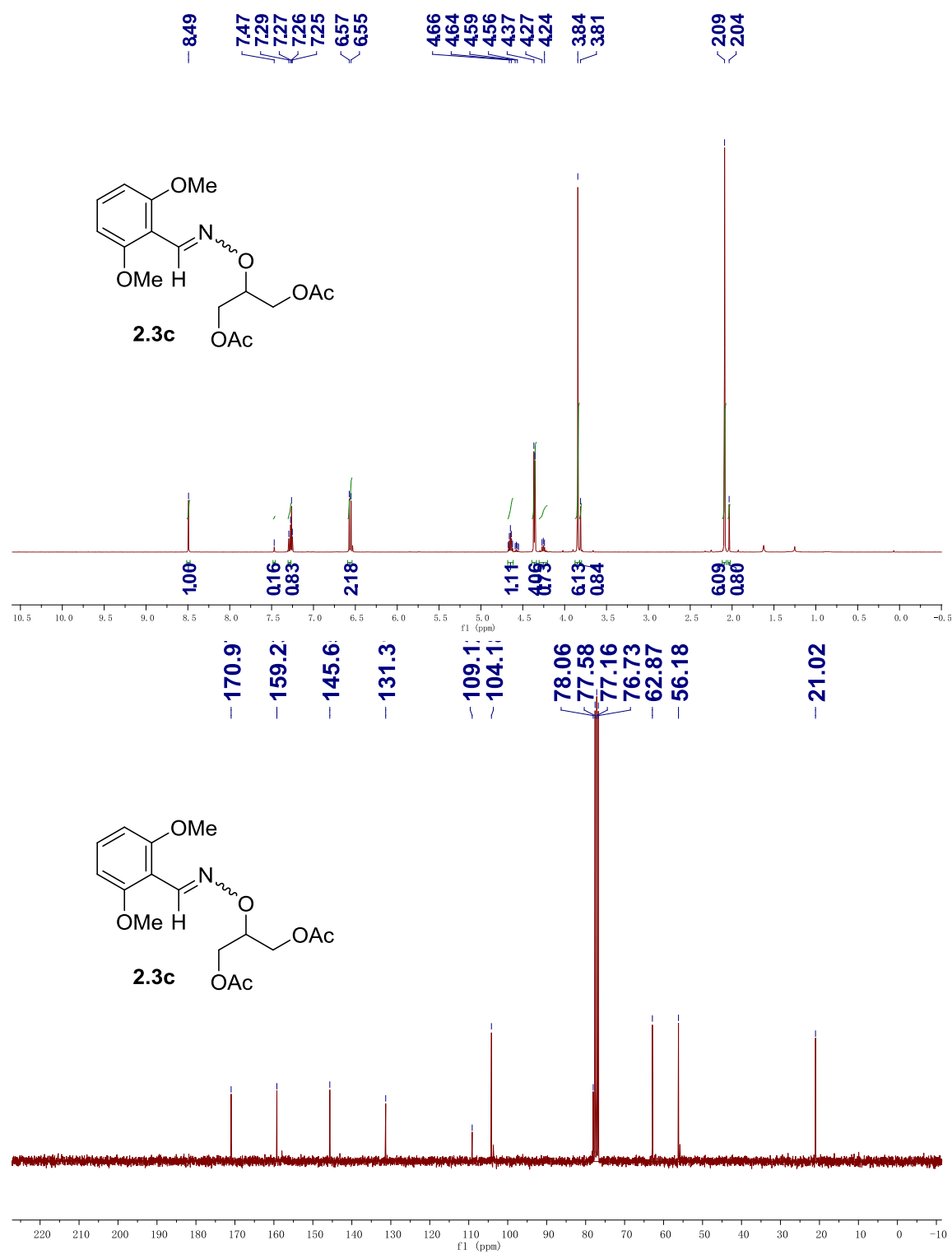


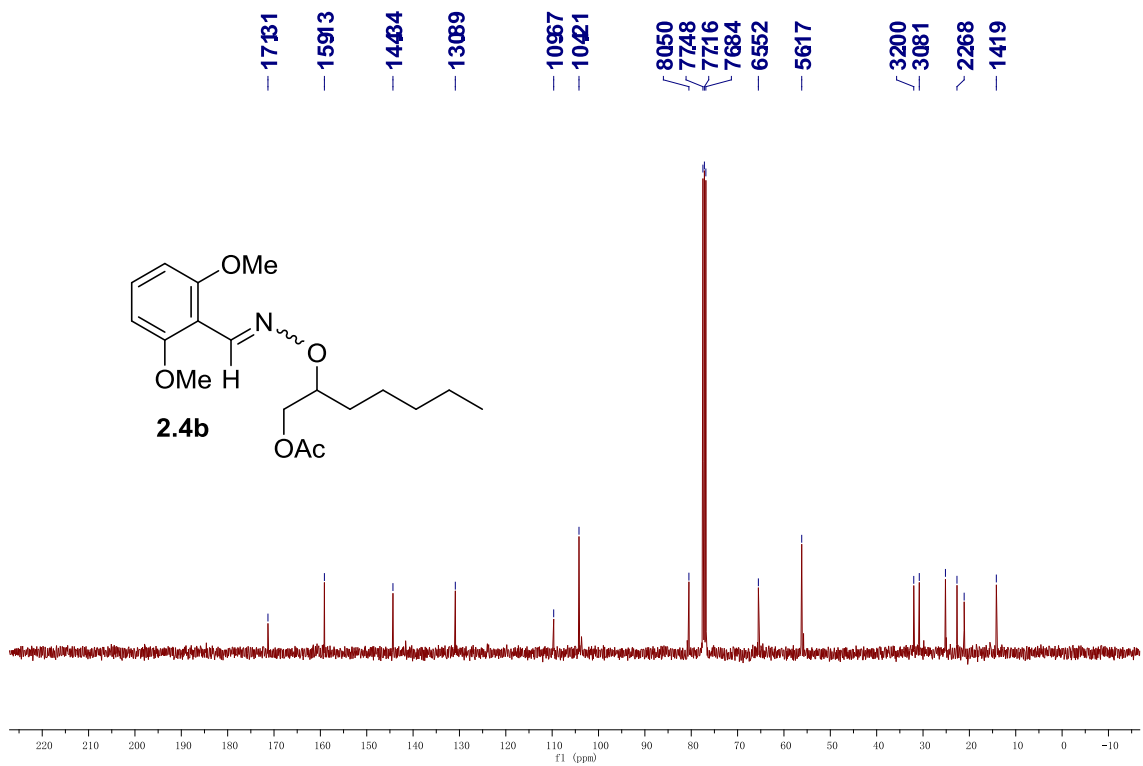
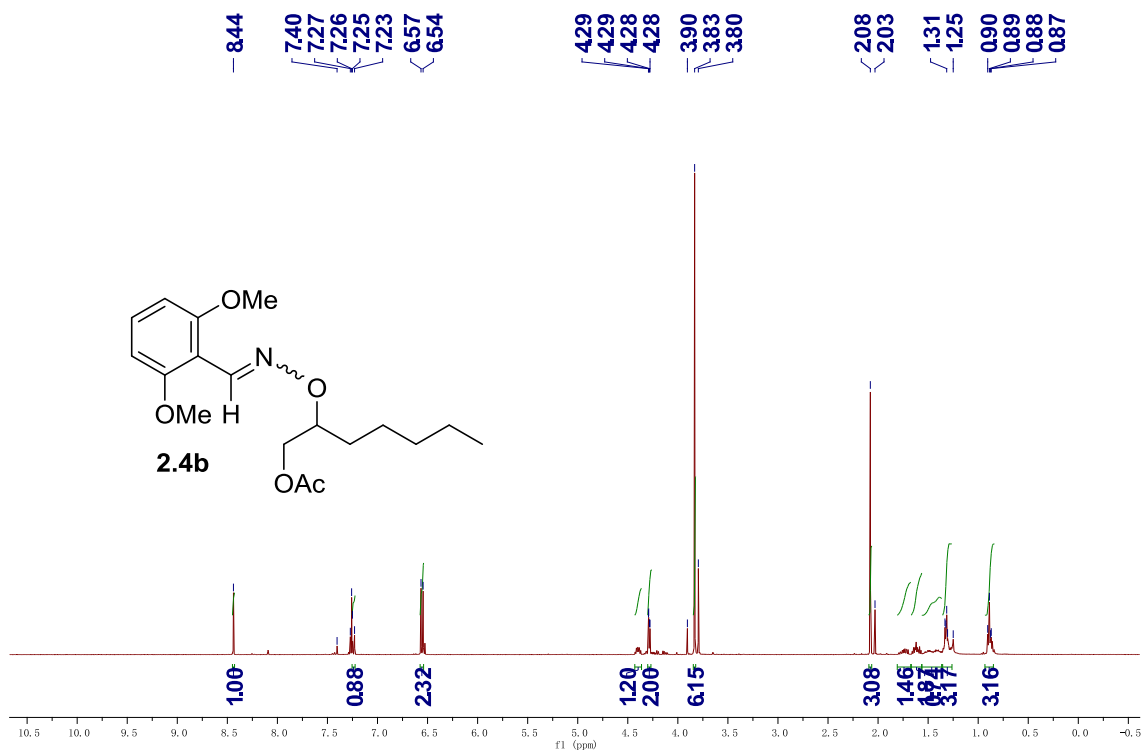


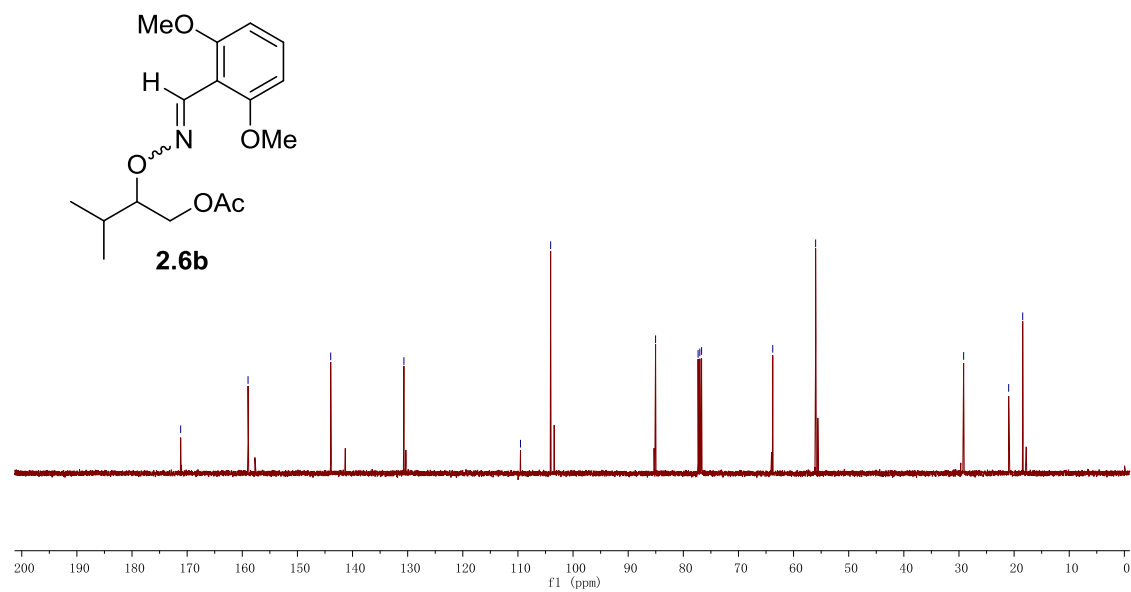
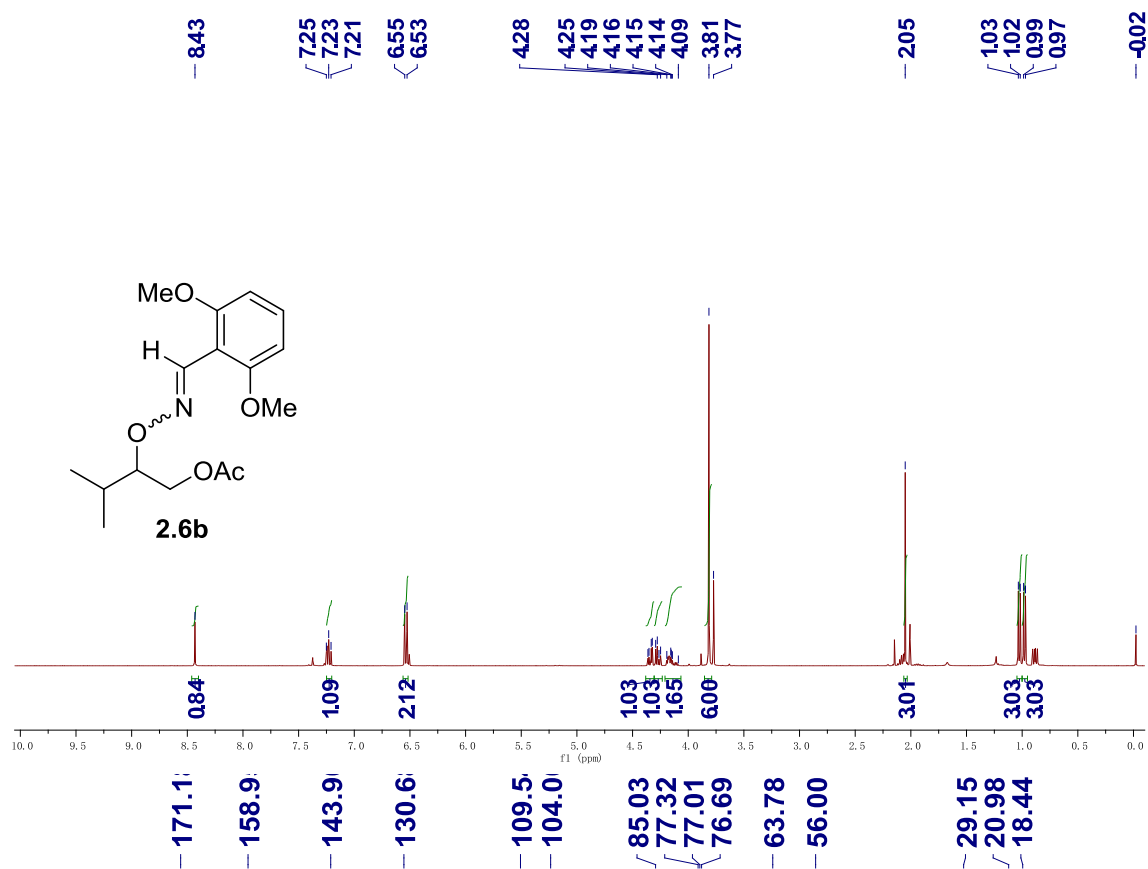


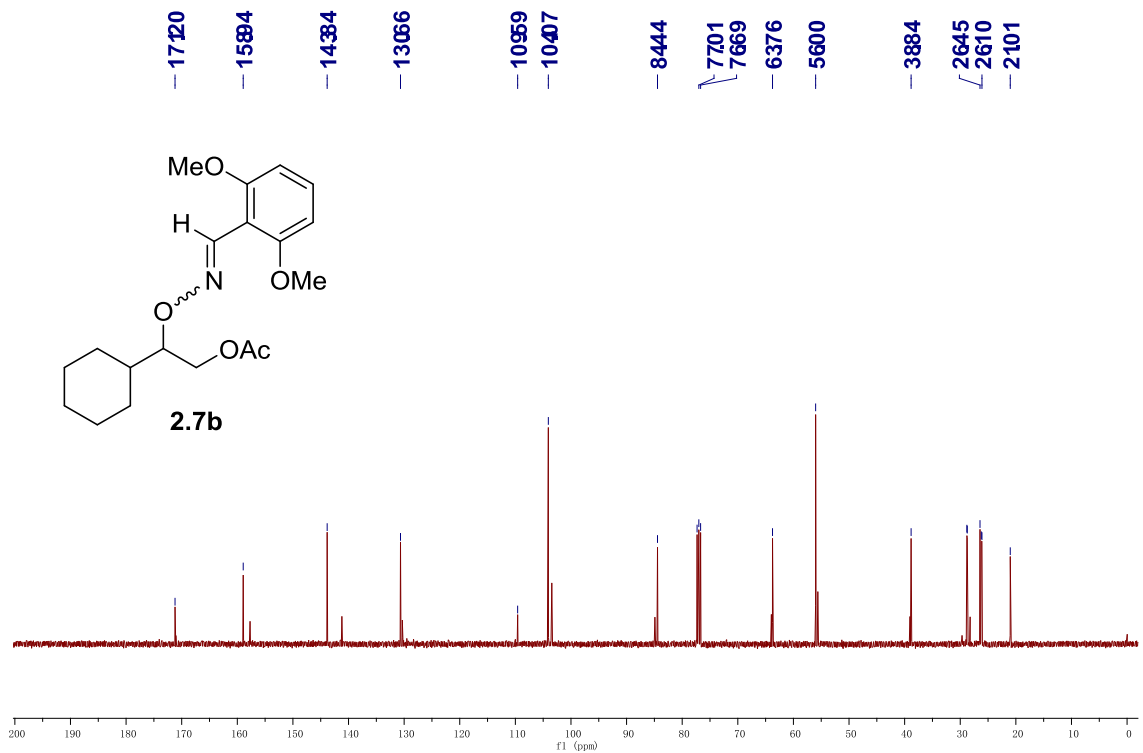
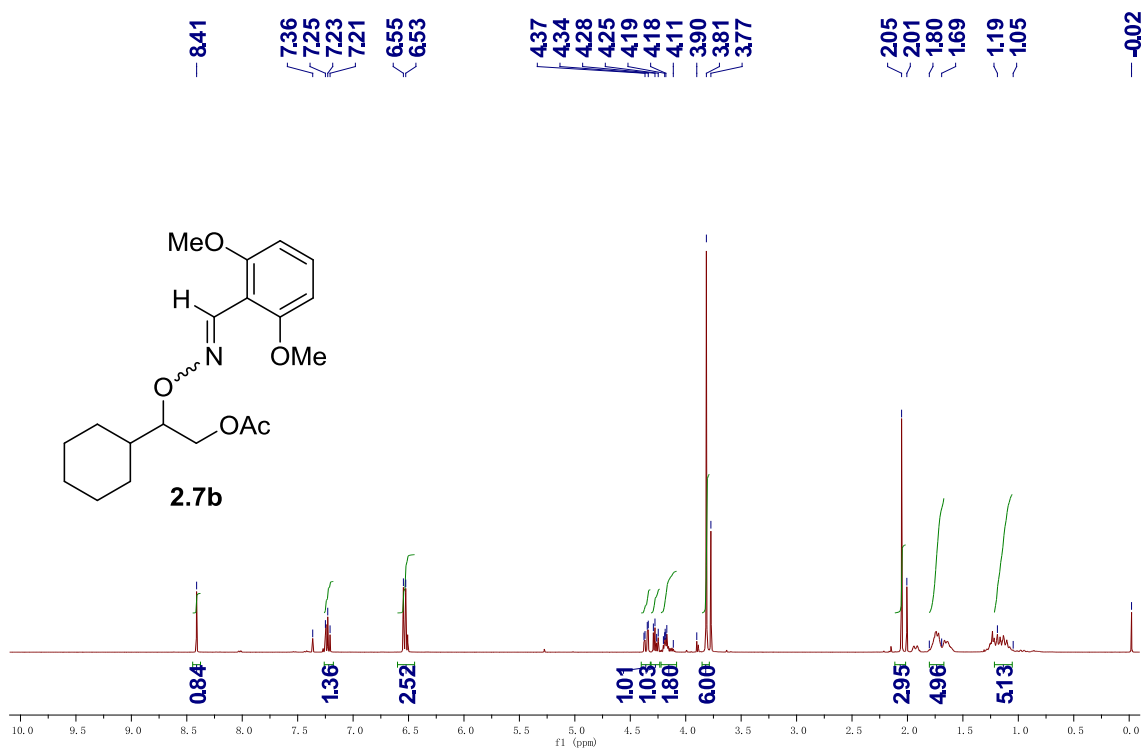


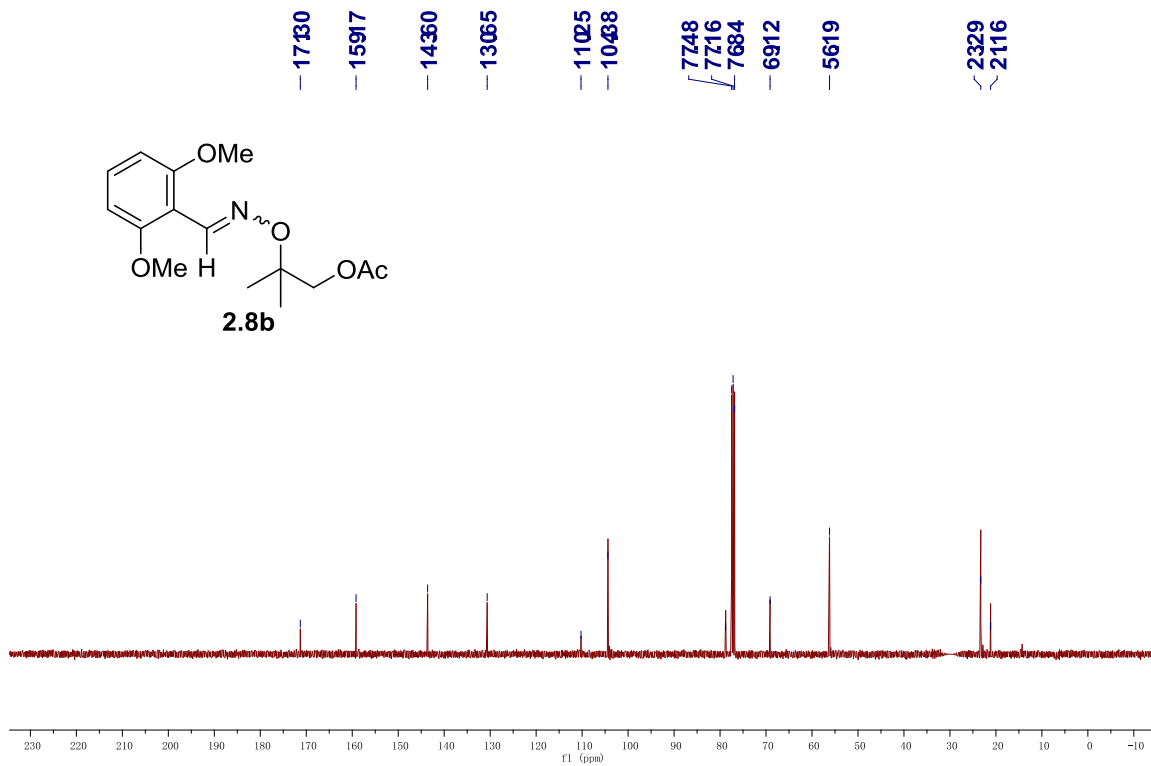
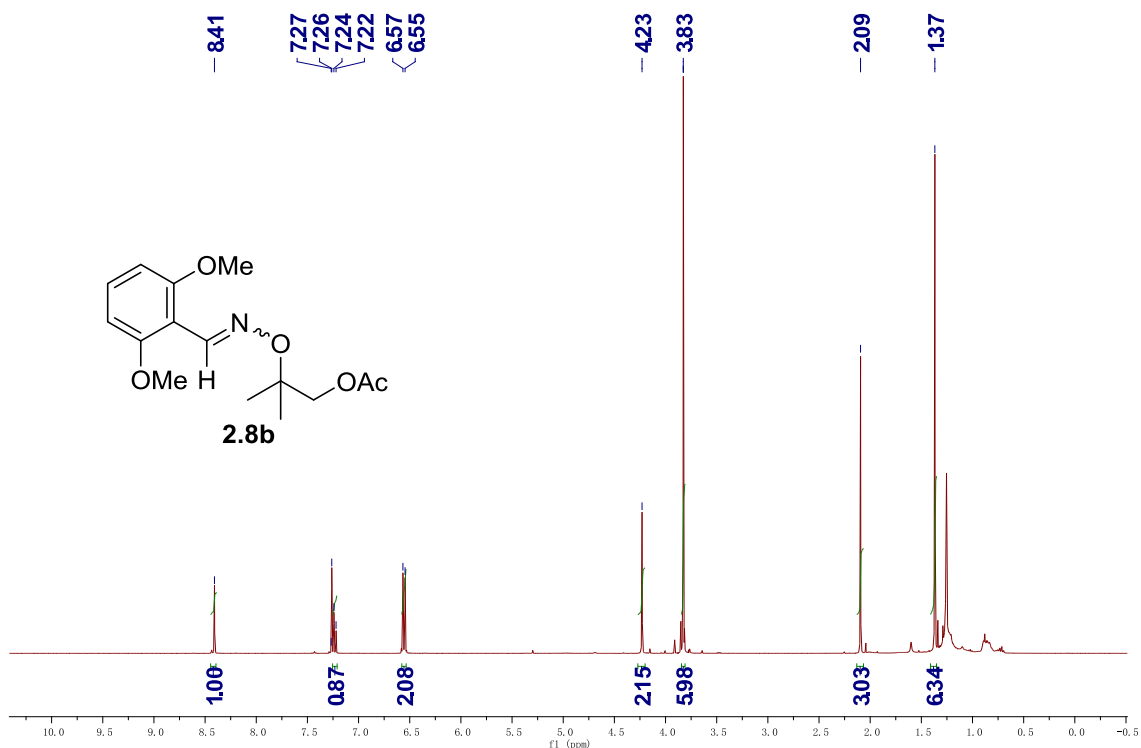


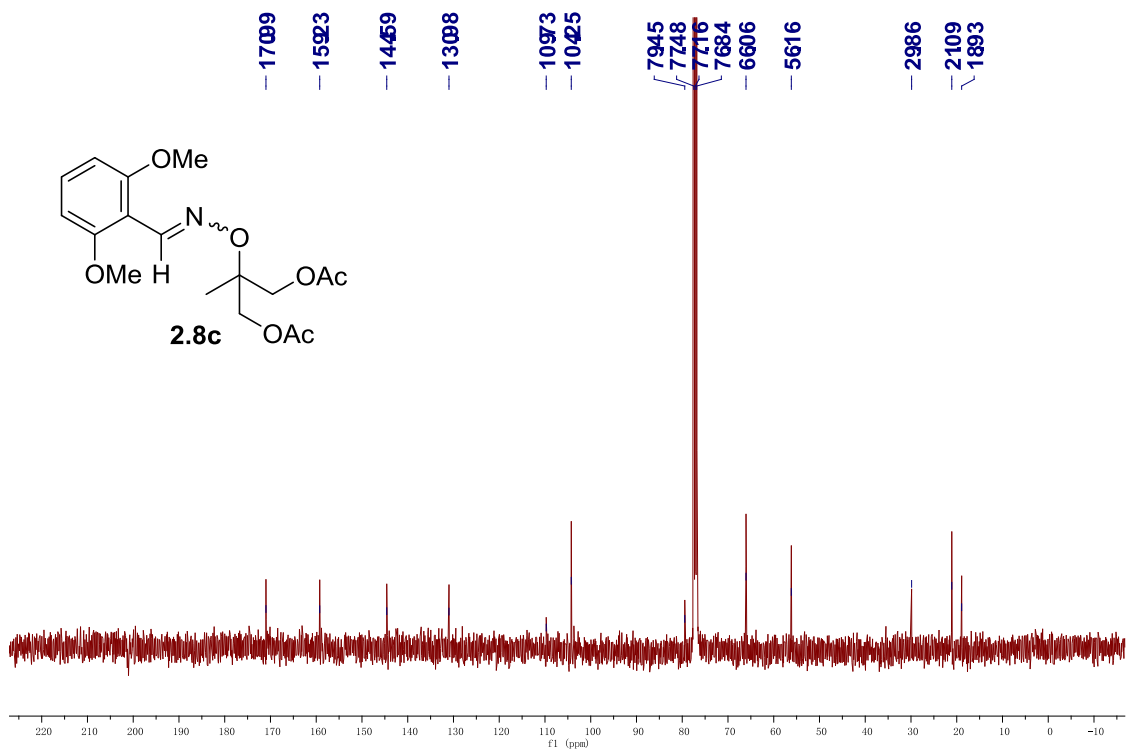
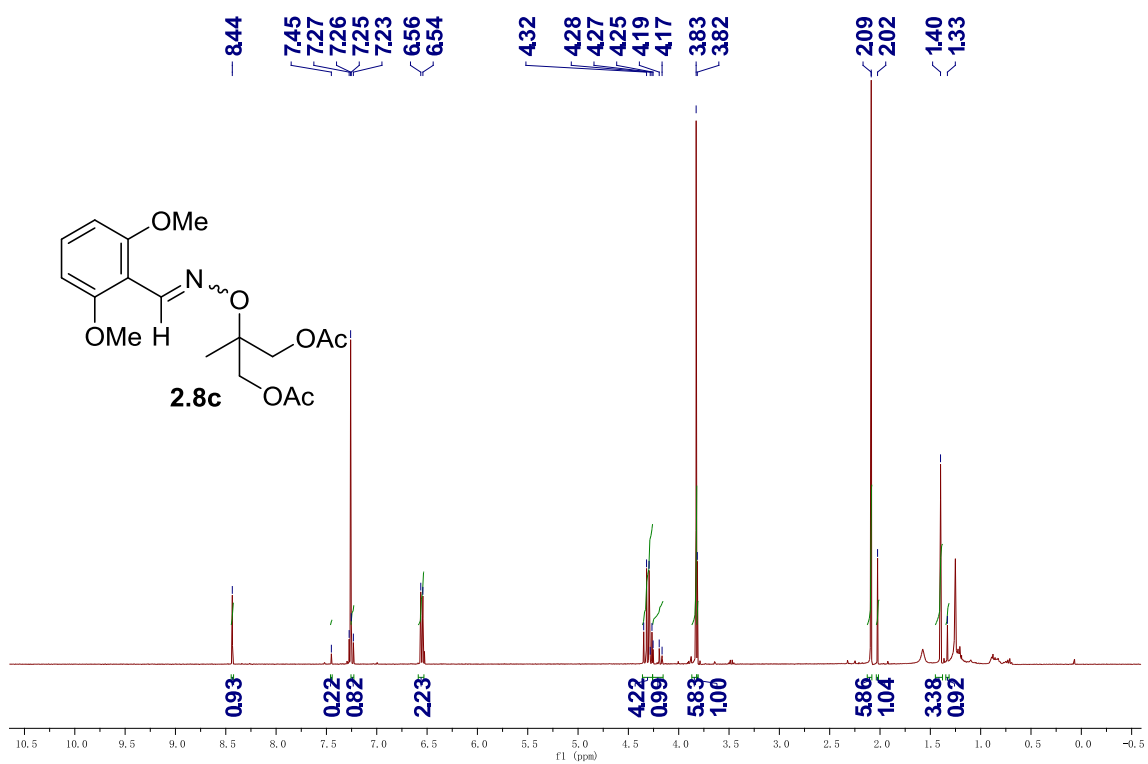


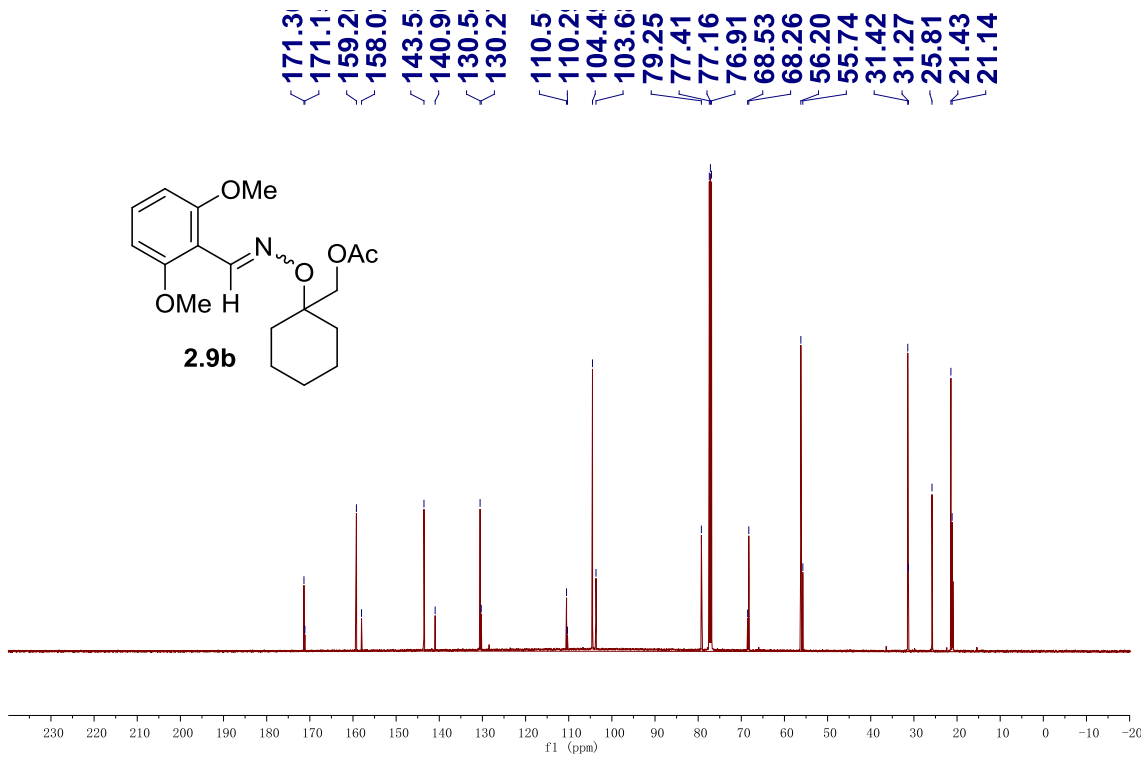
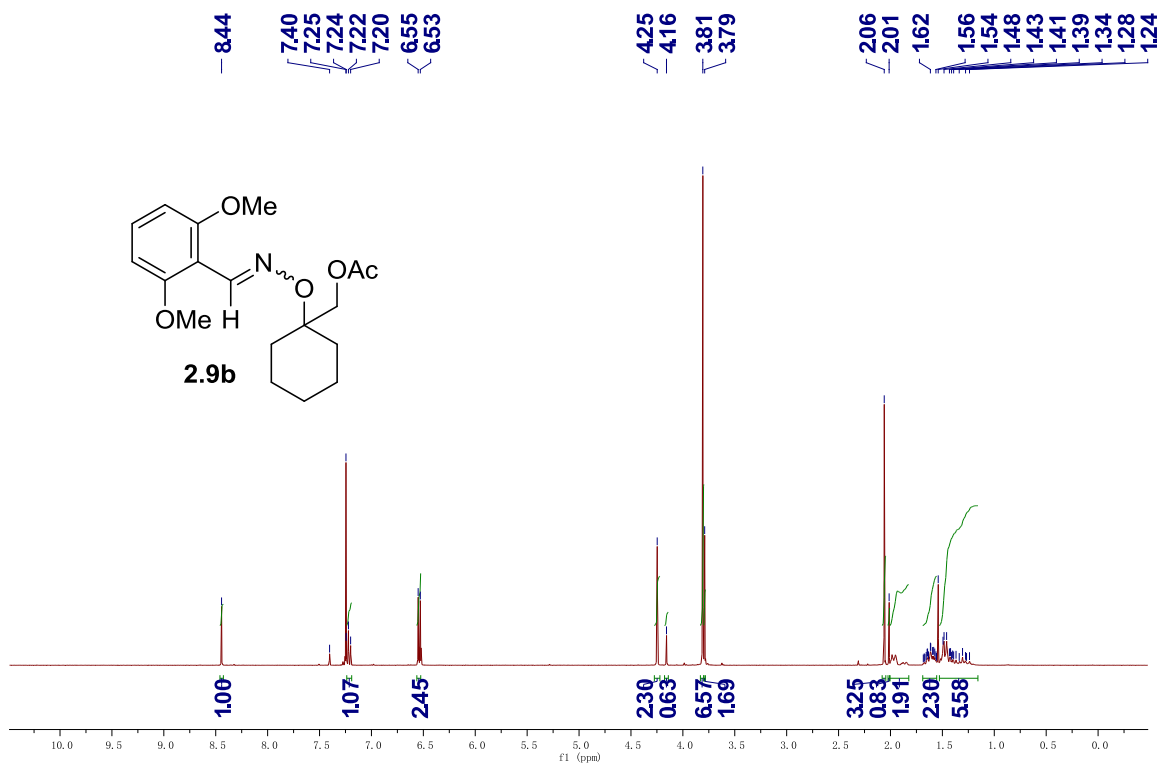


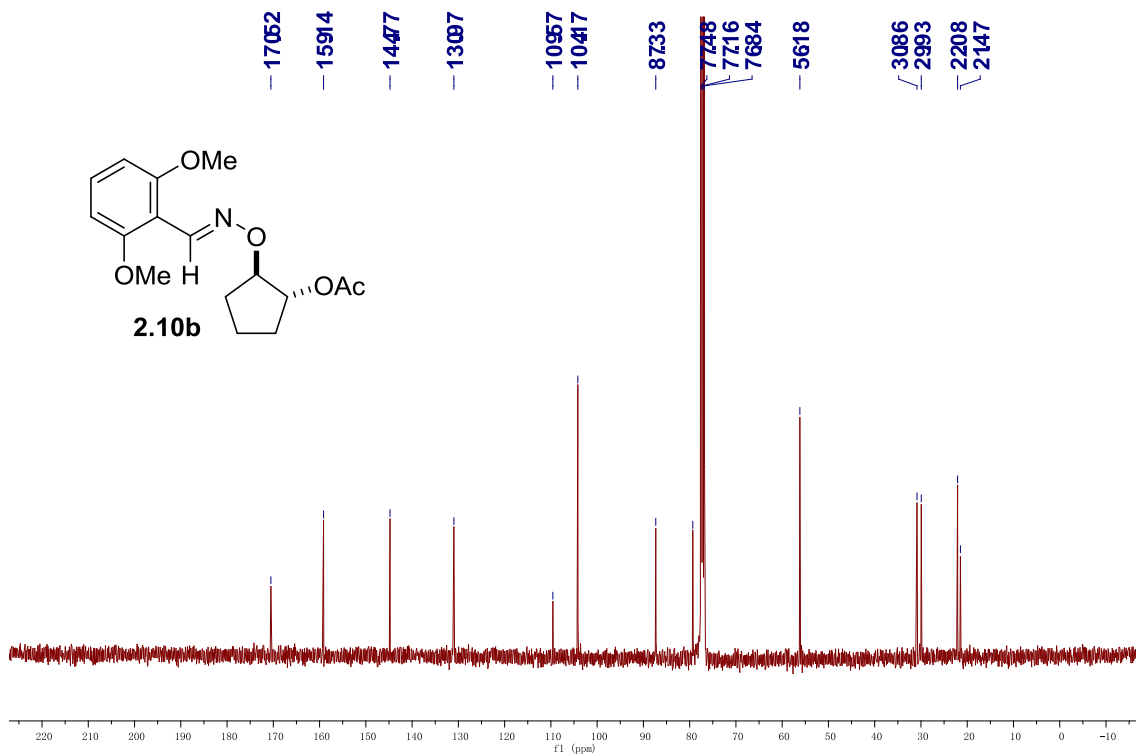
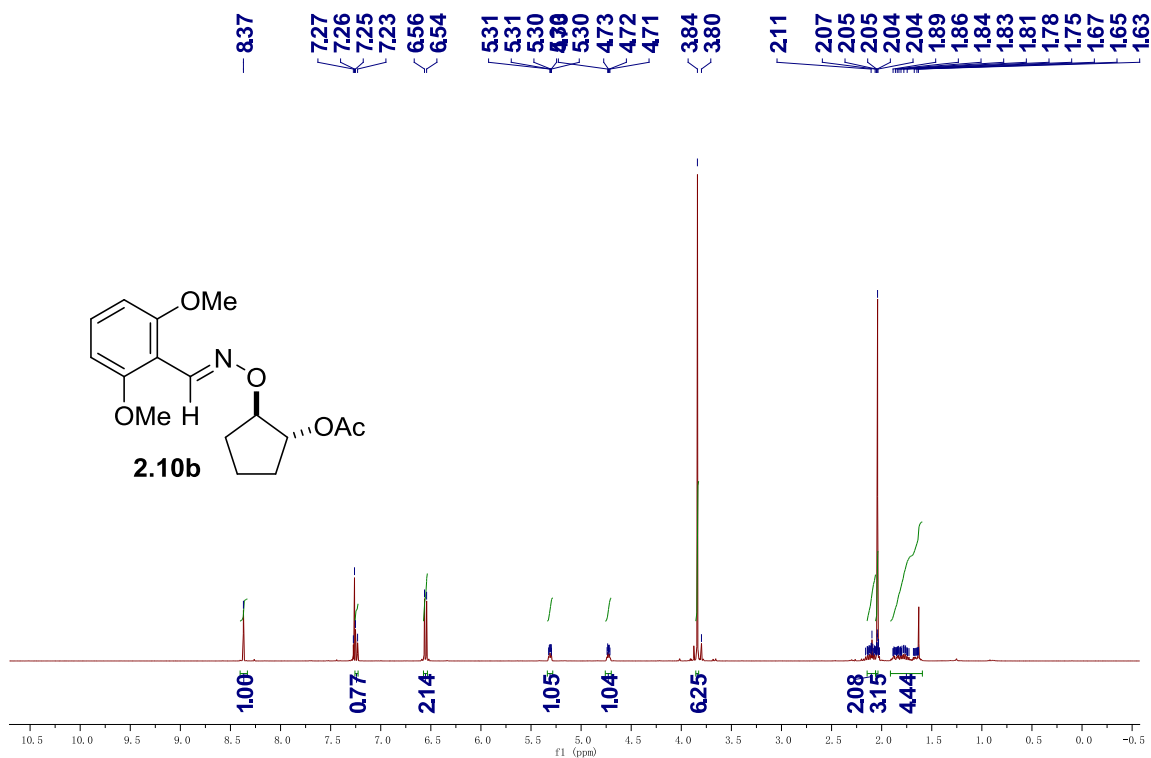


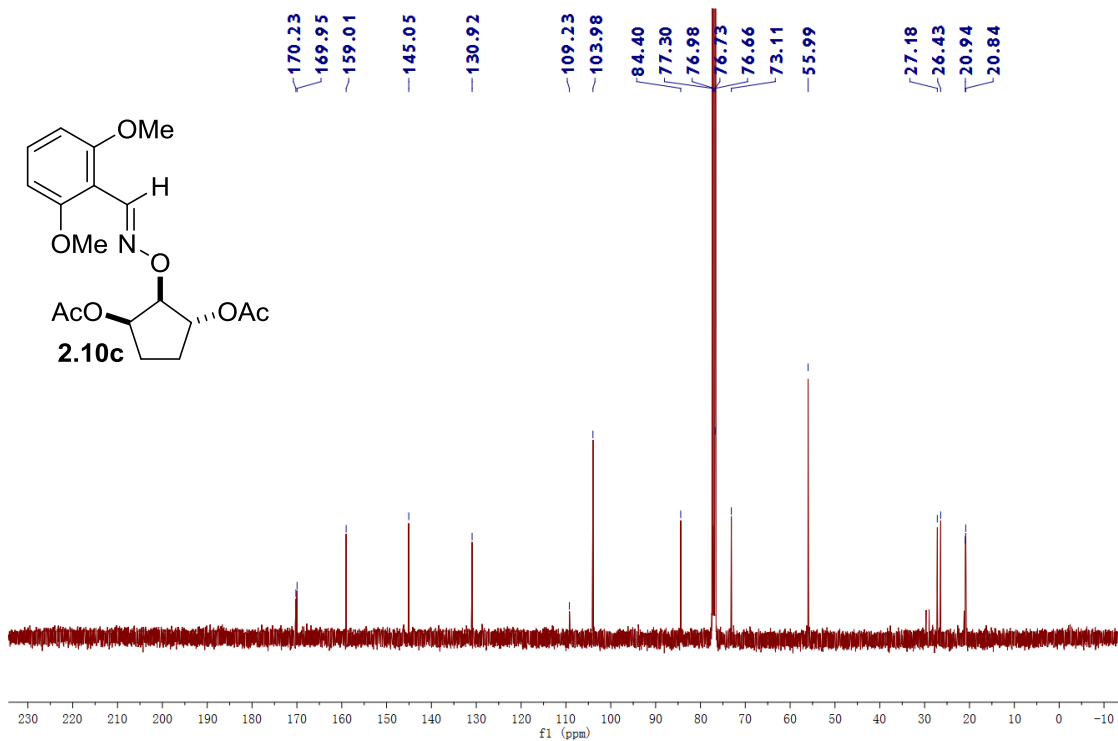
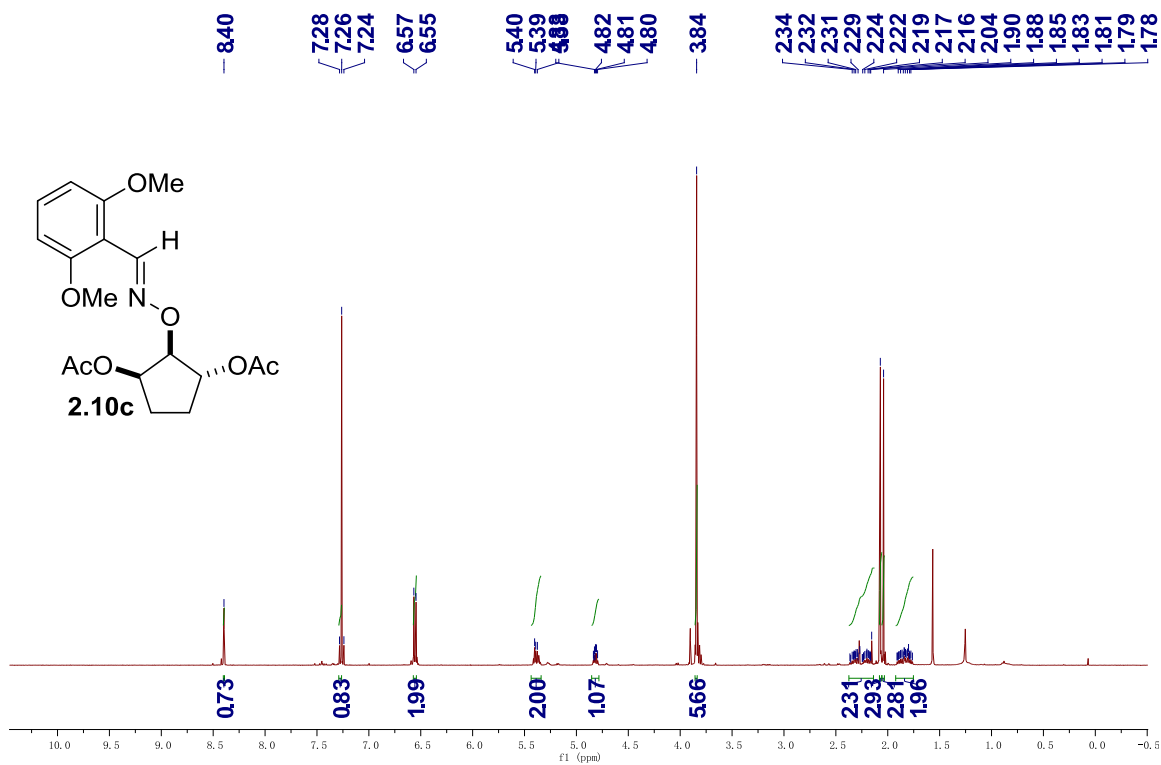


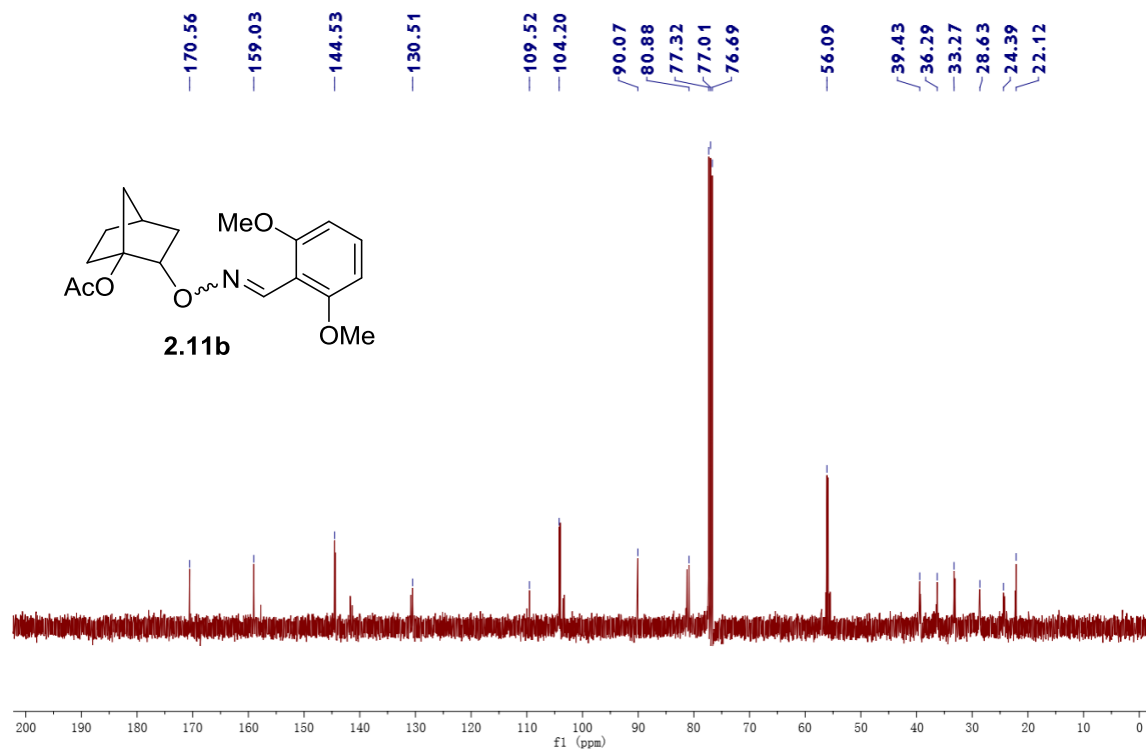
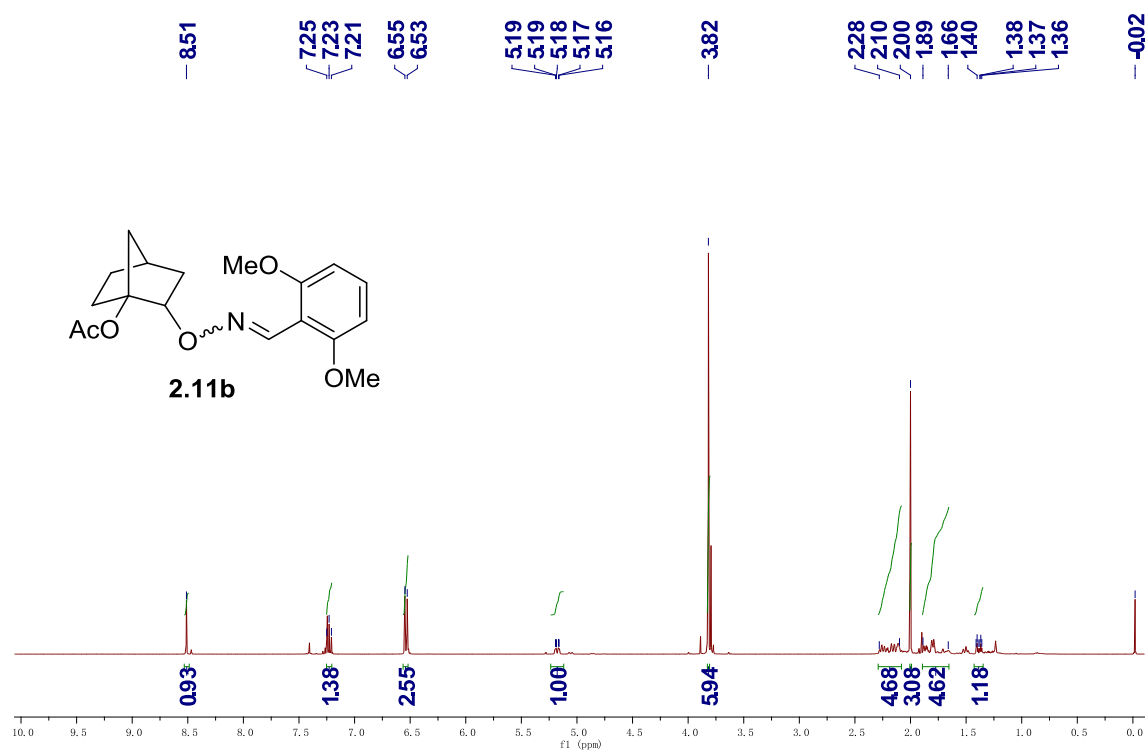


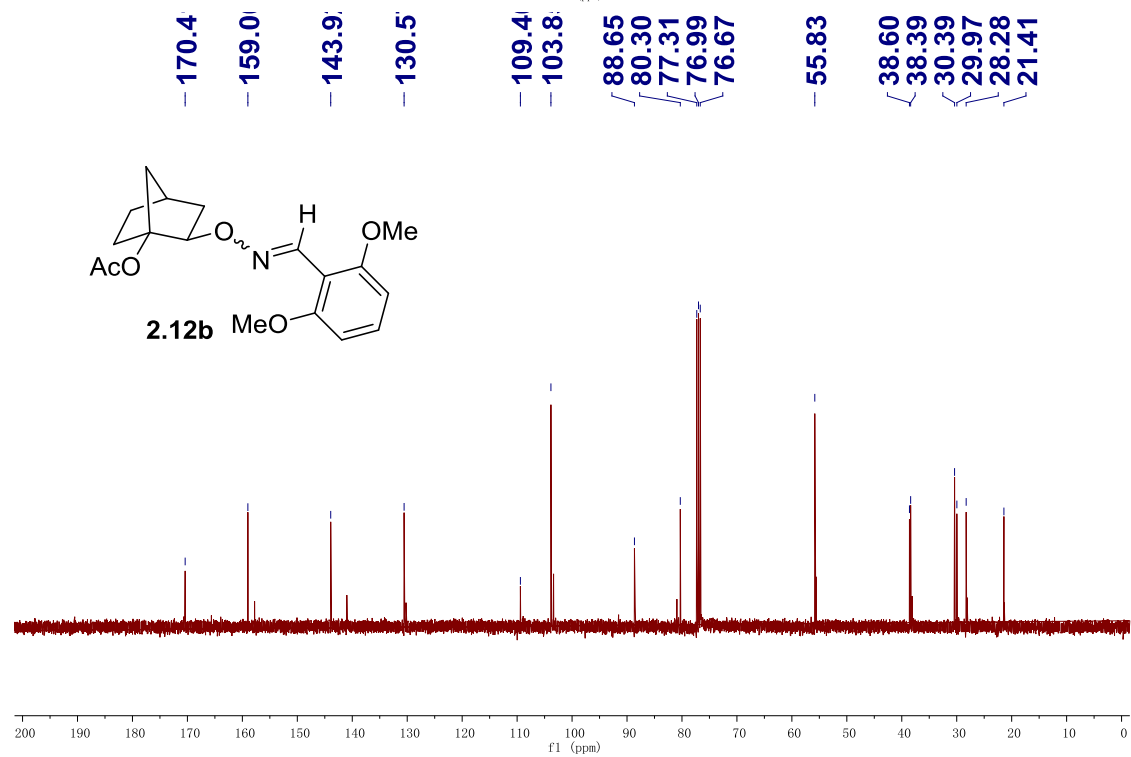
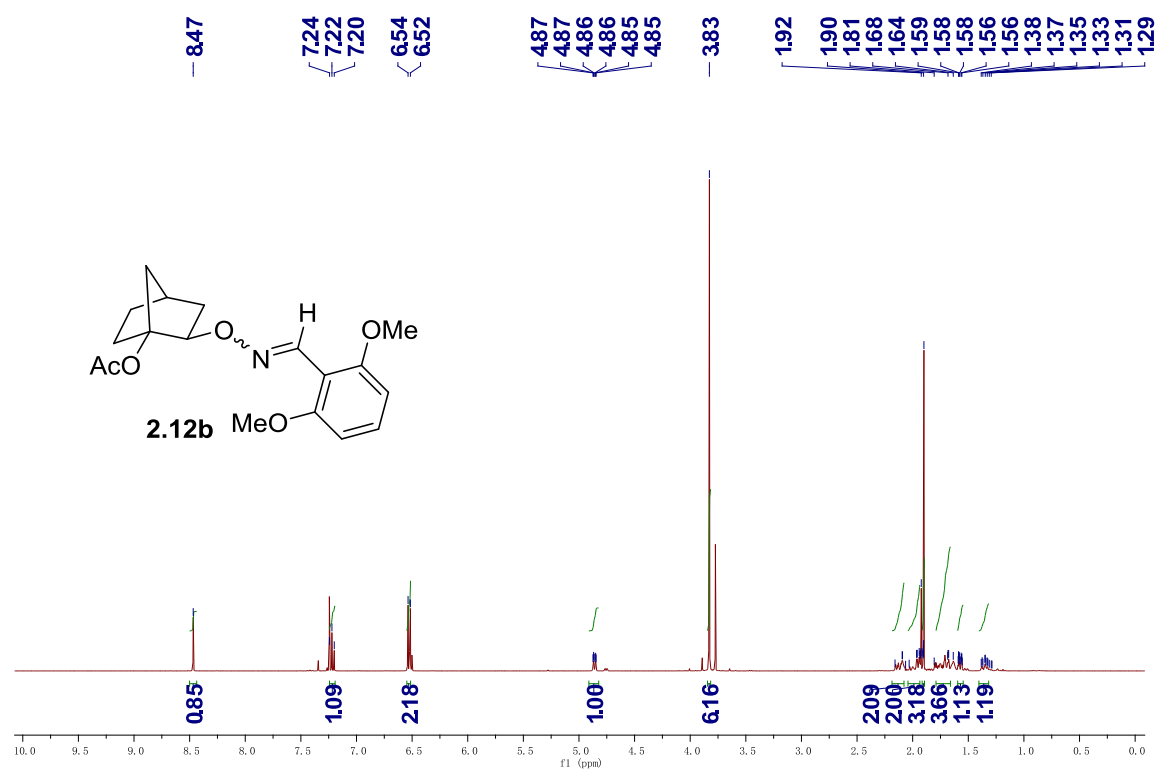


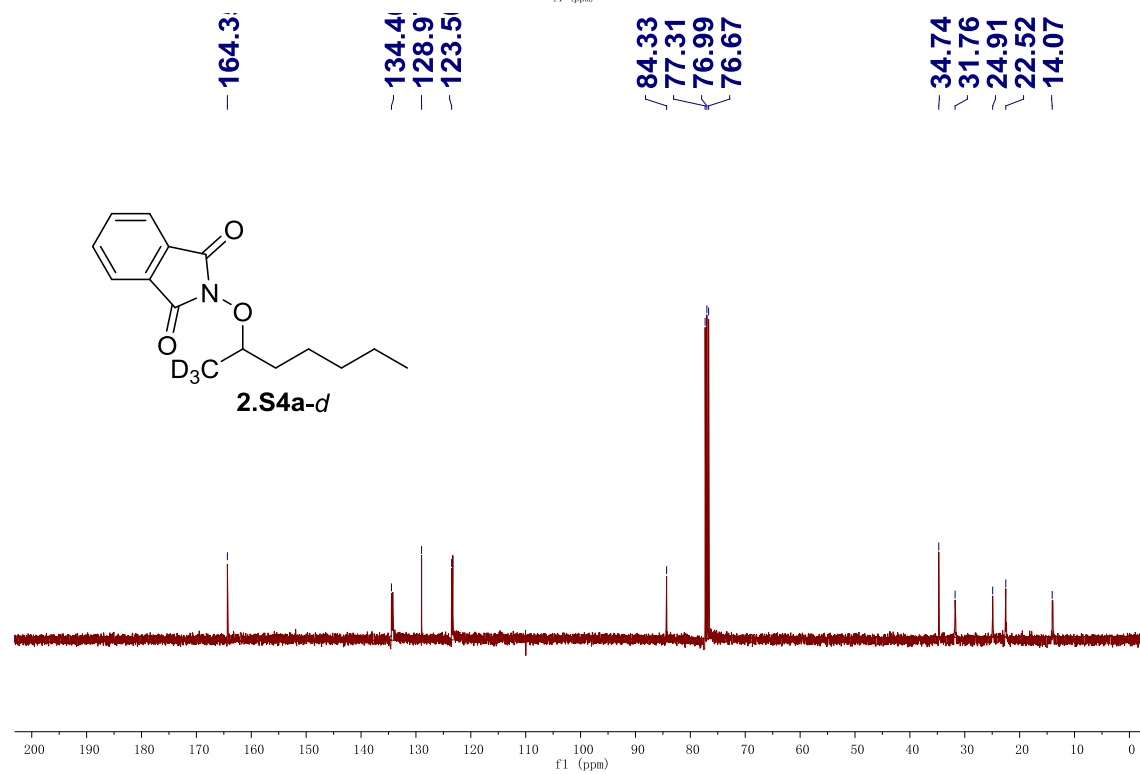
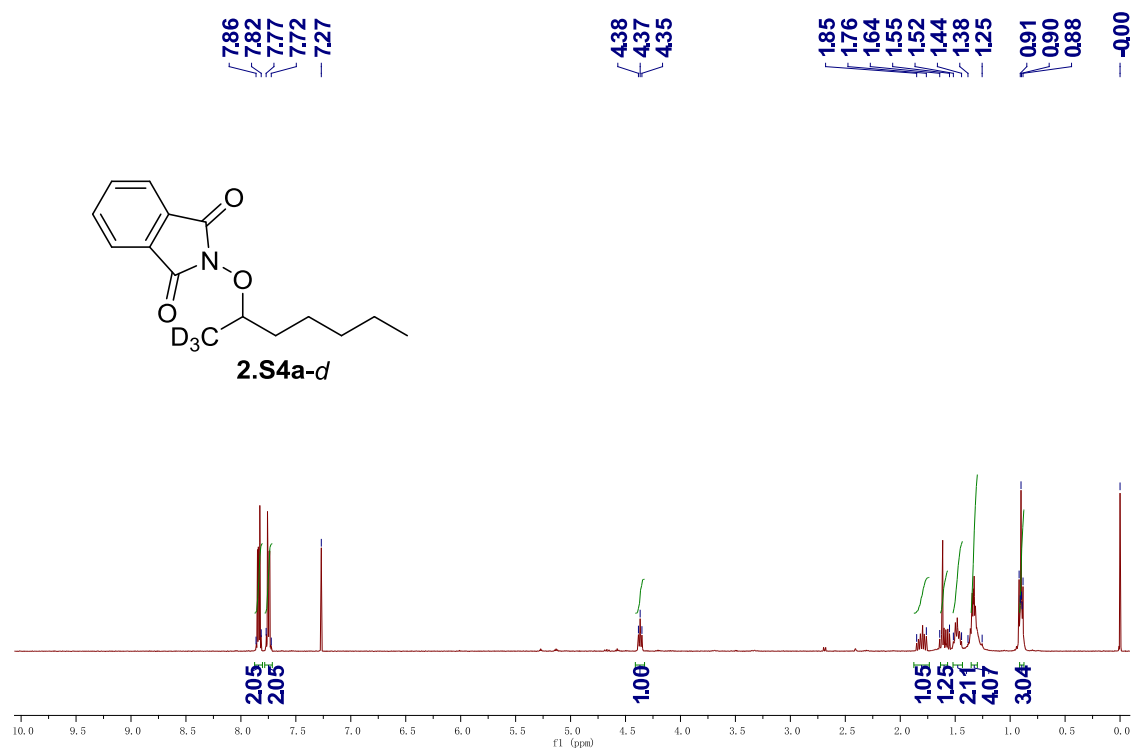


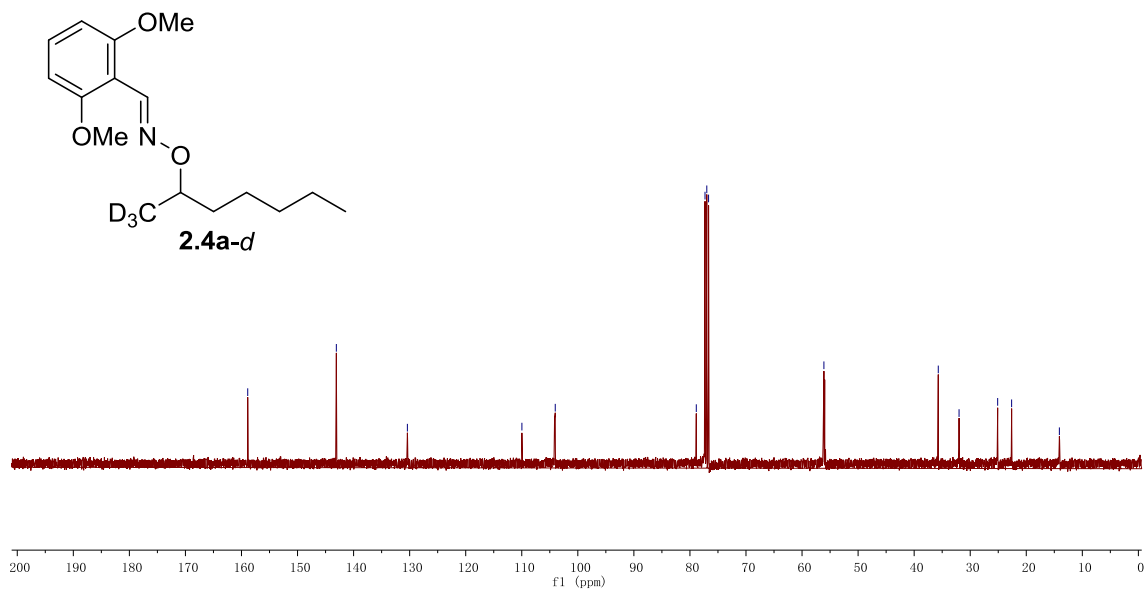
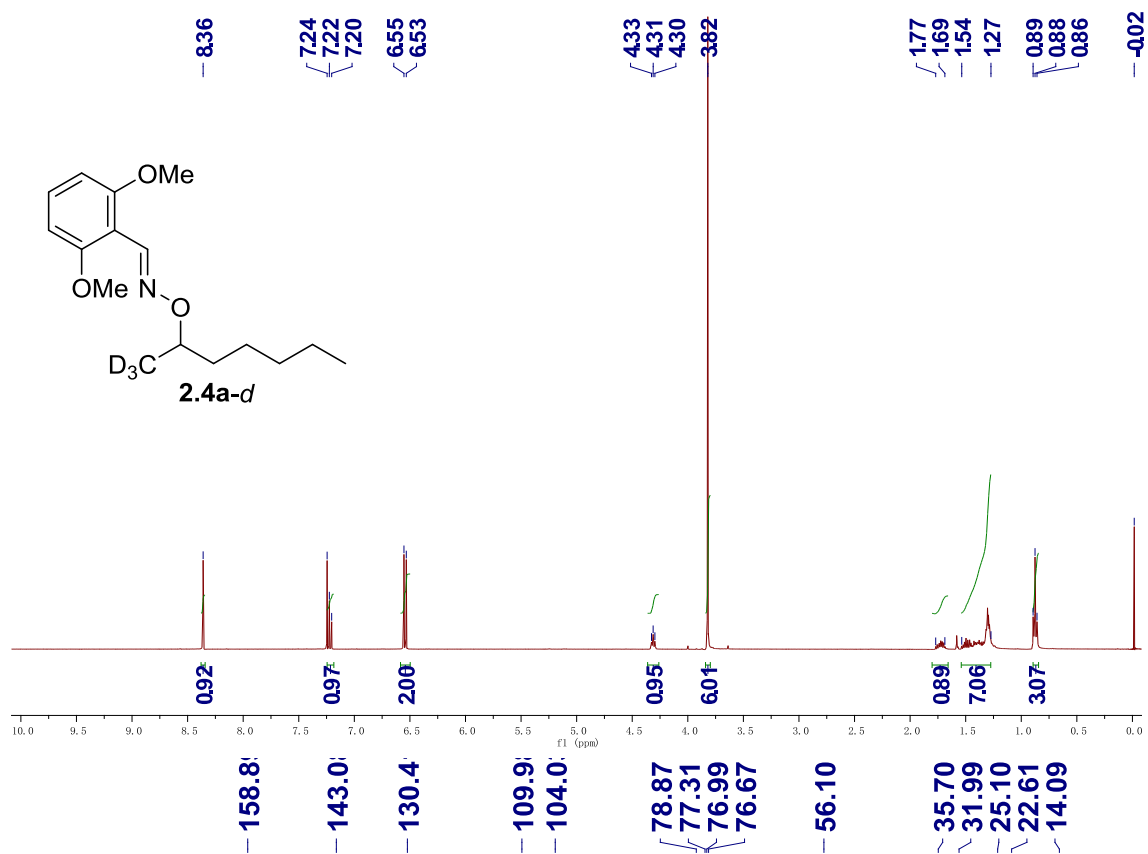


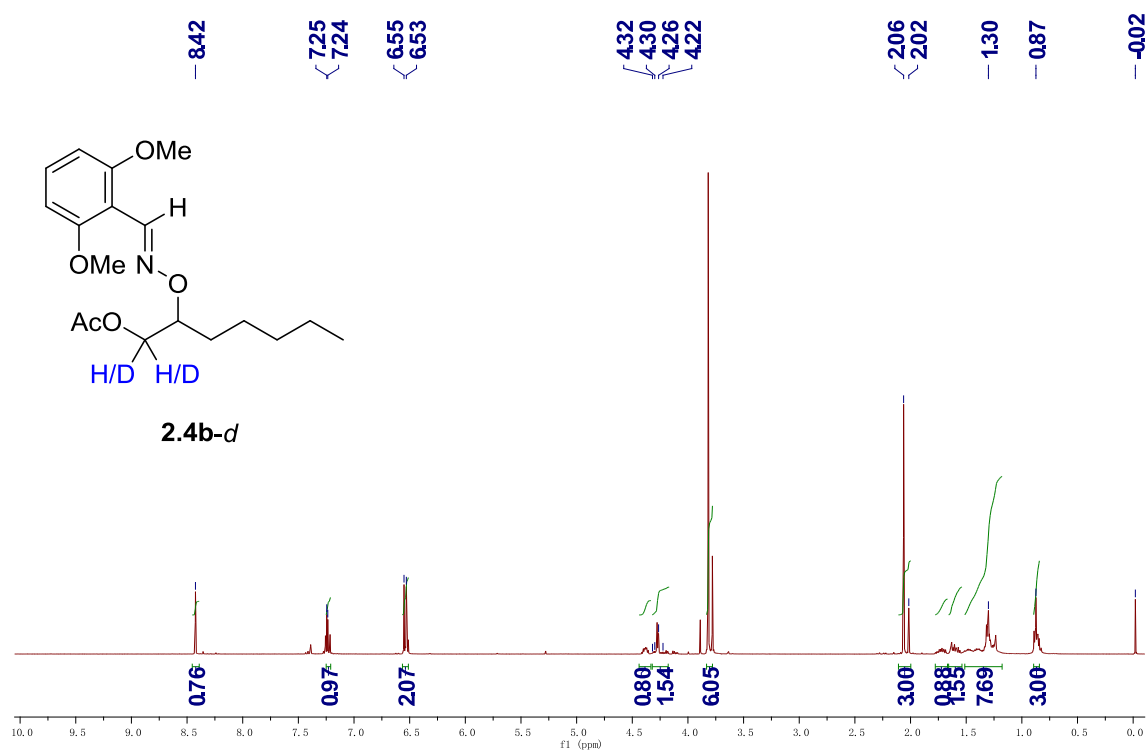


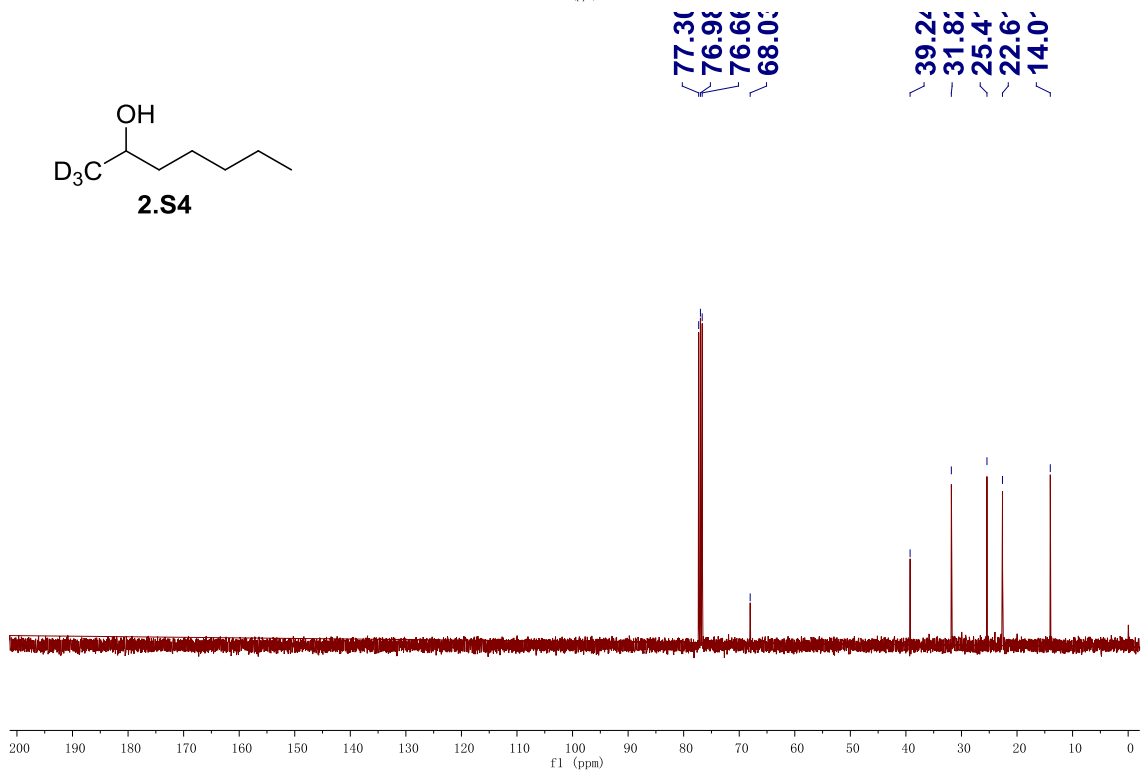
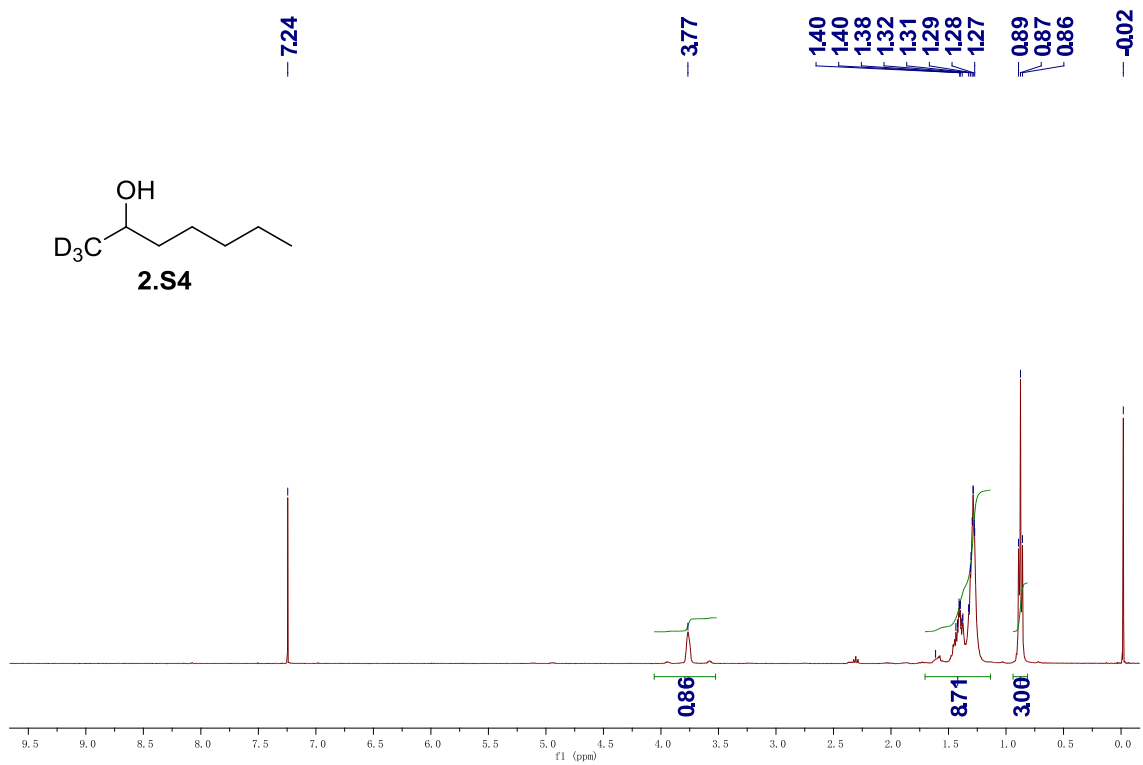


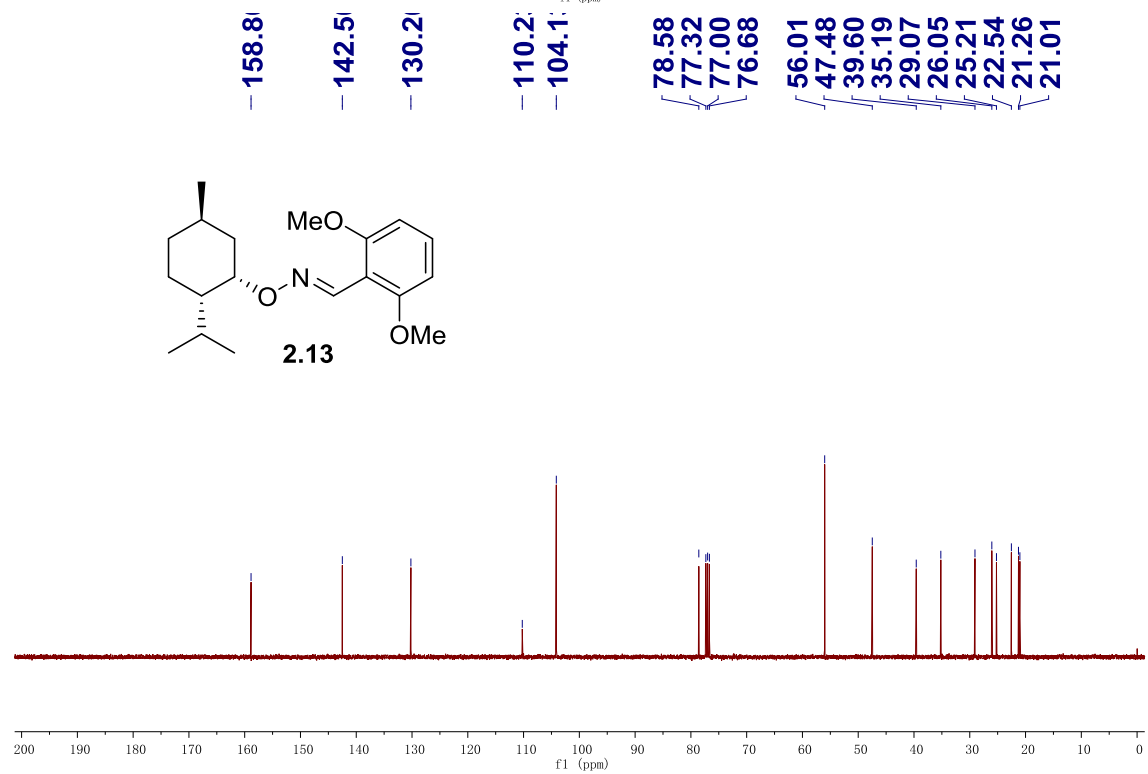
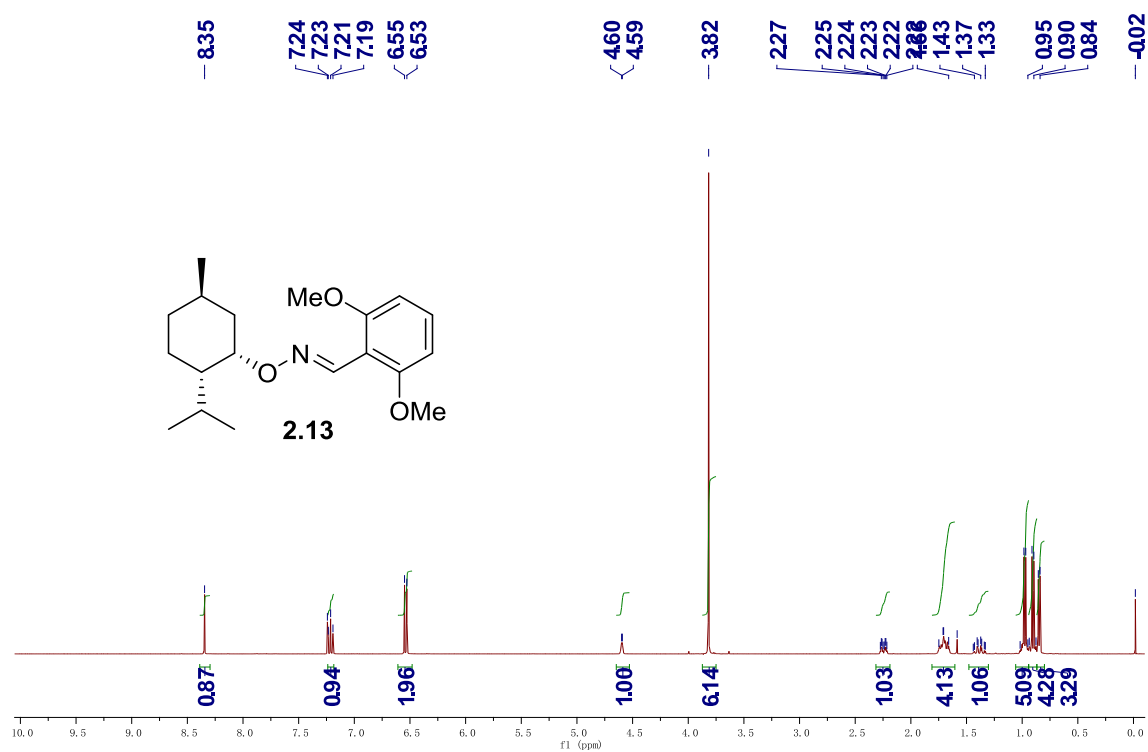


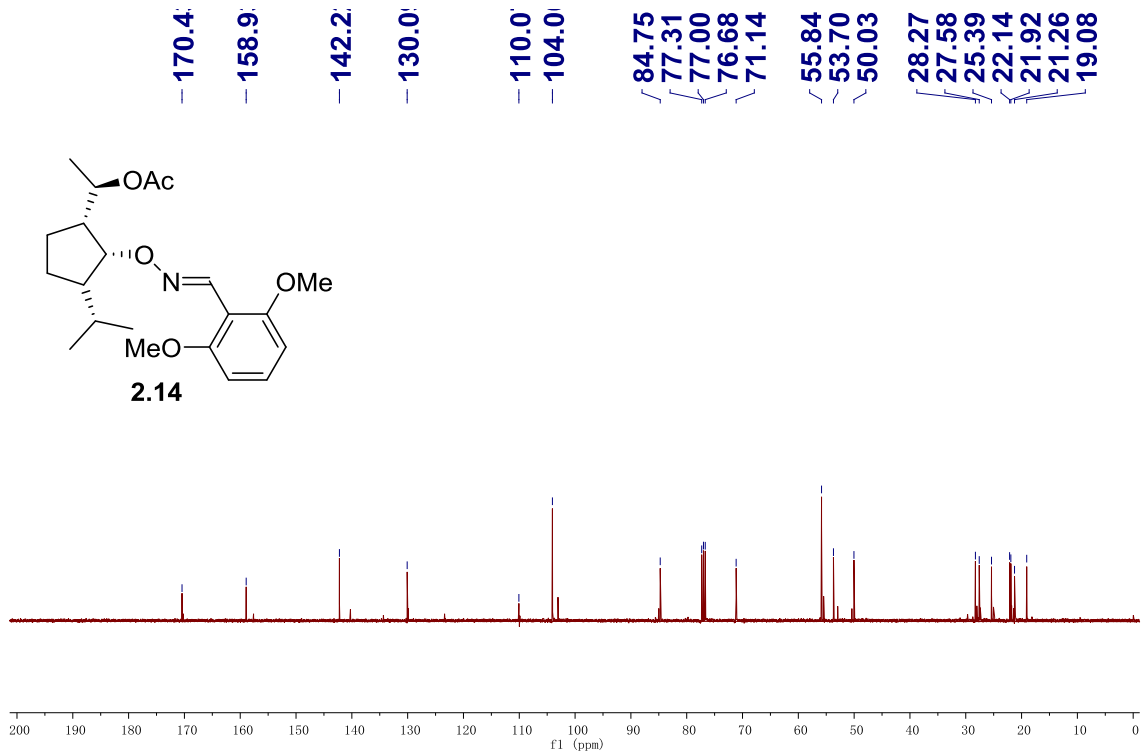
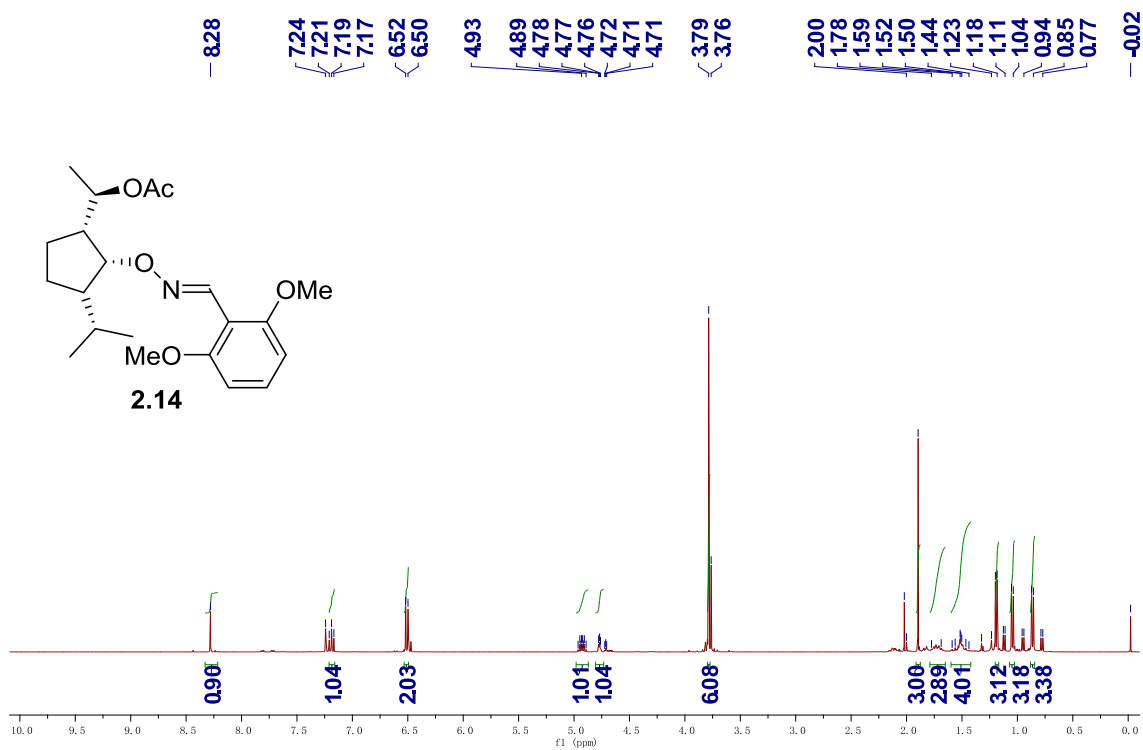


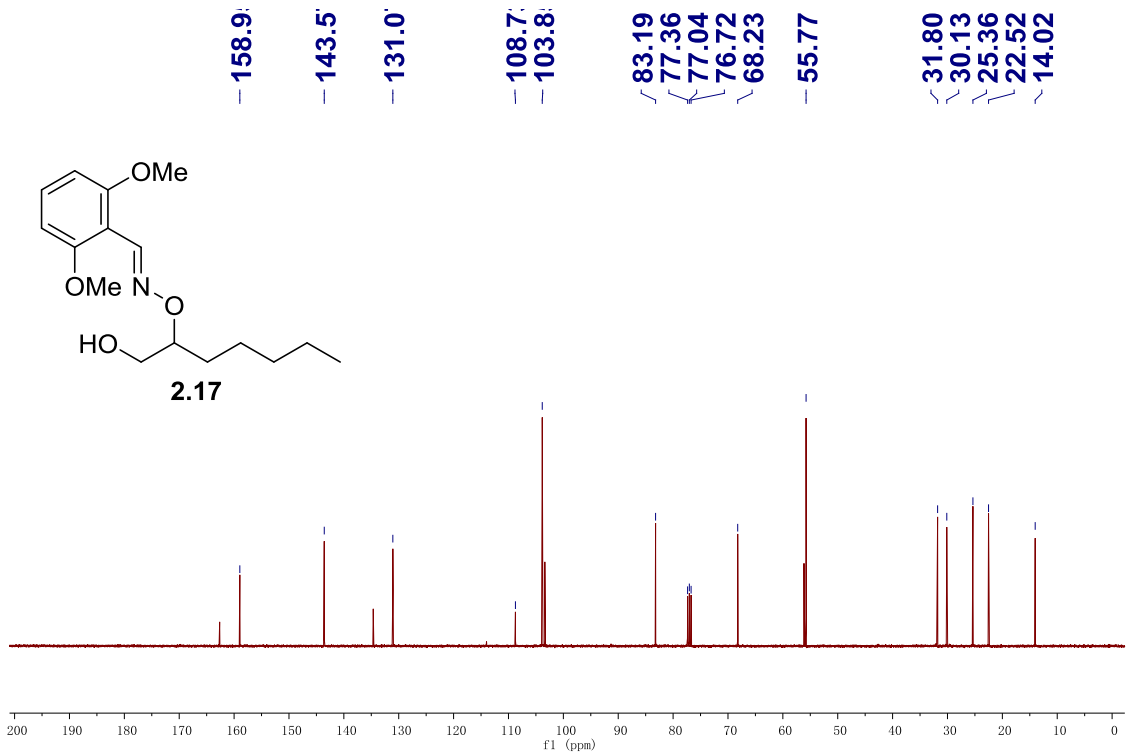
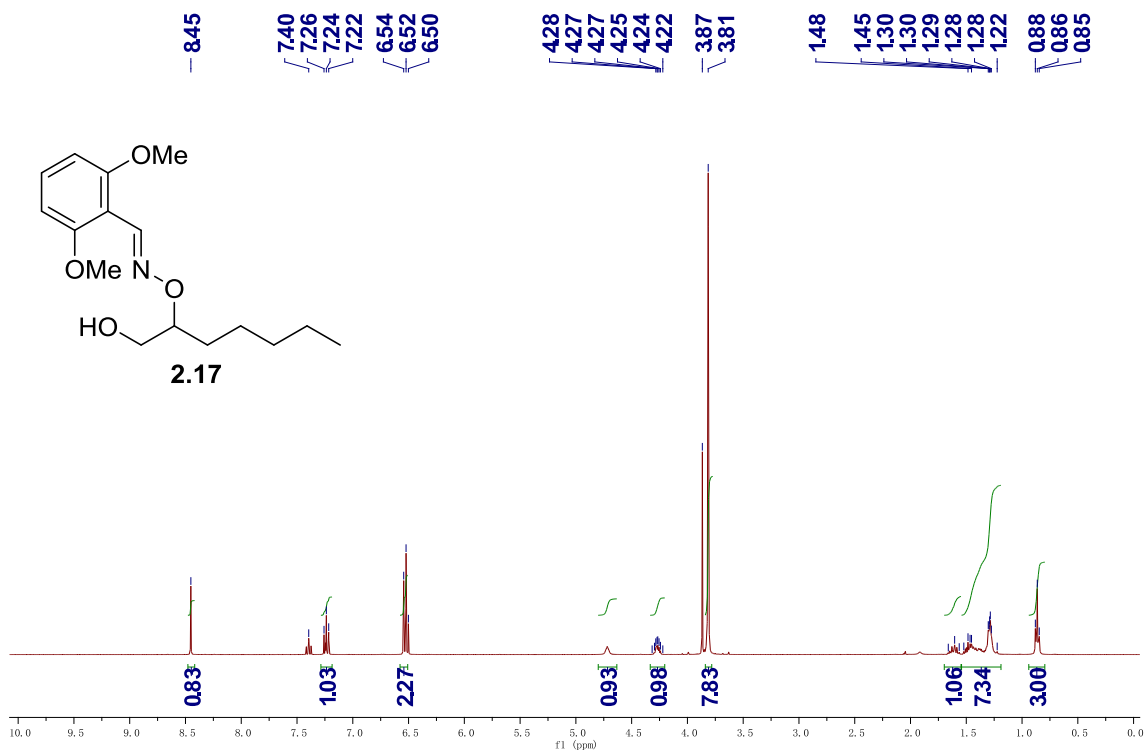


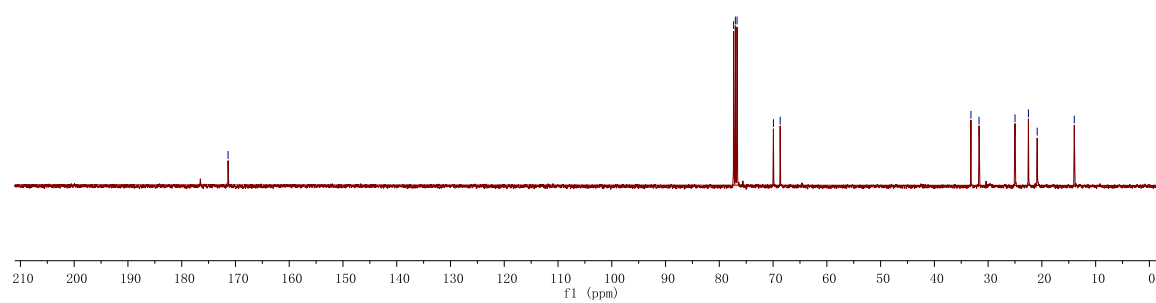
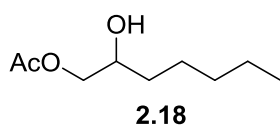
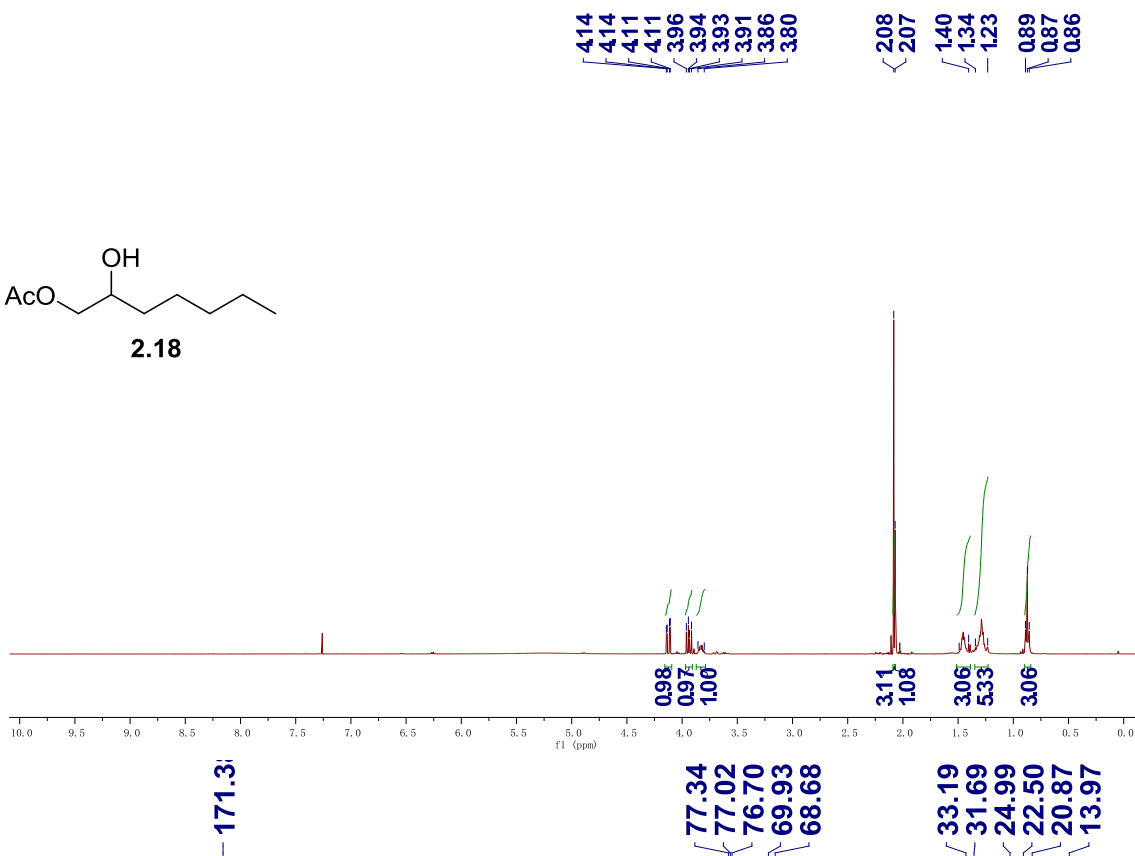
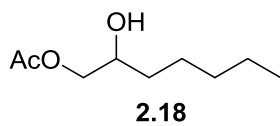


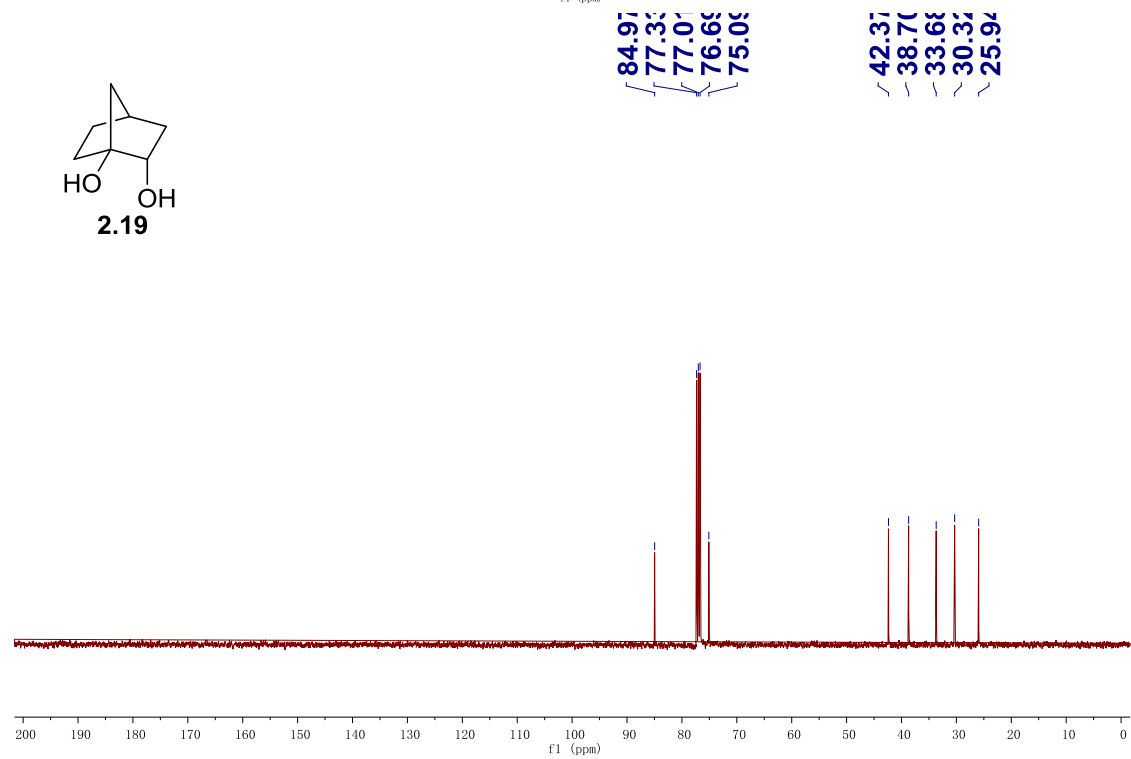
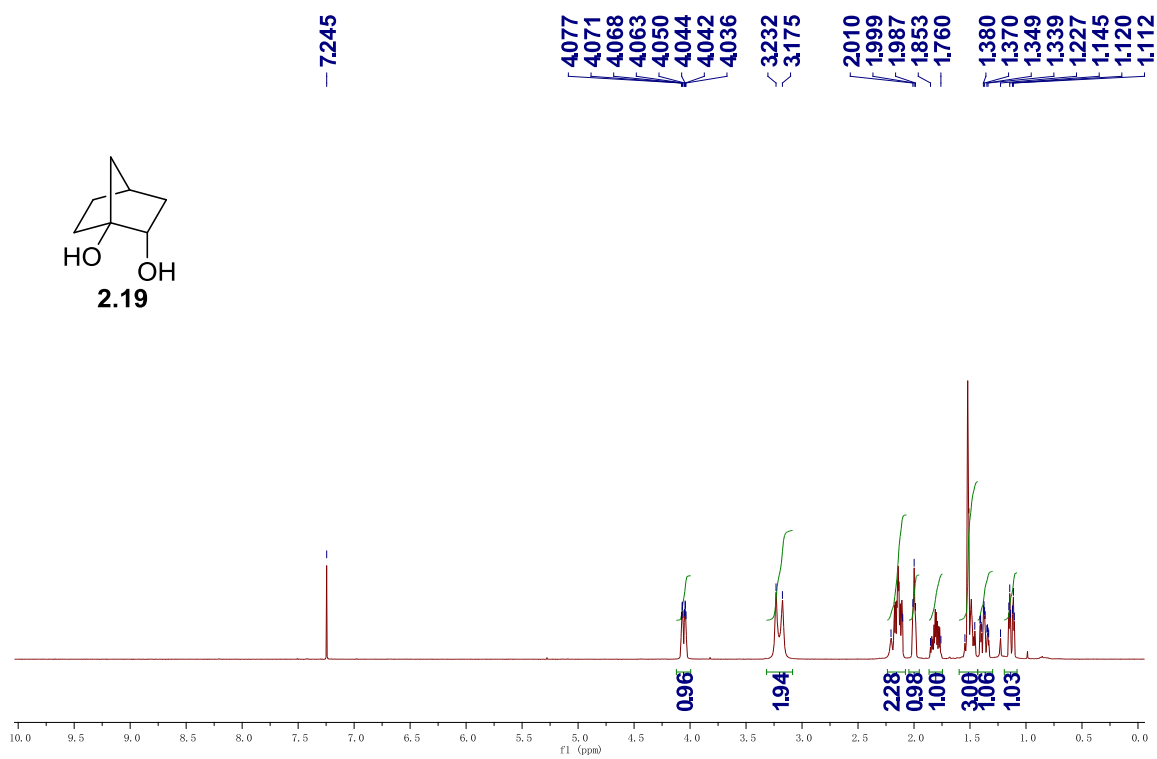


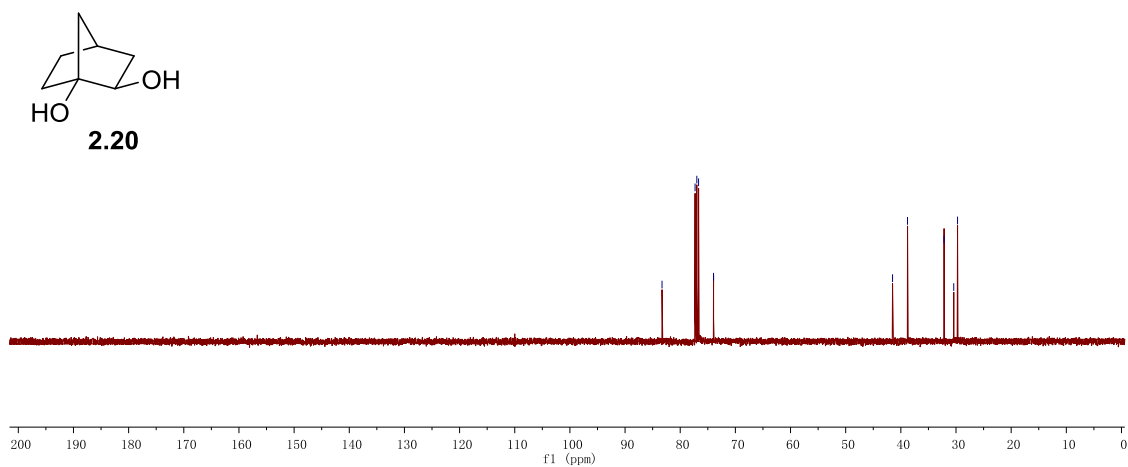
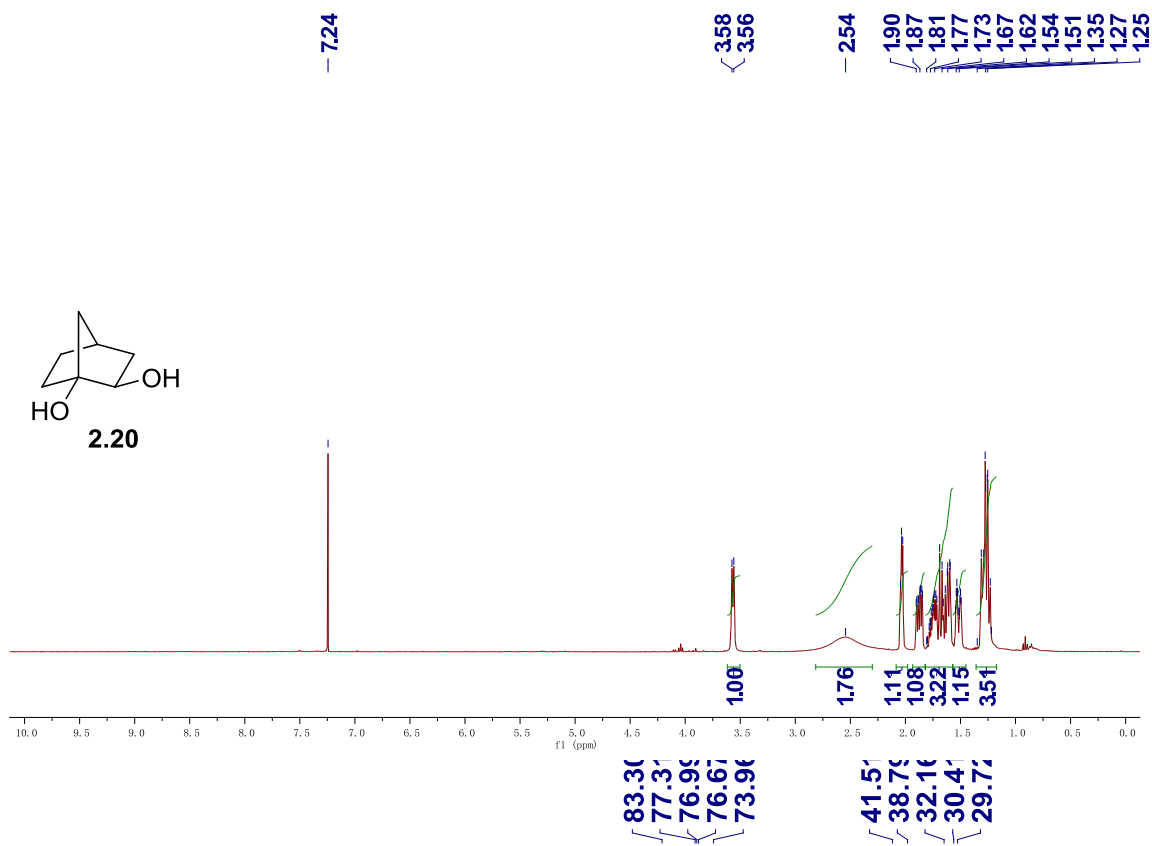


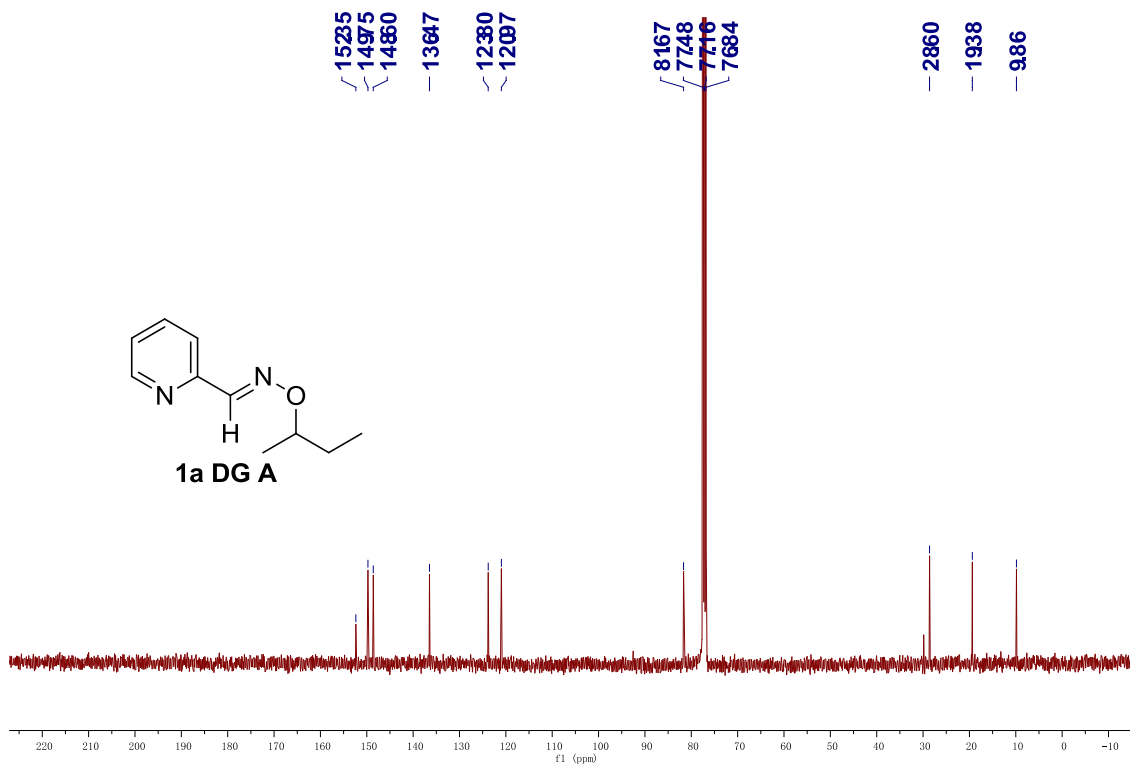
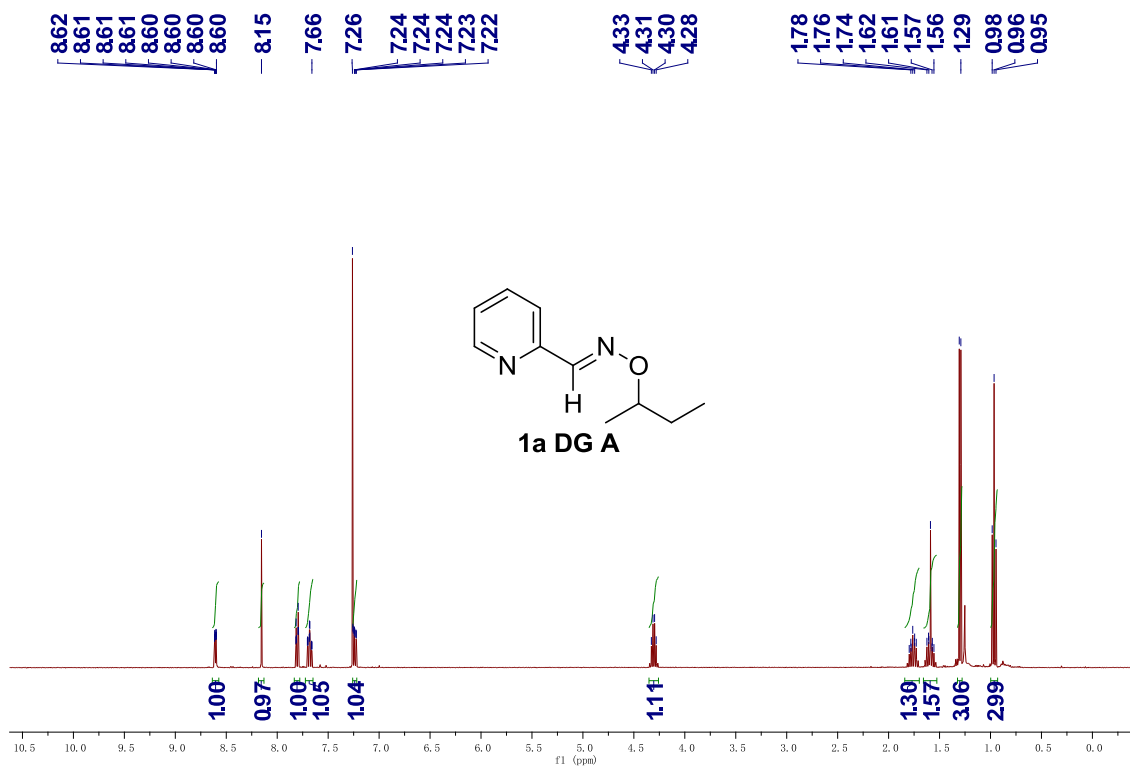


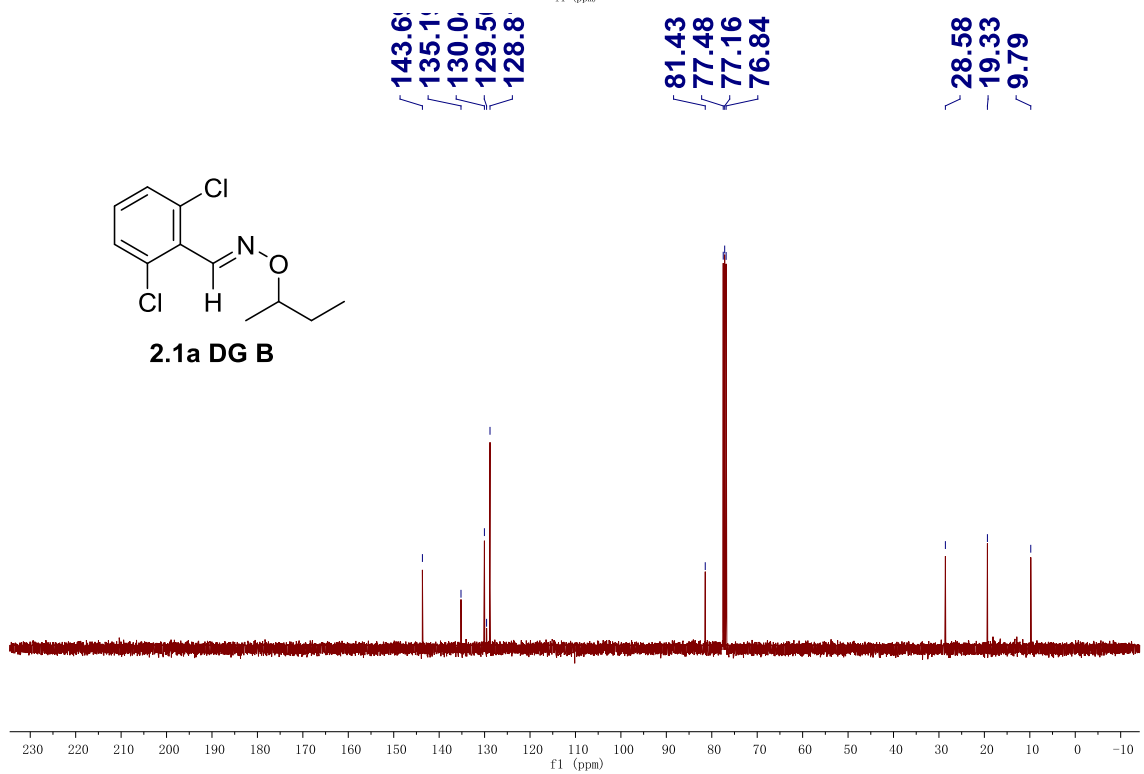
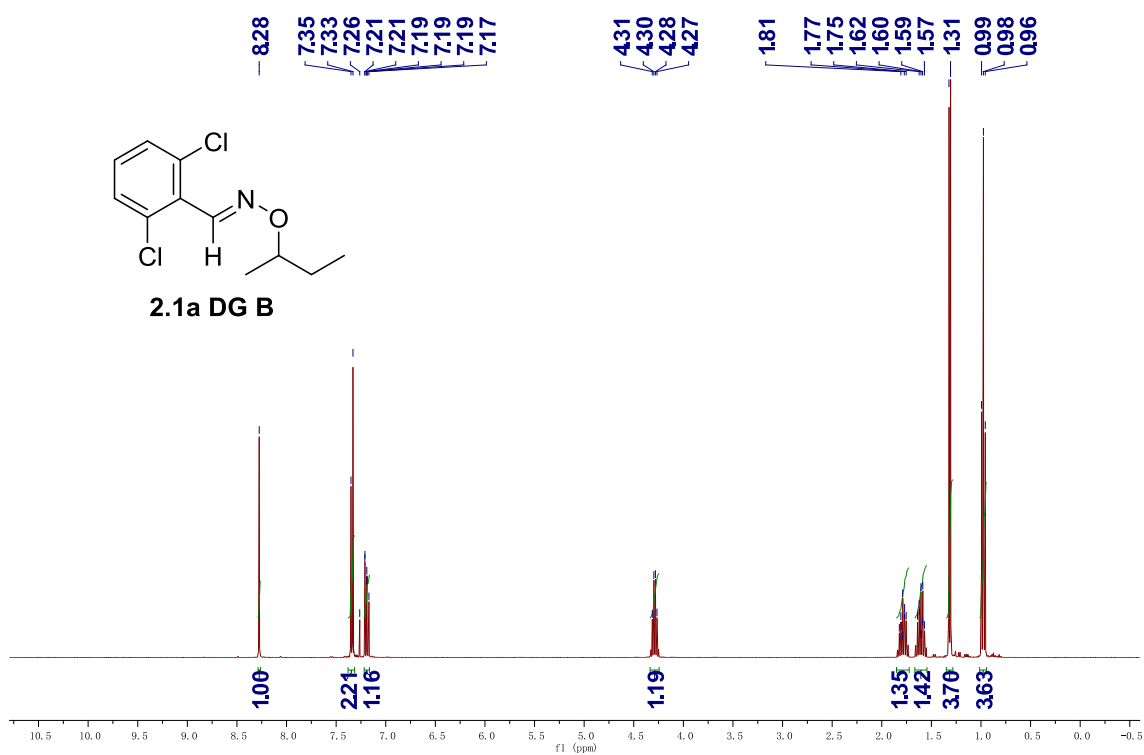










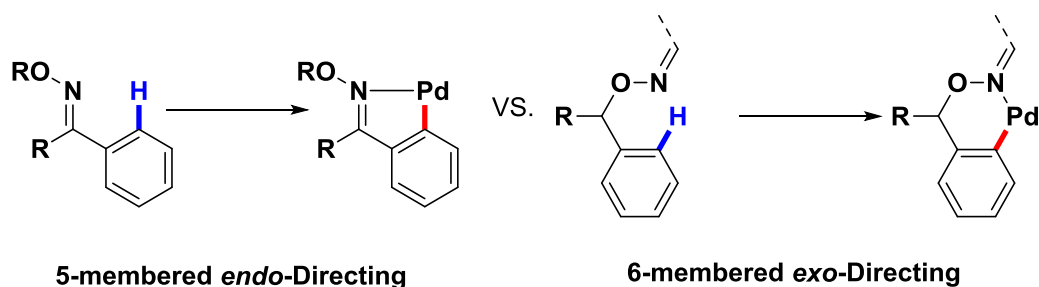


CHAPTER 3: PALLADIUM-CATALYZED *ORTHO*-ACETOXYLATION OF MASKED BENZYL ALCOHOLS VIA AN *EXO*-DIRECTING MODE

3.1 Introduction

Directing strategy has been widely applied to control the site-selectivity in transition metal (TM)-catalyzed aromatic C–H bond activation for various carbon-heteroatom bond formation reactions.¹ For nitrogen based directing groups (DGs), the *endo*-directing strategy has been studied and utilized by many other groups.² Our group has come up with a novel *exo*-directing strategy for C–H bonds activation for carbon-oxygen bonds formation.³ The ring size for the *exo*-directing strategy is a six-membered metallocycle instead of five-membered metallocycle (Scheme 3.1).

Scheme 3.1. Different directing modes in aromatic palladation.



The pioneer DGs, such as pyridine, generally requires harsh conditions to remove, while that would limit the application of those methods.⁴ Therefore, many efforts were attempted to utilize advanced DG, which should be easy to remove or even through temporary functional groups.⁵ Considered the prevalence of hydroxyl groups in bioactive compounds, e.g. Salbutamol (anti-asthma) and Simocyclinone D8 (antibiotic),⁶ the alcohols or masked alcohols based directing strategies would provide rapid access to functionalize the C–H bonds in late stage. As demonstrated by few established examples

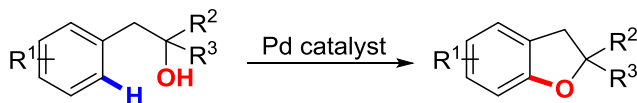
in this area, the elimination of hydroxyl group is one of the obstacles in the development of alcohol-based DGs for oxidation of C–H bonds.⁷

3.2 Background

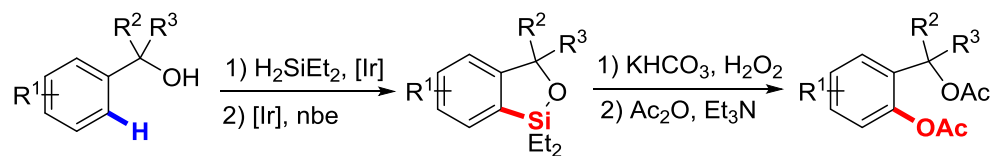
Among various oxidation methods of aromatic C–H bonds at *ortho* position have been achieved, only two methods were developed using free or masked alcohols as DGs. In 2008, Yu developed a synthesis of dihydrobenzofurans via free alcohol-directed intramolecular C–H cyclization (Scheme 3.2.A).⁷ This method works well on tertiary alcohol substrates, but the secondary alcohol suffers from lower yield and side reaction. Later, Hartwig and coworkers reported an Ir-catalyzed *ortho*-silylation of aromatic C–H bond, and after the Tamao-Fleming oxidation step, the C–Si bond was transferred into a C–O bond. (Scheme 3.2.B).⁸

Scheme 3.2. Alcohol or masked alcohol-directed arene C–H oxidation.

(A) Yu's method



(B) Hartwig's approach



Oxime has been documented as a ligand for Pd and Pt since 1970,⁹ while the catalytic aliphatic and aromatic C–H oxidation reactions were developed by Sanford and coworkers in 2006 and 2008 respectively.^{2, 4a} Especially, from a mechanistic point of view, there was one example of using 2-heptanone oxime as DG for directed *ortho*-arene oxidation.¹⁰ In 2012, the catalytic activation of an aliphatic C–H bond to form the C–O

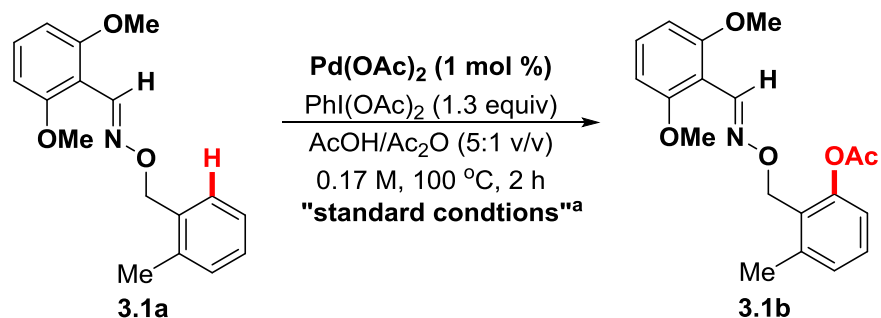
bonds at β -position of the masked alcohol was developed by our group, in which the use of a 2,6-dimethoxybenzaloxime as the DG was found efficient.³ We hypothesized that this special aldoxime DG has an advantageous for aromatic C–H oxidation, because 1) the potential oxidation of DG would be avoided, as the ketoximes would have acidic α -hydrogens that are known to be oxidized under strong oxidative conditions;¹¹ 2) the weak chelation from the methoxy groups on the DG could enhance the catalyst stability during the catalytic cycle to give a higher catalyst turnover.

3.3 Reaction development and scope

The substrate **3.1a** was used as the standard substrate to test our hypothesis. After a series of optimizations, when using 1 mol % Pd(OAc)₂ as the catalyst and 1.3 equiv of PhI(OAc)₂ as the oxidant in AcOH/Ac₂O (5:1) at 100 °C, the desired *ortho*-acetoxyated product (**3.1b**) was isolated in 87 % yield (Table 3.1). A series of control experiments were conducted to gain further insights into this reaction. No desired product was observed without the Pd catalyst or the oxidant (entry 2 and 3). A 10 mol % catalyst loading gave a faster reaction but a lower yield (entry 4), which is due to the elimination of aldoxime in the presence of Pd catalyst. In the absence of Ac₂O, the yield was decreased dramatically, suggesting that water might hamper the reaction (entry 5).¹² Other metal salts, such as Co(II) or Ag(I) acetate, did not give any desirable products under these conditions (entry 6 and 7). When K₂S₂O₈ was used as the oxidant, the yield was decreased to only 30 % (entry 8). However, the addition of a catalytic amount of PhI(OAc)₂ or PhI (10 mol %) along with K₂S₂O₈ increased the yield to 79 % and 72 % respectively (entries 9 and 10). Presumably, under these conditions, the more effective

oxidant, $\text{PhI}(\text{OAc})_2$, was generated *in situ* from a more practical oxidant.¹³ Moreover, by using 2.5 equiv of $\text{K}_2\text{S}_2\text{O}_8$, the isolated yield can reach 85 % (entry 11).

Table 3.1. Selected Optimization of Reaction Conditions.



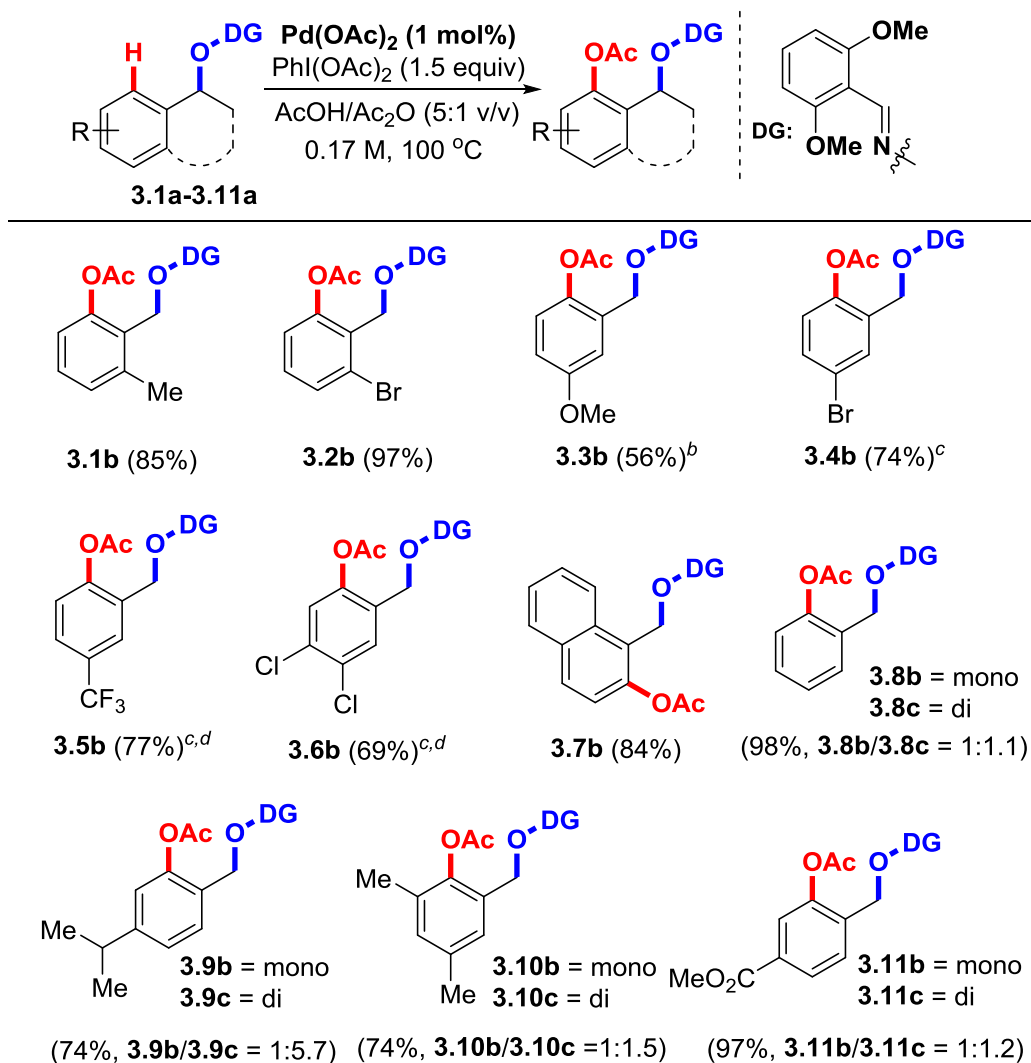
entry	variation from the "standard conditions"	yield ^{a,b,c}
1	none	87% ^d
2	no Pd(OAc)_2	0%
3	no PhI(OAc)_2	0%
4	10% Pd(OAc)_2	68%
5	no Ac_2O	61%
6	Co(OAc)_2 (10 mol%) instead of Pd(OAc)_2	0%
7	AgOAc (10 mol%) instead of Pd(OAc)_2	0%
8	$\text{K}_2\text{S}_2\text{O}_8$ instead of PhI(OAc)_2	30%
9	$\text{K}_2\text{S}_2\text{O}_8$ (2 equiv) and PhI(OAc)_2 (10 mol %)	79%
10	$\text{K}_2\text{S}_2\text{O}_8$ (2 equiv) and PhI (10 mol %)	72%
11	$\text{K}_2\text{S}_2\text{O}_8$ (2.5 equiv) and PhI(OAc)_2 (10 mol %)	85% ^d

^aReaction conditions: all the reactions were run on a 0.1 mmol scale with 0.6 mL of solvents. ^bNMR yields with 1,1,2,2-tetrachloroethane as the internal standard. ^cProduct 3.1b consisted of a mixture of oxime E/Z stereoisomers.

^dIsolated yield.

Three general ways are developed to prepare the benzyl alcohol-derived oxime substrates to test the substrate scope. The first protocol is the previously demonstrated procedure, through a Mitsunobu reaction between the corresponding alcohol and hydroxy phthalimide followed by a one-pot deprotection/condensation.^{3a} The second is via an $\text{S}_{\text{N}}2$ reaction between the corresponding benzyl halides and 2,6-dimethoxybenzaldoxime. Alternatively, by adopting Ellman's oxaziridine,¹⁴ the oxime substrates can be prepared in one-pot from the corresponding benzyl alcohols via electrophilic amination followed by condensation.

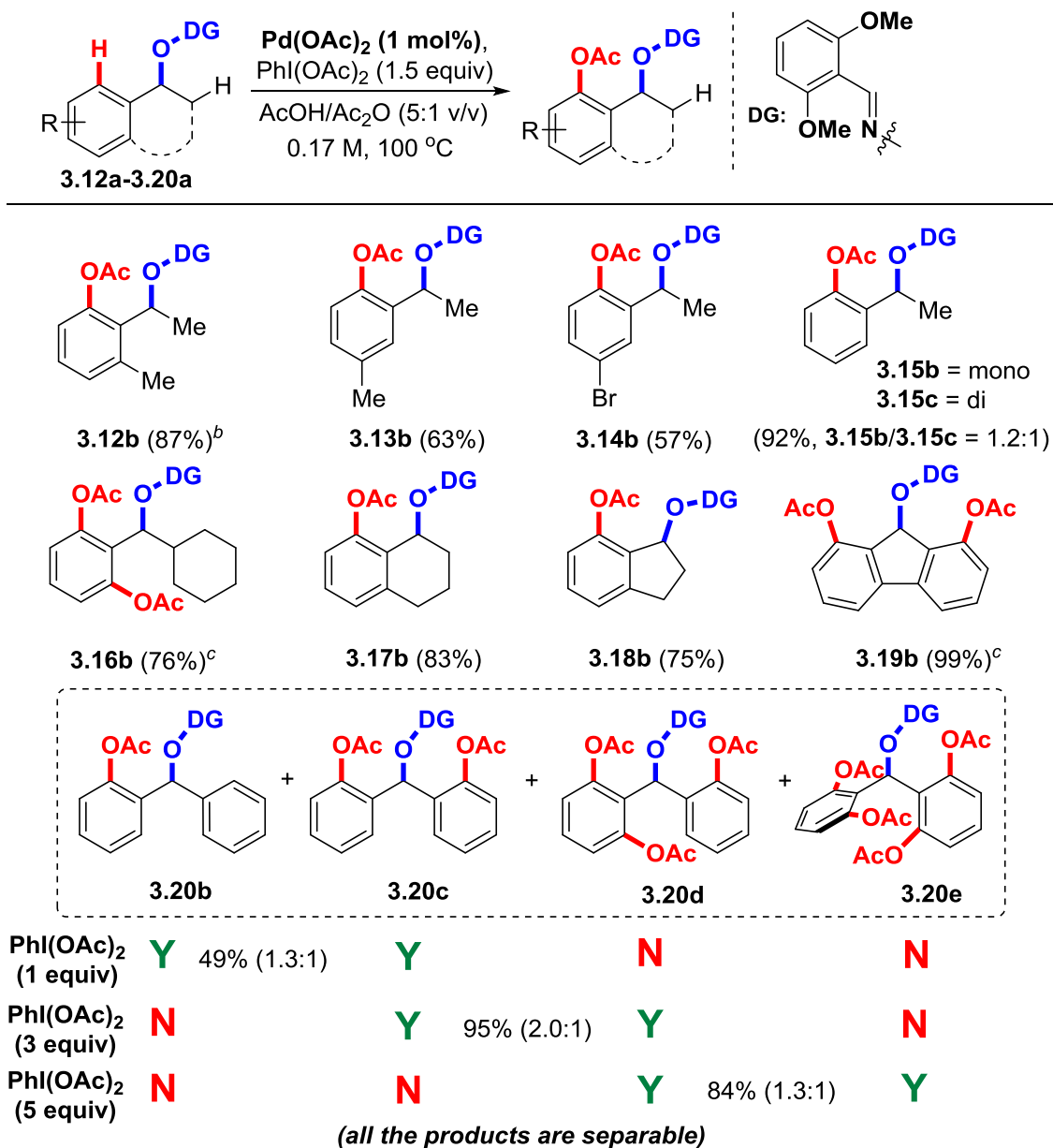
Scheme 3.3. The scope with primary alcohol-derived substrates.



^aIsolated yields. Product consists of a mixture of oxime E/Z stereoisomers

^bK₂S₂O₈ (2.5 equiv) and PhI(OAc)₂ (10 mol %) was used. ^c80 °C. ^d5 mol % Pd(OAc)₂ were used.

Scheme 3.4. The scope with secondary alcohol-derived substrates.



^aIsolated yields. Product consists of a mixture of oxime E/Z stereoisomers. ^bOxidation of the sp³ C-H bond was observed. ^c3 equiv of PhI(OAc)₂ were used.

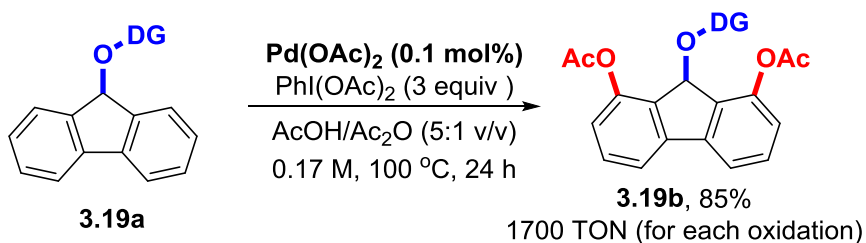
The results with masked primary benzyl alcohol substrates were shown in Table 3.2. Benzylic alcohols with various electronic and steric properties all reacted to give the *ortho*-acetoxylation, in the presence of just 1 mol % catalyst loading, the corresponding 2-hydroxymethylphenol derivatives can be isolated in good to excellent yields. A number of FGs can be tolerated, including aryl bromides and chlorides, trifluoromethyl, anisole, naphthalene, and esters. Mono-oxidation can be achieved when there is an *ortho*- or *meta*-substituent. While bis-oxidation was observed when possible, the isolation of products is easy, due to their significant difference of polarity introduced by acetate groups. Moreover, by controlling the loading of the catalyst and oxidant, the mono-oxidation product can also be obtained with a good selectivity (Scheme 3.5). In addition, a lower reaction temperature (e.g. 80 °C) can be used to enhance the regioselectivity. Notably, with the sterically hindered substrates, such as **3.10a**, the oxidation occurs selectively at *ortho* position.

The masked secondary alcohol-derived substrates were subsequently examined (Scheme 3.4). Either acyclic or cyclic benzyl alcohols gave the desired *ortho*-oxidation products in good to excellent yields. While the substrates contain β -aliphatic C–H bonds that are available for the Pd-catalyzed vicinal oxidation,^{3, 15} only a small amount of the *sp*³ C–H activation product (7.5 % yield) was observed in substrate **3.12a** along with an 87 % yield on the aromatic oxidation. Obviously, the aromatic C–H functionalization is much more favorable. Both the α -tetralol (**3.17b**) and 1-indanol (**3.18b**) derived oximes proved to be excellent substrates. It is exciting to find that the 9-fluorenol-derived substrate gave the desired 1,8-di-*O*-substituted product **3.19b** in almost a quantitative yield, which is difficult to prepare by other means.¹⁶ In the case of the diphenylmethanol substrate, by choosing different amounts of oxidants, mono- to tetra-acetoxylation products **20b-e** can be formed with different selectivity. It is noteworthy that the second

oxidation took place on the other phenyl group. The fourth oxidation was much slower which could be the result of a higher rotation barrier, and all these products can be easily separated.

Scheme 3.5. Reaction TON test and mono-oxidation.

Reaction TON Test



Mono-Oxidation

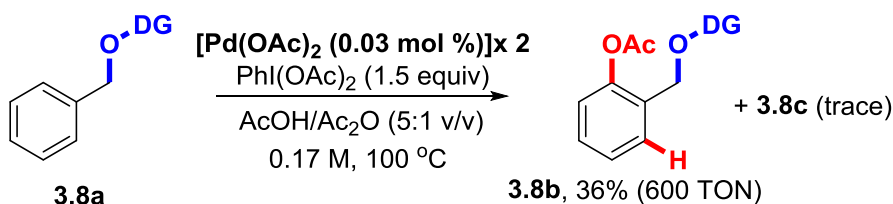
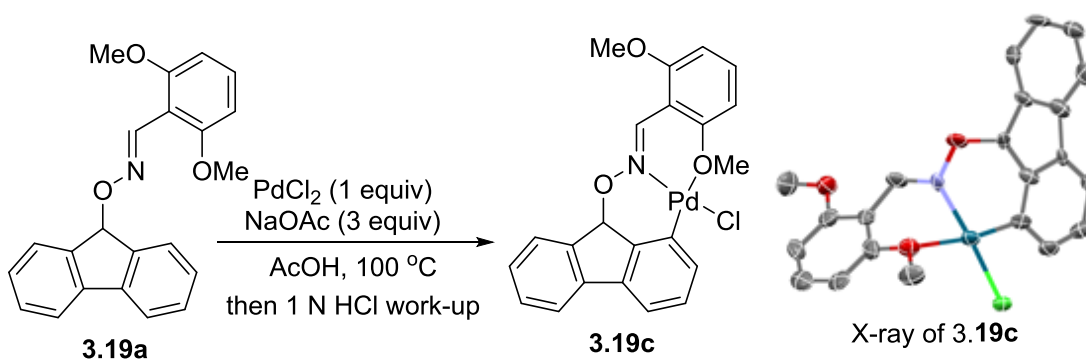


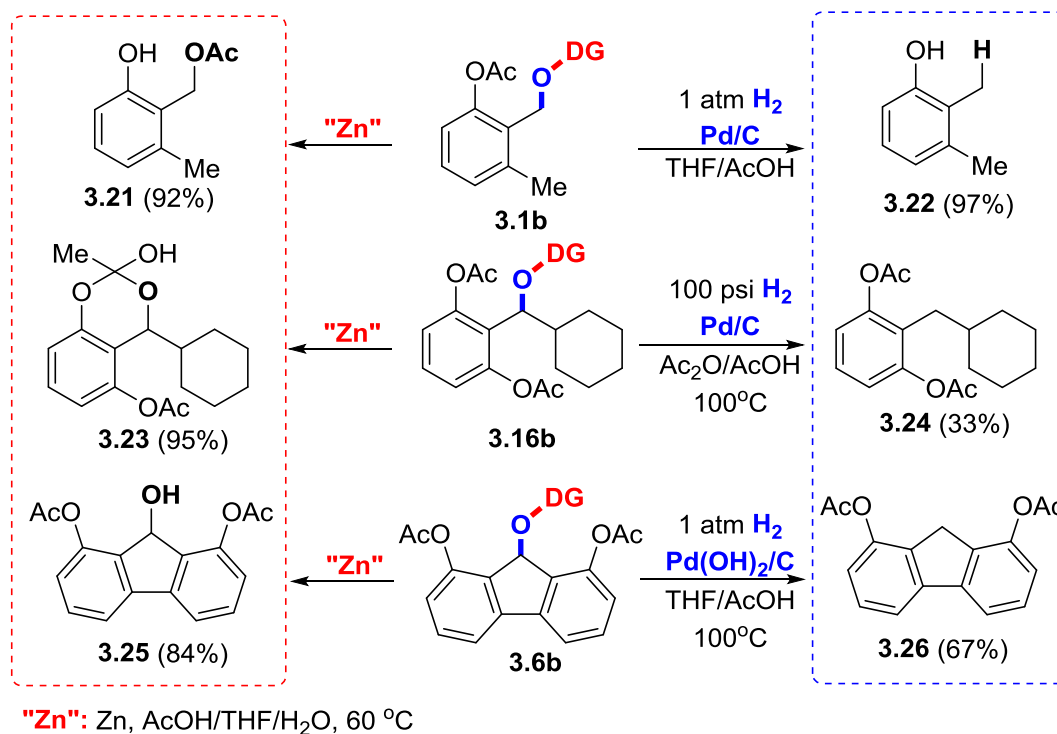
Figure 3.1. Isolation of Palladacycle **3.19c**.



As shown in scheme 3.5, the turnover number (TON) of the catalyst was examined with substrate **3.19a**. Indeed, using our 2,6-dimethoxyl benzaldoxime DG, the TON can reach 1700 for each acetoxylation with 0.1 mol % of the catalyst. By using a lower catalyst loading (0.06 mol %) and less oxidant, the mono-oxidation product **3.8b**

can be selectively obtained with 600 TON with $\text{Pd}(\text{OAc})_2$ catalyst (Scheme 3.5). The coordination mode of the DG during the C–H activation step was investigated by obtaining a palladacycle intermediate for substrate **3.19a** (Figure 3.1). After HCl workup, the palladium chloride species as a mononuclear pseudo-square planar *exo*-palladacycle **3.19c** was obtained and confirmed by X-ray crystallography. The high catalyst turnover of this reaction is presumably due to the chelation of the methoxy group as a weak ligand to further stabilize the palladacycle.

Scheme 3.6. Cleavage of the Directing Group



There are two strategies that have been demonstrated to remove the DG through either N–O bond or C–O bond cleavage (Scheme 3.6). As our established method, the N–O bond of the oximes was selectively cleaved using inexpensive zinc metal.¹⁷ It is interesting to know that, after the N–O bond cleavage, a free phenol was obtained through transesterification of the resulting benzyl alcohol from **3.1b**, while an orthoacetate **3.23**

was obtained for substrate **3.16b**. On the other hand, a Pd-catalyzed hydrogenolysis can be applied to the benzyl C–O bond cleavage.¹⁸ As the oxime substrates can be ultimately synthesized from the corresponding benzylic halides followed by an S_N2 reaction, this approach can provide the highly substituted phenols in a traceless fashion.

3.4. Conclusion

In conclusion, a Pd-catalyzed *ortho*-acetoxylation of masked benzyl alcohols has been developed, and the *exo*-directing strategy can be extended to aromatic C–H functionalization. A variety of 2-hydroxyalkyl phenol derivatives can be synthesized in good to excellent yields under optimized condition. The methoxy group on the 2,6-dimethoxybenzaloxime has been proved to be important during the C–H activation step. The DG can be removed either by N–O bond to provide the benzyl alcohols, or in a traceless fashion to give highly substituted phenols.

3.5. Experiment Results

3.5.1 GENERAL CONSIDERATION

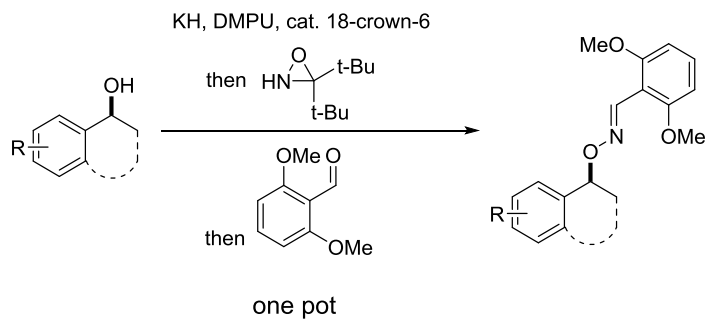
Unless otherwise noted, all experiments were carried out under air atmosphere. Tetrahydrofuran (THF) were distilled over sodium. The other reagents and solvents were directly used from the supplier without further purification unless noted. Analytical thin-layer chromatography (TLC) was carried out using 0.2 mm commercial silica gel plates (silica gel 60, F254, EMD chemical). The vials (1 dram, 15×45 mm with PTFE-lined cap attached) were purchased from Qorpak and dried in an oven overnight and cooled in air. Infrared spectra were recorded on a Nicolet iS5 FT-IR Spectrometer using neat thin film technique. High-resolution mass spectra (HRMS) were obtained on a Karatos MS9 and are reported as m/z (relative intensity). Accurate masses are reported for the molecular ion [M+Na]⁺ or [M+H]⁺. Nuclear magnetic resonance spectra (¹H NMR and ¹³C NMR)

were recorded with Varian Gemini (400 MHz, ^1H at 400 MHz, ^{13}C at 100 MHz). For CDCl_3 solutions, the chemical shifts are reported as parts per million (ppm) referenced to residual protium or carbon of the solvents; CHCl_3 δ H (7.26 ppm) and CDCl_3 δ C (77.16 ppm). Coupling constants are reported in Hertz (Hz). Data for ^1H NMR spectra are reported as follows: chemical shift (ppm, referenced to protium; s = singlet, d = doublet, t = triplet, q = quartet, p = pentet (quintet), dd = doublet of doublets, td = triplet of doublets, ddd = doublet of doublet of doublets, m = multiplet, coupling constant (Hz), and integration).

3.5.2 GENERAL PROCEDURE AND CHARACTERIZATION

General procedure for oxime substrates with three approaches

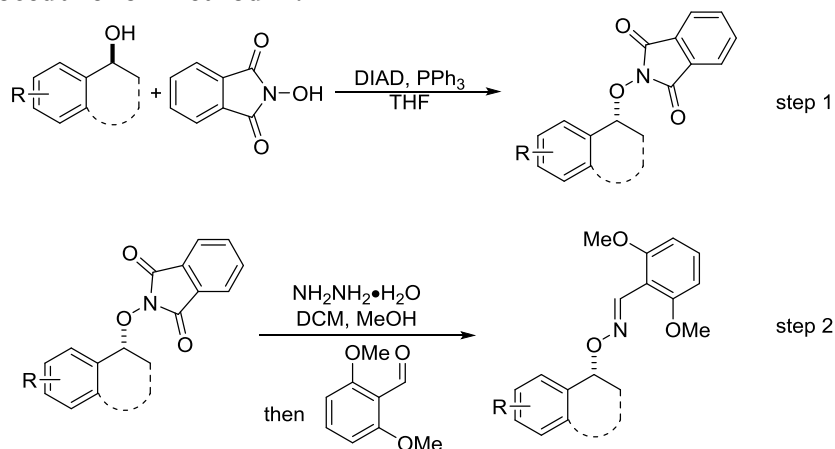
General procedure for method A:



3,3'-Di-tert-butyl oxaziridine was prepared according to the modified Ellman's procedure, and the amination procedure was adopted from the Ellman's publication.¹⁴

To a suspension of KH (1.5 equiv) and 18-crown-6 (0.1 equiv) in DMPU (3ml/1mmol alcohol) was added the alcohol (1.0 equiv) under a nitrogen atmosphere at room temperature. After stirring at room temperature for 1h and no gas evolution was observed, the resulting solution was slowly added into a DMPU solution (1.5ml/1mmol alcohol) of 3,3'-di-tert-butyl oxaziridine (2.5 equiv) at -40 °C. The reaction was then warmed to room temperature and stirred for another 1.5 h. Several drops of HOAc were added in, followed by the addition of 2,6-dimethoxy benzaldehyde (1.3 equiv). The mixture was stirred for 0.5 h and then diluted with 1M NaOH, extracted with EtOAc and washed with water and brine. The combined organic extracts were dried over Na₂SO₄ and concentrated under reduced pressure. The desired compound was purified by flash column chromatography on silica gel. **All the yields are not optimized.**

General procedure for method B:

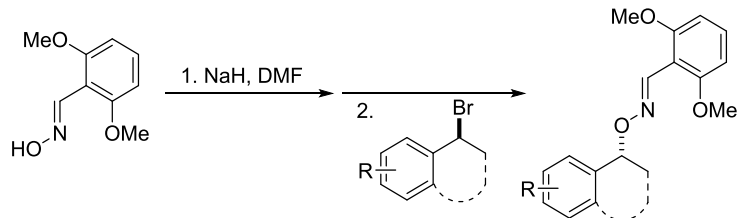


Step 1: To a solution of the alcohol (10 mmol, 1.0 equiv), *N*-hydroxy phthalimide (1.956g, 12 mmol, 1.2 equiv) and PPh_3 (3.144 g, 12 mmol, 1.2 equiv) in 20 mL THF was added diisopropyl azodicarboxylate (2.4 mL, 12 mmol, 1.2 equiv) dropwise at 0 °C. The reaction was then allowed to warm to room temperature and stirred overnight. After the reaction is finished, hexanes were added, and the precipitation was collected and directly used in the next step without further purification.

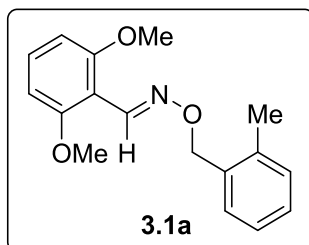
Step 2: To a solution of *N*-alkoxy phthalimide (1.1 equiv) in DCM/MeOH=1:1 (10 mL/mmol) was added hydrazine monohydrate (1.15 equiv) at room temperature. The reaction was monitored by TLC and usually completed in 20 min. The 2,6-dimethoxybenzaldehyde (1.0 equiv) was then added. The reaction was monitored by TLC. After 0.5 h the solvent was removed under reduced pressure. The desired oxime product was purified by flash column chromatography on silica gel. **All the yields are not optimized.**

General procedure for method C:

2,6-dimethoxy benzaldehyde oxime was prepared according to the literature procedure.¹⁹



In a pre-dried flask, 2,6-dimethoxy benzaldehyde oxime (1.25 equiv) and sodium hydride (1 equiv) was added, followed by addition of DMF (2mL/1mmol). After 0.5 h, the corresponding benzyl bromide was added and heated to 80°C overnight. After the reaction was complete, the reaction mixture was diluted by EA and washed with excess water and brine. The desired compound was purified by flash column chromatography (15:1 to 5:1 Hexanes: EA) on silica gel. **All the yields are not optimized.**



(E)-2,6-dimethoxybenzaldehyde O-(2-methylbenzyl) oxime (3.1a)

White solid. General Method **B**: yield 80%. General Method **C**: yield 74%. E/Z > 19:1.

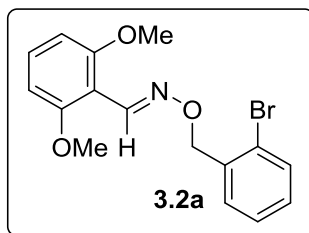
Mp. 71-72 °C. R_f = 0.5 (Hex/EA=3:1).

IR (KBr) 3005, 2937, 2838, 1595, 1578, 1469, 1432, 1255 cm^{-1} .

^1H NMR (400 MHz, CDCl_3) δ 8.53 (s, 1H), 7.43 (d, J = 7.3 Hz, 1H), 7.27 (t, J = 8.4 Hz, 1H), 7.21 (dd, J = 4.0, 3.1 Hz, 2H), 6.57 (d, J = 8.4 Hz, 2H), 5.27 (s, 2H), 3.84 (s, 6H), 2.43 (s, 3H).

^{13}C NMR (100 MHz, CDCl_3) δ 159.17, 144.71, 137.24, 135.72, 130.99, 130.27, 129.59, 128.14, 125.91, 109.45, 104.18, 74.37, 56.19, 19.23.

HRMS calcd. for $\text{C}_{17}\text{H}_{19}\text{NO}_3^+$ $[\text{M}+\text{H}]^+$: 286.1438. Found: 286.1440.



(E)-2,6-dimethoxybenzaldehyde O-(2-bromobenzyl) oxime (3.2a)

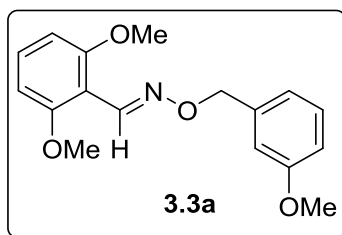
White solid. General Method **B**: yield 84%. E/Z > 19:1. Mp. 91-92 °C. R_f = 0.5 (Hex/EA=3:1).

IR (KBr) 2937, 2837, 1595, 1470, 1432, 1360, 1256, 1208 cm^{-1} .

^1H NMR (400 MHz, CDCl_3) δ 8.58 (s, 1H), 7.62 – 7.52 (m, 2H), 7.32 (td, J = 7.5, 1.2 Hz, 1H), 7.27 (t, J = 8.4 Hz, 1H), 7.15 (ddd, J = 8.0, 7.4, 1.7 Hz, 1H), 6.57 (d, J = 8.4 Hz, 2H), 5.34 (s, 2H), 3.84 (s, 6H).

^{13}C NMR (100 MHz, CDCl_3) δ 159.16, 145.20, 137.66, 132.57, 131.13, 129.92, 129.02, 127.31, 122.95, 109.28, 104.15, 75.19, 56.19.

HRMS calcd. for $\text{C}_{16}\text{H}_{17}\text{BrNO}_3^+$ $[\text{M}+\text{H}]^+$: 350.0386. Found: 350.0387.



(E)-2,6-dimethoxybenzaldehyde O-(3-methoxybenzyl) oxime (3.3a)

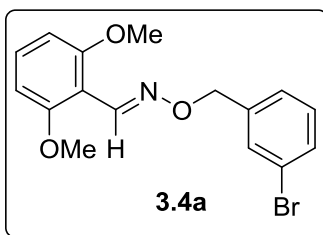
Colorless oil. General Method C: yield 82%. E/Z > 19:1. R_f = 0.45 (Hex/EA=3:1).

IR 3002, 2938, 2837, 1595, 1470, 1432, 1360, 1340, 1307, 1286, 1186 (KBr) cm^{-1} .

^1H NMR (400 MHz, CDCl_3) δ 8.54 (s, 1H), 7.31 – 7.24 (m, 2H), 7.07 – 7.03 (m, 2H), 6.86 (ddd, J = 8.3, 2.5, 1.1 Hz, 1H), 6.57 (d, J = 8.4 Hz, 2H), 5.24 (s, 2H), 3.84 (s, 6H), 3.82 (s, 3H).

^{13}C NMR (100 MHz, CDCl_3) δ 159.68, 159.09, 144.86, 139.40, 131.00, 129.40, 120.78, 113.84, 113.55, 109.32, 104.11, 75.95, 56.11, 55.28.

HRMS calcd. for $\text{C}_{17}\text{H}_{20}\text{NO}_4^+$ $[\text{M}+\text{H}]^+$: 302.1387. Found: 302.1391.



(E)-2,6-dimethoxybenzaldehyde O-(3-bromobenzyl) oxime (3.4a)

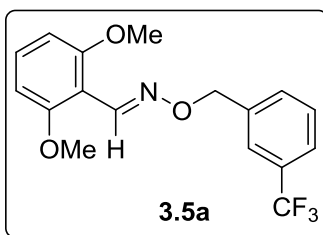
Colorless oil. General Method C: yield 73%. E/Z > 19:1. R_f = 0.5 (Hex/EA=3:1).

IR (KBr) 3003, 2936, 2837, 1595, 1571, 1470, 1431, 1257, 1270, 1114 cm^{-1} .

^1H NMR (400 MHz, CDCl_3) δ 8.53 (s, 1H), 7.66 (t, J = 1.7 Hz, 1H), 7.46 – 7.40 (m, 1H), 7.37 (d, J = 7.7 Hz, 1H), 7.30 – 7.19 (m, 2H), 6.56 (dd, J = 8.4, 3.3 Hz, 2H), 5.21 (s, 2H), 3.83 (s, 6H).

^{13}C NMR (100 MHz, CDCl_3) δ 159.04, 145.06, 140.41, 131.41, 131.09, 130.75, 129.90, 126.89, 122.40, 109.08, 104.04, 74.97, 56.09.

HRMS calcd. for $\text{C}_{16}\text{H}_{16}\text{BrNO}_3\text{Na}^+$ $[\text{M}+\text{Na}]^+$: 372.0206. Found: 372.0203.



(E)-2,6-dimethoxybenzaldehyde O-(3-(trifluoromethyl)benzyl) oxime (3.5a)

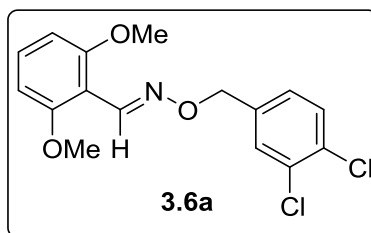
White solid. General Method C: yield 77%. E/Z > 19:1. Mp. 74-77 °C. R_f = 0.65 (Hex/EA=3:1).

IR (KBr) 3006, 2962, 2939, 2840, 1596, 1471, 1433, 1363, 1329, 1285, 1258 cm^{-1} .

^1H NMR (400 MHz, CDCl_3) δ 8.53 (s, 1H), 7.75 (s, 1H), 7.65 – 7.61 (m, 1H), 7.56 (d, J = 7.8 Hz, 1H), 7.48 (t, J = 7.7 Hz, 1H), 7.27 (t, J = 8.4 Hz, 1H), 6.57 (d, J = 8.4 Hz, 2H), 5.28 (s, 2H), 3.83 (s, 6H).

^{13}C NMR (100 MHz, CDCl_3) δ 159.23, 145.36, 139.27, 131.71 (d, J = 1.2 Hz), 131.21, 130.76 (q, J = 32.2 Hz), 128.83, 125.24 (q, J = 3.8 Hz), 124.59 (q, J = 3.8 Hz), 124.36 (q, J = 272.2 Hz), 109.27, 104.22, 75.13, 56.17.

HRMS calcd. for $\text{C}_{17}\text{H}_{17}\text{F}_3\text{NO}_3$ $[\text{M}+\text{H}]^+$: 340.1155. Found: 340.1158.



(E)-2,6-dimethoxybenzaldehyde O-(3,4-dichlorobenzyl) oxime (3.6a)

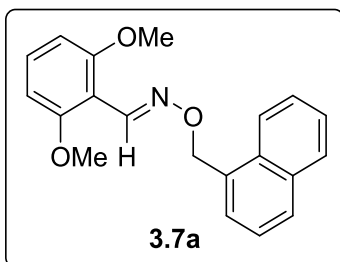
White solid. General Method **B**: yield 81%. E/Z > 19:1. Mp. 61-63 °C. R_f = 0.45 (Hex/EA=3:1).

IR (KBr) 3004, 2937, 2838, 1595, 1470, 1432, 1398, 1257, 1114 cm^{-1} .

^1H NMR (400 MHz, CDCl_3) δ 8.50 (s, 1H), 7.59 (d, $J=2.0$, 1H), 7.42 (d, $J=8.2$, 1H), 7.30 – 7.25 (m, 2H), 6.56 (d, $J=8.4$, 2H), 5.16 (d, $J=0.6$, 2H), 3.84 (s, 6H).

^{13}C NMR (100 MHz, CDCl_3) δ 159.15, 145.37, 138.58, 132.39, 131.69, 131.26, 130.45, 130.33, 127.70, 109.08, 104.13, 74.41, 56.18.

HRMS calcd. for $\text{C}_{16}\text{H}_{16}\text{Cl}_2\text{NO}_3^+$ $[\text{M}+\text{H}]^+$: 340.0502. Found: 340.0502.



(E)-2,6-dimethoxybenzaldehyde O-naphthalen-1-ylmethyl oxime (3.7a)

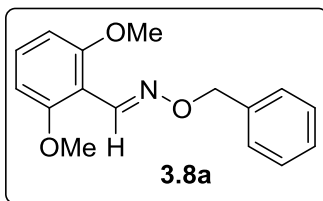
White solid. General Method **B**: yield 90%. E/Z > 19:1. Mp. 129-131 °C. R_f = 0.5 (Hex/EA=3:1).

IR (KBr) 3005, 2937, 2837, 1595, 1470, 1257, 1113, 1028 cm^{-1} .

^1H NMR (400 MHz, CDCl_3) δ 8.56 (s, 1H), 8.23 (dd, J = 8.5, 0.9 Hz, 1H), 7.91 – 7.81 (m, 2H), 7.65 – 7.61 (m, 1H), 7.58 – 7.44 (m, 3H), 7.25 (dd, J = 11.0, 5.8 Hz, 1H), 6.55 (d, J = 8.4 Hz, 2H), 5.72 (s, 2H), 3.83 (s, 6H).

^{13}C NMR (100 MHz, CDCl_3) δ 159.15, 144.91, 133.83, 133.32, 132.06, 131.03, 128.88, 128.57, 127.44, 126.31, 125.80, 125.40, 124.45, 109.34, 104.14, 74.46, 56.15.

HRMS calcd. for $\text{C}_{20}\text{H}_{19}\text{NO}_3\text{Na}^+$ $[\text{M}+\text{Na}]^+$: 344.1257. Found: 344.1258.



(E)-2,6-dimethoxybenzaldehyde O-benzyl oxime (3.8a)

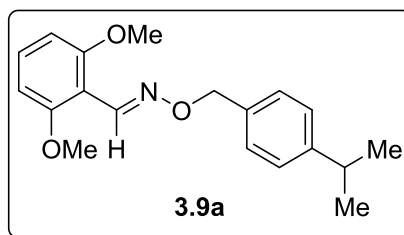
Colorless oil. General Method **B**: yield 93%. E/Z > 19:1. R_f = 0.5 (Hex/EA=3:1).

IR (KBr) 3062, 3004, 2937, 2838, 1595, 1496, 1470, 1432, 1366, 1342 cm^{-1} .

^1H NMR (400 MHz, CDCl_3) δ 8.53 (s, 1H), 7.50 – 7.45 (m, 2H), 7.41 – 7.35 (m, 2H), 7.35 – 7.29 (m, 1H), 7.27 (t, $J=8.4$, 1H), 6.57 (d, $J=8.4$, 2H), 5.26 (s, 2H), 3.84 (s, 6H).

^{13}C NMR (100 MHz, CDCl_3) δ 159.03, 144.71, 137.78, 130.94, 128.55, 128.33, 127.81, 109.28, 104.06, 76.04, 56.06.

HRMS calcd. for $\text{C}_{16}\text{H}_{17}\text{NO}_3\text{Na}^+$ $[\text{M}+\text{Na}]^+$: 294.1101. Found: 294.1114.



(E)-2,6-dimethoxybenzaldehyde O-(4-isopropylbenzyl) oxime (3.9a)

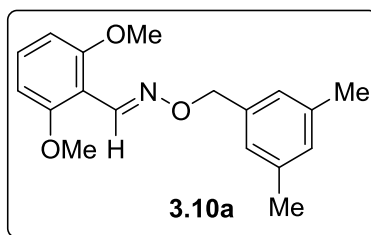
Colorless oil. General Method **B**: yield 92%. E/Z > 19:1. Mp. 41-44 °C. R_f = 0.5 (Hex/EA=3:1).

IR (KBr) 3006, 2959, 2869, 2838, 1595, 1578, 1469, 1432, 1255, 1208 cm^{-1} .

^1H NMR (400 MHz, CDCl_3) δ 8.53 (s, 1H), 7.41 (d, J = 8.1 Hz, 2H), 7.30 – 7.22 (m, 3H), 6.57 (d, J = 8.4 Hz, 2H), 5.22 (s, 2H), 3.85 (s, 6H), 2.99 – 2.86 (m, 1H), 1.32 – 1.19 (m, 6H).

^{13}C NMR (100 MHz, CDCl_3) δ 159.14, 148.67, 144.71, 135.08, 130.95, 128.89, 126.53, 109.49, 104.16, 76.10, 56.17, 34.05, 24.15.

HRMS calcd. for $\text{C}_{19}\text{H}_{24}\text{NO}_3^+$ $[\text{M}+\text{H}]^+$: 314.1751. Found: 314.1752.



(E)-2,6-dimethoxybenzaldehyde O-(3,5-dimethylbenzyl) oxime (3.10a)

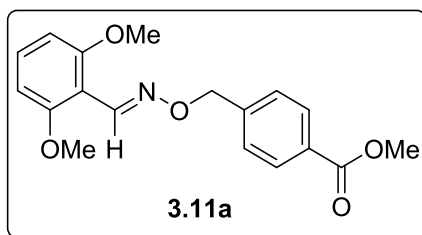
White solid. General Method C: yield 75%. E/Z > 19:1. Mp. 58-60 °C. R_f = 0.5 (Hex/EA=3:1).

IR (KBr) 3004, 2937, 2838, 1595, 1470, 1432, 1356, 1257, 1207, 1113, 1034 cm^{-1} .

^1H NMR (400 MHz, CDCl_3) δ 8.53 (s, 1H), 7.27 (t, J = 8.4 Hz, 1H), 7.10 (dd, J = 1.0, 0.5 Hz, 2H), 6.96 (s, 1H), 6.57 (d, J = 8.4 Hz, 2H), 5.18 (s, 2H), 3.85 (s, 6H), 2.34 (d, J = 0.6 Hz, 6H).

^{13}C NMR (100 MHz, CDCl_3) δ 159.15, 144.76, 137.97, 137.46, 130.96, 129.61, 126.59, 109.49, 104.16, 76.33, 56.18, 21.42.

HRMS calcd. for $\text{C}_{18}\text{H}_{22}\text{NO}_3^+$ $[\text{M}+\text{H}]^+$: 300.1594. Found: 300.1598.



Methyl (E)-4-((((2,6-dimethoxybenzylidene)amino)oxy)methyl)benzoate (3.11a)

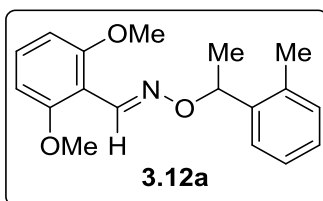
White solid. General Method C: yield 82%. E/Z > 12:1. Mp. 71-73 °C. R_f = 0.3 (Hex/EA=3:1).

IR (KBr) 2949, 2839, 1720, 1595, 1471, 1433, 1279, 1257, 1209, 1113 cm^{-1} .

^1H NMR (400 MHz, CDCl_3) δ 8.51 (s, 1H), 8.01 (dq, $J=8.2, 1.8$, 2H), 7.54 – 7.46 (m, 2H), 7.28 – 7.20 (m, 1H), 6.53 (d, $J=8.4$, 2H), 5.27 (s, 2H), 3.88 (s, 3H), 3.80 (s, 6H).

^{13}C NMR (100 MHz, CDCl_3) δ 167.06, 159.08, 145.13, 143.41, 131.14, 129.64, 129.38, 127.99, 109.12, 104.09, 75.20, 56.11, 52.14.

HRMS calcd. for $\text{C}_{18}\text{H}_{20}\text{NO}_5^+$ $[\text{M}+\text{H}]^+$: 330.1336. Found: 330.1339.



(E)-2,6-dimethoxybenzaldehyde O-(1-(o-tolyl)ethyl) oxime (3.12a)

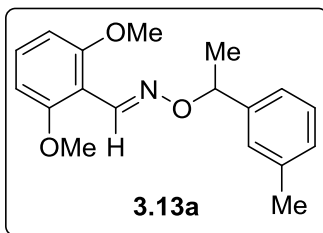
Colorless oil. General Method **B**: yield 78%. E/Z > 19:1. R_f = 0.5 (Hex/EA=3:1).

IR (KBr) 2973, 2935, 2837, 1595, 1470, 1432, 1306, 1285, 1257, 1207 cm^{-1} .

^1H NMR (400 MHz, CDCl_3) δ 8.49 (s, 1H), 7.51 – 7.46 (m, 1H), 7.26 – 7.13 (m, 4H), 6.55 (d, J =8.4, 2H), 5.64 (q, J =6.5, 1H), 3.80 (s, 6H), 2.43 (s, 3H), 1.63 (d, J =6.6, 3H).

^{13}C NMR (100 MHz, CDCl_3) δ 159.08, 144.14, 141.38, 135.33, 130.73, 130.33, 127.17, 126.06, 109.89, 104.27, 77.63, 56.14, 21.02, 19.40.

HRMS calcd. for $\text{C}_{18}\text{H}_{21}\text{NO}_3\text{Na}^+$ $[\text{M}+\text{Na}]^+$: 322.1414. Found: 322.1414.



(E)-2,6-dimethoxybenzaldehyde O-(1-(m-tolyl)ethyl) oxime (3.13a)

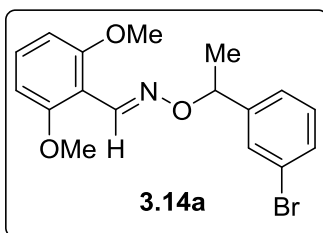
Colorless oil. General Method **B**: yield 67%. E/Z > 19:1. Mp. 41-44 °C. R_f = 0.5 (Hex/EA=3:1).

IR (KBr) 2973, 2934, 2837, 1595, 1432, 1368, 1341, 1306, 1257, 1207 cm^{-1} .

^1H NMR (400 MHz, CDCl_3) δ 8.47 (s, 1H), 7.28 – 7.21 (m, 4H), 7.12 – 7.07 (m, 1H), 6.55 (t, J = 5.7 Hz, 2H), 5.38 (q, J = 6.6 Hz, 1H), 3.79 (s, 6H), 2.37 (s, 3H), 1.63 (d, J = 6.6 Hz, 3H).

^{13}C NMR (100 MHz, CDCl_3) δ 159.10, 144.18, 143.28, 137.82, 130.73, 128.22, 128.17, 127.46, 123.80, 109.93, 104.28, 80.86, 56.16, 22.04, 21.64.

HRMS calcd. for $\text{C}_{18}\text{H}_{21}\text{NO}_3\text{Na}^+$ $[\text{M}+\text{Na}]^+$: 322.1414. Found: 322.1414.



(E)-2,6-dimethoxybenzaldehyde O-(1-(3-bromophenyl)ethyl) oxime (3.14a)

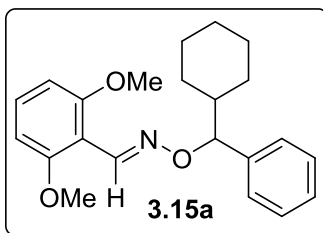
Colorless oil. General Method **B**: yield 96%. E/Z > 19:1. R_f = 0.45 (Hex/EA=3:1).

IR (KBr) 2974, 2934, 2837, 1595, 1470, 1431, 1338, 1306, 1256, 1207, 1113 cm^{-1} .

^1H NMR (400 MHz, CDCl_3) δ 8.46 (s, 1H), 7.58 (q, J = 1.7 Hz, 1H), 7.39 (ddd, J = 7.9, 2.0, 1.1 Hz, 1H), 7.35 – 7.31 (m, 1H), 7.25 – 7.17 (m, 2H), 6.54 (d, J = 8.4 Hz, 2H), 5.35 (q, J = 6.6 Hz, 1H), 3.79 (s, 6H), 1.60 (d, J = 6.6 Hz, 3H).

^{13}C NMR (100 MHz, CDCl_3) δ 159.12, 146.11, 144.65, 130.94, 130.37, 129.92, 129.89, 125.32, 122.43, 109.65, 104.25, 80.03, 56.18, 22.04.

HRMS calcd. for $\text{C}_{17}\text{H}_{18}\text{BrNO}_3\text{Na}^+$ $[\text{M}+\text{Na}]^+$: 386.0362. Found: 386.0362.



(E)-2,6-dimethoxybenzaldehyde O-(cyclohexyl(phenyl)methyl) oxime (3.15a)

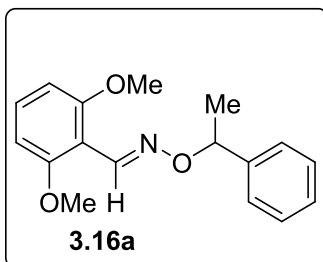
White solid. General Method **B**: yield 67%. E/Z > 19:1. Mp. 109-110 °C. R_f = 0.5 (Hex/EA=3:1).

IR (KBr) 2926, 2851, 1595, 1470, 1451, 1431, 1256, 1207, 1114 cm^{-1} .

^1H NMR (400 MHz, CDCl_3) δ 8.44 (s, 1H), 7.33 (d, $J=0.5$, 2H), 7.32 – 7.30 (m, 2H), 7.24 (ddd, $J=4.9$, 3.6, 2.6, 1H), 7.20 (t, $J=8.3$, 1H), 6.50 (d, $J=8.4$, 2H), 4.99 (d, $J=7.3$, 1H), 3.73 (s, 6H), 2.12 – 2.02 (m, 1H), 1.88 (dtd, $J=11.4$, 7.7, 3.4, 1H), 1.81 – 1.73 (m, 1H), 1.66 (dddd, $J=15.4$, 11.1, 5.5, 2.9, 3H), 1.51 (ddt, $J=12.8$, 3.5, 1.9, 1H), 1.30 – 1.14 (m, 4H).

^{13}C NMR (100 MHz, CDCl_3) δ 159.07, 143.72, 141.82, 130.58, 128.32, 127.81, 127.54, 126.96, 126.76, 110.18, 104.42, 89.62, 79.53, 77.48, 77.36, 77.16, 76.84, 56.14, 45.11, 43.20, 29.50, 29.46, 29.24, 28.97, 26.68, 26.56, 26.35, 26.32, 26.24, 26.15.

HRMS calcd. for $\text{C}_{22}\text{H}_{27}\text{NO}_3\text{Na}^+$ $[\text{M}+\text{Na}]^+$: 376.1883. Found: 376.1884.



(E)-2,6-dimethoxybenzaldehyde O-(1-phenylethyl) oxime (3.16a)

Colorless oil. General Method **B**: yield 74%. E/Z= 14:1. R_f = 0.5 (Hex/EA=3:1).

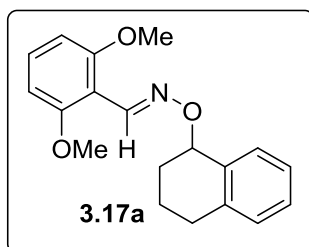
IR (KBr) 2973, 2935, 2837, 1595, 1470, 1432, 1306, 1257, 1209, 1113 cm^{-1} .

Major isomer:

^1H NMR (400 MHz, CDCl_3) δ 8.49 (s, 1H), 7.45 (ddd, J = 6.1, 1.3, 0.6 Hz, 2H), 7.41 – 7.33 (m, 2H), 7.29 (dt, J = 4.4, 1.8 Hz, 1H), 7.24 (t, J = 8.4 Hz, 1H), 6.55 (d, J = 8.4 Hz, 2H), 5.43 (q, J = 6.6 Hz, 1H), 3.79 (s, 6H), 1.66 (d, J = 6.6 Hz, 3H).

^{13}C NMR (100 MHz, CDCl_3) δ 159.07, 144.19, 143.46, 130.75, 128.28, 127.36, 126.70, 109.86, 104.27, 80.78, 56.13, 22.06.

HRMS calcd. for $\text{C}_{17}\text{H}_{20}\text{NO}_3^+$ $[\text{M}+\text{H}]^+$: 308.1257. Found: 308.1258.



**(E)-2,6-dimethoxybenzaldehyde O-(1,2,3,4-tetrahydronaphthalen-1-yl) oxime
(3.17a)**

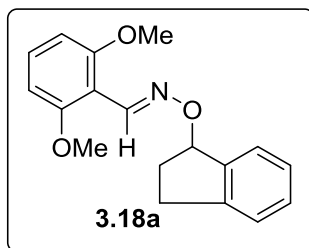
White solid. General Method **A**: 38%. General Method **B**: yield 80%. E/Z > 19:1. Mp. 104-105 °C. R_f = 0.45 (Hex/EA=3:1).

IR (KBr) 3003, 2936, 2836, 1595, 1470, 1432, 1306, 1256 cm^{-1} .

^1H NMR (400 MHz, CDCl_3) δ 8.48 (s, 1H), 7.59 – 7.53 (m, 1H), 7.25 (t, J =8.4, 1H), 7.22 – 7.16 (m, 2H), 7.12 (dd, J =6.6, 2.3, 1H), 6.56 (d, J =8.4, 2H), 5.37 (t, J =4.0, 1H), 3.85 (s, 6H), 2.86 (dt, J =17.0, 4.5, 1H), 2.81 – 2.69 (m, 1H), 2.42 – 2.28 (m, 1H), 2.08 – 1.93 (m, 2H), 1.79 (tdd, J =10.4, 6.7, 4.0, 1H).

^{13}C NMR (100 MHz, CDCl_3) δ 159.11, 144.11, 138.24, 135.39, 130.75, 130.60, 129.02, 127.90, 125.86, 109.88, 104.22, 78.38, 56.20, 29.53, 28.83, 18.53.

HRMS calcd. for $\text{C}_{19}\text{H}_{21}\text{NO}_3\text{Na}^+$ $[\text{M}+\text{Na}]^+$: 334.1414. Found: 334.1418.



(E)-2,6-dimethoxybenzaldehyde O-(2,3-dihydro-1H-inden-1-yl) oxime (3.18a)

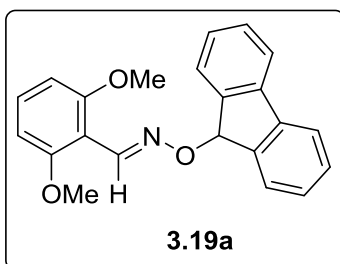
White solid. General Method **B**: yield 78%. E/Z > 19:1. Mp. 154-156 °C. R_f = 0.45 (Hex/EA=3:1).

IR (KBr) 2994, 2946, 2905, 2838, 1608, 1595, 1584, 1260 cm^{-1} .

^1H NMR (400 MHz, CDCl_3) δ 8.37 (s, 1H), 7.30 – 7.24 (m, 3H), 7.21 – 7.17 (m, 2H), 6.57 (d, $J=8.4$, 2H), 5.27 – 5.21 (m, 1H), 3.85 (s, 6H), 3.35 – 3.21 (m, 4H).

^{13}C NMR (100 MHz, CDCl_3) δ 159.06, 144.62, 141.45, 130.84, 126.55, 124.90, 109.74, 104.19, 83.20, 56.19, 39.33.

HRMS calcd. for $\text{C}_{18}\text{H}_{19}\text{NO}_3\text{Na}^+$ $[\text{M}+\text{Na}]^+$: 320.1257. Found: 320.1262.



(E)-2,6-dimethoxybenzaldehyde O-(9H-fluoren-9-yl) oxime (3.19a)

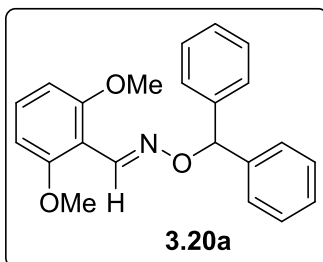
White solid. General Method **B**: yield 94%. E/Z > 19:1. Mp. 151-153 °C. R_f = 0.45 (Hex/EA=3:1).

IR (KBr) 3003, 2938, 2837, 1595, 1470, 1452, 1431, 1303, 1256, 1207, 1186 cm^{-1} .

^1H NMR (400 MHz, CDCl_3) δ 8.56 (s, 1H), 7.87 (ddt, J = 7.4, 1.3, 0.7 Hz, 2H), 7.68 (dd, J = 6.7, 0.8 Hz, 2H), 7.41 (tdd, J = 7.5, 1.2, 0.5 Hz, 2H), 7.34 – 7.28 (m, 3H), 6.61 (d, J = 8.4 Hz, 2H), 6.33 (s, 1H), 3.91 (s, 6H).

^{13}C NMR (100 MHz, CDCl_3) δ 159.25, 145.52, 143.26, 141.05, 131.12, 129.22, 127.61, 126.51, 119.94, 109.52, 104.21, 83.97, 56.21.

HRMS calcd. for $\text{C}_{22}\text{H}_{19}\text{NO}_3\text{Na}^+$ $[\text{M}+\text{Na}]^+$: 368.1257. Found: 368.1261.



(E)-2,6-dimethoxybenzaldehyde O-benzhydryl oxime (3.20a)

White solid. General Method **B**: yield 94%. E/Z > 19:1. Mp. 104-106 °C. R_f = 0.5 (Hex/EA=3:1).

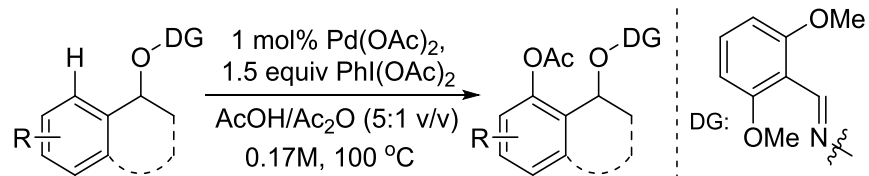
IR (KBr) 3027, 2937, 2837, 1595, 1470, 1431, 1346, 1256, 1113 cm^{-1} .

^1H NMR (400 MHz, CDCl_3) δ 8.59 (s, 1H), 7.48 – 7.40 (m, 4H), 7.38 – 7.32 (m, 4H), 7.30 – 7.26 (m, 2H), 7.24 (dd, J = 11.7, 5.0 Hz, 1H), 6.53 (d, J = 8.4 Hz, 2H), 6.41 (s, 1H), 3.75 (s, 6H).

^{13}C NMR (100 MHz, CDCl_3) δ 159.15, 144.93, 141.77, 130.91, 128.30, 127.82, 127.48, 109.78, 104.34, 86.44, 56.15.

HRMS calcd. for $\text{C}_{22}\text{H}_{22}\text{NO}_3^+$ $[\text{M}+\text{H}]^+$: 348.1594. Found: 348.1596.

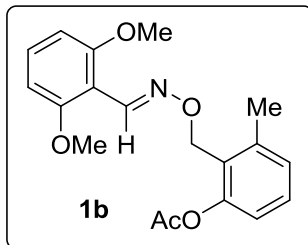
Pd-catalyzed oxidation of *ortho* C–H bonds in benzyl oximes:



General Procedure:

Iodosobenzene diacetate (1.5 equiv) and oxime (0.1 mmol, 1 equiv) were charged in a scintillation vial, followed by 0.5 mL 2mM Pd(OAc)₂ in AcOH solution (0.22 mg, 0.001 mmol, 1 mol%) and 100 μ L Ac₂O. The vial was tightly capped and stirred at 100 °C. The reaction was monitored by TLC. Upon done, the mixture was directly purified by flash column chromatography on silica gel. The E/Z ratio was determined by ¹H NMR spectrum.

Primary Alcohol-Derived Substrates:



1b: Yellow solid. Yield 85%. E/Z = 6.1:1. Mp. 106-108 °C. R_f = 0.3 (Hex/EA=3:1).

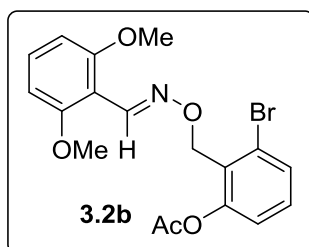
IR (KBr) 2934, 2840, 1763, 1595, 1581, 1468, 1433, 1367, 1256, 1205, 1186 cm^{-1} .

Major isomer:

^1H NMR (400 MHz, CDCl_3) δ 8.45 (s, 1H), 7.25 (td, J = 8.1, 2.4 Hz, 2H), 7.10 (d, J = 7.3 Hz, 1H), 6.94 (d, J = 8.0 Hz, 1H), 6.55 (d, J = 8.4 Hz, 2H), 5.23 (s, 2H), 3.83 (s, 6H), 2.52 (s, 3H), 2.33 (s, 3H).

^{13}C NMR (100 MHz, CDCl_3) δ 169.89, 159.12, 150.32, 144.72, 140.42, 130.97, 129.08, 128.15, 127.59, 120.23, 109.30, 104.11, 67.77, 56.08, 21.10, 19.71.

HRMS calcd. for $\text{C}_{19}\text{H}_{21}\text{NO}_5\text{Na}^+$ $[\text{M}+\text{Na}]^+$: 366.1312. Found: 366.1253.



**(E)-3-bromo-2-((((2,6-dimethoxybenzylidene)amino)oxy)methyl)phenyl acetate
(3.2b)**

White solid. Yield 97%. E/Z = 8.2:1. Mp. 83-85 °C. R_f = 0.3 (Hex/EA=3:1).

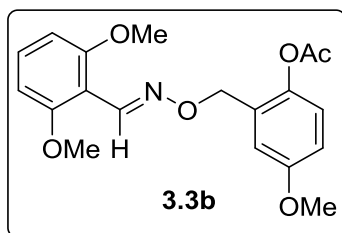
IR (KBr) 3004, 2941, 2894, 2838, 1769, 1595, 1572, 1471, 1447, 1432, 1368, 1257 cm^{-1} .

Major isomer:

^1H NMR (400 MHz, CDCl_3) δ 8.44 (s, 1H), 7.50 (dd, J = 8.0, 1.1 Hz, 1H), 7.24 (dt, J = 12.9, 8.2 Hz, 2H), 7.08 (dd, J = 8.1, 1.1 Hz, 1H), 6.55 (d, J = 8.4 Hz, 2H), 5.37 (s, 2H), 3.83 (s, 6H), 2.33 (s, 3H).

^{13}C NMR (100 MHz, CDCl_3) δ 169.39, 159.19, 151.08, 145.10, 131.07, 130.68, 130.22, 129.58, 126.35, 122.39, 109.24, 104.13, 70.57, 56.11, 21.03.

HRMS calcd. for $\text{C}_{18}\text{H}_{18}\text{BrNO}_5\text{Na}^+$ $[\text{M}+\text{Na}]^+$: 430.0261. Found: 430.0262.



**(E)-2-((((2,6-dimethoxybenzylidene)amino)oxy)methyl)-4-methoxyphenyl acetate
(3.3b)**

Colorless oil. Yield 58%. E/Z = 10:1. R_f = 0.3 (Hex/EA=3:1).

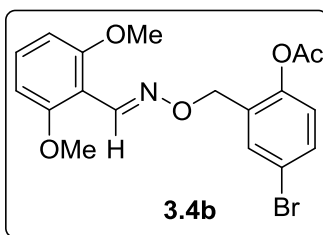
IR (KBr) 2924, 2839, 1759, 1595, 1496, 1469, 1432, 1368, 1257 cm^{-1} .

Major isomer:

^1H NMR (400 MHz, CDCl_3) δ 8.51 (s, 1H), 7.28 (d, J =8.4, 1H), 7.10 (d, J =3.1, 1H), 7.00 (d, J =8.8, 1H), 6.84 (dd, J =8.8, 3.0, 1H), 6.56 (d, J =8.4, 2H), 5.17 (s, 2H), 3.84 (s, 6H), 3.81 (s, 3H), 2.30 (s, 3H).

^{13}C NMR (100 MHz, CDCl_3) δ 169.77, 159.01, 157.25, 144.98, 142.16, 130.96, 130.81, 122.94, 114.90, 113.96, 109.11, 104.00, 70.88, 56.01, 55.57, 20.82.

HRMS calcd. for $\text{C}_{19}\text{H}_{21}\text{NO}_6\text{Na}^+$ $[\text{M}+\text{Na}]^+$: 382.1261. Found: 382.1261.



**(E)-4-bromo-2-((((2,6-dimethoxybenzylidene)amino)oxy)methyl)phenyl acetate
(3.4b)**

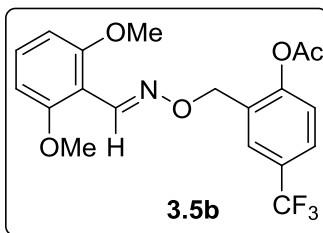
Colorless oil. Yield 74%. E/Z = 14:1. R_f = 0.6 (Hex/EA=3:1).

IR (KBr) 3004, 2934, 2839, 1763, 1595, 1472, 1432, 1368, 1257, 1204, 1171 cm^{-1} .

Major isomer: ^1H NMR (400 MHz, CDCl_3) δ 8.49 (s, 1H), 7.73 (d, J = 2.4 Hz, 1H), 7.44 (dd, J = 8.6, 2.5 Hz, 1H), 7.27 (t, J = 8.4 Hz, 1H), 6.98 (d, J = 8.6 Hz, 1H), 6.56 (d, J = 8.4 Hz, 2H), 5.15 (s, 2H), 3.85 (s, 6H), 2.31 (s, 3H).

^{13}C NMR (100 MHz, CDCl_3) δ 168.95, 159.01, 147.58, 145.28, 132.76, 132.37, 131.56, 131.10, 123.93, 119.04, 108.92, 103.97, 70.06, 56.05, 20.82.

HRMS calcd. for $\text{C}_{18}\text{H}_{18}\text{BrNO}_5\text{Na}^+$ $[\text{M}+\text{Na}]^+$: 430.0261. Found: 430.0260.



(E)-2-((((2,6-dimethoxybenzylidene)amino)oxy)methyl)-4-(trifluoromethyl)phenyl acetate (3.5b)

Colorless oil. Yield 77%. E/Z = 13:1. R_f = 0.3 (Hex/EA=3:1).

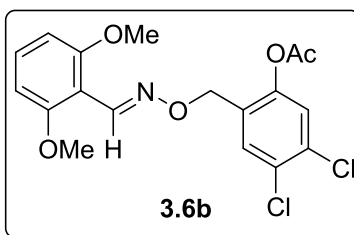
IR (KBr) 2940, 2841, 1770, 1596, 1500, 1472, 1433, 1330 cm^{-1} .

Major isomer:

^1H NMR (400 MHz, CDCl_3) δ 8.49 (s, 1H), 7.85 (dd, J =1.8, 1.0, 1H), 7.61 – 7.55 (m, 1H), 7.27 (d, J =8.4, 1H), 7.21 (dd, J =8.5, 0.9, 1H), 6.54 (d, J =8.5, 2H), 5.21 (s, 2H), 3.81 (s, 6H), 2.33 (s, 3H).

^{13}C NMR (100 MHz, CDCl_3) δ 168.81, 159.23, 151.23 (d, J =1.7), 145.63, 131.48, 131.31, 128.31 (q, J =32.7), 127.35 (q, J =3.7), 125.93 (q, J =3.8), 122.98, 123.88 (q, J =225.4), 109.10, 104.19, 70.32, 56.15, 20.99. ^{19}F NMR (375 MHz, CDCl_3) δ -62.20 (s).

HRMS calcd. for $\text{C}_{19}\text{H}_{19}\text{F}_3\text{NO}_5$ $^+ [\text{M}+\text{H}]^+$: 398.1210. Found: 398.1211.



(E)-4,5-dichloro-2-((((2,6-dimethoxybenzylidene)amino)oxy)methyl)phenyl acetate (3.6b)

White solid. Yield 69%. E/Z = 8.2:1. Mp. 108-109 °C. R_f = 0.25 (Hex/EA=3:1).

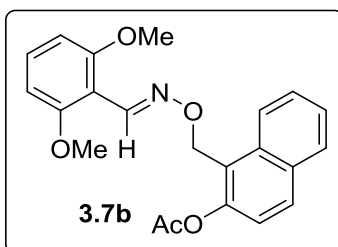
IR (KBr) 2926, 2840, 1768, 1596, 1472, 1432, 1286, 1197, 1114 cm^{-1} .

Major isomer:

^1H NMR (400 MHz, CDCl_3) δ 8.48 (s, 1H), 7.69 (s, 1H), 7.28 (t, J = 8.4 Hz, 1H), 7.24 (s, 1H), 6.57 (d, J = 8.4 Hz, 2H), 5.12 (s, 2H), 3.85 (s, 6H), 2.32 (s, 3H).

^{13}C NMR (100 MHz, CDCl_3) δ 168.63, 159.00, 147.05, 145.47, 131.83, 131.19, 131.12, 130.68, 129.72, 124.34, 108.78, 103.95, 69.62, 56.02, 20.74.

HRMS calcd. for $\text{C}_{18}\text{H}_{17}\text{Cl}_2\text{NO}_5\text{Na}^+$ $[\text{M}+\text{Na}]^+$: 420.0376. Found: 420.0379.



**(E)-1-(((2,6-dimethoxybenzylidene)amino)oxy)methyl)naphthalen-2-yl acetate
(3.7b)**

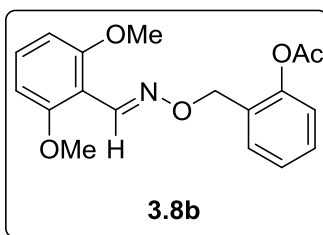
Colorless oil. Yield 84%. E/Z = 6.1:1. R_f = 0.6 (Hex/EA=3:1).

IR (KBr) 3057, 3004, 2940, 2898, 2838, 1762, 1624, 1595, 1471, 1432, 1367, 1257 cm^{-1} .

Major isomer: ^1H NMR (400 MHz, CDCl_3) δ 8.49 (s, 1H), 8.35 – 8.30 (m, 1H), 7.89 – 7.84 (m, 2H), 7.58 (ddd, J =8.4, 6.9, 1.4, 1H), 7.49 (ddd, J =8.0, 6.8, 1.2, 1H), 7.29 – 7.24 (m, 2H), 6.56 (d, J =8.4, 2H), 5.66 (s, 2H), 3.83 (s, 6H), 2.41 (s, 3H).

^{13}C NMR (100 MHz, CDCl_3) δ 169.79, 159.05, 147.62, 144.94, 133.26, 131.92, 130.94, 130.19, 128.31, 126.85, 125.52, 125.03, 123.20, 121.48, 109.12, 103.99, 66.77, 55.99, 21.05.

HRMS calcd. for $\text{C}_{22}\text{H}_{22}\text{NO}_5^+$ $[\text{M}+\text{H}]^+$: 380.1492. Found: 380.1493.



(E)-2-((((2,6-dimethoxybenzylidene)amino)oxy)methyl)phenyl acetate (3.8b)

Colorless oil. Yield 47%. E/Z = 12:1. R_f = 0.3 (Hex/EA=3:1).

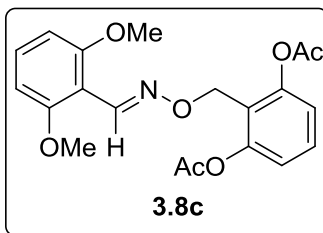
IR (KBr) 3005, 2924, 2852, 1763, 1591, 1472, 1433, 1368, 1254, 1205, 1175, 1113, 1061, 1034 cm^{-1} .

Major isomer:

^1H NMR (400 MHz, CDCl_3) δ 8.50 (s, 1H), 7.59 – 7.54 (m, 1H), 7.34 (ddd, J =8.1, 7.5, 1.8, 1H), 7.28 (d, J =8.3, 1H), 7.24 (dd, J =7.5, 1.3, 1H), 7.10 (dd, J =8.0, 1.3, 1H), 6.56 (d, J =8.4, 2H), 5.21 (s, 2H), 3.84 (s, 6H), 2.32 (s, 3H).

^{13}C NMR (100 MHz, CDCl_3) δ 169.36, 159.00, 148.88, 144.85, 130.93, 130.19, 129.81, 128.86, 125.93, 122.31, 109.16, 104.02, 70.99, 56.01, 20.89.

HRMS calcd. for $\text{C}_{18}\text{H}_{19}\text{NO}_5\text{Na}^+$ $[\text{M}+\text{Na}]^+$: 352.1155. Found: 352.1155.



**(E)-2-((((2,6-dimethoxybenzylidene)amino)oxy)methyl)-1,3-phenylene diacetate
(3.8c)**

Colorless oil. Yield 51%. E/Z = 7.7:1. R_f = 0.1 (Hex/EA=3:1).

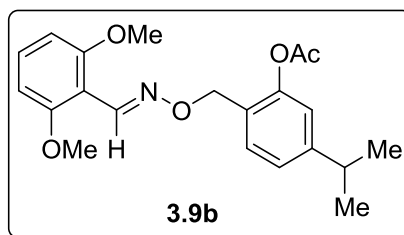
IR (KBr) 3004, 2924, 2851, 1764, 1595, 1470, 1432, 1257, 1206, 1176, 1112 cm^{-1} .

Major isomer:

^1H NMR (400 MHz, CDCl_3) δ 8.39 (s, 1H), 7.37 (dd, J =8.4, 8.0, 1H), 7.26 (t, J =8.4, 1H), 7.04 (d, J =8.2, 2H), 6.56 (d, J =8.4, 2H), 5.17 (s, 2H), 3.83 (s, 6H), 2.32 (s, 6H).

^{13}C NMR (100 MHz, CDCl_3) δ 169.20, 159.02, 150.54, 144.79, 130.95, 129.21, 122.35, 120.37, 109.12, 104.02, 65.73, 55.98, 20.92.

HRMS calcd. for $\text{C}_{20}\text{H}_{21}\text{NO}_7\text{Na}^+$ $[\text{M}+\text{Na}]^+$: 410.1210. Found: 410.1210.



(E)-2-((((2,6-dimethoxybenzylidene)amino)oxy)methyl)-5-isopropylphenyl acetate (3.9b)

Colorless oil. Yield 11%. E/Z >19:1. R_f = 0.3 (Hex/EA=3:1).

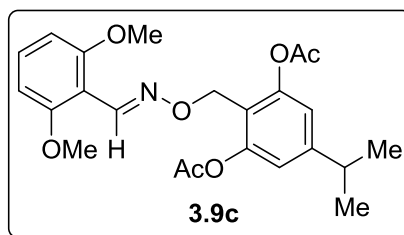
IR (KBr) 3003, 2961, 2934, 2872, 2839, 1767, 1620, 1595, 1577, 1506, 1471, 1432, 1368, 1257 cm^{-1} .

Major isomer:

^1H NMR (400 MHz, CDCl_3) δ 8.49 (s, 1H), 7.47 (d, $J=7.9$, 1H), 7.29 – 7.23 (m, 1H), 7.12 (dd, $J=7.9$, 1.7, 1H), 6.95 (d, $J=1.7$, 1H), 6.56 (d, $J=8.4$, 2H), 5.17 (s, 2H), 3.84 (s, 6H), 2.91 (hept, $J=6.9$, 1H), 2.31 (s, 3H), 1.25 (d, $J=6.9$, 6H).

^{13}C NMR (100 MHz, CDCl_3) δ 169.30, 158.99, 150.84, 150.35, 144.61, 130.86, 119.44, 118.49, 109.17, 103.99, 65.80, 55.97, 33.81, 23.54, 20.92.

HRMS calcd. for $\text{C}_{21}\text{H}_{26}\text{NO}_5$ $[\text{M}+\text{H}]^+$: 372.1805. Found: 372.1806.



(E)-2-((((2,6-dimethoxybenzylidene)amino)oxy)methyl)-5-isopropyl-1,3-phenylene diacetate (3.9c)

Colorless oil. Yield 63%. E/Z > 19:1. R_f = 0.1 (Hex/EA=3:1).

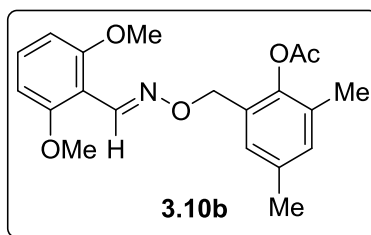
IR (KBr) 3003, 2962, 2935, 2872, 2840, 1769, 1626, 1596, 1577, 1471, 1432, 1368 cm^{-1} .

Major isomer:

^1H NMR (400 MHz, CDCl_3) δ 8.39 (s, 1H), 7.29 – 7.24 (m, 1H), 6.89 (s, 2H), 6.56 (d, J = 8.4 Hz, 2H), 5.12 (s, 2H), 3.83 (s, 6H), 2.96 – 2.85 (m, 1H), 2.31 (s, 6H), 1.24 (d, J = 6.9 Hz, 6H).

^{13}C NMR (100 MHz, CDCl_3) δ 169.30, 158.99, 150.84, 150.35, 144.61, 130.86, 119.44, 118.49, 109.17, 103.99, 65.80, 55.97, 33.81, 23.54, 20.92.

HRMS calcd. for $\text{C}_{23}\text{H}_{28}\text{NO}_7^+$ $[\text{M}+\text{H}]^+$: 430.1860. Found: 430.1862.



**(E)-2-((((2,6-dimethoxybenzylidene)amino)oxy)methyl)-4,6-dimethylphenyl acetate
(3.10b)**

Colorless oil. Yield 55%. E/Z = 14:1. R_f = 0.6 (Hex/EA=3:1).

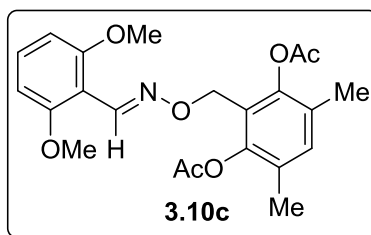
IR (KBr) 2936, 2839, 1758, 1595, 1472, 1432, 1368, 1257, 1213, 1188 cm^{-1} .

Major isomer:

^1H NMR (400 MHz, CDCl_3) δ 8.49 (s, 1H), 7.27 (t, J = 8.4 Hz, 1H), 7.18 (d, J = 1.5 Hz, 1H), 7.01 (s, 1H), 6.56 (d, J = 8.4 Hz, 2H), 5.14 (s, 2H), 3.84 (s, 6H), 2.32 (s, 3H), 2.32 (s, 3H), 2.14 (s, 3H).

^{13}C NMR (100 MHz, CDCl_3) δ 169.13, 159.00, 145.63, 144.74, 135.42, 131.39, 130.86, 130.17, 129.22, 128.46, 109.25, 104.02, 71.48, 56.01, 20.86, 20.53, 16.13.

HRMS calcd. for $\text{C}_{20}\text{H}_{23}\text{NO}_5\text{Na}^+$ $[\text{M}+\text{Na}]^+$: 380.1468. Found: 380.1470.



(E)-2-((((2,6-dimethoxybenzylidene)amino)oxy)methyl)-4,6-dimethyl-1,3-phenylene diacetate (3.10c)

Colorless oil. Yield 30%. E/Z > 19:1. R_f = 0.6 (Hex/EA=3:1).

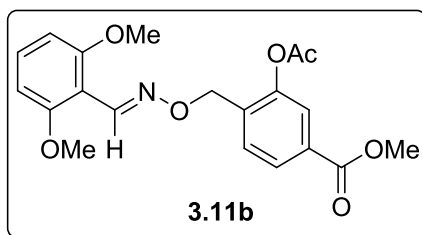
IR (KBr) 3005, 2989, 1762, 1595, 1472, 1433, 1275, 1259, 1193, 1113 cm^{-1} .

Major isomer:

^1H NMR (400 MHz, CDCl_3) δ 8.37 (s, 1H), 7.24 (t, J = 8.4 Hz, 2H), 7.09 (s, 1H), 6.54 (d, J = 8.4 Hz, 2H), 5.07 (s, 2H), 3.81 (s, 6H), 2.31 (s, 6H), 2.12 (d, J = 0.7 Hz, 6H).

^{13}C NMR (100 MHz, CDCl_3) δ 169.17, 159.30, 147.30, 144.97, 132.91, 131.11, 128.66, 122.26, 109.57, 104.33, 66.75, 56.24, 20.79, 16.33.

HRMS calcd. for $\text{C}_{22}\text{H}_{25}\text{NO}_7\text{Na}^+$ $[\text{M}+\text{Na}]^+$: 438.1523. Found: 438.1524.



Methyl (E)-3-acetoxy-4-(((2,6-dimethoxybenzylidene)amino)oxy)methyl)benzoate (3.11b)

Colorless oil. Yield 44%. E/Z = 7.9:1. R_f = 0.2 (Hex/EA=3:1).

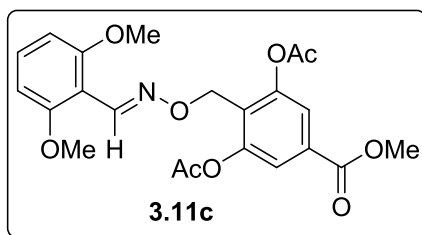
IR (KBr) 3004, 2951, 2840, 1769, 1723, 1596, 1501, 1472, 1434, 1415, 1369, 1289, 1258 cm^{-1} .

Major isomer:

^1H NMR (400 MHz, CDCl_3) δ 8.52 (s, 1H), 7.93 (dd, J =8.0, 1.7, 1H), 7.76 (d, J =1.6, 1H), 7.67 – 7.64 (m, 1H), 7.27 (t, J =8.4, 1H), 6.56 (d, J =8.4, 2H), 5.24 (s, 2H), 3.91 (s, 3H), 3.83 (s, 6H), 2.34 (s, 3H).

^{13}C NMR (100 MHz, CDCl_3) δ 168.98, 166.11, 159.00, 148.33, 145.26, 135.45, 131.12, 130.61, 129.57, 127.04, 123.49, 108.90, 103.99, 70.44, 56.02, 52.24, 20.80.

HRMS calcd. for $\text{C}_{20}\text{H}_{22}\text{NO}_7$ $[\text{M}+\text{H}]^+$: 388.1391. Found: 388.1390.



(E)-2-((((2,6-dimethoxybenzylidene)amino)oxy)methyl)-5-(methoxycarbonyl)-1,3-phenylene diacetate (3.11c)

Colorless oil. Yield 53%. E/Z > 19:1. R_f = 0.35 (Hex/EA=1:1).

IR (KBr) 2952, 2841, 1771, 1725, 1596, 1434, 1421, 1368, 1308 cm^{-1} .

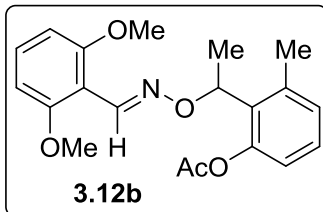
Major isomer:

^1H NMR (400 MHz, CDCl_3) δ 8.37 (s, 1H), 7.70 (s, 2H), 7.29 – 7.23 (m, 1H), 6.55 (d, J = 8.4 Hz, 2H), 5.18 (s, 2H), 3.90 (s, 3H), 3.82 (s, 6H), 2.34 (s, 6H).

^{13}C NMR (100 MHz, CDCl_3) δ 168.89, 165.25, 159.03, 150.37, 145.12, 131.28, 131.07, 127.50, 121.57, 108.91, 104.01, 65.60, 55.97, 52.47, 20.84.

HRMS calcd. for $\text{C}_{22}\text{H}_{23}\text{NO}_9\text{Na}^+$ $[\text{M}+\text{Na}]^+$: 468.1265. Found: 468.1263.

Secondary Alcohol-Derived Substrates:



**(E)-2-(1-(((2,6-dimethoxybenzylidene)amino)oxy)ethyl)-3-methylphenyl acetate
(3.12b)**

Colorless oil. Yield 87%. E/Z = 14:1. R_f = 0.6 (Hex/EA=3:1).

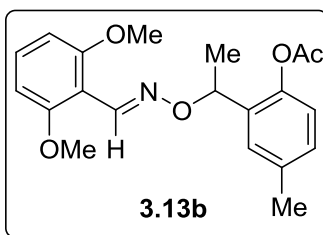
IR (KBr) 2972, 2937, 2838, 1766, 1595, 1471, 1432, 1367, 1306, 1284, 1256, 1206 cm^{-1} .

Major isomer:

^1H NMR (400 MHz, CDCl_3) δ 8.36 (s, 1H), 7.22 (t, $J=8.4$, 1H), 7.17 (t, $J=7.8$, 1H), 7.04 (ddd, $J=7.6$, 1.4, 0.7, 1H), 6.90 – 6.85 (m, 1H), 6.52 (d, $J=8.4$, 2H), 5.74 (q, $J=6.9$, 1H), 3.77 (s, 6H), 2.49 (s, 3H), 2.34 (s, 3H), 1.65 (d, $J=6.9$, 3H).

^{13}C NMR (100 MHz, CDCl_3) δ 169.95, 159.13, 149.13, 143.90, 137.93, 133.02, 130.76, 128.78, 127.87, 121.18, 109.89, 104.40, 76.36, 56.18, 21.47, 20.43, 19.31.

HRMS calcd. for $\text{C}_{20}\text{H}_{24}\text{NO}_5^+$ $[\text{M}+\text{H}]^+$: 358.1649. Found: 358.1651.



**(E)-2-(1-(((2,6-dimethoxybenzylidene)amino)oxy)ethyl)-4-methylphenyl acetate
(3.13b)**

Colorless oil. Yield 52%. E/Z= 16:1. R_f = 0.6 (Hex/EA=3:1).

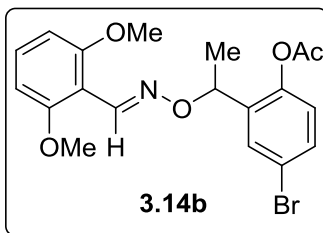
IR (KBr) 2975, 2934, 2839, 1762, 1595, 1496, 1471, 1433, 1369, 1306, 1285, 1257, 1190, 1158, 1113 cm^{-1} .

Major isomer:

^1H NMR (400 MHz, CDCl_3) δ 8.45 (s, 1H), 7.34 (d, J =1.9, 1H), 7.23 (d, J =8.4, 1H), 7.09 (ddd, J =8.2, 2.2, 0.6, 1H), 6.94 (d, J =8.2, 1H), 6.54 (d, J =8.4, 2H), 5.51 (q, J =6.6, 1H), 3.80 (s, 6H), 2.36 (s, 3H), 2.31 (s, 3H), 1.58 (d, J =6.6, 3H).

^{13}C NMR (100 MHz, CDCl_3) δ 169.84, 159.11, 145.74, 144.43, 135.77, 134.63, 130.84, 128.87, 128.11, 122.20, 109.79, 104.30, 75.57, 56.17, 21.24, 21.19, 21.17.

HRMS calcd. for $\text{C}_{20}\text{H}_{24}\text{NO}_5^+$ $[\text{M}+\text{H}]^+$: 358.1649. Found: 358.1650.



**(E)-4-bromo-2-(1-(((2,6-dimethoxybenzylidene)amino)oxy)ethyl)phenyl acetate
(3.14b)**

Colorless oil. Yield 57%. E/Z > 19:1. R_f = 0.6 (Hex/EA=3:1).

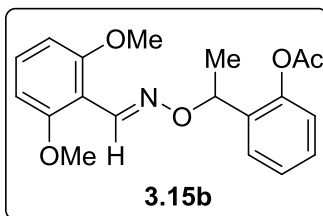
IR (KBr) 2932, 2838, 1764, 1595, 1472, 1432, 1257, 1203, 1172, 1113, 1088 cm^{-1} .

Major isomer:

^1H NMR (400 MHz, CDCl_3) δ 8.46 (s, 1H), 7.67 (d, J = 2.4 Hz, 1H), 7.38 (s, 1H), 7.25 (t, J = 8.4 Hz, 1H), 6.96 (d, J = 8.6 Hz, 1H), 6.54 (d, J = 8.4 Hz, 2H), 5.49 (q, J = 6.6 Hz, 1H), 3.80 (s, 6H), 2.32 (s, 3H), 1.55 (d, J = 6.6 Hz, 3H).

^{13}C NMR (100 MHz, CDCl_3) δ 169.01, 158.98, 146.72, 144.82, 137.56, 130.88, 130.87, 130.62, 124.09, 119.21, 109.36, 104.10, 74.95, 56.02, 20.96.

HRMS calcd. for $\text{C}_{19}\text{H}_{20}\text{BrNO}_5\text{Na}^+$ $[\text{M}+\text{Na}]^+$: 444.0417. Found: 444.0411.



(E)-2-(1-(((2,6-dimethoxybenzylidene)amino)oxy)ethyl)phenyl acetate (3.15b)

Colorless oil. Yield 50%. E/Z= 9.6:1. R_f = 0.6 (Hex/EA=3:1).

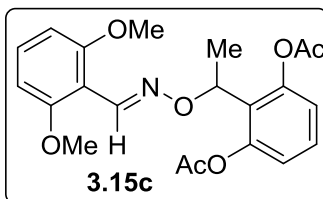
IR (KBr) 2959, 2931, 1764, 1595, 1472, 1257, 1205, 1113, 1075 cm^{-1} .

Major isomer:

^1H NMR (400 MHz, CDCl_3) δ 8.45 (s, 1H), 7.56 – 7.52 (m, 1H), 7.31 – 7.27 (m, 1H), 7.26 – 7.24 (m, 1H), 7.22 (d, $J=8.3$, 1H), 7.08 – 7.04 (m, 1H), 6.54 (d, $J=8.4$, 2H), 5.55 (q, $J=6.6$, 1H), 3.79 (s, 6H), 2.32 (s, 3H), 1.59 (d, $J=6.6$, 3H).

^{13}C NMR (100 MHz, CDCl_3) δ 169.43, 158.98, 147.87, 144.32, 135.09, 130.71, 128.05, 127.54, 126.03, 122.35, 109.66, 104.20, 75.41, 56.04, 21.04, 20.98.

HRMS calcd. for $\text{C}_{19}\text{H}_{22}\text{NO}_5^+$ $[\text{M}+\text{H}]^+$: 344.1492. Found: 344.1497.



**(E)-2-(1-(((2,6-dimethoxybenzylidene)amino)oxy)ethyl)-1,3-phenylene diacetate
(3.15c)**

Colorless oil. Yield 42%. E/Z > 19:1. R_f = 0.6 (Hex/EA=3:1).

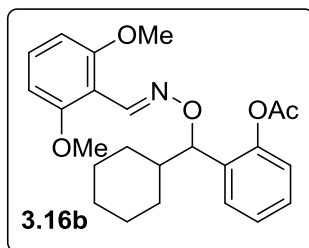
IR (KBr) 2938, 2840, 1767, 1595, 1470, 1433, 1368, 1258, 1188, 1112, 1033 cm^{-1} .

Major isomer:

^1H NMR (400 MHz, CDCl_3) δ 8.30 (s, 1H), 7.33 – 7.28 (m, 1H), 7.22 (t, J = 8.4 Hz, 1H), 6.97 (d, J = 8.2 Hz, 2H), 6.52 (d, J = 8.4 Hz, 2H), 5.61 (q, J = 6.8 Hz, 1H), 3.78 (s, 6H), 2.35 (s, 6H), 1.66 (d, J = 6.8 Hz, 3H).

^{13}C NMR (100 MHz, CDCl_3) δ 169.25, 158.99, 149.30, 144.02, 130.69, 128.15, 127.61, 120.93, 109.58, 104.27, 74.25, 56.05, 21.15, 19.16.

HRMS calcd. for $\text{C}_{21}\text{H}_{23}\text{NO}_7\text{Na}^+$ $[\text{M}+\text{Na}]^+$: 424.1367. Found: 424.1370.



**(E)-2-(cyclohexyl(((2,6-dimethoxybenzylidene)amino)oxy)methyl)phenyl acetate
(3.16b)**

With 3 equiv $\text{PhI}(\text{OAc})_2$. Yellow wax. Yield 76%. E/Z > 19:1. R_f = 0.1 (Hex/EA=3:1).

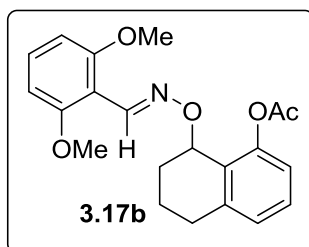
IR (KBr) 2929, 2851, 1771, 1595, 1469, 1432, 1367, 1257, 1185 cm^{-1} .

Major isomer:

^1H NMR (400 MHz, CDCl_3) δ 8.24 (s, 1H), 7.30 – 7.27 (m, 1H), 7.17 (t, J =8.4, 1H), 6.97 (d, J =8.1, 2H), 6.48 (d, J =8.4, 2H), 5.30 (d, J =9.7, 1H), 3.73 (s, 6H), 2.34 (s, 6H), 2.32 – 2.22 (m, 1H), 1.85 – 1.74 (m, 1H), 1.71 – 1.56 (m, 3H), 1.38 – 1.13 (m, 5H), 0.86 (qd, J =12.8, 12.3, 3.2, 1H).

^{13}C NMR (100 MHz, CDCl_3) δ 168.88, 159.00, 149.71, 143.54, 130.46, 127.66, 126.32, 120.63, 109.81, 104.39, 82.96, 56.00, 41.11, 30.73, 29.44, 26.42, 26.14, 26.03, 21.32.

HRMS calcd. for $\text{C}_{21}\text{H}_{23}\text{NO}_5\text{Na}^+$ $[\text{M}+\text{Na}]^+$: 392.1468. Found: 392.1470.



(E)-8-(((2,6-dimethoxybenzylidene)amino)oxy)-5,6,7,8-tetrahydronaphthalen-1-yl acetate (3.17b)

White solid. Yield 83%. E/Z > 19:1. Mp. 161-163 °C. R_f = 0.35 (Hex/EA=3:1).

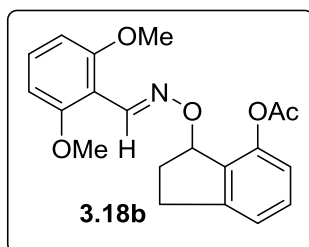
IR (KBr) 2937, 2838, 1763, 1654, 1594, 1472, 1432, 1369, 1256, 1202, 1112 cm^{-1} .

Major isomer:

^1H NMR (400 MHz, CDCl_3) δ 8.37 (s, 1H), 7.30 – 7.26 (m, 1H), 7.05 (d, J = 7.7 Hz, 1H), 6.95 (d, J = 7.9 Hz, 1H), 6.57 (d, J = 8.4 Hz, 2H), 5.46 (t, J = 2.9 Hz, 1H), 3.91 (s, 1H), 3.84 (s, 6H), 3.73 (s, 1H), 2.88 (d, J = 16.7 Hz, 1H), 2.56 – 2.47 (m, 1H), 2.27 (s, 3H), 2.13 – 1.91 (m, 2H), 1.82 – 1.72 (m, 2H).

^{13}C NMR (100 MHz, CDCl_3) δ 169.87, 158.91, 150.55, 143.93, 140.56, 130.62, 128.52, 126.75, 126.72, 120.34, 109.77, 104.10, 73.02, 56.01, 29.41, 28.19, 20.86, 17.26.

HRMS calcd. for $\text{C}_{21}\text{H}_{23}\text{NO}_5\text{Na}^+$ $[\text{M}+\text{Na}]^+$: 392.1468. Found: 392.1470.



**(E)-3-(((2,6-dimethoxybenzylidene)amino)oxy)-2,3-dihydro-1H-inden-4-yl acetate
(3.18b)**

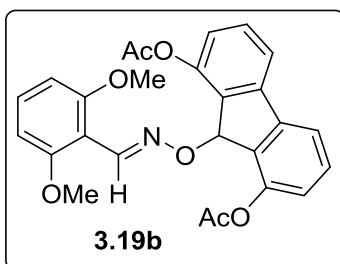
Colorless oil. Yield 75%. E/Z = 11:1. R_f = 0.35 (Hex/EA=3:1).

IR (KBr) 2940, 2839, 1762, 1595, 1470, 1432, 1256, 1207 cm^{-1} .

^1H NMR (400 MHz, CDCl_3) δ 8.39 (s, 1H), 7.30 (ddd, J =8.0, 7.5, 0.5, 1H), 7.25 (t, J =8.4, 1H), 7.15 (ddd, J =7.5, 1.0, 0.5, 1H), 6.93 (dq, J =8.0, 0.8, 1H), 6.56 (d, J =8.4, 2H), 5.90 – 5.83 (m, 1H), 3.83 (s, 6H), 3.18 (dddt, J =14.3, 8.5, 6.7, 0.9, 1H), 2.88 (dddt, J =16.2, 8.6, 4.6, 0.8, 1H), 2.55 – 2.34 (m, 2H), 2.26 (s, 3H).

^{13}C NMR (100 MHz, CDCl_3) δ 169.54, 159.10, 148.32, 147.75, 144.19, 133.73, 130.83, 130.21, 122.66, 120.08, 109.78, 104.25, 85.16, 56.14, 32.20, 30.71, 21.01.

HRMS calcd. for $\text{C}_{20}\text{H}_{21}\text{NO}_5\text{Na}^+$ $[\text{M}+\text{Na}]^+$: 378.1312. Found: 378.1311.



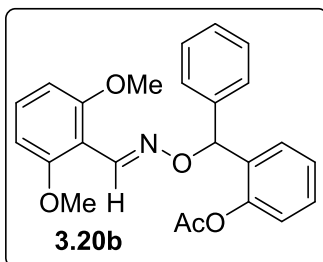
(E)-9-(((2,6-dimethoxybenzylidene)amino)oxy)-9H-fluorene-1,8-diyl diacetate (3.19b)

With 3 equiv $\text{PhI}(\text{OAc})_2$. Yellow wax. Yield 99%. E/Z=6.0:1. R_f = 0.1 (Hex/EA=3:1).

IR (KBr) 3009, 2937, 2840, 1759, 1591, 1480, 1470, 1433, 1368, 1256, 1194 cm^{-1} . Major isomer: ^1H NMR (400 MHz, CDCl_3) δ 8.45 (s, 1H), 7.53 (dd, J = 7.5, 0.8 Hz, 2H), 7.41 (dd, J = 11.8, 4.1 Hz, 2H), 7.27 (t, J = 8.4 Hz, 1H), 7.01 (dd, J = 8.0, 0.8 Hz, 2H), 6.56 (d, J = 8.4 Hz, 2H), 6.48 (s, 1H), 3.80 (s, 6H), 2.20 (s, 6H).

^{13}C NMR (100 MHz, CDCl_3) δ 169.24, 159.15, 148.67, 144.25, 142.45, 134.60, 131.00, 130.81, 122.00, 118.00, 109.46, 104.23, 83.64, 56.01, 20.94.

HRMS calcd. for $\text{C}_{26}\text{H}_{24}\text{NO}_7^+$ $[\text{M}+\text{H}]^+$: 462.1547. Found: 462.1546.



(E)-2-((((2,6-dimethoxybenzylidene)amino)oxy)(phenyl)methyl)phenyl acetate (3.20b)

With 1 equiv $\text{PhI}(\text{OAc})_2$. Colorless oil. Yield 45%. E/Z > 19:1. R_f = 0.3 (Hex/EA=3:1).

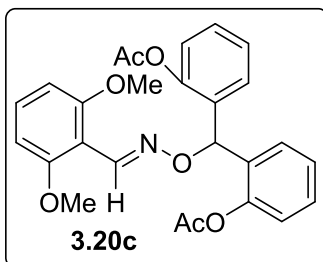
IR (KBr) 2934, 2839, 1766, 1595, 1471, 1453, 1432, 1257, 1202, 1171, 1113 cm^{-1} .

Major isomer:

^1H NMR (400 MHz, CDCl_3) δ 8.55 (s, 1H), 7.49 (dd, J = 7.7, 1.8 Hz, 1H), 7.38 (dt, J = 2.9, 1.9 Hz, 2H), 7.36 – 7.27 (m, 4H), 7.26 – 7.21 (m, 2H), 7.10 (dd, J = 8.0, 1.3 Hz, 1H), 6.56 (s, 1H), 6.53 (t, J = 5.6 Hz, 2H), 3.76 (s, 6H), 2.16 (d, J = 1.3 Hz, 3H).

^{13}C NMR (100 MHz, CDCl_3) δ 168.95, 159.00, 148.33, 144.95, 140.25, 133.29, 130.83, 128.87, 128.34, 128.15, 127.82, 127.59, 125.72, 122.66, 109.47, 104.14, 81.47, 55.98, 20.87.

HRMS calcd. for $\text{C}_{24}\text{H}_{24}\text{NO}_5^+$ $[\text{M}+\text{H}]^+$: 406.1649. Found: 406.1648.



(E)-(((2,6-dimethoxybenzylidene)amino)oxy)methylene)bis(2,1-phenylene) diacetate (3.20c)

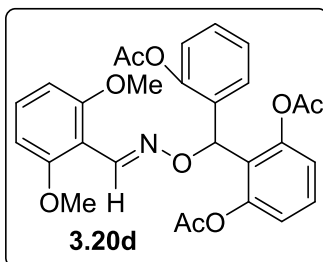
With 1 equiv $\text{PhI}(\text{OAc})_2$. Colorless oil. Yield 49%. E/Z > 19:1. R_f = 0.1 (Hex/EA=3:1).

IR (KBr) 2936, 2840, 1766, 1595, 1471, 1432, 1369, 1257 cm^{-1} .

Major isomer: ^1H NMR (400 MHz, CDCl_3) δ 8.51 (s, 1H), 7.37 – 7.31 (m, 4H), 7.25 – 7.19 (m, 3H), 7.14 – 7.10 (m, 2H), 6.73 (s, 1H), 6.53 (d, J = 8.4 Hz, 2H), 3.76 (s, 6H), 2.15 (s, 6H).

^{13}C NMR (100 MHz, CDCl_3) δ 169.20, 159.15, 148.81, 145.21, 131.87, 131.06, 129.38, 128.87, 125.86, 122.84, 109.52, 104.26, 77.18, 56.10, 20.90.

HRMS calcd. for $\text{C}_{26}\text{H}_{26}\text{NO}_7^+$ $[\text{M}+\text{H}]^+$: 464.1704. Found: 464.1702.



(E)-2-((2-acetoxyphenyl)(((2,6-dimethoxybenzylidene)amino)oxy)methyl)-1,3-phenylene diacetate (3.20d)

With 5 equiv $\text{PhI}(\text{OAc})_2$. Colorless oil. Yield 47%. E/Z = 7.0:1. R_f = 0.45 (Hex/EA=1:1).

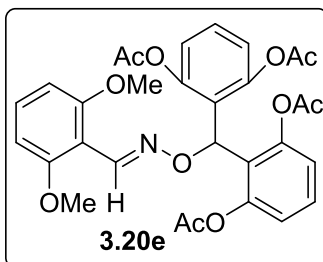
IR (KBr) 3062, 3007, 2939, 2840, 1768, 1595, 1471, 1433, 1369, 1257, 1179, 1113, 1025 cm^{-1} .

Major isomer:

^1H NMR (400 MHz, CDCl_3) δ 8.45 (s, 1H), 7.58 – 7.52 (m, 1H), 7.38 – 7.33 (m, 1H), 7.33 – 7.28 (m, 1H), 7.26 – 7.20 (m, 2H), 7.07 (dd, J =8.0, 1.3, 1H), 7.03 (d, J =8.2, 2H), 6.79 (s, 1H), 6.52 (d, J =8.4, 2H), 3.77 (s, 6H), 2.13 (s, 3H), 2.12 (s, 6H).

^{13}C NMR (100 MHz, CDCl_3) δ 169.05, 168.64, 159.05, 149.82, 148.16, 144.89, 131.77, 130.87, 128.71, 128.61, 128.36, 125.37, 124.56, 122.53, 120.81, 109.28, 104.13, 75.28, 55.92, 20.84, 20.76.

HRMS calcd. for $\text{C}_{28}\text{H}_{28}\text{NO}_9$ $[\text{M}+\text{H}]^+$: 522.1759. Found: 522.1755.



(E)-((((2,6-dimethoxybenzylidene)amino)oxy)methylene)bis(benzene-2,1,3-triyl) tetraacetate (3.20e)

With 5 equiv $\text{PhI}(\text{OAc})_2$. White solid. Yield 37%. E/Z > 19:1. Mp. > 200 °C. R_f = 0.35 (Hex/EA=1:1).

IR (KBr) 2924, 2849, 1762, 1607, 1593, 1577, 1470, 1435, 1256, 1182, 1110, 1044, 1022 cm^{-1} .

Major isomer:

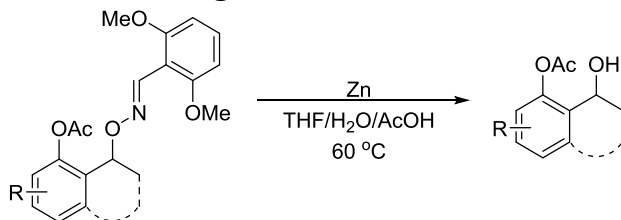
^1H NMR (400 MHz, CDCl_3) δ 8.26 (s, 1H), 7.33 (t, J = 8.2 Hz, 2H), 7.21 (t, J = 8.4 Hz, 1H), 7.01 (d, J = 8.2 Hz, 4H), 6.90 (s, 1H), 6.50 (d, J = 8.4 Hz, 2H), 3.74 (s, 6H), 2.12 (s, 12H).

^{13}C NMR (100 MHz, CDCl_3) δ 168.99, 159.20, 149.76, 144.92, 131.02, 128.46, 124.61, 120.94, 109.33, 104.29, 74.46, 56.03, 21.03.

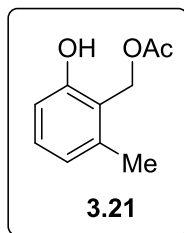
HRMS calcd. for $\text{C}_{28}\text{H}_{27}\text{NO}_9\text{Na}^+$ $[\text{M}+\text{Na}]^+$: 602.1633. Found: 602.1631.

Removal of the directing group: N–O bond cleavage and C–O bond cleavage:

General procedure for N–O cleavage:



To a solution of oxime (0.1 mmol, 1 equiv) in 1.2 mL AcOH-THF-water (3:1:1), zinc powder (65 mg, 1 mmol, 10 equiv) was added in one portion at room temperature. Then the mixture was stirred at 60 °C. The reaction was monitored by TLC. After 2.5 h, the mixture was quenched with 5 mL water and extracted with EA (10 mL×3), the combined organic layer was dried over Na₂SO₄, the solvent was removed under reduced pressure. The desired compound was purified by flash column chromatography on silica gel (Hex/EA 10:1 to 5:1).



2-hydroxy-6-methylbenzyl acetate (3.21)

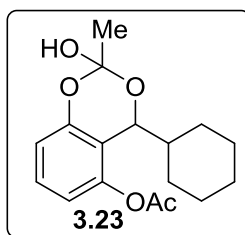
Colorless oil. Yield 92%. $R_f = 0.45$ (Hex/EA=1:1).

IR (KBr) 3354, 2923, 2853, 1710, 1611, 1591, 1468, 1384, 1362 cm^{-1} .

^1H NMR (400 MHz, CDCl_3) δ 7.98 (s, broad, 1H), 7.17 (dd, $J=8.4, 7.4$, 1H), 6.80 (dddd, $J=14.8, 7.5, 1.2, 0.6$, 2H), 5.19 (s, 2H), 2.41 (t, $J=0.7$, 3H), 2.10 (s, 3H).

^{13}C NMR (100 MHz, CDCl_3) δ 173.97, 156.01, 139.83, 130.57, 122.47, 120.83, 115.88, 59.87, 20.87, 19.27.

HRMS: calcd. $\text{C}_{10}\text{H}_{12}\text{O}_3^+ [\text{M}]^+$: 180.0786. Found: 180.0785.



4-cyclohexyl-2-hydroxy-2-methyl-4H-benzo[d][1,3]dioxin-5-yl acetate (3.23)

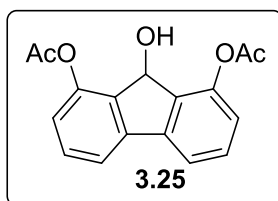
Colorless oil. Yield 95%. $R_f = 0.45$ (Hex/EA=1:1).

IR (KBr) 3426, 2930, 2852, 1765, 1740, 1612, 1594, 1466, 1370 cm^{-1} .

^1H NMR (400 MHz, CDCl_3) δ 7.17 (t, $J=8.2$, 1H), 6.76 (dd, $J=8.3$, 1.1, 1H), 6.63 (dd, $J=8.1$, 1.1, 1H), 6.61 (s, 1H), 5.80 (d, $J=9.8$, 1H), 2.33 (s, 3H), 2.06 (s, 3H), 1.81 – 1.73 (m, 1H), 1.72 – 1.58 (m, 3H), 1.36 – 1.28 (m, 1H), 1.24 – 1.11 (m, 3H), 1.08 – 0.83 (m, 2H).

^{13}C NMR (100 MHz, CDCl_3) δ 169.22, 155.93, 149.29, 129.37, 115.38, 115.35, 115.32, 115.18, 74.25, 40.21, 29.97, 28.82, 26.10, 25.69, 25.54, 21.09, 20.77.

HRMS: calcd. $\text{C}_{17}\text{H}_{22}\text{O}_5\text{Na}^+$ $[\text{M}+\text{Na}]^+$: 329.1359. Found: 329.1347. *The compound is unstable.*



9-hydroxy-9H-fluorene-1,8-diyl diacetate (3.25)

White solid. Yield 84%. R_f = 0.45 (Hex/EA=1:1). Mp. 165-167°C.

IR (KBr) 3452, 2924, 2360, 1759, 1619, 1586, 1481, 1207 cm^{-1} .

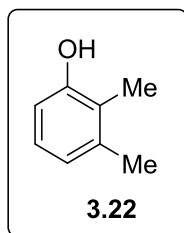
^1H NMR (400 MHz, CDCl_3) δ 7.56 – 7.51 (m, 2H), 7.45 – 7.38 (m, 2H), 7.02 – 6.98 (m, 2H), 5.73 (s, 1H), 2.38 (s, 6H), 1.97 (s, 1H).

^{13}C NMR (100 MHz, CDCl_3) δ 169.85, 148.49, 141.84, 135.99, 130.92, 122.13, 118.29, 73.23, 21.15.

HRMS: calcd. $\text{C}_{17}\text{H}_{14}\text{O}_5\text{Na}^+$ $[\text{M}+\text{Na}]^+$: 321.0733. Found: 321.0735.

General procedure for C–O bond cleavage:

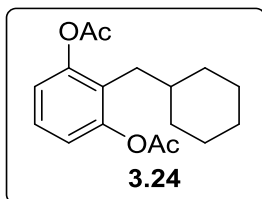
To a 2 mL solution (solvent varies) of the oxime (0.1 mmol, 1 equiv) was added to a tube charged with corresponding Pd catalyst (1:1 to oxime by weight). The reaction was run under a hydrogen atmosphere. After the reaction was completed, the mixture was filtrated through a short pipette of Celite, and then the solvent was removed under reduced pressure. The desired compound was purified by flash column chromatography on silica gel (Hex/EA 10:1 to 5:1).

**2,3-dimethylphenol (3.22)**

THF/AcOH=1:1 as a solvent, 1 atm hydrogen gas with Pd/C (10% w/w) was used.

White solid. Yield 97%. R_f = 0.45 (Hex/EA=3:1).

^1H NMR (400 MHz, CDCl_3) δ 6.96 (d, J =7.8, 1H), 6.79 – 6.74 (m, 1H), 6.66 – 6.62 (m, 1H), 4.61 (s, 1H), 2.28 (s, 3H), 2.17 (s, 3H). Match the literature.²⁰



2-(cyclohexylmethyl)-1,3-phenylene diacetate (3.24)

Ac₂O/AcOH=1:1 as solvent, 100 psi hydrogen gas with Pd/C (10% w/w) was used, reaction conducted at 100°C in Q-tube with freeze-pump-thaw three times.

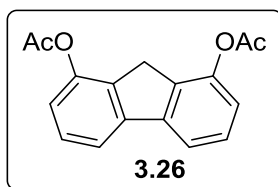
Colorless oil. Yield 33%. R_f = 0.5 (Hex/EA=3:1).

IR (KBr) 2925, 2850, 1769, 1463, 1449, 1369, 1204, 1190 cm⁻¹.

¹H NMR (400 MHz, CDCl₃) δ 7.20 (dd, J =8.5, 7.8, 1H), 6.97 – 6.93 (m, 2H), 2.35 – 2.32 (m, 2H), 2.29 (s, 6H), 1.73 – 1.57 (m, 5H), 1.48 – 1.35 (m, 1H), 1.20 – 1.07 (m, 3H), 0.91 (td, J =13.3, 12.8, 6.5, 2H).

¹³C NMR (100 MHz, CDCl₃) δ 169.20, 150.11, 126.61, 126.38, 120.10, 38.59, 33.64, 32.63, 26.50, 26.41, 21.16.

HRMS: calcd. C₁₇H₂₂O₄Na⁺ [M+Na]⁺: 313.1410. Found: 313.1398.



9H-fluorene-1,8-diyl diacetate (3.26)

THF/AcOH=1:1 as solvent, 1 atm hydrogen gas with Pd(OH)₂/C (20% w/w) was used and reaction conducted at 100°C.

Colorless oil. Yield 67%. R_f = 0.5 (Hex/EA=3:1).

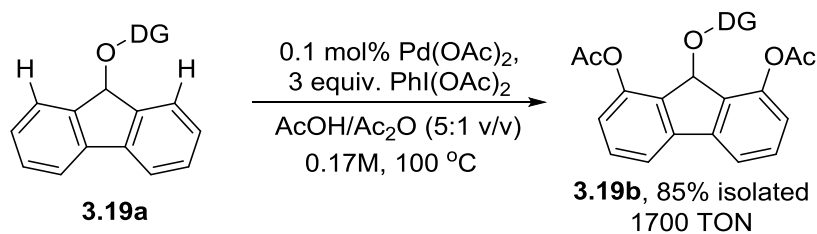
IR (KBr) 2937, 1758, 1581, 1480, 1436, 1369, 1214, 1187 cm⁻¹.

¹H NMR (400 MHz, CDCl₃) δ 7.67 (dd, J =7.6, 0.9, 2H), 7.46 – 7.36 (m, 2H), 7.06 (dd, J =8.0, 0.9, 2H), 3.71 (s, 2H), 2.39 (s, 6H).

¹³C NMR (100 MHz, CDCl₃) δ 168.88, 147.65, 143.71, 134.36, 128.66, 120.51, 118.21, 32.23, 21.18.

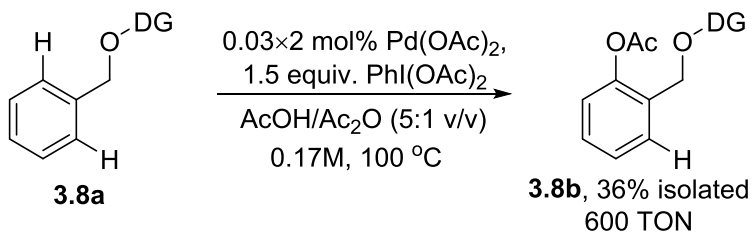
HRMS: calcd. C₁₇H₁₄O₄Na⁺ [M+Na]⁺: 305.0784. Found: 305.0789.

Reaction TON test:



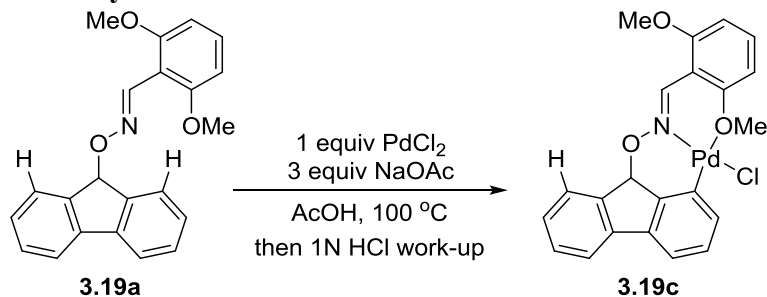
Iodosobenzene diacetate (48.3 mg, 1.5 equiv in most cases) and oxime **3.19a** (34.5mg, 0.1 mmol, 1 equiv) were charged in a scintillation vial, followed by 50 μ L 2mM Pd(OAc)₂ solution in AcOH (0.0001 mmol, 0.1 mol%) and followed by 450 μ L AcOH and 0.1 mL Ac₂O. The vial was tightly capped and stirred at 100 °C for 24h. Upon done, the mixture was directly purified by flash column chromatography on silica gel (Hex/EA= about 10:1 to 3:1) to give the compounds **3.19b** in 85% yield with E/Z = 4.2:1. The TON for each oxidation catalytic cycle is 1700. *Note this reaction was not monitored by TLC due to the very low catalyst loading.*

Mono-Oxidation Procedure:



Iodosobenzene diacetate (48.3 mg, 1.5 equiv in most cases) and the oxime **3.8a** (34.5mg, 0.1 mmol, 1 equiv) were charged in a scintillation vial, followed by 15 μL 2mM $\text{Pd}(\text{OAc})_2$ solution in AcOH (0.0001 mmol, 0.1 mol%) and followed by 485 μL AcOH and 0.1 mL Ac_2O . The vial was tightly capped and stirred at 100 °C for 4h. The vial was then opened and added another 15 μL 2mM $\text{Pd}(\text{OAc})_2$ solution. The vial was resealed and stirred at 100°C for 4h. Upon done, the mixture was directly purified by flash column chromatography on silica gel (Hex/EA= about 10:1 to 3:1) to give the compounds **3.8b** in 36% yield with E/Z = 5.6:1. The TON for each oxidation catalytic cycle is 600. The bisoxidized product was generated in a trace amount and observable on LC-MS but not isolatable. *Note this reaction was not monitored by TLC due to the very low catalyst loading.*

Preparation and X-ray structure data of 3.19c:



The oxime **3.19a** (345mg, 1 mmol, 1 equiv), PdCl₂ (212mg, 1.2 mmol, 1.2 equiv) and NaOAc (246 mg, 3 mmol, 3 equiv) was added into a 20 mL vial, followed by 5 mL acetic acid. The vial was added stir-bar and then sealed. The reaction was conducted at 100°C, and monitored by TLC. After 1h, the reaction was complete and the solvent was removed under reduced pressure. The residue was dissolved in chloroform and washed with 1N HCl. The organic layer was dried over MgSO₄, and the solvent was removed under reduced pressure. The desired compound was purified by flash column chromatography on silica gel (Hex/EA 10:1 to 3:1) to give the yellow solid. The crystal was obtained by slow evaporation DCM solvent.

HRMS: calcd. C₂₂H₁₈NO₃Pd⁺ [M-Cl]⁺: 450.0325. Found: 450.0319.

X-ray structure of Compound **3.19c**:

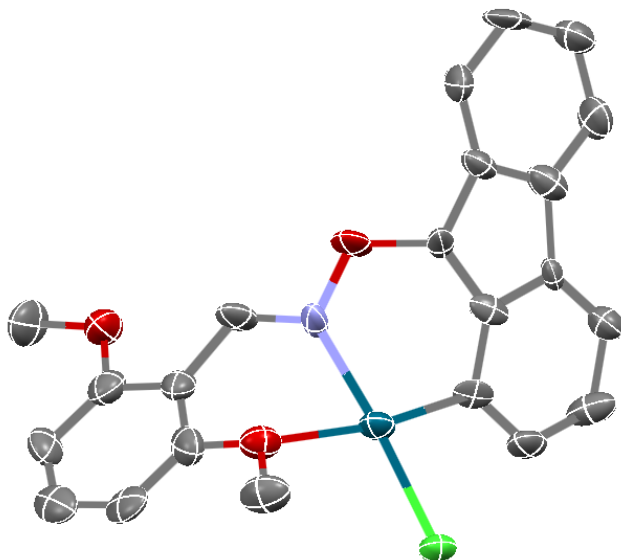


Table 1. Crystal data and structure refinement for **3.19c**.

Empirical formula	C ₂₂ H ₁₈ Cl N O ₃ Pd
Formula weight	486.22
Temperature	100(2) K
Wavelength	0.71073 Å
Crystal system	monoclinic
Space group	P 2 ₁ /c
Unit cell dimensions	a = 19.306(8) Å = 90°.
	b = 4.5687(19) Å = 103.674(8)°.
	c = 22.128(9) Å = 90°.
Volume	1896.5(14) Å ³
Z	4
Density (calculated)	1.703 Mg/m ³
Absorption coefficient	1.143 mm ⁻¹

F(000) 976

Crystal size 0.300 x 0.020 x 0.020 mm

Theta range for data collection 3.202 to 25.349°.

Index ranges $-22 \leq h \leq 23$, $-5 \leq k \leq 5$, $-26 \leq l \leq 25$

Reflections collected 10572

Independent reflections 3475 [R(int) = 0.1525]

Completeness to theta = 25.242° 99.8 %

Absorption correction Semi-empirical from equivalents

Max. and min. transmission 1.00 and 0.513

Refinement method Full-matrix least-squares on F2

Data / restraints / parameters 3475 / 0 / 255

Goodness-of-fit on F2 1.017

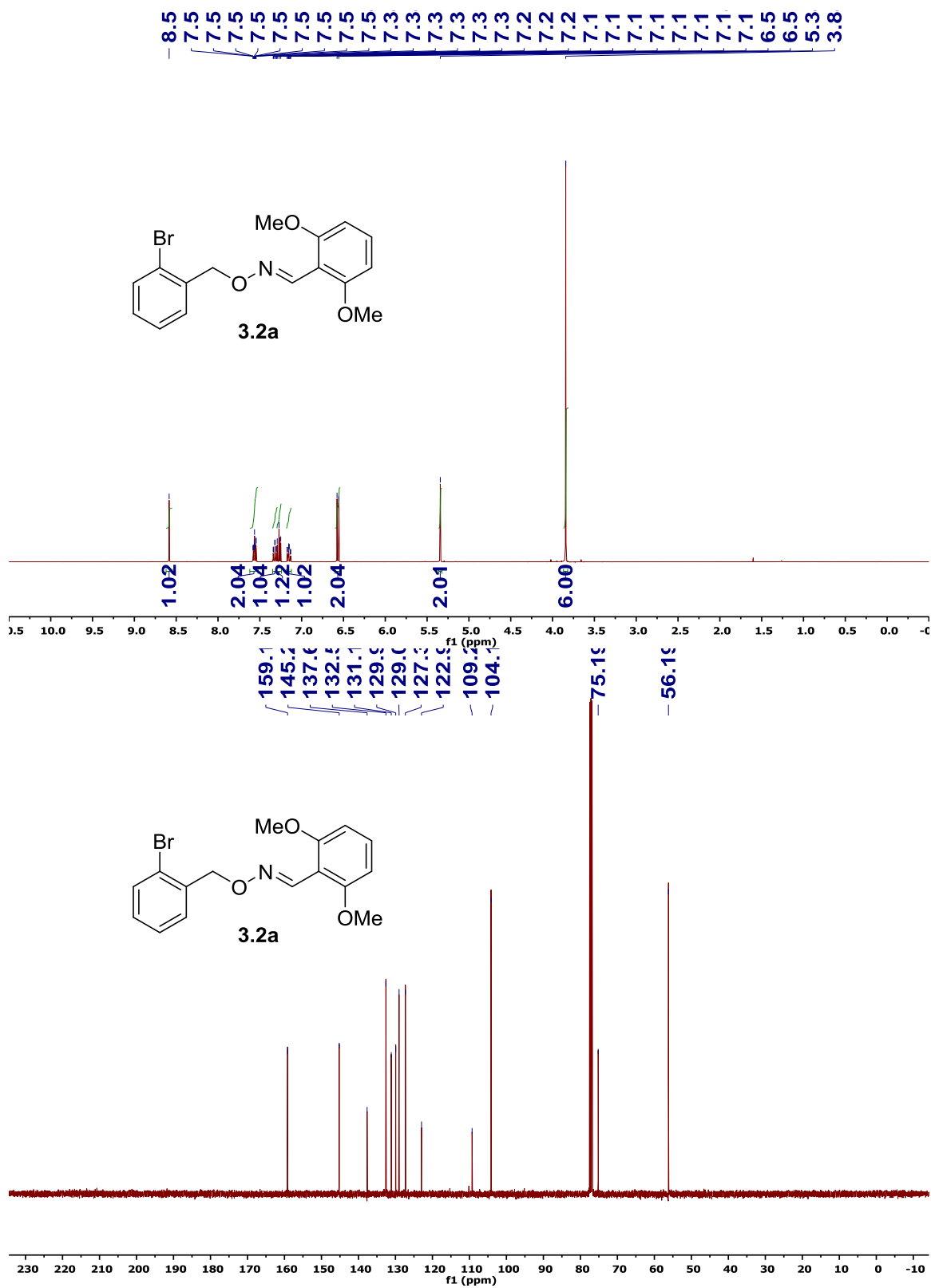
Final R indices [$I > 2\sigma(I)$] R1 = 0.0771, wR2 = 0.1476

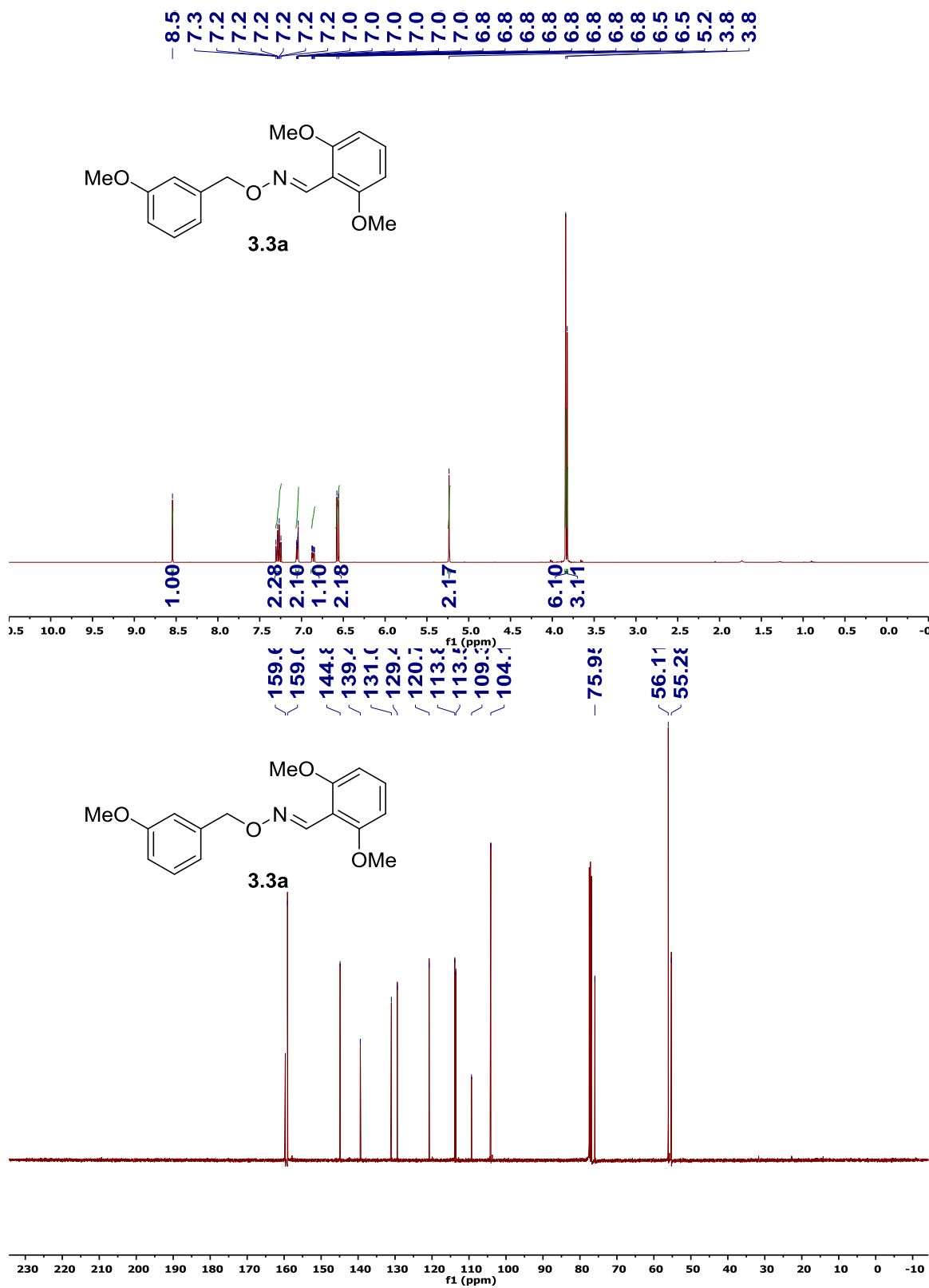
R indices (all data) R1 = 0.1351, wR2 = 0.1706

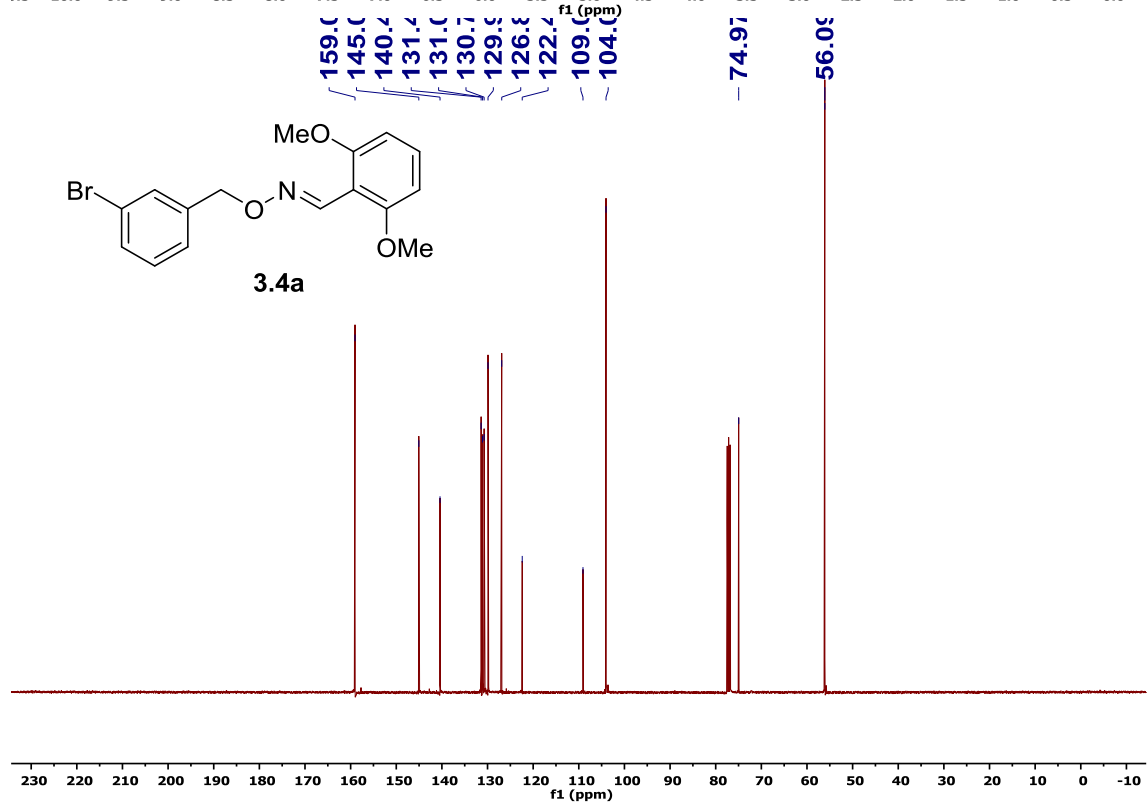
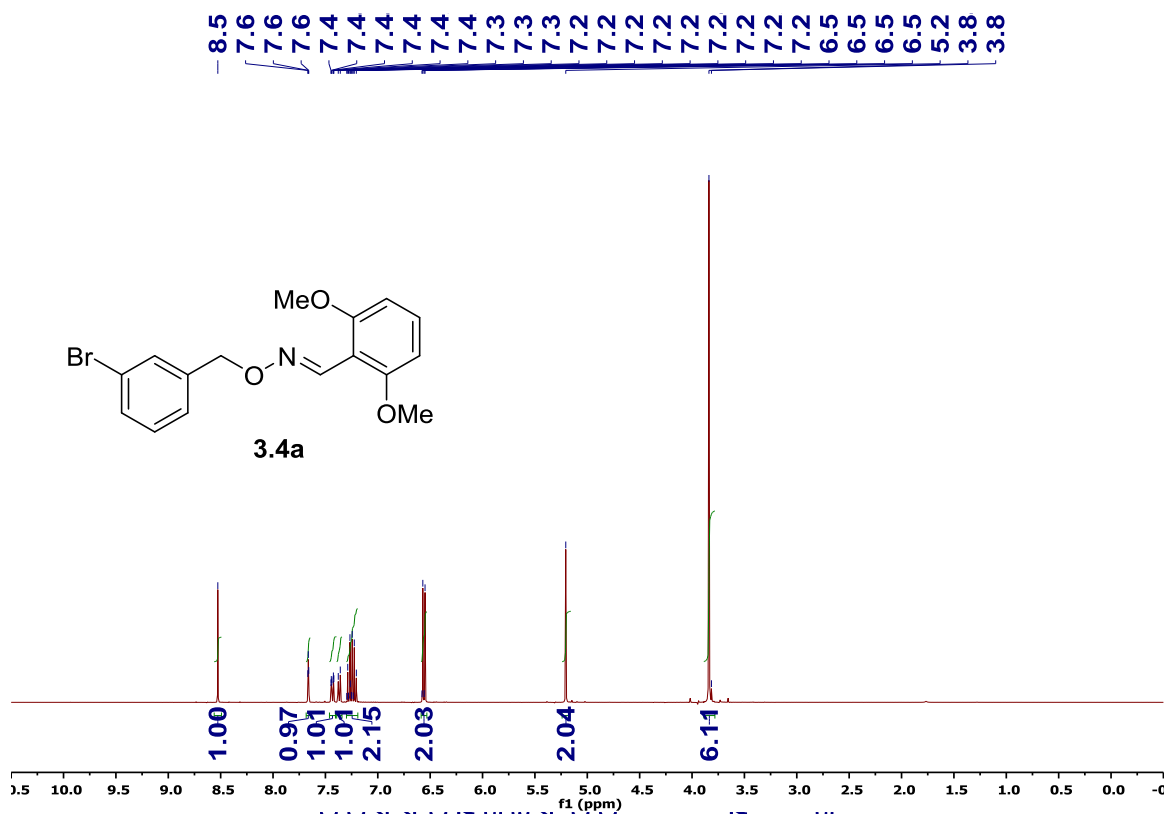
Extinction coefficient n/a

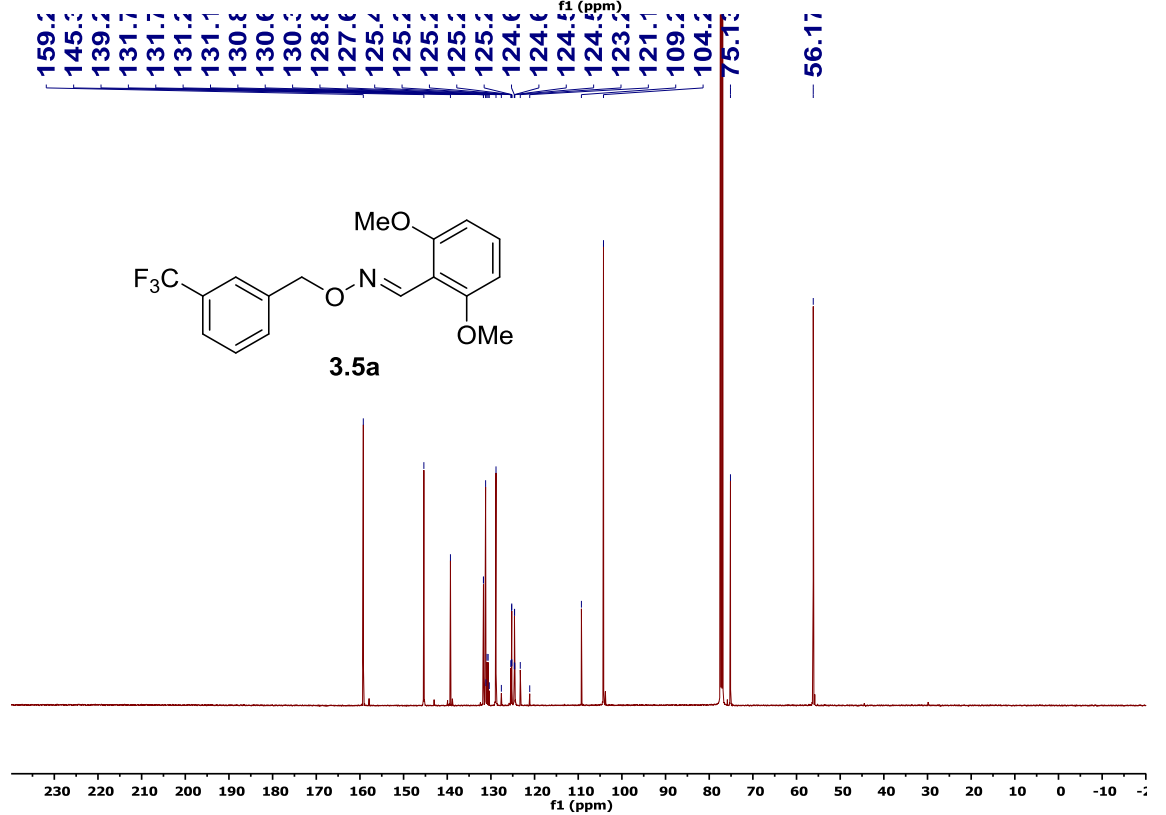
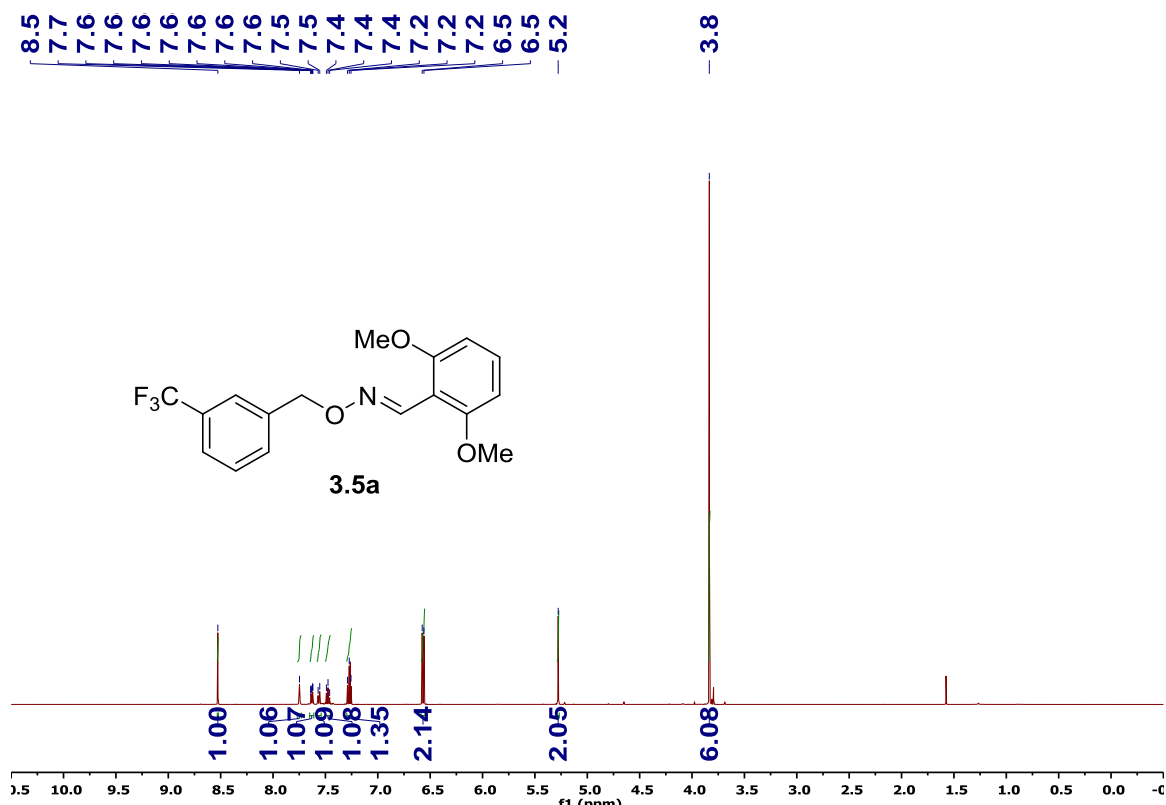
Largest diff. peak and hole 0.930 and -1.213 e.Å⁻³

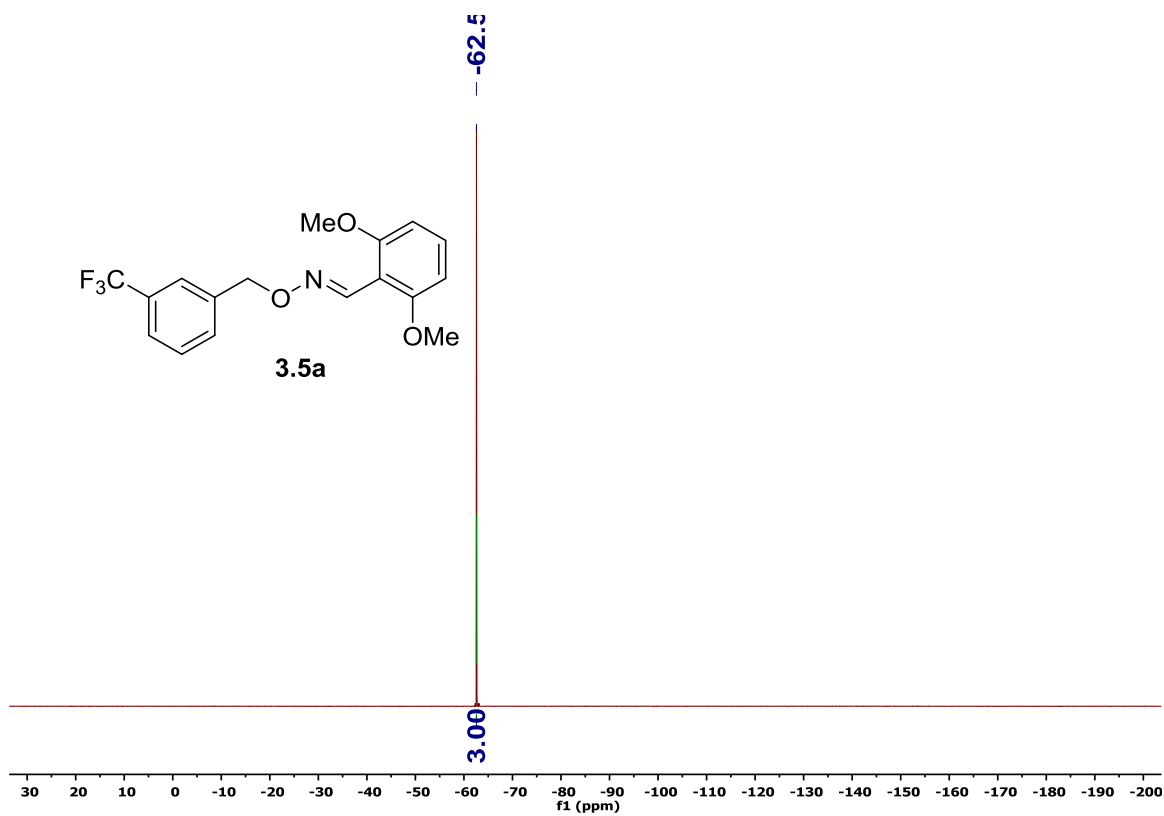


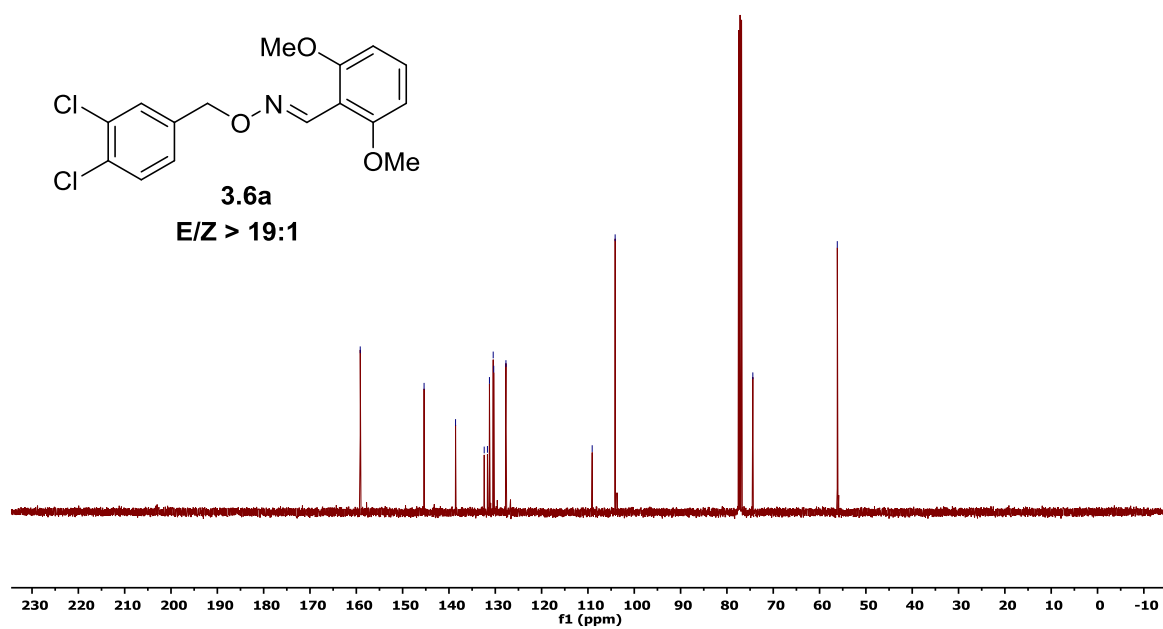
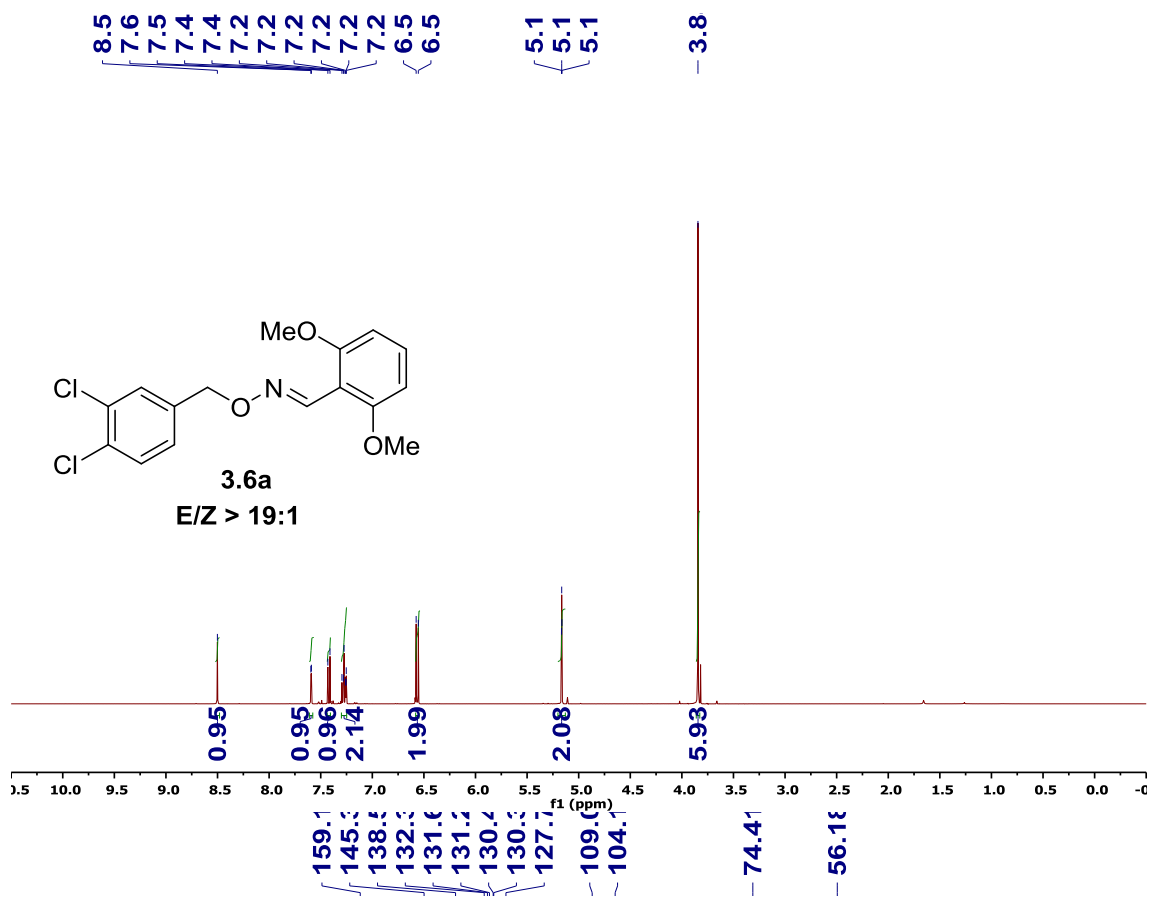


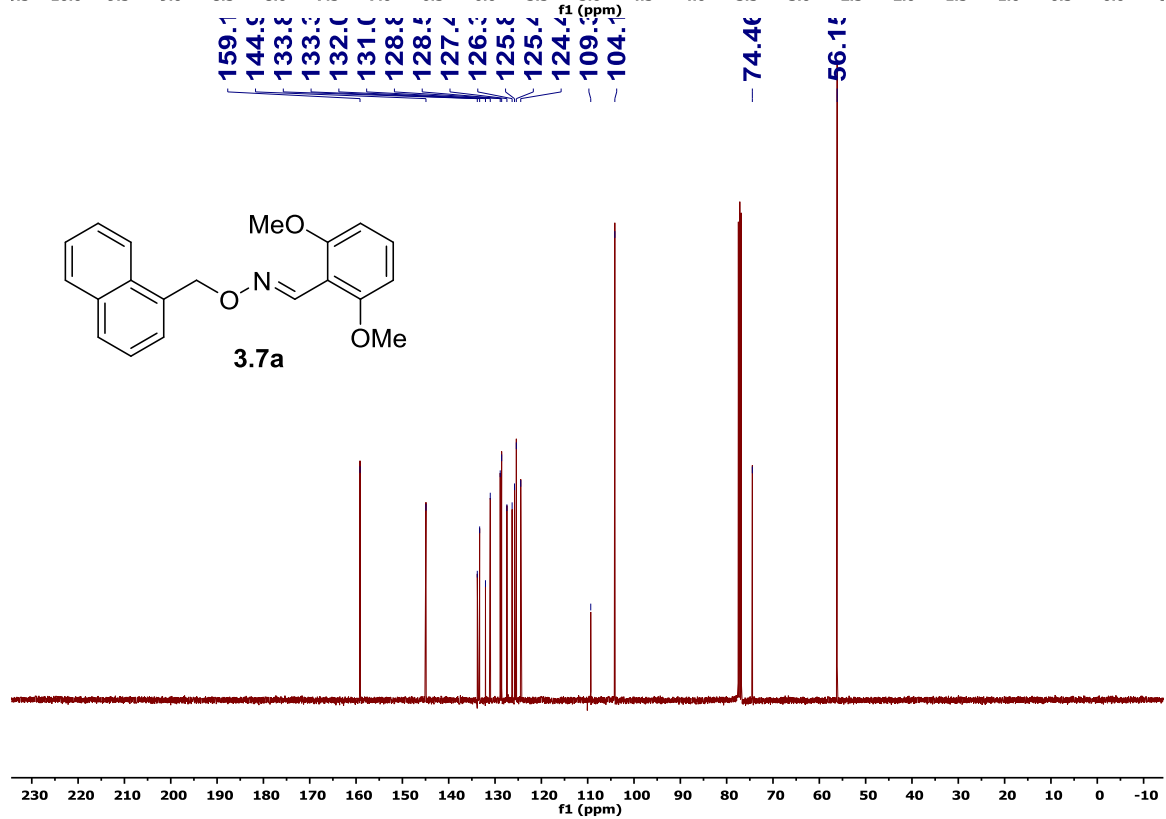
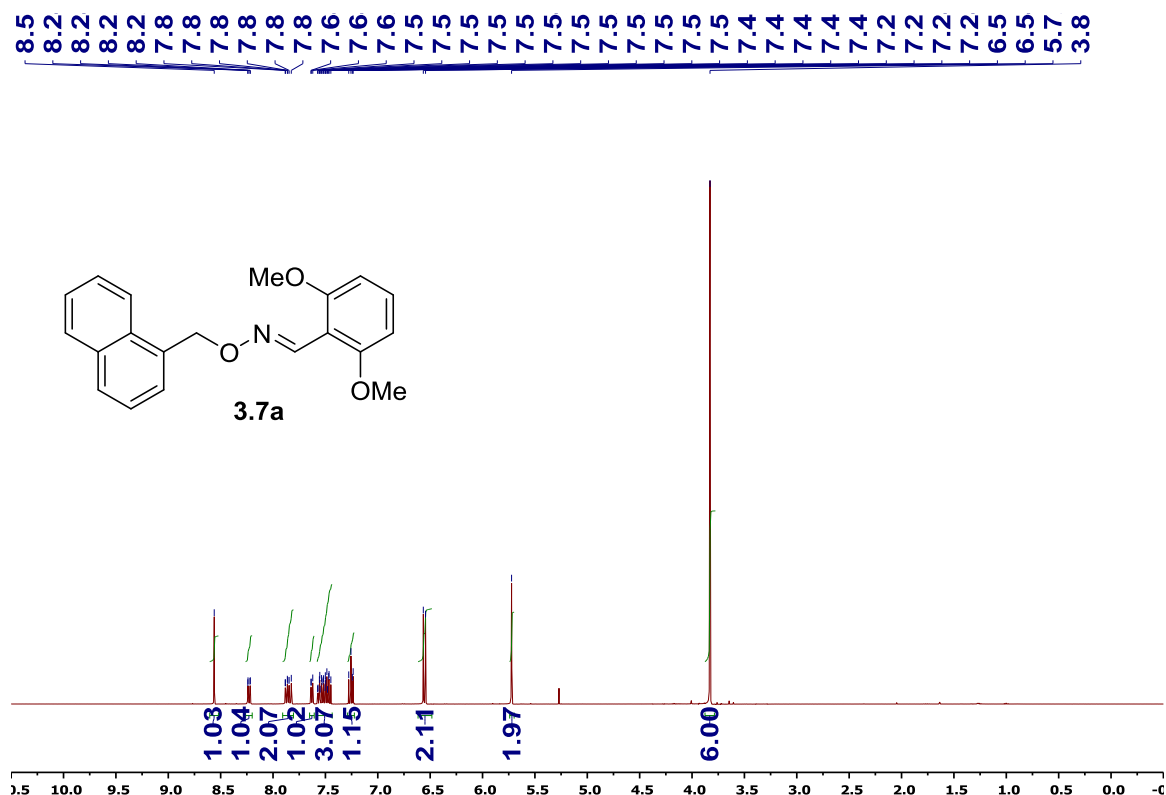


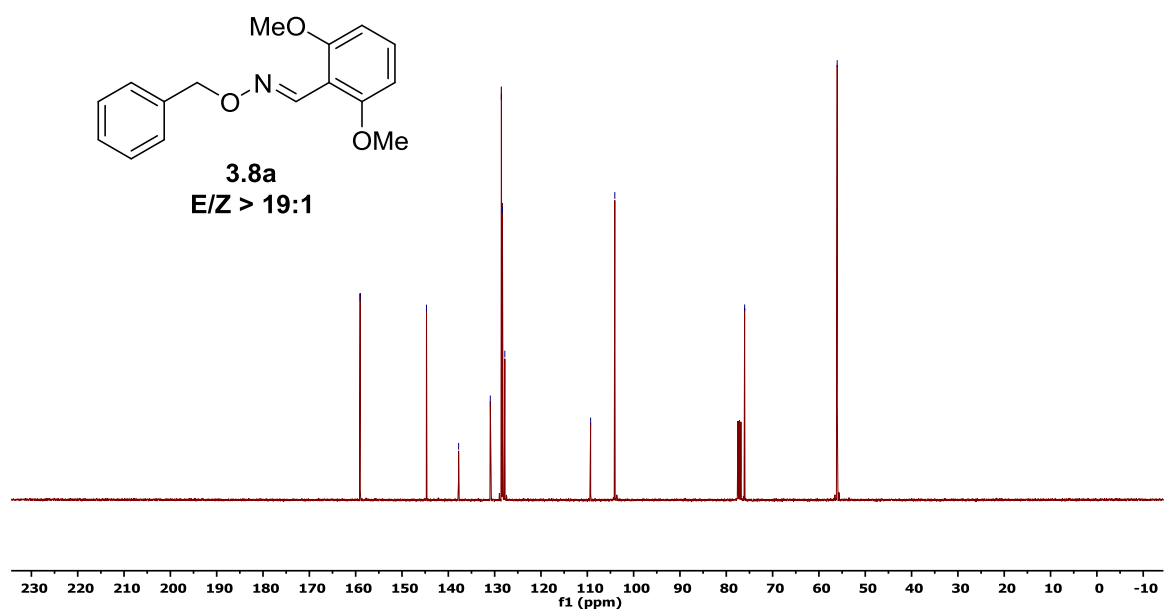
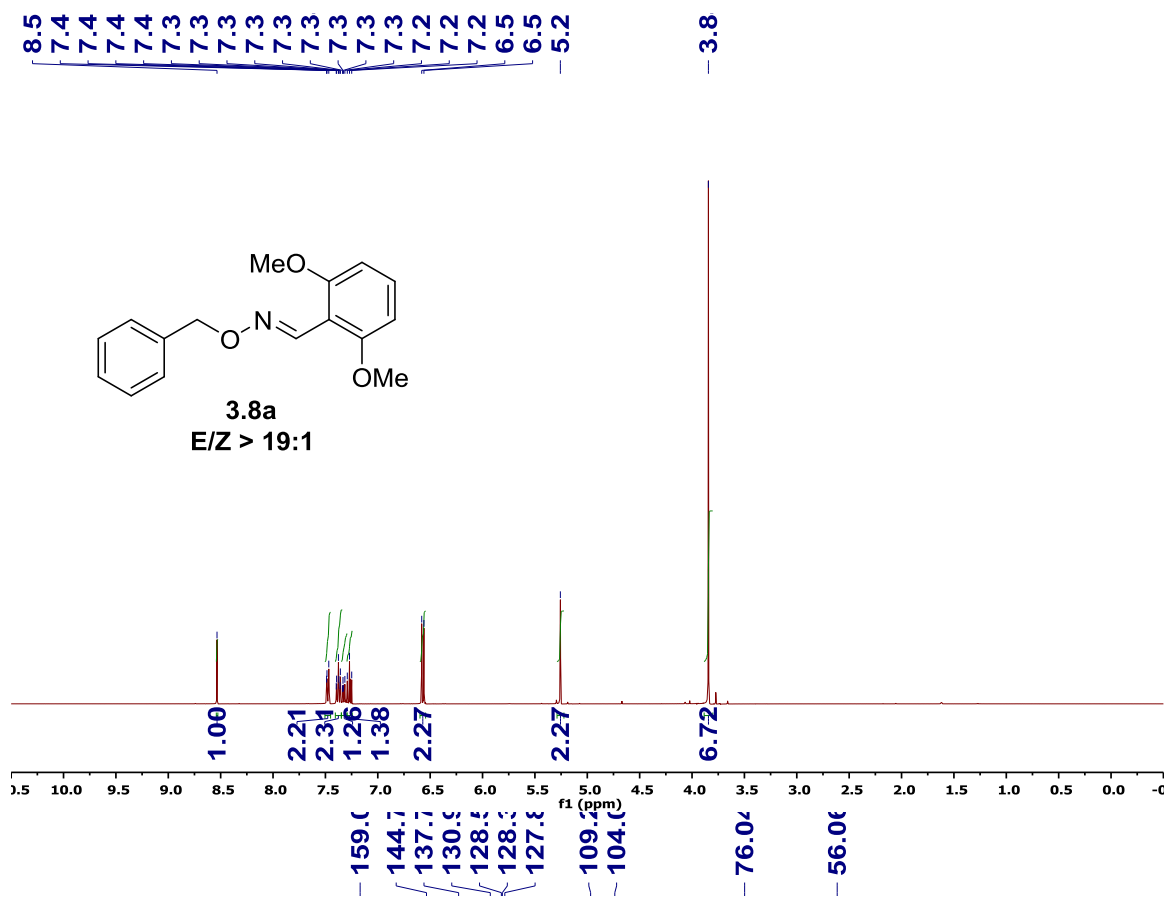


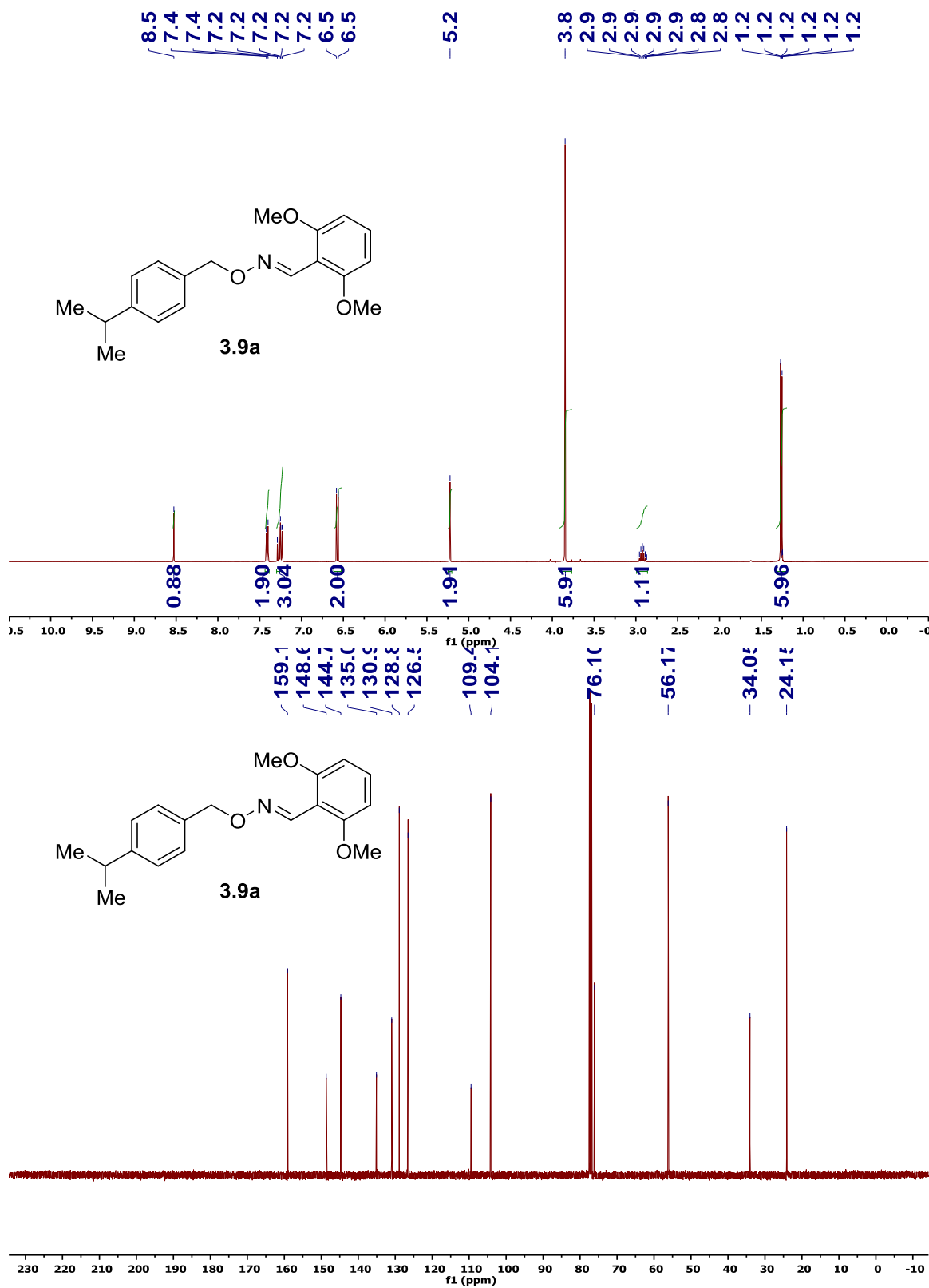


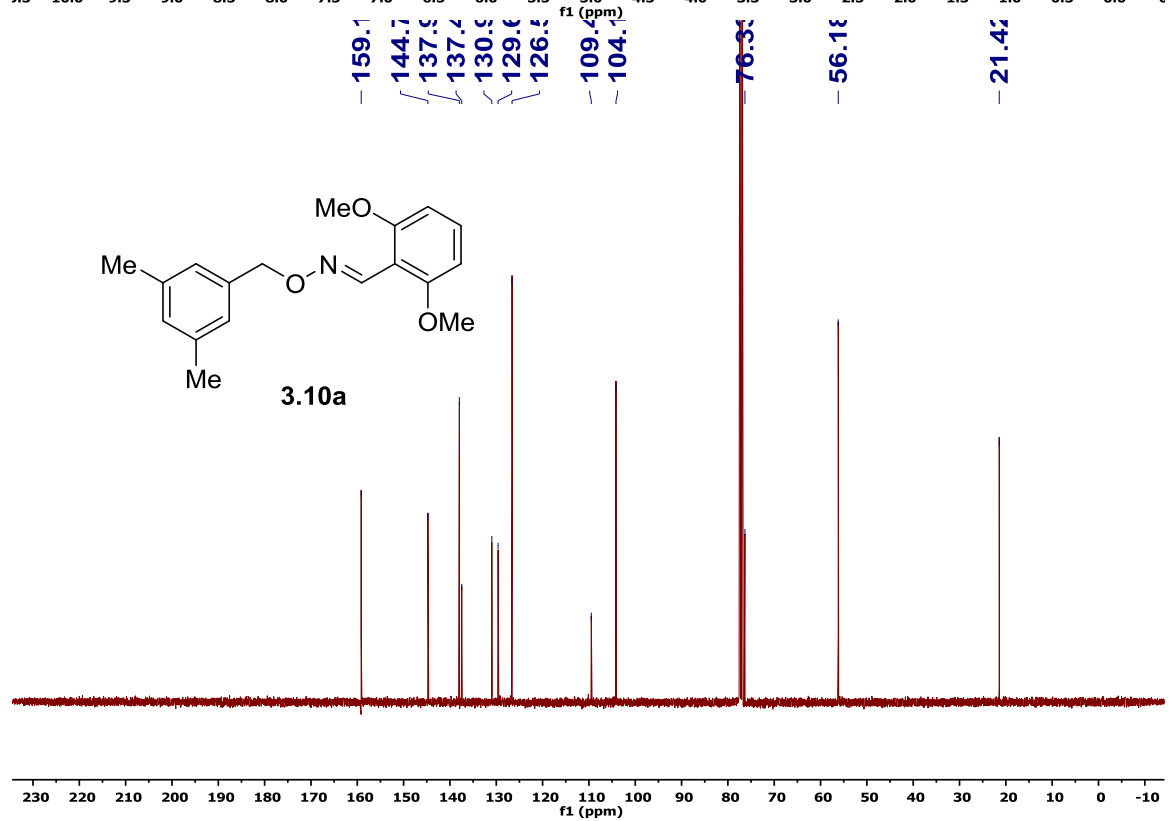
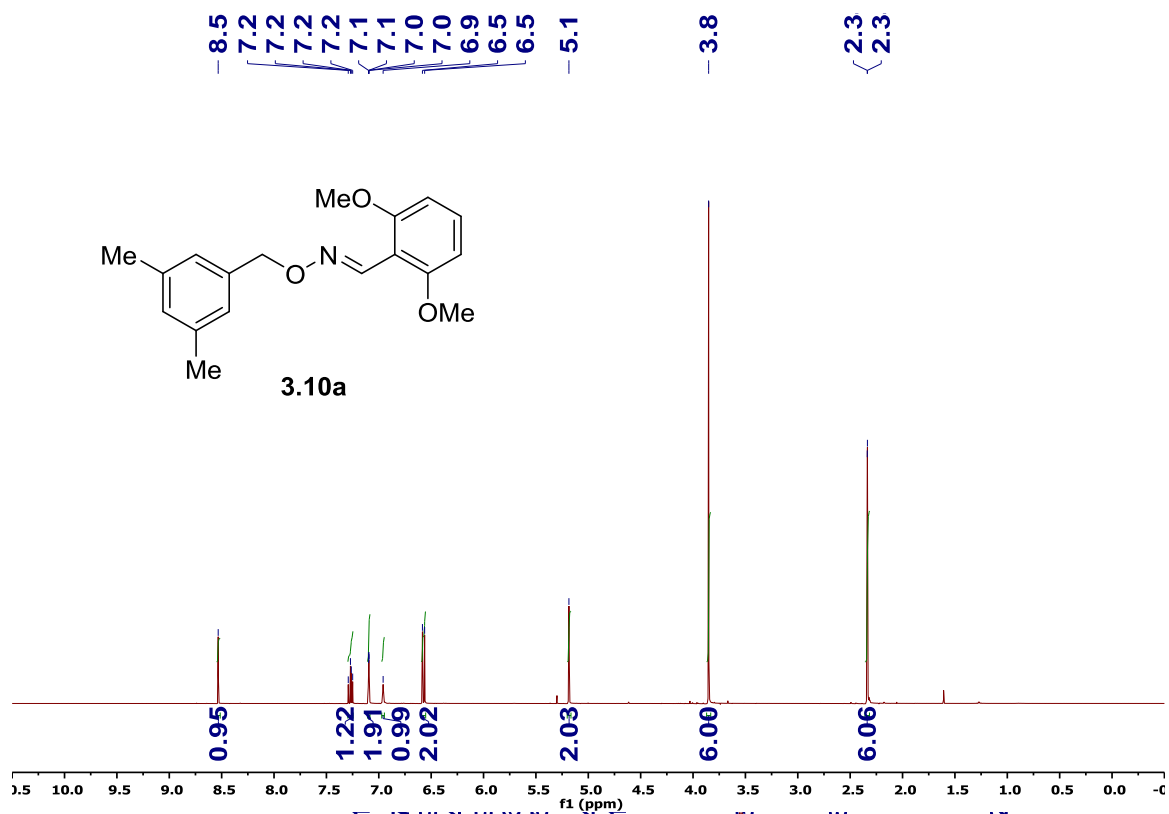


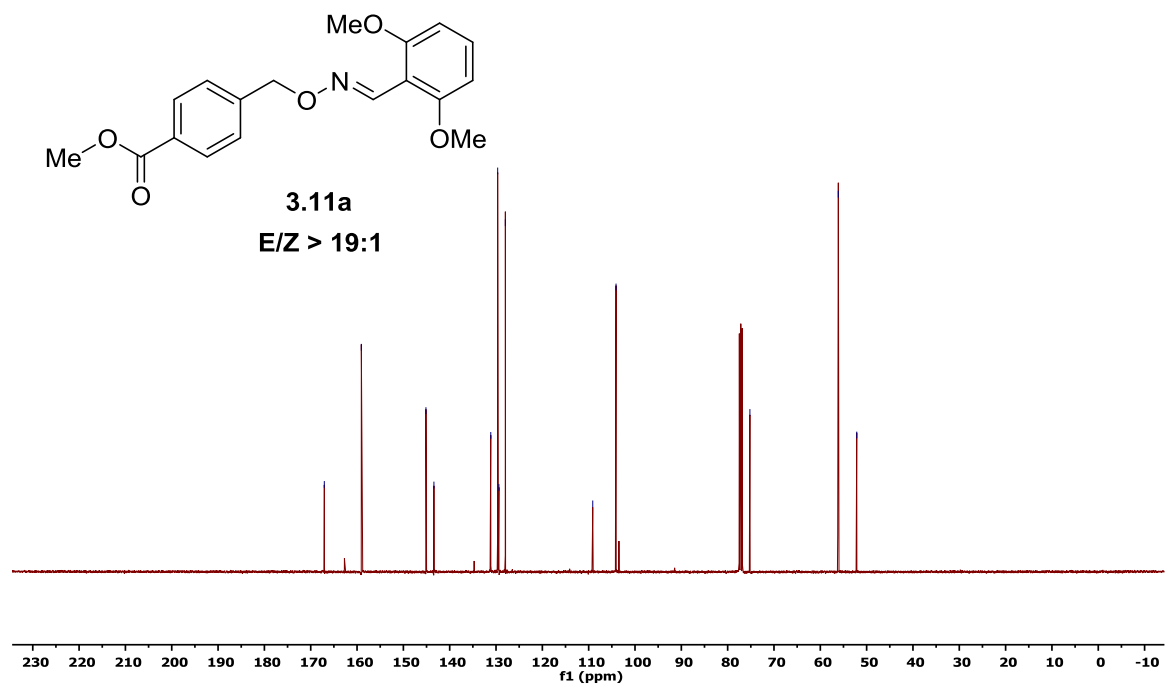
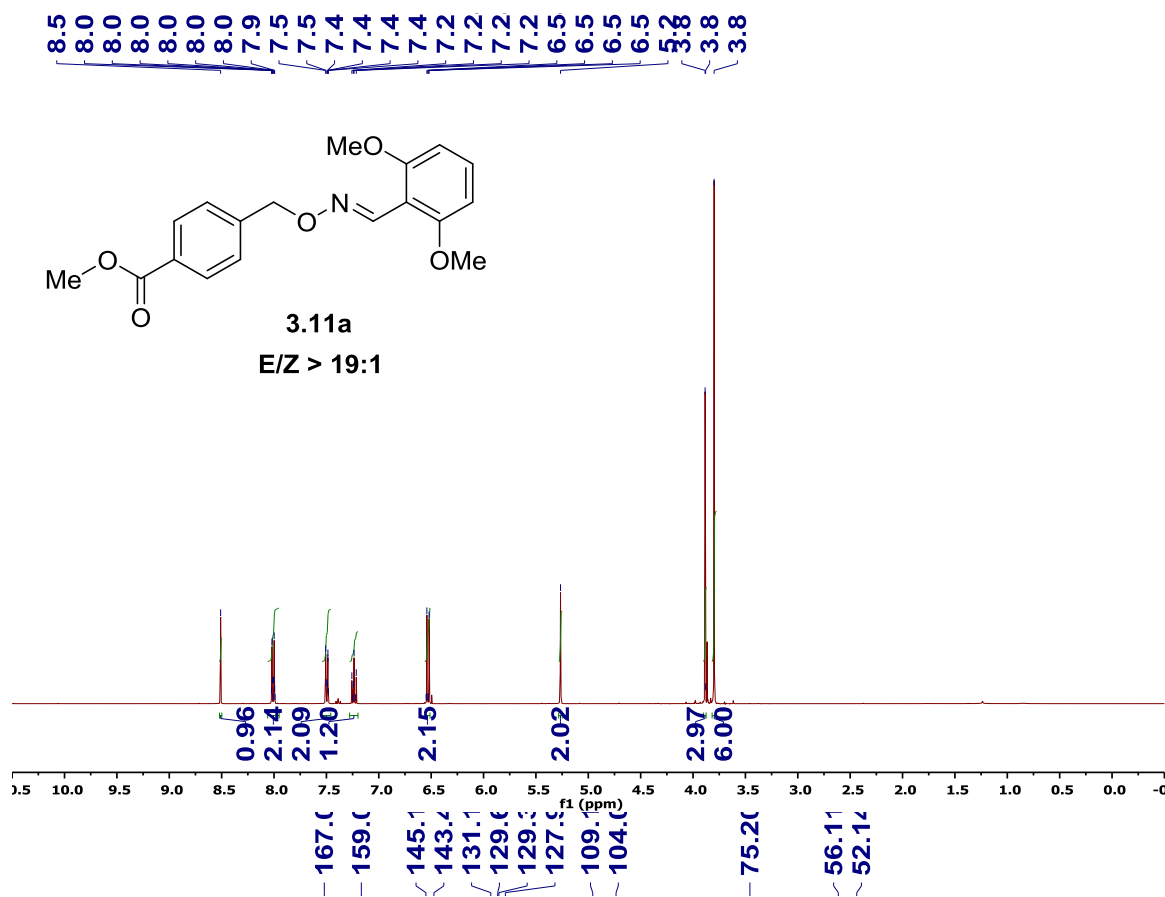


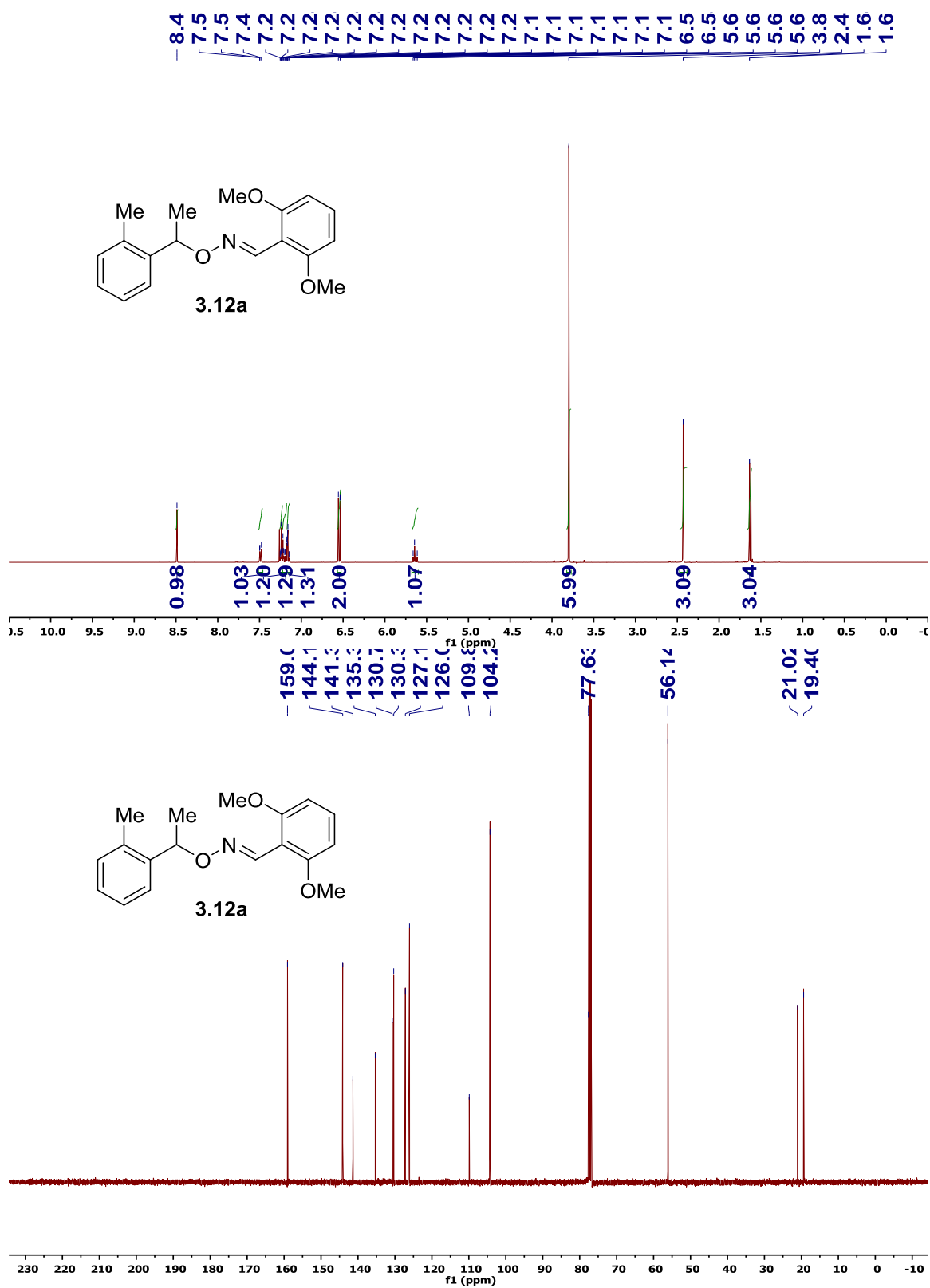


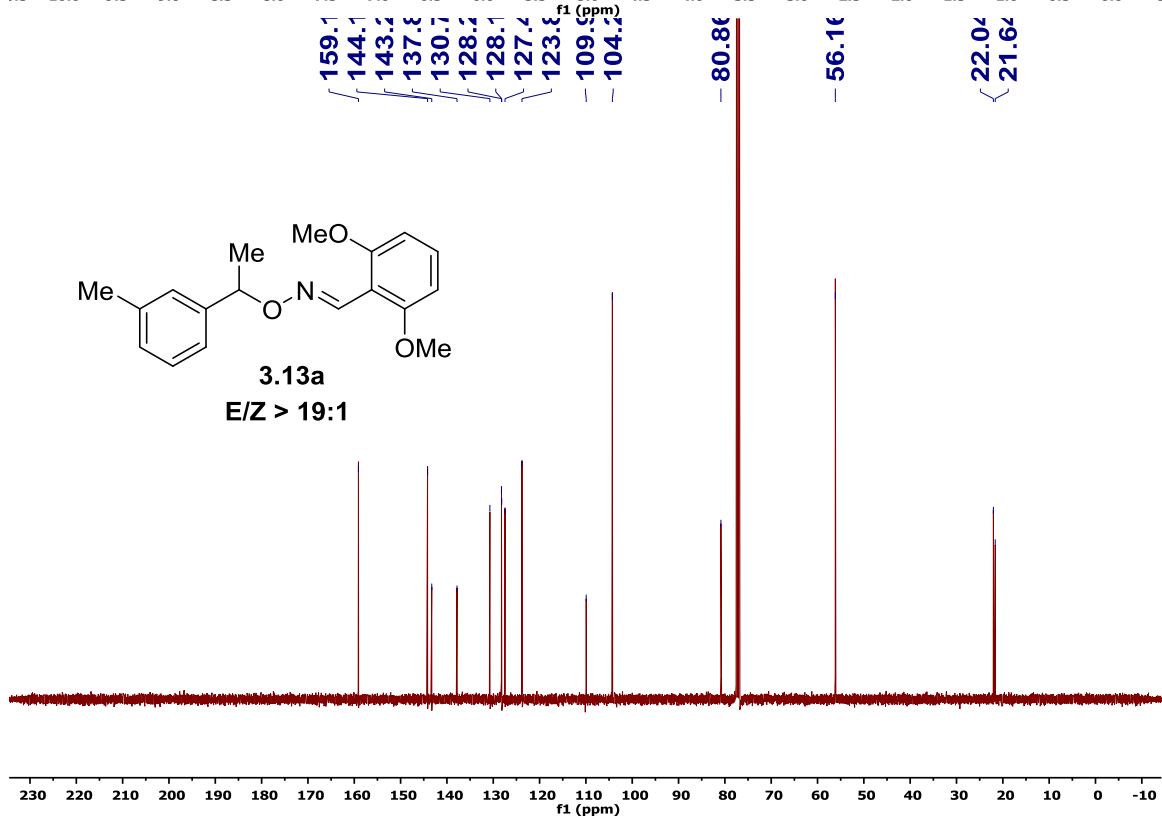
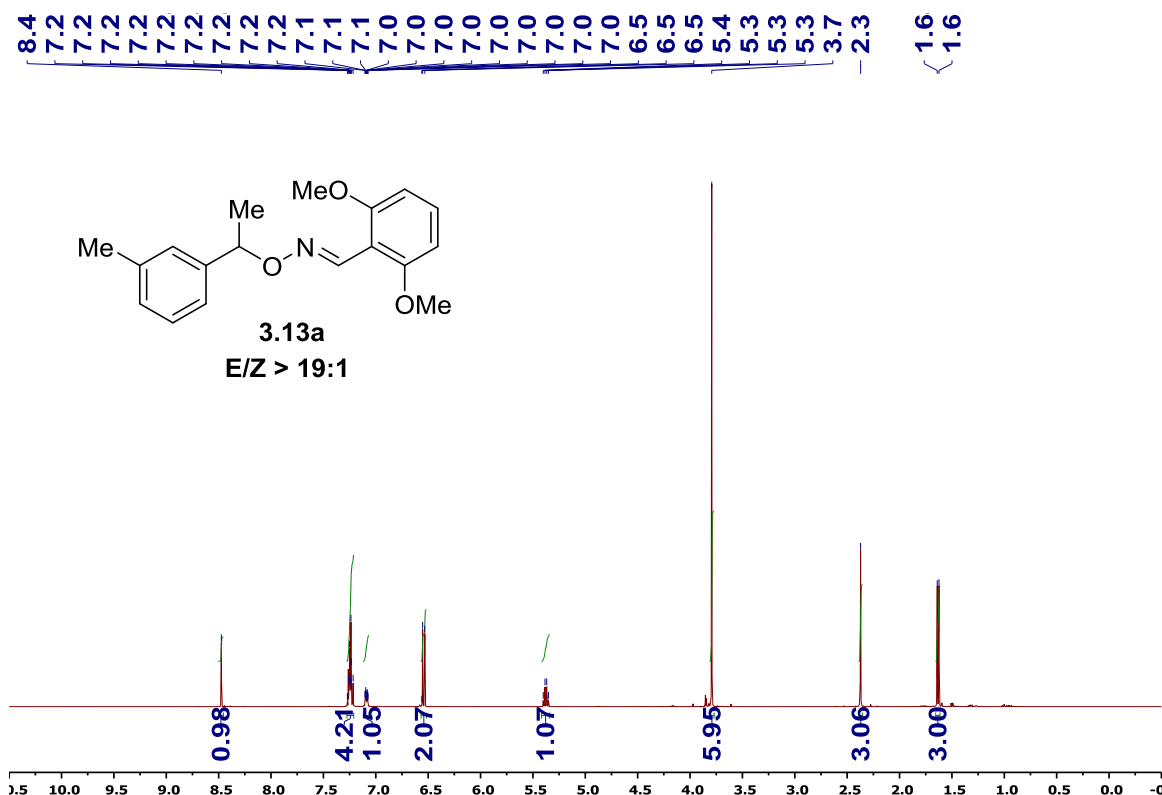


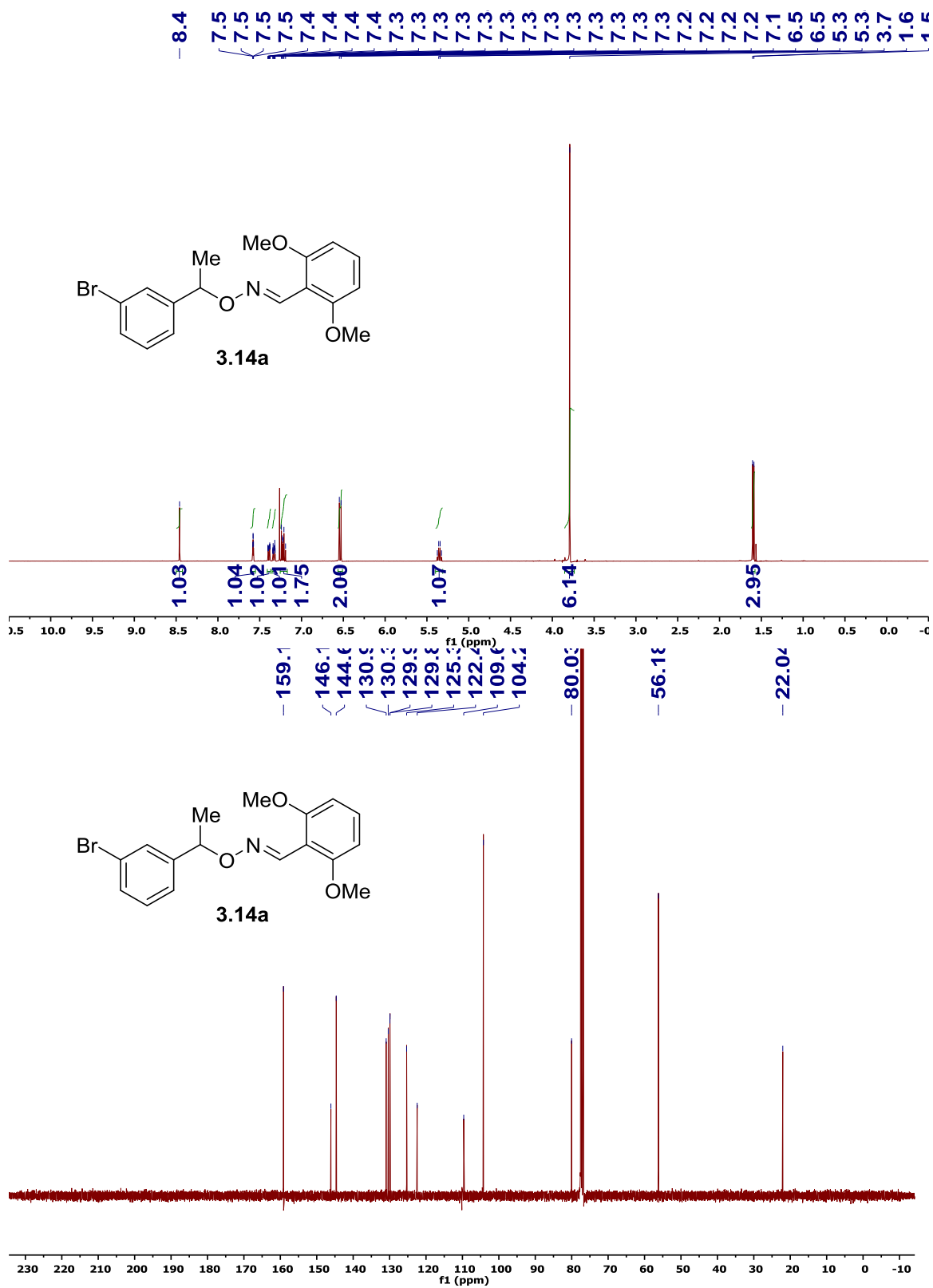


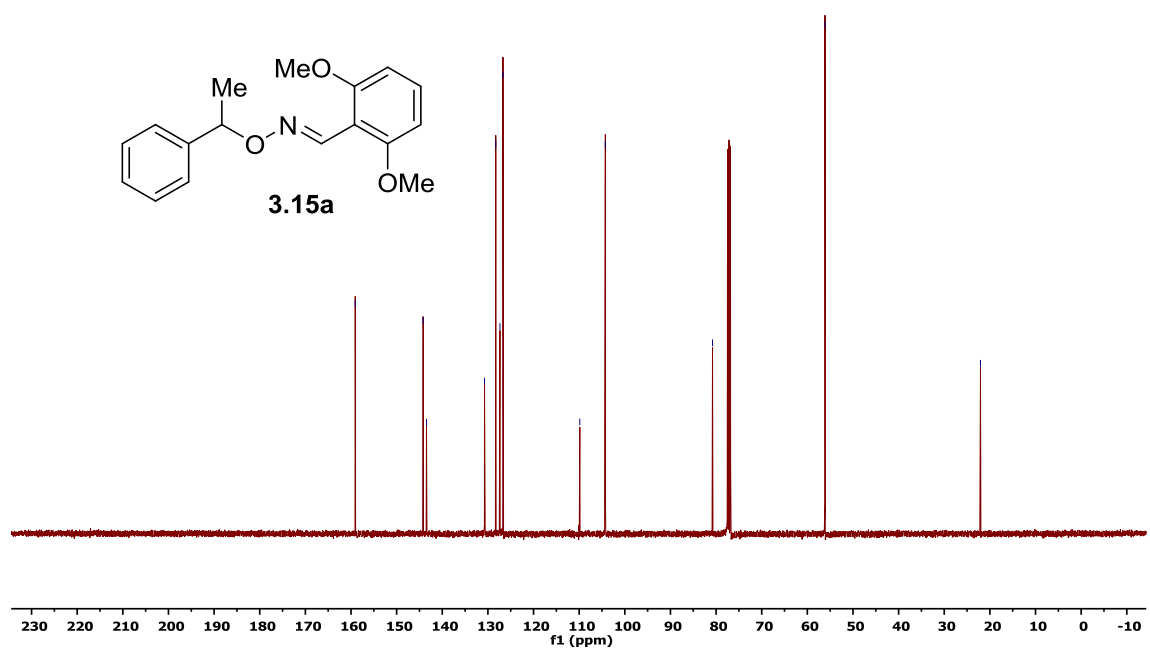
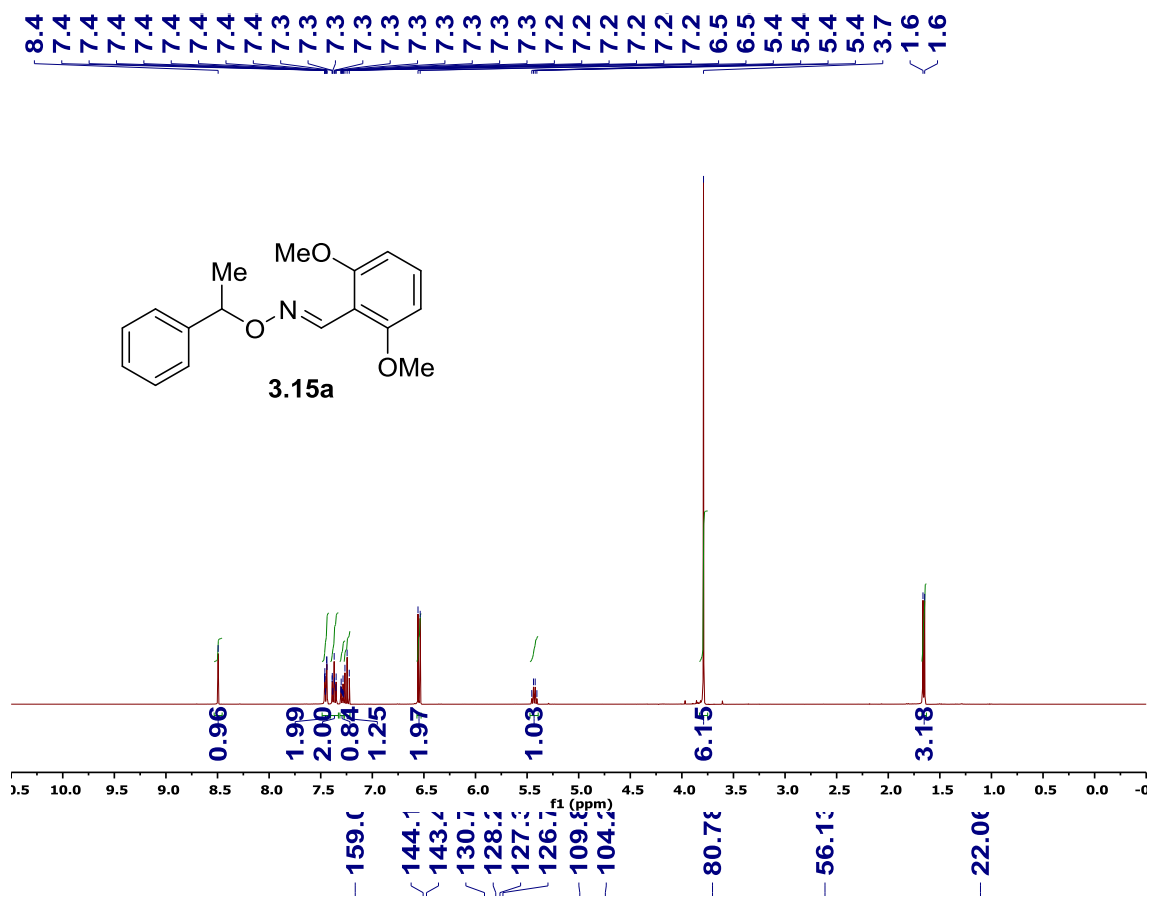


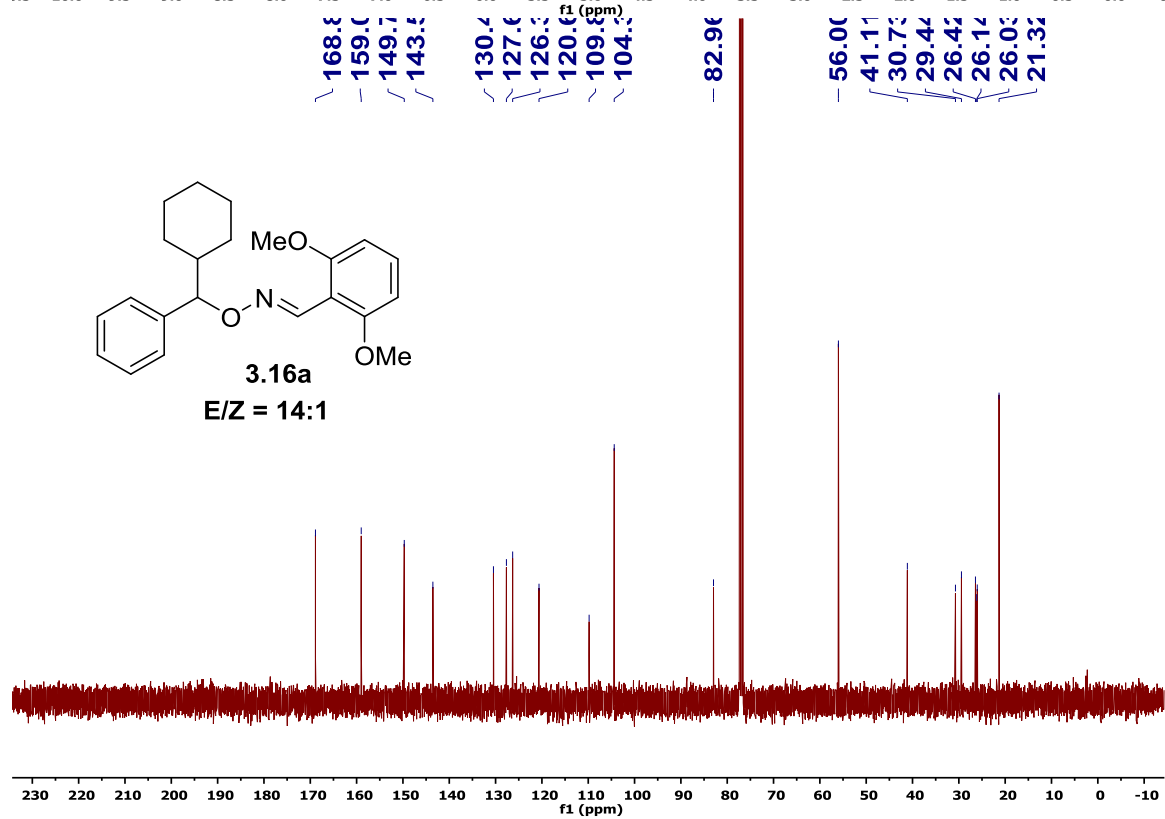
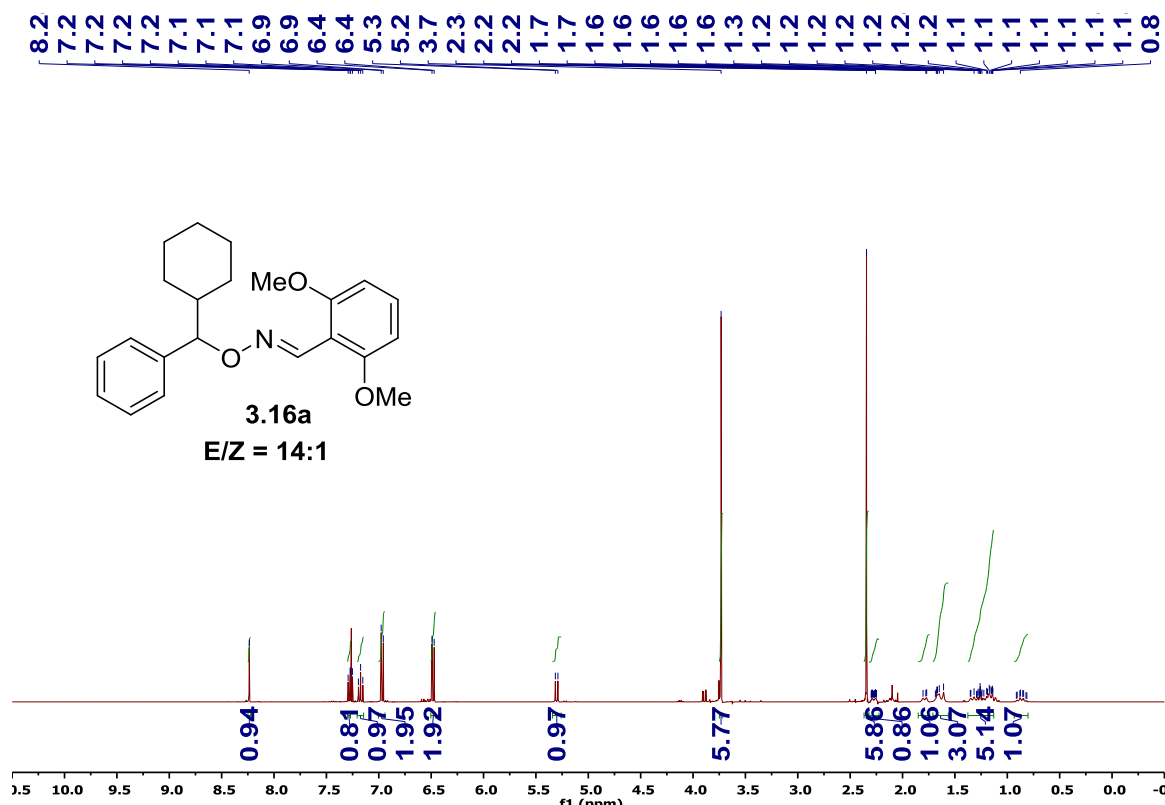


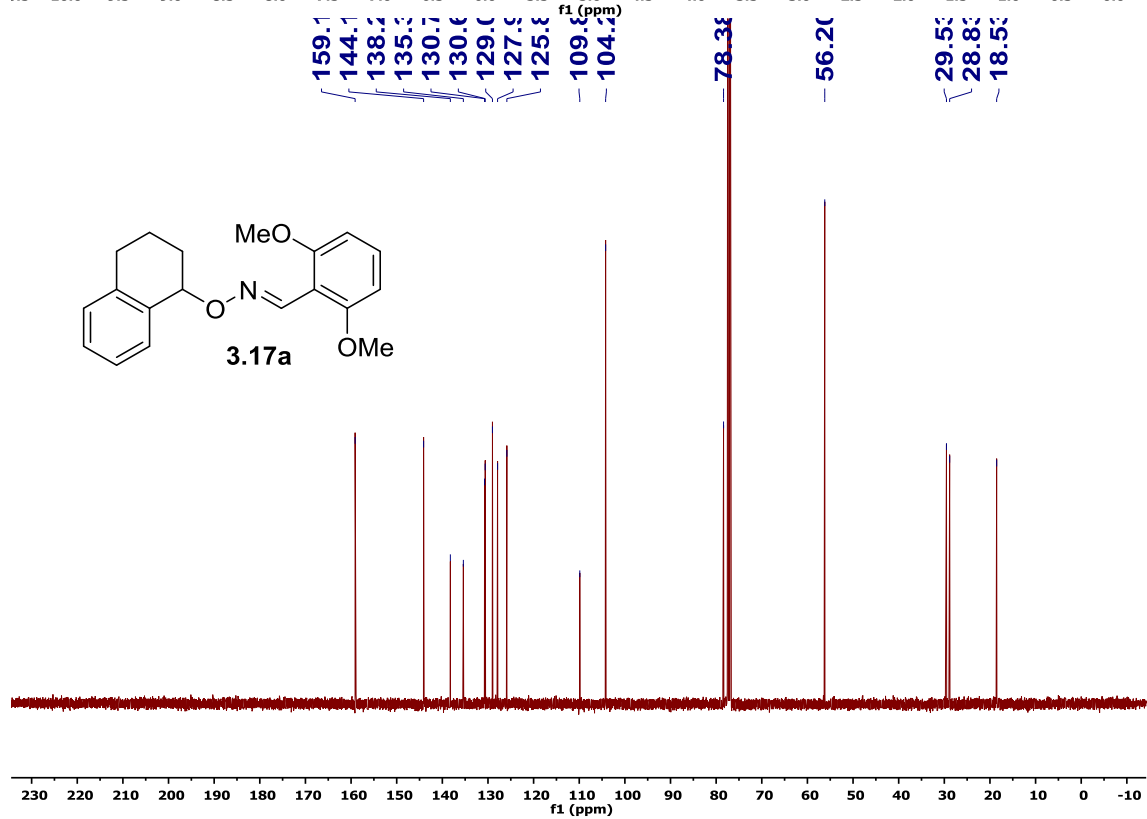
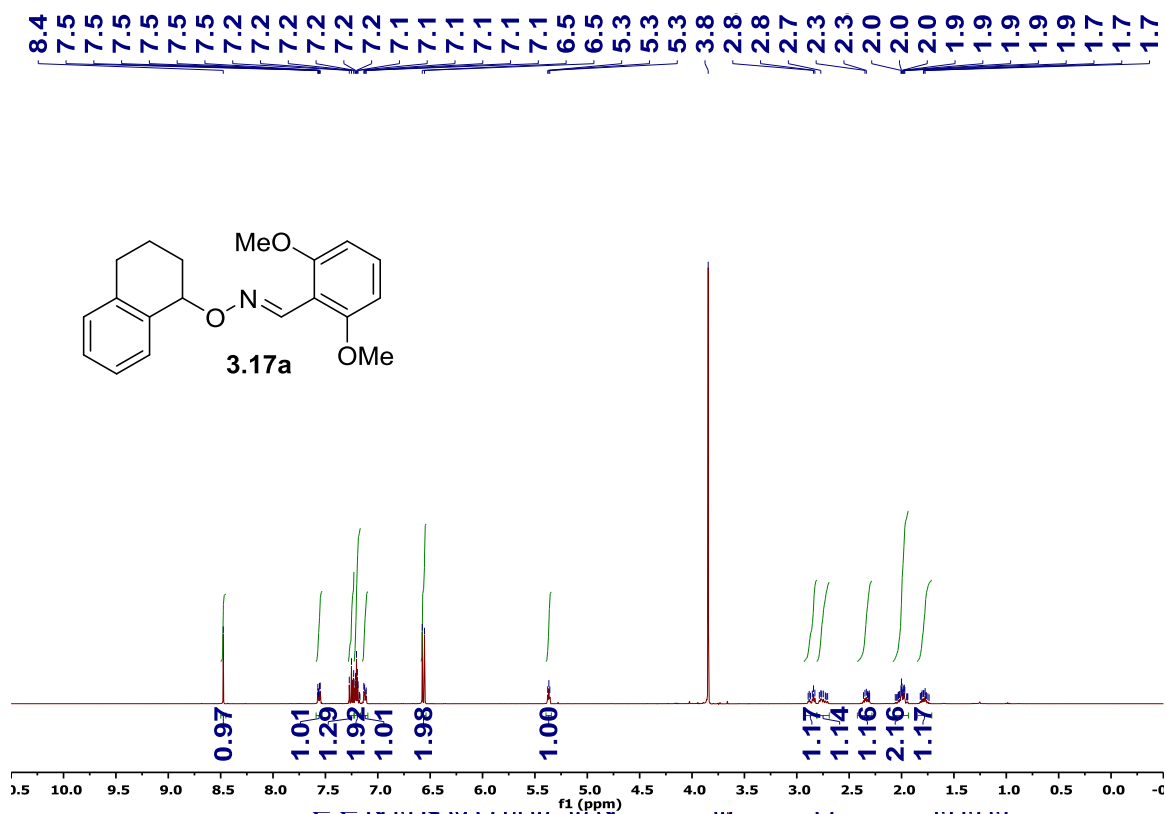


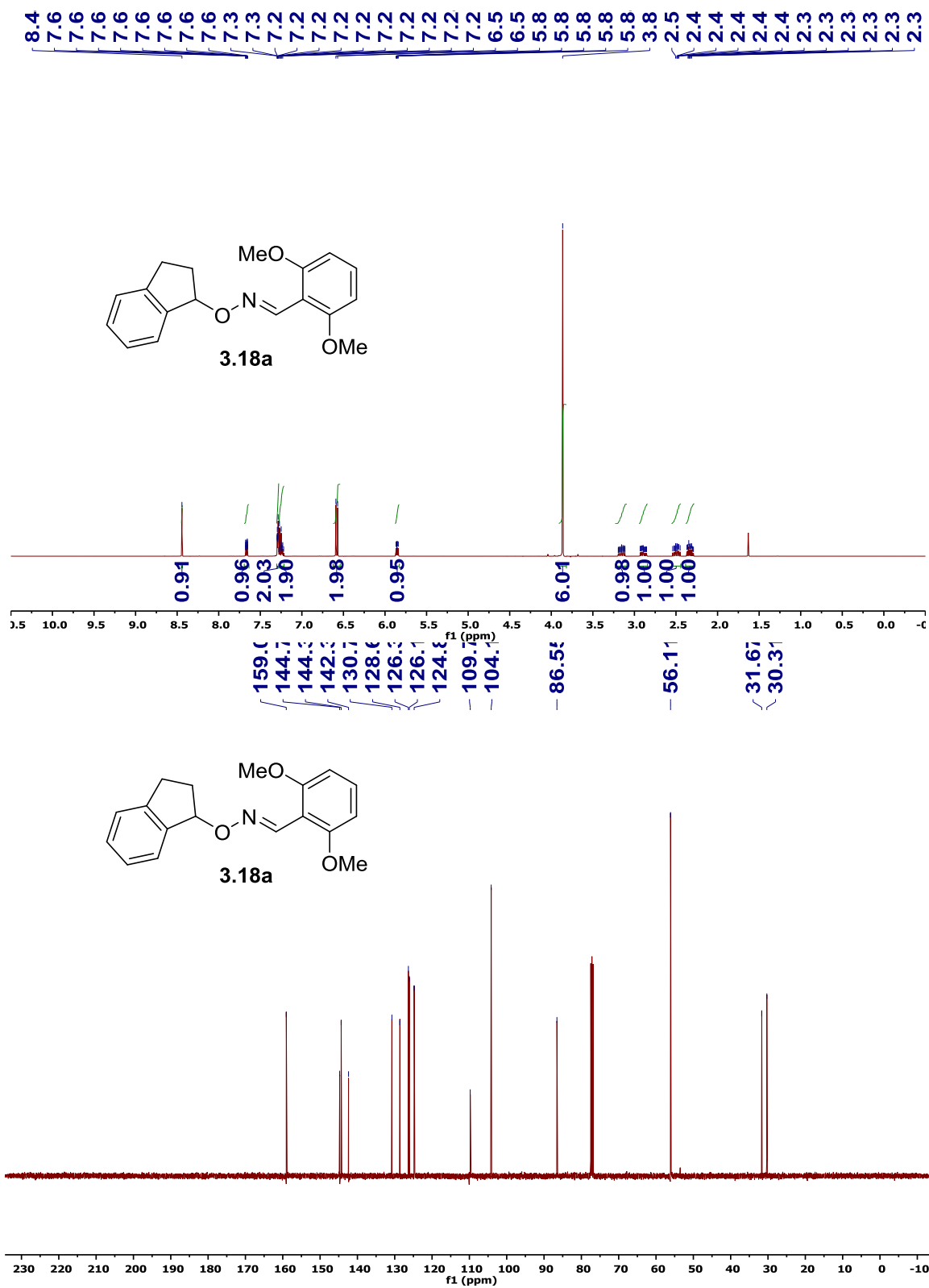


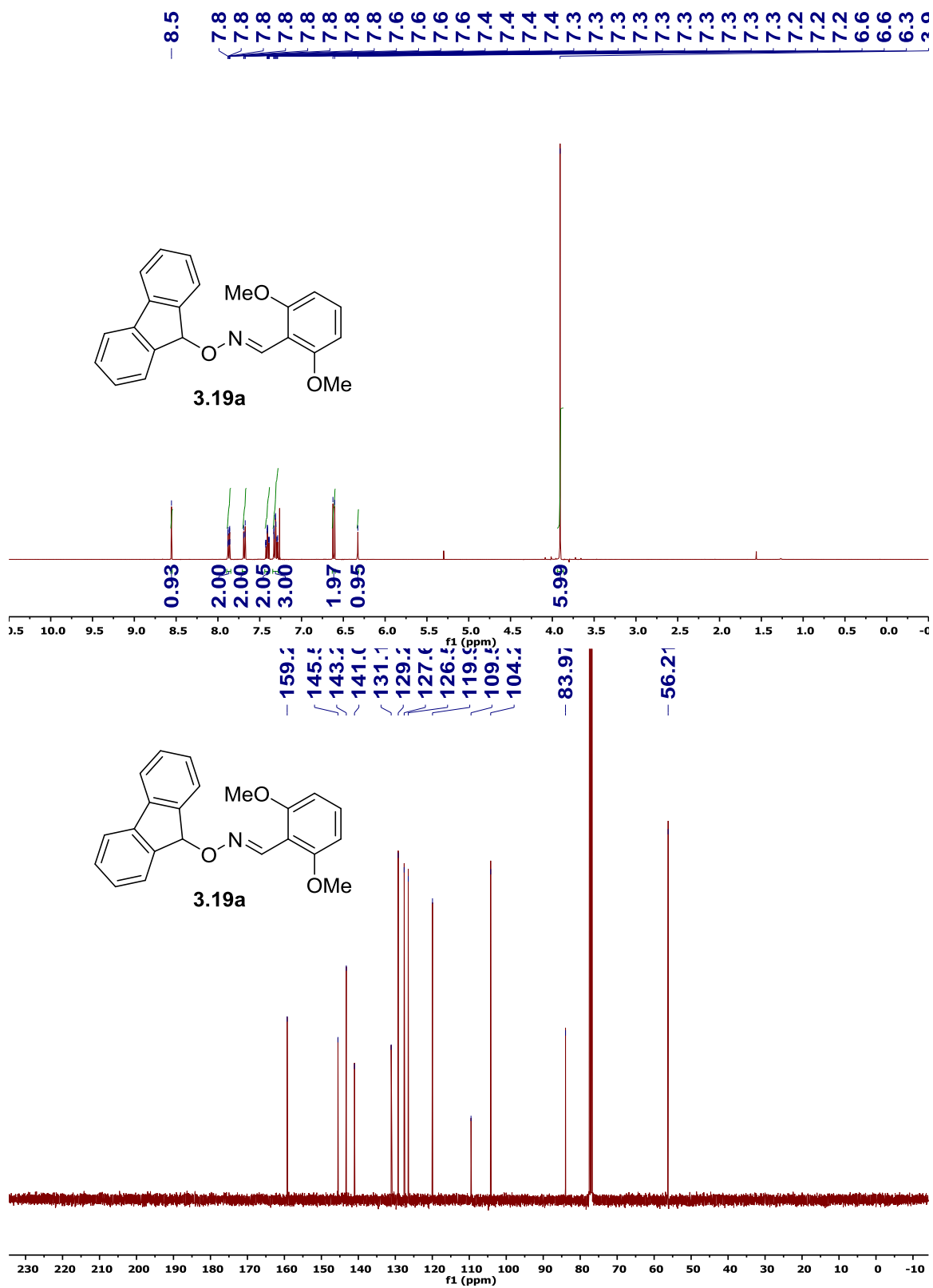


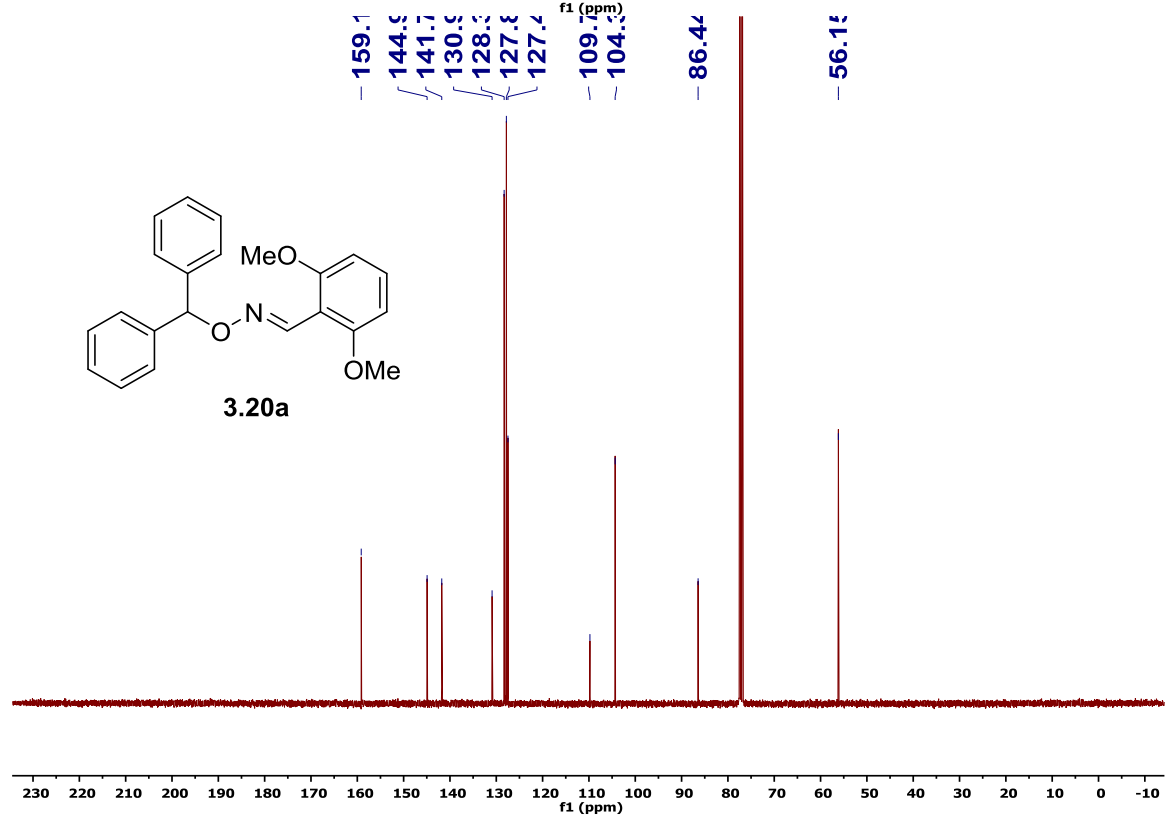
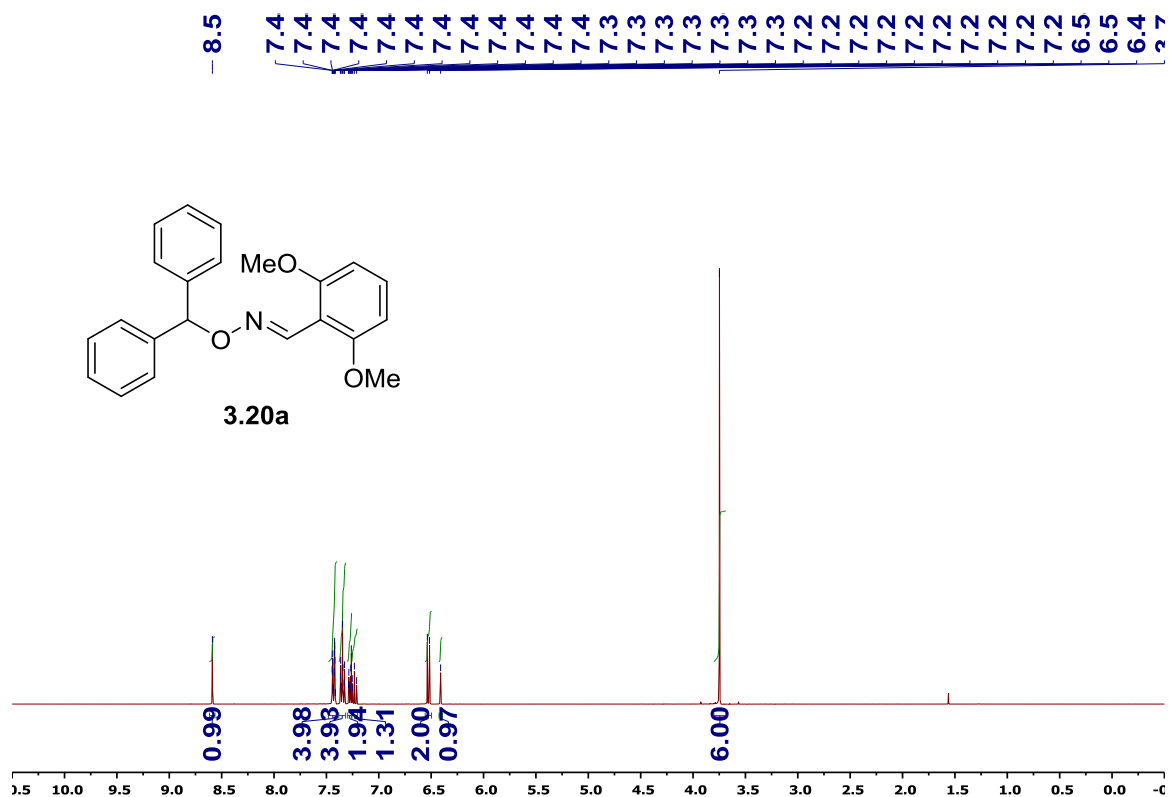


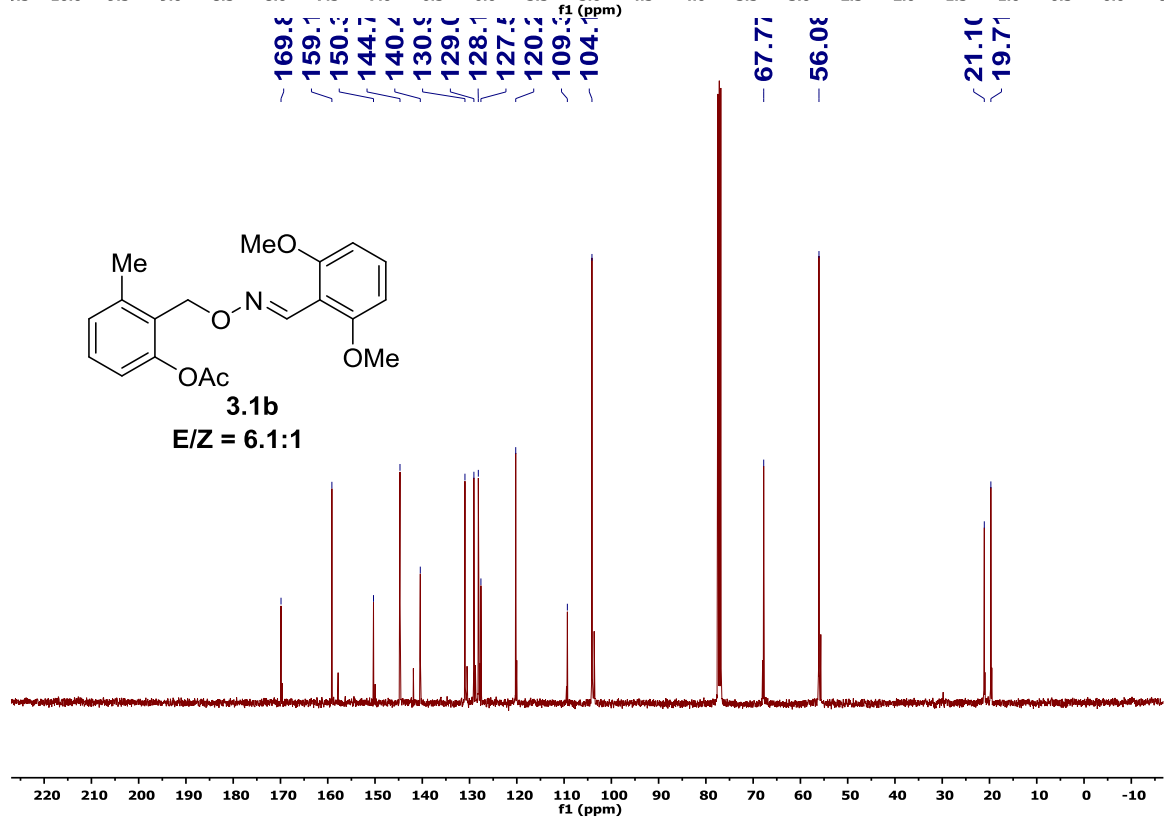
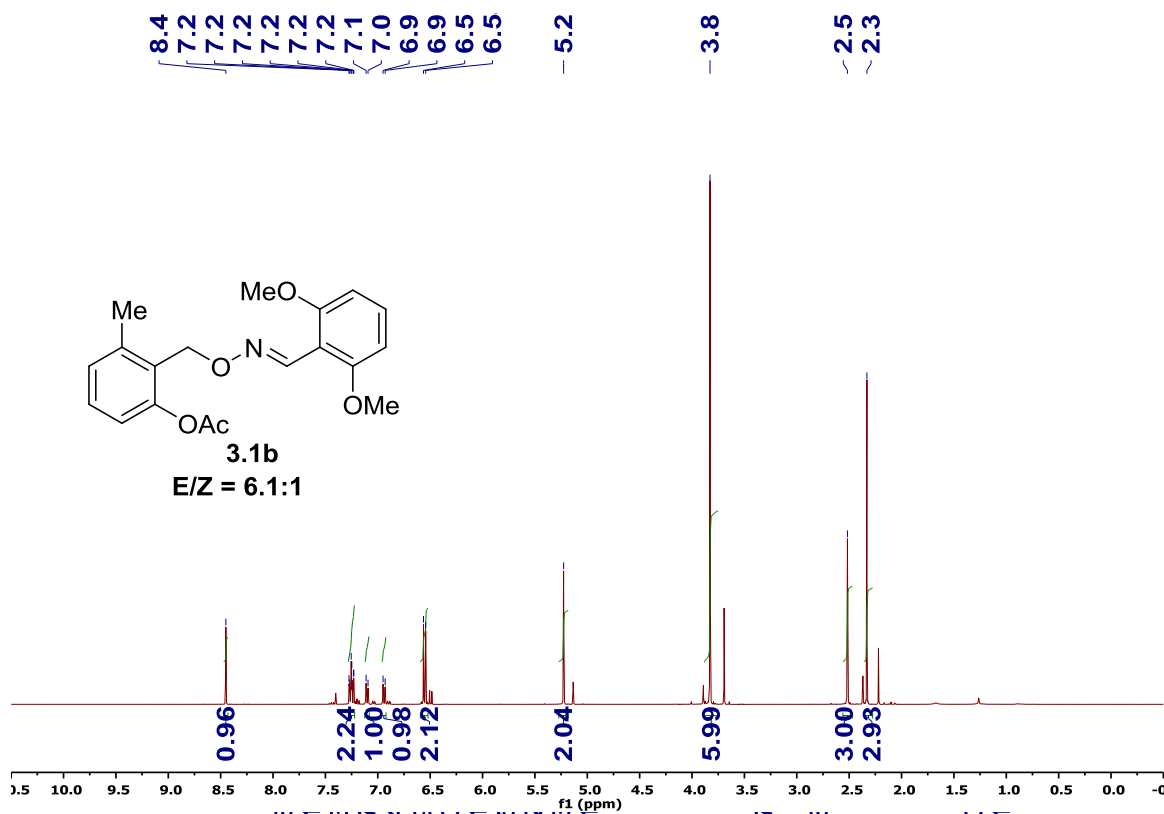


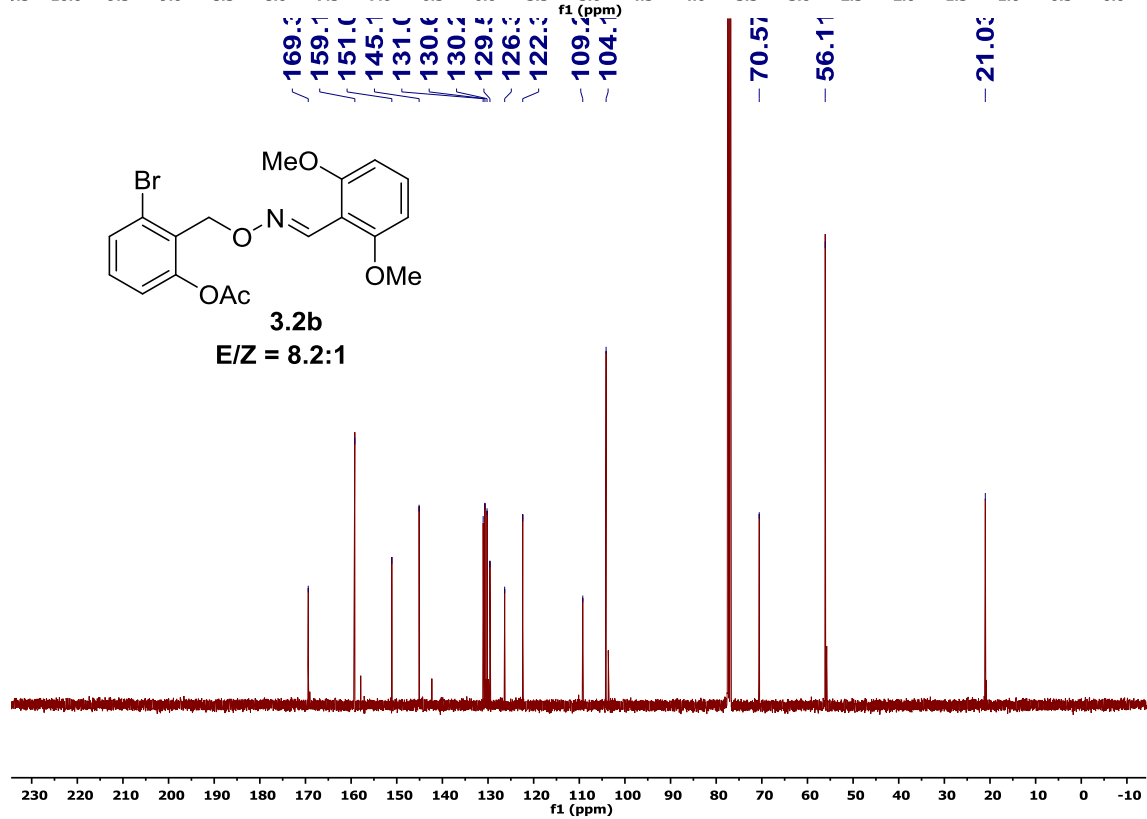
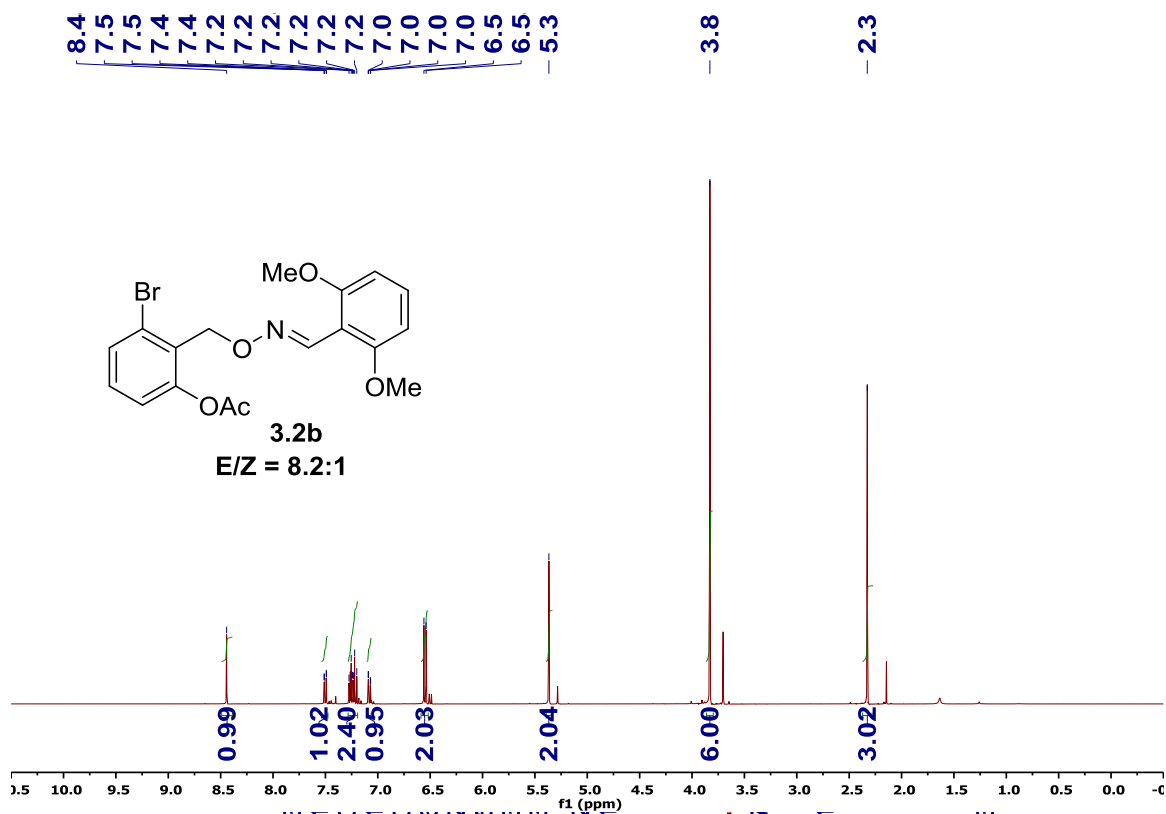


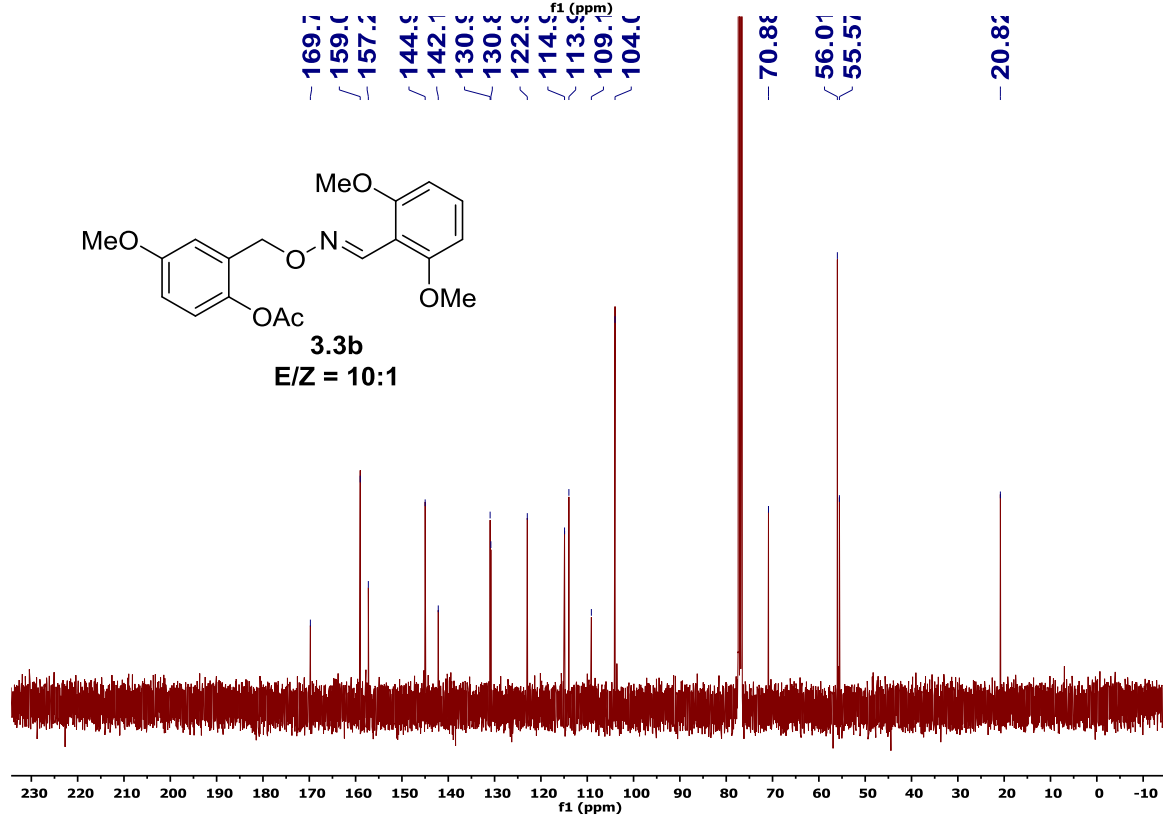
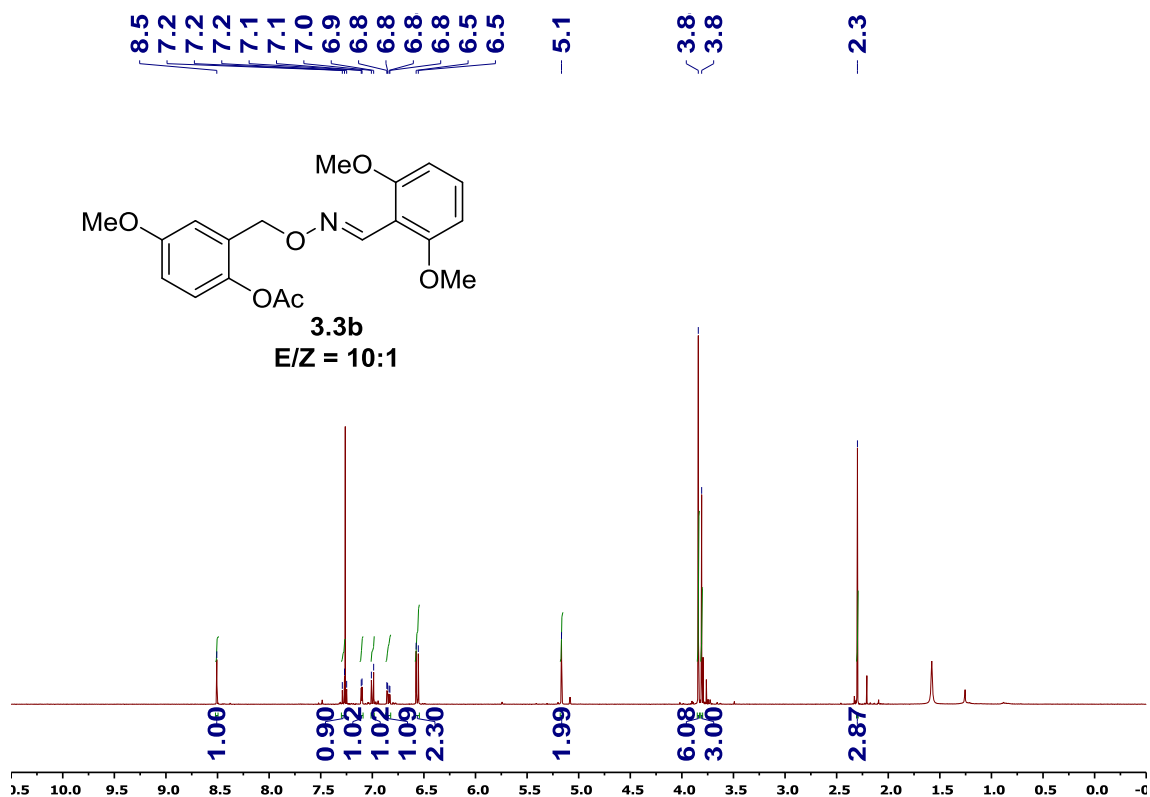


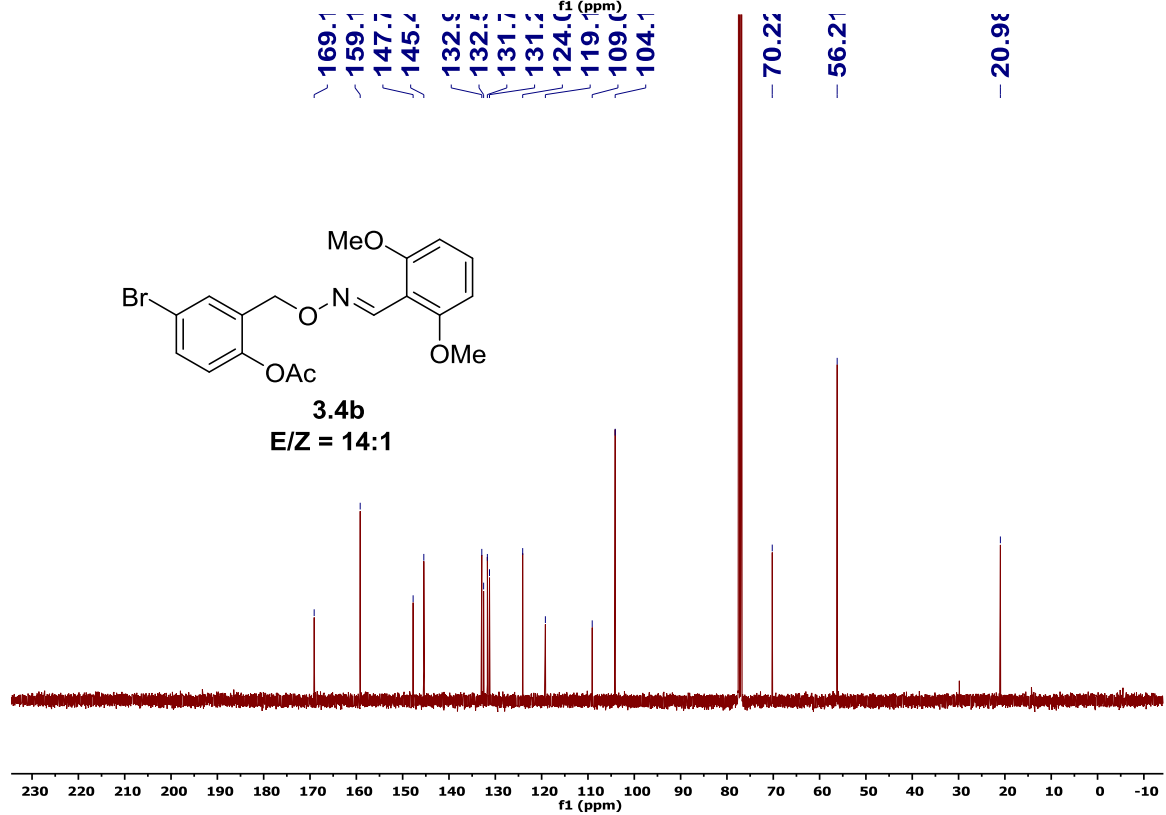
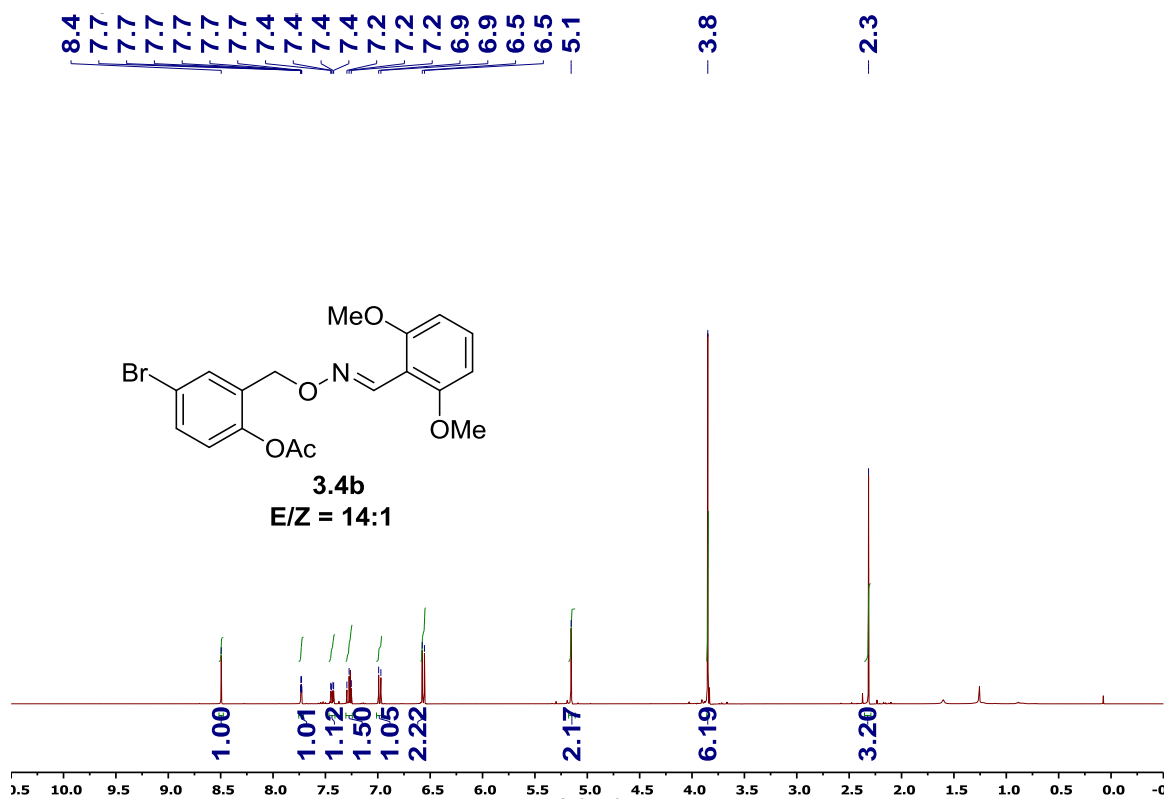


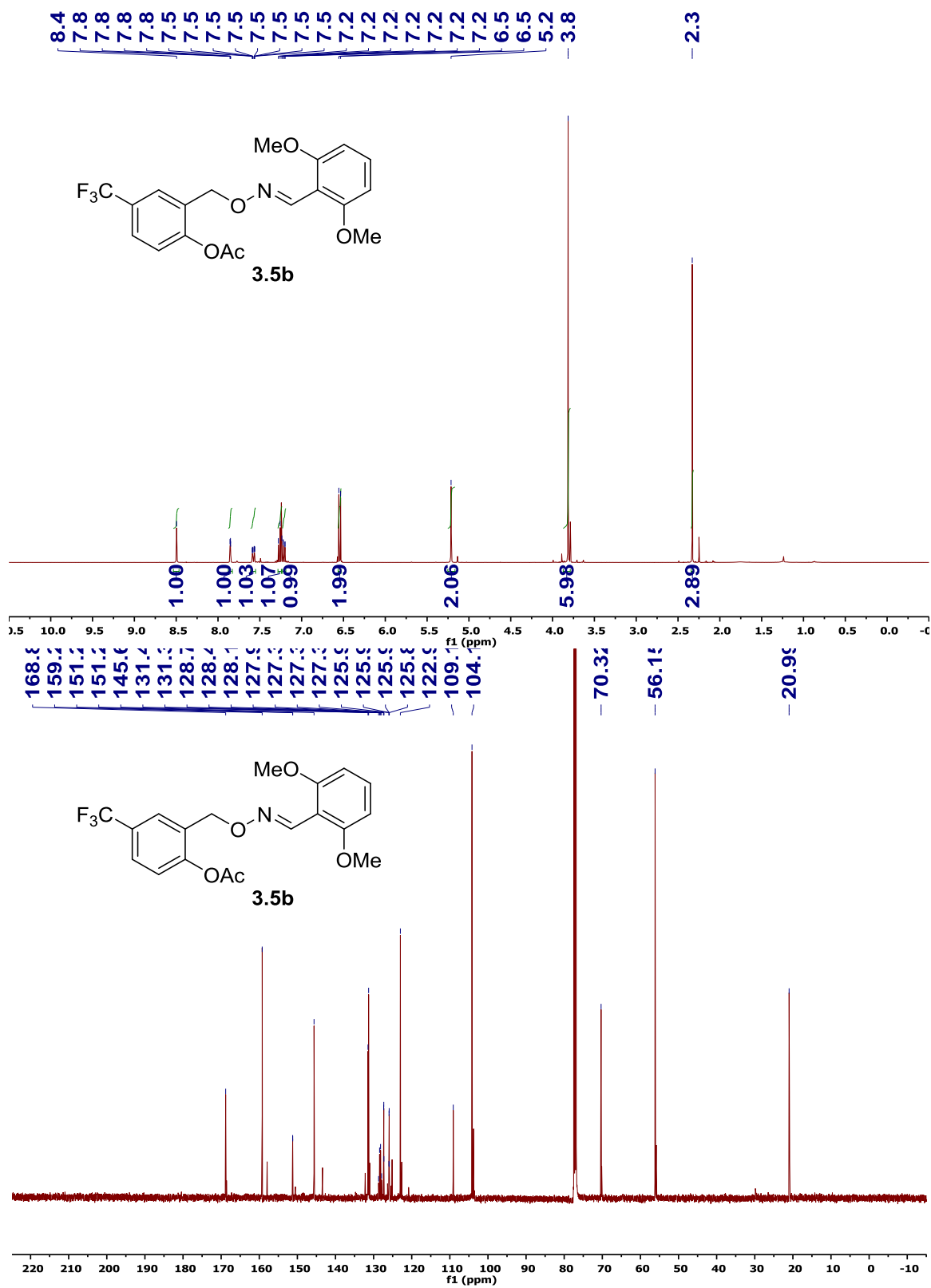


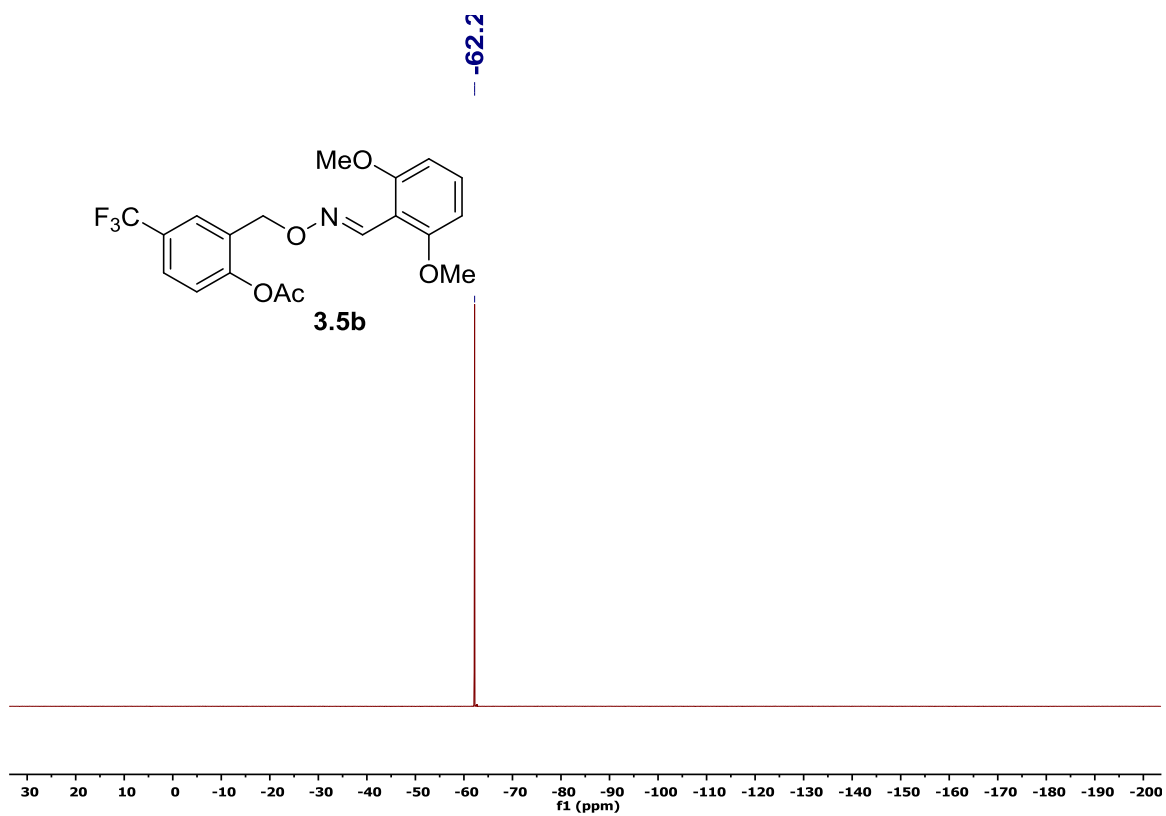


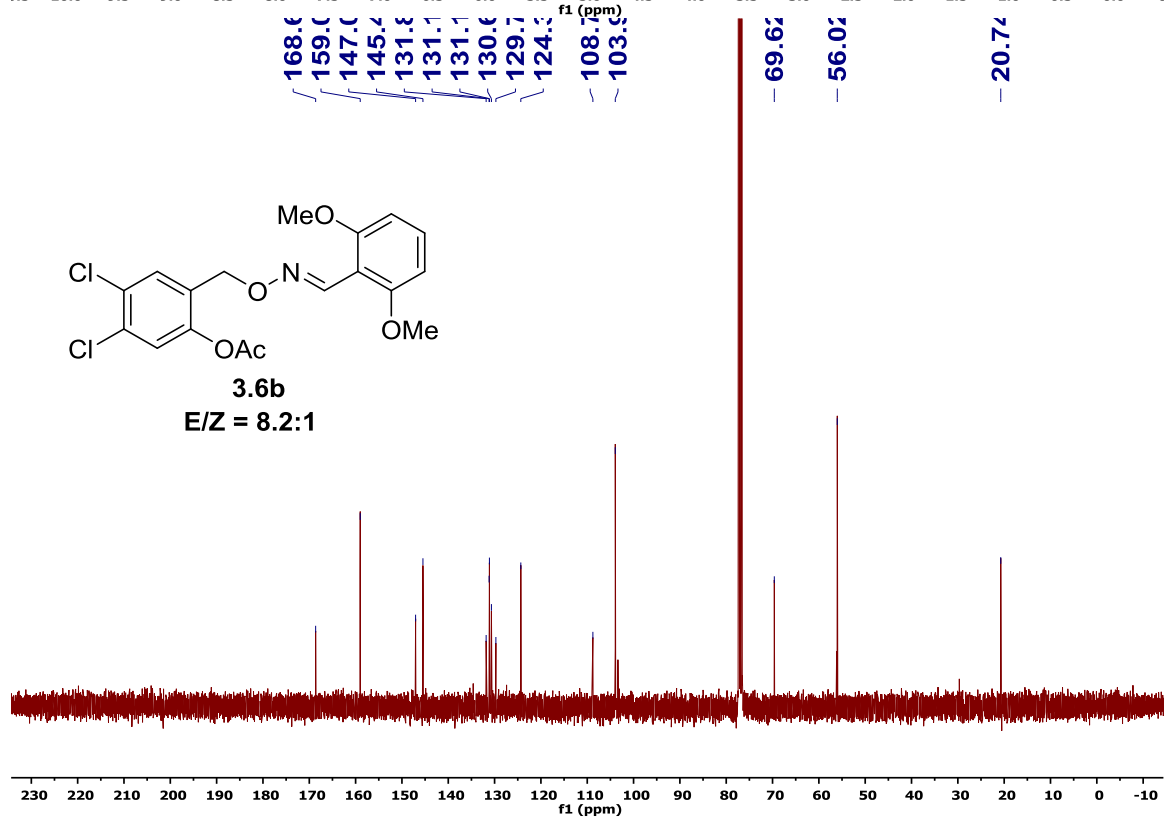
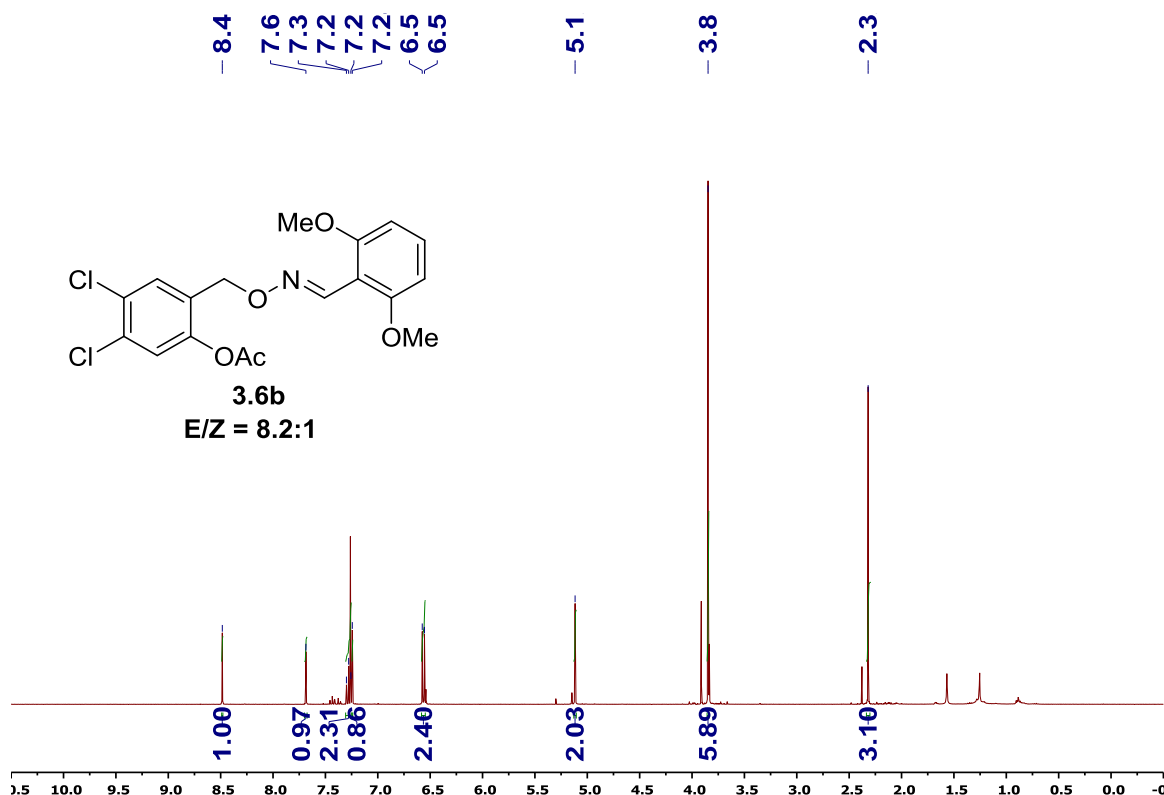


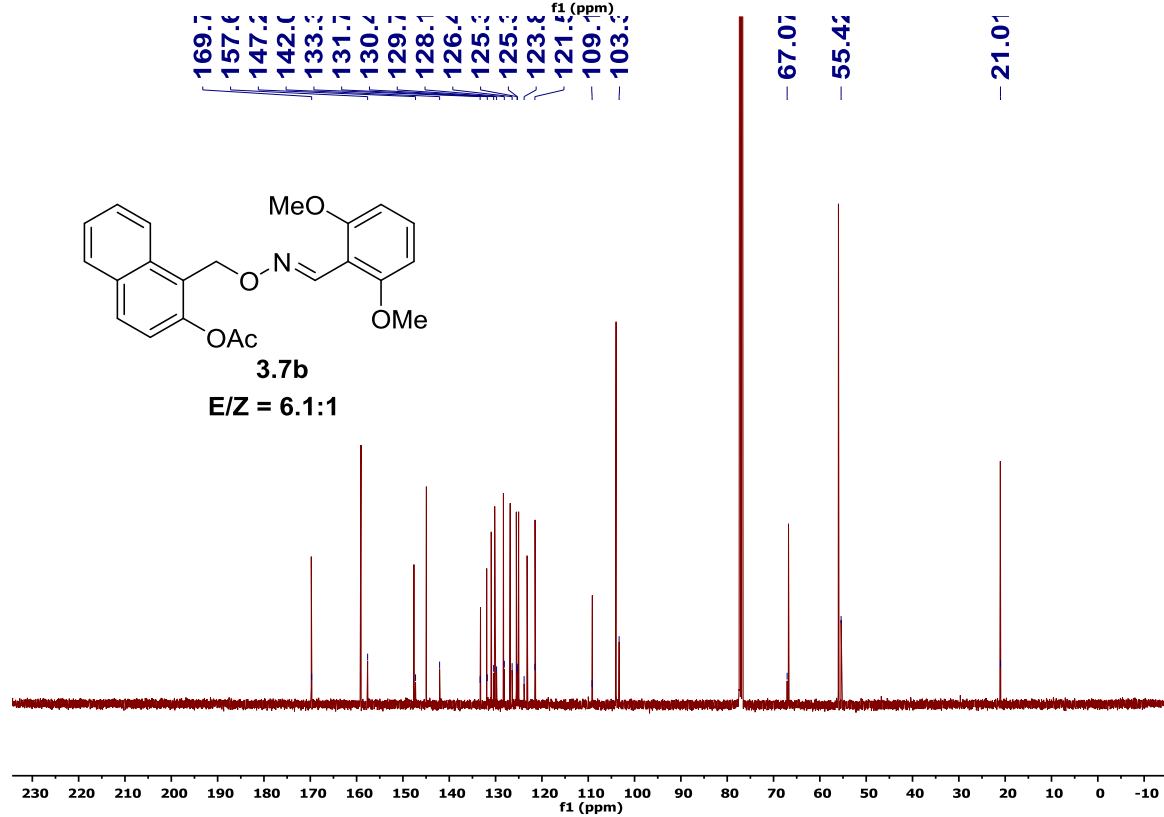
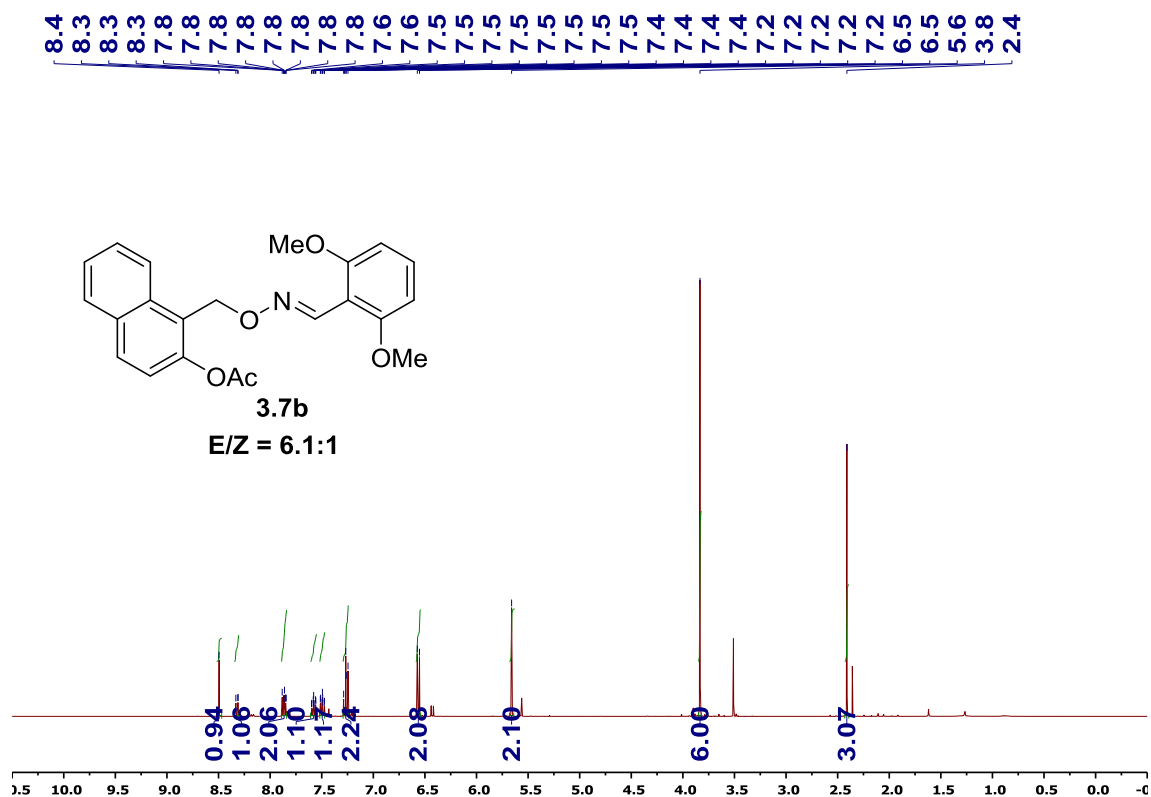


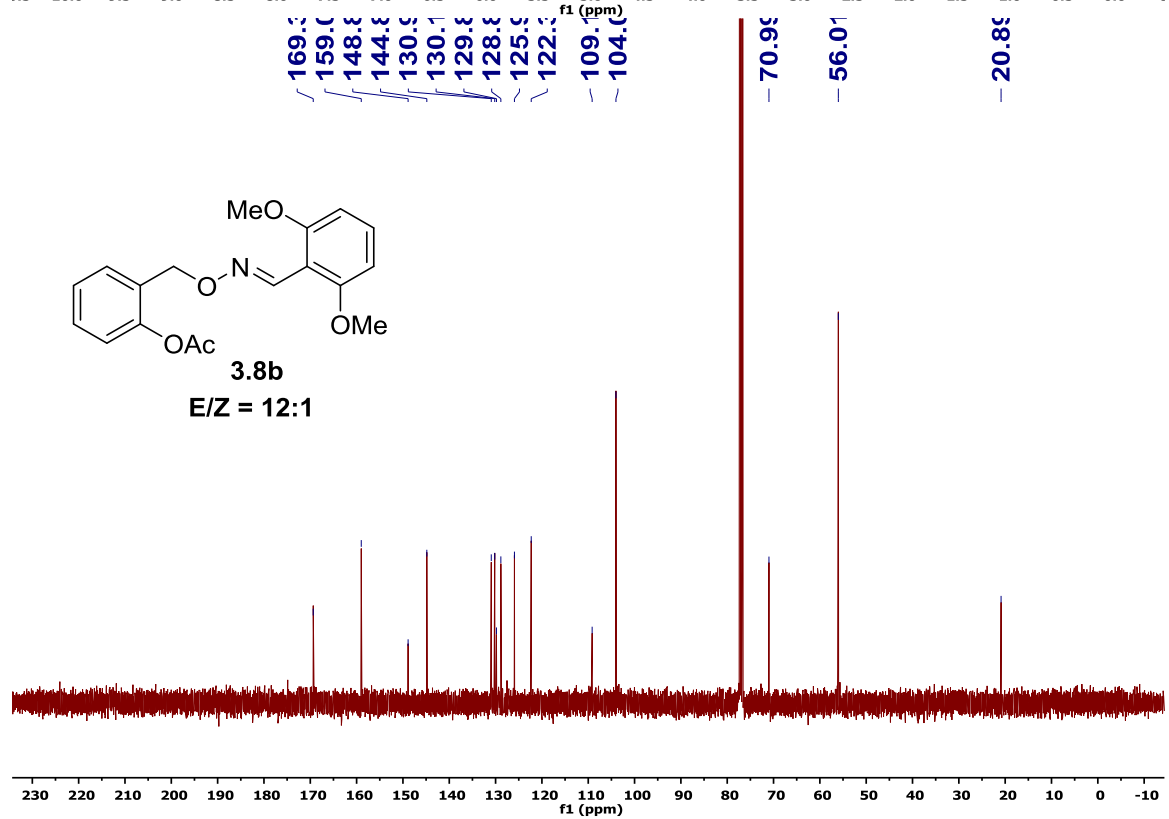
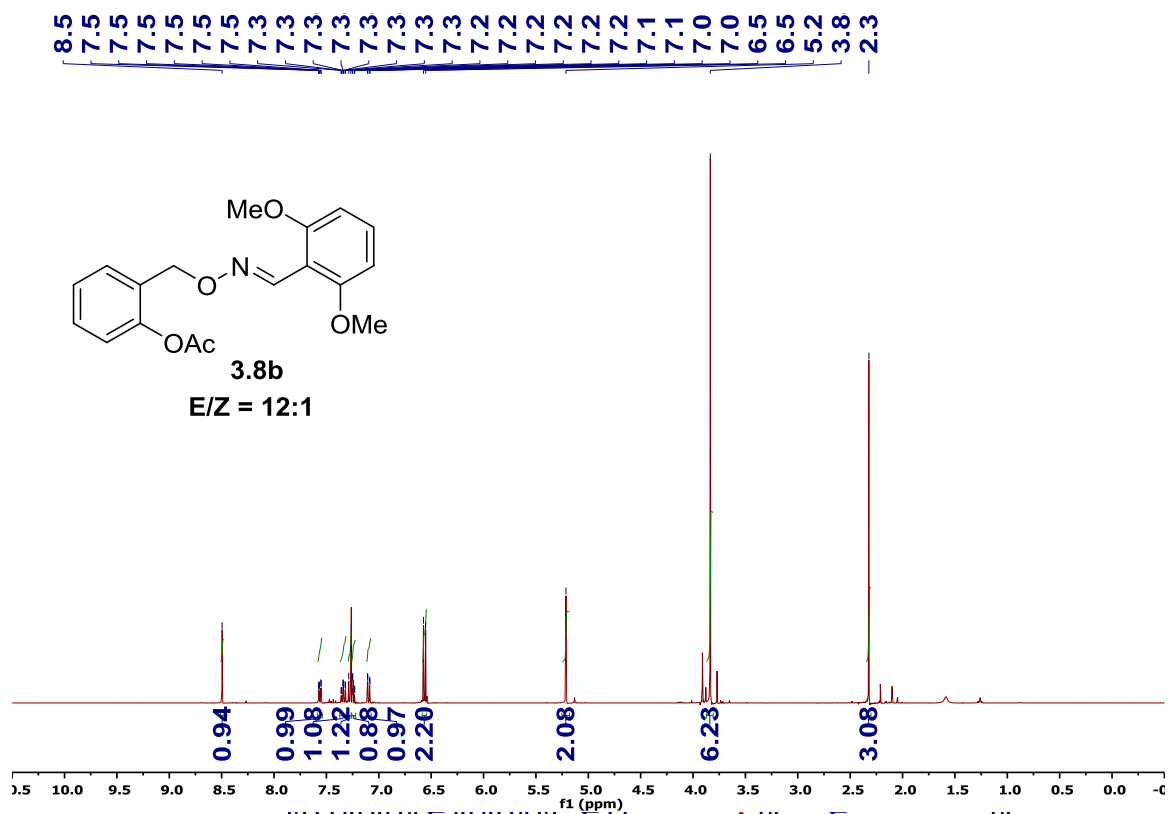


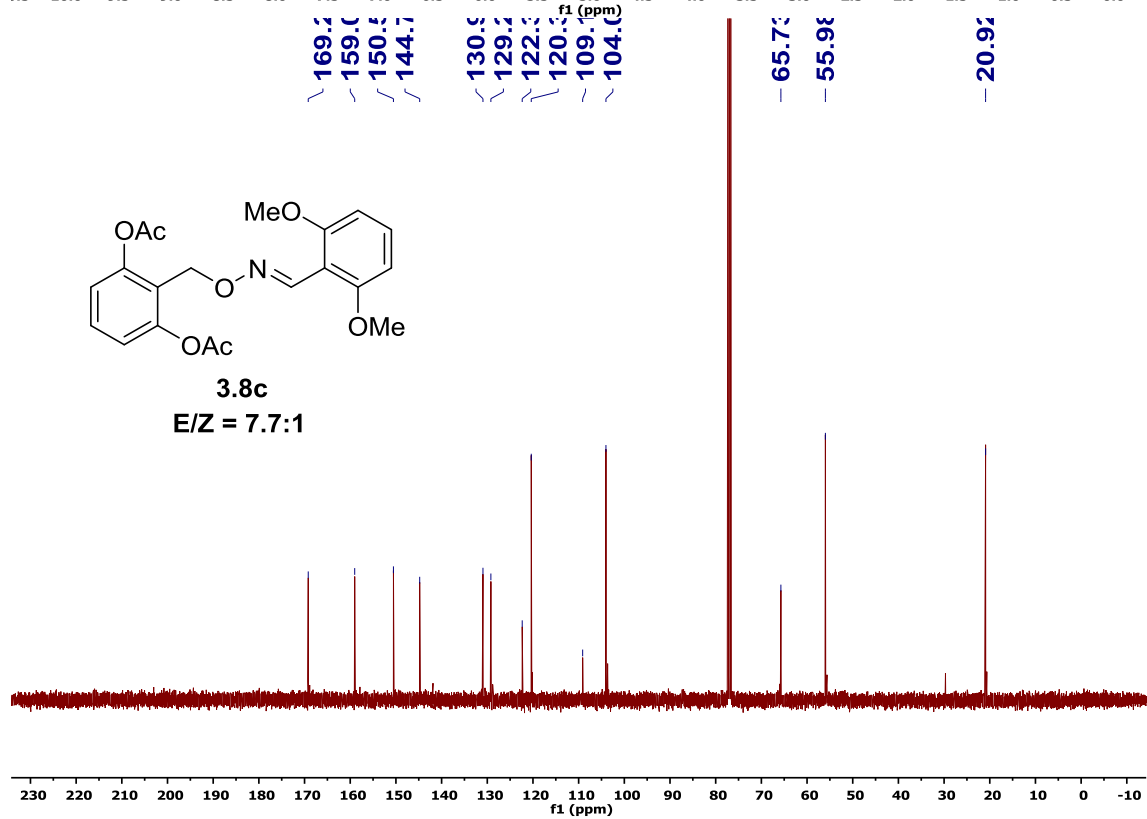
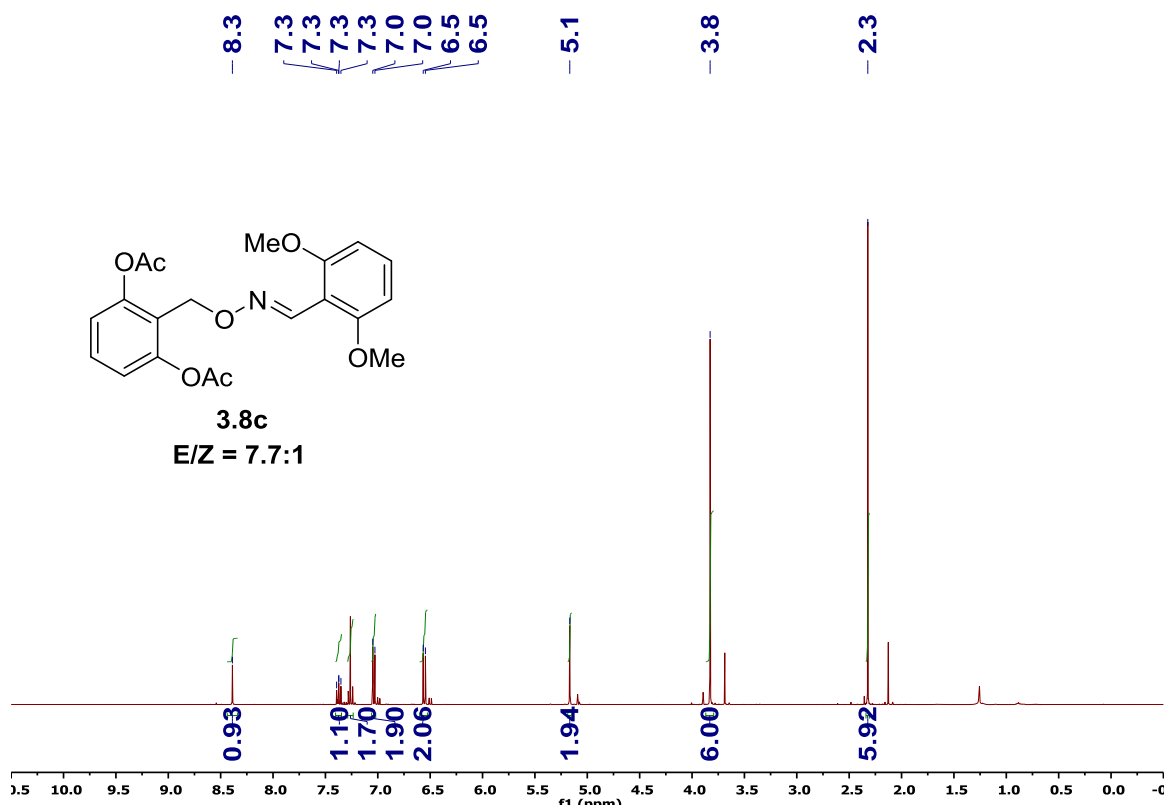


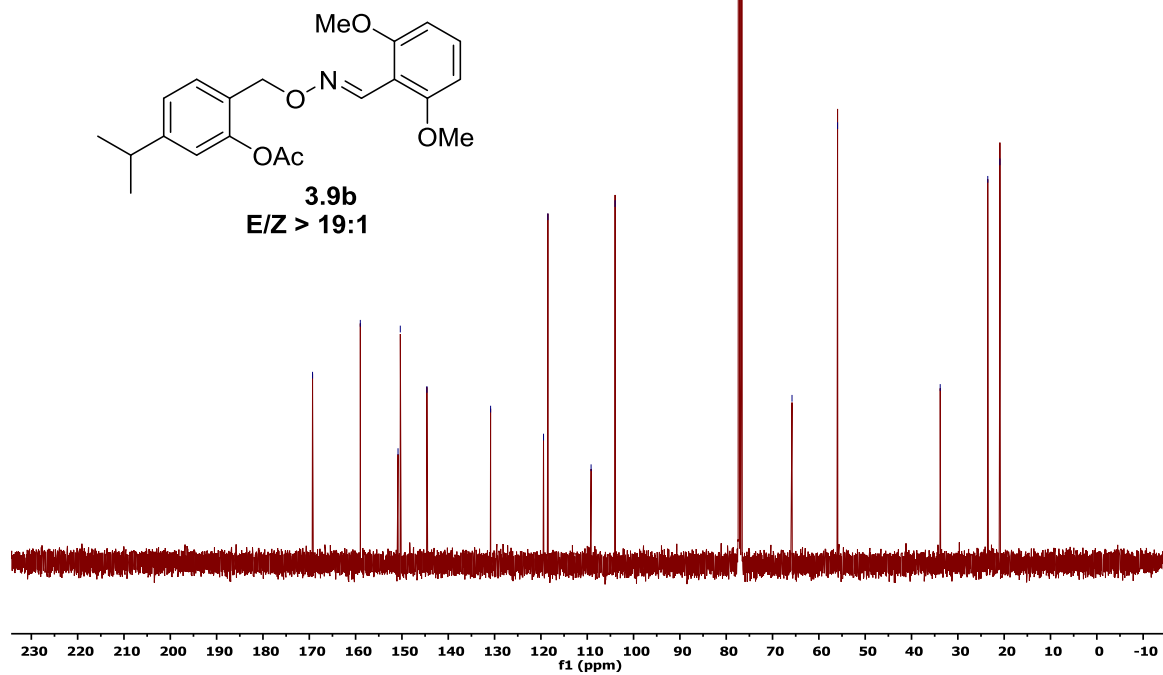
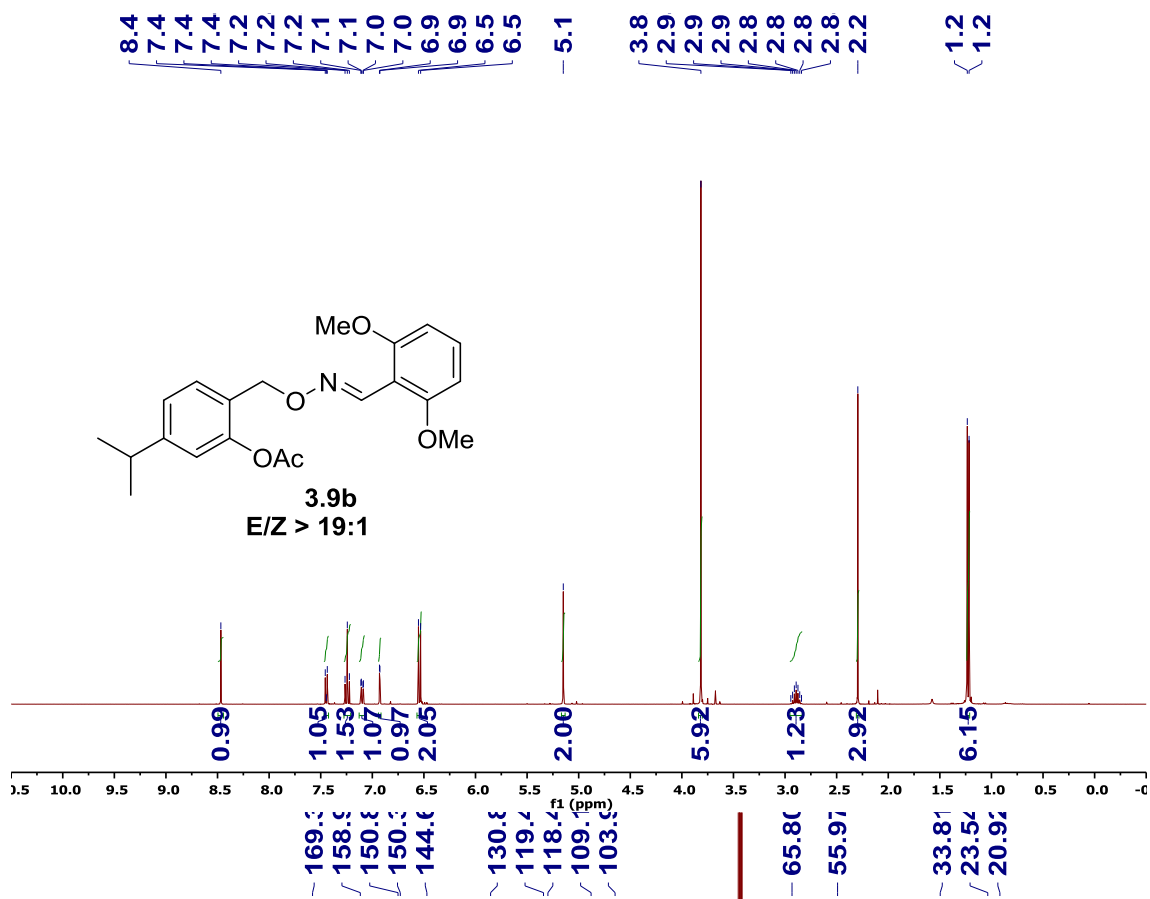


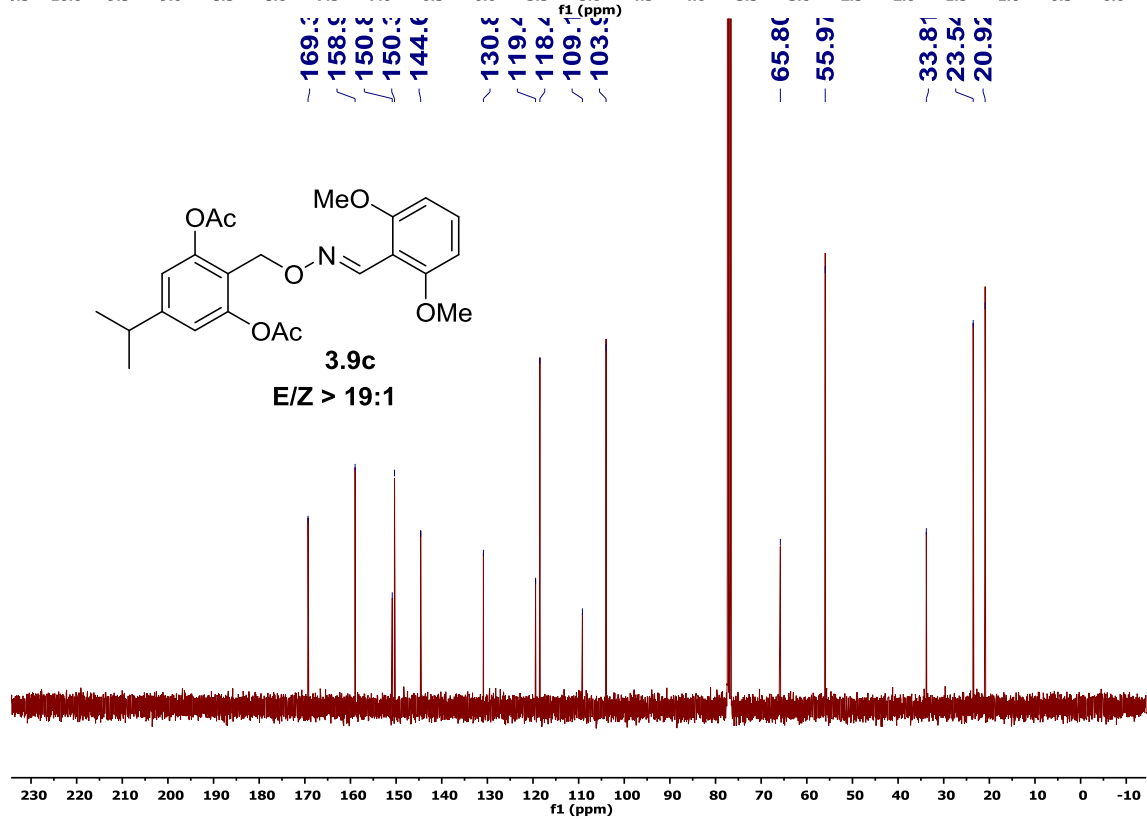
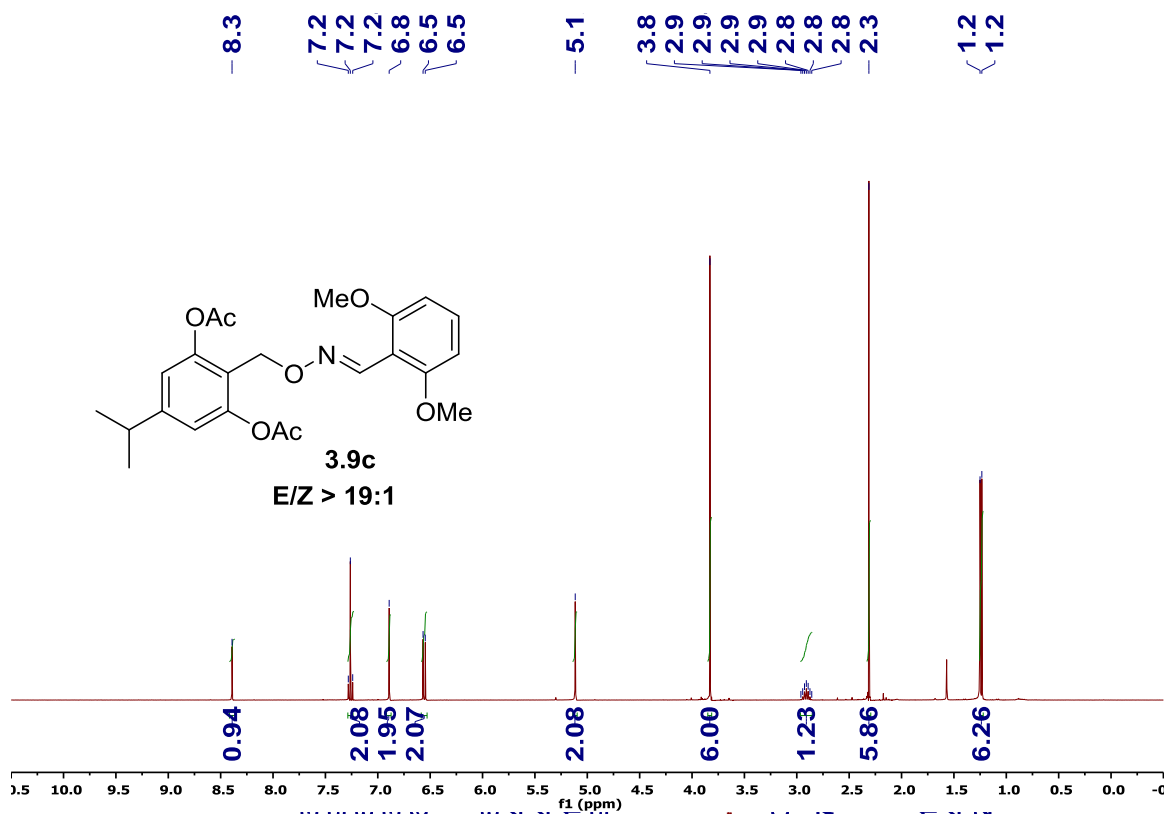


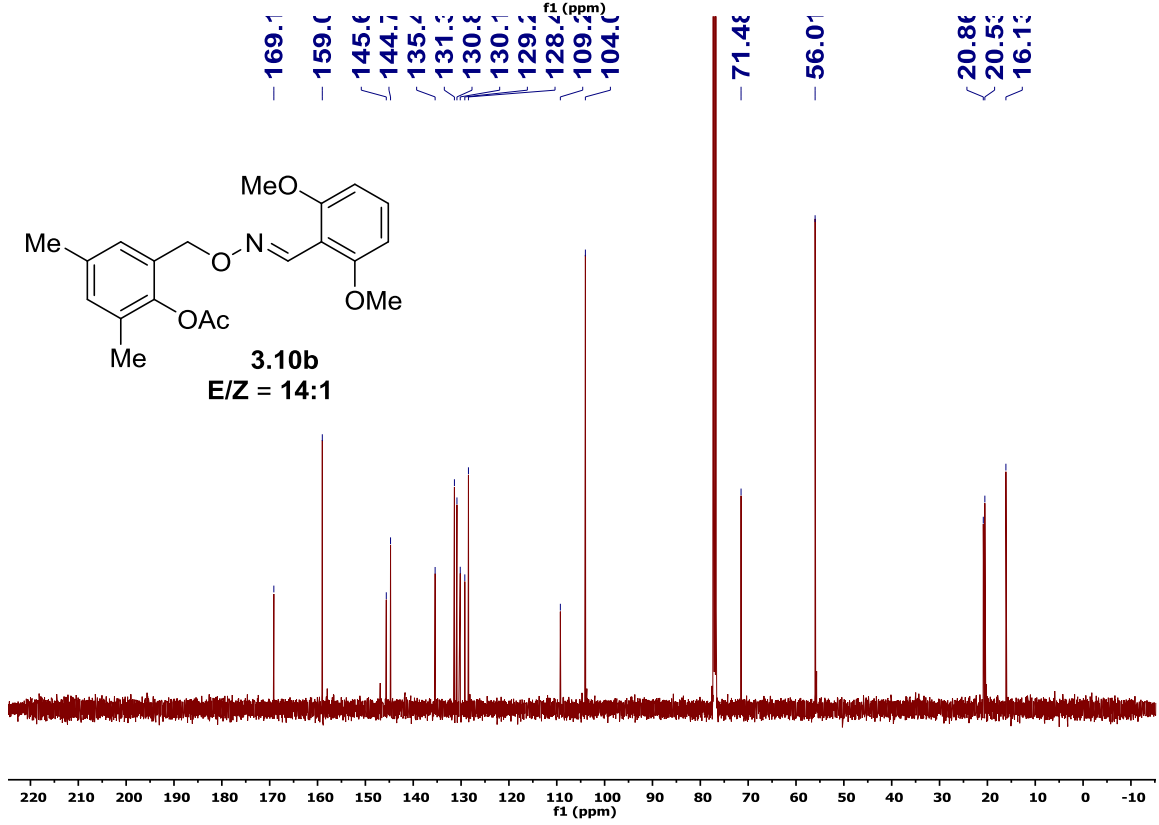
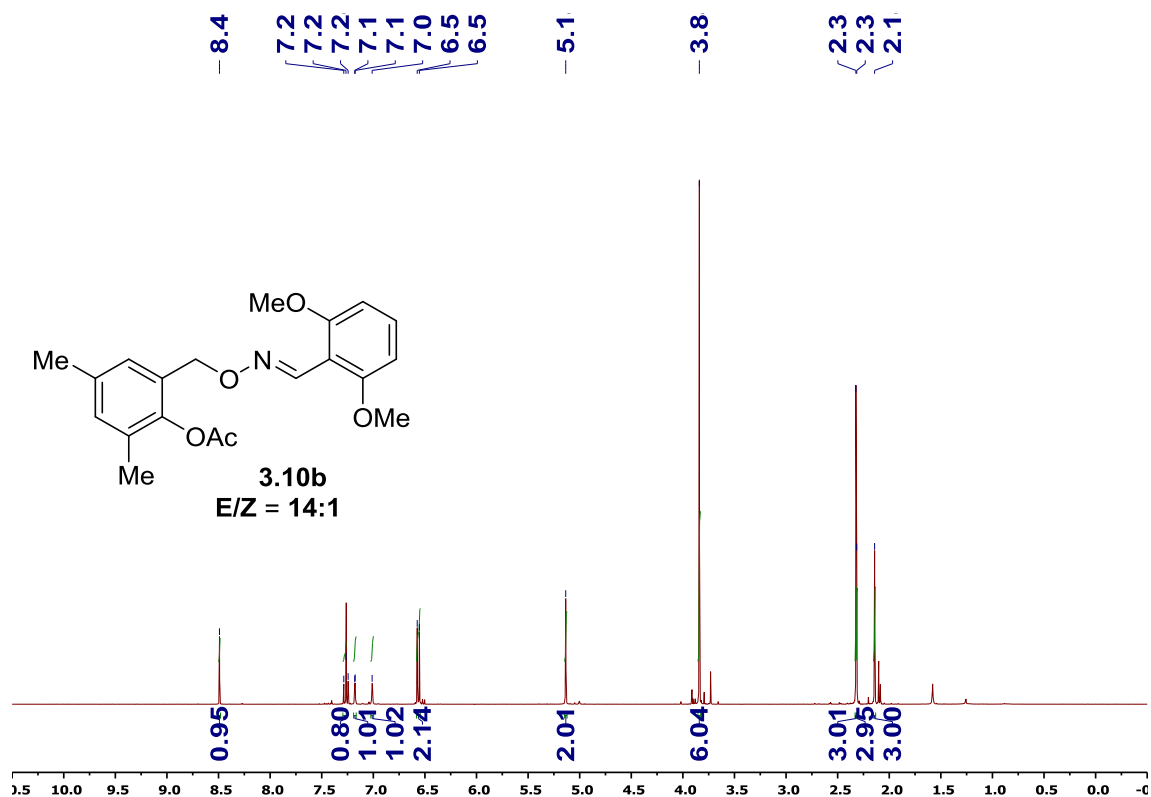


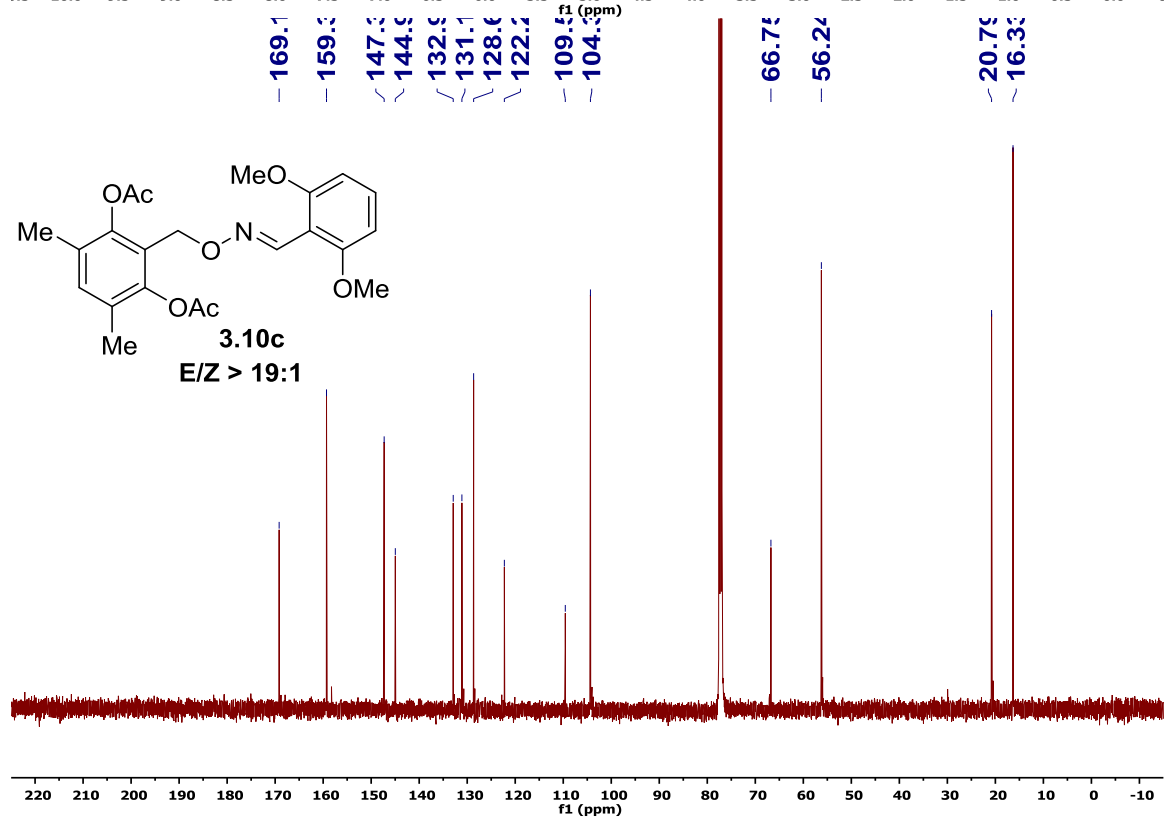
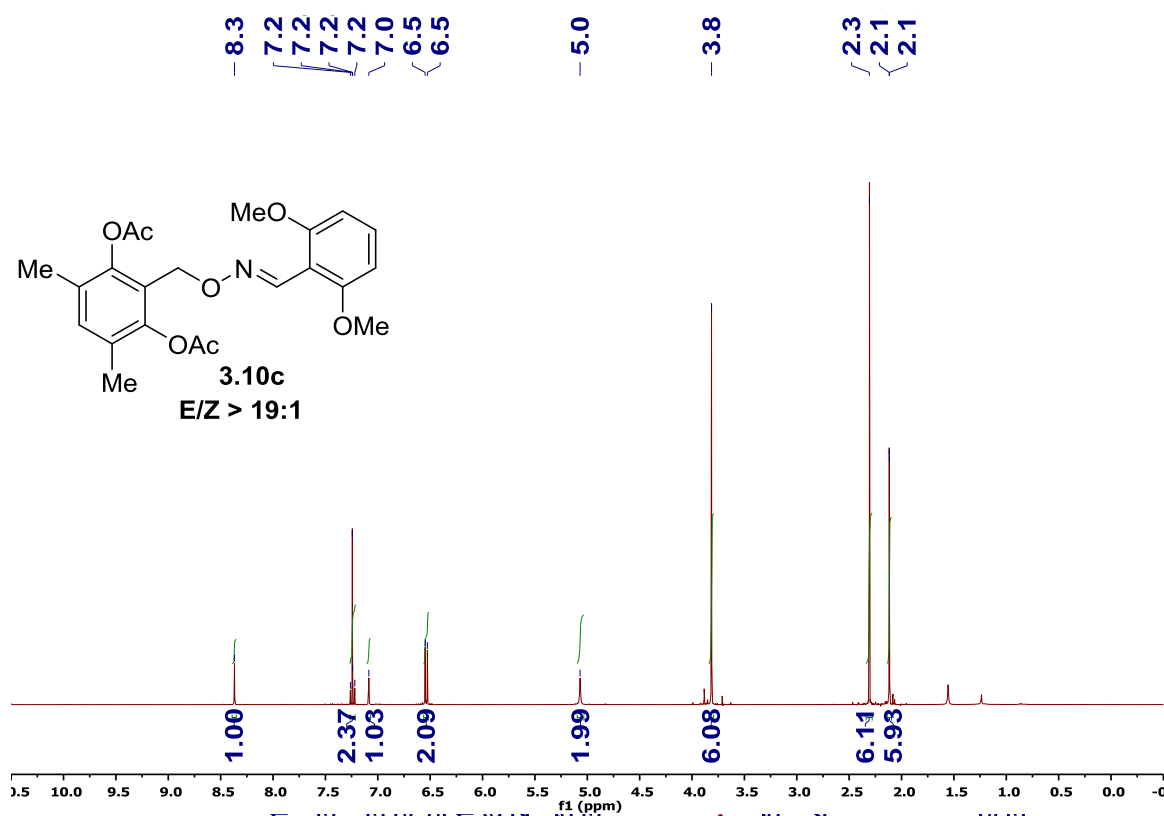


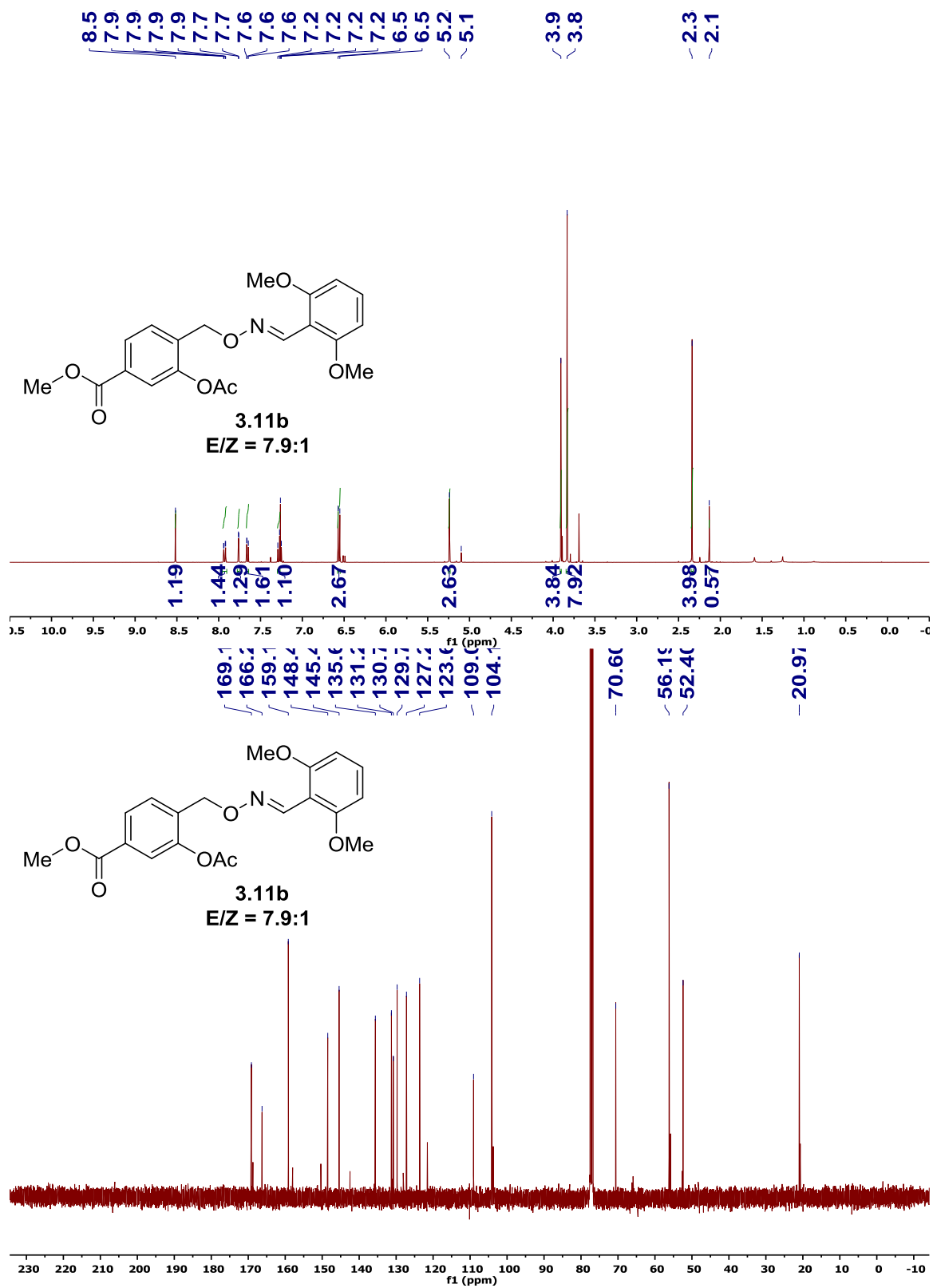


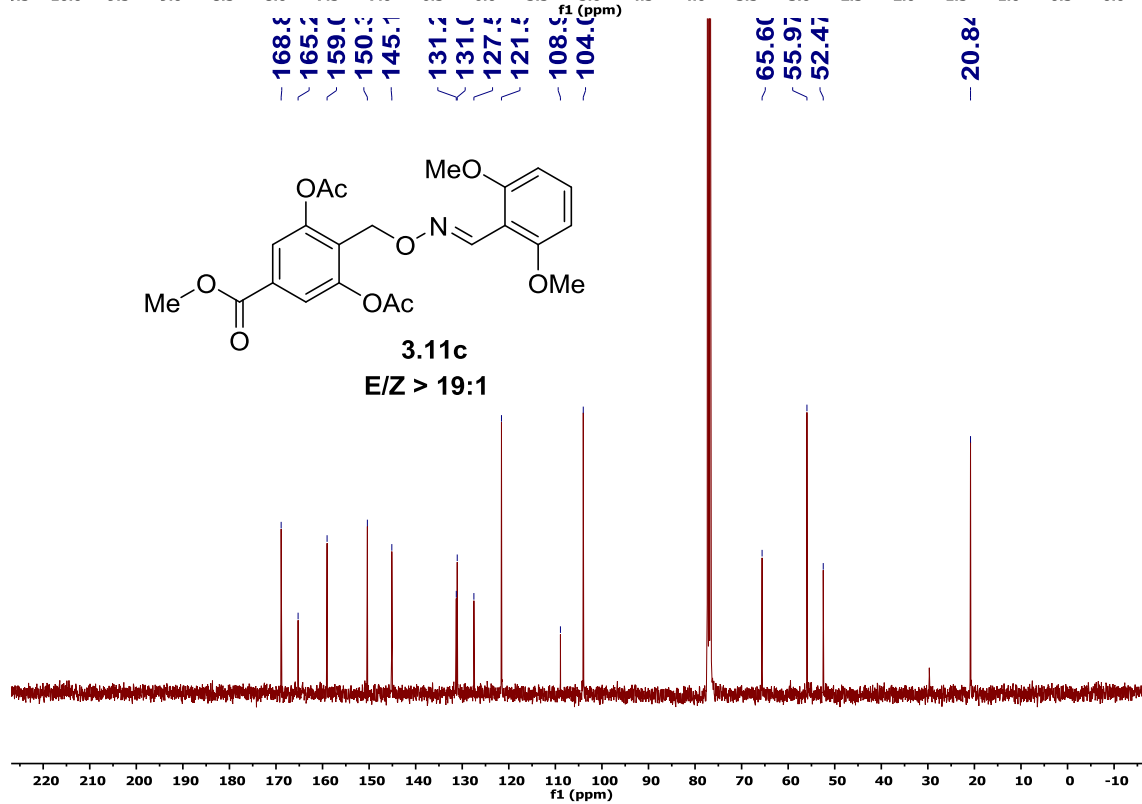
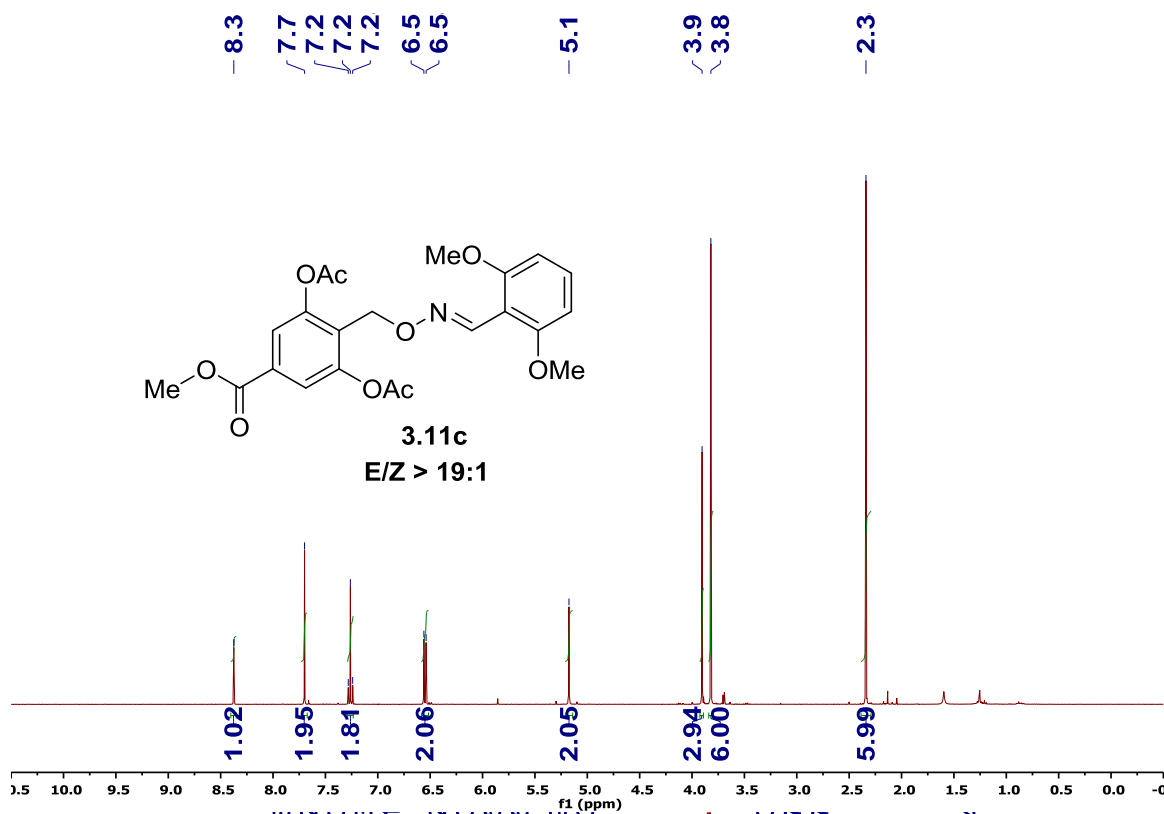


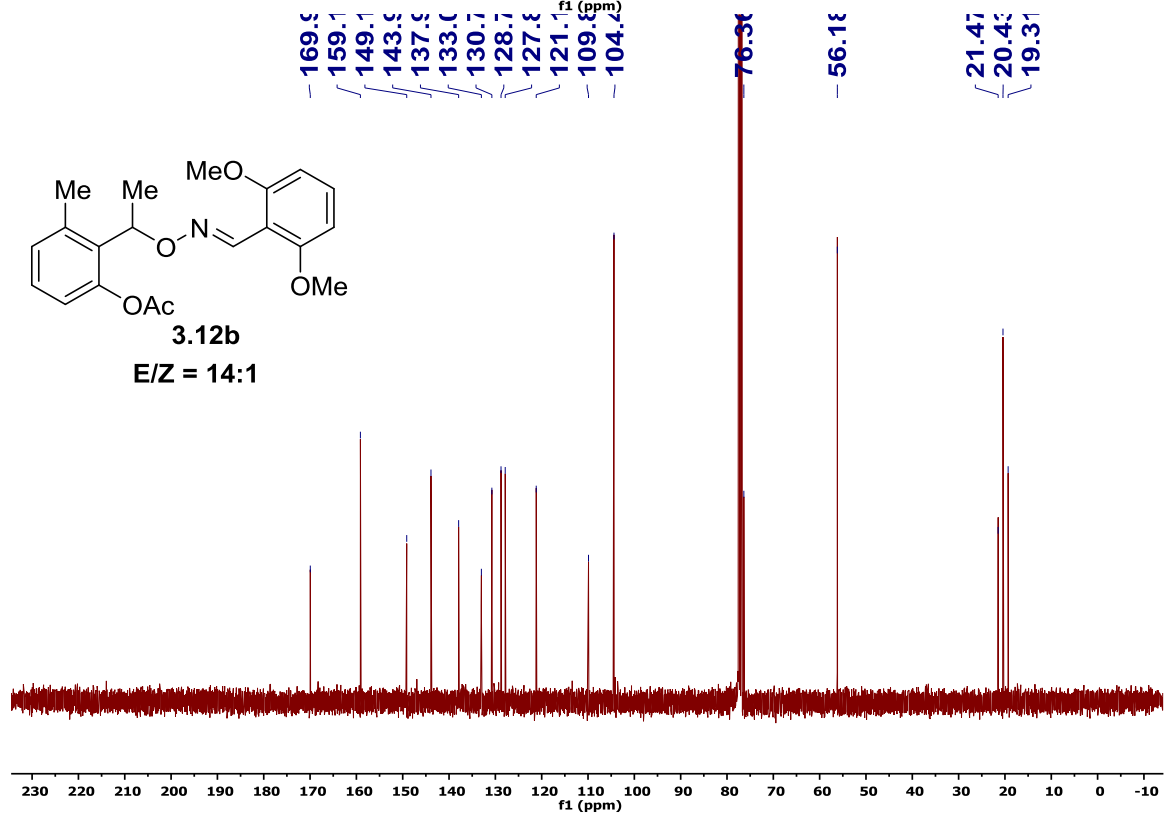
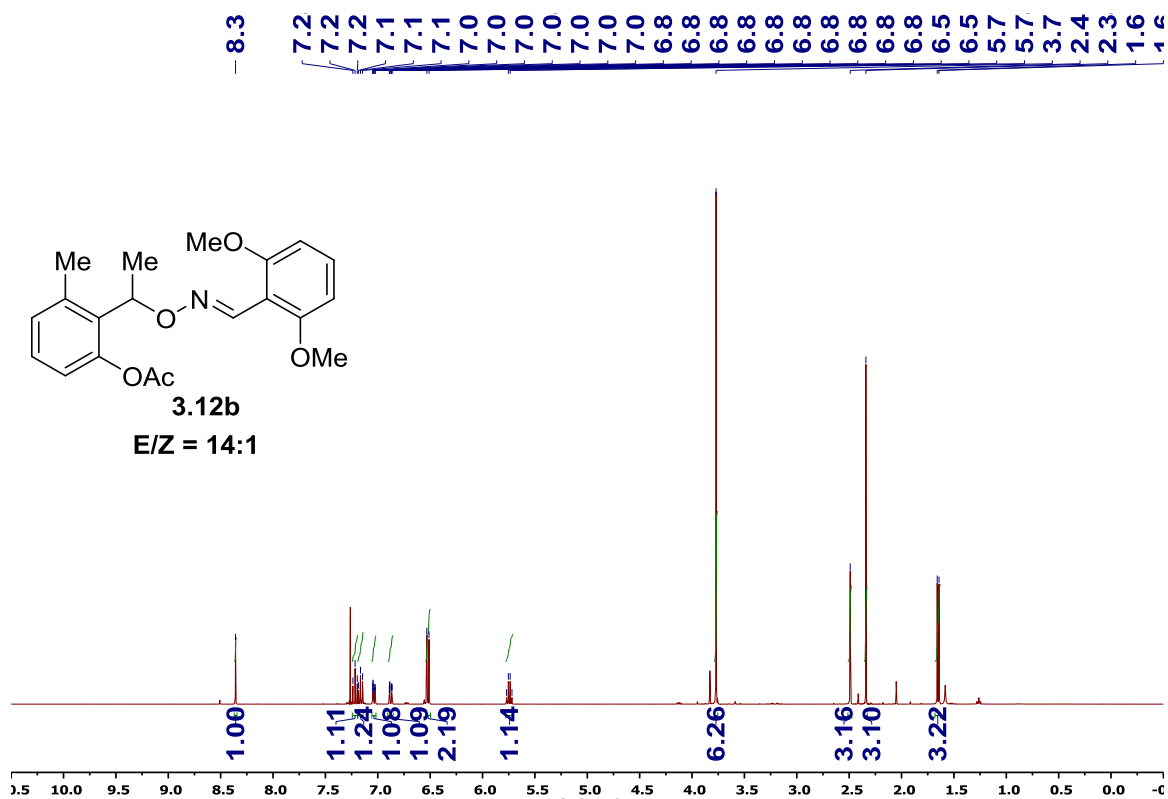


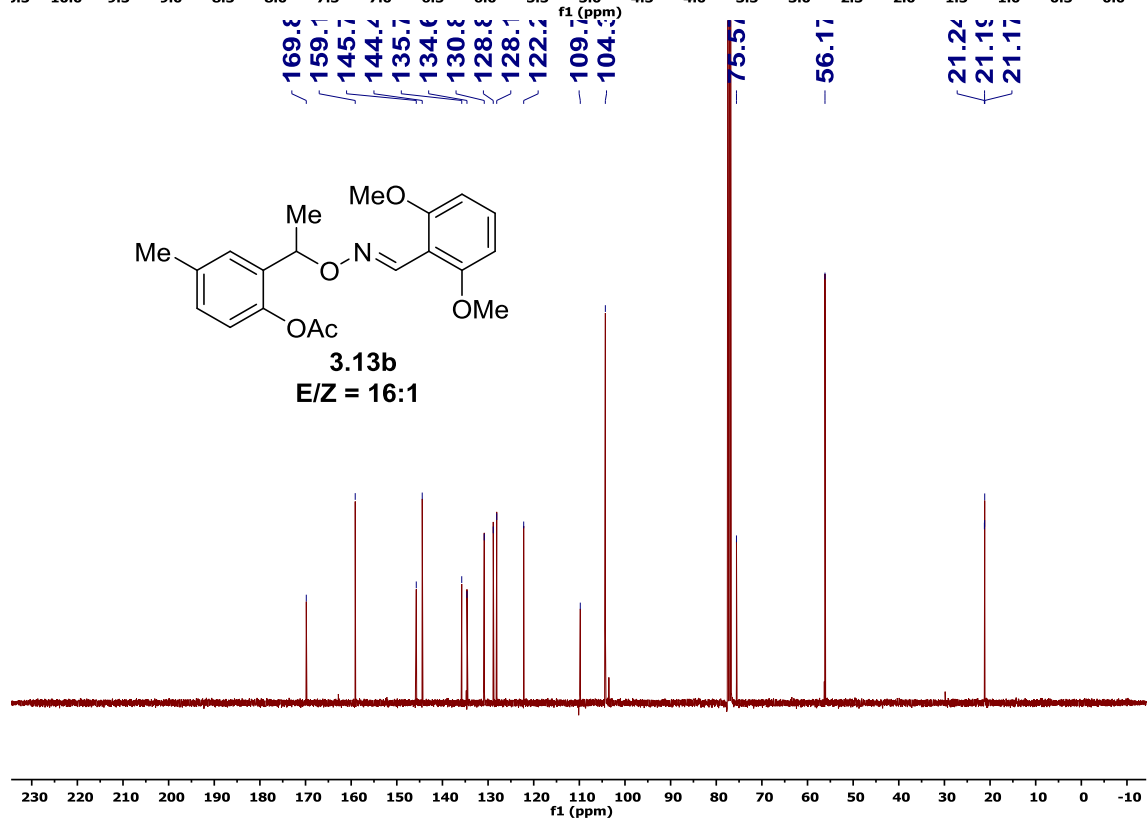
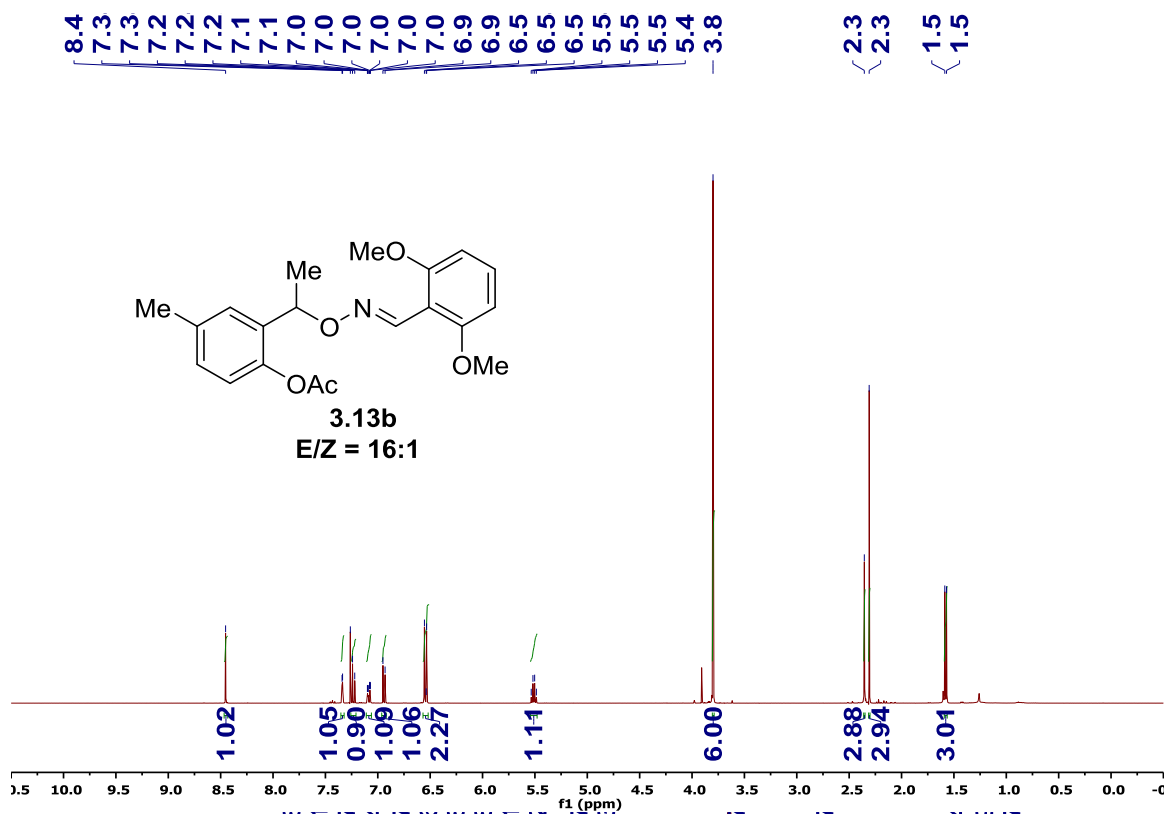


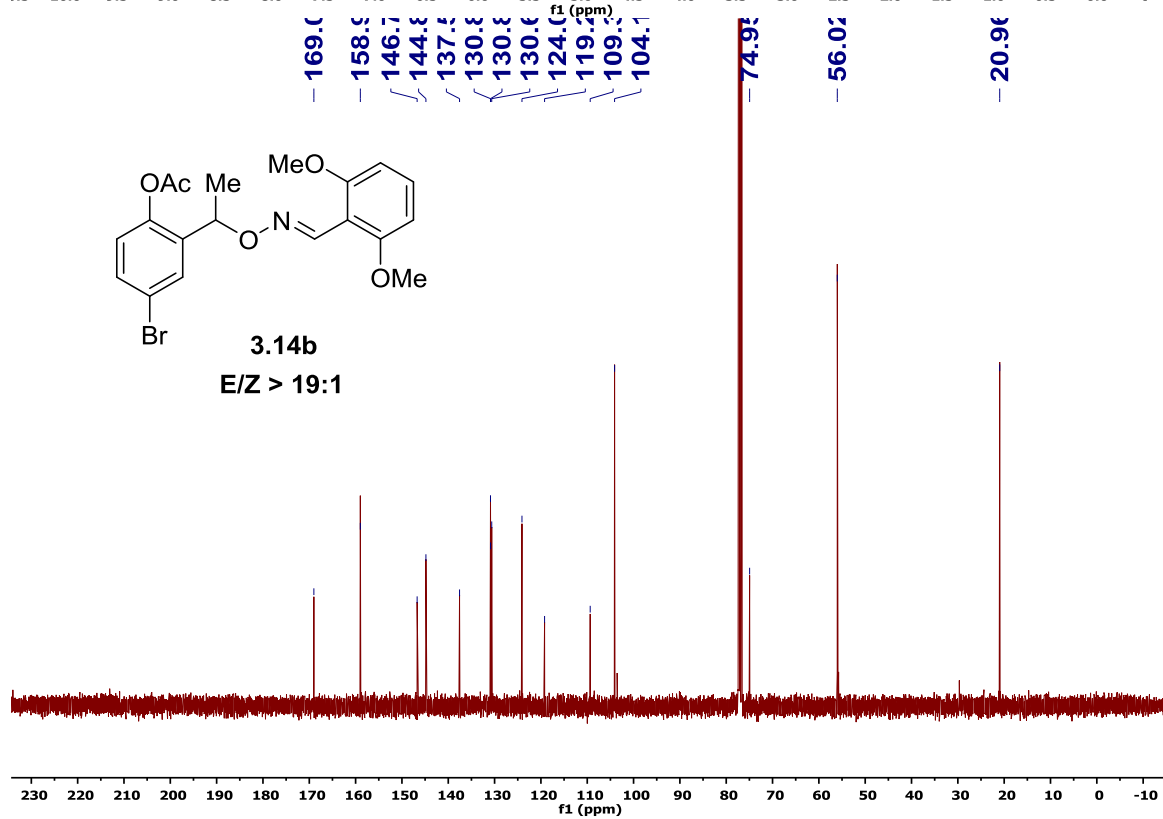
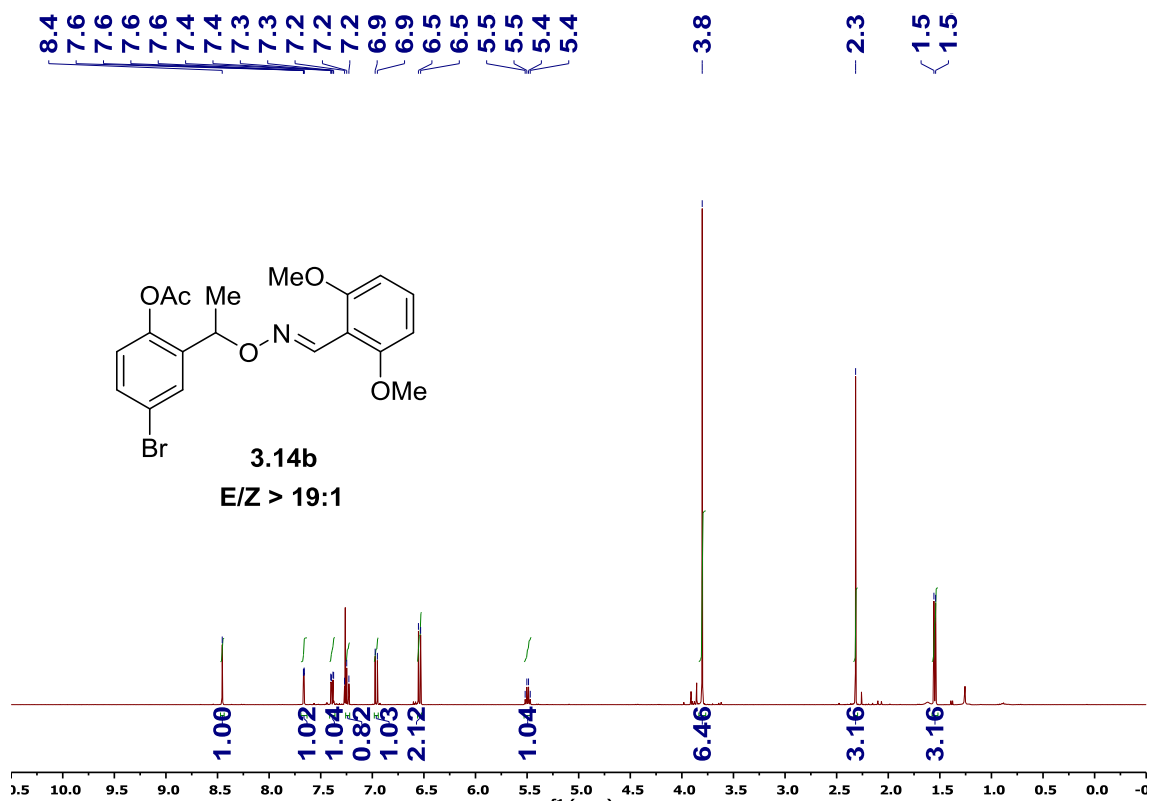


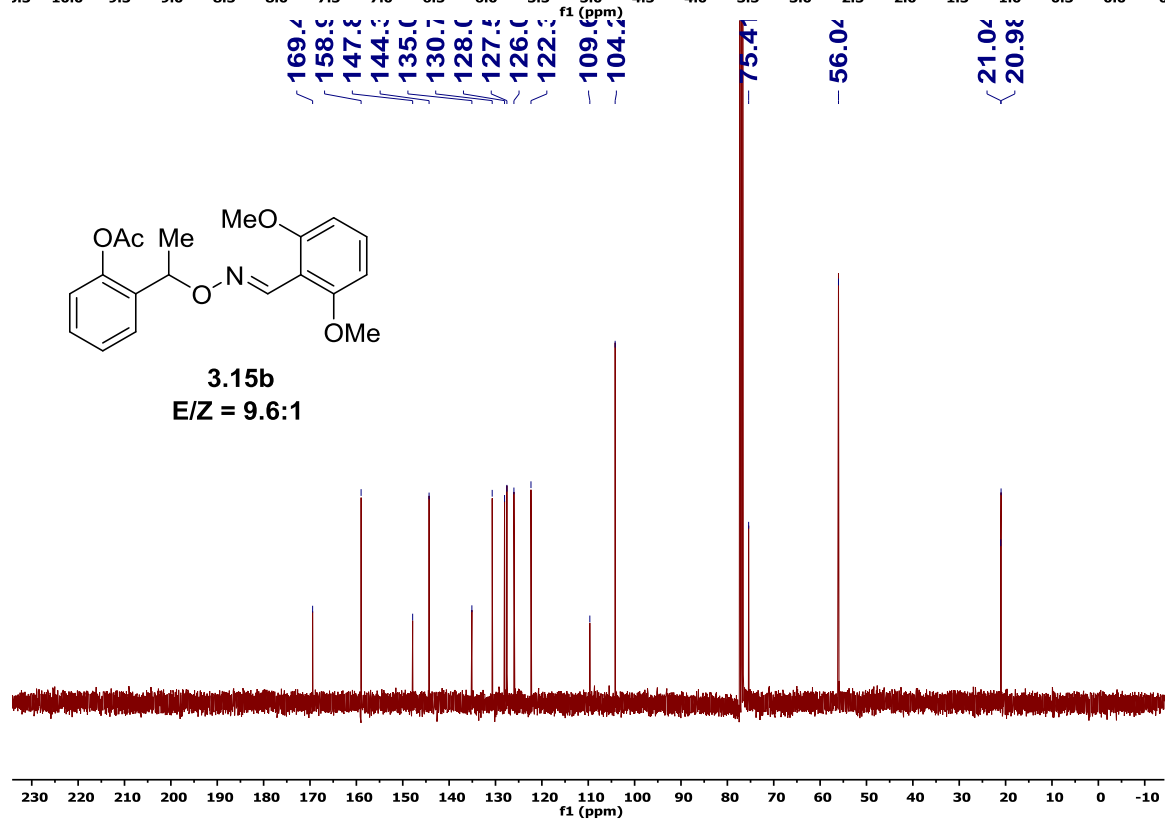
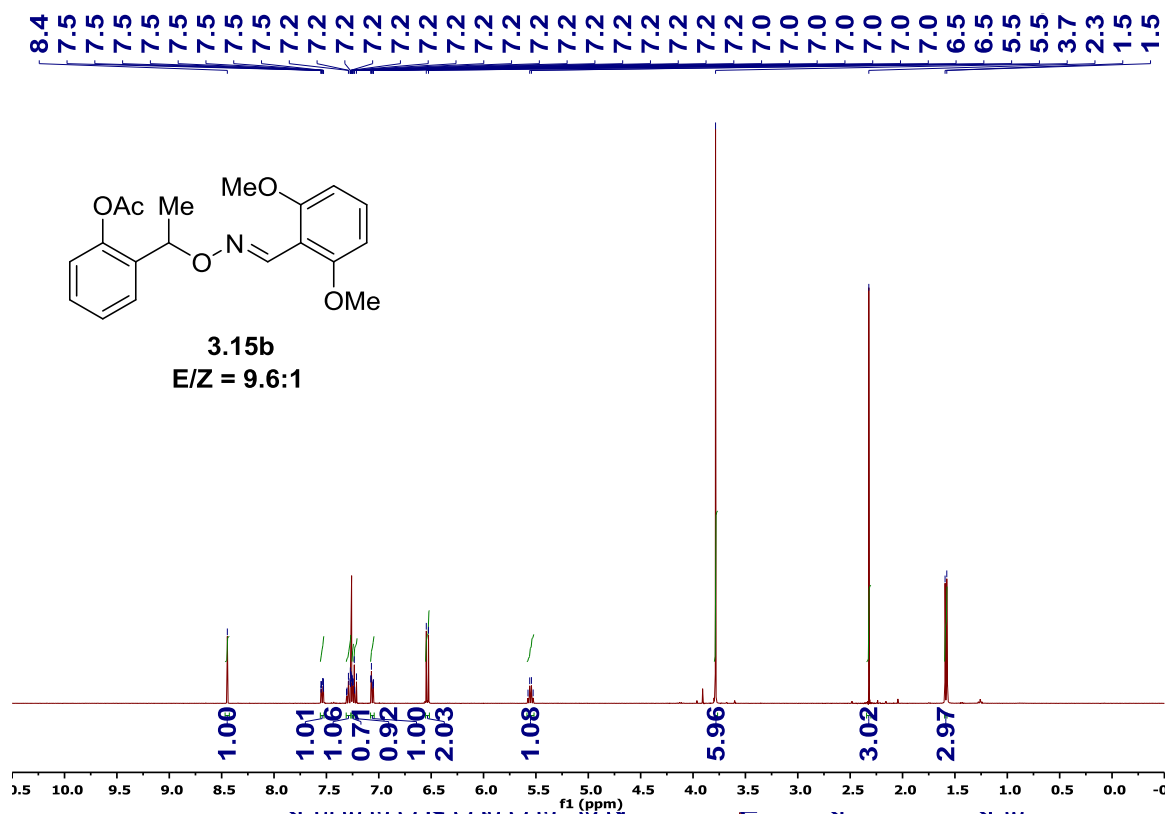


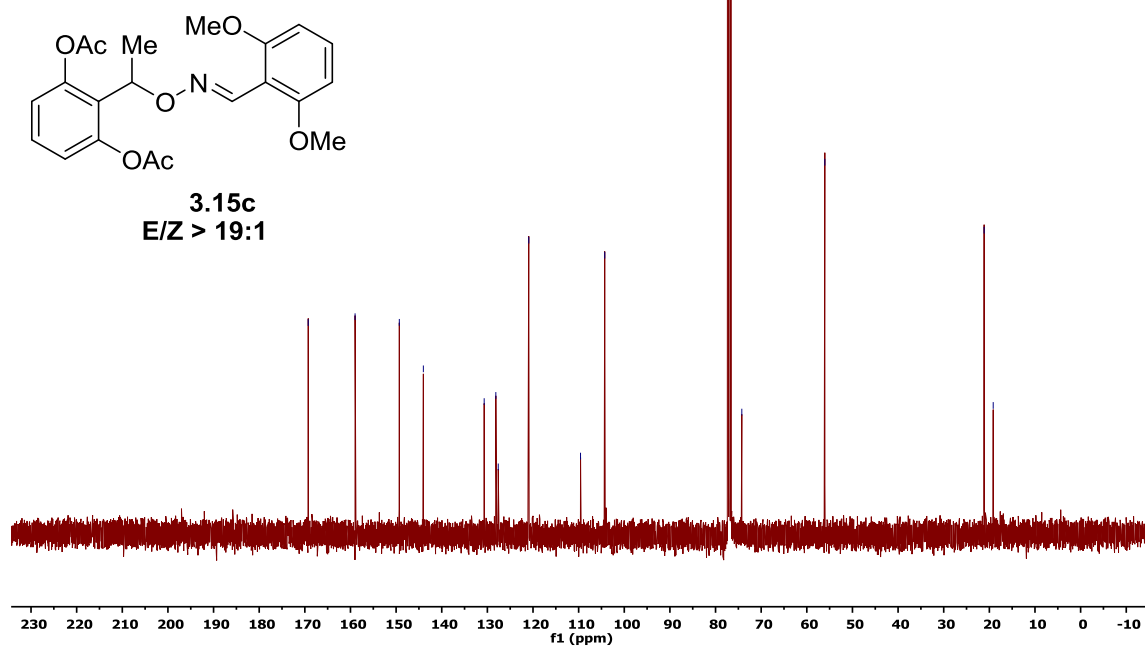
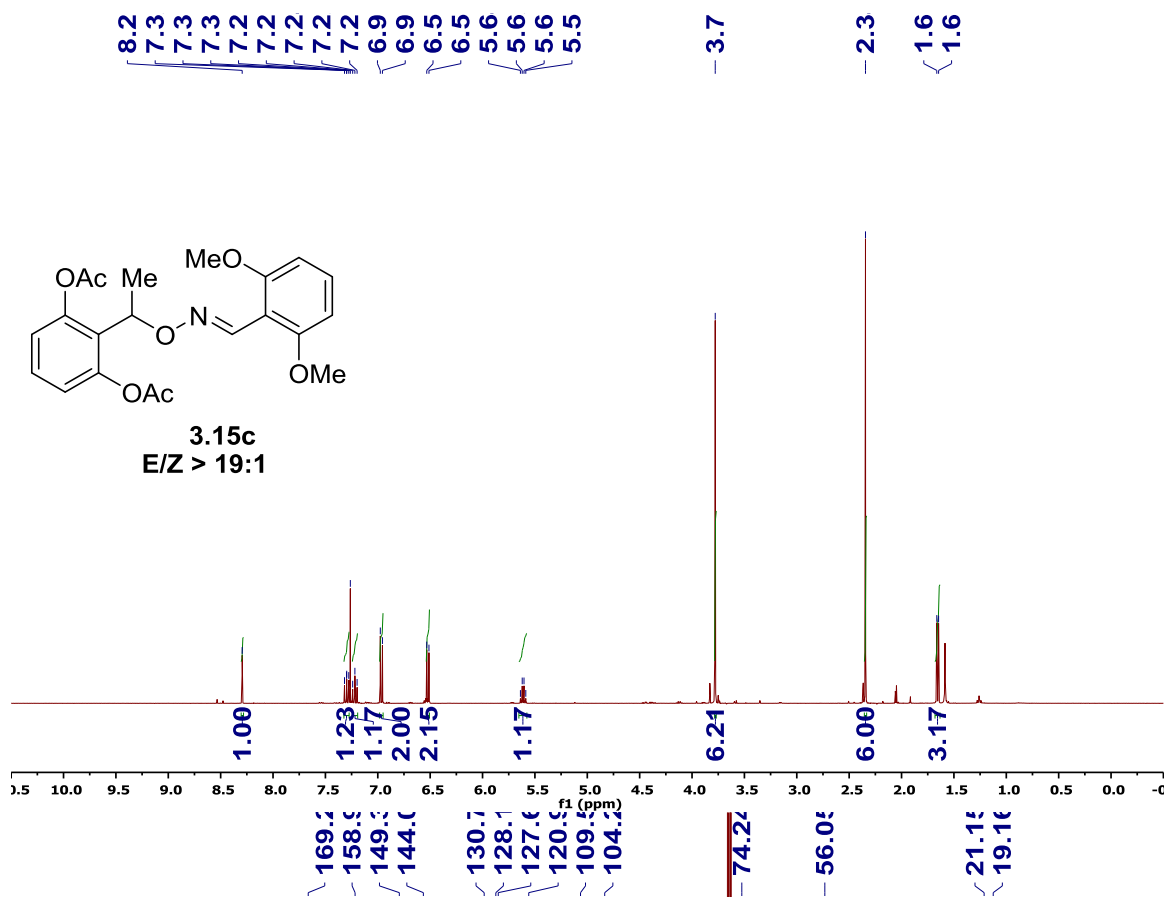


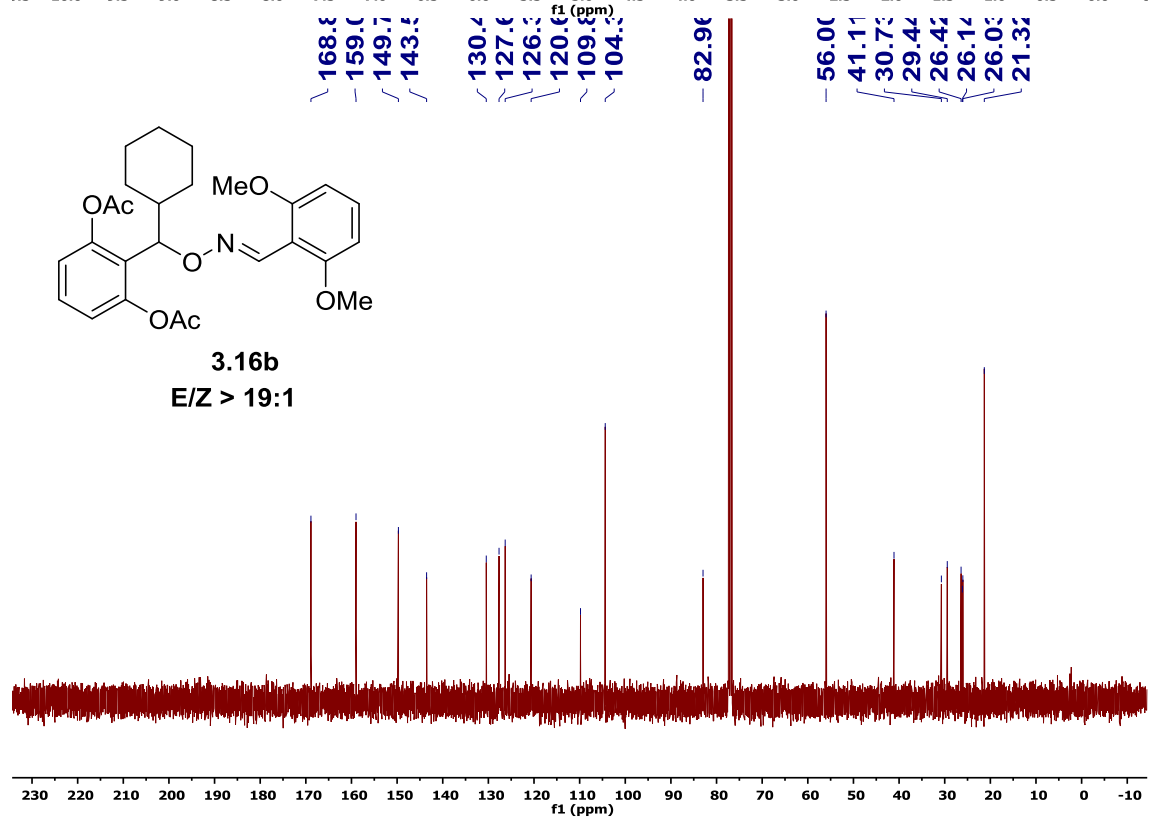
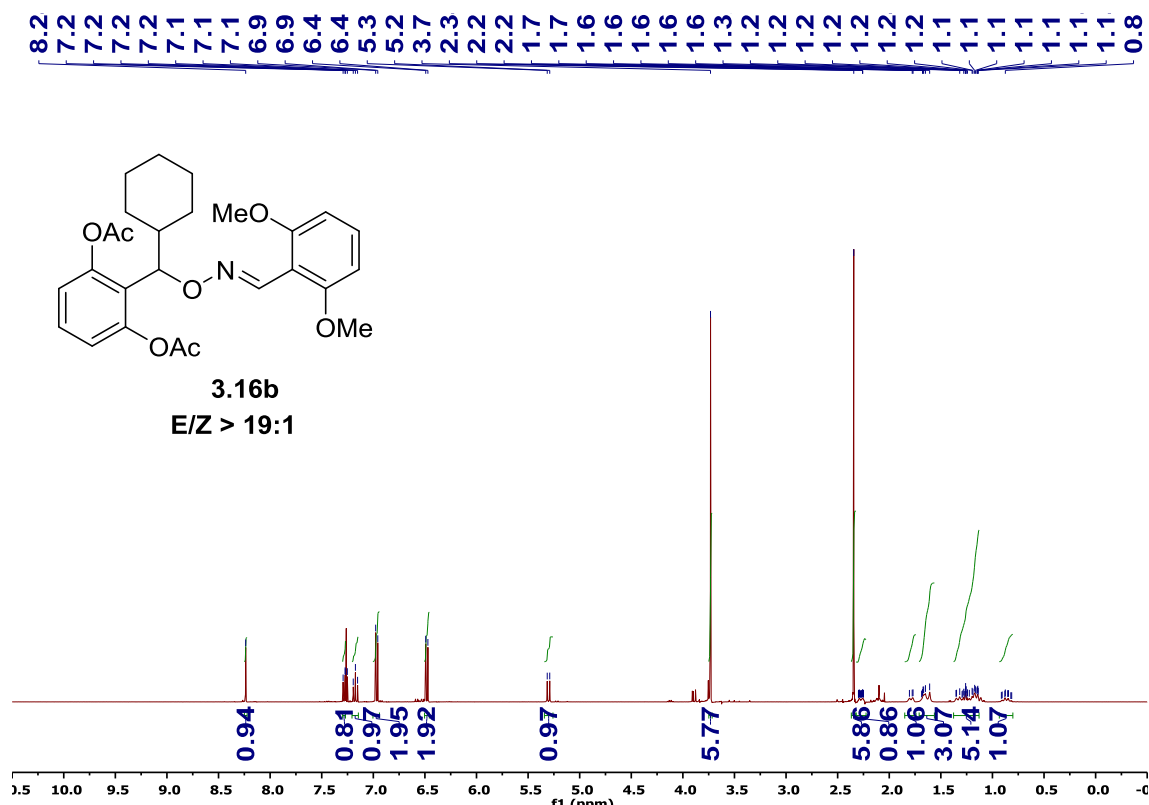


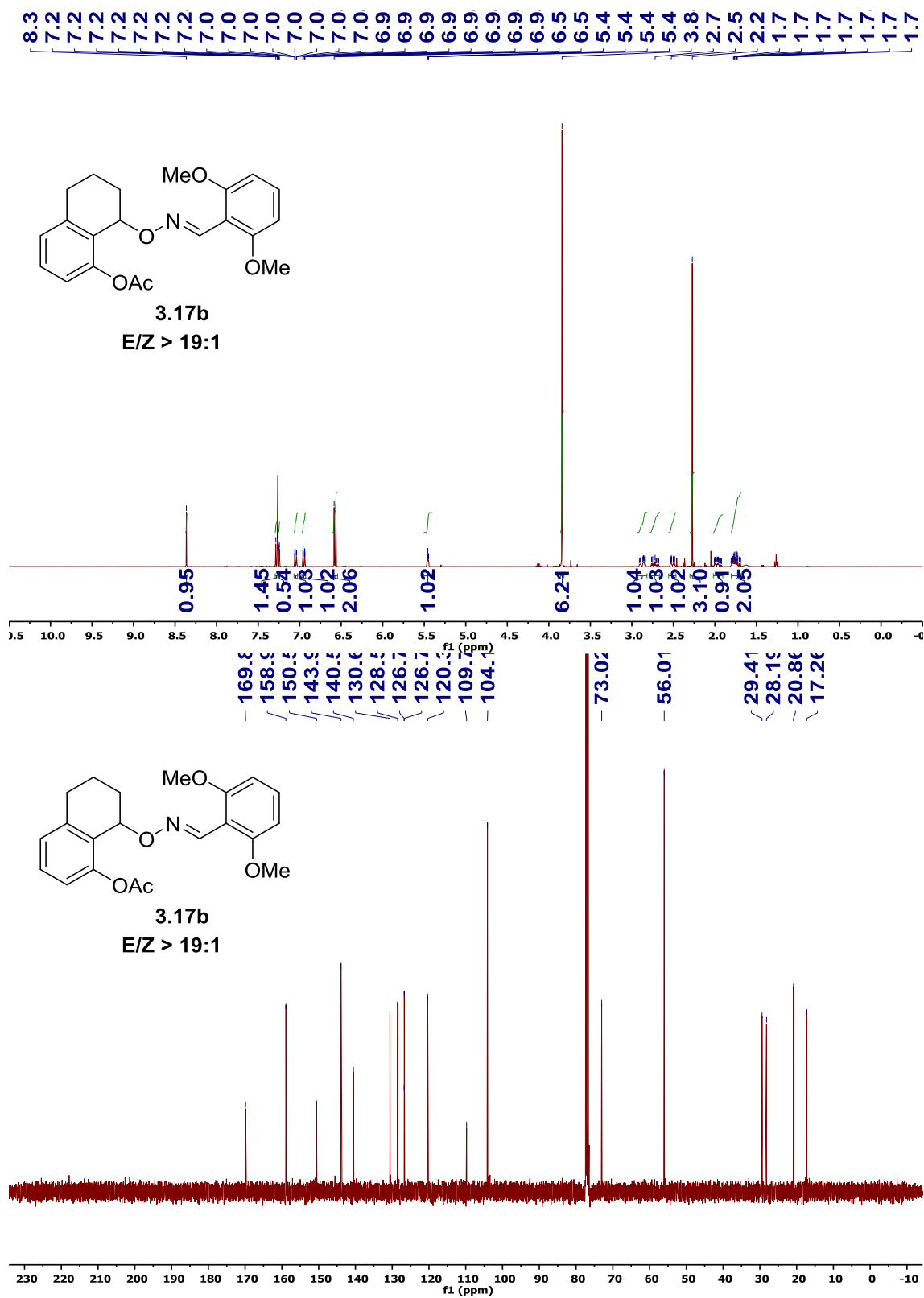


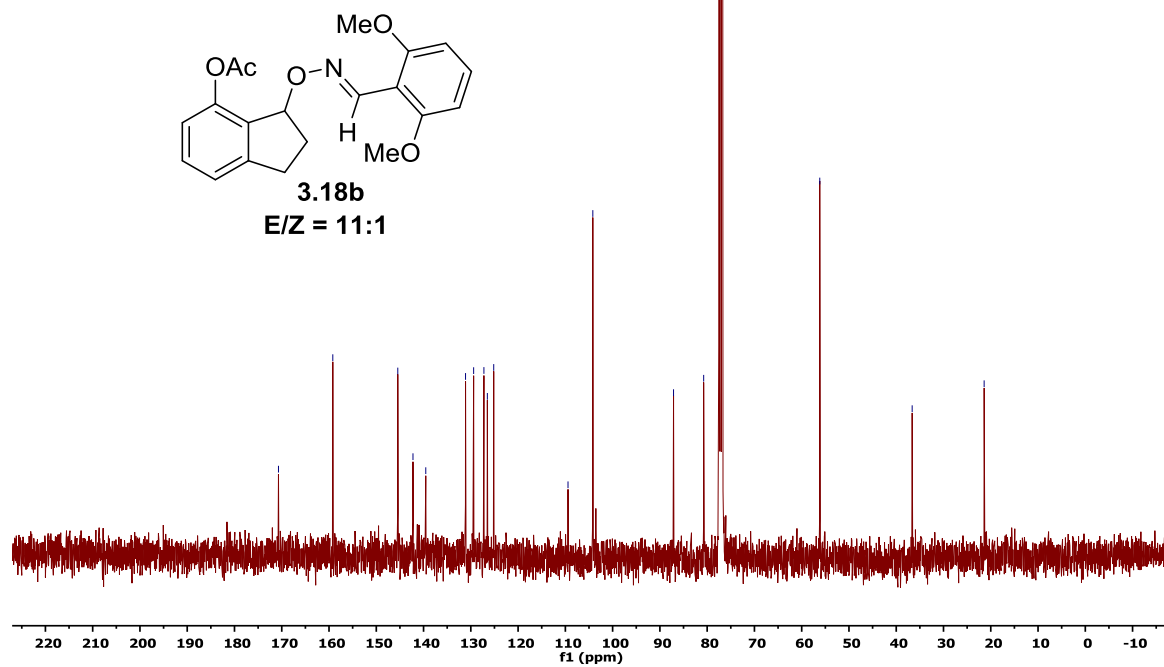
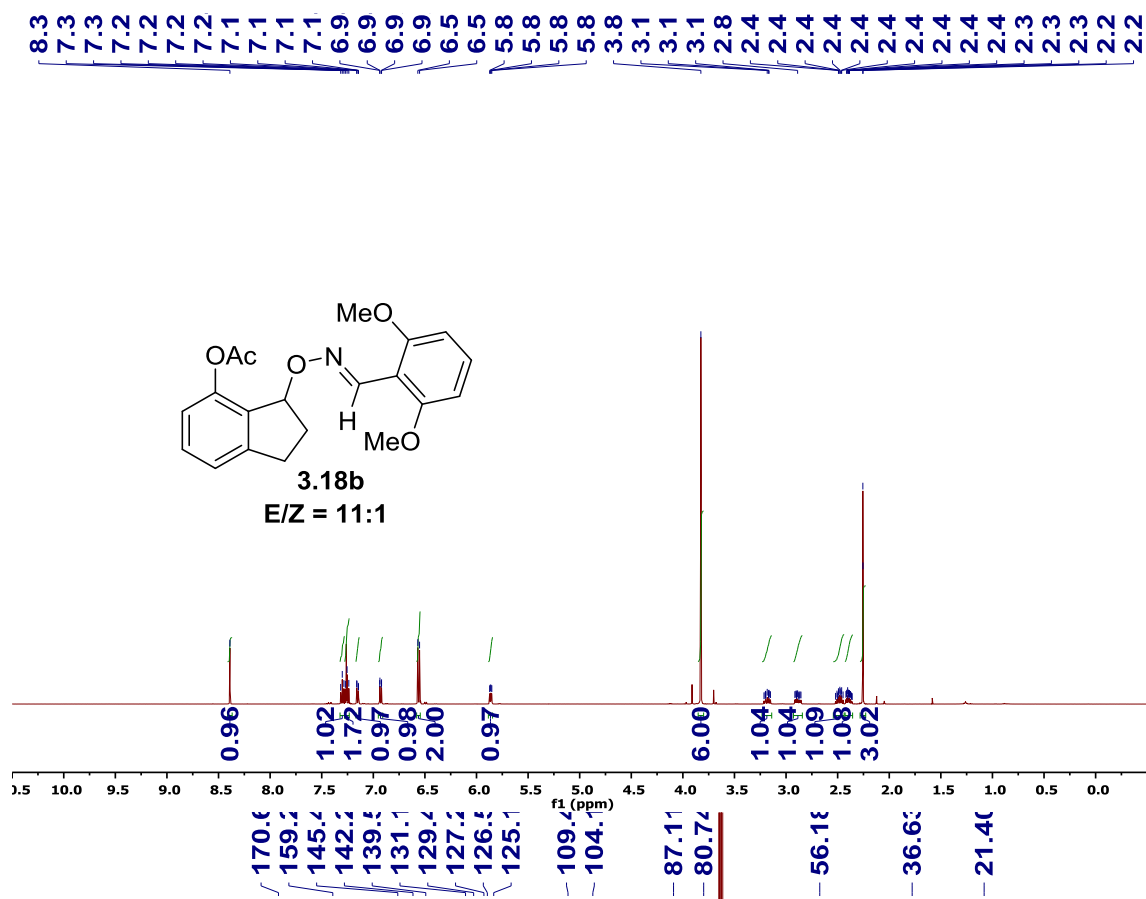


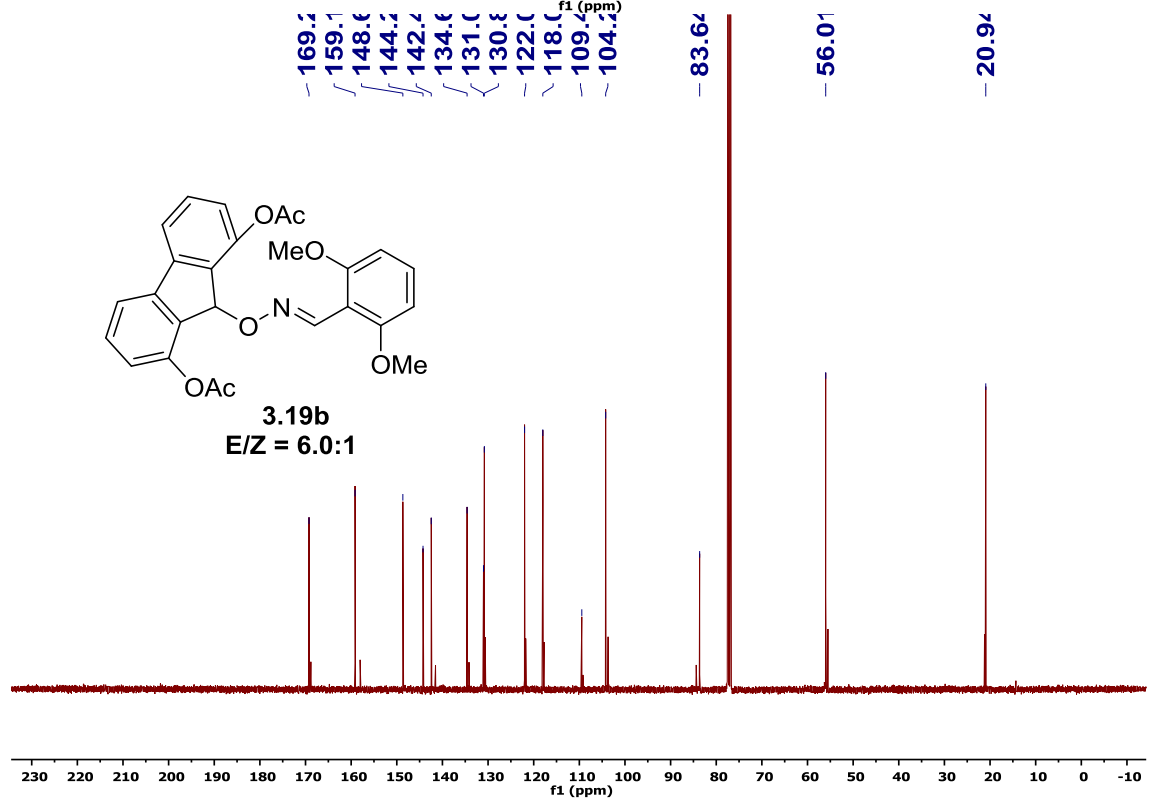
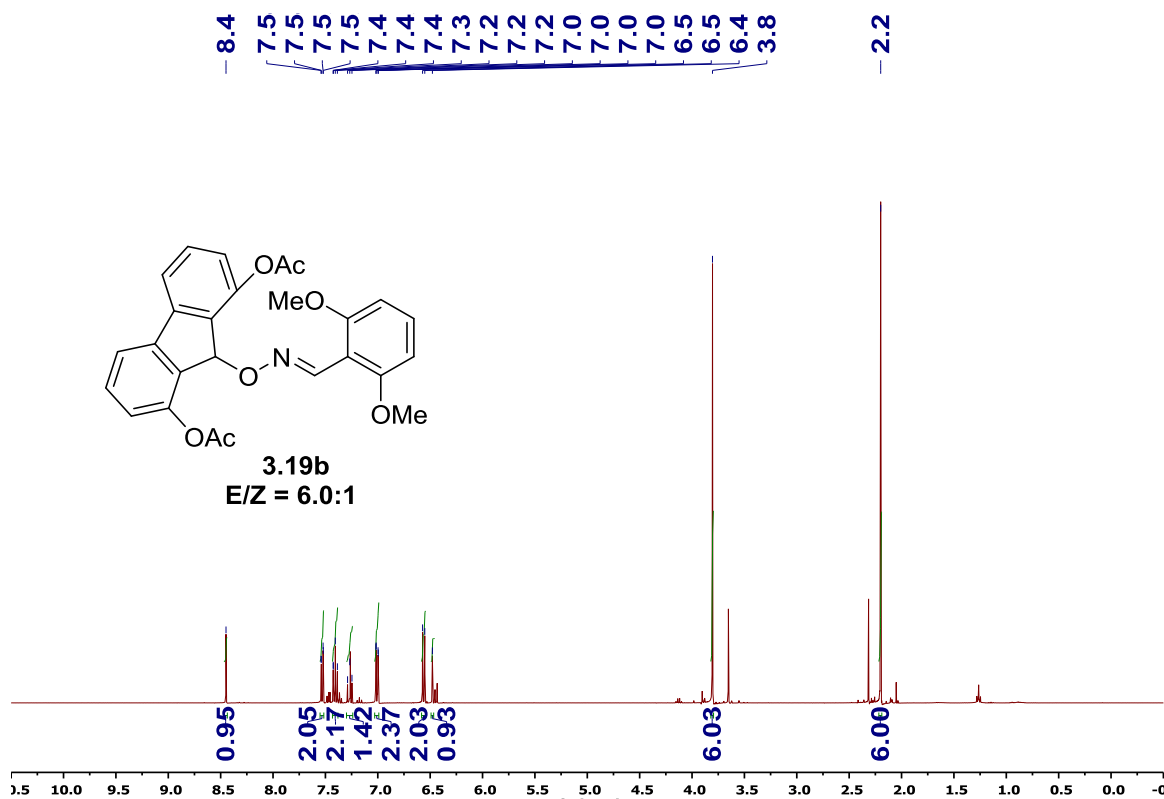


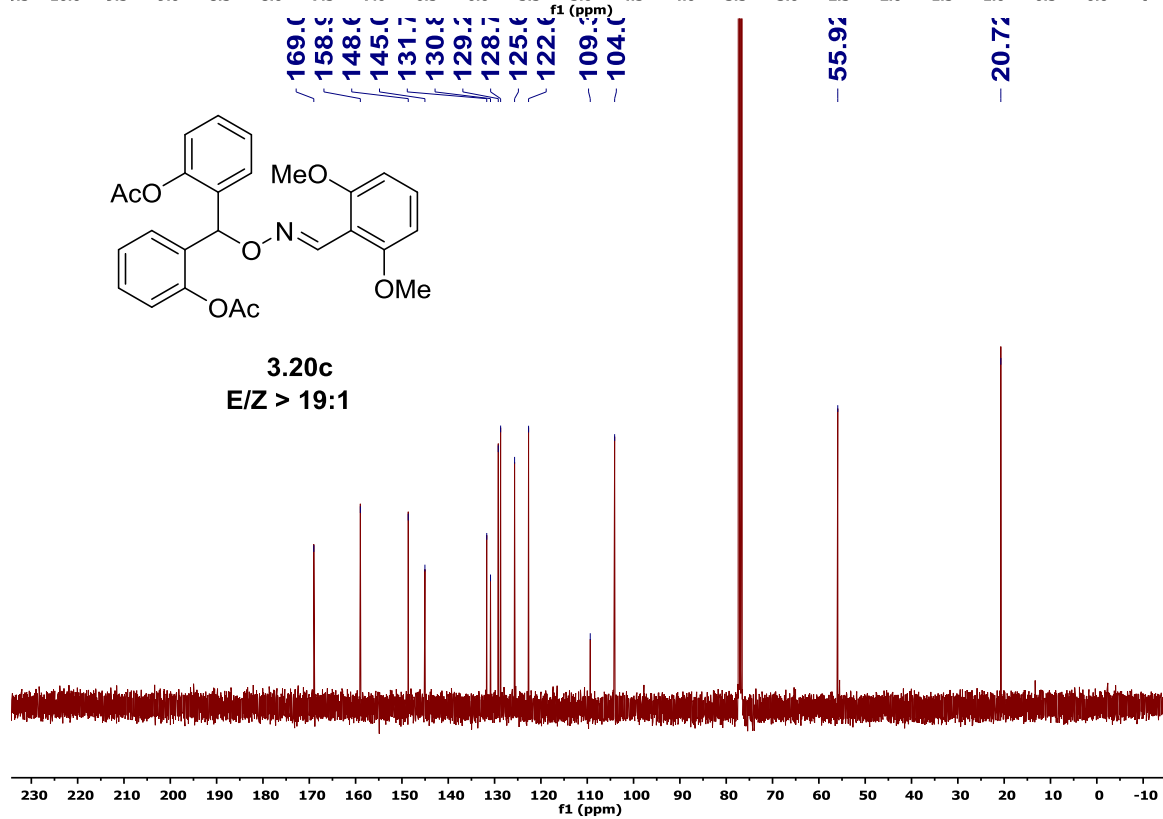
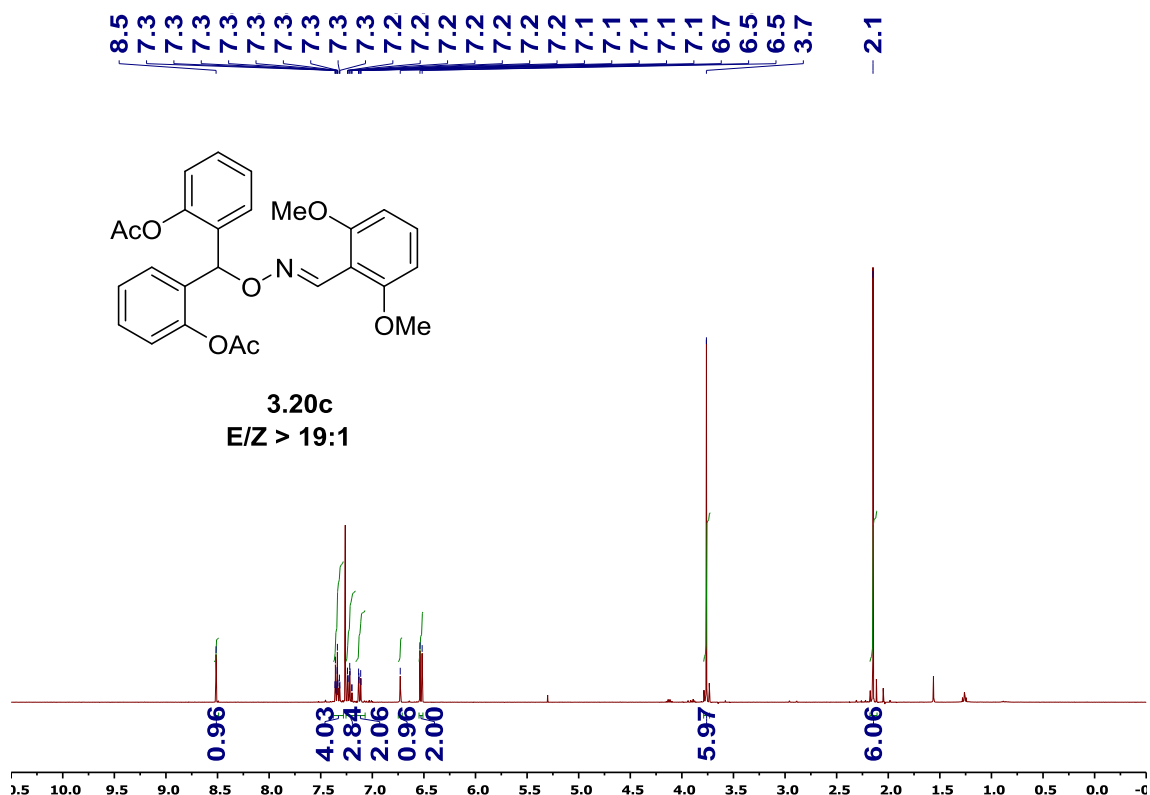


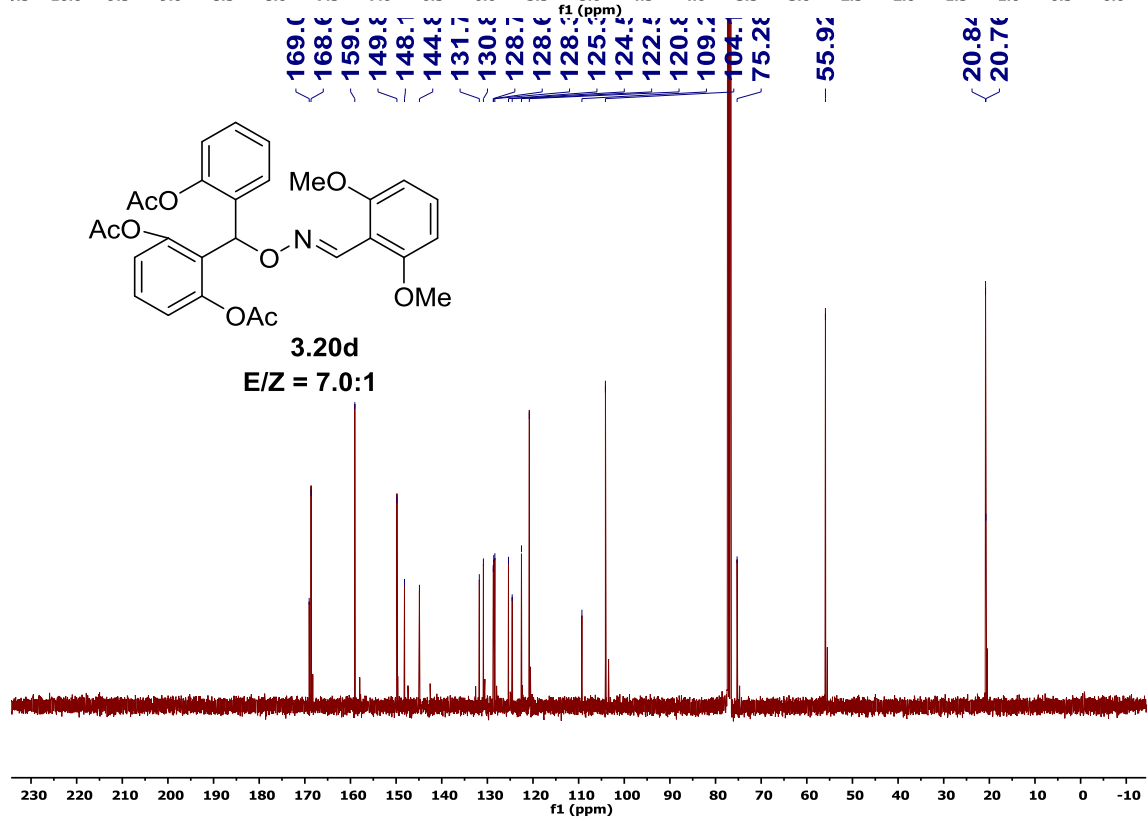
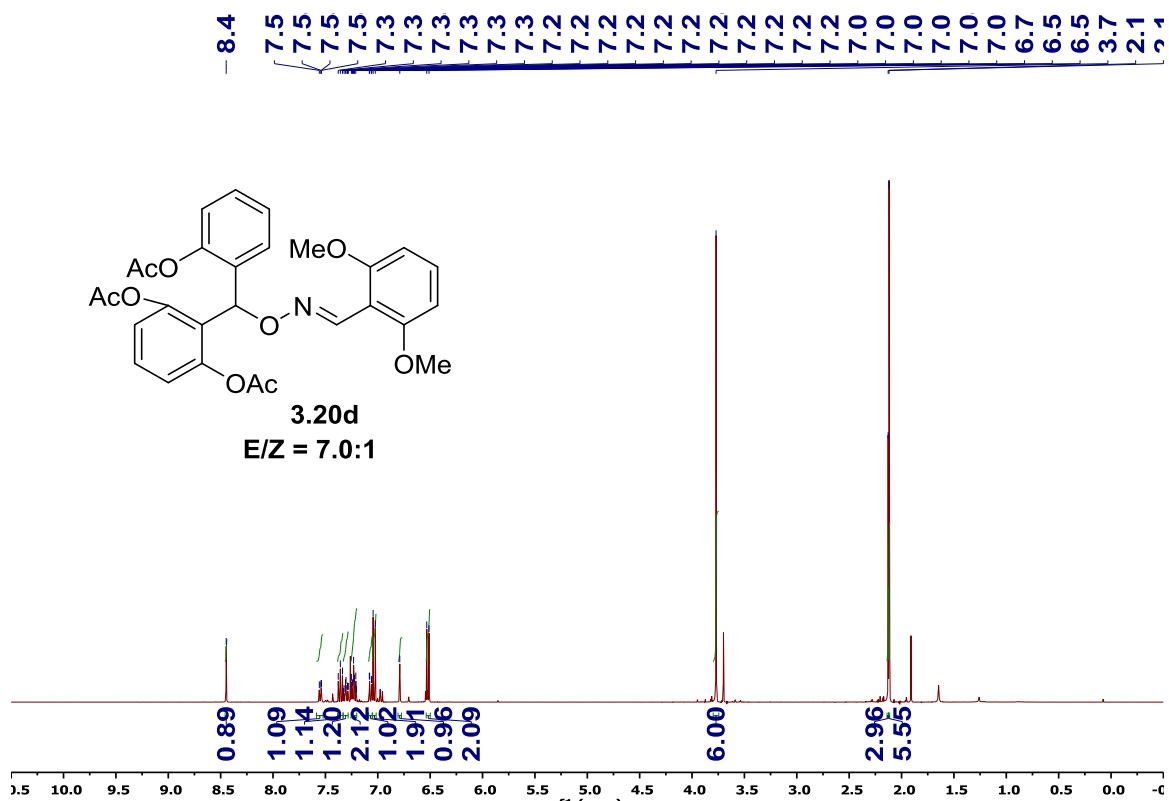


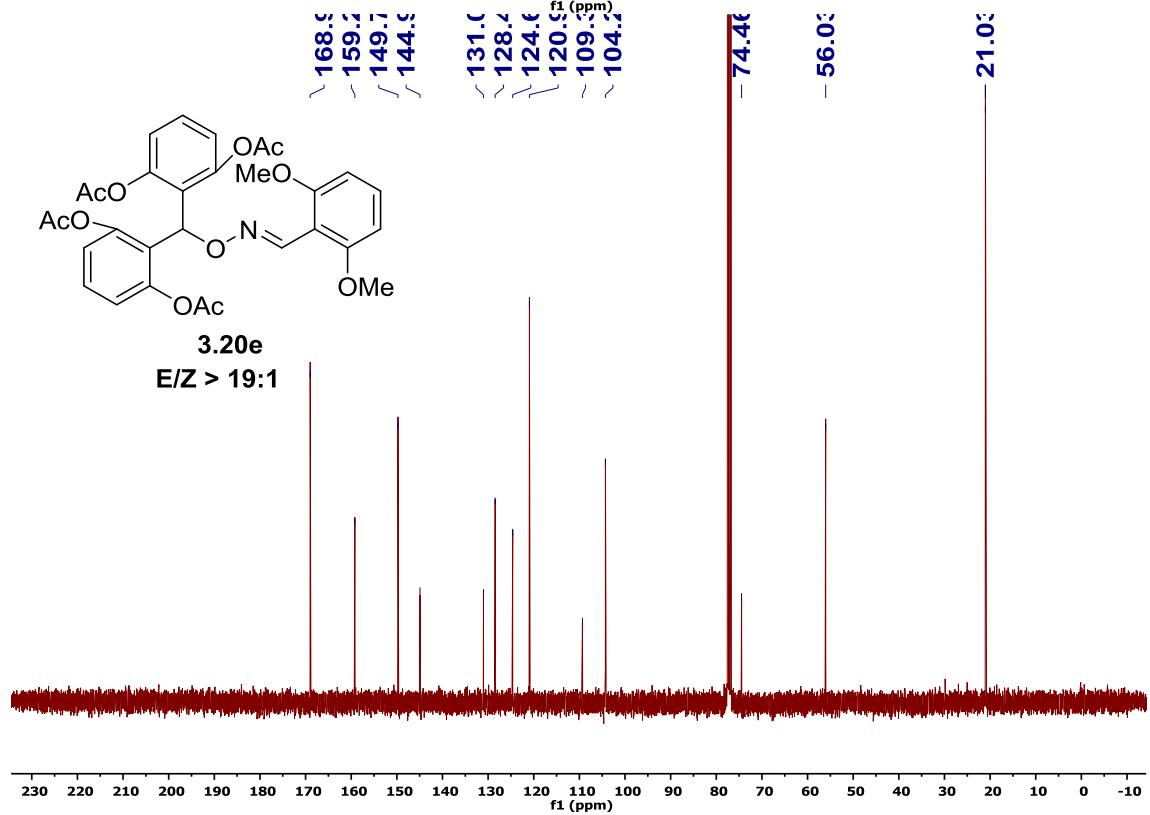
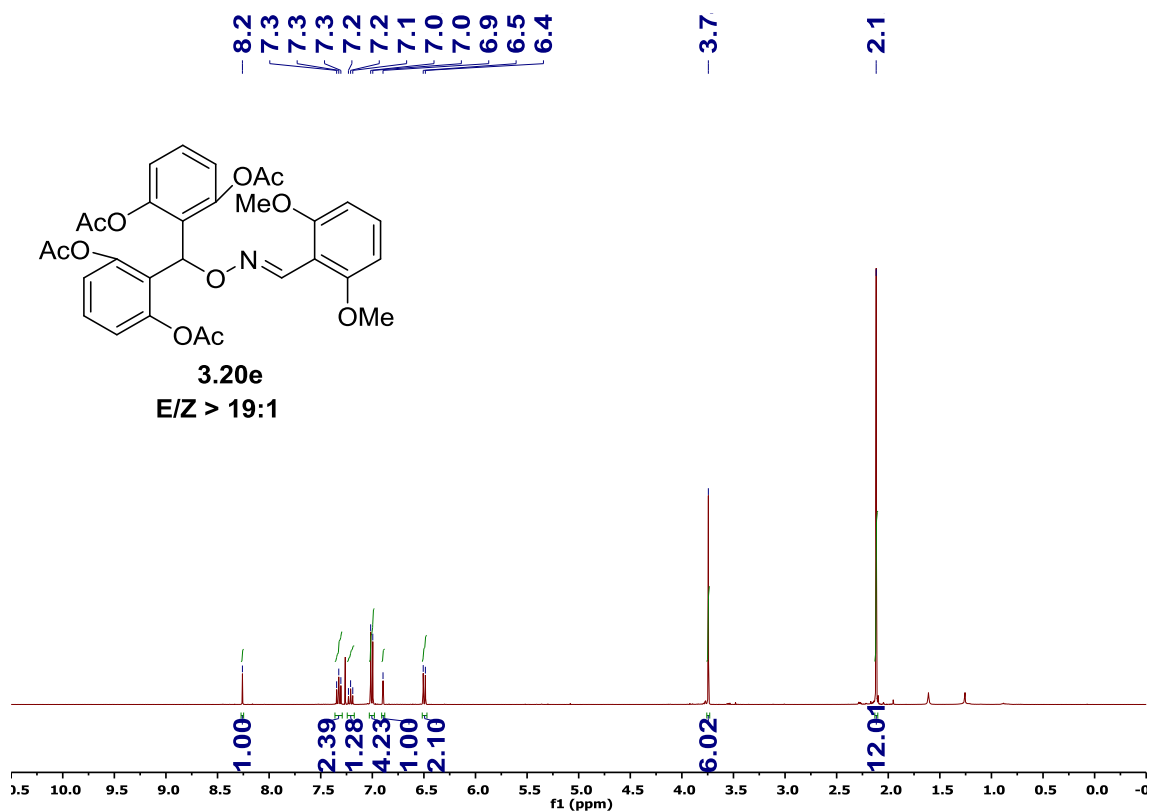


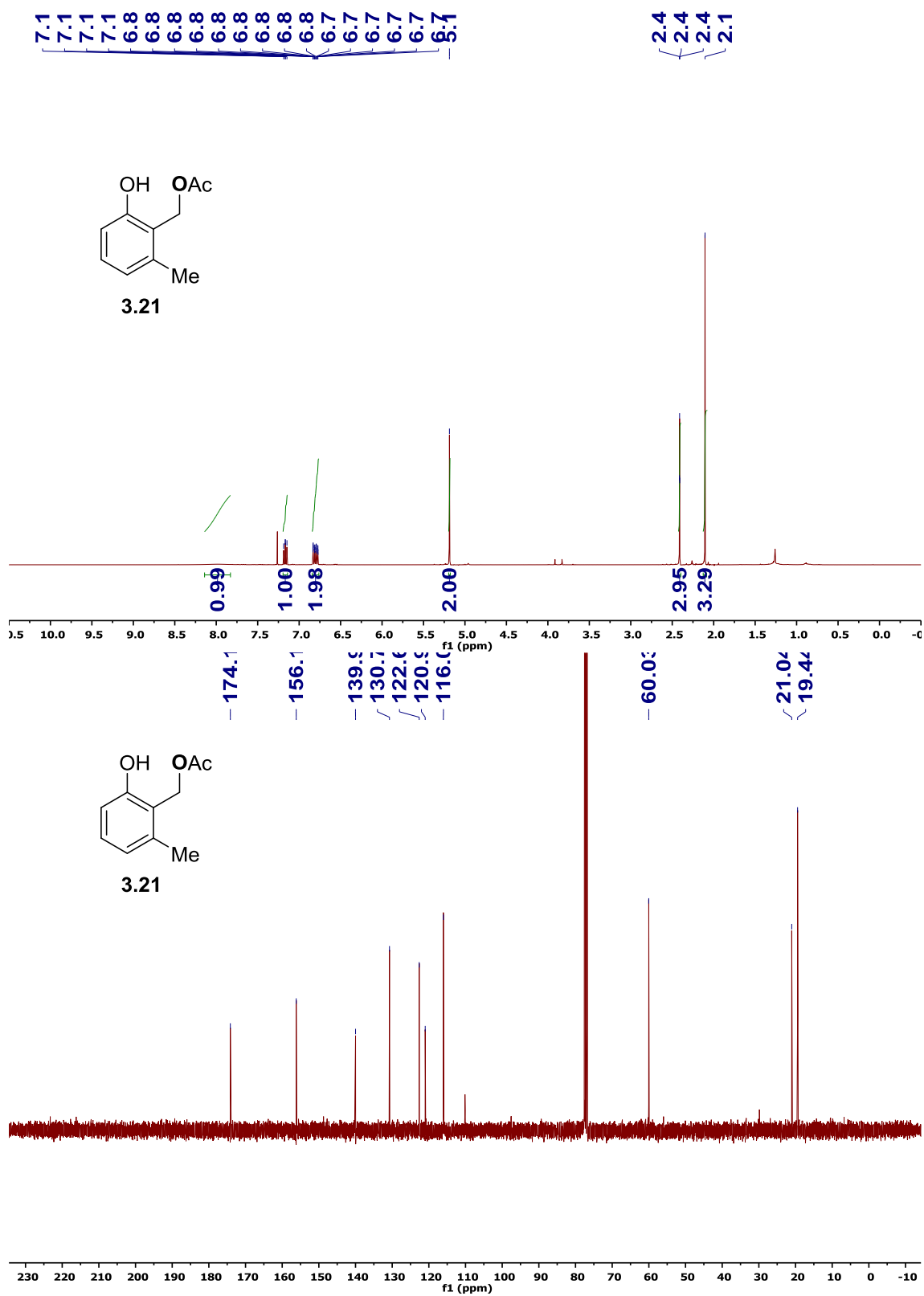


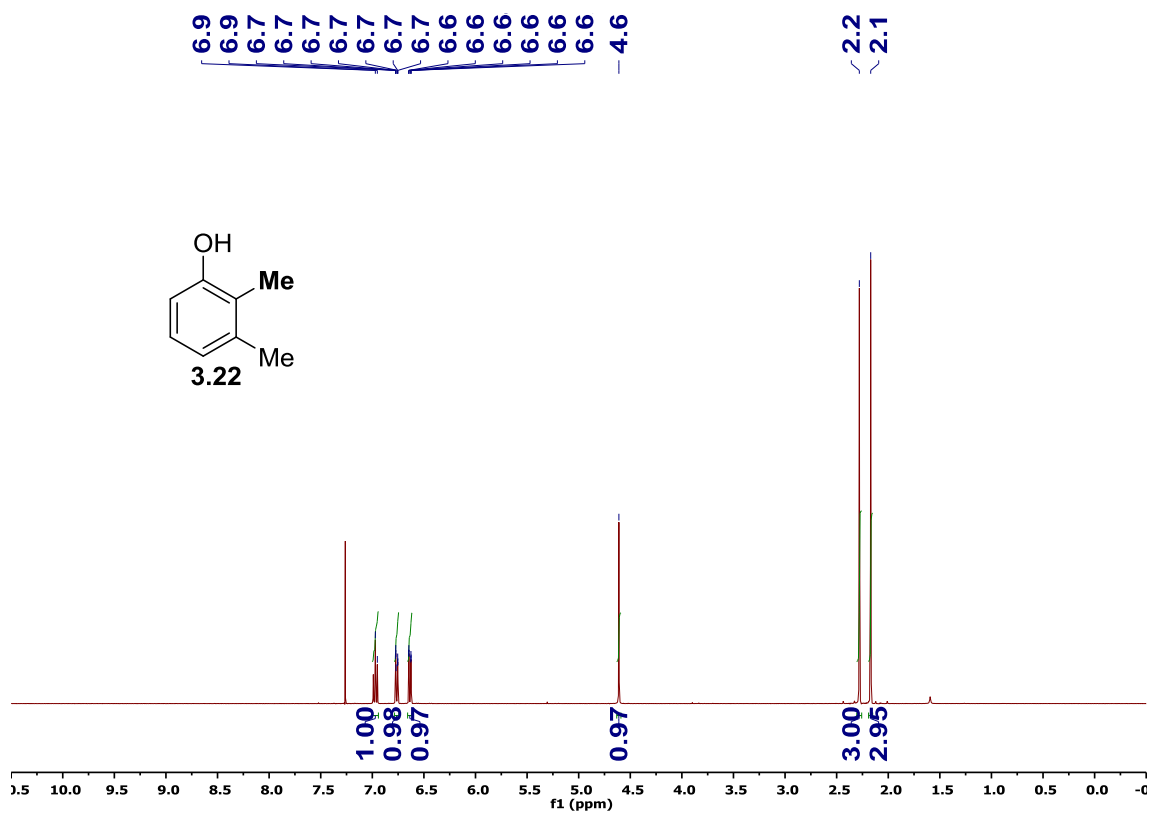


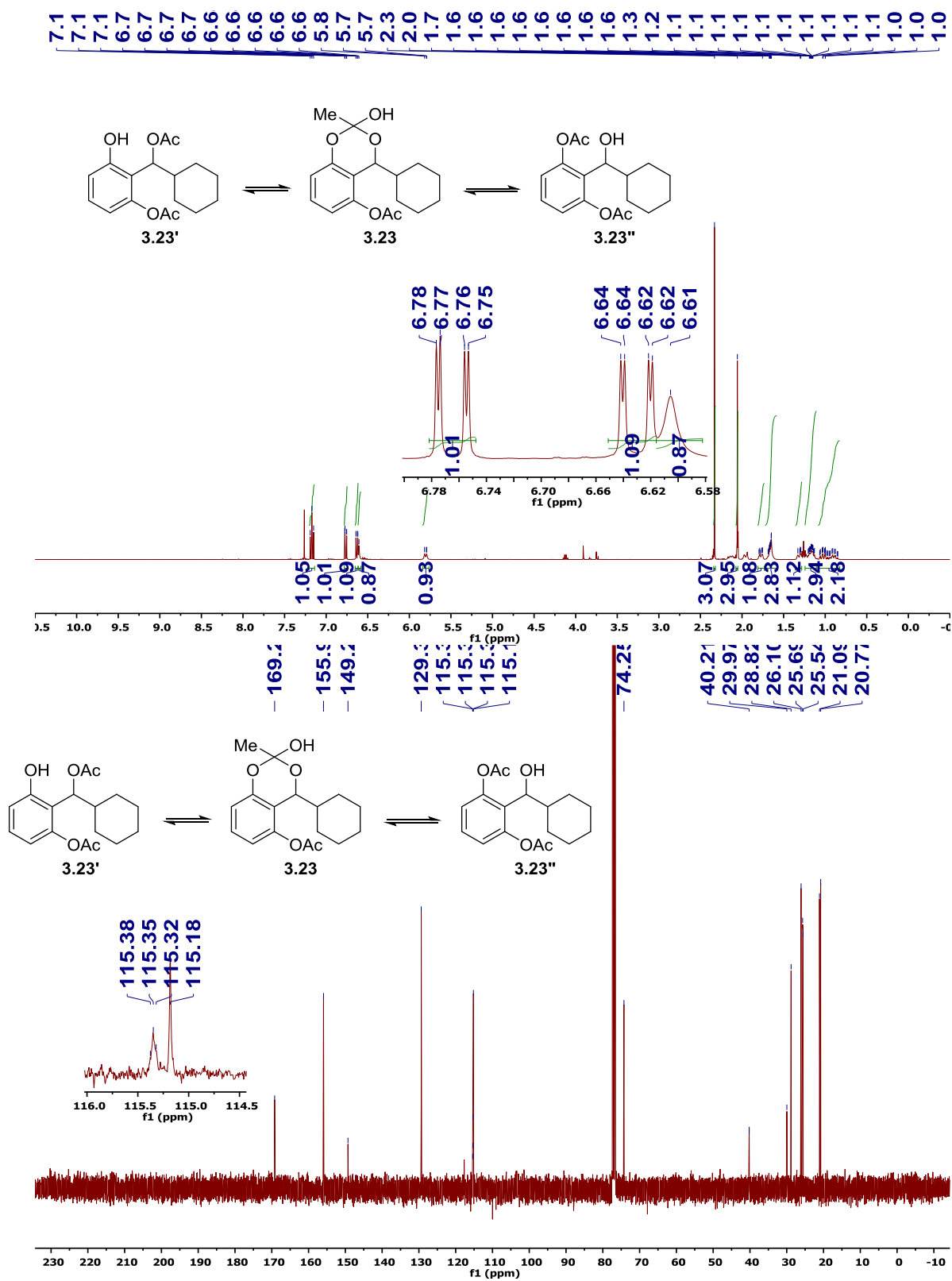


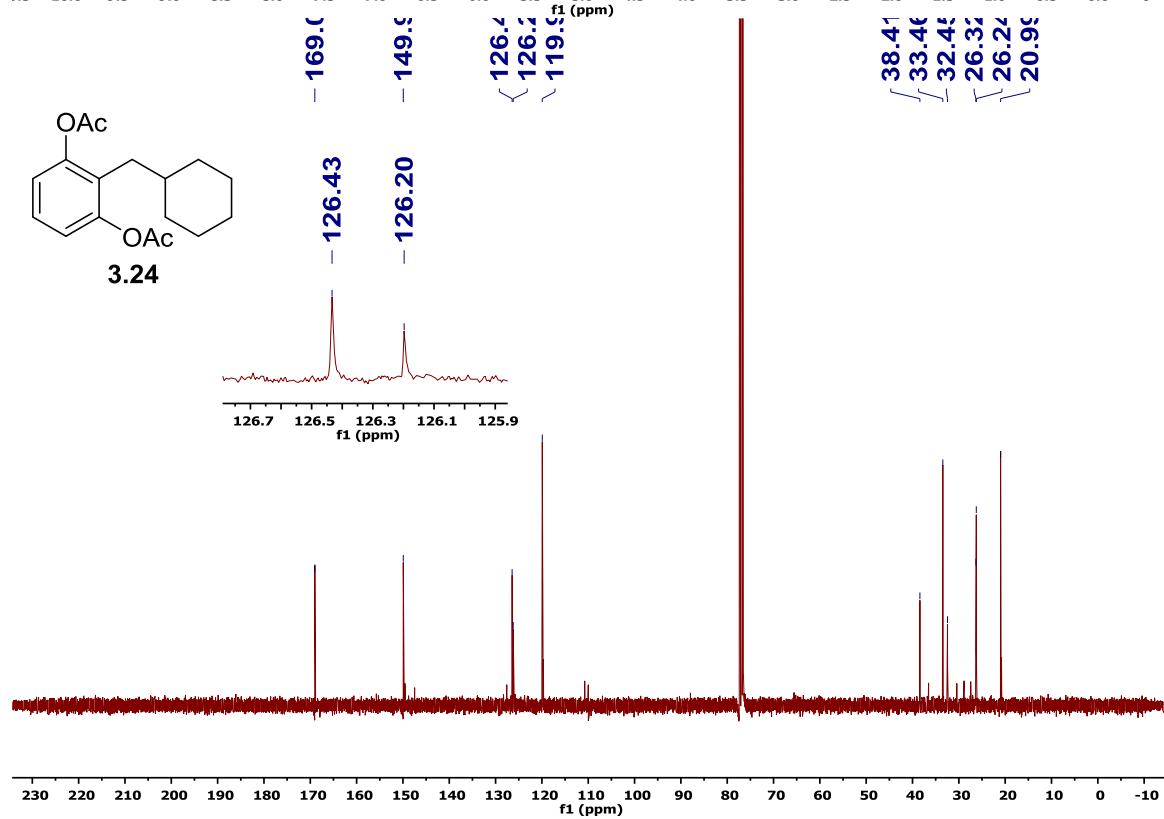
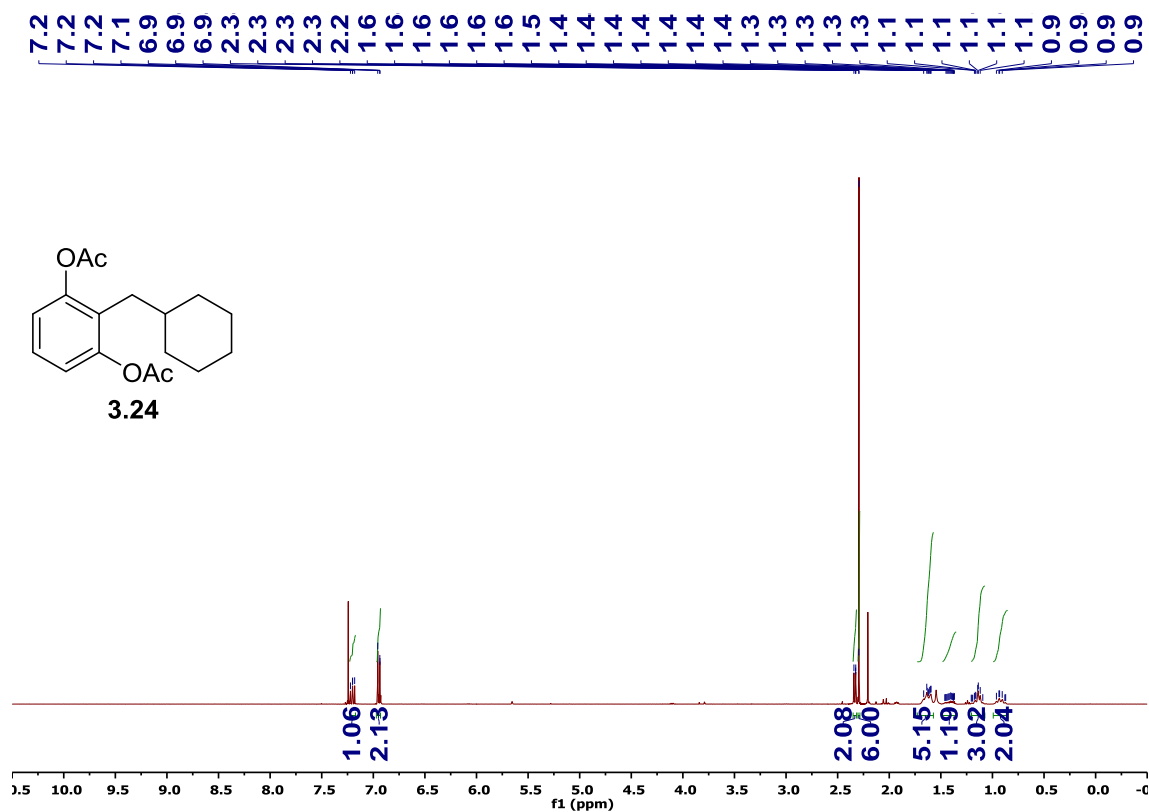


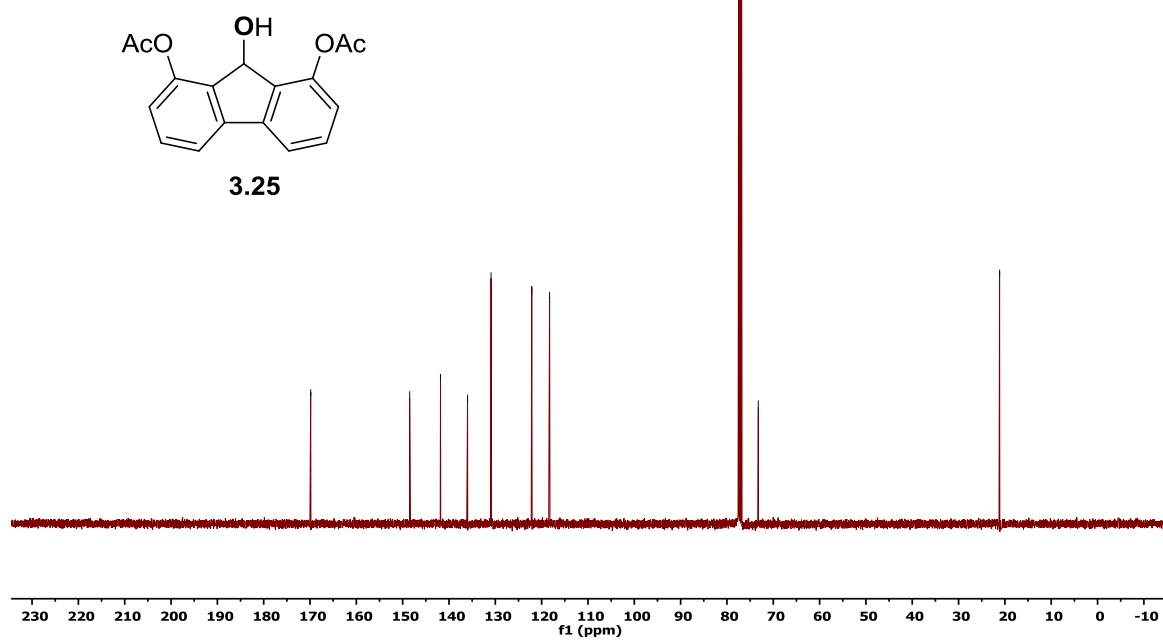
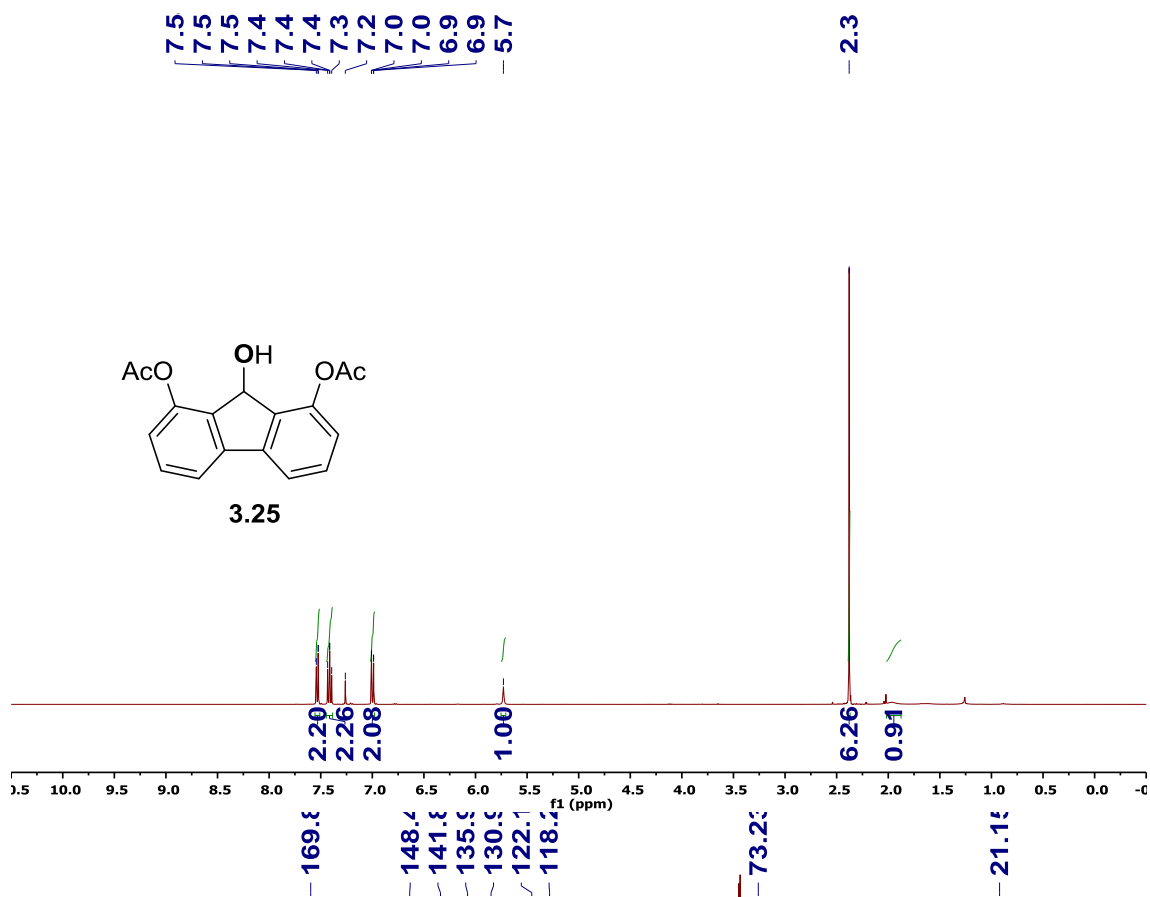


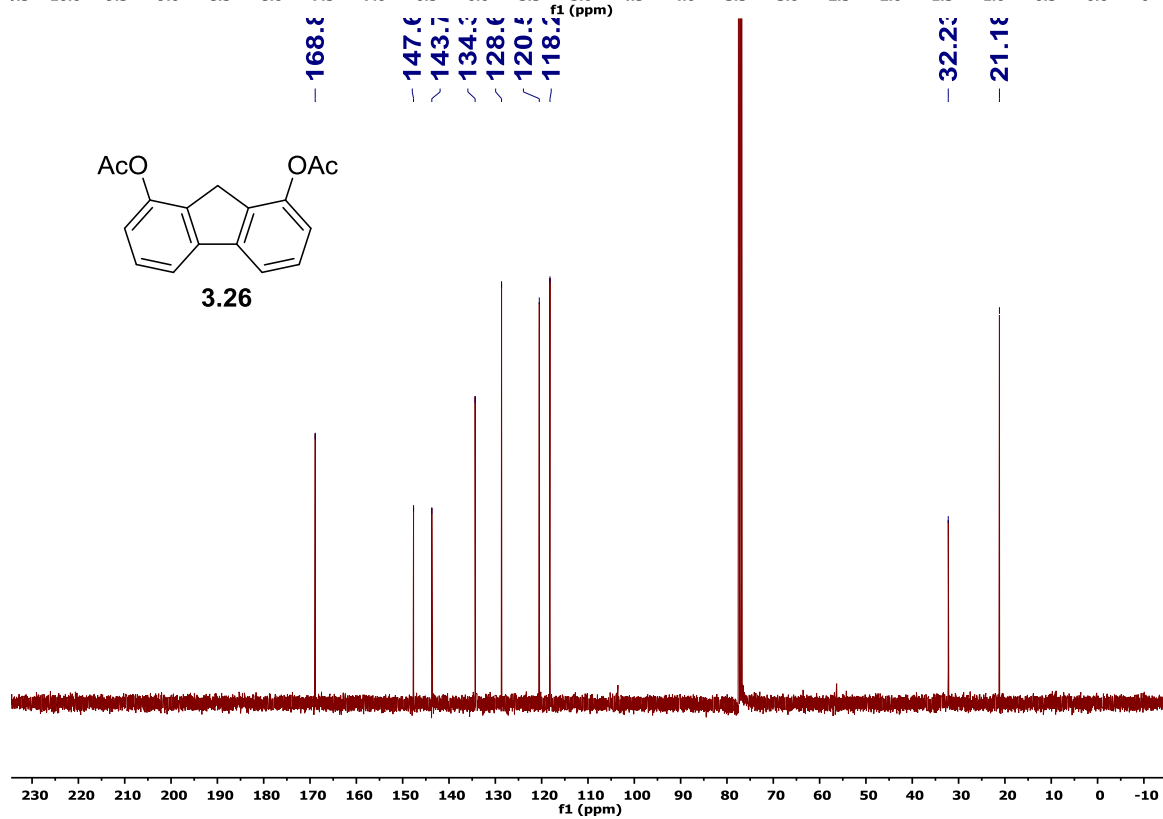
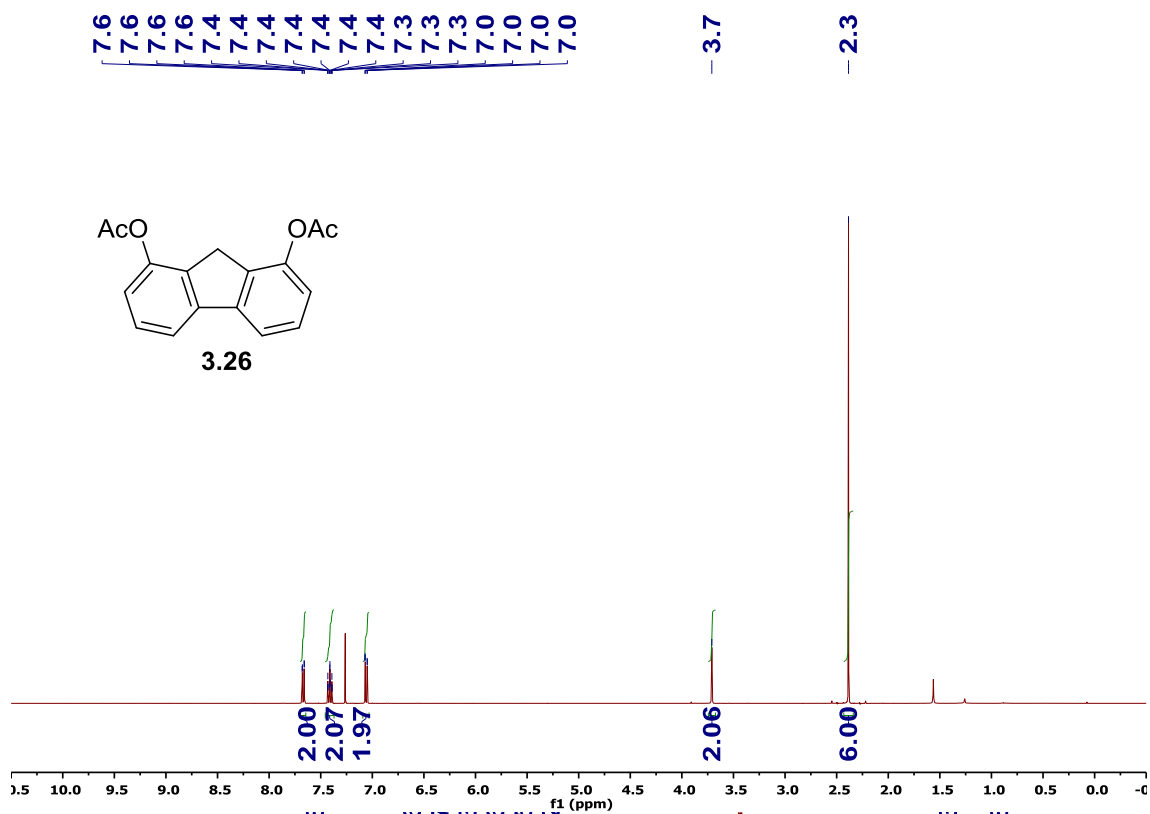












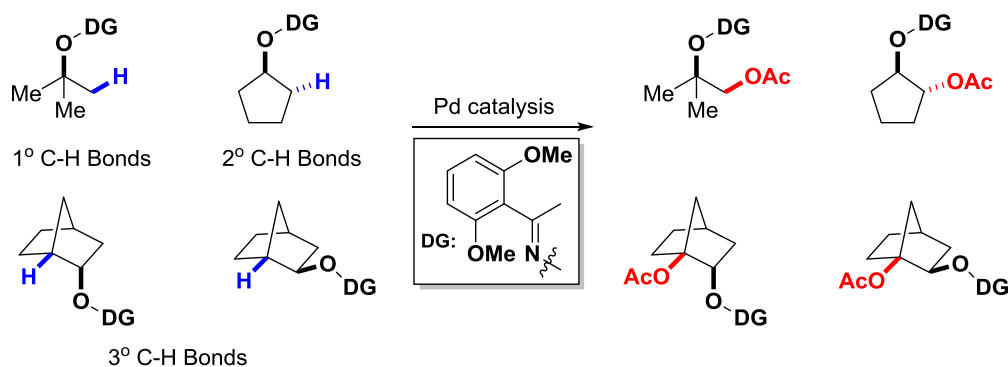
CHAPTER 4: PRELIMINARY MECHANISTIC STUDIES ON PALLADIUM CATALYZED C–H BOND ACTIVATION WITH *EXO*-DIRECTING GROUPS

4.1 Introduction

Pd-catalyzed C–H bond activation and carbon-heteroatom bond formation reactions are demonstrated as efficient transformations.¹ Site selectivity is one of the grand challenges for developing synthetic methods because the wide existence of C–H bonds in molecules and their subtle differences.² To achieve such selectivity, directing groups (DGs) are introduced, and among those, the *endo*-DGs are well established and studied by many other groups.³ The emergence of *exo*-directing strategy, as demonstrated for both aliphatic and aromatic C–H functionalization, has a significant impact on the late-stage C–H activation.⁴

As demonstrated in previous chapters, by using oximes as DGs, there are three types of C–H bonds at β -position of masked alcohols can be activated, and they are methyl, cyclic methylene, and bridgehead methine C–H bonds (Scheme 4.1).^{4f}

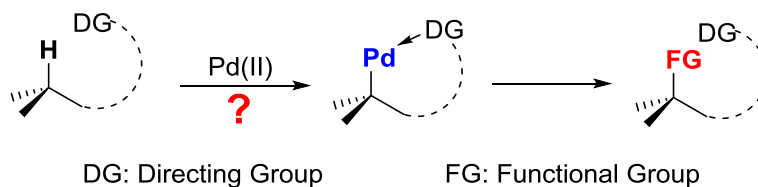
Scheme 4.1. Pd-Catalyzed C–H oxidation with *exo*-directing strategy.



As the tertiary carbon radicals are stabilized by hyperconjugation, the methine C–H bonds are the weakest among all unactivated aliphatic C–H bonds (93 kcal/mol). Thus, the main obstacle to preparing the methine complex should not be thermodynamic

but due to the steric hindrance of the regular tertiary C–H bond. Since there is no precedent evidence that direct C–H activation could occur at methine C–H bonds with Pd precursor, the mechanistic pathway for this reaction is in doubt (Figure 4.1). Therefore, stoichiometric studies of the preparation of tertiary alkyl palladacycles through activation of a bridgehead C–H bond would provide important mechanistic information for palladium-catalyzed methine C–H activation.

Figure 4.1. The mechanism for C–H activation at tertiary carbon center.

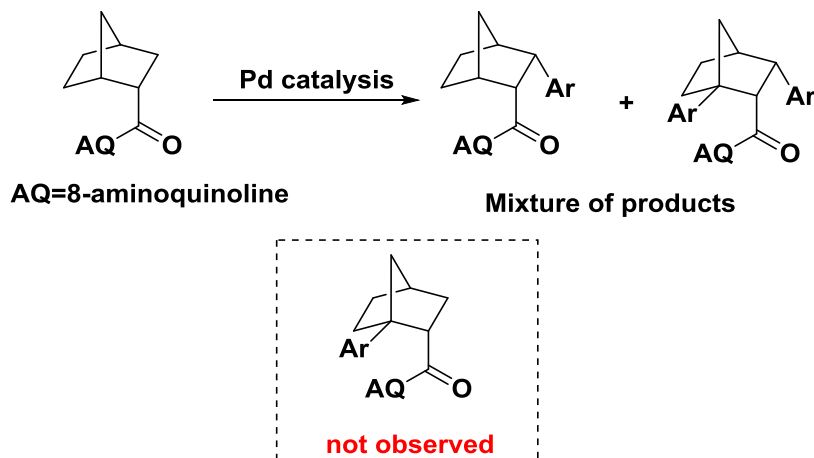
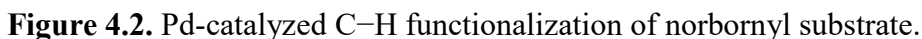


4.2 Background

With the efforts of many research groups, Pd-catalyzed functionalization of primary methyl C–H bonds has been extensively studied and several seminar works have also been realized for secondary methylene C–H bonds.^{2,5} Nevertheless, few examples have been developed for activating an unactivated tertiary C–H bond with Pd catalysis (Scheme 4.2).^{4b, 6}

In particularly, Babu and co-worker also demonstrated that using bidentate DG for the functionalization of the methine C–H bonds at bridgehead in norbornyl substrate in 2014. In this case, the methylene C–H bonds are more reactive than the methine ones (Figure 4.2). Interestingly, this result is a controversy to our observation using *exo*-DG that oxidation exclusively occurs at bridgehead C–H bonds. Therefore, to demonstrate the unique feature of our *exo*-directing strategy, it is important to obtain the Pd intermediate before the oxidation, to avoid the interference of any potential oxidative rearrangement.

Bridgehead Position of Norbornyl:

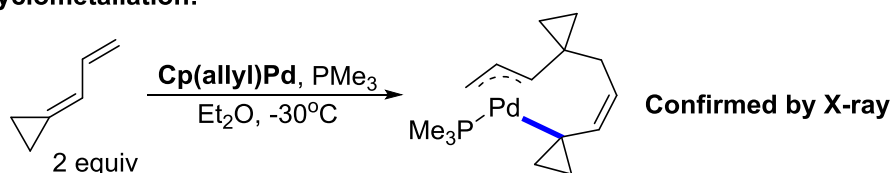


282

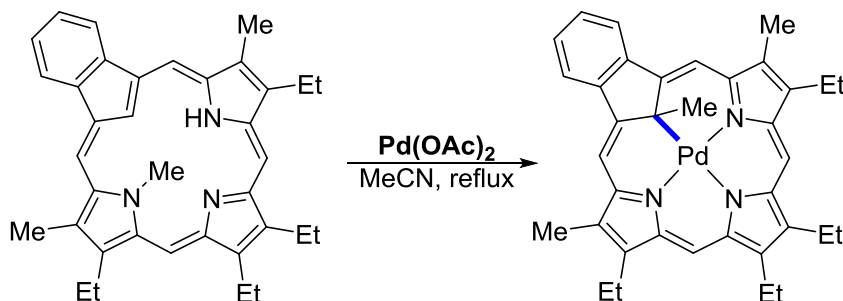
acidic carbon nucleophile;⁷ 2) cyclometallation with alkylidene cyclopropanes;⁸ and 3) alkyl group migration.⁹ These methods all requires special electronic or steric properties of the methine C–H bonds, and direct C–H activation at tertiary positions has not been reported previously. Thus, the success in obtaining a tertiary alkyl Pd complex would not only help to explain the mechanism of our reaction but answer a long existing organometallic question.

Scheme 4.3. Representative tertiary alkyl Pd complexes.

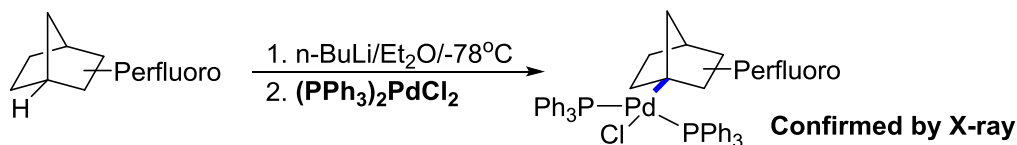
Cyclometallation:



Alkyl Group Migration:



Transmetalation:

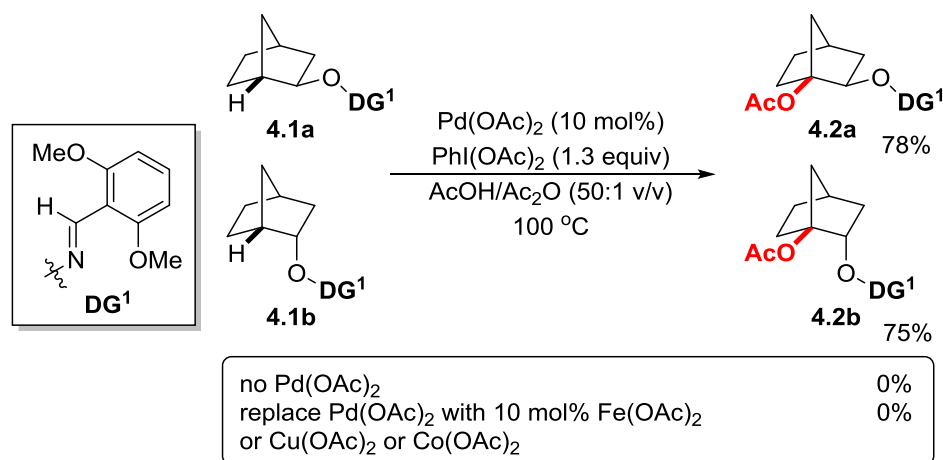


4.3 Reaction Design and Discussion

As the mechanism of the reaction is not clear, the reaction could undergo radical pathway, which would make the attempts to isolate Pd complex pointless. Therefore, some preliminary studies were required to exclude the typical radical pathway through a

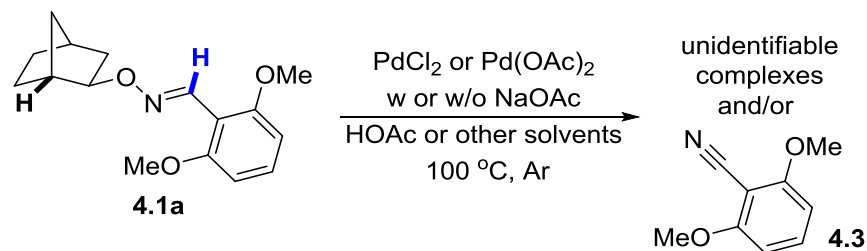
series of control experiments with substrates **4.1a** and **4.1b**. As shown in scheme 4.2, under the metal-free condition, or with other metal salts that typically promote radical formation, such as Cu(II), Fe(II) and Co(II), there was no desired product was observed. These results suggest a radical approach for C–H abstraction is disfavored. Thus, a cyclopalladation pathway is worth to explore.

Scheme 4.4. Pd-catalyzed oxidation of bridgehead C–H bonds via an *exo*-DG.



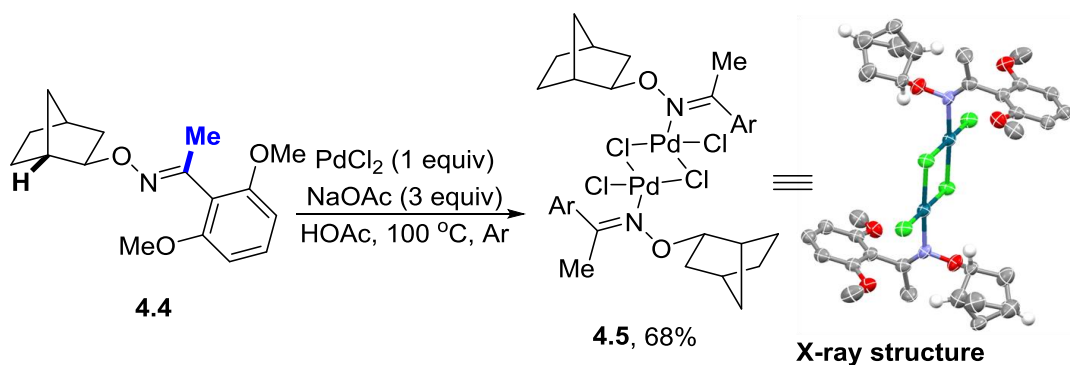
However, using oxime **4.1a** substrate under various conditions to form a cyclopalladation complex remained unfruitful. In the absence of strong oxidants, e.g. $\text{PhI}(\text{OAc})_2$, the major reaction was found to be the Pd-mediated elimination of aldoxime to give 2,6-dimethoxynitrile (Figure 4.3). These unsuccessful results suggest that the active Pd complex with the 2,6-dimethoxylaldoxime DG was too reactive to isolate, and a more stable DG was required.

Figure 4.3. Pd-mediated elimination of aldoxime to give 2,6-dimethoxynitrile.



When the more stable ketoxime **4.4** was used to avoid the potential elimination, the C–H activation Pd complex was expected to be formed. However, the complex obtained in 68% yield was a chloride-bridged palladium dimer, Pd complex **4.5**, which precipitated during the reaction (Scheme 4.3). The absence of OAc group in complex **4.5** was unexpected as the reaction was carried out with 3 equiv of NaOAc and the solvent amount of HOAc and without HCl workup. We hypothesized the further reaction did not occur as its solubility is too low in organic solvents.

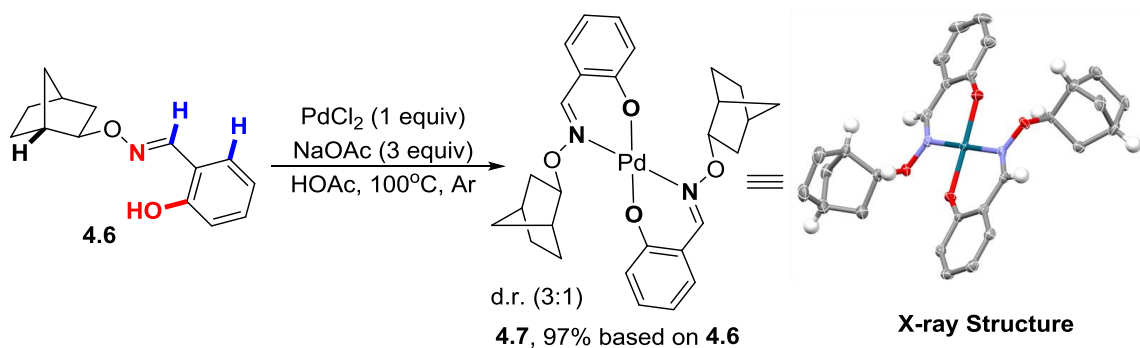
Scheme 4.5. Preparation of Pd complex **4.5**.



The low solubility of Pd complex **4.5** is presumably due to the inorganic nature of the chloride as X ligand, which leads us to consider the role of X ligands on Pd metal. Therefore, it is critical to apply an X ligand that could enable the concerted metalation-deprotonation (CMD) pathway and stabilize the pallacycle intermediate. According to this analysis, we replaced an L ligand, the methoxy group on the 2,6-dimethoxyaloxime

DG, with an X ligand would provide a more suitable DG. To test this hypothesis, the salicylaldehyde aldoxime **4.6** was introduced as the substrate for cyclopalladation (Scheme 4.4), which contains one L ligand, the sp^2 nitrogen of oxime, and one X ligand, the hydroxyl group. Although the salicylaldehyde-based DG has an available *ortho*-aryl C–H bond at the *endo* position, it is expected that the chelation between the phenoxide and imine nitrogen would overcome the *endo* effect to inhibit the potential *ortho*-metalation. Upon treating the aldoxime **4.6** with PdCl₂ and NaOAc in HOAc, there is no *ortho* C–H activation which is consistent with our speculation. However, the Pd species obtained are square planar complexes coordinated with two oxime substrates as inseparable diastereomers, in which the C–H bond remained intact.

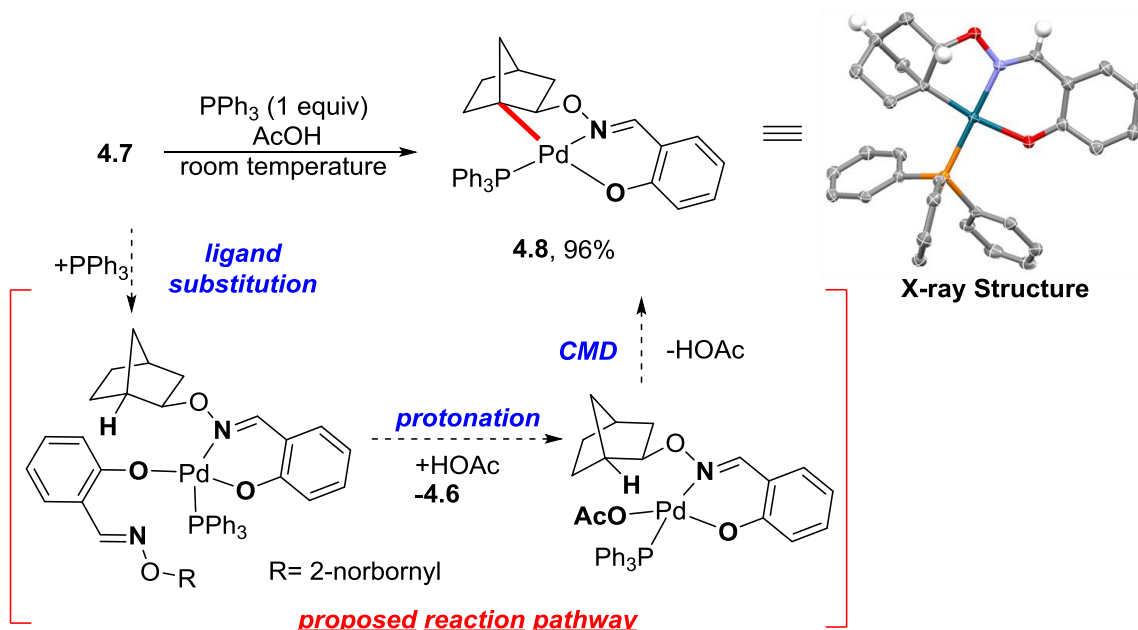
Scheme 4.6. Preparation of Pd complex **4.7**.



With this discouraging while inspiring result, we hypothesized that the formation of complex **4.7** was likely due to the lack of OAc group for the CMD process. Therefore, it is critical to remove one strong bidentate salicylaldehyde substrate from the Pd center for C–H cyclometalation to occur. Therefore, one equivalent of triphenylphosphine as an incoming strong L ligand was subsequently added at room temperature to compete with one oxime ligand in the presence of HOAc. To our delight, the desired tertiary alkyl palladacycle, Pd complex **4.8**, was formed in high yield via an intramolecular C–H

abstraction, which was confirmed and characterized via crystallography (Scheme 4.5). Unfortunately, complex **4.8** exhibits low solubility in most organic solvents that become an obstacle for NMR characterization and further experiments with this complex.

Scheme 4.7. C–H cyclopalladation at tertiary sp^3 positions with substrate **4.6**

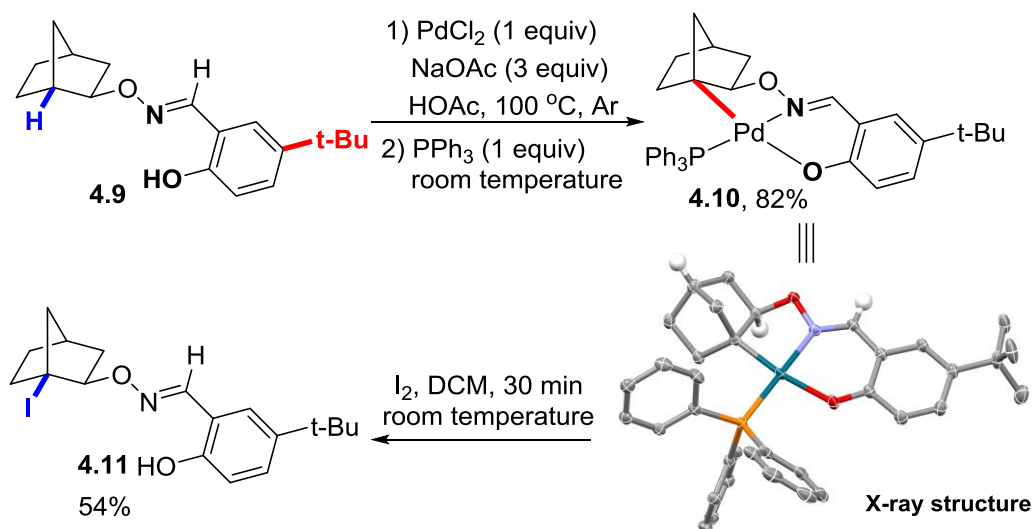


To overcome the solubility problem, the 5-tert-butylsalicylaldoxime was employed as DG in substrate **4.9**, after many failed attempts. Following the similar two-step procedure for preparation of complex **4.8**, the desired palladacycle **4.10** was isolated in high yield (Scheme 4.6). With this new DG, the Pd complex **4.10** exhibits good solubility in most solvents, which allows full NMR characterization in addition to X-ray crystallography. According to the data obtained from the X-ray structure, there is no torsion for the spare planar Pd(II) complex, which could be a possible explanation of the unique site selectivity.

It is worth to note that mix the triphenylphosphine at the beginning of the reaction with PdCl_2 did not provide any cyclometalation complex, because of the reduction of

Pd(II) to Pd(0) by phosphine ligand. The reactivity of the Pd complex **4.10** was also tested by treating the complex with I₂ at room temperature. The iodination smoothly furnished the tertiary C–H functionalization product, giving the C1-iodinated norbornene product **4.11**, which is tedious to prepare through the carbon skeleton rearrangement through a carbocation.¹⁰

Scheme 4.8. C–H cyclopalladation at tertiary *sp*³ positions with substrate **4.9**



4.4 Conclusion

In summary, it is the first report of prepared and characterization of tertiary alkyl-Pd(II) complexes via C–H activation, which is enabled by *exo*-DGs. This study indicates that C–H cyclopalladation can occur at tertiary *sp*³ positions in the present of cyclic methylene C–H bonds. The catalytic Pd functionalization of tertiary *sp*³ C–H bonds with different reactivity is under developing. This study would provide a solid basis for the further studies toward the mechanistic understanding of *exo*-directing strategy.

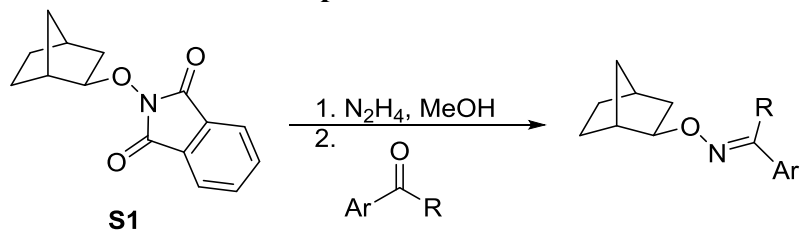
4.5 Experiment results

4.5.1 GENERAL CONSIDERATIONS

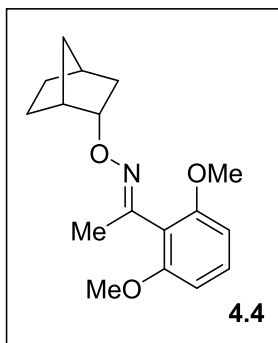
Unless otherwise noted, all experiments were carried out under air atmosphere. The other reagents and solvents were directly used from the supplier without further purification unless noted. Analytical thin-layer chromatography (TLC) was carried out using 0.2 mm commercial silica gel plates (silica gel 60, F254, EMD chemical). The vials (1 dram, 15×45 mm with PTFE-lined cap attached) were purchased from Qorpak and dried in an oven overnight and cooled in air. Infrared spectra were recorded on a Nicolet iS5 FT-IR Spectrometer using neat thin film technique. High-resolution mass spectra (HRMS) were obtained on a Karatos MS9 and are reported as m/z (relative intensity). Accurate masses are reported for the molecular ion $[M+Na]^+$, $[M+H]^+$ or $[2M-Cl]^+$. Nuclear magnetic resonance spectra (1H NMR and ^{13}C NMR) were recorded with Varian Gemini (400 MHz, 1H at 400 MHz, ^{13}C at 100 MHz) or Varian Gemini (500 MHz, 1H at 500 MHz, ^{13}C at 125 MHz). For $CDCl_3$ solutions, the chemical shifts are reported as parts per million (ppm) referenced to residual protium or carbon of the solvents; $CHCl_3$ 1H (7.26 ppm) and $CDCl_3$ ^{13}C (77.16 ppm). Coupling constants are reported in Hertz (Hz). Data for 1H NMR spectra are reported as follows: chemical shift (ppm, referenced to protium; s = singlet, d = doublet, t = triplet, q = quartet, p = pentet (quintet), dd = doublet of doublets, td = triplet of doublets, ddd = doublet of doublet of doublets, m = multiplet, coupling constant (Hz), and integration).

4.5.2 GENERAL PROCEDURE AND CHARACTERIZATION

General Procedure Preparation and Characterization of Oxime Starting Materials



To a solution of compound **S1** (1 equiv) in MeOH (1.5 mL/mmol) was added hydrazine hydrate (1 equiv) at room temperature. After 1.5 h, the corresponding aldehyde or ketone was added (when ketone was used, 2 drops of AcOH were added). After the reaction was complete (30 mins for aldehyde and overnight for ketone), the solvent was removed under *vacuo*. The desired oxime product was further purified by flash column chromatography on silica gel. Compounds **S1** and **1a** were prepared according to our previous reported procedure.^{4b}



(E)-1-(2,6-dimethoxyphenyl)ethan-1-one O-(endo-bicyclo[2.2.1]heptan-2-yl) oxime (4.4)

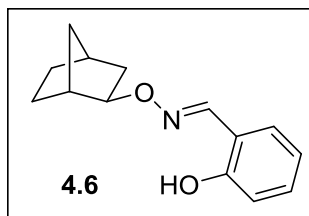
The reaction was conducted on a 1.5 mmol scale with 2,6-dimethoxyacetophenone. The title compound was isolated as a white solid (0.4023 g, 93%). **R_f value**= 0.1 in Hexanes/EA= 10:1. **Melting Point** (air): 87-89 °C.

IR (neat): 2955, 2870, 2836, 1709, 1595, 1471, 1432, 1351, 1304, 1250 cm⁻¹.

¹H NMR (400 MHz, CDCl₃) δ 7.22 (t, *J* = 8.4 Hz, 1H), 6.55 (d, *J* = 8.4 Hz, 2H), 4.29 (ddt, *J* = 7.2, 2.3, 1.0 Hz, 1H), 3.79 (s, 6H), 2.50 – 2.44 (m, 1H), 2.27 (td, *J* = 4.1, 1.7 Hz, 1H), 2.07 (s, 3H), 1.67 – 1.41 (m, 5H), 1.15 – 1.03 (m, 3H).

¹³C NMR (100 MHz, CDCl₃) δ 158.33, 152.37, 129.72, 116.36, 104.27, 85.31, 56.11, 41.21, 38.30, 35.53, 34.89, 28.80, 24.29, 16.64.

HRMS (ESI) Calcd. For C₁₇H₂₃NO₃Na⁺ [*M*+Na]⁺: 312.1570, Found: 312.1579.



(E)-2-hydroxybenzaldehyde O-(*exo*-bicyclo[2.2.1]heptan-2-yl) oxime (4.6)

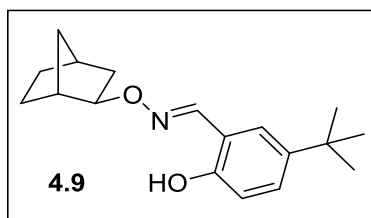
The reaction was conducted on a 1.0 mmol scale with salicylaldehyde. The title compound was isolated as a colorless oil (0.2119 g, 92%). **R_f value**= 0.6 in Hexanes/EA= 10:1.

IR (neat): 3188, 2960, 2872, 1622, 1609, 1494, 1394, 1354, 1264 cm⁻¹.

¹H NMR (400 MHz, CDCl₃) δ 10.08 (d, *J* = 0.4 Hz, 1H), 8.14 (s, 1H), 7.29 – 7.24 (m, 1H), 7.14 (ddt, *J* = 7.7, 1.7, 0.5 Hz, 1H), 6.98 (ddt, *J* = 8.3, 1.1, 0.5 Hz, 1H), 6.93 – 6.87 (m, 1H), 4.25 (ddt, *J* = 7.1, 2.3, 1.0 Hz, 1H), 2.53 – 2.47 (m, 1H), 2.34 – 2.28 (m, 1H), 1.72 – 1.65 (m, 1H), 1.60 – 1.45 (m, 4H), 1.18 – 1.06 (m, 3H).

¹³C NMR (100 MHz, CDCl₃) δ 157.56, 151.29, 131.05, 130.67, 119.63, 116.78, 116.77, 86.81, 40.87, 37.96, 35.45, 34.71, 28.60, 24.23.

HRMS (ESI) Calcd. For C₁₄H₁₇NO₂⁺ [M+H]⁺: 232.1332, Found: 232.1331.



(E)-5-(tert-butyl)-2-hydroxybenzaldehyde O-(*exo*-bicyclo[2.2.1]heptan-2-yl) oxime (4.9)

The reaction was conducted on a 10.0 mmol scale with 5-(*tert*-butyl)-2-hydroxybenzaldehyde. The title compound was isolated as a yellow oil (2.4041 g, 84%).

R_f value= 0.5 in Hexanes/EA= 10:1.

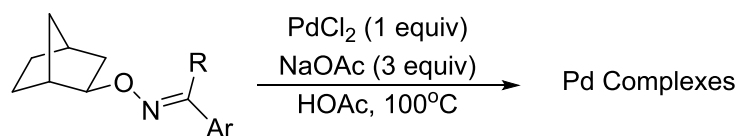
¹H NMR (400 MHz, CDCl₃) δ 9.90 (s, 1H), 8.14 (s, 1H), 7.30 (dd, *J* = 8.6, 2.5 Hz, 1H), 7.11 (d, *J* = 2.5 Hz, 1H), 6.94 – 6.89 (m, 1H), 4.24 (ddt, *J* = 7.1, 2.2, 1.0 Hz, 1H), 2.49 (d, *J* = 4.9 Hz, 1H), 2.34 – 2.26 (m, 1H), 1.67 (ddd, *J* = 13.4, 7.1, 2.5 Hz, 1H), 1.56 – 1.41 (m, 4H), 1.29 (s, 9H), 1.12 (dddd, *J* = 11.5, 6.8, 3.8, 2.1 Hz, 3H).

¹³C NMR (100 MHz, CDCl₃) δ 155.29, 151.75, 142.32, 128.32, 127.23, 116.31, 116.04, 86.69, 40.86, 37.97, 35.46, 34.69, 34.09, 31.55, 28.63, 24.24.

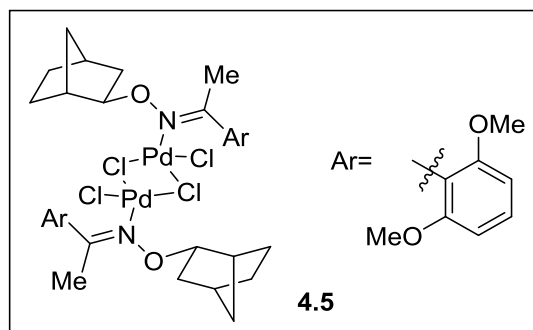
IR (neat): 3188, 2960, 2872, 1622, 1609, 1494, 1394, 1354, 1264 cm⁻¹.

HRMS (ESI) Calcd. For C₁₈H₂₅NO₂Na⁺ [*M*+Na]⁺: 310.1778, Found: 310.1785.

General Procedure Preparation Procedure for the Palladium Complexes



PdCl_2 (17.7 mg, 0.1 mmol, 1 equiv), NaOAc (24.6mg, 0.3 mmol, 3 equiv) and the oxime substrate (0.1 mmol, 1 equiv) were added in a Schlenk flask, followed by 0.5 mL AcOH . The flask was freeze-pump-thawed for three times and charged with Ar, and then the reaction was stirred at 100°C . The reaction was monitored by TLC and generally finished within 2. The mixture was purified according to the specific procedure in each case. In general, the crystal structures are obtained by slow evaporation of DCM and hexanes unless otherwise mentioned.

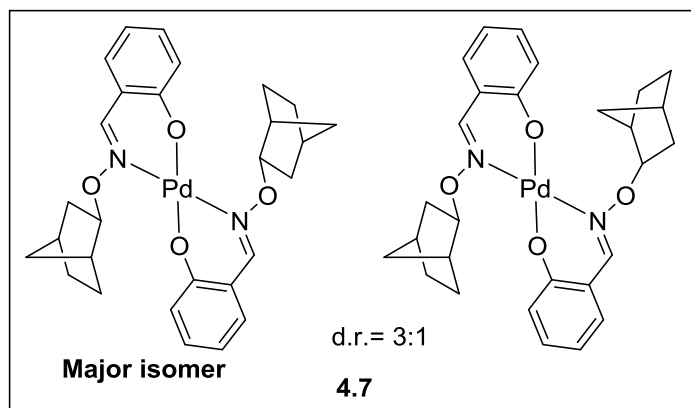


Pd complex **4.5**

The reaction was conducted on a 0.1 mmol scale. After the reaction was complete in 2h, the reaction was diluted with DCM and sequentially washed with water, and brine. The crude mixture was purified by column chromatography to give the title complex as a yellow solid (0.0319 g, 68%). However, the complex could form a number of isomers in solution, and the NMR spectra (-50 °C) are difficult to understand. **R_f value**= 0.27 in Hexanes/EA= 3:1. **Melting Point** (air): decompose at 120 °C.

IR (neat): 2959, 2872, 2837, 1623, 1596, 1474, 1431, 1356, 1306, 1291, 1257 cm⁻¹.

HRMS (ESI) Calcd. For C₃₄H₃₆Cl₃N₄O₂Pd₂⁺ [2M-Cl]⁺: 850.9970, Found: 850.9978.



Pd complex **4.7**

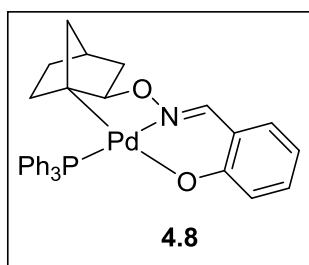
The reaction was conducted on a 0.1 mmol scale. After the reaction was finished in 1h, the reaction was diluted with DCM and sequentially washed with water, and brine. The crude mixture was purified by column chromatography to give the title compound as a yellow-orange solid (0.0137 g, 97%). The mixture contains inseparable diastereomers in 3:1 ratio, which is determined by NMR. Both of the diastereomers are **not** C2-symmetrical according to the X-ray structure presumably due to the steric hindrance of the norbornyl skeleton. **R_f value**= 0.4 in Hexanes/EA= 5:1. **Melting Point** (air): decompose at 205 °C.

IR (neat): 2958, 2870, 1602, 1533, 1465, 1440, 1350, 1307, 1194, 1149, 1128, 1070, 1031 cm⁻¹.

¹H NMR for the distinctive peaks of major isomer (400 MHz, CDCl₃) δ 7.97 (s, 1H), 7.29 (ddd, *J* = 8.7, 4.5, 2.6 Hz, 1H), 7.14 (ddd, *J* = 7.9, 3.1, 1.8 Hz, 1H), 6.91 (d, *J* = 8.5 Hz, 1H), 6.61 (dddd, *J* = 7.9, 6.8, 2.0, 1.1 Hz, 1H), 4.58 (ddt, *J* = 15.0, 7.4, 2.1 Hz, 1H), 2.40 (dd, *J* = 23.7, 4.9 Hz, 1H), 2.34 (s, 1H), 1.76 (ddt, *J* = 13.7, 7.3, 2.3 Hz, 1H), 1.64 (dd, *J* = 5.4, 2.7 Hz, 2H), 1.56 – 1.41 (m, 3H), 1.13 – 1.03 (m, 2H).

^{13}C NMR for the distinctive peaks of major isomer (125 MHz, CDCl_3) δ 164.56, 164.54, 157.52, 135.10, 133.41, 120.41, 120.37, 115.49, 115.46, 114.63, 114.55, 88.25, 88.19, 39.05, 38.79, 37.63, 37.55, 35.52, 35.50, 35.00, 34.83, 28.43, 28.42, 24.09, 23.95.

HRMS (ESI) Calcd. For $\text{C}_{26}\text{H}_{36}\text{ClN}_2\text{O}_6\text{Pd}_2^+$ $[\text{M}]^+$: 721.0337, Found: 721.0331.

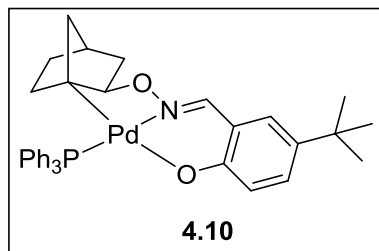


Pd complex **4.8**

The reaction was conducted on a 0.5 mmol scale. After the reaction was finished in 1h, 1 equiv of PPh_3 was added, and the reaction was stirred for another 30 mins. The solid was suspended in the large excess amount of DCM and washed with hexanes and water three times. After addition of hexanes to the solution, a yellow solid was precipitated and collected to give Pd complex **4.8** as a yellow solid (0.1435 g, 96%). The crystal was obtained by dissolving the complex in a large amount of DCM, and then slowly diffusion with hexanes. The complex **4.8** has low solubility in most organic solvents for NMR characterization. Melting Point (air): decompose at 200 $^\circ\text{C}$.

FT-IR (neat): 2955, 2870, 2836, 1709, 1595, 1471, 1432, 1351, 1304, 1250 cm^{-1} .

HRMS (ESI) Calcd. For $\text{C}_{32}\text{H}_{30}\text{NO}_2\text{PPd}^+$ $[\text{M}+\text{H}]^+$: 598.1134, Found: 598.1128.



Pd complex **4.10**

The reaction was conducted on a 0.1 mmol scale. After the reaction was finished in 2h, 1 equiv of PPh₃ was added, and the reaction was purified by column chromatography to give the title complex as a yellow solid (0.0269 g, 82%). **R_f value**= 0.4 in Hexanes/EA= 3:1. **Melting Point** (air): decompose at 215 °C.

IR (neat): 3054, 2952, 2860, 1612, 1518, 1469, 1435 cm⁻¹.

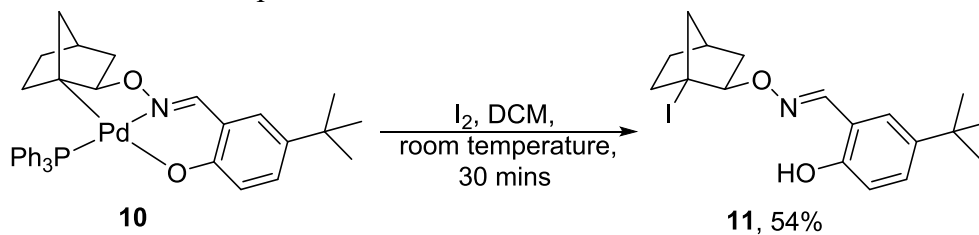
¹H NMR (400 MHz, CDCl₃) δ 8.09 (d, *J* = 8.3 Hz, 1H), 7.77 (ddd, *J* = 11.1, 8.0, 1.6 Hz, 6H), 7.55 – 7.32 (m, 9H), 7.21 (dd, *J* = 8.9, 2.7 Hz, 1H), 6.99 (d, *J* = 2.7 Hz, 1H), 6.49 (d, *J* = 8.9 Hz, 1H), 4.05 (dt, *J* = 6.3, 1.6 Hz, 1H), 1.90 (t, *J* = 4.3 Hz, 1H), 1.56 (ddt, *J* = 13.0, 4.3, 2.5 Hz, 1H), 1.44 – 1.39 (m, 1H), 1.37 – 1.32 (m, 1H), 1.25 (s, 9H), 1.03 – 0.91 (m, 2H), 0.81 (ddd, *J* = 11.2, 6.8, 4.1 Hz, 1H), 0.67 – 0.56 (m, 1H), 0.21 (dq, *J* = 9.7, 1.3 Hz, 1H).

¹³C NMR (100 MHz, CDCl₃) δ 165.31, 148.62 (d, *J* = 2.8 Hz), 135.43, 135.22 (d, *J* = 12.3 Hz), 131.21, 130.48 (d, *J* = 46.1 Hz), 130.44 (d, *J* = 2.4 Hz), 128.80, 128.06 (d, *J* = 10.5 Hz), 122.30, 115.24, 92.43, 60.93 (d, *J* = 5.0 Hz), 39.03, 35.11, 34.21, 33.62, 32.46 (d, *J* = 6.1 Hz), 31.56, 29.64 (d, *J* = 3.5 Hz).

^{31}P NMR (160 MHz, CDCl_3) δ 34.93.

HRMS (ESI) Calcd. For $\text{C}_{36}\text{H}_{38}\text{NO}_2\text{PPd}^+$ $[\text{M}+\text{H}]^+$: 654.1761, Found: 654.1776.

Reaction of Pd complex **10** with Iodine



In a vial charged with Pd complex **10** (0.0654 g, 0.1 mmol, 1 equiv) and I_2 (0.0284g, 0.1 mmol, 1 equiv), 1 mL of DCM was added as solvent. The reaction was stirred at room temperature for 30 min. After the reaction had been finished, the reaction was purified by column chromatography to give the title compound as a dark oil light sensitive (0.0222 g, 54%). R_f value= 0.3 in Hexanes/EA= 10:1.

IR (neat): 3217, 2961, 2871, 1621, 1608, 1580, 1494, 1462, 1439, 1384, 1364, 1262 cm^{-1} .

^1H NMR (400 MHz, CDCl_3) δ 9.65 (s, 1H), 8.25 (s, 1H), 7.31 (dd, J = 8.7, 2.5 Hz, 1H), 7.13 (d, J = 2.4 Hz, 1H), 6.92 (dd, J = 8.6, 0.5 Hz, 1H), 4.21 (td, J = 4.9, 1.4 Hz, 1H), 2.24 – 2.17 (m, 1H), 2.14 – 2.04 (m, 2H), 1.87 – 1.78 (m, 3H), 1.74 – 1.53 (m, 3H), 1.29 (s, 9H).

^{13}C NMR (100 MHz, CDCl_3) δ 155.22, 152.38, 142.42, 128.61, 127.49, 116.38, 115.89, 87.91, 47.05, 40.39, 39.45, 39.22, 34.81, 34.11, 31.55, 31.43.

HRMS (ESI) Calcd. For $\text{C}_{18}\text{H}_{24}\text{INO}_2^+$ $[\text{M}+\text{H}]^+$: 414.0924, Found: 414.0924.

X-ray Structures Data:

X-ray structure data of Pd complex **4.5**:

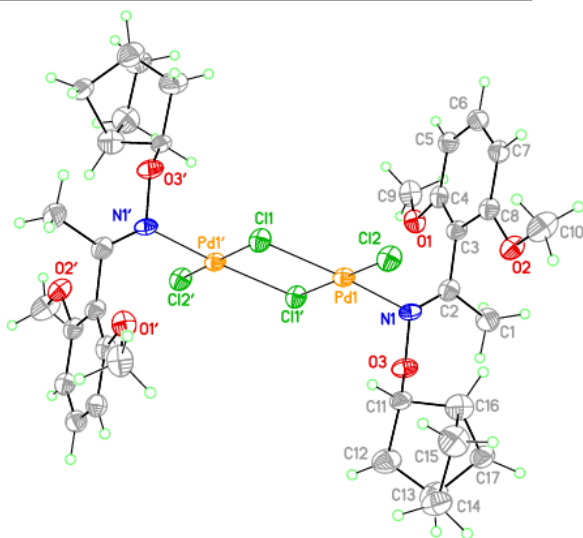
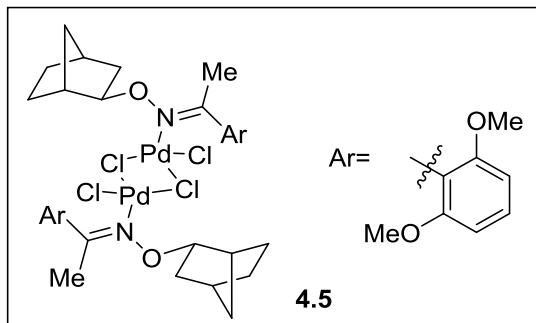


Table 4.1.1. Crystal data and structure refinement for Pd complex **4.5**.

Empirical formula	C ₃₄ H ₄₆ Cl ₄ N ₂ O ₆ Pd ₂	
Formula weight	933.33	
Temperature	100(2) K	
Wavelength	1.54184 Å	
Crystal system	monoclinic	
Space group	P 2 ₁ /n	
Unit cell dimensions	a = 14.9412(8) Å	= 90°.
	b = 8.7902(6) Å	= 116.895(6)°.

	$c = 15.9120(9) \text{ \AA}$	$= 90^\circ$.
Volume	1863.8(2) \AA^3	
Z	2	
Density (calculated)	1.663 Mg/m^3	
Absorption coefficient	10.797 mm^{-1}	
F(000)	944	
Crystal size	0.076 x 0.051 x 0.025 mm^3	
Theta range for data collection	3.370 to 74.553°.	
Index ranges	$-18 \leq h \leq 18$, $-10 \leq k \leq 7$, $-19 \leq l \leq 19$	
Reflections collected	8709	
Independent reflections	3662 [R(int) = 0.0431]	
Completeness to theta = 67.684°	99.5 %	
Absorption correction Gaussian		
Max. and min. transmission	0.940 and 0.872	
Refinement method	Full-matrix least-squares on F ²	
Data / restraints / parameters	3662 / 0 / 220	
Goodness-of-fit on F ²	1.051	
Final R indices [I > 2sigma(I)]	R1 = 0.0498, wR2 = 0.1102	
R indices (all data)	R1 = 0.0687, wR2 = 0.1201	
Extinction coefficient	n/a	
Largest diff. peak and hole	0.727 and -0.782 e.\AA^{-3}	

Table 4.1.2. Atomic coordinates and equivalent isotropic displacement parameters for Pd complex **4.5**.

U(eq) is defined as one third of the trace of the orthogonalized U_{ij} tensor. Atomic coordinates ($\times 10^4$) and equivalent isotropic displacement parameters ($\text{\AA}^2 \times 10^3$)

Atom	x	y	z	U(eq)
C1	8725(5)	2004(9)	6363(4)	63(2)
C2	7684(4)	2404(8)	5623(4)	45(1)
C3	7040(4)	1147(7)	5010(4)	41(1)
C4	6529(4)	164(7)	5331(4)	42(1)
C5	5971(5)	-1035(7)	4770(4)	46(1)
C6	5958(4)	-1264(8)	3904(4)	47(2)
C7	6485(4)	-349(7)	3596(4)	46(2)
C8	7050(4)	858(7)	4156(4)	42(1)
C9	6380(6)	-736(9)	6671(5)	61(2)
C10	7600(6)	1654(11)	3034(4)	74(2)
C11	8073(4)	6142(7)	5569(4)	45(2)
C12	8657(6)	7410(10)	6288(5)	71(2)
C13	9589(6)	7589(11)	6243(5)	74(2)
C14	9377(5)	8344(9)	5305(5)	67(2)
C15	8826(7)	7080(11)	4587(6)	82(3)
C16	8781(6)	5746(10)	5152(5)	67(2)
C17	9833(5)	5988(8)	6083(5)	59(2)
N1	7324(3)	3740(6)	5467(3)	38(1)

O1	6642(3)	458(5)	6213(3)	51(1)
O2	7671(3)	1763(6)	3964(3)	50(1)
O3	7960(3)	4859(5)	6079(3)	50(1)
Cl1	4270(1)	5363(2)	3918(1)	45(1)
Cl2	6011(1)	4434(2)	3318(1)	50(1)
Pd1	5903(1)	4450(1)	4695(1)	38(1)

Table 4.1.3. Bond lengths [Å] and angles [°] for Pd complex **4.5**.

		C6-H6	0.9500
C1-C2	1.507(8)	C7-C8	1.397(8)
C1-H1A	0.98	C7-H7	0.9500
C1-H1B	0.98	C8-O2	1.357(7)
C1-H1C	0.98	C9-O1	1.430(8)
C2-N1	1.268(8)	C9-H9A	0.98
C2-C3	1.500(8)	C9-H9B	0.98
C3-C8	1.390(8)	C9-H9C	0.98
C3-C4	1.394(9)	C10-O2	1.439(7)
C4-O1	1.361(7)	C10-H10A	0.98
C4-C5	1.389(9)	C10-H10B	0.98
C5-C6	1.383(8)	C10-H10C	0.98
C5-H5	0.9500	C11-O3	1.443(7)
C6-C7	1.362(9)	C11-C16	1.522(10)

C11-C12	1.552(9)	C2-C1-H1B	109.5
C11-H11	1.00	H1A-C1-H1B	109.5
C12-C13	1.434(11)	C2-C1-H1C	109.5
C12-H12A	0.99	H1A-C1-H1C	109.5
C12-H12B	0.99	H1B-C1-H1C	109.5
C13-C17	1.505(11)	N1-C2-C3	117.6(5)
C13-C14	1.530(10)	N1-C2-C1	124.5(6)
C13-H13	1.00	C3-C2-C1	117.9(6)
C14-C15	1.539(11)	C8-C3-C4	119.7(6)
C14-H14A	0.99	C8-C3-C2	118.9(6)
C14-H14B	0.99	C4-C3-C2	121.0(5)
C15-C16	1.497(11)	O1-C4-C5	124.5(6)
C15-H15A	0.99	O1-C4-C3	115.3(5)
C15-H15B	0.99	C5-C4-C3	120.2(5)
C16-C17	1.614(9)	C6-C5-C4	119.0(6)
C16-H16	1.00	C6-C5-H5	120.5
C17-H17A	0.99	C4-C5-H5	120.5
C17-H17B	0.99	C7-C6-C5	121.5(6)
N1-O3	1.408(6)	C7-C6-H6	119.3
N1-Pd1	2.012(5)	C5-C6-H6	119.3
Cl1-Pd1	2.3223(14)	C6-C7-C8	120.0(6)
Cl1-Pd1#1	2.3408(15)	C6-C7-H7	120.0
Cl2-Pd1	2.2698(15)	C8-C7-H7	120.0
Pd1-Cl1#1	2.3408(15)	O2-C8-C3	115.1(5)
C2-C1-H1A	109.5	O2-C8-C7	125.4(5)

C3-C8-C7	119.4(6)	C12-C13-C17	102.8(7)
O1-C9-H9A	109.5	C12-C13-C14	108.6(7)
O1-C9-H9B	109.5	C17-C13-C14	101.5(7)
H9A-C9-H9B	109.5	C12-C13-H13	114.2
O1-C9-H9C	109.5	C17-C13-H13	114.2
H9A-C9-H9C	109.5	C14-C13-H13	114.2
H9B-C9-H9C	109.5	C13-C14-C15	102.5(7)
O2-C10-H10A	109.5	C13-C14-H14A	111.3
O2-C10-H10B	109.5	C15-C14-H14A	111.3
H10A-C10-H10B	109.5	C13-C14-H14B	111.3
O2-C10-H10C	109.5	C15-C14-H14B	111.3
H10A-C10-H10C	109.5	H14A-C14-H14B	109.2
H10B-C10-H10C	109.5	C16-C15-C14	105.9(6)
O3-C11-C16	110.3(6)	C16-C15-H15A	110.6
O3-C11-C12	108.5(5)	C14-C15-H15A	110.6
C16-C11-C12	102.5(6)	C16-C15-H15B	110.6
O3-C11-H11	111.7	C14-C15-H15B	110.6
C16-C11-H11	111.7	H15A-C15-H15B	108.7
C12-C11-H11	111.7	C15-C16-C11	108.2(7)
C13-C12-C11	106.1(7)	C15-C16-C17	99.1(6)
C13-C12-H12A	110.5	C11-C16-C17	98.6(6)
C11-C12-H12A	110.5	C15-C16-H16	116.1
C13-C12-H12B	110.5	C11-C16-H16	116.1
C11-C12-H12B	110.5	C17-C16-H16	116.1
H12A-C12-H12B	108.7	C13-C17-C16	93.9(6)

C13-C17-H17A	112.9	C8-O2-C10	116.9(5)
C16-C17-H17A	112.9	N1-O3-C11	111.8(4)
C13-C17-H17B	112.9	Pd1-Cl1-Pd1#1	93.42(4)
C16-C17-H17B	112.9	N1-Pd1-Cl2	94.06(14)
H17A-C17-H17B	110.4	N1-Pd1-Cl1	175.22(14)
C2-N1-O3	114.7(4)	Cl2-Pd1-Cl1	90.27(5)
C2-N1-Pd1	130.1(4)	N1-Pd1-Cl1#1	89.00(14)
O3-N1-Pd1	113.7(4)	Cl2-Pd1-Cl1#1	175.82(6)
C4-O1-C9	116.9(5)	Cl1-Pd1-Cl1#1	86.58(4)

Symmetry transformations used to generate equivalent atoms:

#1 -x+1,-y+1,-z+1

Table 4.1.4. Anisotropic displacement parameters for Pd complex **4.5**.

The anisotropic displacement factor exponent takes the form: $-2\pi^2 [h^2 a^{*2} U^{11} + \dots + 2 h k a^* b^* U^{12}]$. Anisotropic displacement parameters ($\text{\AA}^2 \times 10^3$).

Atom	U^{11}	U^{22}	U^{33}	U^{23}	U^{13}	U^{12}
C1	46(4)	74(5)	44(3)	-8(3)	0(3)	11(3)
C2	39(3)	58(4)	33(3)	2(3)	11(2)	3(3)
C3	34(3)	49(3)	32(3)	0(2)	8(2)	0(3)
C4	38(3)	54(4)	31(2)	5(3)	15(2)	10(3)
C5	42(3)	45(3)	46(3)	4(3)	15(3)	5(3)
C6	44(3)	50(4)	40(3)	-1(3)	14(3)	3(3)
C7	42(3)	61(4)	32(3)	-4(3)	13(2)	5(3)
C8	35(3)	54(4)	30(2)	4(3)	8(2)	6(3)
C9	72(5)	68(5)	45(3)	16(3)	29(3)	15(4)
C10	61(4)	120(7)	43(3)	6(4)	27(3)	-16(5)
C11	33(3)	44(3)	48(3)	-4(3)	7(2)	-5(3)
C12	67(5)	84(6)	56(4)	-12(4)	22(4)	-17(4)
C13	60(5)	97(7)	60(4)	-8(4)	23(4)	-8(5)
C14	56(4)	63(5)	66(4)	9(4)	14(3)	-10(4)
C15	87(6)	95(7)	63(5)	-1(5)	34(4)	-1(5)
C16	74(5)	70(5)	58(4)	0(4)	31(4)	-8(4)
C17	39(3)	58(4)	65(4)	0(3)	11(3)	-2(3)
N1	36(2)	42(3)	28(2)	-3(2)	7(2)	-10(2)

O1	59(3)	59(3)	35(2)	2(2)	22(2)	7(2)
O2	42(2)	71(3)	37(2)	2(2)	17(2)	-5(2)
O3	46(2)	57(3)	33(2)	-3(2)	6(2)	-12(2)
Cl1	40(1)	57(1)	29(1)	7(1)	9(1)	8(1)
Cl2	46(1)	67(1)	30(1)	5(1)	11(1)	4(1)
Pd1	36(1)	40(1)	27(1)	2(1)	6(1)	-2(1)

Table 4.1.5. H coordinates and isotropic displacement parameters for Pd complex **4.5**.

Hydrogen coordinates (x 10⁴) and isotropic displacement parameters (Å²x 10³)

Hydrogen	x	y	z	U(eq)
H1A	9093	1501	6064	94
H1B	8678	1316	6827	94
H1C	9079	2933	6679	94
H5	5605	-1688	4977	56
H6	5573	-2077	3516	56
H7	6468	-533	3001	55
H9A	5649	-859	6370	91
H9B	6618	-479	7338	91
H9C	6693	-1688	6621	91
H10A	7859	666	2960	110
H10B	7995	2469	2943	110
H10C	6896	1753	2564	110

H11	7410	6514	5076	55
H12A	8272	8373	6119	85
H12B	8779	7111	6931	85
H13	10128	8096	6808	89
H14A	10007	8638	5287	80
H14B	8947	9255	5190	80
H15A	8142	7413	4140	98
H15B	9197	6812	4226	98
H16	8679	4729	4840	80
H17A	9920	5288	6602	71
H17B	10421	5929	5954	71

Table 4.1.6. Torsion angles [°] for Pd complex **4.5**.

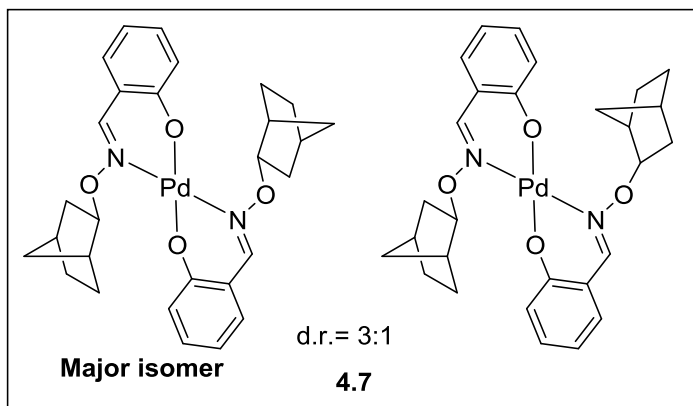
N1-C2-C3-C8	85.9(8)	C4-C5-C6-C7	0.5(9)
C1-C2-C3-C8	-92.3(7)	C5-C6-C7-C8	-0.4(9)
N1-C2-C3-C4	-101.6(7)	C4-C3-C8-O2	-171.9(5)
C1-C2-C3-C4	80.1(8)	C2-C3-C8-O2	0.6(8)
C8-C3-C4-O1	173.9(5)	C4-C3-C8-C7	4.8(8)
C2-C3-C4-O1	1.5(8)	C2-C3-C8-C7	177.4(5)
C8-C3-C4-C5	-4.7(9)	C6-C7-C8-O2	174.1(6)
C2-C3-C4-C5	-177.1(5)	C6-C7-C8-C3	-2.3(9)
O1-C4-C5-C6	-176.5(5)	O3-C11-C12-C13	115.2(7)
C3-C4-C5-C6	2.0(9)	C16-C11-C12-C13	-1.4(8)

C11-C12-C13-C17	-35.9(8)	C11-C16-C17-C13	-54.8(7)
C11-C12-C13-C14	71.1(9)	C3-C2-N1-O3	178.9(5)
C12-C13-C14-C15	-70.0(9)	C1-C2-N1-O3	-3.0(9)
C17-C13-C14-C15	37.8(8)	C3-C2-N1-Pd1	14.3(9)
C13-C14-C15-C16	-0.7(9)	C1-C2-N1-Pd1	-167.6(5)
C14-C15-C16-C11	68.8(8)	C5-C4-O1-C9	15.8(8)
C14-C15-C16-C17	-33.5(8)	C3-C4-O1-C9	-162.8(5)
O3-C11-C16-C15	176.9(5)	C3-C8-O2-C10	-171.3(6)
C12-C11-C16-C15	-67.8(7)	C7-C8-O2-C10	12.1(9)
O3-C11-C16-C17	-80.5(6)	C2-N1-O3-C11	129.1(6)
C12-C11-C16-C17	34.8(7)	Pd1-N1-O3-C11	-63.8(5)
C12-C13-C17-C16	55.7(7)	C16-C11-O3-N1	-76.4(6)
C14-C13-C17-C16	-56.6(7)	C12-C11-O3-N1	172.1(5)
C15-C16-C17-C13	55.3(7)		

Symmetry transformations used to generate equivalent atoms:

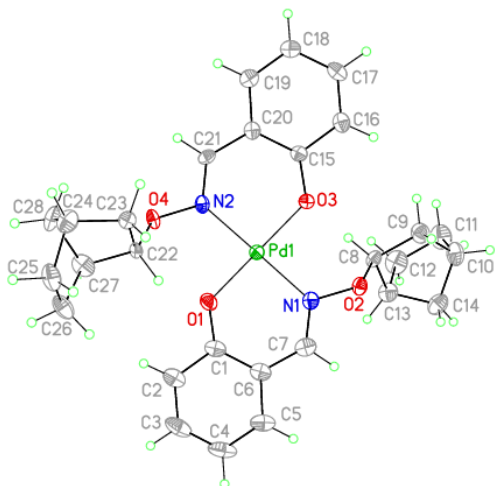
#1 -x+1,-y+1,-z+1

X-ray structure data of Pd complex **4.7**:



The major diastereomer of Pd complex

4.7:



The minor diastereomer of Pd complex

4.7:

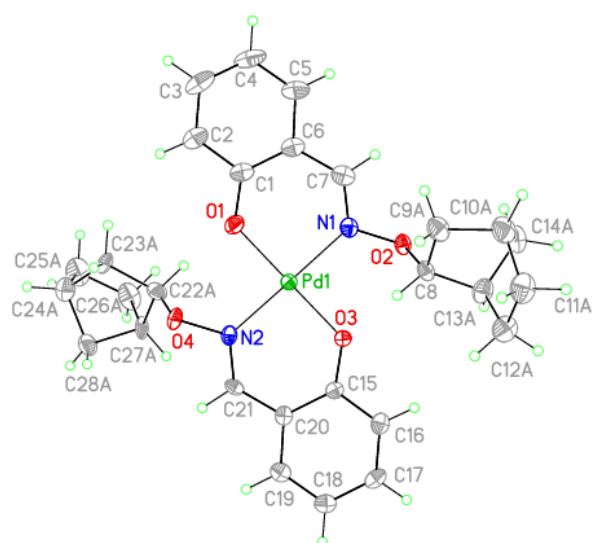


Table 4.2.1. Crystal data and structure refinement for Pd complex **4.7**.

Empirical formula	C ₂₈ H ₃₂ N ₂ O ₄ Pd
Formula weight	566.95
Temperature	100(2) K
Wavelength	0.71073 Å
Crystal system	orthorhombic
Space group	P 21 21 21
Unit cell dimensions	a = 5.8758(11) Å = 90°. b = 17.966(4) Å = 90°. c = 23.513(4) Å = 90°.
Volume	2482.2(8) Å ³
Z	4
Density (calculated)	1.517 Mg/m ³
Absorption coefficient	0.785 mm ⁻¹
F(000)	1168
Crystal size	0.230 x 0.070 x 0.040 mm ³
Theta range for data collection	3.450 to 27.463°.
Index ranges	-7<= <i>h</i> <=7, -23<= <i>k</i> <=23, -29<= <i>l</i> <=30
Reflections collected	39216
Independent reflections	5677 [R(int) = 0.0590]
Completeness to theta = 25.242°	99.7 %
Absorption correction	Semi-empirical from equivalents
Max. and min. transmission	1.00 and 0.800
Refinement method	Full-matrix least-squares on F ²
Data / restraints / parameters	5677 / 375 / 438
Goodness-of-fit on F ²	1.163

Final R indices [$I > 2\sigma(I)$]	R1 = 0.0343, wR2 = 0.0650
R indices (all data)	R1 = 0.0374, wR2 = 0.0660
Absolute structure parameter	-0.033(15)
Extinction coefficient	n/a
Largest diff. peak and hole	0.419 and -0.807 e.Å ⁻³

Table 4.2.2. Atomic coordinates and equivalent isotropic displacement parameters for **4.7**.

U(eq) is defined as one-third of the trace of the orthogonalized U_{ij} tensor.

Atomic coordinates ($\times 10^4$) and equivalent isotropic displacement parameters (Å² $\times 10^3$)

Atom	x	y	z	U(eq)
C1	3196(9)	454(2)	7596(2)	24(1)
C2	2642(10)	489(3)	8182(2)	31(1)
C3	4161(9)	262(3)	8591(3)	39(1)
C4	6294(10)	2(3)	8447(2)	40(2)
C5	6894(10)	-35(3)	7887(2)	32(1)
C6	5384(9)	187(3)	7450(2)	23(1)
C7	6187(9)	108(3)	6881(2)	24(1)
C8	5265(8)	-383(3)	5567(2)	20(1)
C9	6280(20)	-309(7)	4975(6)	30(2)
C10	7496(14)	-1047(4)	4870(3)	34(2)
C11	5680(30)	-1647(8)	4796(8)	40(2)
C12	4684(16)	-1723(5)	5398(4)	40(2)
C13	6040(20)	-1169(8)	5755(6)	27(2)
C14	8332(13)	-1218(5)	5471(3)	33(2)

C9A	5520(40)	-1163(17)	5813(11)	31(4)
C10A	7020(30)	-1564(7)	5385(6)	36(2)
C11A	5630(50)	-1691(13)	4846(15)	39(3)
C12A	5310(30)	-897(8)	4618(6)	35(3)
C13A	6670(40)	-404(11)	5022(12)	30(4)
C14A	8550(20)	-923(9)	5198(7)	35(3)
C15	1092(8)	1302(2)	5226(2)	18(1)
C16	1648(8)	1273(2)	4638(2)	23(1)
C17	141(9)	1515(3)	4231(2)	24(1)
C18	-1985(9)	1807(2)	4383(2)	24(1)
C19	-2556(8)	1843(2)	4948(2)	22(1)
C20	-1060(8)	1600(2)	5377(2)	18(1)
C21	-1809(8)	1688(2)	5950(2)	18(1)
C22	-660(40)	2140(12)	7270(11)	14(4)
C23	-634(17)	2942(6)	7036(4)	23(2)
C24	-2101(17)	3373(4)	7461(3)	30(2)
C25	-760(20)	3439(6)	8012(5)	31(3)
C26	-756(17)	2630(5)	8251(4)	34(2)
C27	-2100(30)	2210(8)	7804(7)	29(4)
C28	-3894(16)	2793(6)	7613(6)	31(2)
C22A	-1050(60)	2110(17)	7280(17)	25(9)
C23A	-2160(50)	2019(11)	7861(9)	20(4)
C24A	-3420(20)	2756(7)	7963(6)	32(3)
C25A	-1660(30)	3365(12)	8083(8)	43(6)
C26A	-410(20)	3456(8)	7506(7)	38(3)
C27A	-1650(20)	2922(8)	7116(6)	24(4)
C28A	-4070(20)	2964(9)	7349(6)	30(4)

O1	1653(6)	671(2)	7232(1)	25(1)
O2	6318(5)	183(2)	5921(1)	20(1)
O3	2633(5)	1059(2)	5584(1)	20(1)
O4	-1941(7)	1607(2)	6905(1)	22(1)
Pd1	2157(1)	878(1)	6409(1)	16(1)
N1	5063(6)	289(2)	6428(2)	20(1)
N2	-696(6)	1489(2)	6399(2)	18(1)

Table 4.2.3. Bond lengths [Å] and angles [°] for **4.7**.

C1-O1	1.307(5)	C8-C9	1.519(16)
C1-C2	1.416(6)	C8-C13A	1.52(3)
C1-C6	1.415(7)	C8-C9A	1.52(3)
C2-C3	1.374(7)	C8-C13	1.549(15)
C2-H2	0.95	C8-H8	0.96(5)
C3-C4	1.380(8)	C9-C10	1.525(13)
C3-H3	0.95	C9-H9A	0.99
C4-C5	1.365(7)	C9-H9B	0.99
C4-H4	0.95	C10-C11	1.526(15)
C5-C6	1.415(7)	C10-C14	1.527(10)
C5-H5	0.95	C10-H10	1.00
C6-C7	1.426(7)	C11-C12	1.54(2)
C7-N1	1.295(6)	C11-H11A	0.99
C7-H7	0.95	C11-H11B	0.99
C8-O2	1.454(5)	C12-C13	1.526(17)

C12-H12A	0.99	C17-C18	1.401(7)
C12-H12B	0.99	C17-H17	0.95
C13-C14	1.507(13)	C18-C19	1.371(6)
C13-H13	1.00	C18-H18	0.95
C14-H14A	0.99	C19-C20	1.409(6)
C14-H14B	0.99	C19-H19	0.95
C9A-C10A	1.519(18)	C20-C21	1.425(6)
C9A-H9A1	0.99	C21-N2	1.292(6)
C9A-H9A2	0.99	C21-H21	0.95
C10A-C11A	1.524(18)	C22-O4	1.49(2)
C10A-C14A	1.528(13)	C22-C27	1.52(3)
C10A-H10A	1.00	C22-C23	1.54(3)
C11A-C12A	1.54(3)	C22-H22	1.00
C11A-H11C	0.99	C23-C24	1.531(12)
C11A-H11D	0.99	C23-H23A	0.99
C12A-C13A	1.52(2)	C23-H23B	0.99
C12A-H12C	0.99	C24-C25	1.523(14)
C12A-H12D	0.99	C24-C28	1.524(12)
C13A-C14A	1.507(17)	C24-H24	1.00
C13A-H13A	1.00	C25-C26	1.558(15)
C14A-H14C	0.99	C25-H25A	0.99
C14A-H14D	0.99	C25-H25B	0.99
C15-O3	1.310(5)	C26-C27	1.517(19)
C15-C20	1.419(6)	C26-H26A	0.99
C15-C16	1.421(6)	C26-H26B	0.99
C16-C17	1.374(7)	C27-C28	1.552(17)
C16-H16	0.95	C27-H27	1.00

C28-H28A	0.99	C25A-H25D	0.99
C28-H28B	0.99	C26A-C27A	1.513(19)
C22A-O4	1.37(3)	C26A-H26C	0.99
C22A-C23A	1.52(4)	C26A-H26D	0.99
C22A-C27A	1.55(3)	C27A-C28A	1.527(17)
C22A-H22A	1.00	C27A-H27A	1.00
C23A-C24A	1.54(2)	C28A-H28C	0.99
C23A-H23C	0.99	C28A-H28D	0.99
C23A-H23D	0.99	O1-Pd1	1.991(3)
C24A-C25A	1.531(18)	O2-N1	1.413(5)
C24A-C28A	1.539(16)	O3-Pd1	1.988(3)
C24A-H24A	1.00	O4-N2	1.412(5)
C25A-C26A	1.55(2)	Pd1-N2	2.004(3)
C25A-H25C	0.99	Pd1-N1	2.009(3)
O1-C1-C2	117.7(5)	C4-C5-C6	121.6(6)
O1-C1-C6	124.9(4)	C4-C5-H5	119.2
C2-C1-C6	117.4(5)	C6-C5-H5	119.2
C3-C2-C1	121.2(6)	C1-C6-C5	119.3(5)
C3-C2-H2	119.4	C1-C6-C7	124.2(5)
C1-C2-H2	119.4	C5-C6-C7	116.5(5)
C2-C3-C4	121.3(6)	N1-C7-C6	125.3(5)
C2-C3-H3	119.3	N1-C7-H7	117.3
C4-C3-H3	119.3	C6-C7-H7	117.3
C5-C4-C3	119.2(5)	O2-C8-C9	107.2(6)
C5-C4-H4	120.4	O2-C8-C13A	105.6(9)
C3-C4-H4	120.4	O2-C8-C9A	112.6(12)

C13A-C8-C9A	104.1(8)	C13-C12-H12A	110.9
O2-C8-C13	110.4(6)	C11-C12-H12A	110.9
C9-C8-C13	103.1(6)	C13-C12-H12B	110.9
O2-C8-H8	106(3)	C11-C12-H12B	110.9
C9-C8-H8	113(3)	H12A-C12-H12B	108.9
C13A-C8-H8	123(3)	C14-C13-C12	100.6(9)
C9A-C8-H8	106(3)	C14-C13-C8	100.9(9)
C13-C8-H8	117(3)	C12-C13-C8	106.5(9)
C8-C9-C10	104.9(8)	C14-C13-H13	115.6
C8-C9-H9A	110.8	C12-C13-H13	115.6
C10-C9-H9A	110.8	C8-C13-H13	115.6
C8-C9-H9B	110.8	C13-C14-C10	96.4(8)
C10-C9-H9B	110.8	C13-C14-H14A	112.5
H9A-C9-H9B	108.8	C10-C14-H14A	112.5
C11-C10-C9	107.8(9)	C13-C14-H14B	112.5
C11-C10-C14	100.8(10)	C10-C14-H14B	112.5
C9-C10-C14	100.1(7)	H14A-C14-H14B	110.0
C11-C10-H10	115.4	C10A-C9A-C8	104.0(14)
C9-C10-H10	115.4	C10A-C9A-H9A1	111.0
C14-C10-H10	115.4	C8-C9A-H9A1	111.0
C10-C11-C12	103.0(8)	C10A-C9A-H9A2	111.0
C10-C11-H11A	111.2	C8-C9A-H9A2	111.0
C12-C11-H11A	111.2	H9A1-C9A-H9A2	109.0
C10-C11-H11B	111.2	C9A-C10A-C11A	108.2(15)
C12-C11-H11B	111.2	C9A-C10A-C14A	100.1(13)
H11A-C11-H11B	109.1	C11A-C10A-C14A	100.9(16)
C13-C12-C11	104.4(8)	C9A-C10A-H10A	115.2

C11A-C10A-H10A	115.2	O3-C15-C16	116.9(4)
C14A-C10A-H10A	115.2	C20-C15-C16	117.6(4)
C10A-C11A-C12A	102.5(10)	C17-C16-C15	121.2(5)
C10A-C11A-H11C	111.3	C17-C16-H16	119.4
C12A-C11A-H11C	111.3	C15-C16-H16	119.4
C10A-C11A-H11D	111.3	C16-C17-C18	121.1(5)
C12A-C11A-H11D	111.3	C16-C17-H17	119.5
H11C-C11A-H11D	109.2	C18-C17-H17	119.5
C13A-C12A-C11A	105.1(11)	C19-C18-C17	118.8(5)
C13A-C12A-H12C	110.7	C19-C18-H18	120.6
C11A-C12A-H12C	110.7	C17-C18-H18	120.6
C13A-C12A-H12D	110.7	C18-C19-C20	121.9(5)
C11A-C12A-H12D	110.7	C18-C19-H19	119.1
H12C-C12A-H12D	108.8	C20-C19-H19	119.1
C14A-C13A-C8	100.5(15)	C19-C20-C15	119.5(4)
C14A-C13A-C12A	101.2(13)	C19-C20-C21	116.8(4)
C8-C13A-C12A	104.9(16)	C15-C20-C21	123.6(4)
C14A-C13A-H13A	116.0	N2-C21-C20	125.9(4)
C8-C13A-H13A	116.0	N2-C21-H21	117.1
C12A-C13A-H13A	116.0	C20-C21-H21	117.1
C13A-C14A-C10A	96.4(11)	O4-C22-C27	104.2(18)
C13A-C14A-H14C	112.5	O4-C22-C23	113.4(17)
C10A-C14A-H14C	112.5	C27-C22-C23	102.9(9)
C13A-C14A-H14D	112.5	O4-C22-H22	111.9
C10A-C14A-H14D	112.5	C27-C22-H22	111.9
H14C-C14A-H14D	110.0	C23-C22-H22	111.9
O3-C15-C20	125.5(4)	C24-C23-C22	103.5(10)

C24-C23-H23A	111.1	C22-C27-H27	114.3
C22-C23-H23A	111.1	C28-C27-H27	114.3
C24-C23-H23B	111.1	C24-C28-C27	93.4(9)
C22-C23-H23B	111.1	C24-C28-H28A	113.0
H23A-C23-H23B	109.0	C27-C28-H28A	113.0
C25-C24-C28	102.3(8)	C24-C28-H28B	113.0
C25-C24-C23	107.7(8)	C27-C28-H28B	113.0
C28-C24-C23	101.4(7)	H28A-C28-H28B	110.4
C25-C24-H24	114.7	O4-C22A-C23A	110(3)
C28-C24-H24	114.7	O4-C22A-C27A	112(3)
C23-C24-H24	114.7	C23A-C22A-C27A	103.2(14)
C24-C25-C26	103.5(7)	O4-C22A-H22A	110.4
C24-C25-H25A	111.1	C23A-C22A-H22A	110.4
C26-C25-H25A	111.1	C27A-C22A-H22A	110.4
C24-C25-H25B	111.1	C22A-C23A-C24A	104.7(16)
C26-C25-H25B	111.1	C22A-C23A-H23C	110.8
H25A-C25-H25B	109.0	C24A-C23A-H23C	110.8
C27-C26-C25	102.4(8)	C22A-C23A-H23D	110.8
C27-C26-H26A	111.3	C24A-C23A-H23D	110.8
C25-C26-H26A	111.3	H23C-C23A-H23D	108.9
C27-C26-H26B	111.3	C25A-C24A-C23A	108.6(15)
C25-C26-H26B	111.3	C25A-C24A-C28A	99.7(14)
H26A-C26-H26B	109.2	C23A-C24A-C28A	100.5(13)
C26-C27-C22	108.7(15)	C25A-C24A-H24A	115.3
C26-C27-C28	102.6(10)	C23A-C24A-H24A	115.3
C22-C27-C28	101.3(14)	C28A-C24A-H24A	115.3
C26-C27-H27	114.3	C24A-C25A-C26A	103.4(12)

C24A-C25A-H25C	111.1	C27A-C28A-H28D	112.7
C26A-C25A-H25C	111.1	C24A-C28A-H28D	112.7
C24A-C25A-H25D	111.1	H28C-C28A-H28D	110.2
C26A-C25A-H25D	111.1	C1-O1-Pd1	126.1(3)
H25C-C25A-H25D	109.0	N1-O2-C8	110.9(3)
C27A-C26A-C25A	103.7(11)	C15-O3-Pd1	125.7(3)
C27A-C26A-H26C	111.0	C22A-O4-N2	116.4(16)
C25A-C26A-H26C	111.0	N2-O4-C22	108.6(10)
C27A-C26A-H26D	111.0	O3-Pd1-O1	178.55(13)
C25A-C26A-H26D	111.0	O3-Pd1-N2	90.95(15)
H26C-C26A-H26D	109.0	O1-Pd1-N2	89.40(15)
C26A-C27A-C28A	101.4(11)	O3-Pd1-N1	89.27(15)
C26A-C27A-C22A	109.7(17)	O1-Pd1-N1	90.41(16)
C28A-C27A-C22A	99.7(16)	N2-Pd1-N1	178.48(16)
C26A-C27A-H27A	114.8	C7-N1-O2	113.1(3)
C28A-C27A-H27A	114.8	C7-N1-Pd1	125.7(4)
C22A-C27A-H27A	114.8	O2-N1-Pd1	119.8(3)
C27A-C28A-C24A	95.3(11)	C21-N2-O4	112.7(3)
C27A-C28A-H28C	112.7	C21-N2-Pd1	125.7(3)
C24A-C28A-H28C	112.7	O4-N2-Pd1	120.3(3)

Table 4.2.4. Anisotropic displacement parameters for **4.7**.

The anisotropic displacement ($\text{\AA}^2 \times 10^3$) factor exponent takes the form: $-2\pi^2 [h^2 a^{*2} U^{11} + \dots + 2 h k a^* b^* U^{12}]$

Atom	U11	U22	U33	U23	U13	U12
C1	30(3)	17(2)	24(2)	3(2)	-6(2)	-7(2)
C2	37(3)	32(3)	24(2)	2(2)	-3(2)	-9(2)
C3	52(3)	46(3)	20(2)	7(3)	-5(3)	-19(3)
C4	42(3)	49(3)	29(3)	16(2)	-16(2)	-17(3)
C5	33(3)	30(3)	31(3)	9(2)	-12(2)	-9(2)
C6	31(3)	13(2)	25(3)	3(2)	-4(2)	-7(2)
C7	26(3)	14(2)	32(3)	1(2)	-5(2)	-5(2)
C8	15(2)	18(2)	26(3)	-5(2)	-1(2)	0(2)
C9	35(5)	27(4)	29(4)	-3(3)	2(4)	4(4)
C10	39(4)	28(3)	34(3)	-7(3)	9(3)	2(3)
C11	52(4)	24(4)	45(5)	-14(4)	4(4)	-1(4)
C12	45(4)	24(4)	51(4)	-7(3)	1(4)	-4(3)
C13	34(5)	14(3)	34(4)	-2(3)	-1(4)	2(4)
C14	32(4)	23(3)	45(4)	0(3)	-1(3)	7(3)
C9A	35(7)	20(5)	37(6)	-3(5)	0(6)	4(6)
C10A	42(5)	23(4)	42(4)	-3(4)	2(4)	6(4)
C11A	49(6)	25(5)	43(6)	-9(5)	3(5)	-3(5)
C12A	45(5)	24(5)	36(5)	-3(5)	-1(4)	-2(5)
C13A	34(6)	28(6)	28(6)	-9(5)	2(5)	-5(5)
C14A	30(5)	37(5)	36(5)	-7(5)	11(4)	5(5)

C15	23(2)	12(2)	18(2)	0(2)	-1(2)	0(2)
C16	27(3)	18(2)	24(2)	-2(2)	3(2)	-2(2)
C17	32(3)	23(3)	18(2)	1(2)	-1(2)	-7(2)
C18	26(2)	20(2)	25(2)	1(2)	-5(2)	-3(2)
C19	20(3)	18(2)	27(2)	-1(2)	-2(2)	-5(2)
C20	20(2)	14(2)	21(2)	-1(2)	1(2)	-4(2)
C21	16(2)	14(2)	24(2)	0(2)	-4(2)	1(2)
C22	11(6)	16(6)	15(6)	-9(4)	-1(4)	-4(4)
C23	23(5)	25(4)	21(5)	0(4)	0(4)	3(4)
C24	33(5)	16(4)	40(5)	1(3)	1(4)	1(4)
C25	41(7)	18(5)	33(5)	-15(4)	6(5)	-8(5)
C26	47(5)	31(5)	24(4)	-12(4)	0(4)	-9(4)
C27	40(6)	18(6)	30(6)	0(5)	0(5)	-11(6)
C28	20(5)	28(5)	43(7)	-8(5)	9(5)	4(4)
C22A	25(13)	21(11)	29(12)	3(8)	-3(9)	7(9)
C23A	28(8)	19(9)	14(7)	-8(6)	4(6)	-5(7)
C24A	33(7)	32(7)	31(7)	-5(6)	6(6)	-1(5)
C25A	40(10)	39(9)	51(9)	-26(7)	-3(8)	-7(8)
C26A	34(8)	24(7)	56(8)	-15(6)	2(7)	-4(6)
C27A	30(8)	17(6)	27(7)	-2(5)	13(6)	8(6)
C28A	27(7)	28(8)	33(8)	-4(6)	2(6)	8(6)
O1	31(2)	25(2)	18(2)	4(1)	3(1)	3(1)
O2	19(2)	17(2)	23(2)	-6(1)	2(1)	-1(1)
O3	21(2)	24(2)	16(1)	1(1)	0(1)	5(1)
O4	26(2)	23(2)	17(2)	-6(1)	6(2)	-1(2)

Pd1	18(1)	13(1)	16(1)	1(1)	0(1)	1(1)
N1	23(2)	14(2)	22(2)	-1(2)	1(2)	0(1)
N2	21(2)	16(2)	19(2)	-4(2)	3(2)	0(1)

Table 4.2.5. H coordinates and isotropic displacement parameters for **4.7**.

H coordinates ($\times 10^4$) and isotropic displacement parameters ($\text{\AA}^2 \times 10^3$)

Atom	x	y	z	U(eq)
H2	1193	672	8294	37
H3	3734	285	8980	47
H4	7332	-150	8734	48
H5	8363	-214	7788	38
H7	7669	-93	6830	29
H9A	7373	111	4960	36
H9B	5077	-226	4689	36
H10	8702	-1036	4570	41
H11A	6361	-2121	4667	48
H11B	4502	-1489	4521	48
H12A	3043	-1597	5401	48
H12B	4880	-2236	5544	48
H13	6033	-1262	6175	33
H14A	9014	-1720	5502	40
H14B	9413	-839	5614	40
H9A1	6252	-1147	6192	37

H9A2	4020	-1411	5848	37
H10A	7830	-2013	5535	43
H11C	4152	-1928	4932	47
H11D	6474	-2005	4571	47
H12C	5906	-855	4225	42
H12D	3686	-757	4620	42
H13A	7153	90	4867	36
H14C	9476	-722	5515	41
H14D	9555	-1062	4876	41
H16	3085	1082	4525	28
H17	548	1485	3841	29
H18	-3013	1978	4099	29
H19	-4000	2038	5052	26
H21	-3256	1912	6006	22
H22	912	1956	7358	17
H23A	934	3142	7023	27
H23B	-1299	2962	6649	27
H24	-2726	3853	7314	36
H25A	-1509	3786	8280	37
H25B	813	3615	7939	37
H26A	812	2433	8284	41
H26B	-1509	2605	8627	41
H27	-2766	1729	7940	35
H28A	-4800	2628	7281	37
H28B	-4910	2954	7925	37

H22A	636	2047	7310	30
H23C	-993	1935	8158	24
H23D	-3232	1595	7861	24
H24A	-4717	2730	8237	39
H25C	-594	3209	8386	52
H25D	-2412	3835	8198	52
H26C	-534	3973	7364	45
H26D	1213	3321	7540	45
H27A	-1505	3036	6701	29
H28C	-5103	2595	7171	35
H28D	-4733	3469	7319	35
H8	3670(80)	-280(30)	5570(20)	22

Table 4.2.6. Torsion angles [°] for **4.7**.

O1-C1-C2-C3	179.2(4)	C4-C5-C6-C1	0.0(7)
C6-C1-C2-C3	-0.9(7)	C4-C5-C6-C7	-178.8(5)
C1-C2-C3-C4	0.9(8)	C1-C6-C7-N1	2.1(8)
C2-C3-C4-C5	-0.5(8)	C5-C6-C7-N1	-179.1(5)
C3-C4-C5-C6	0.0(8)	O2-C8-C9-C10	117.5(7)
O1-C1-C6-C5	-179.7(4)	C13-C8-C9-C10	1.0(8)
C2-C1-C6-C5	0.4(6)	C8-C9-C10-C11	70.1(12)
O1-C1-C6-C7	-1.0(7)	C8-C9-C10-C14	-34.7(9)
C2-C1-C6-C7	179.1(4)	C9-C10-C11-C12	-69.8(12)

C14-C10-C11-C12	34.5(10)	C8-C13A-C14A-C10A	54.8(13)
C10-C11-C12-C13	-0.7(12)	C12A-C13A-C14A-C10A	-52.8(17)
C11-C12-C13-C14	-33.9(11)	C9A-C10A-C14A-C13A	-55.2(17)
C11-C12-C13-C8	70.9(10)	C11A-C10A-C14A-C13A	55.7(15)
O2-C8-C13-C14	-80.6(9)	O3-C15-C16-C17	-180.0(4)
C9-C8-C13-C14	33.6(8)	C20-C15-C16-C17	-0.8(6)
O2-C8-C13-C12	174.8(6)	C15-C16-C17-C18	0.7(7)
C9-C8-C13-C12	-71.0(9)	C16-C17-C18-C19	-0.5(7)
C12-C13-C14-C10	54.6(9)	C17-C18-C19-C20	0.5(7)
C8-C13-C14-C10	-54.7(9)	C18-C19-C20-C15	-0.6(6)
C11-C10-C14-C13	-55.4(9)	C18-C19-C20-C21	178.0(4)
C9-C10-C14-C13	55.1(9)	O3-C15-C20-C19	179.8(4)
O2-C8-C9A-C10A	-114.6(15)	C16-C15-C20-C19	0.8(6)
C13A-C8-C9A-C10A	-0.6(18)	O3-C15-C20-C21	1.3(7)
C8-C9A-C10A-C11A	-71(2)	C16-C15-C20-C21	-177.7(4)
C8-C9A-C10A-C14A	34.5(19)	C19-C20-C21-N2	179.0(4)
C9A-C10A-C11A-C12A	68(3)	C15-C20-C21-N2	-2.5(7)
C14A-C10A-C11A-C12A	-37(2)	O4-C22-C23-C24	111.2(13)
C10A-C11A-C12A-C13A	4(3)	C27-C22-C23-C24	-0.7(16)
O2-C8-C13A-C14A	84.8(11)	C22-C23-C24-C25	71.2(12)
C9A-C8-C13A-C14A	-34.0(14)	C22-C23-C24-C28	-35.7(12)
O2-C8-C13A-C12A	-170.5(9)	C28-C24-C25-C26	35.8(10)
C9A-C8-C13A-C12A	70.7(17)	C23-C24-C25-C26	-70.6(10)
C11A-C12A-C13A-C14A	31(2)	C24-C25-C26-C27	-0.1(12)
C11A-C12A-C13A-C8	-73.1(19)	C25-C26-C27-C22	71.8(14)

C25-C26-C27-C28	-34.9(13)	C25A-C24A-C28A-C27A	56.4(13)
O4-C22-C27-C26	169.9(11)	C23A-C24A-C28A-C27A	-54.7(15)
C23-C22-C27-C26	-71.5(16)	C2-C1-O1-Pd1	166.7(3)
O4-C22-C27-C28	-82.5(15)	C6-C1-O1-Pd1	-13.2(6)
C23-C22-C27-C28	36.1(16)	C9-C8-O2-N1	164.2(5)
C25-C24-C28-C27	-55.1(10)	C13A-C8-O2-N1	176.0(8)
C23-C24-C28-C27	56.1(10)	C9A-C8-O2-N1	-71.0(9)
C26-C27-C28-C24	55.5(11)	C13-C8-O2-N1	-84.2(6)
C22-C27-C28-C24	-56.9(13)	C20-C15-O3-Pd1	11.5(6)
O4-C22A-C23A-C24A	-116(2)	C16-C15-O3-Pd1	-169.4(3)
C27A-C22A-C23A-C24A	4(3)	C23A-C22A-O4-N2	-164.0(13)
C22A-C23A-C24A-C25A	-72(2)	C27A-C22A-O4-N2	82(2)
C22A-C23A-C24A-C28A	32(2)	C27-C22-O4-N2	-178.6(10)
C23A-C24A-C25A-C26A	67.8(19)	C23-C22-O4-N2	70.3(12)
C28A-C24A-C25A-C26A	-36.8(16)	C6-C7-N1-O2	177.3(4)
C24A-C25A-C26A-C27A	2.5(18)	C6-C7-N1-Pd1	11.0(7)
C25A-C26A-C27A-C28A	33.3(16)	C8-O2-N1-C7	115.8(4)
C25A-C26A-C27A-C22A	-72(2)	C8-O2-N1-Pd1	-77.0(4)
O4-C22A-C27A-C26A	-173.8(19)	C20-C21-N2-O4	-176.3(4)
C23A-C22A-C27A-C26A	68(2)	C20-C21-N2-Pd1	-9.3(6)
O4-C22A-C27A-C28A	80(2)	C22A-O4-N2-C21	-116.4(17)
C23A-C22A-C27A-C28A	-38(2)	C22-O4-N2-C21	-119.2(10)
C26A-C27A-C28A-C24A	-55.5(13)	C22A-O4-N2-Pd1	75.8(17)
C22A-C27A-C28A-C24A	57.0(17)	C22-O4-N2-Pd1	73.0(10)

X-ray structure data of Pd complex **4.8**:

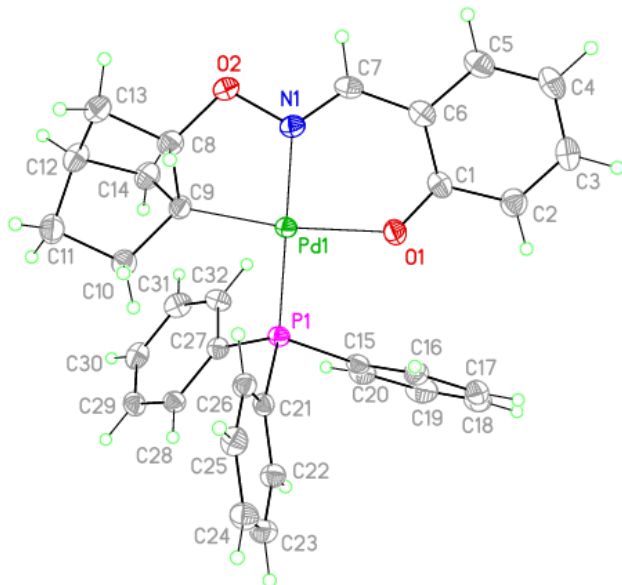
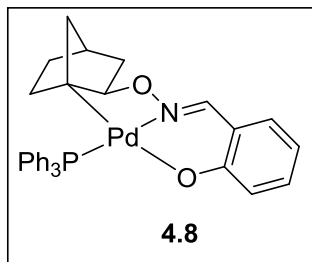


Table 4.3.1. Crystal data and structure refinement for Pd complex **4.8**.

Empirical formula	C ₃₂ H ₃₀ N O ₂ P Pd	
Formula weight	597.94	
Temperature	100(2) K	
Wavelength	1.54184 Å	
Crystal system	triclinic	
Space group	P -1	
Unit cell dimensions	a = 9.1130(9) Å	= 109.376(3)°.
	b = 11.3390(11) Å	= 105.198(4)°.
	c = 13.8100(12) Å	= 93.408(3)°.
Volume	1282.2(2) Å ³	

Z	2
Density (calculated)	1.549 Mg/m ³
Absorption coefficient	6.669 mm ⁻¹
F(000)	612
Crystal size	0.190 x 0.100 x 0.067 mm ³
Theta range for data collection	3.556 to 76.893°.
Index ranges	-10 ≤ h ≤ 11, -13 ≤ k ≤ 14, -17 ≤ l ≤ 16
Reflections collected	15182
Independent reflections	5283 [R(int) = 0.0188]
Completeness to theta = 67.684°	100.0 %
Absorption correction Gaussian	
Max. and min. transmission	0.689 and 0.459
Refinement method	Full-matrix least-squares on F ²
Data / restraints / parameters	5283 / 0 / 334
Goodness-of-fit on F ²	1.080
Final R indices [I > 2σ(I)]	R1 = 0.0207, wR2 = 0.0543
R indices (all data)	R1 = 0.0210, wR2 = 0.0544
Extinction coefficient	n/a
Largest diff. peak and hole	0.410 and -0.498 e.Å ⁻³

Table 4.3.2. Atomic coordinates and equivalent isotropic displacement parameters for **4.8**.

U(eq) is defined as one-third of the trace of the orthogonalized U^{ij} tensor.

Atomic coordinates ($\times 10^4$) and equivalent isotropic displacement parameters ($\text{\AA}^2 \times 10^3$)

Atom	x	y	z	U(eq)
C1	1077(2)	2475(2)	880(2)	23(1)
C2	-473(2)	1847(2)	500(2)	27(1)
C3	-1575(2)	2086(2)	-272(2)	28(1)
C4	-1208(2)	2936(2)	-734(2)	31(1)
C5	282(2)	3536(2)	-409(2)	29(1)
C6	1455(2)	3336(2)	396(1)	22(1)
C7	2973(2)	4013(2)	657(1)	22(1)
C8	6810(2)	3970(2)	1752(2)	24(1)
C9	6656(2)	3549(2)	2683(1)	20(1)
C10	7949(2)	2778(2)	2873(2)	25(1)
C11	9450(2)	3787(2)	3414(2)	29(1)
C12	8837(2)	5011(2)	3417(2)	28(1)
C13	8290(2)	4953(2)	2246(2)	28(1)
C14	7288(2)	4811(2)	3644(2)	26(1)
C15	2792(2)	1125(2)	3454(2)	20(1)
C16	1629(2)	336(2)	2542(2)	25(1)
C17	204(2)	-41(2)	2618(2)	30(1)
C18	-90(2)	380(2)	3597(2)	35(1)
C19	1048(3)	1171(2)	4507(2)	36(1)
C20	2498(2)	1543(2)	4442(2)	26(1)

C21	5168(2)	81(2)	2627(1)	18(1)
C22	5045(2)	-913(2)	3000(2)	22(1)
C23	5410(2)	-2076(2)	2472(2)	25(1)
C24	5880(2)	-2258(2)	1562(2)	26(1)
C25	6000(2)	-1282(2)	1181(2)	24(1)
C26	5640(2)	-114(2)	1711(1)	20(1)
C27	5909(2)	2309(2)	4624(1)	19(1)
C28	6990(2)	1711(2)	5126(1)	21(1)
C29	7906(2)	2348(2)	6181(2)	25(1)
C30	7753(2)	3577(2)	6738(2)	26(1)
C31	6688(2)	4175(2)	6247(2)	27(1)
C32	5772(2)	3543(2)	5195(2)	23(1)
N1	4184(2)	3866(1)	1306(1)	20(1)
O1	2022(2)	2228(1)	1644(1)	28(1)
O2	5552(2)	4621(1)	1424(1)	25(1)
Pd1	4381(1)	2810(1)	2240(1)	16(1)
P1	4615(1)	1597(1)	3260(1)	16(1)

Table 4.3.3. Bond lengths [Å] and angles [°] for **4.8**.

C1-O1	1.297(2)	C3-C4	1.389(3)
C1-C2	1.422(3)	C3-H3	0.95
C1-C6	1.426(3)	C4-C5	1.369(3)
C2-C3	1.372(3)	C4-H4	0.95
C2-H2	0.95	C5-C6	1.414(3)

C5-H5	0.95	C16-C17	1.384(3)
C6-C7	1.435(3)	C16-H16	0.95
C7-N1	1.285(2)	C17-C18	1.379(3)
C7-H7	0.95	C17-H17	0.95
C8-O2	1.453(2)	C18-C19	1.385(4)
C8-C13	1.537(3)	C18-H18	0.95
C8-C9	1.548(2)	C19-C20	1.398(3)
C8-H8	1.00	C19-H19	0.95
C9-C10	1.528(2)	C20-H20	0.95
C9-C14	1.543(2)	C21-C26	1.395(2)
C9-Pd1	2.0404(17)	C21-C22	1.396(2)
C10-C11	1.565(3)	C21-P1	1.8195(17)
C10-H10A	0.99	C22-C23	1.387(3)
C10-H10B	0.99	C22-H22	0.95
C11-C12	1.525(3)	C23-C24	1.387(3)
C11-H11A	0.99	C23-H23	0.95
C11-H11B	0.99	C24-C25	1.384(3)
C12-C13	1.540(3)	C24-H24	0.95
C12-C14	1.544(3)	C25-C26	1.390(2)
C12-H12	1.00	C25-H25	0.95
C13-H13A	0.99	C26-H26	0.95
C13-H13B	0.99	C27-C32	1.392(2)
C14-H14A	0.99	C27-C28	1.395(2)
C14-H14B	0.99	C27-P1	1.8168(18)
C15-C20	1.390(3)	C28-C29	1.391(3)
C15-C16	1.397(3)	C28-H28	0.95
C15-P1	1.8282(18)	C29-C30	1.386(3)

C29-H29	0.95	C32-H32	0.95
C30-C31	1.378(3)	N1-O2	1.4099(19)
C30-H30	0.95	N1-Pd1	2.0149(15)
C31-C32	1.387(3)	O1-Pd1	2.0682(13)
C31-H31	0.95	Pd1-P1	2.2549(5)
O1-C1-C2	117.37(17)	O2-C8-C13	106.90(15)
O1-C1-C6	125.53(17)	O2-C8-C9	111.26(14)
C2-C1-C6	117.09(17)	C13-C8-C9	104.40(15)
C3-C2-C1	121.77(19)	O2-C8-H8	111.3
C3-C2-H2	119.1	C13-C8-H8	111.3
C1-C2-H2	119.1	C9-C8-H8	111.3
C2-C3-C4	121.02(19)	C10-C9-C14	101.84(15)
C2-C3-H3	119.5	C10-C9-C8	105.77(14)
C4-C3-H3	119.5	C14-C9-C8	100.28(14)
C5-C4-C3	118.91(18)	C10-C9-Pd1	122.86(13)
C5-C4-H4	120.5	C14-C9-Pd1	119.02(12)
C3-C4-H4	120.5	C8-C9-Pd1	104.21(11)
C4-C5-C6	122.24(19)	C9-C10-C11	104.27(15)
C4-C5-H5	118.9	C9-C10-H10A	110.9
C6-C5-H5	118.9	C11-C10-H10A	110.9
C5-C6-C1	118.94(18)	C9-C10-H10B	110.9
C5-C6-C7	116.82(17)	C11-C10-H10B	110.9
C1-C6-C7	124.24(16)	H10A-C10-H10B	108.9
N1-C7-C6	124.64(17)	C12-C11-C10	102.44(15)
N1-C7-H7	117.7	C12-C11-H11A	111.3
C6-C7-H7	117.7	C10-C11-H11A	111.3

C12-C11-H11B	111.3	C18-C17-C16	120.1(2)
C10-C11-H11B	111.3	C18-C17-H17	119.9
H11A-C11-H11B	109.2	C16-C17-H17	119.9
C11-C12-C13	108.04(17)	C17-C18-C19	120.00(19)
C11-C12-C14	101.98(16)	C17-C18-H18	120.0
C13-C12-C14	101.46(16)	C19-C18-H18	120.0
C11-C12-H12	114.6	C18-C19-C20	120.3(2)
C13-C12-H12	114.6	C18-C19-H19	119.8
C14-C12-H12	114.6	C20-C19-H19	119.8
C8-C13-C12	103.13(15)	C15-C20-C19	119.7(2)
C8-C13-H13A	111.1	C15-C20-H20	120.1
C12-C13-H13A	111.1	C19-C20-H20	120.1
C8-C13-H13B	111.1	C26-C21-C22	119.32(16)
C12-C13-H13B	111.1	C26-C21-P1	119.13(13)
H13A-C13-H13B	109.1	C22-C21-P1	121.45(13)
C9-C14-C12	94.81(14)	C23-C22-C21	120.17(17)
C9-C14-H14A	112.8	C23-C22-H22	119.9
C12-C14-H14A	112.8	C21-C22-H22	119.9
C9-C14-H14B	112.8	C24-C23-C22	119.94(18)
C12-C14-H14B	112.8	C24-C23-H23	120.0
H14A-C14-H14B	110.2	C22-C23-H23	120.0
C20-C15-C16	119.27(17)	C25-C24-C23	120.47(17)
C20-C15-P1	123.63(15)	C25-C24-H24	119.8
C16-C15-P1	117.05(14)	C23-C24-H24	119.8
C17-C16-C15	120.57(19)	C24-C25-C26	119.72(17)
C17-C16-H16	119.7	C24-C25-H25	120.1
C15-C16-H16	119.7	C26-C25-H25	120.1

C25-C26-C21	120.37(17)	C31-C32-H32	119.5
C25-C26-H26	119.8	C27-C32-H32	119.5
C21-C26-H26	119.8	C7-N1-O2	114.50(14)
C32-C27-C28	118.87(16)	C7-N1-Pd1	129.45(13)
C32-C27-P1	116.00(13)	O2-N1-Pd1	115.92(10)
C28-C27-P1	125.13(14)	C1-O1-Pd1	126.70(12)
C29-C28-C27	119.96(17)	N1-O2-C8	106.50(13)
C29-C28-H28	120.0	N1-Pd1-C9	82.31(7)
C27-C28-H28	120.0	N1-Pd1-O1	88.86(6)
C30-C29-C28	120.33(17)	C9-Pd1-O1	171.17(6)
C30-C29-H29	119.8	N1-Pd1-P1	178.82(4)
C28-C29-H29	119.8	C9-Pd1-P1	97.51(5)
C31-C30-C29	120.08(18)	O1-Pd1-P1	91.31(4)
C31-C30-H30	120.0	C27-P1-C21	107.88(8)
C29-C30-H30	120.0	C27-P1-C15	103.40(8)
C30-C31-C32	119.77(18)	C21-P1-C15	102.57(8)
C30-C31-H31	120.1	C27-P1-Pd1	116.39(6)
C32-C31-H31	120.1	C21-P1-Pd1	112.49(6)
C31-C32-C27	120.99(17)	C15-P1-Pd1	112.86(6)

Table 4.3.4. Anisotropic displacement parameters for **4.8**.

The anisotropic displacement ($\text{\AA}^2 \times 10^3$) factor exponent takes the form: $-2\pi^2 [h^2 a^{*2} U^{11} + \dots + 2 h k a^* b^* U^{12}]$

Atom	U ¹¹	U ²²	U ³³	U ²³	U ¹³	U ¹²
------	-----------------	-----------------	-----------------	-----------------	-----------------	-----------------

C1	21(1)	27(1)	22(1)	9(1)	6(1)	7(1)
C2	25(1)	30(1)	27(1)	11(1)	8(1)	4(1)
C3	21(1)	34(1)	23(1)	5(1)	5(1)	4(1)
C4	26(1)	40(1)	23(1)	12(1)	2(1)	8(1)
C5	32(1)	34(1)	24(1)	15(1)	8(1)	10(1)
C6	25(1)	24(1)	19(1)	7(1)	8(1)	8(1)
C7	29(1)	21(1)	19(1)	10(1)	10(1)	8(1)
C8	24(1)	25(1)	26(1)	12(1)	10(1)	5(1)
C9	18(1)	21(1)	21(1)	8(1)	6(1)	1(1)
C10	22(1)	29(1)	27(1)	13(1)	9(1)	4(1)
C11	21(1)	38(1)	30(1)	16(1)	7(1)	2(1)
C12	26(1)	29(1)	28(1)	8(1)	8(1)	-3(1)
C13	26(1)	30(1)	32(1)	14(1)	10(1)	1(1)
C14	26(1)	26(1)	24(1)	6(1)	8(1)	0(1)
C15	20(1)	21(1)	27(1)	14(1)	12(1)	9(1)
C16	23(1)	24(1)	31(1)	13(1)	10(1)	6(1)
C17	21(1)	30(1)	46(1)	21(1)	9(1)	6(1)
C18	25(1)	38(1)	61(1)	32(1)	25(1)	14(1)
C19	40(1)	40(1)	48(1)	26(1)	32(1)	19(1)
C20	30(1)	28(1)	31(1)	15(1)	16(1)	10(1)
C21	16(1)	17(1)	20(1)	5(1)	6(1)	3(1)
C22	23(1)	21(1)	23(1)	9(1)	9(1)	5(1)
C23	26(1)	20(1)	31(1)	10(1)	10(1)	6(1)
C24	26(1)	19(1)	29(1)	4(1)	10(1)	8(1)
C25	23(1)	23(1)	24(1)	4(1)	11(1)	4(1)
C26	19(1)	19(1)	21(1)	7(1)	7(1)	3(1)
C27	20(1)	20(1)	19(1)	7(1)	9(1)	4(1)

C28	21(1)	22(1)	24(1)	11(1)	9(1)	6(1)
C29	21(1)	34(1)	25(1)	16(1)	6(1)	5(1)
C30	26(1)	33(1)	18(1)	9(1)	6(1)	-4(1)
C31	35(1)	23(1)	22(1)	5(1)	13(1)	4(1)
C32	28(1)	22(1)	21(1)	10(1)	9(1)	9(1)
N1	22(1)	19(1)	20(1)	9(1)	8(1)	3(1)
O1	19(1)	37(1)	33(1)	22(1)	4(1)	2(1)
O2	23(1)	24(1)	30(1)	16(1)	7(1)	2(1)
Pd1	17(1)	16(1)	16(1)	7(1)	6(1)	4(1)
P1	18(1)	16(1)	17(1)	7(1)	8(1)	5(1)

Table 4.3.5. H coordinates and isotropic displacement parameters for **4.8**.

Hydrogen coordinates (x 10⁴) and isotropic displacement parameters (Å²x 10³)

Atom	x	y	z	U(eq)
H2	-753	1247	790	32
H3	-2604	1662	-495	33
H4	-1978	3100	-1266	37
H5	537	4105	-735	34
H7	3090	4611	326	26
H8	6887	3237	1128	28
H10A	7983	2150	2185	30
H10B	7808	2327	3354	30
H11A	9962	3829	4154	35
H11B	10185	3601	2987	35
H12	9551	5802	3934	34

H13A	8074	5787	2216	34
H13B	9068	4675	1872	34
H14A	7415	4714	4346	31
H14B	6664	5484	3585	31
H16	1817	56	1863	30
H17	-574	-591	1995	37
H18	-1072	127	3646	42
H19	841	1462	5180	43
H20	3279	2079	5069	32
H22	4711	-792	3618	26
H23	5339	-2748	2732	30
H24	6121	-3058	1198	31
H25	6327	-1411	560	28
H26	5717	555	1448	23
H28	7100	869	4748	25
H29	8642	1938	6522	30
H30	8382	4007	7458	32
H31	6583	5017	6628	32
H32	5039	3959	4860	28

Table 4.3.6. Torsion angles [°] for **4.8**.

O1-C1-C2-C3	177.13(18)	C2-C3-C4-C5	0.3(3)
C6-C1-C2-C3	-2.1(3)	C3-C4-C5-C6	-1.2(3)
C1-C2-C3-C4	1.4(3)	C4-C5-C6-C1	0.5(3)

C4-C5-C6-C7	179.44(18)	C13-C12-C14-C9	55.71(17)
O1-C1-C6-C5	-178.00(18)	C20-C15-C16-C17	-0.8(3)
C2-C1-C6-C5	1.1(3)	P1-C15-C16-C17	-178.59(14)
O1-C1-C6-C7	3.1(3)	C15-C16-C17-C18	1.2(3)
C2-C1-C6-C7	-177.75(17)	C16-C17-C18-C19	-0.7(3)
C5-C6-C7-N1	-174.45(17)	C17-C18-C19-C20	-0.2(3)
C1-C6-C7-N1	4.4(3)	C16-C15-C20-C19	-0.1(3)
O2-C8-C9-C10	174.83(14)	P1-C15-C20-C19	177.54(15)
C13-C8-C9-C10	-70.21(18)	C18-C19-C20-C15	0.6(3)
O2-C8-C9-C14	-79.63(17)	C26-C21-C22-C23	0.8(3)
C13-C8-C9-C14	35.33(18)	P1-C21-C22-C23	177.13(14)
O2-C8-C9-Pd1	44.05(16)	C21-C22-C23-C24	-0.8(3)
C13-C8-C9-Pd1	159.01(12)	C22-C23-C24-C25	0.5(3)
C14-C9-C10-C11	-32.33(18)	C23-C24-C25-C26	-0.3(3)
C8-C9-C10-C11	72.07(18)	C24-C25-C26-C21	0.3(3)
Pd1-C9-C10-C11	-168.84(12)	C22-C21-C26-C25	-0.6(3)
C9-C10-C11-C12	-2.63(19)	P1-C21-C26-C25	-176.99(14)
C10-C11-C12-C13	-69.68(19)	C32-C27-C28-C29	0.1(3)
C10-C11-C12-C14	36.74(19)	P1-C27-C28-C29	-179.14(14)
O2-C8-C13-C12	117.55(16)	C27-C28-C29-C30	0.0(3)
C9-C8-C13-C12	-0.44(19)	C28-C29-C30-C31	0.0(3)
C11-C12-C13-C8	72.05(19)	C29-C30-C31-C32	0.0(3)
C14-C12-C13-C8	-34.73(19)	C30-C31-C32-C27	0.0(3)
C10-C9-C14-C12	53.46(17)	C28-C27-C32-C31	0.0(3)
C8-C9-C14-C12	-55.22(16)	P1-C27-C32-C31	179.24(15)
Pd1-C9-C14-C12	-167.92(13)	C6-C7-N1-O2	179.04(15)
C11-C12-C14-C9	-55.76(17)	C6-C7-N1-Pd1	-5.4(3)

C2-C1-O1-Pd1	172.17(13)	C26-C21-P1-C27	-119.04(14)
C6-C1-O1-Pd1	-8.7(3)	C22-C21-P1-C27	64.64(16)
C7-N1-O2-C8	-154.96(15)	C26-C21-P1-C15	132.22(14)
Pd1-N1-O2-C8	28.83(16)	C22-C21-P1-C15	-44.11(16)
C13-C8-O2-N1	-161.23(14)	C26-C21-P1-Pd1	10.68(15)
C9-C8-O2-N1	-47.83(18)	C22-C21-P1-Pd1	-165.64(13)
C32-C27-P1-C21	173.02(14)	C20-C15-P1-C27	13.81(17)
C28-C27-P1-C21	-7.77(18)	C16-C15-P1-C27	-168.55(14)
C32-C27-P1-C15	-78.81(15)	C20-C15-P1-C21	125.92(16)
C28-C27-P1-C15	100.40(16)	C16-C15-P1-C21	-56.44(15)
C32-C27-P1-Pd1	45.52(15)	C20-C15-P1-Pd1	-112.79(15)
C28-C27-P1-Pd1	-135.27(14)	C16-C15-P1-Pd1	64.85(14)

X-ray structure data of Pd complex **4.10**:

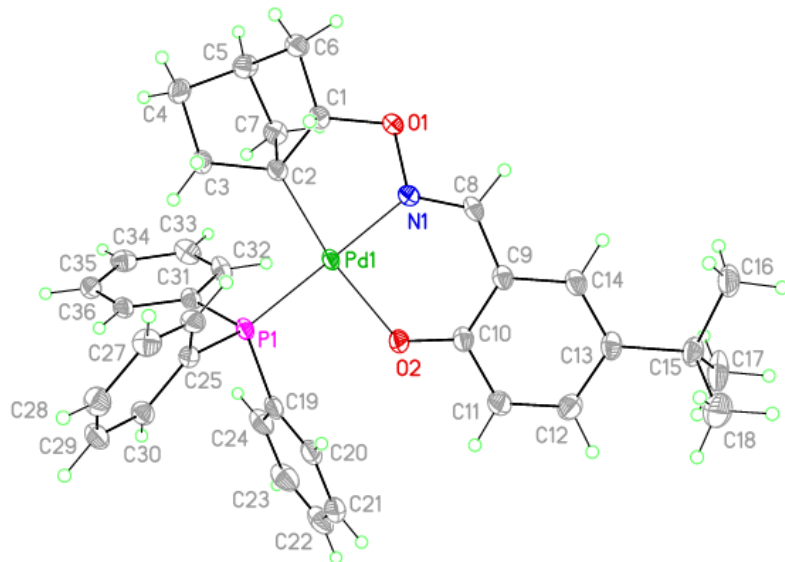
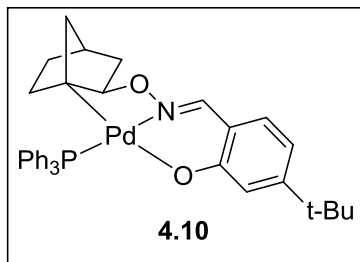


Table 4.4.1. Crystal data and structure refinement for Pd complex **4.10**.

Empirical formula	C ₄₂ H ₅₂ N O ₂ P Pd	
Formula weight	740.21	
Temperature	100(2) K	
Wavelength	1.54184 Å	
Crystal system	triclinic	
Space group	P -1	
Unit cell dimensions	a = 9.224(2) Å	= 105.095(3)°.
	b = 11.291(2) Å	= 99.285(3)°.
	c = 18.410(3) Å	= 92.776(3)°.
Volume	1818.7(6) Å ³	
Z	2	

Density (calculated)	1.352 Mg/m ³
Absorption coefficient	4.802 mm ⁻¹
F(000)	776
Crystal size	0.170 x 0.120 x 0.050 mm ³
Theta range for data collection	2.527 to 74.418°.
Index ranges	-11 ≤ h ≤ 11, -14 ≤ k ≤ 14, -22 ≤ l ≤ 22
Reflections collected	33905
Independent reflections	7207 [R(int) = 0.0262]
Completeness to theta = 67.684°	99.4 %
Absorption correction	Semi-empirical from equivalents
Max. and min. transmission	1.00 and 0.813
Refinement method	Full-matrix least-squares on F ²
Data / restraints / parameters	7207 / 35 / 427
Goodness-of-fit on F ²	1.039
Final R indices [I > 2σ(I)]	R1 = 0.0236, wR2 = 0.0593
R indices (all data)	R1 = 0.0238, wR2 = 0.0595
Extinction coefficient	n/a
Largest diff. peak and hole	0.506 and -0.653 e.Å ⁻³

Table 4.4.2. Atomic coordinates and equivalent isotropic displacement parameters for **4.10**.

U(eq) is defined as one third of the trace of the orthogonalized U_{ij} tensor.

	x	y	z	U(eq)
C1	1015(2)	3573(2)	2741(1)	19(1)
C2	1780(2)	4698(2)	3396(1)	18(1)
C3	608(2)	5627(2)	3497(1)	20(1)

C4	-535(2)	5045(2)	3875(1)	24(1)
C5	70(2)	3815(2)	3910(1)	24(1)
C6	-143(2)	2974(2)	3088(1)	23(1)
C7	1753(2)	4178(2)	4092(1)	23(1)
C8	4083(2)	2642(2)	1993(1)	19(1)
C9	5424(2)	3082(2)	1808(1)	19(1)
C10	6099(2)	4317(2)	2117(1)	20(1)
C11	7348(2)	4618(2)	1817(1)	24(1)
C12	7914(2)	3774(2)	1280(1)	25(1)
C13	7291(2)	2538(2)	991(1)	22(1)
C14	6057(2)	2235(2)	1259(1)	22(1)
C15	8042(2)	1596(2)	445(1)	26(1)
C16	7045(2)	399(2)	67(1)	33(1)
C17	9448(3)	1314(2)	907(1)	42(1)
C18	8415(3)	2117(2)	-205(1)	43(1)
C19	6135(2)	7652(2)	3993(1)	22(1)
C20	6821(2)	7687(2)	3379(1)	27(1)
C21	8308(2)	8095(2)	3506(1)	34(1)
C22	9111(2)	8471(2)	4247(2)	38(1)
C23	8453(2)	8444(2)	4858(1)	36(1)
C24	6963(2)	8038(2)	4737(1)	28(1)
C25	3273(2)	8107(2)	3306(1)	18(1)
C26	2181(2)	7618(2)	2661(1)	21(1)
C27	1470(2)	8388(2)	2269(1)	24(1)
C28	1848(2)	9649(2)	2513(1)	26(1)
C29	2950(2)	10147(2)	3149(1)	25(1)
C30	3663(2)	9381(2)	3542(1)	21(1)

C31	3731(2)	7433(2)	4755(1)	19(1)
C32	4150(2)	6630(2)	5199(1)	25(1)
C33	3943(2)	6881(2)	5950(1)	28(1)
C34	3314(2)	7934(2)	6269(1)	25(1)
C35	2872(2)	8726(2)	5831(1)	24(1)
C36	3082(2)	8482(2)	5076(1)	19(1)
C37	2098(6)	4870(4)	841(2)	50(1)
C38	3244(4)	4446(3)	316(2)	46(1)
C39	2621(5)	3330(3)	-322(2)	45(1)
C40	3735(4)	2746(3)	-788(2)	40(1)
C41	3093(4)	1712(3)	-1492(2)	45(1)
C42	4396(6)	1026(5)	-1817(3)	53(2)
C37A	2575(13)	4886(8)	853(5)	44(3)
C38A	2756(10)	3602(8)	287(4)	47(2)
C39A	2228(11)	3503(8)	-534(5)	48(2)
C40A	2509(9)	2365(7)	-1114(5)	45(2)
C41A	4126(9)	2163(8)	-1160(5)	50(2)
C42A	4061(14)	947(9)	-1859(6)	40(3)
N1	3319(2)	3308(1)	2442(1)	18(1)
O1	2041(1)	2664(1)	2532(1)	21(1)
O2	5676(1)	5166(1)	2645(1)	24(1)
P1	4186(1)	7062(1)	3798(1)	16(1)
Pd1	3744(1)	5074(1)	3088(1)	15(1)

Table 4.4.3. Bond lengths [Å] and angles [°] for **4.10**.

C1-O1	1.451(2)	C10-C11	1.420(3)
C1-C6	1.544(2)	C11-C12	1.372(3)
C1-C2	1.550(2)	C11-H11	0.95
C1-H1	1.0000	C12-C13	1.413(3)
C2-C3	1.541(2)	C12-H12	0.95
C2-C7	1.546(2)	C13-C14	1.375(3)
C2-Pd1	2.0412(17)	C13-C15	1.536(2)
C3-C4	1.560(2)	C14-H14	0.95
C3-H3A	0.99	C15-C17	1.527(3)
C3-H3B	0.99	C15-C16	1.530(3)
C4-C5	1.534(3)	C15-C18	1.542(3)
C4-H4A	0.99	C16-H16A	0.98
C4-H4B	0.99	C16-H16B	0.98
C5-C6	1.539(2)	C16-H16C	0.98
C5-C7	1.546(3)	C17-H17A	0.98
C5-H5	1.00	C17-H17B	0.98
C6-H6A	0.99	C17-H17C	0.98
C6-H6B	0.99	C18-H18A	0.98
C7-H7A	0.99	C18-H18B	0.98
C7-H7B	0.99	C18-H18C	0.98
C8-N1	1.288(2)	C19-C20	1.391(3)
C8-C9	1.435(3)	C19-C24	1.403(3)
C8-H8	0.95	C19-P1	1.8323(19)
C9-C14	1.420(2)	C20-C21	1.388(3)
C9-C10	1.430(2)	C20-H20	0.95
C10-O2	1.300(2)	C21-C22	1.391(3)

C21-H21	0.95	C35-C36	1.392(3)
C22-C23	1.369(4)	C35-H35	0.95
C22-H22	0.95	C36-H36	0.95
C23-C24	1.390(3)	C37-C38	1.556(5)
C23-H23	0.95	C37-H37A	0.98
C24-H24	0.95	C37-H37B	0.98
C25-C26	1.396(2)	C37-H37C	0.98
C25-C30	1.400(2)	C38-C39	1.497(5)
C25-P1	1.8244(18)	C38-H38A	0.99
C26-C27	1.391(3)	C38-H38B	0.99
C26-H26	0.95	C39-C40	1.510(5)
C27-C28	1.385(3)	C39-H39A	0.99
C27-H27	0.95	C39-H39B	0.99
C28-C29	1.392(3)	C40-C41	1.514(4)
C28-H28	0.95	C40-H40A	0.99
C29-C30	1.390(3)	C40-H40B	0.99
C29-H29	0.95	C41-C42	1.576(5)
C30-H30	0.95	C41-H41A	0.99
C31-C36	1.389(2)	C41-H41B	0.99
C31-C32	1.399(2)	C42-H42A	0.98
C31-P1	1.8237(18)	C42-H42B	0.98
C32-C33	1.385(3)	C42-H42C	0.98
C32-H32	0.95	C37A-C38A	1.584(8)
C33-C34	1.381(3)	C37A-H37D	0.98
C33-H33	0.95	C37A-H37E	0.98
C34-C35	1.387(3)	C37A-H37F	0.98
C34-H34	0.95	C38A-C39A	1.484(8)

C38A-H38C	0.99	C41A-H41C	0.99
C38A-H38D	0.99	C41A-H41D	0.99
C39A-C40A	1.506(8)	C42A-H42D	0.98
C39A-H39C	0.99	C42A-H42E	0.98
C39A-H39D	0.99	C42A-H42F	0.98
C40A-C41A	1.532(8)	N1-O1	1.4102(18)
C40A-H40C	0.99	N1-Pd1	2.0206(14)
C40A-H40D	0.99	O2-Pd1	2.0844(13)
C41A-C42A	1.609(8)	P1-Pd1	2.2637(5)
O1-C1-C6	106.74(14)	H3A-C3-H3B	108.9
O1-C1-C2	111.21(14)	C5-C4-C3	102.69(14)
C6-C1-C2	104.94(13)	C5-C4-H4A	111.2
O1-C1-H1	111.2	C3-C4-H4A	111.2
C6-C1-H1	111.2	C5-C4-H4B	111.2
C2-C1-H1	111.2	C3-C4-H4B	111.2
C3-C2-C7	101.55(14)	H4A-C4-H4B	109.1
C3-C2-C1	105.11(14)	C4-C5-C6	108.03(15)
C7-C2-C1	100.16(13)	C4-C5-C7	101.72(14)
C3-C2-Pd1	122.89(12)	C6-C5-C7	101.92(14)
C7-C2-Pd1	119.90(12)	C4-C5-H5	114.6
C1-C2-Pd1	104.16(11)	C6-C5-H5	114.6
C2-C3-C4	104.33(14)	C7-C5-H5	114.6
C2-C3-H3A	110.9	C5-C6-C1	102.64(14)
C4-C3-H3A	110.9	C5-C6-H6A	111.2
C2-C3-H3B	110.9	C1-C6-H6A	111.2
C4-C3-H3B	110.9	C5-C6-H6B	111.2

C1-C6-H6B	111.2	C13-C14-H14	118.2
H6A-C6-H6B	109.2	C9-C14-H14	118.2
C5-C7-C2	95.03(13)	C17-C15-C16	109.26(18)
C5-C7-H7A	112.7	C17-C15-C13	108.05(15)
C2-C7-H7A	112.7	C16-C15-C13	111.99(16)
C5-C7-H7B	112.7	C17-C15-C18	110.30(19)
C2-C7-H7B	112.7	C16-C15-C18	106.82(17)
H7A-C7-H7B	110.2	C13-C15-C18	110.42(17)
N1-C8-C9	124.70(15)	C15-C16-H16A	109.5
N1-C8-H8	117.6	C15-C16-H16B	109.5
C9-C8-H8	117.6	H16A-C16-H16B	109.5
C14-C9-C10	119.52(16)	C15-C16-H16C	109.5
C14-C9-C8	116.65(15)	H16A-C16-H16C	109.5
C10-C9-C8	123.77(16)	H16B-C16-H16C	109.5
O2-C10-C11	118.20(16)	C15-C17-H17A	109.5
O2-C10-C9	125.85(16)	C15-C17-H17B	109.5
C11-C10-C9	115.95(16)	H17A-C17-H17B	109.5
C12-C11-C10	122.58(17)	C15-C17-H17C	109.5
C12-C11-H11	118.7	H17A-C17-H17C	109.5
C10-C11-H11	118.7	H17B-C17-H17C	109.5
C11-C12-C13	122.01(17)	C15-C18-H18A	109.5
C11-C12-H12	119.0	C15-C18-H18B	109.5
C13-C12-H12	119.0	H18A-C18-H18B	109.5
C14-C13-C12	116.34(16)	C15-C18-H18C	109.5
C14-C13-C15	123.35(17)	H18A-C18-H18C	109.5
C12-C13-C15	120.20(17)	H18B-C18-H18C	109.5
C13-C14-C9	123.52(16)	C20-C19-C24	119.14(18)

C20-C19-P1	118.52(14)	C27-C28-H28	120.0
C24-C19-P1	122.32(16)	C29-C28-H28	120.0
C21-C20-C19	120.0(2)	C30-C29-C28	120.08(17)
C21-C20-H20	120.0	C30-C29-H29	120.0
C19-C20-H20	120.0	C28-C29-H29	120.0
C20-C21-C22	120.0(2)	C29-C30-C25	120.38(16)
C20-C21-H21	120.0	C29-C30-H30	119.8
C22-C21-H21	120.0	C25-C30-H30	119.8
C23-C22-C21	120.7(2)	C36-C31-C32	118.91(16)
C23-C22-H22	119.6	C36-C31-P1	124.32(13)
C21-C22-H22	119.6	C32-C31-P1	116.66(14)
C22-C23-C24	119.7(2)	C33-C32-C31	120.83(17)
C22-C23-H23	120.2	C33-C32-H32	119.6
C24-C23-H23	120.2	C31-C32-H32	119.6
C23-C24-C19	120.5(2)	C34-C33-C32	119.94(17)
C23-C24-H24	119.8	C34-C33-H33	120.0
C19-C24-H24	119.8	C32-C33-H33	120.0
C26-C25-C30	118.97(16)	C33-C34-C35	119.79(17)
C26-C25-P1	118.93(13)	C33-C34-H34	120.1
C30-C25-P1	122.07(13)	C35-C34-H34	120.1
C27-C26-C25	120.44(16)	C34-C35-C36	120.54(17)
C27-C26-H26	119.8	C34-C35-H35	119.7
C25-C26-H26	119.8	C36-C35-H35	119.7
C28-C27-C26	120.21(17)	C31-C36-C35	119.98(16)
C28-C27-H27	119.9	C31-C36-H36	120.0
C26-C27-H27	119.9	C35-C36-H36	120.0
C27-C28-C29	119.91(17)	C38-C37-H37A	109.5

C38-C37-H37B	109.5	C42-C41-H41B	109.9
H37A-C37-H37B	109.5	H41A-C41-H41B	108.3
C38-C37-H37C	109.5	C41-C42-H42A	109.5
H37A-C37-H37C	109.5	C41-C42-H42B	109.5
H37B-C37-H37C	109.5	H42A-C42-H42B	109.5
C39-C38-C37	110.9(3)	C41-C42-H42C	109.5
C39-C38-H38A	109.5	H42A-C42-H42C	109.5
C37-C38-H38A	109.5	H42B-C42-H42C	109.5
C39-C38-H38B	109.5	C38A-C37A-H37D	109.5
C37-C38-H38B	109.5	C38A-C37A-H37E	109.5
H38A-C38-H38B	108.1	H37D-C37A-H37E	109.5
C38-C39-C40	114.1(3)	C38A-C37A-H37F	109.5
C38-C39-H39A	108.7	H37D-C37A-H37F	109.5
C40-C39-H39A	108.7	H37E-C37A-H37F	109.5
C38-C39-H39B	108.7	C39A-C38A-C37A	114.7(7)
C40-C39-H39B	108.7	C39A-C38A-H38C	108.6
H39A-C39-H39B	107.6	C37A-C38A-H38C	108.6
C39-C40-C41	114.9(3)	C39A-C38A-H38D	108.6
C39-C40-H40A	108.5	C37A-C38A-H38D	108.6
C41-C40-H40A	108.5	H38C-C38A-H38D	107.6
C39-C40-H40B	108.5	C38A-C39A-C40A	117.8(8)
C41-C40-H40B	108.5	C38A-C39A-H39C	107.8
H40A-C40-H40B	107.5	C40A-C39A-H39C	107.8
C40-C41-C42	108.7(3)	C38A-C39A-H39D	107.8
C40-C41-H41A	109.9	C40A-C39A-H39D	107.8
C42-C41-H41A	109.9	H39C-C39A-H39D	107.2
C40-C41-H41B	109.9	C39A-C40A-C41A	116.7(7)

C39A-C40A-H40C	108.1	C8-N1-O1	114.02(13)
C41A-C40A-H40C	108.1	C8-N1-Pd1	130.19(12)
C39A-C40A-H40D	108.1	O1-N1-Pd1	115.61(10)
C41A-C40A-H40D	108.1	N1-O1-C1	106.60(12)
H40C-C40A-H40D	107.3	C10-O2-Pd1	126.78(11)
C40A-C41A-C42A	104.9(7)	C31-P1-C25	106.97(8)
C40A-C41A-H41C	110.8	C31-P1-C19	102.01(8)
C42A-C41A-H41C	110.8	C25-P1-C19	103.34(8)
C40A-C41A-H41D	110.8	C31-P1-Pd1	117.55(6)
C42A-C41A-H41D	110.8	C25-P1-Pd1	112.13(6)
H41C-C41A-H41D	108.8	C19-P1-Pd1	113.45(6)
C41A-C42A-H42D	109.5	N1-Pd1-C2	82.32(6)
C41A-C42A-H42E	109.5	N1-Pd1-O2	88.15(5)
H42D-C42A-H42E	109.5	C2-Pd1-O2	170.43(6)
C41A-C42A-H42F	109.5	N1-Pd1-P1	178.95(4)
H42D-C42A-H42F	109.5	C2-Pd1-P1	97.30(5)
H42E-C42A-H42F	109.5	O2-Pd1-P1	92.21(4)

Table 4.4.4. Anisotropic displacement parameters for **4.10**.

The anisotropic displacement ($\text{\AA}^2 \times 10^3$) factor exponent takes the form: $-2\pi^2 [h^2 a^{*2} U^{11} + \dots + 2 h k a^* b^* U^{12}]$

Atom	U^{11}	U^{22}	U^{33}	U^{23}	U^{13}	U^{12}
C1	20(1)	17(1)	18(1)	1(1)	4(1)	2(1)

C2	18(1)	15(1)	18(1)	2(1)	2(1)	1(1)
C3	19(1)	18(1)	21(1)	1(1)	4(1)	3(1)
C4	23(1)	24(1)	22(1)	0(1)	7(1)	2(1)
C5	26(1)	26(1)	19(1)	5(1)	6(1)	0(1)
C6	24(1)	20(1)	23(1)	2(1)	7(1)	-1(1)
C7	25(1)	23(1)	20(1)	5(1)	3(1)	1(1)
C8	23(1)	13(1)	18(1)	0(1)	1(1)	2(1)
C9	20(1)	18(1)	18(1)	2(1)	2(1)	3(1)
C10	18(1)	19(1)	19(1)	1(1)	1(1)	4(1)
C11	21(1)	21(1)	26(1)	1(1)	3(1)	-1(1)
C12	20(1)	28(1)	23(1)	3(1)	5(1)	1(1)
C13	22(1)	24(1)	17(1)	0(1)	3(1)	5(1)
C14	23(1)	18(1)	19(1)	0(1)	2(1)	3(1)
C15	24(1)	30(1)	20(1)	-5(1)	7(1)	3(1)
C16	28(1)	32(1)	30(1)	-8(1)	8(1)	4(1)
C17	30(1)	50(1)	32(1)	-15(1)	1(1)	16(1)
C18	53(2)	44(1)	31(1)	0(1)	21(1)	-1(1)
C19	17(1)	13(1)	33(1)	2(1)	1(1)	4(1)
C20	23(1)	15(1)	40(1)	1(1)	6(1)	2(1)
C21	27(1)	20(1)	56(1)	6(1)	16(1)	6(1)
C22	20(1)	19(1)	68(2)	6(1)	-5(1)	3(1)
C23	26(1)	24(1)	50(1)	8(1)	-10(1)	0(1)
C24	25(1)	17(1)	38(1)	4(1)	-5(1)	2(1)
C25	17(1)	17(1)	19(1)	4(1)	4(1)	2(1)
C26	21(1)	18(1)	22(1)	3(1)	3(1)	-1(1)
C27	22(1)	27(1)	23(1)	8(1)	0(1)	1(1)
C28	28(1)	26(1)	26(1)	12(1)	5(1)	7(1)

C29	30(1)	16(1)	28(1)	7(1)	7(1)	3(1)
C30	22(1)	17(1)	22(1)	3(1)	2(1)	1(1)
C31	17(1)	16(1)	19(1)	1(1)	-2(1)	1(1)
C32	29(1)	18(1)	25(1)	2(1)	-2(1)	7(1)
C33	32(1)	25(1)	24(1)	9(1)	-4(1)	1(1)
C34	25(1)	27(1)	20(1)	3(1)	1(1)	-5(1)
C35	22(1)	20(1)	26(1)	1(1)	5(1)	0(1)
C36	16(1)	16(1)	24(1)	3(1)	0(1)	1(1)
N1	18(1)	15(1)	19(1)	2(1)	3(1)	0(1)
O1	21(1)	14(1)	26(1)	1(1)	8(1)	-1(1)
O2	20(1)	17(1)	28(1)	-4(1)	8(1)	0(1)
P1	16(1)	12(1)	19(1)	0(1)	0(1)	2(1)
Pd1	15(1)	11(1)	16(1)	0(1)	2(1)	2(1)

Table 4.4.5. H coordinates and isotropic displacement parameters for **4.10**.

Hydrogen coordinates ($\times 10^4$) and isotropic displacement parameters ($\text{\AA}^2 \times 10^3$)

Atom	x	y	z	U(eq)
H1	540	3834	2287	23
H3A	136	5727	2997	24
H3B	1053	6441	3831	24
H4A	-571	5571	4393	29
H4B	-1535	4913	3559	29
H5	-311	3429	4282	28
H6A	-1154	2972	2807	27

H6B	52	2119	3085	27
H7A	2333	3459	4074	27
H7B	2072	4811	4586	27
H8	3733	1800	1769	23
H11	7811	5437	1994	29
H12	8749	4028	1097	30
H14	5602	1415	1067	26
H16A	6867	-9	458	49
H16B	7526	-146	-309	49
H16C	6102	586	-189	49
H17A	10101	2076	1140	64
H17B	9952	721	569	64
H17C	9193	965	1310	64
H18A	7506	2304	-493	65
H18B	8891	1506	-549	65
H18C	9086	2871	12	65
H20	6272	7432	2872	33
H21	8778	8118	3086	41
H22	10129	8749	4330	46
H23	9010	8700	5363	43
H24	6503	8022	5161	34
H26	1922	6753	2488	25
H27	722	8048	1833	29
H28	1357	10173	2246	31
H29	3215	11011	3314	30
H30	4418	9724	3974	25
H32	4582	5904	4982	30

H33	4233	6329	6246	33
H34	3184	8114	6787	30
H35	2423	9442	6048	28
H36	2781	9032	4781	23
H37A	1195	5029	535	75
H37B	2509	5626	1238	75
H37C	1868	4223	1082	75
H38A	3528	5122	100	55
H38B	4142	4256	622	55
H39A	1813	3562	-666	54
H39B	2189	2710	-104	54
H40A	4476	2423	-456	48
H40B	4256	3394	-950	48
H41A	2524	2049	-1883	54
H41B	2418	1127	-1357	54
H42A	5129	1629	-1883	79
H42B	4009	433	-2312	79
H42C	4861	590	-1459	79
H37D	3256	5526	786	66
H37E	2799	4832	1382	66
H37F	1559	5094	743	66
H38C	3812	3454	359	57
H38D	2209	2942	426	57
H39C	2688	4226	-651	58
H39D	1150	3565	-608	58
H40C	1999	2393	-1625	53
H40D	2049	1639	-1000	53

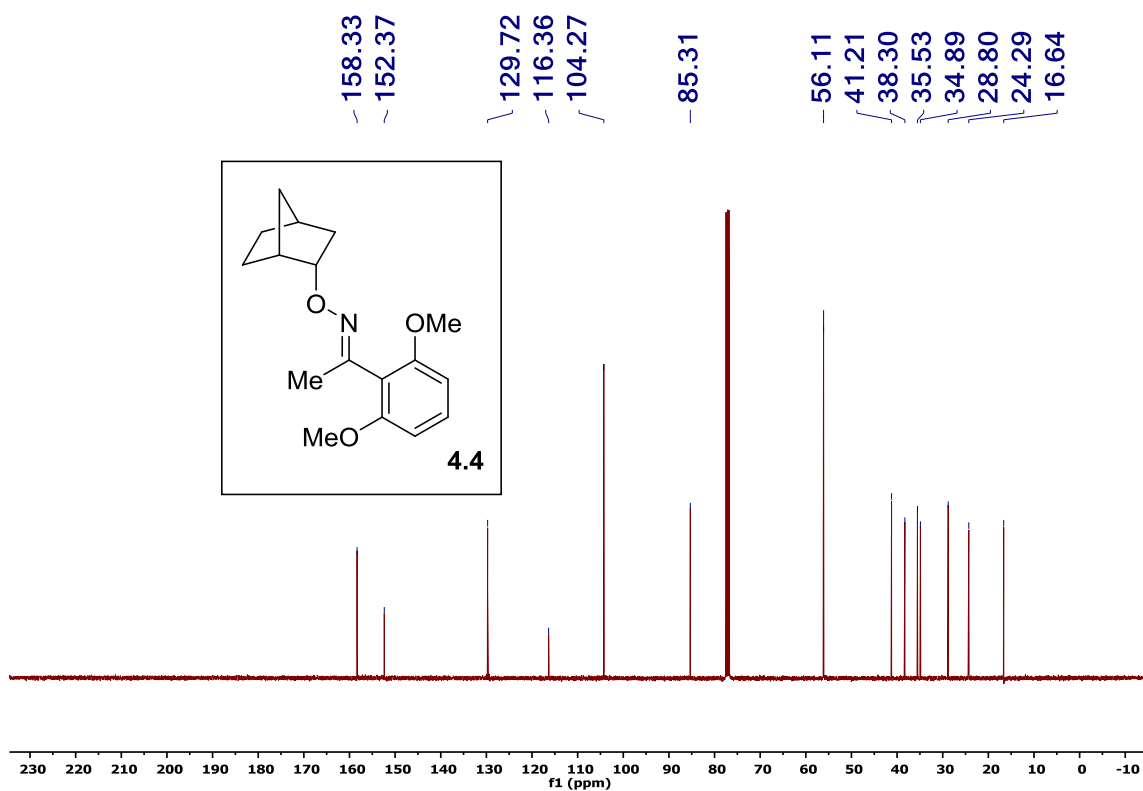
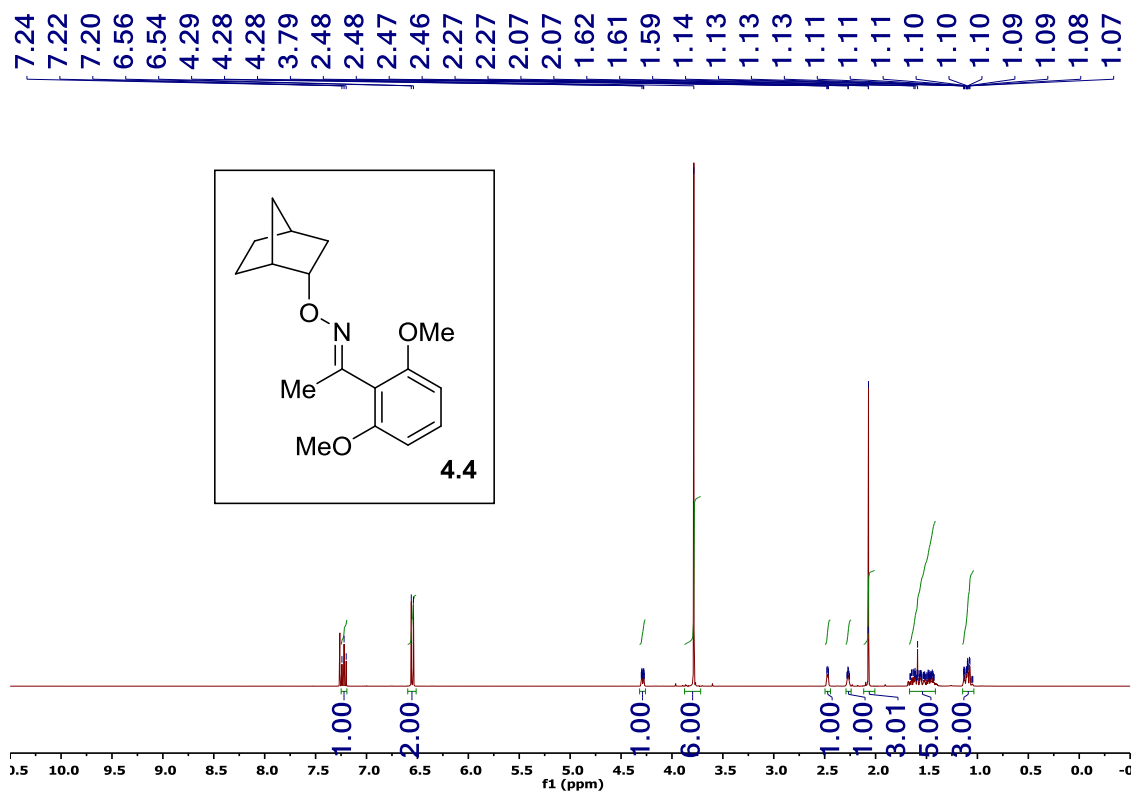
H41C	4652	2036	-677	59
H41D	4636	2879	-1262	59
H42D	3038	583	-2038	60
H42E	4667	349	-1686	60
H42F	4440	1168	-2278	60

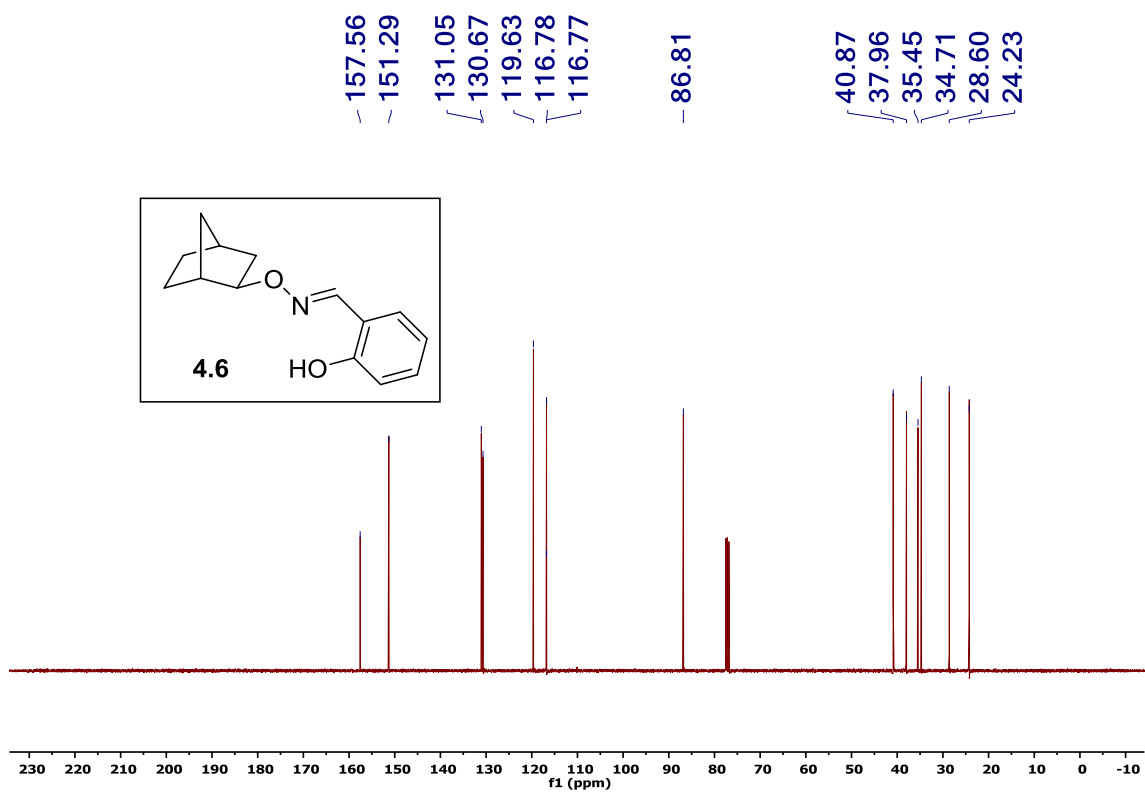
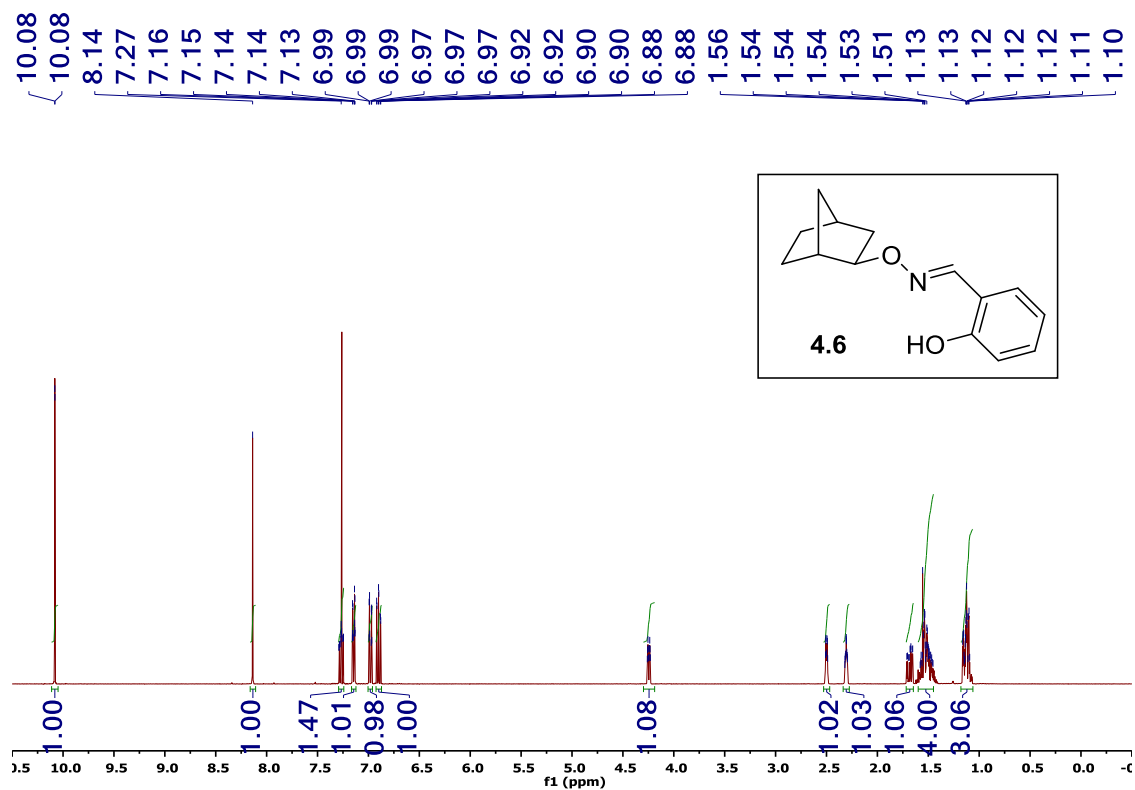
Table 4.4.6. Torsion angles [°] for **4.10**.

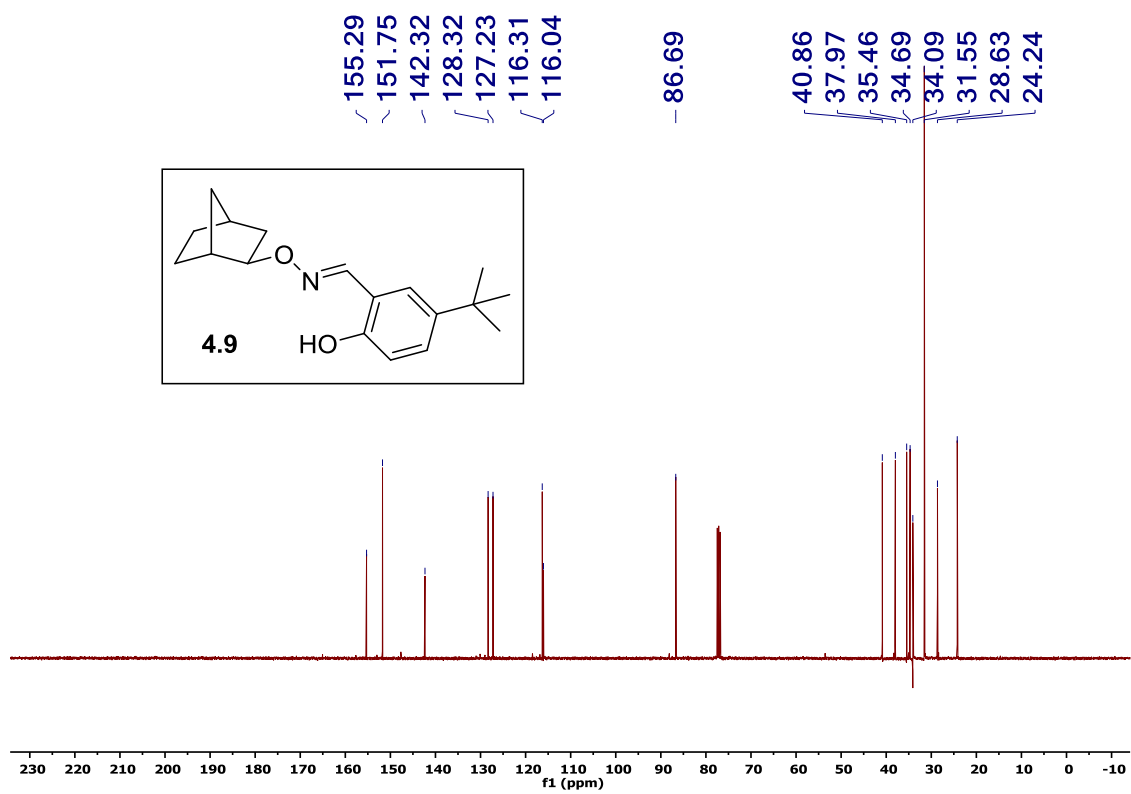
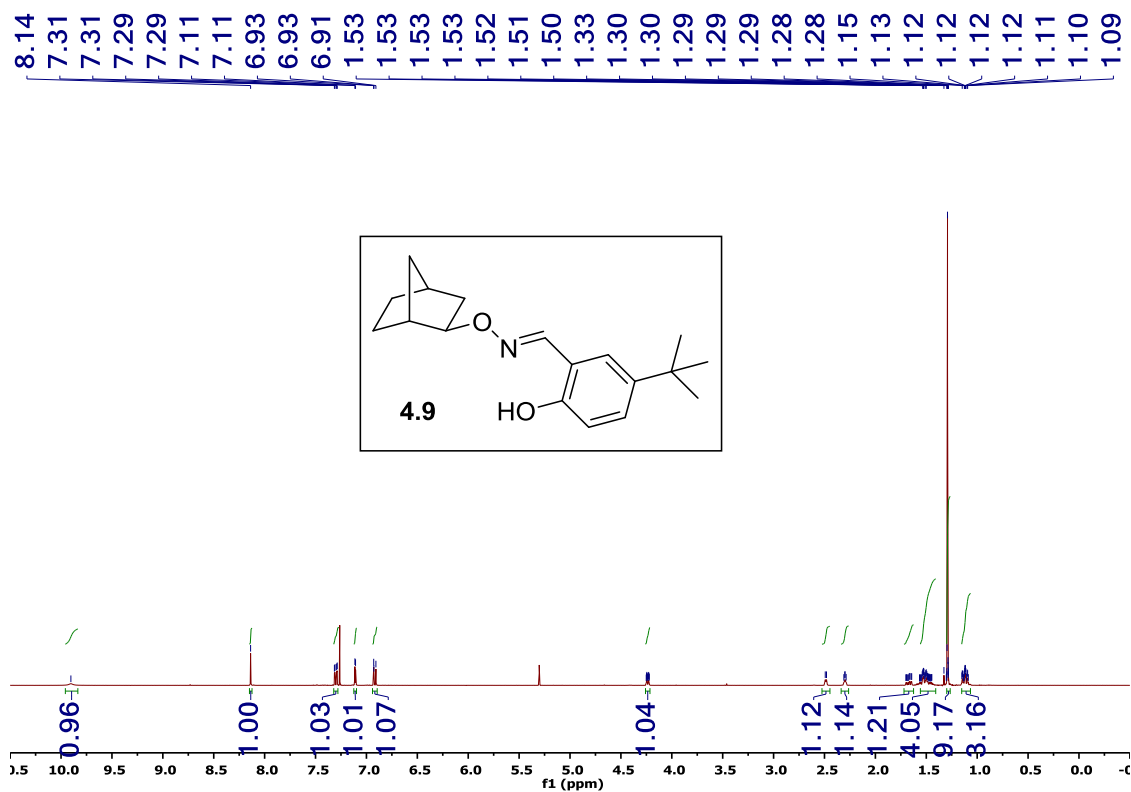
O1-C1-C2-C3	174.59(13)	C3-C2-C7-C5	53.42(15)
C6-C1-C2-C3	-70.37(17)	C1-C2-C7-C5	-54.45(15)
O1-C1-C2-C7	-80.39(16)	Pd1-C2-C7-C5	-167.39(12)
C6-C1-C2-C7	34.64(17)	N1-C8-C9-C14	-175.60(17)
O1-C1-C2-Pd1	44.19(15)	N1-C8-C9-C10	1.7(3)
C6-C1-C2-Pd1	159.22(12)	C14-C9-C10-O2	-176.78(16)
C7-C2-C3-C4	-32.15(16)	C8-C9-C10-O2	6.0(3)
C1-C2-C3-C4	71.84(16)	C14-C9-C10-C11	2.7(2)
Pd1-C2-C3-C4	-169.72(11)	C8-C9-C10-C11	-174.49(16)
C2-C3-C4-C5	-2.78(17)	O2-C10-C11-C12	177.50(17)
C3-C4-C5-C6	-69.99(17)	C9-C10-C11-C12	-2.1(3)
C3-C4-C5-C7	36.83(16)	C10-C11-C12-C13	-0.3(3)
C4-C5-C6-C1	71.79(18)	C11-C12-C13-C14	2.0(3)
C7-C5-C6-C1	-34.88(17)	C11-C12-C13-C15	-174.48(18)
O1-C1-C6-C5	118.11(15)	C12-C13-C14-C9	-1.2(3)
C2-C1-C6-C5	0.00(18)	C15-C13-C14-C9	175.12(17)
C4-C5-C7-C2	-55.83(15)	C10-C9-C14-C13	-1.2(3)
C6-C5-C7-C2	55.69(16)	C8-C9-C14-C13	176.25(17)

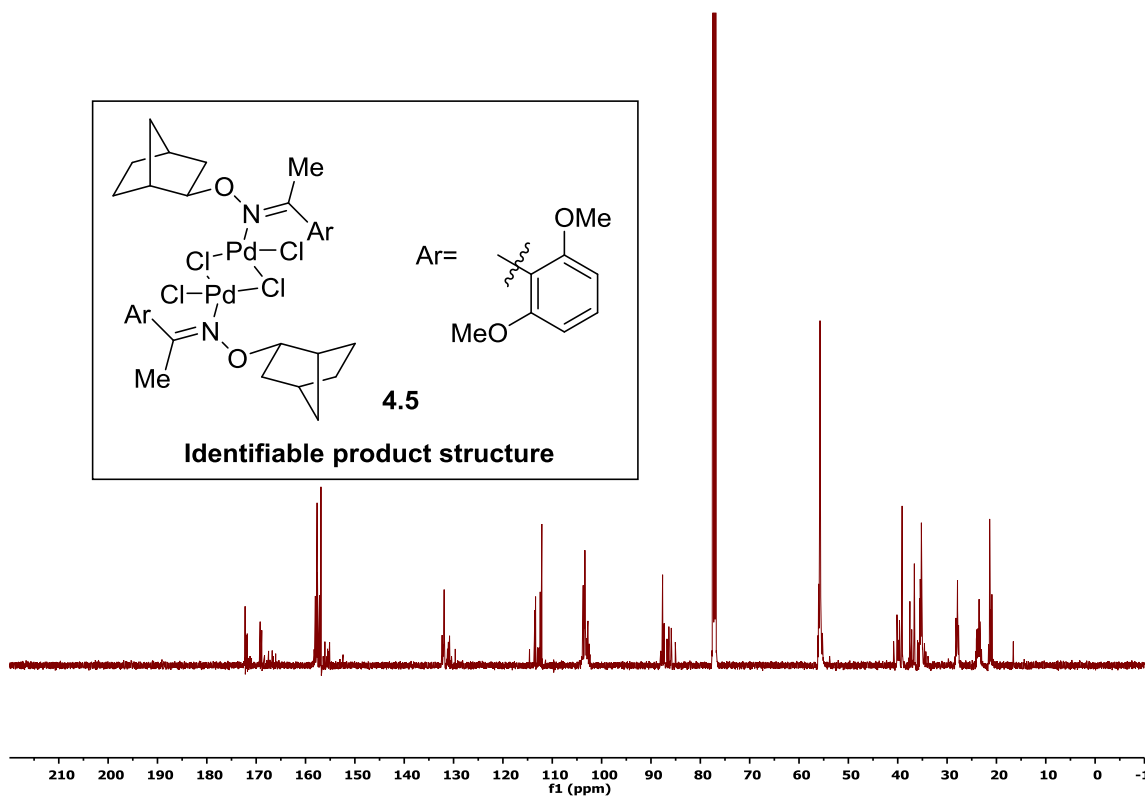
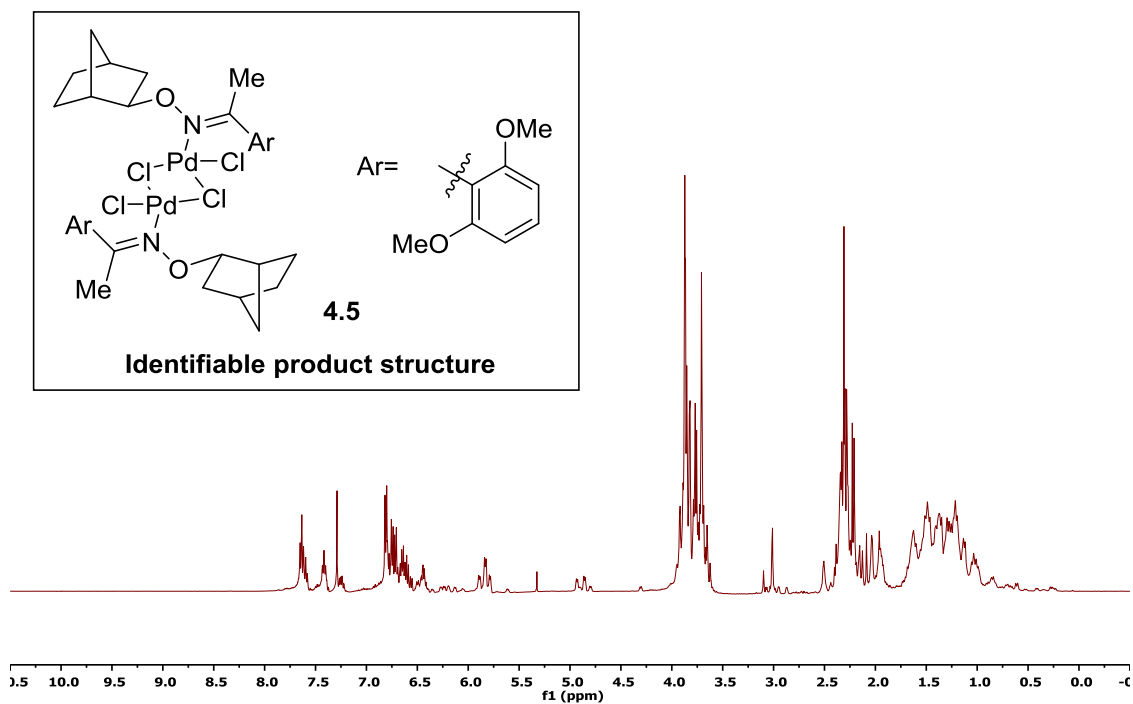
C14-C13-C15-C17	-104.5(2)	C32-C31-C36-C35	0.7(3)
C12-C13-C15-C17	71.7(2)	P1-C31-C36-C35	-175.48(13)
C14-C13-C15-C16	15.9(3)	C34-C35-C36-C31	0.3(3)
C12-C13-C15-C16	-167.88(18)	C37-C38-C39-C40	-171.3(3)
C14-C13-C15-C18	134.8(2)	C38-C39-C40-C41	-173.0(3)
C12-C13-C15-C18	-49.0(2)	C39-C40-C41-C42	-168.5(4)
C24-C19-C20-C21	0.3(3)	C37A-C38A-C39A-C40A	173.6(9)
P1-C19-C20-C21	-178.11(14)	C38A-C39A-C40A-C41A	-64.2(12)
C19-C20-C21-C22	-0.1(3)	C39A-C40A-C41A-C42A	-176.2(8)
C20-C21-C22-C23	0.0(3)	C9-C8-N1-O1	179.88(15)
C21-C22-C23-C24	-0.1(3)	C9-C8-N1-Pd1	-5.3(3)
C22-C23-C24-C19	0.3(3)	C8-N1-O1-C1	-154.98(14)
C20-C19-C24-C23	-0.4(3)	Pd1-N1-O1-C1	29.39(14)
P1-C19-C24-C23	177.96(15)	C6-C1-O1-N1	-162.26(13)
C30-C25-C26-C27	-1.4(3)	C2-C1-O1-N1	-48.34(16)
P1-C25-C26-C27	-179.56(14)	C11-C10-O2-Pd1	171.35(12)
C25-C26-C27-C28	0.5(3)	C9-C10-O2-Pd1	-9.1(3)
C26-C27-C28-C29	0.4(3)	C36-C31-P1-C25	-12.27(17)
C27-C28-C29-C30	-0.4(3)	C32-C31-P1-C25	171.49(13)
C28-C29-C30-C25	-0.4(3)	C36-C31-P1-C19	95.88(16)
C26-C25-C30-C29	1.3(3)	C32-C31-P1-C19	-80.36(15)
P1-C25-C30-C29	179.44(14)	C36-C31-P1-Pd1	-139.38(13)
C36-C31-C32-C33	-0.9(3)	C32-C31-P1-Pd1	44.38(15)
P1-C31-C32-C33	175.56(15)	C26-C25-P1-C31	-116.28(14)
C31-C32-C33-C34	0.1(3)	C30-C25-P1-C31	65.58(16)
C32-C33-C34-C35	1.0(3)	C26-C25-P1-C19	136.50(14)
C33-C34-C35-C36	-1.2(3)	C30-C25-P1-C19	-41.64(17)

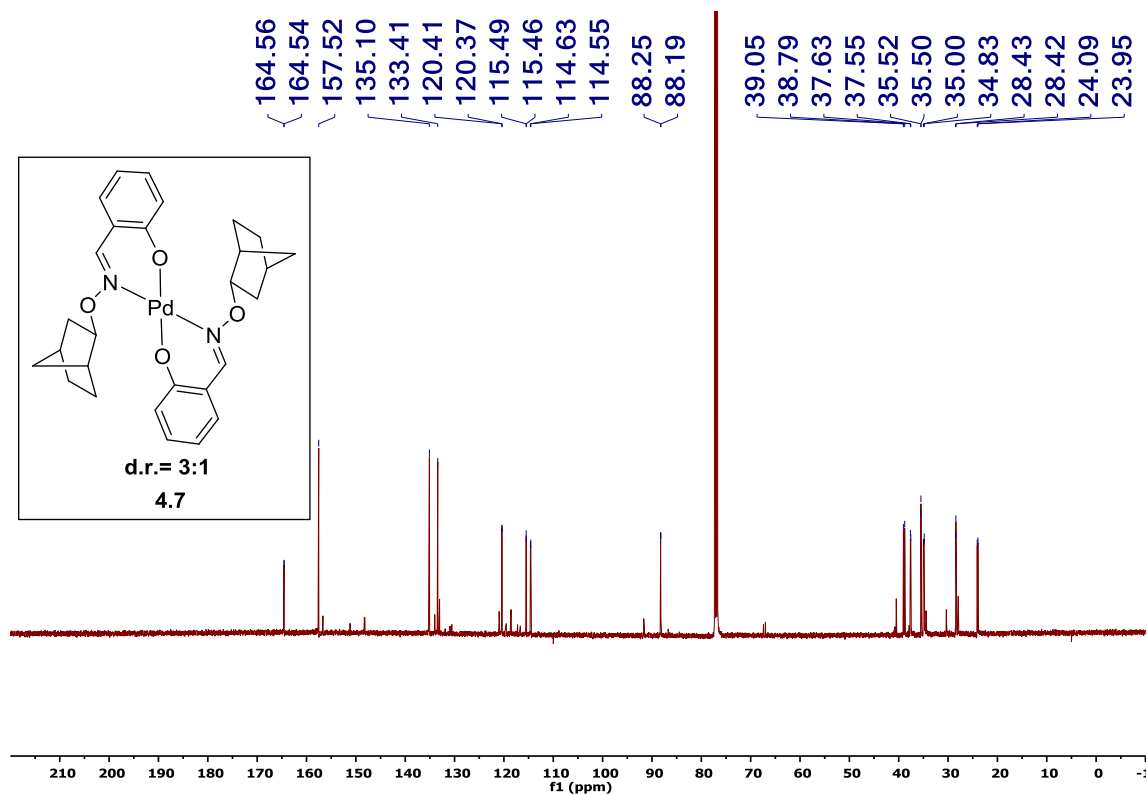
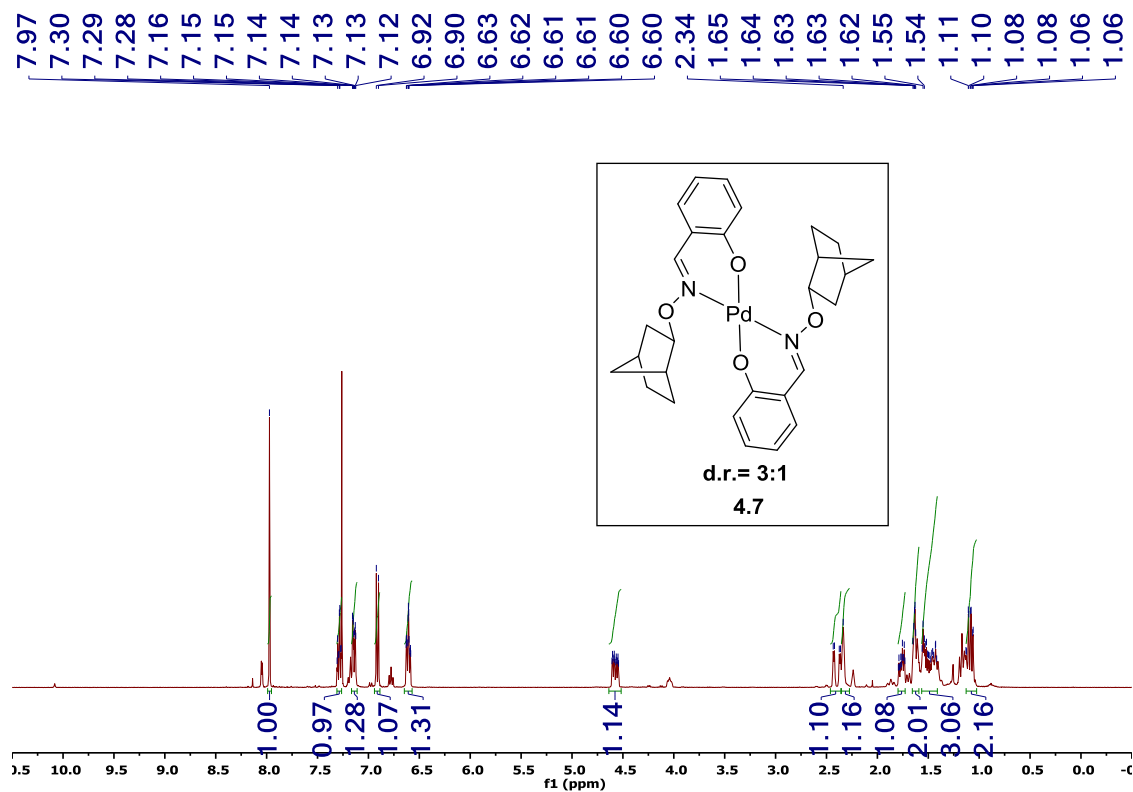
C26-C25-P1-Pd1	13.96(16)	C24-C19-P1-C25	121.49(15)
C30-C25-P1-Pd1	-164.18(13)	C20-C19-P1-Pd1	61.50(15)
C20-C19-P1-C31	-171.08(14)	C24-C19-P1-Pd1	-116.85(14)
C24-C19-P1-C31	10.57(17)		
C20-C19-P1-C25	-60.16(16)		

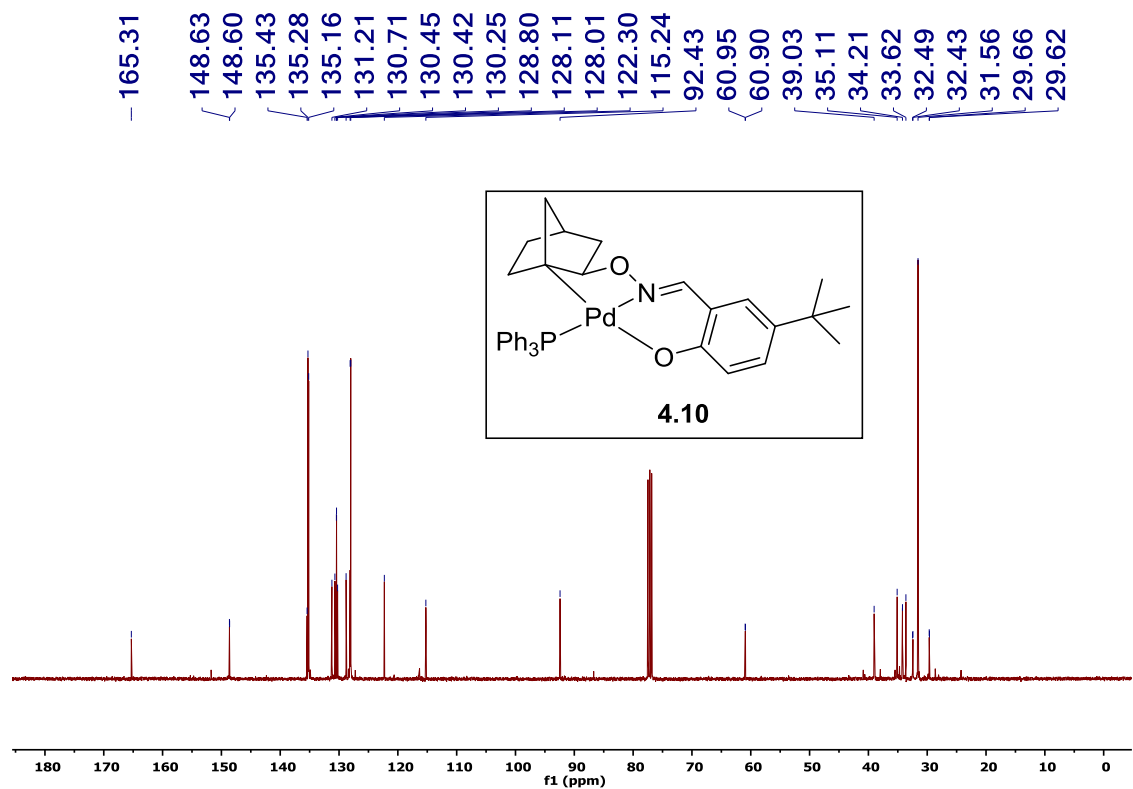
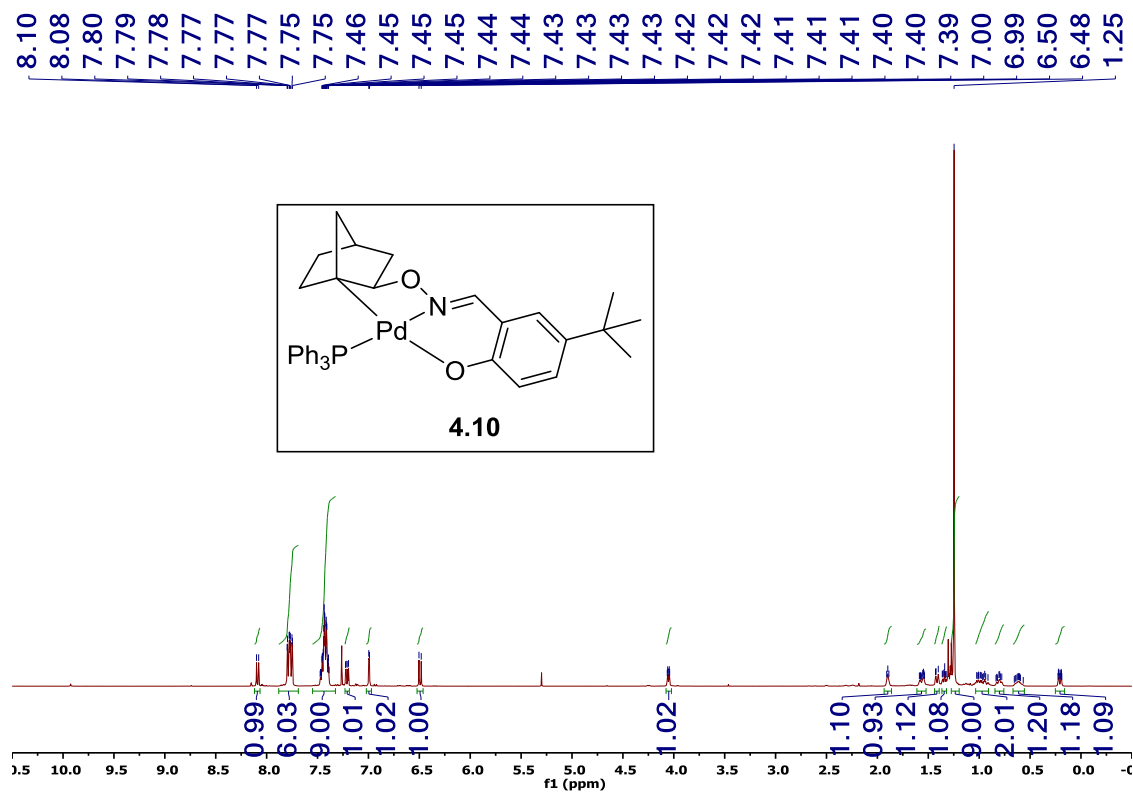


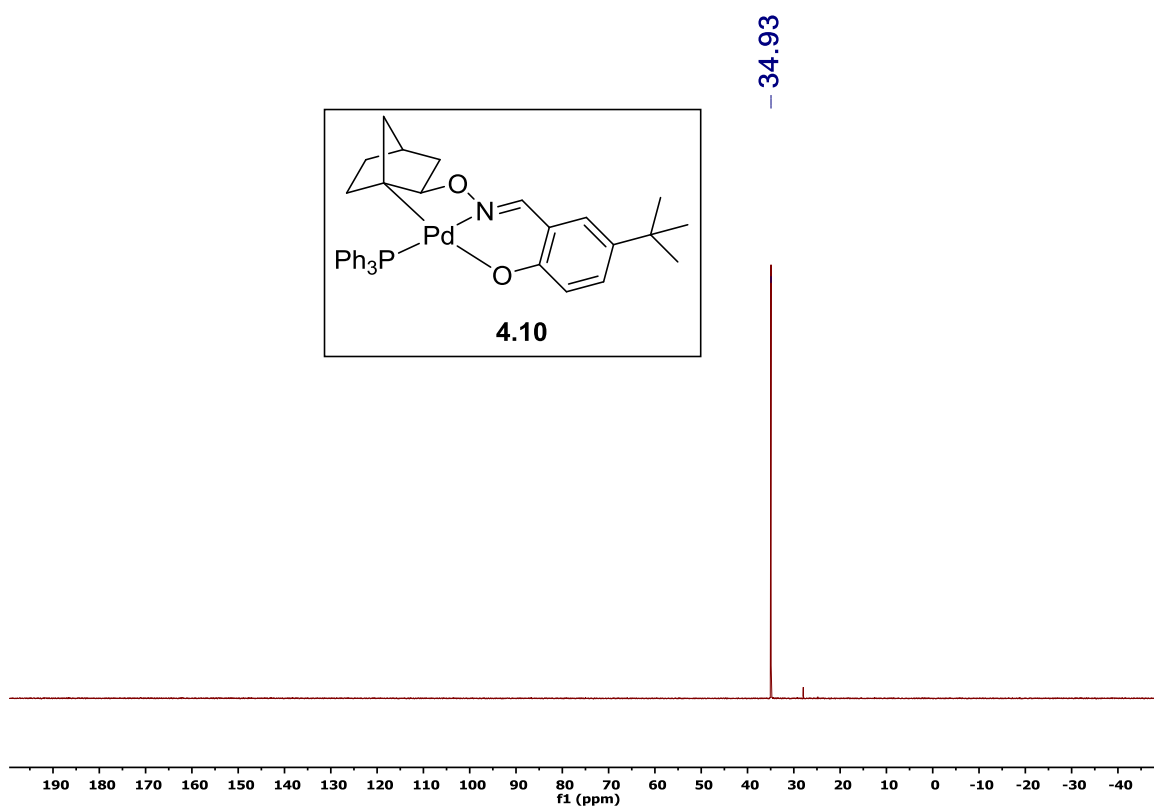


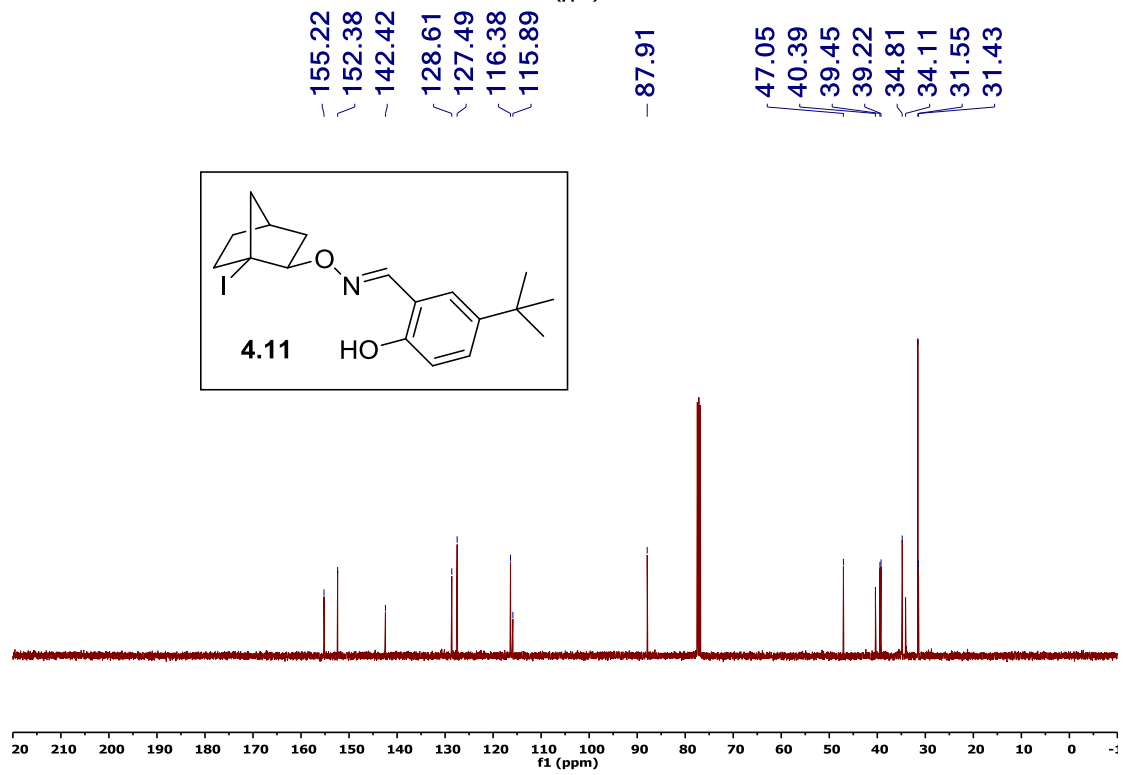
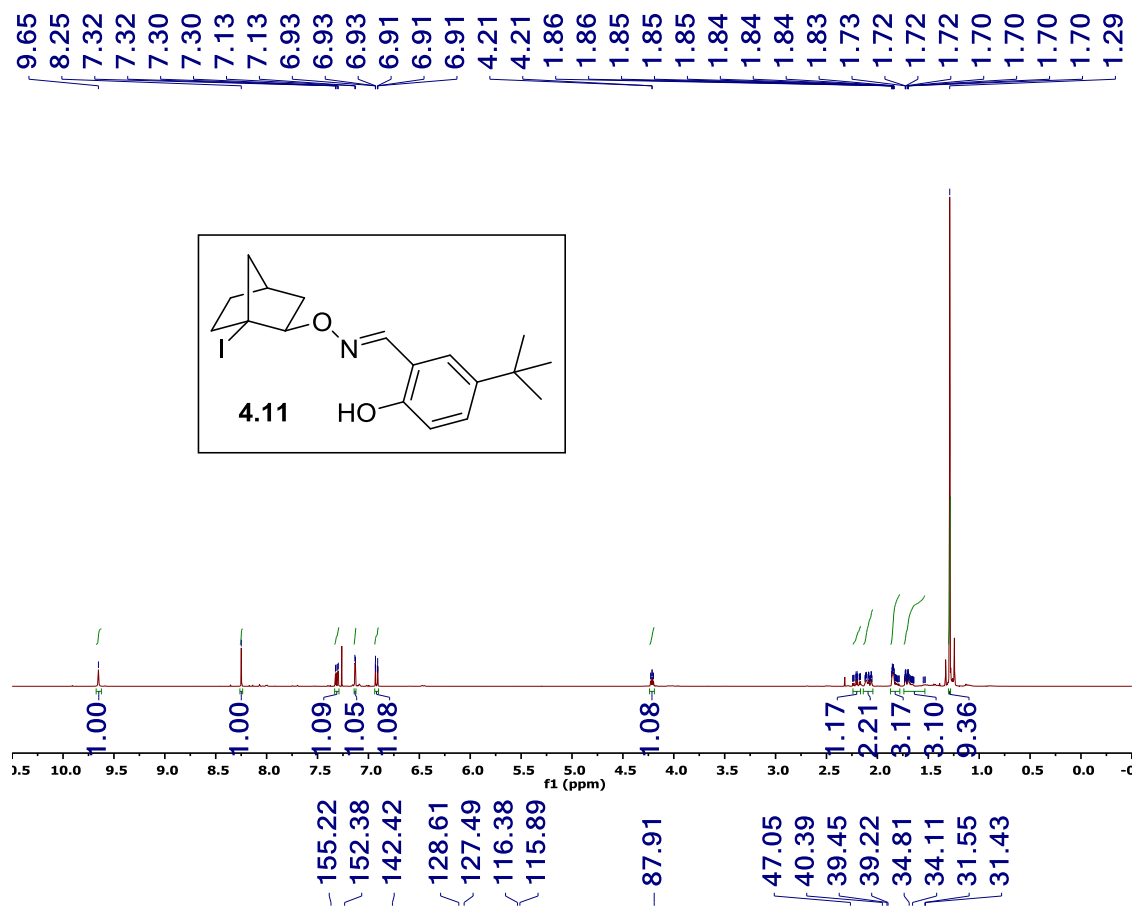












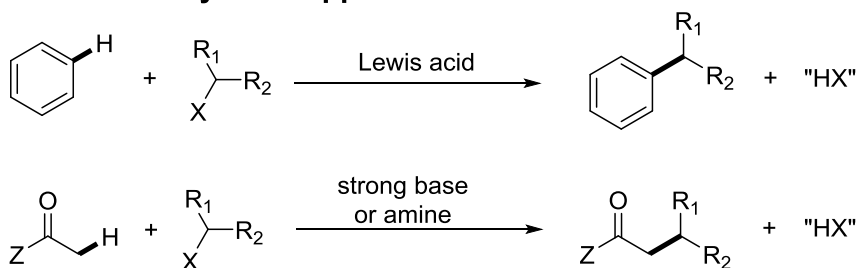
CHAPTER 5: TRANSITION-METALS CATALYZED ALKYLATION OF AROMATIC C–H BONDS WITH SIMPLE OLEFINS

5.1 Introduction

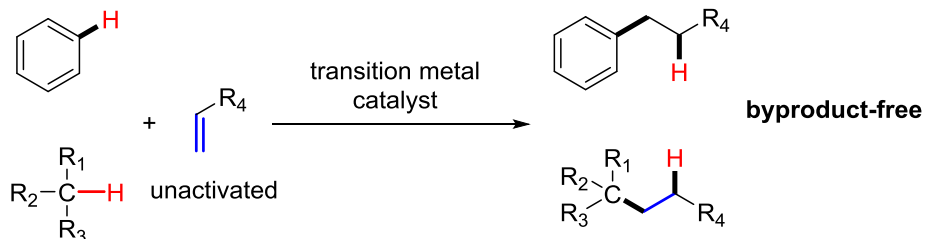
Carbon–carbon bond (C–C) formation is at the forefront of modern organic synthesis.¹ Alkylation reactions, the couplings between a nucleophile and an alkylating agent, clearly constitute one highly important C–C bond-forming reaction and have been widely employed in synthesizing compounds for various purposes. Scheme 1 depicts two most representative alkylation reactions: electrophilic aromatic alkylation² and enolate alkylation.³ Conventionally, both transformations mainly rely on using highly reactive alkylating agents, e.g. alkyl halides and sulfonates, etc. While efficient, these transformations inevitably are concerned about the cost and generation of stoichiometric byproducts.

Scheme 5.1. Two representative alkylation reactions.

A. Classical alkylation approaches to construct C–C bond



B. Olefins as alkylation reagents



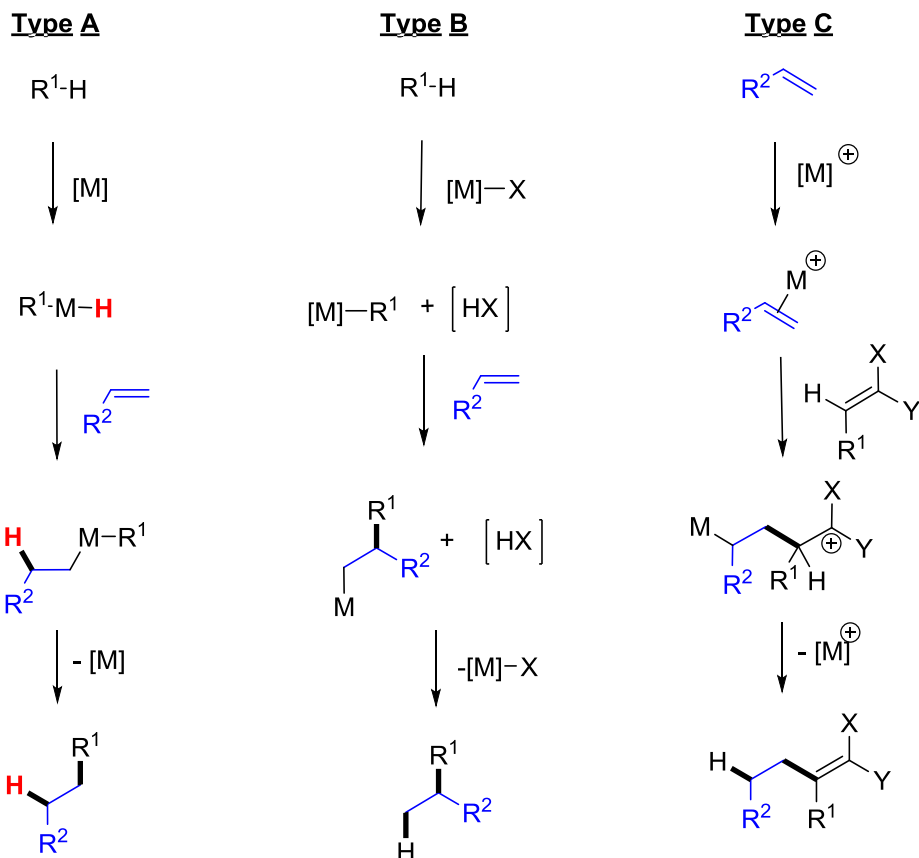
With the advancement of transition-metal chemistry during the last three decades, catalytic carbon–hydrogen bond (C–H) functionalization has become an important tool for synthesizing complex molecules. One intriguing question emerged: can the alkylation reactions be achieved through the addition of a C–H bond across an unactivated alkene? Comparing to the traditional alkylation reagents, a number of attractive features can be envisioned using alkenes: 1) the alkylation reaction would be byproduct-free;⁴ 2) olefins are generally much cheaper and more readily available than the corresponding alkyl halides;⁵ 3) the reactivity of alkenes is *orthogonal* to many functional groups; 4) using olefins can streamline syntheses, whereas many primary alkyl halides or sulfonates are ultimately synthesized from olefins.⁶

Herein, this review will focus on transition metal-catalyzed C–H alkylation using alkenes as the coupling partner. As an overview of this field, three general mechanistic pathways are possible for this transformation (Scheme 2). **Type A** pathway is mediated by a metal–hydride intermediate. In this type, a low-valent transition metal first inserts into a C–H bond to give a metal-hydride intermediate, which then undergoes olefin migratory insertion followed by reductive elimination to afford the alkylation product. The reductive elimination step is generally considered as the most challenging step for **Type A** transformations, where it is often the rate-determining step and therefore controls the regioselectivity of the olefin insertion.⁷

Type B is a pathway involving metalation and net protonation. A carbon–metal bond is formed through an electrophilic metallation of the C–H bond, e.g. concerted metalation deprotonation (CMD). Instead of forming a hydride intermediate, the hydrogen leaves as a proton equivalent. The resulting carbon–metal bond can undergo migratory insertion into the olefin, and the newly generated carbon–metal bond then directly or indirectly gets protonated to offer the alkylation product. Clearly, **type A** and

type B are closely related pathways, and sometimes, are difficult to differentiate through experiments. In this review, we discuss both pathway types in the section of “alkylation via C–H activation”.

Scheme 5.2. Three pathways for the alkylation of aromatic C–H bonds.



Type C involves activation of the alkenes by a π -acidic transition-metal. In this pathway, the alkene becomes more electrophilic, which can be attacked by an electron-rich carbon nucleophile, followed by a proton transfer, to give the alkylation product.^{3b} This type of reactions will be summarized in the section of “alkylation via olefin activation”. Besides the above three major pathways, other mechanisms are also possible, and will be discussed on a case-by-case basis.

5.2 Background

The addition of arene C–H bonds across olefins, also known as hydroarylation, has been studied extensively over the past four decades. A number of regio- and enantioselective hydroarylation methods have been established with various transition-metal catalysts, including Ru, Rh, Ni, Re, Mn, Co, Fe and rare earth metal complexes. Chelation-controlled alkylation has dominated the field since the seminal discovery by Lewis⁸ and Murai.⁹ Alkylation of simple arenes, such as benzene, has also been disclosed with homogeneous catalysts (e.g. the Ir¹⁰ and Ru¹¹ systems), although the efficiency remains to be further improved.¹² Besides regular arenes, heteroarenes can also be alkylated with olefins, with both early (e.g. Sc, Y, Ti, and Zr systems) and late transition metals.⁷ While still in its early stage, the hydroarylation methodology has already been utilized in late-stage functionalization, polymer synthesis/modification, and total synthesis. This section is organized based on the nature of the metal catalysts used. This chapter will focus on Ru and Rh-catalyzed alkylation of aromatic C–H bonds.

5.3 TM-Catalyzed Alkylation of Aromatic C–H Bonds

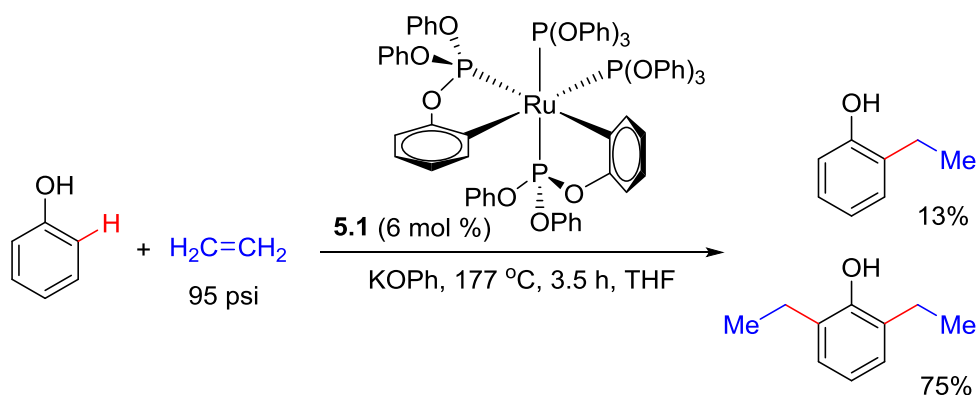
5.3.1 RUTHENIUM CATALYSIS

5.3.1.1 Chelation controlled

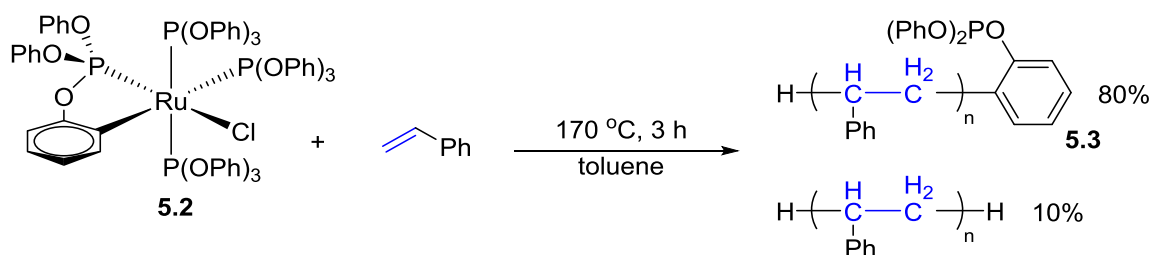
In 1986, Lewis reported the first Ru-catalyzed *ortho*-selective C–H alkylation of phenols with ethylene using complex **5.1** (Scheme 5.3).⁸ The phosphite ligand was critical for the success of this reaction, to install a directing group *in situ* from phenoxide to assist insertion of the ruthenium into the *ortho* C–H bonds. Interestingly, when propylene reacted with complex **5.2**, the branched product was found as the dominating product. Complex **5.2** also reacted with styrene, albeit giving a polymeric product **5.3**

(Scheme 5.4). Other olefins did not react. While the reaction mechanism remains unclear, the metal-hydride pathway (**Type A**, Scheme 5.2) is less likely due to the formation of branched products with propene and the lack of evidence for a Ru–H species. Thus, the authors proposed a **Type B** like mechanism. The significance of this seminal work includes 1) the first use of a temporary directing group to control site-selectivity of C–H functionalization, and 2) the first controlled *ortho* C–H alkylation with olefins, which is distinct from the classical Friedel–Craft reaction. (For an analogous Rh-catalyzed *ortho*-alkylation of phenols, see Scheme 5.38).

Scheme 5.3. Ru-catalyzed *ortho*-selective C–H alkylation of phenols with ethylene.



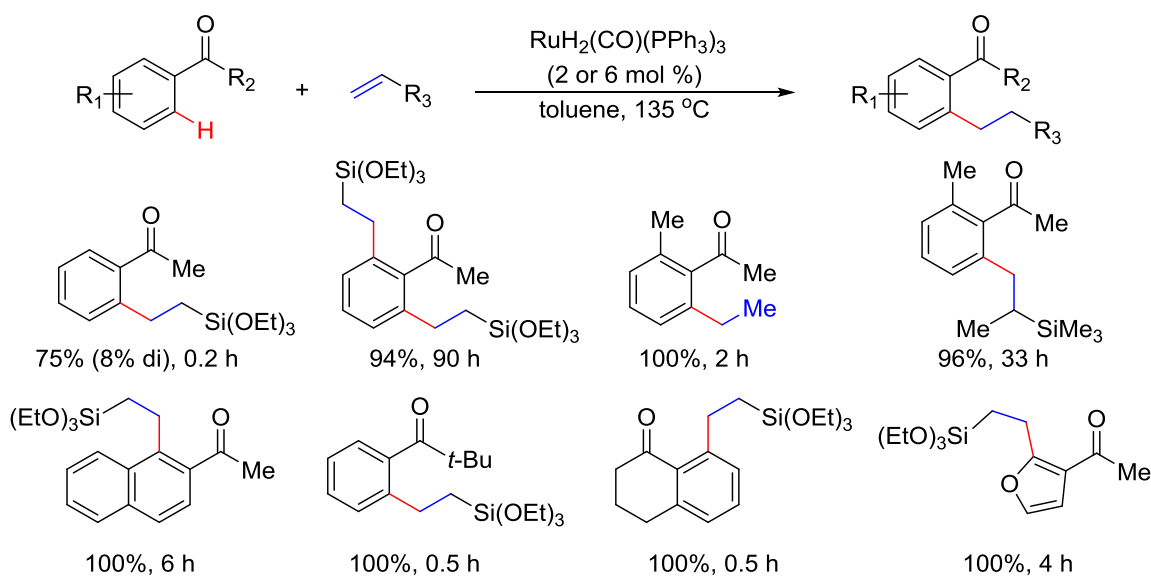
Scheme 5.4. Ru-catalyzed C–H alkylation of phenols with styrene.



In 1993, the Ru-catalyzed *ortho*-alkylation of aromatic ketones with olefins, reported by Murai and coworkers, represents another milestone in the field.⁹ Many aromatic and heteroaromatic ketones were successfully alkylated (Scheme 5.5). When 2-

acetylnaphthalene was used as the substrate, the alkylation occurred site-selectively at the C1 position. The chelation effect is crucial, and ketones that cannot generate strongly chelated five-membered metallocycles, e.g. 1-indanone, do not react. A range of unisomerizable olefins can be used as the coupling partner, giving linear, anti-Markovnikov addition products.¹³

Scheme 5.5. Ru-catalyzed *ortho*-alkylation of aromatic ketones with olefins.

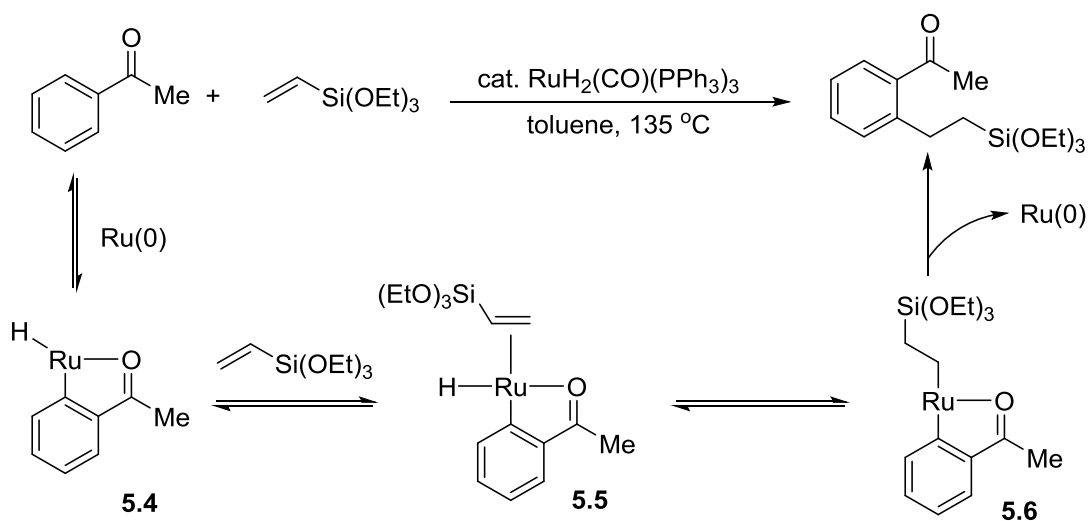


The proposed mechanism is illustrated in Scheme 5.6, which is a **Type A** mechanism. The reaction was initiated by a ketone-assisted oxidative addition into the *ortho* C–H bond, giving a ruthenium–hydride complex (**5.5**). Subsequent migratory insertion into the olefin, followed by reductive elimination, provides the alkylation product.

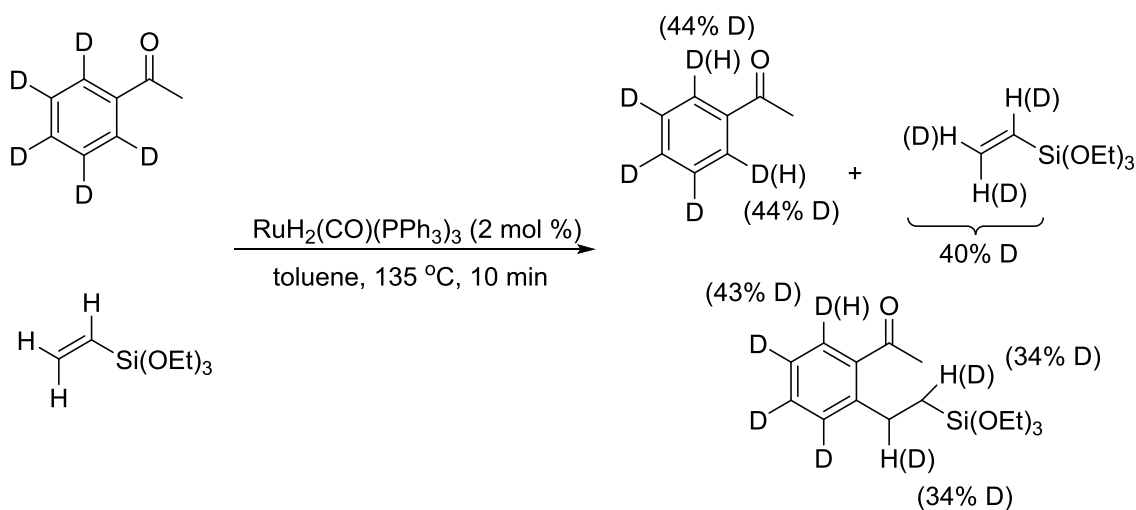
As depicted in Scheme 5.7, deuterium scrambling was observed between the starting materials and products when using *d*₅-acetophenone, which supports the proposed metal–hydride-involved mechanism. In 1998, the DFT study by Koga and

Morokuma indicated that the Ru–H species, generated via oxidative addition of Ru(0) into the *ortho* C–H bond, was a feasible intermediate in the catalytic cycle.¹⁴ The chelation effect is critical for decreasing the activation energy for the C–H activation step. Later, a detailed DFT study by Matsubara, Morokuma and coworkers revealed that reductive elimination is the rate determining step.¹⁵

Scheme 5.6. Proposed mechanism for Ru-catalyzed *ortho*-alkylation of aromatic ketones.

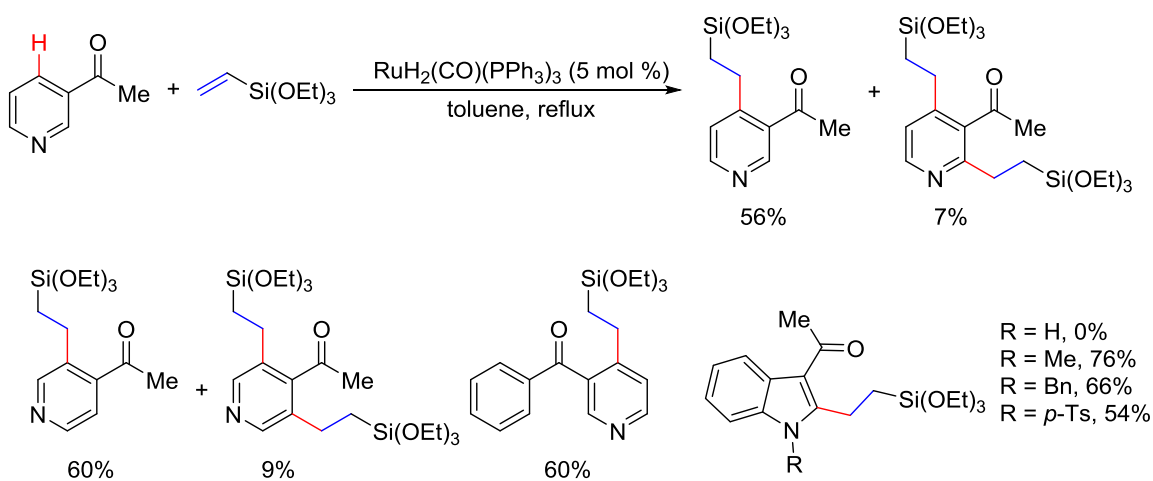


Scheme 5.7. The deuterium scrambling experiment for Ru alkylation.



After Murai's seminal work, Grigg and coworkers in 1997 successfully extended the scope of the ketone substrates to heterocycles, such as pyridine- and indole-based ketones (Scheme 5.8).¹⁶ High site-selectivity was observed using 3-acetylpyridine, with a small amount of bis-alkylated products. Chemo- and site-selective alkylation of the pyridine ring instead of the phenyl ring can be achieved.

Scheme 5.8. Ru-catalyzed alkylation of heterocycles with silylated olefins.

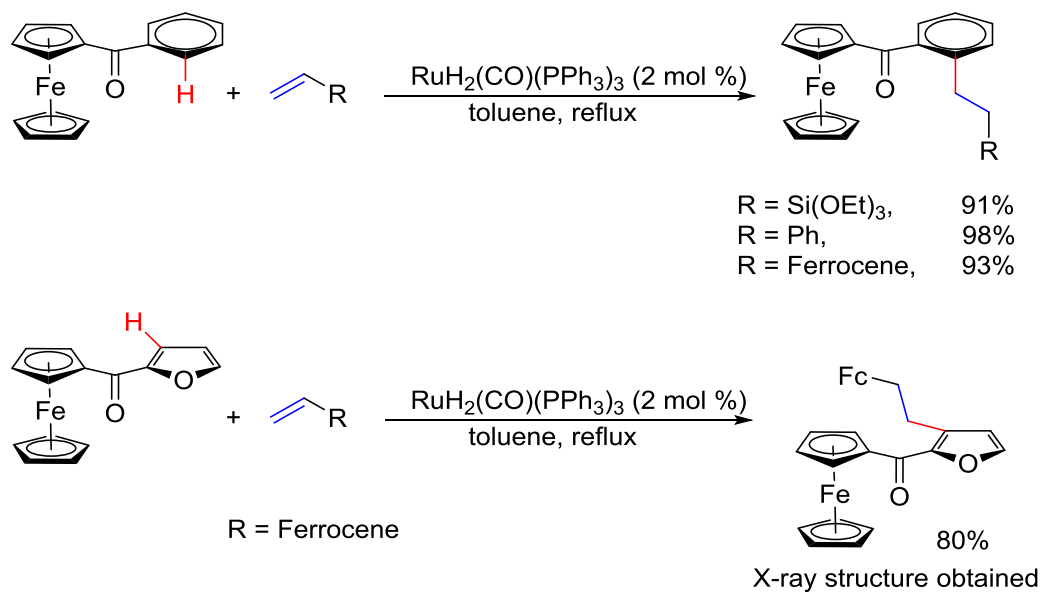


The Ru-catalyzed alkylation of aromatic ketones containing 9-ferrocenyl groups was developed by Du and co-workers in 2001 (Scheme 5.9).¹⁷ The alkylation with various terminal olefins gave a good to excellent yield. The alkylation occurred chemoselectively at the none-ferrocenyl side, presumably due to its electronic properties.

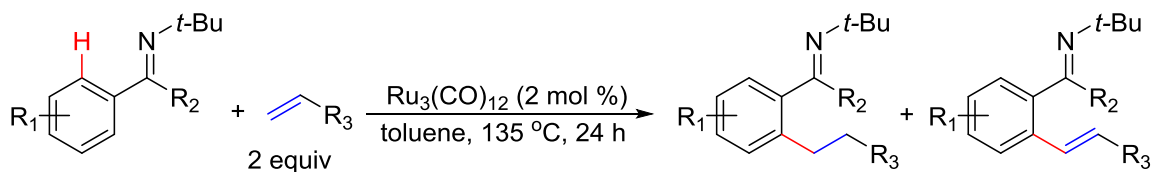
In 1996, Murai and coworkers developed the first Ru-catalyzed *ortho*-alkylation of aromatic imines with simple olefins (Scheme 5.10),¹⁸ in which $\text{Ru}_3(\text{CO})_{12}$ was used as the pre-catalyst. For certain substrates, a few alkenylation products were observed. The alkylation conditions for imine and ketone directing groups are orthogonal to each other,

with chemoselective alkylations achieved by properly choosing the corresponding Ru precatalysts (Scheme 5.11).¹⁹

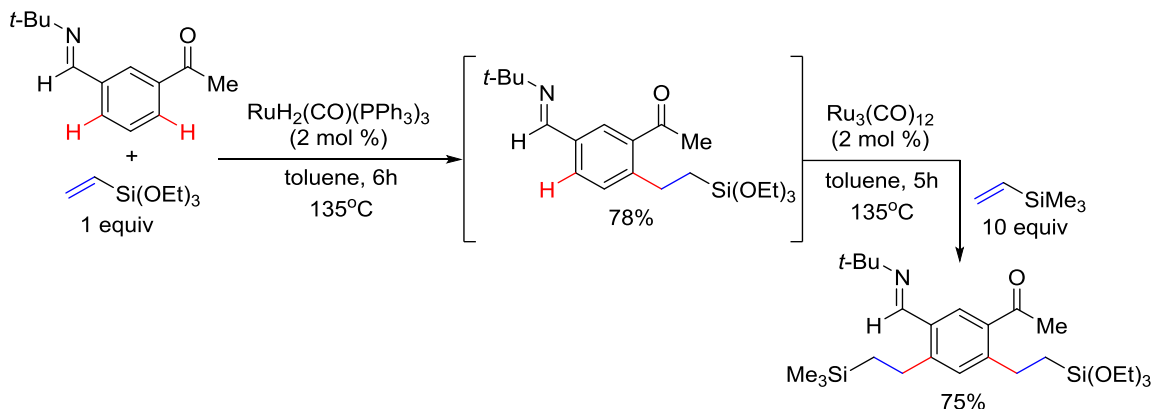
Scheme 5.9. Ru-catalyzed alkylation of aromatic ketones containing 9-ferrocenyl groups.



Scheme 5.10. Ru-catalyzed *ortho*-alkylation of aromatic imines with simple olefins.

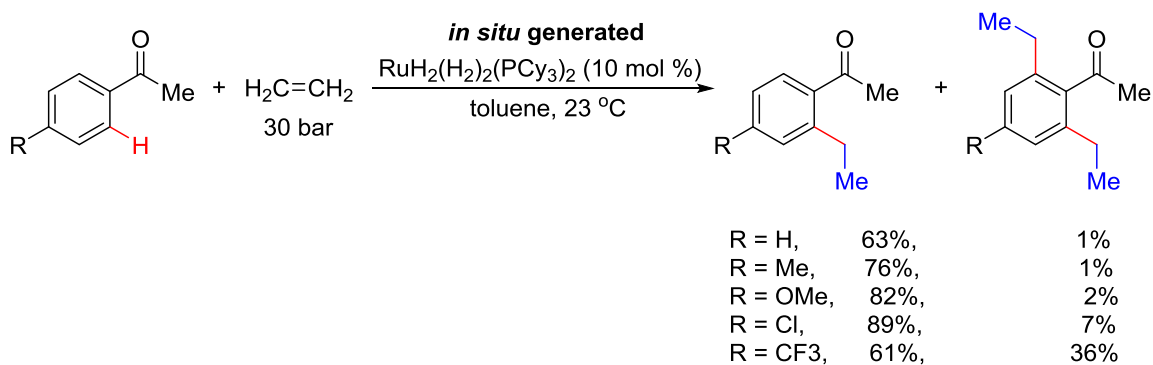


Scheme 5.11. Ru-catalyzed chemoselective alkylations with simple olefins.

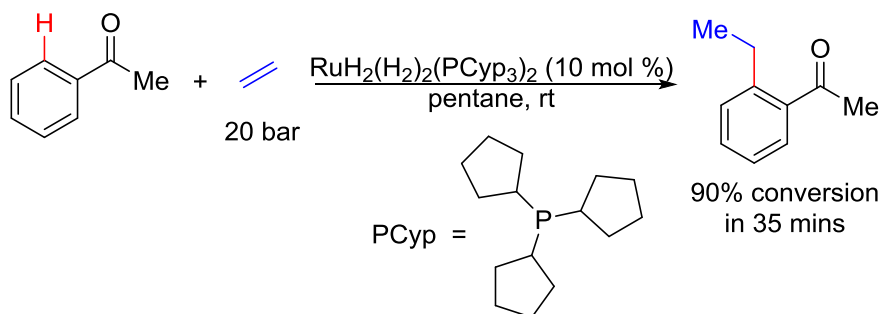


In 2001, the Whittlesey group prepared four new Ru complexes for C–H alkylation, but unfortunately, none of them shown improved reactivity from the $\text{RuH}_2(\text{CO})(\text{PPh}_3)_3$ complex.²⁰ Meanwhile, the Leitner group successfully developed a room temperature alkylation with an *in situ* generated Ru catalyst (Scheme 5.12).²¹ In 2005, Stabo-Etienne and coworkers prepared and isolated the $\text{RuH}_2(\text{H}_2)_2(\text{PCy}_3)_2$ complex, which was confirmed by neutron diffraction analysis (Scheme 5.13).²² With this newly prepared Ru complex, the alkylation of acetophenone can reach 90% conversion within 35 minutes at room temperature, which previously required 10 hours using the Murai's pre-catalyst with heat.

Scheme 5.12. Room temperature alkylation with an *in situ* generated Ru catalyst.

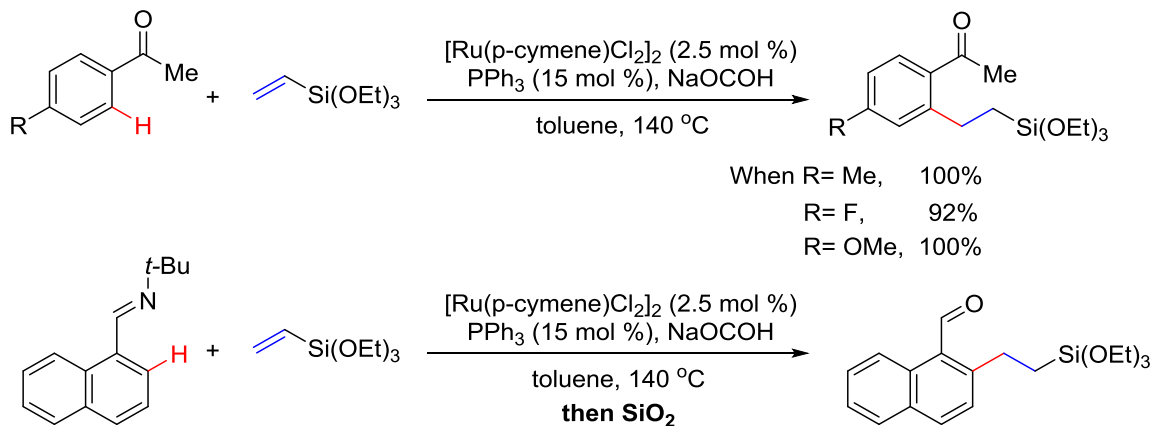


Scheme 5.13. Room temperature alkylation with a fully characterized Ru catalyst.



In 2006, the Darses and Genet group utilized the $[\text{Ru}(\text{p-cymene})\text{Cl}_2]_2$ as a versatile catalyst for both ketone and imine directed alkylations.²³ By combining the Ru pre-catalyst with a reductant, sodium formate, many aromatic ketones and imines were successfully alkylated (Scheme 5.14). According to the kinetic studies, a 1:3 ruthenium/phosphine ratio gave the best result. Later in 2008, the alkylation with styrenes was achieved with an electron-poor phosphine ligand, $\text{P}(\text{4-CF}_3\text{C}_6\text{H}_4)_3$, in which linear products were the major isomer.²⁴

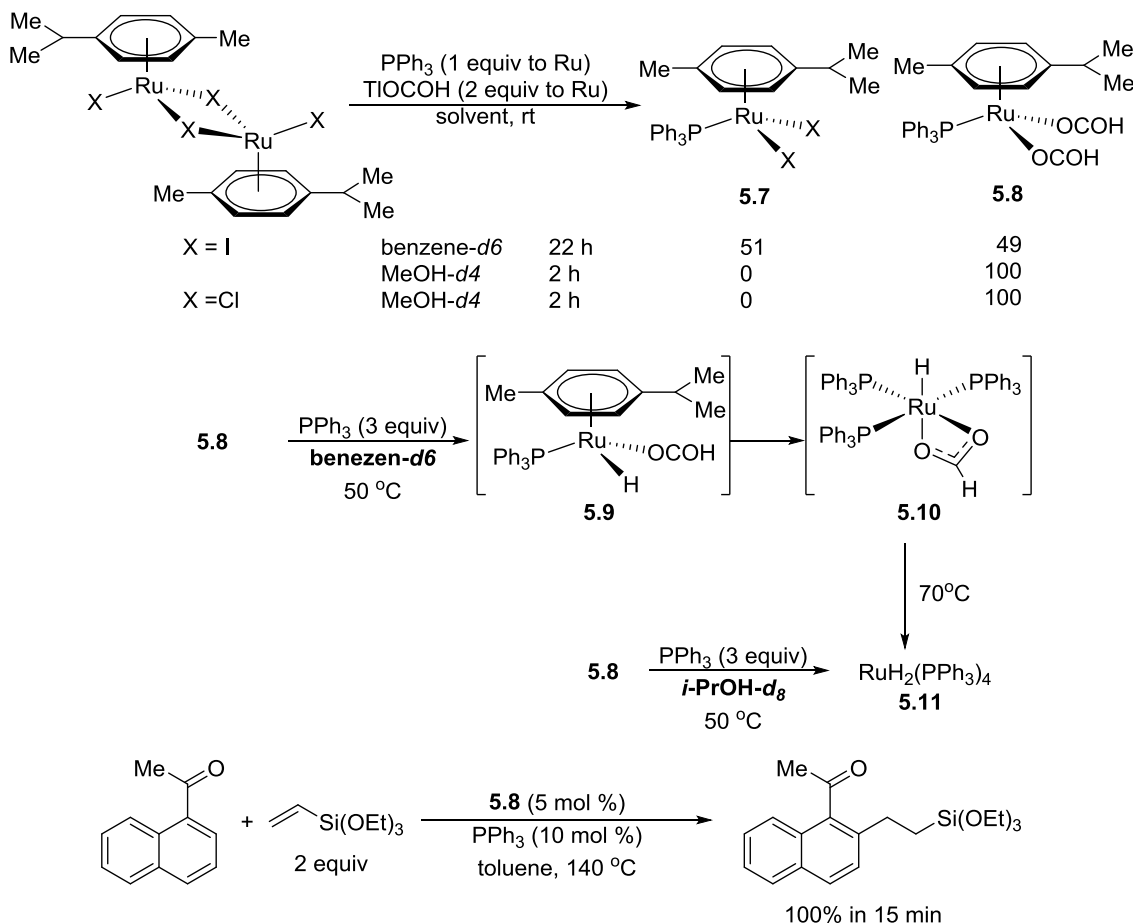
Scheme 5.14. A versatile Ru catalyst for alkylations of both aromatic ketones and imines.



To investigate the role of the formate salt, complexes **5.7** and **5.8** were synthesized as shown in Scheme 5.15.²⁵ Complex **5.8** exhibits higher reactivity for alkylation reaction, as the rapid decarboxylation of the formate intermediate gives a

monohydride ruthenium complex **5.9**, which can form **5.10** through ligand exchange with PPh_3 . Complex **5.10** can form the known dihydride ruthenium complex **5.11**.

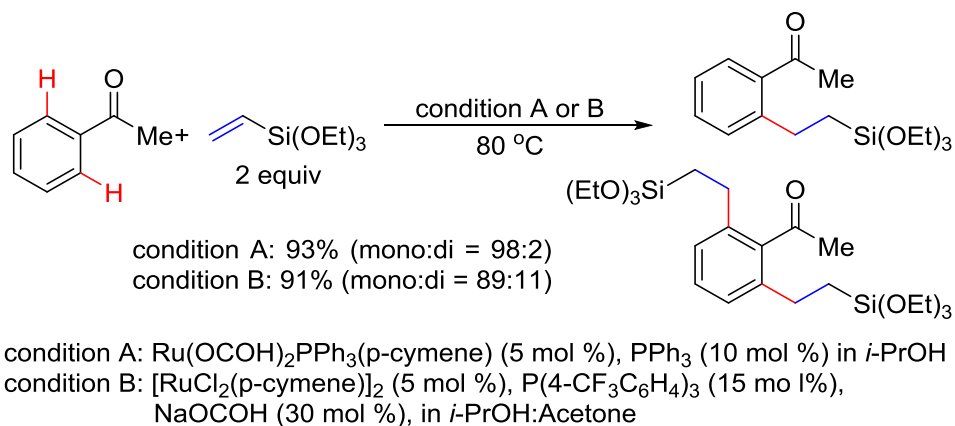
Scheme 5.15. Mechanistic study of formate salt in Ru-catalyzed alkylation.



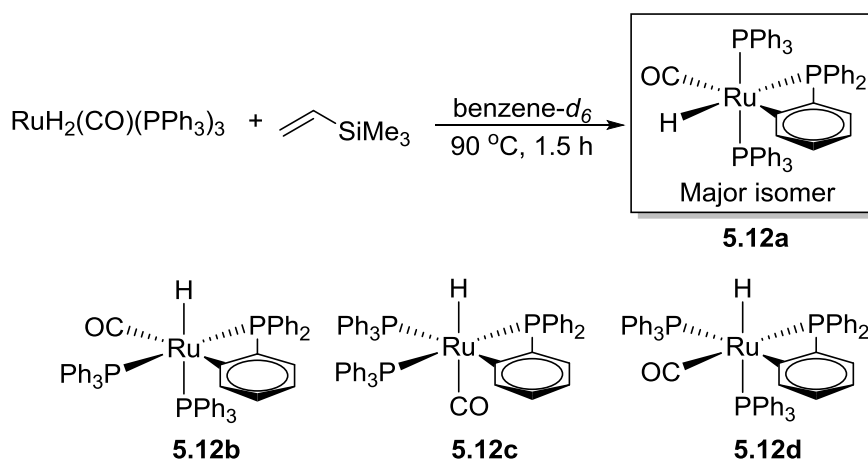
In 2009, the Darses group found that using isopropanol as a solvent could lower the temperature of the Ru-catalyzed alkylation reaction.²⁶ Either the pre-made or *in situ* generated catalyst can be used, affording the desired products in high yield (Scheme 5.16). Since the ketone can be reduced by the metal hydride species, acetone was introduced as a co-solvent and hydride acceptor to suppress the reduction. One year later, the tandem oxidation of benzylic alcohols to the corresponding ketones, and then

alkylation was achieved by the same group, using the less expensive RuCl_3 species as a precatalyst.²⁷

Scheme 5.16. Ru-catalyzed alkylation with isopropanol to lower the temperature.



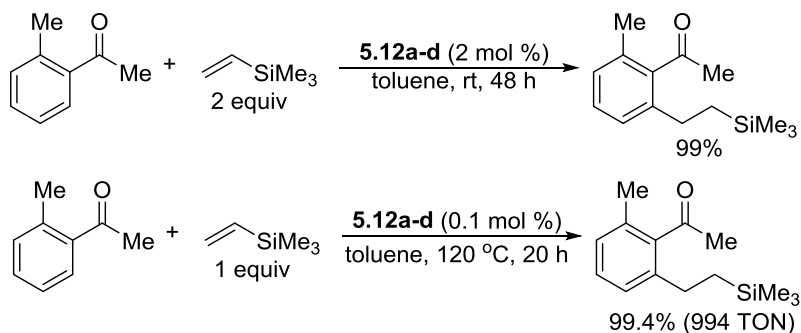
Scheme 5.17. Ru-catalyzed room temperature C–H alkylation of aromatic ketones.



In 2010, Murai, Kakiuchi, and coworkers reported a Ru-catalyzed room temperature C–H alkylation of aromatic ketones.²⁸ When treating $\text{RuH}_2(\text{CO})(\text{PPh}_3)_3$ with vinyl silane in benzene- d_6 at 90 °C for 1.5 h, a mixture of four Ru complexes was formed (Scheme 5.17). Using the mixture of Ru complexes, the alkylation can be carried out at

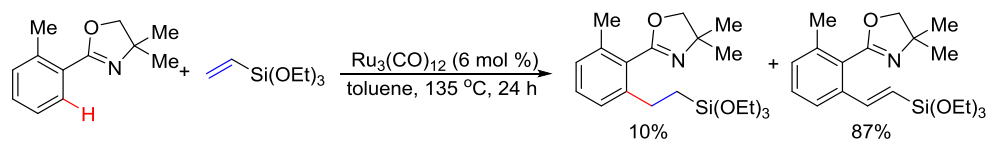
room temperature in excellent yield, or even with low catalyst loadings (0.1 mol%, 994 turnovers at 120°C) in excellent yields (Scheme 5.18).

Scheme 5.18. Reactivity in alkylation with new Ru catalysts.

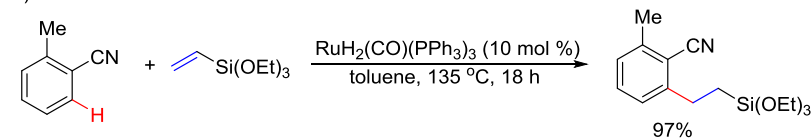


Scheme 5.19. Ru-catalyzed alkylation with various functional groups.

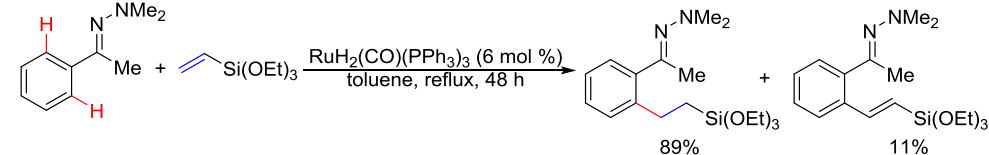
A) Oxazoline



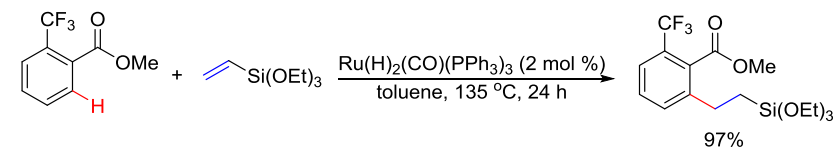
B) Nitrile



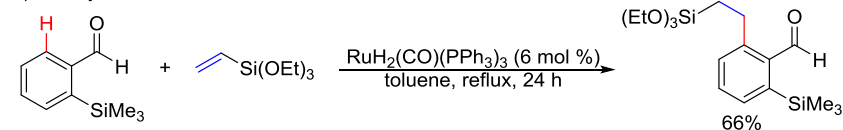
C) Hydrazone



D) Esters

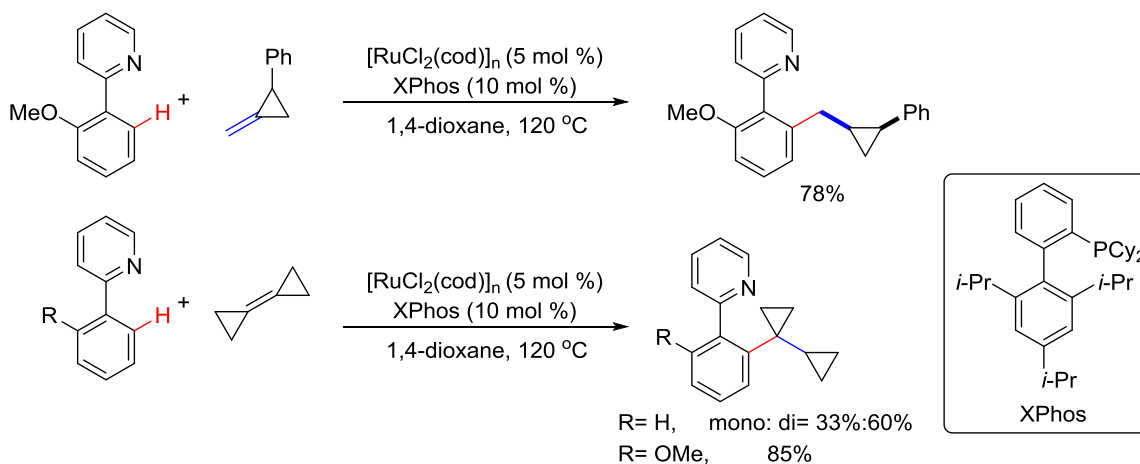


E) Aldehyde



Besides aryl ketones and imines, other types of substrates have also been employed for the Murai-type reaction. Functional groups, such as oxazolines²⁹, nitriles³⁰, hydrazones³¹, esters³², and aldehydes³³, can effectively assist chelation for the *ortho*-alkylation reactions (Scheme 5.19).

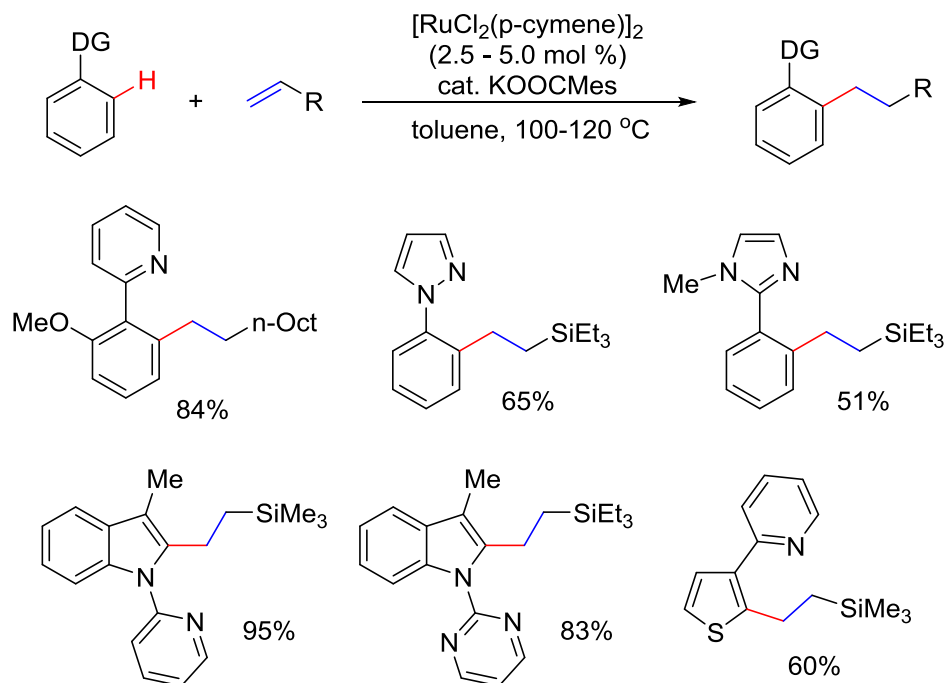
Scheme 5.20. Ru-catalyzed alkylation of 2-phenylpyridine derivatives.



In 2008, Ackermann and coworkers reported a Ru-catalyzed alkylation of 2-phenylpyridine derivatives.³⁴ The highly strained methylenecyclopropanes were used as the alkylation reagent without ring opening (Scheme 5.20). A *cis*-product was obtained and confirmed by X-ray crystallography. A mechanism similar to **Type A**, involving a ruthenium–hydride intermediate, was proposed for this transformation.

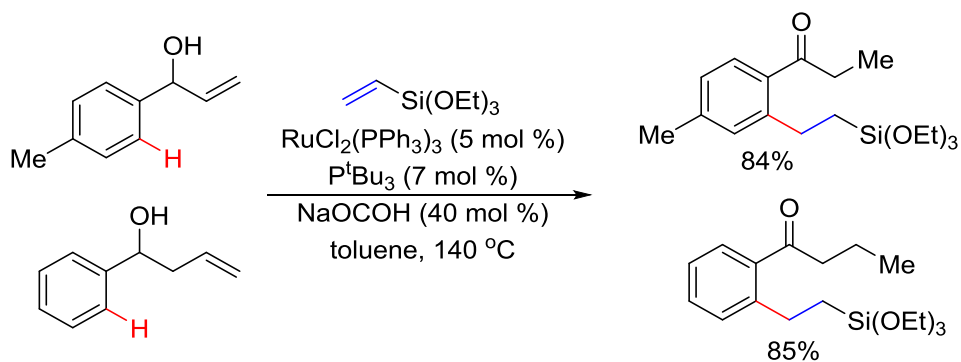
Later in 2013, Ackermann extended the Ru-catalyzed alkylation scope to simple olefins by using pyridine, pyrazole, indole, and imidazoline as the directing groups (Scheme 5.21).³⁵ Inspired by the role of carbonate ligands in Ru-mediated deprotonation/metalation pathways, the Ackermann group came up with a bulky carboxylate additive, KCO_2Mes . This additive was found to be crucial for this C–H alkylation reaction during the deprotonation of the C–H bond. Noteworthy, this reaction can tolerate water as cosolvent.

Scheme 5.21. Ru-catalyzed alkylation using heterocycles as the directing groups.



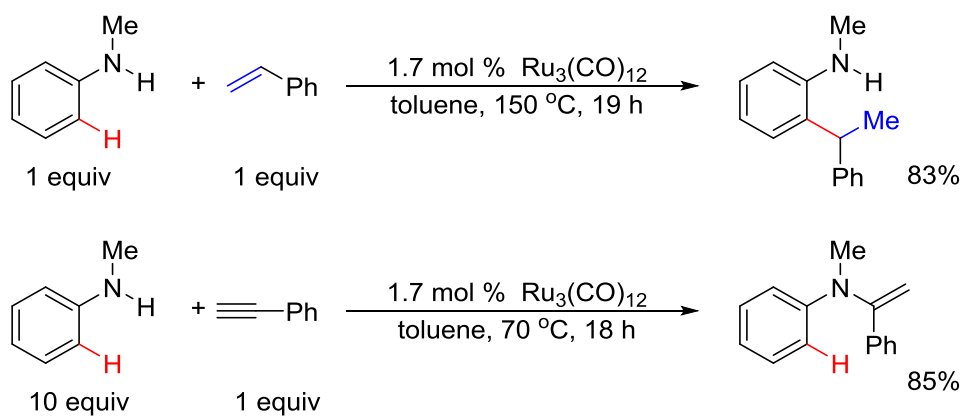
In 2009, through merging the olefin redox isomerization and *ortho* C–H alkylation transformations, the Martín-Matute group reported a Ru-catalyzed *ortho*-alkylation/tautomerization reaction of allylic and homoallylic alcohols (Scheme 5.22).³⁶ Aryl group with various electronic properties can be tolerated. High mono-alkylation selectivity can be achieved for most substrates.

Scheme 5.22. Ru-catalyzed alkylation/tautomerization reaction of allylic and homoallylic alcohols.



In 1999, Uchimaru reported one example of *N*-methyl aniline reacting with styrene to give an *ortho*-alkylated product with Ru catalysis (Scheme 5.23).³⁷ In this reaction, the branched product was obtained, which is due to the benzylic stabilization of the Ru-complex. When an alkyne was applied, hydroamination became the major reaction pathway. The mechanism for this reaction is still not clear.

Scheme 5.23. One example on Ru-catalyzed alkylation of *N*-methyl aniline.

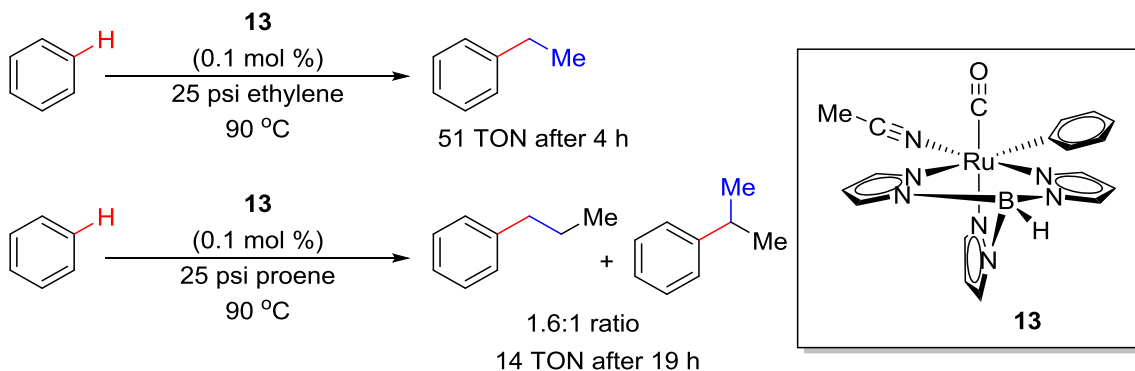


5.3.1.2 Non-chelation control

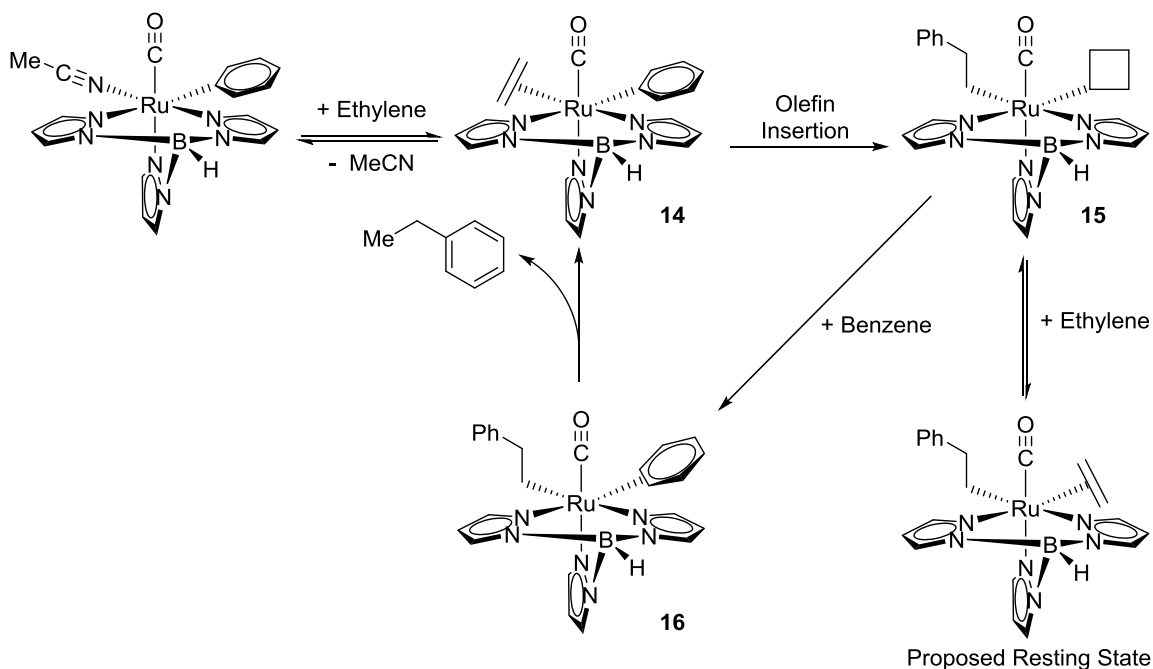
In 2003, Gunnoe and coworkers reported a Ru-catalyzed C–H alkylation of simple benzene (Scheme 5.24).¹¹ The hydridotris(pyrazolyl)borate (TAB) ligand was used to form Ru catalyst **13**, which can catalyze the alkylation of benzene with ethylene gas in 51 turnovers over 4 h. The 1.6:1 linear to branched ratio was observed using propene as the alkylation reagent with 14 turnovers after 19 h. Later DFT study by the Goddard group suggests the rate-determining step of the reaction is the olefin migratory insertion.³⁸ As the ethylene pressure increased, there was a resulting decrease in the reaction rate. The proposed catalytic cycle (Scheme 5.25) starts with ligand exchange

with ethylene, followed by insertion of the olefin with the C–Ru bond, and finally C–H bond activation of the benzene to release of the product.

Scheme 5.24. Ru-catalyzed C–H alkylation of simple benzene.

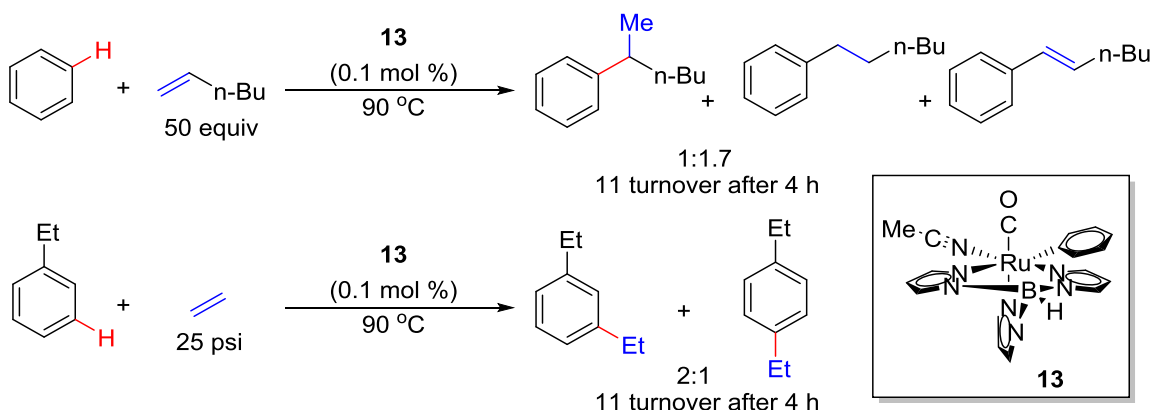


Scheme 5.25. Proposed mechanism for Ru-catalyzed C–H alkylation of simple benzene.



When 1-hexene was used as the alkylation reagent, the linear product was obtained as the major product with benzene as the substrate. The regioselectivity indicates the 2,1-insertion is slightly favored and can be explained by the steric interaction between the substituent groups of the olefin with the pyrazolyl rings on the catalyst. When ethylbenzene was used, the *meta*- and *para*-selective products were obtained, which is a unique difference from typical Friedel-Crafts reactions (Scheme 5.26).

Scheme 5.26. Ru-catalyzed C–H alkylation of simple benzene with 1-hexene.

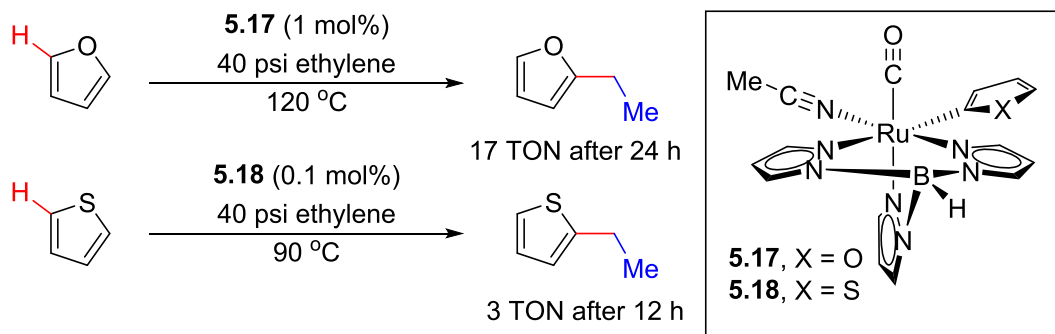


In the same year, Gunnoe, Petersen, and coworkers extended the Ru-catalyzed alkylation to heteroaromatic substrates.³⁹ Catalysts **5.17** and **5.18** containing the corresponding heteroaryl ligands, were used for the alkylation of furans and thiophenes (Scheme 5.27). A DFT study by Goddard and coworker suggested a similar reaction pathway as the previous arene alkylation.⁴⁰

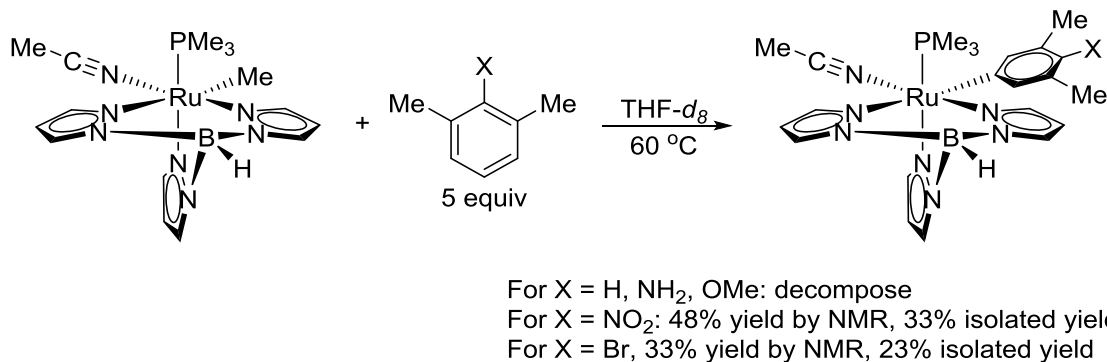
Later in 2007, Gunnoe, Cundari, and coworkers, discovered evidence for a σ -bond metathesis mechanism.⁴¹ The observance of electron-poor arenes affording higher alkylation yields (Scheme 5.28) suggested that the electrophilic aromatic substitution

C–H bond cleavage mechanism could be excluded. The Hammett plot was obtained with a positive ρ -value, suggesting a preference for a σ -bond metathesis mechanism in the C–H activation step.

Scheme 5.27. Ru-catalyzed alkylation of heteroaromatic substrates.



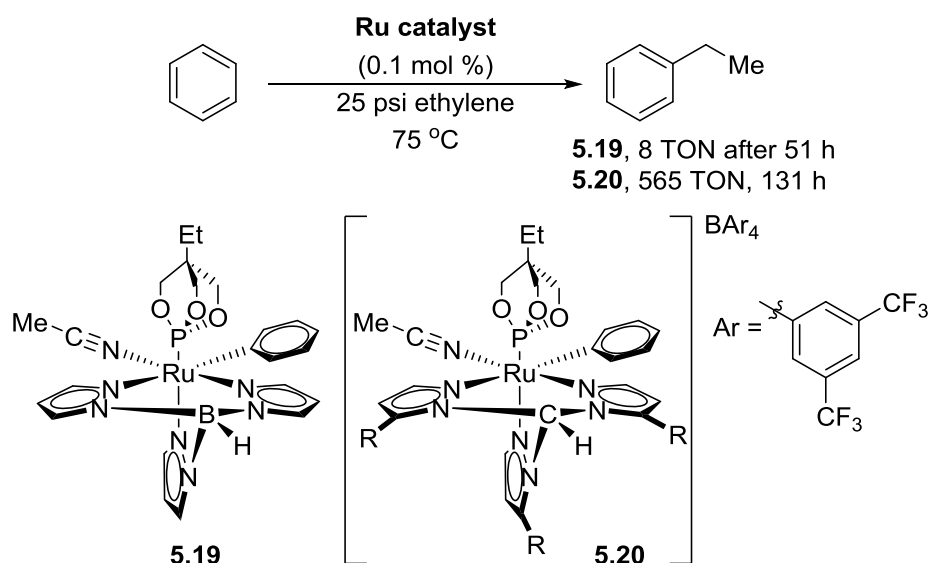
Scheme 5.28. Mechanistic study on Ru-catalyzed alkylation of simple arenes.



In the same year, Gunnoe and co-workers studied the effect of ancillary ligands on the Ru catalyst in the reaction.⁴² The CO ligand was found to promote catalyst decomposition through the formation of CO-bridged multinuclear complexes. Following this observation in 2008, Gunnoe, Cundari and coworkers, developed catalyst **5.19**, which contains a bicyclic phosphite ligand (Scheme 5.29). Using this catalyst the hydroarylation reaction can be achieved at lower temperatures.⁴³ Catalyst **5.19** exhibited enhanced stability compared to the CO-based catalyst. On the other hand, given that the rate-

determining step was found to be the C–H cleavage step, a highly reactive cationic catalyst (**5.20**) was developed by Gunnoe, Cundari and coworkers, which can achieve 565 TON after 131 h.⁴⁴ It's likely the e-deficient nature of the ligand significantly, increased the binding affinity of benzene, which consequently promoted the C–H activation.

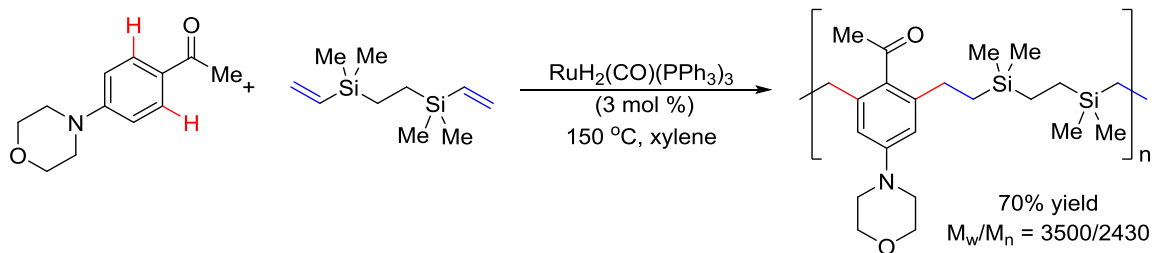
Scheme 5.29. Ru-catalyzed alkylation of simple arenes with high TON.



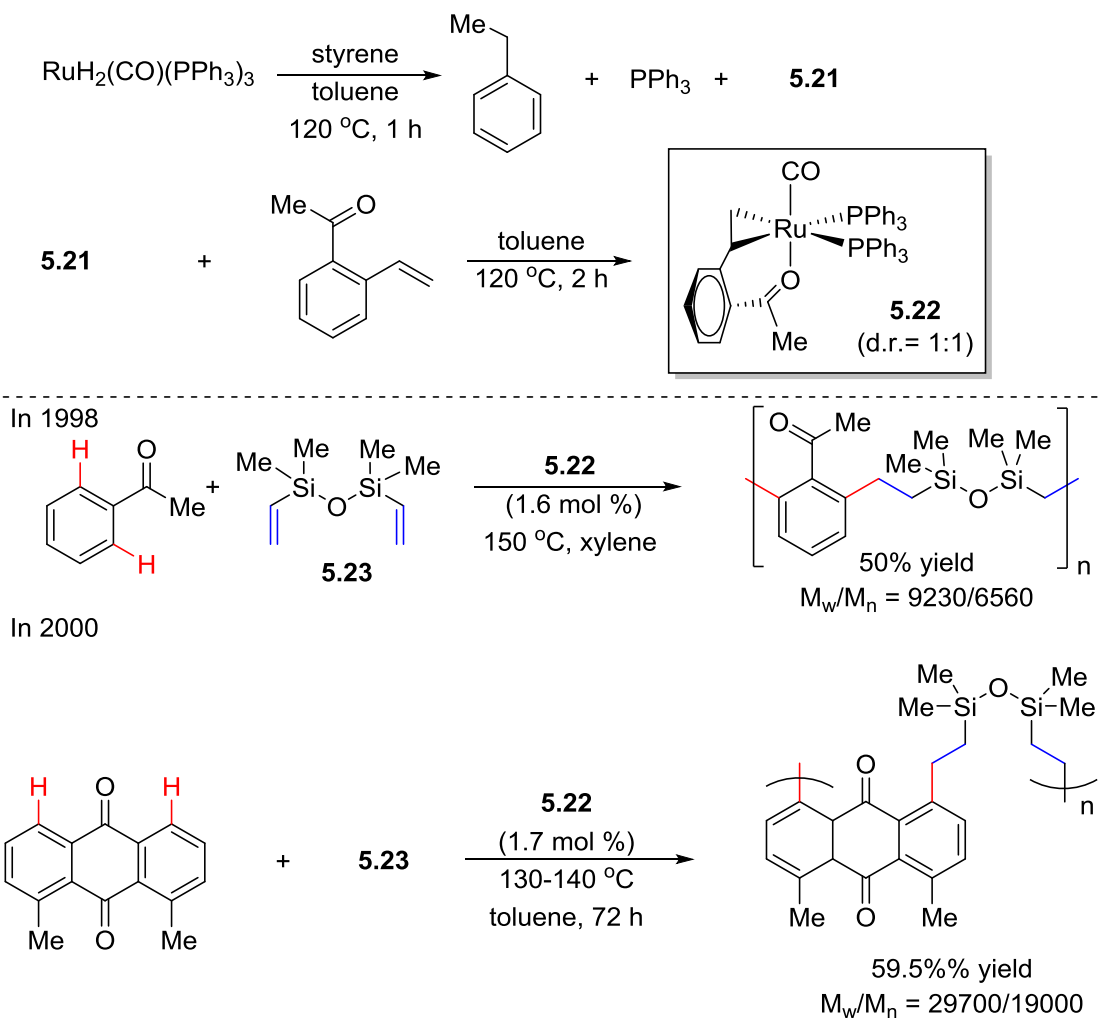
5.3.1.3 Application of Ruthenium-Catalyzed Arene C–H Bond Alkylation

The Ru-catalyzed arene C–H alkylation has been applied in polymer synthesis, Weber and coworkers reported a step-growth copolymerization between an acetophenone and a 1,7-silyldiene in 1995 (Scheme 5.30).⁴⁵ This reaction is sensitive to the electronic properties of acetophenone, where electron rich arenes gave polymers of a higher molecular weight.

Scheme 5.30. Ru-catalyzed step-growth copolymerization with acetophenone.

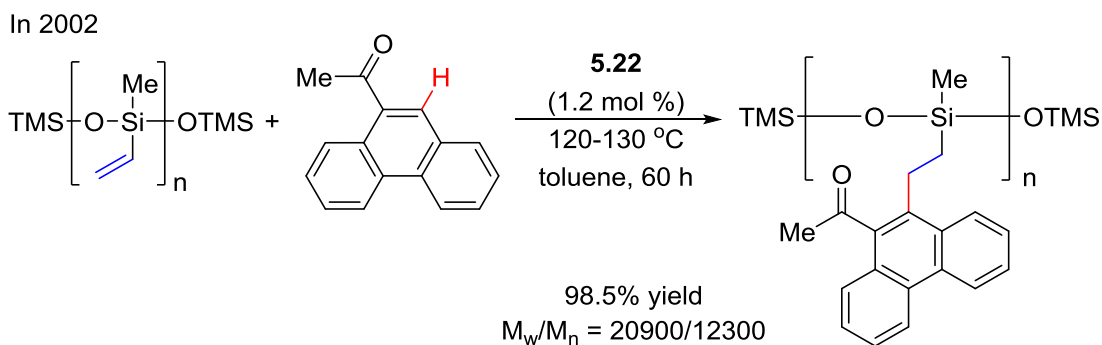


Scheme 5.31. Ru-catalyzed copolymerization with *in situ* generated catalyst.

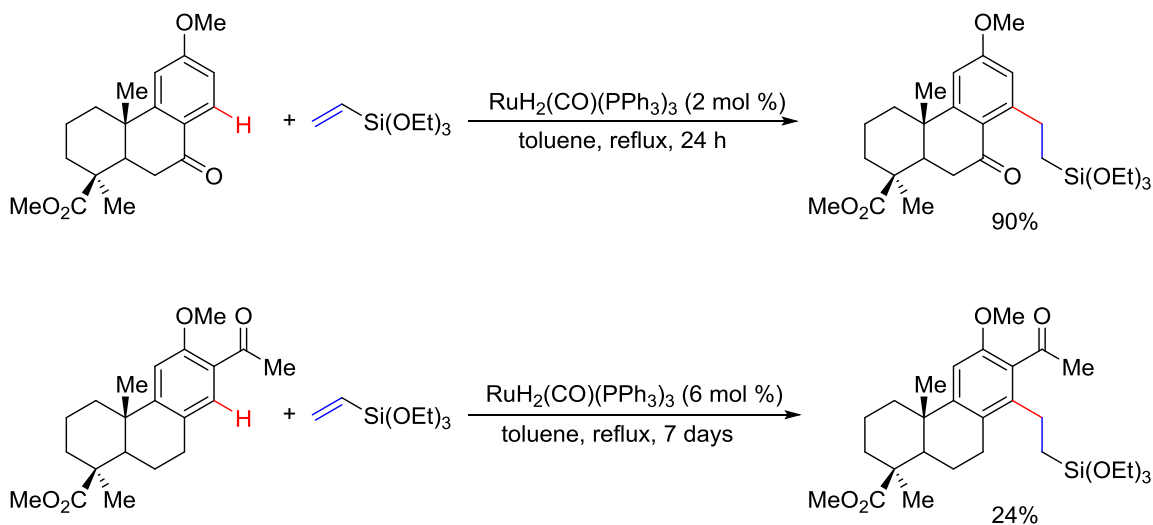


Weber and coworkers further developed a new catalyst for the copolymerization reactions.⁴⁶ Complex **5.22** prepared from complex **5.21** with styrene was able to provide much higher molecular weight polymers than using complex **5.21** for the copolymerization, as shown in Scheme 5.31.⁴⁷ The spectral and thermal properties of these polymers have been studied and reported. It has also been used for post-functionalization of a silicon-based polymer (Scheme 5.32).⁴⁸ In addition, this method has been employed to derivatize diterpenoid natural products (Scheme 5.33).⁴⁹

Scheme 5.32. Ru-catalyzed a post-functionalization with a silicon-based polymer.



Scheme 5.33. Ru-catalyzed derivatization of diterpenoid natural products.

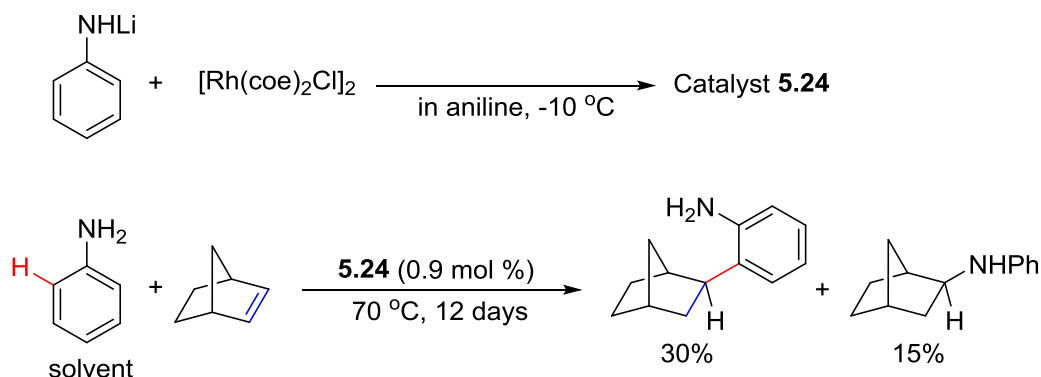


5.3.2 RHODIUM CATALYSIS

5.3.2.1 Electron-Rich Benzene Rings and Heterocycles

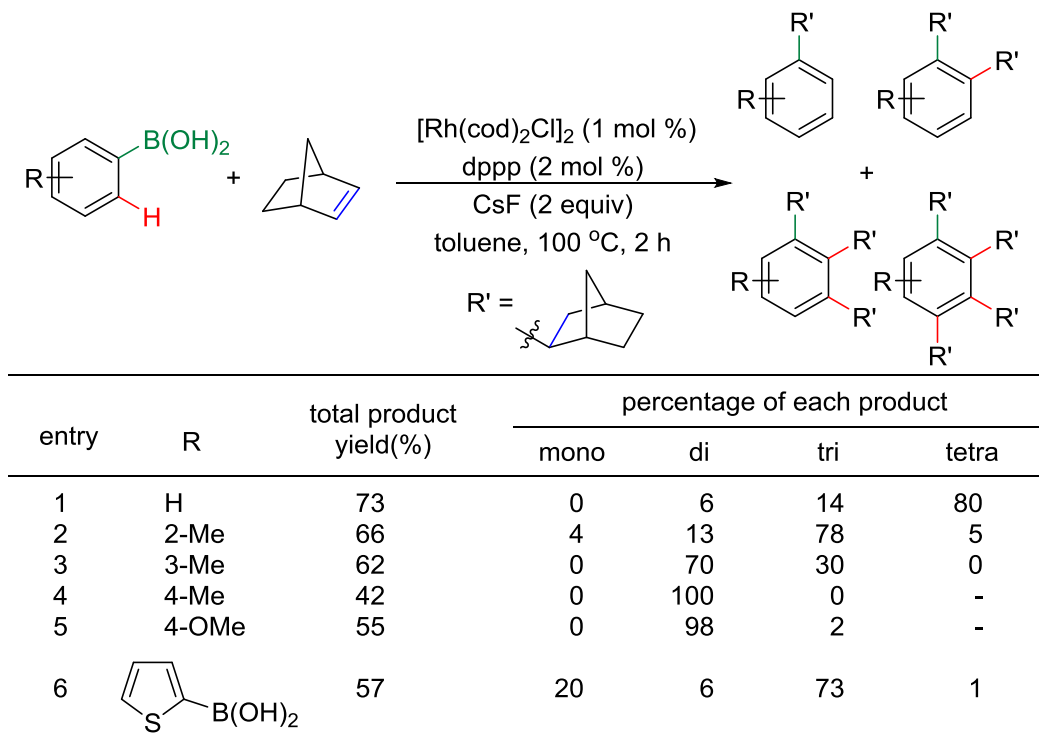
In 1992, Brunet and coworkers discovered an unexpected Rh-catalyzed hydroarylation of norbornene with aniline or diphenylamine.⁵⁰ The catalyst **5.24** was prepared by reacting lithium anilide with $[\text{Rh}(\text{PEt}_3)_2\text{Cl}]_2$ using aniline as a solvent. Attempts to use **5.24** to catalyze the designed hydroamination of norbornene resulted in only 15% yield. However, the *ortho*-alkylation product was isolated in 30% yield (Scheme 5.34). Similarly to the sp^3 nitrogen assisted C–H alkylation with Ru catalyst (see Scheme 5.23), this mechanism has not been fully understood.

Scheme 5.34. Rh-catalyzed hydroarylation of norbornene with aniline or diphenylamine.

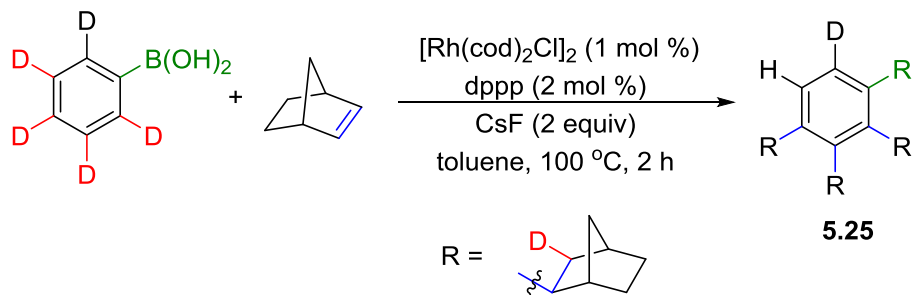


In 2000, Miura and coworkers reported a multi-alkylation reaction of aryl boronic acids with norbornene.⁵¹ Norbornene has previously been shown to couple well with arenes; however, in this case, its unique bicyclic structure allows further alkylations to provide mono-, di-, tri-, and tetrasubstituted products (Scheme 5.35). Mechanistic insights were gained through a deuterium experiment, in which the deuteriums of the starting material were transferred to the C2-position of the norbornyl group (**5.25**) (Scheme 5.36).

Scheme 5.35. Rh-catalyzed multi-alkylation of aryl boronic acids.



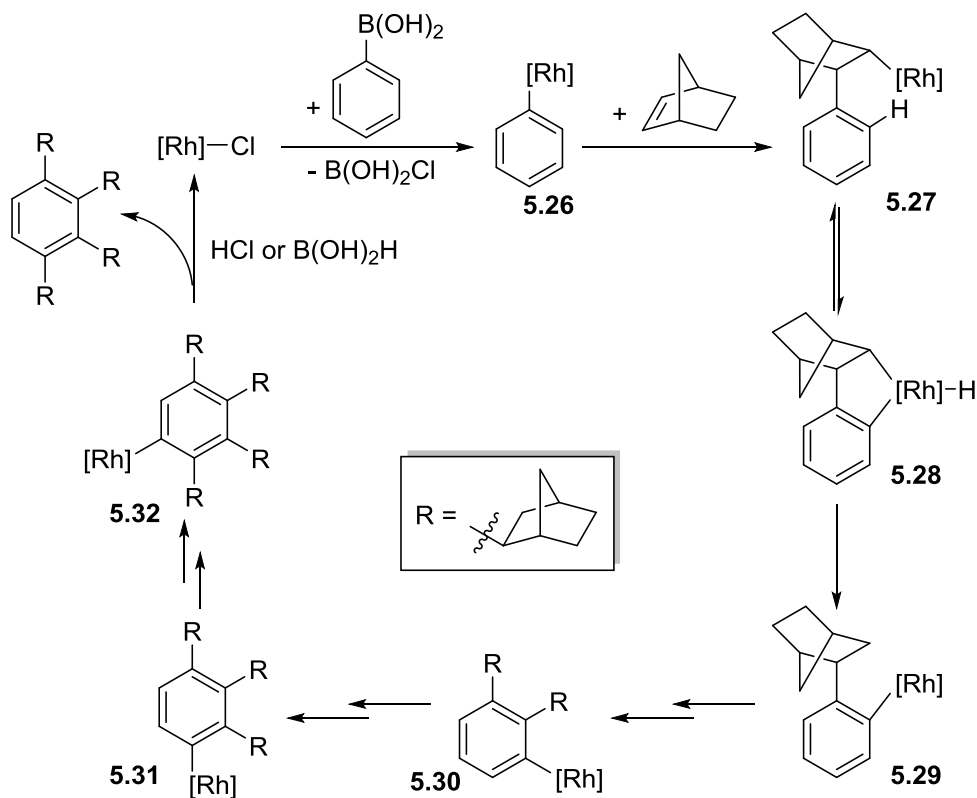
Scheme 5.36. Deuterium labeling in Rh-catalyzed multi-alkylation.



The proposed mechanism is depicted in Scheme 5.37, beginning with transmetalation of the $\text{ArB}(\text{OH})_2$ with the rhodium catalyst to generate an aryl-rhodium species **5.26**. Migratory insertion into norbornene through an *exo*-fashion affords alkyl-rhodium species **5.27**. Sequential C–H bond cleavage then reductive elimination results

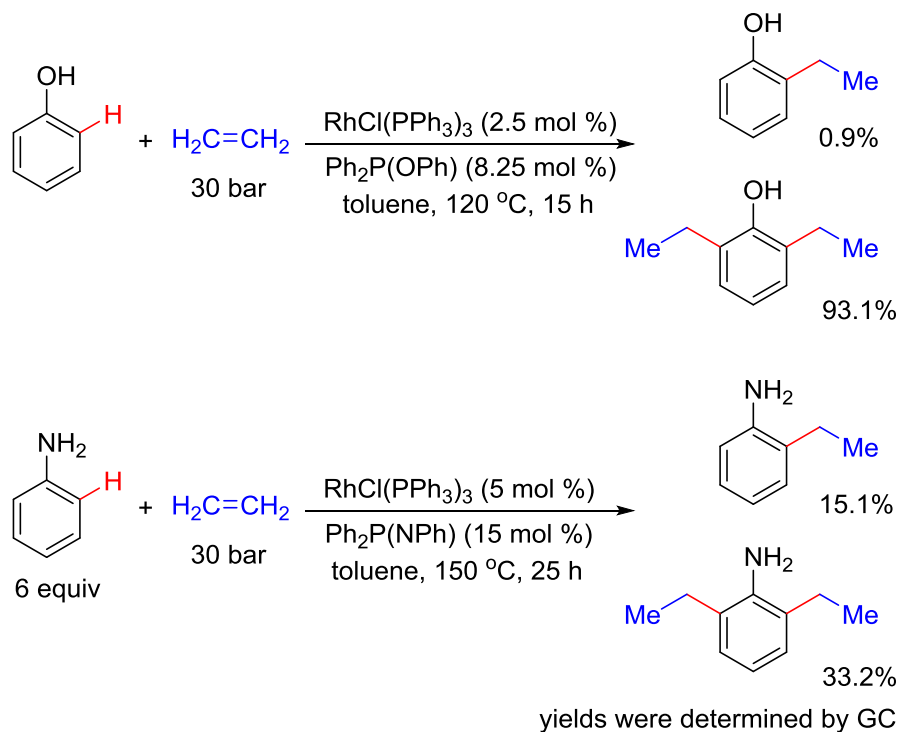
in intermediate **5.29**, which can repeat the insertion and reductive elimination to give multi alkylated arenes **5.30**, **5.31** and **5.32**.

Scheme 5.37. Proposed mechanism for Rh-catalyzed multi-alkylation.

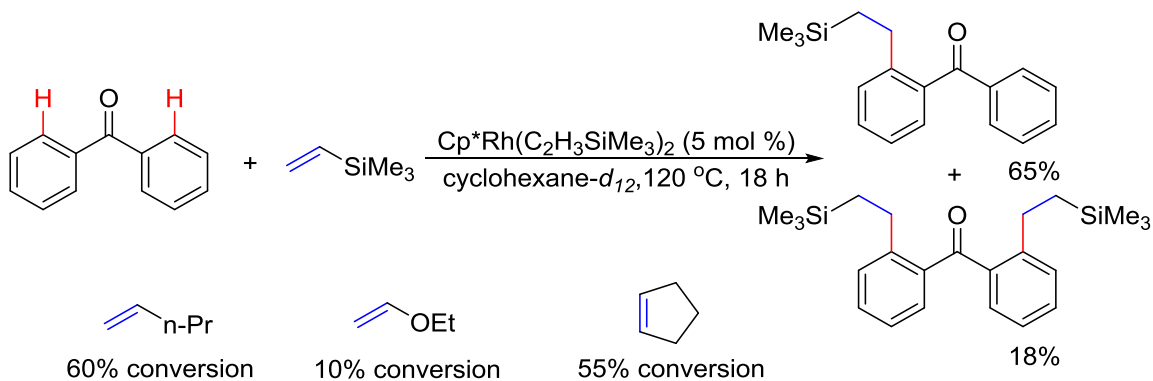


In 2006, the Cole-Hamilton group reported a Rh-catalyzed *ortho*-alkylation of phenols and anilines (Scheme 5.38).⁵² The alkylation of phenols was similar to the Ru-catalyzed reaction by Lewis, using a phosphinite additive to form a covalent bond temporarily with phenol or aniline through transesterification (Scheme 5.3). Thus, the directing group was installed and later removed *in situ*. Other metals such as Ru and Pd were also examined but were found less effective than Rh. Ethylene was the only alkene used in these studies.

Scheme 5.38. Rh-catalyzed *ortho*-alkylation of phenols and anilines.



Scheme 5.39. Rh-catalyzed alkylation of aromatic ketones with new Rh catalyst.

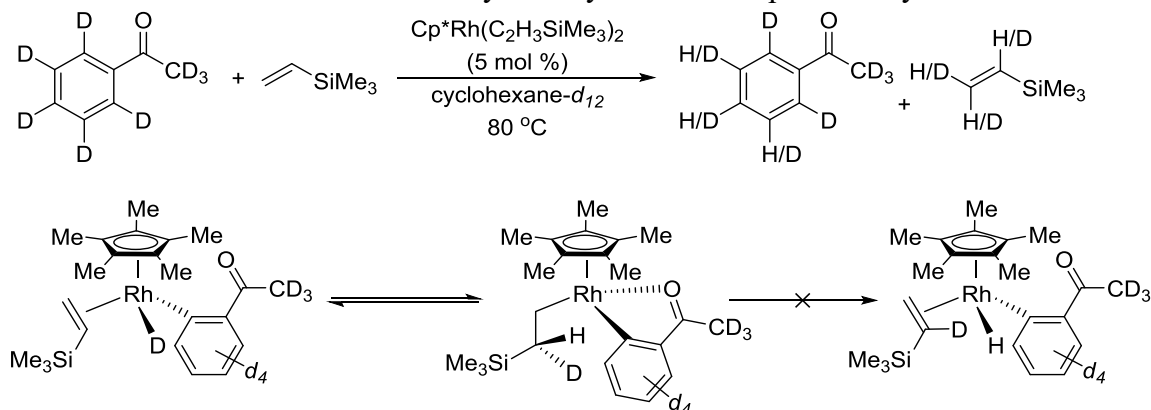


In 1999, Brookhart and coworkers developed an aromatic ketone-directed *ortho*-alkylation with simple olefins using a Rh(I) catalyst (Scheme 5.39).⁵³ Linear products were obtained exclusively, and bulky terminal olefins were found to react faster and give

higher yields. When isomerizable olefins were used, the alkylation gave a moderate conversion, and isomerization to internal olefins was observed.

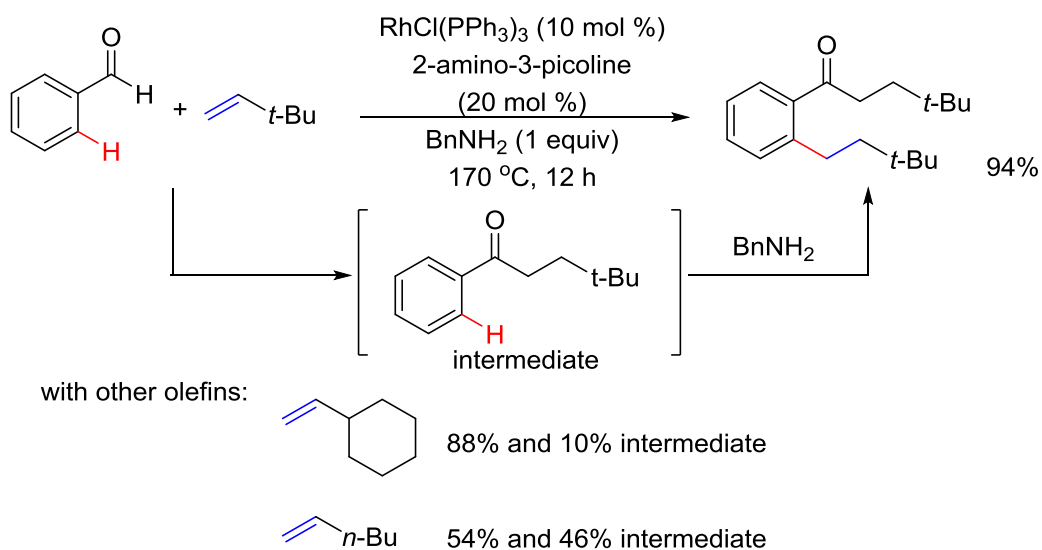
A deuterium study on this transformation suggested that all the C–H bonds on arenes could be activated by the Rh catalyst (Scheme 5.40); however, only the *ortho*-positions favor reductive elimination. This effect can be explained by the chelation effect of the ketone, blocking open coordination sites on the Rh catalyst, forcing β -hydride elimination. The increased steric demands of this intermediate should have a higher tendency to undergo reductive elimination.

Scheme 5.40. Deuterium study on alkylation with Cp^*Rh catalyst.

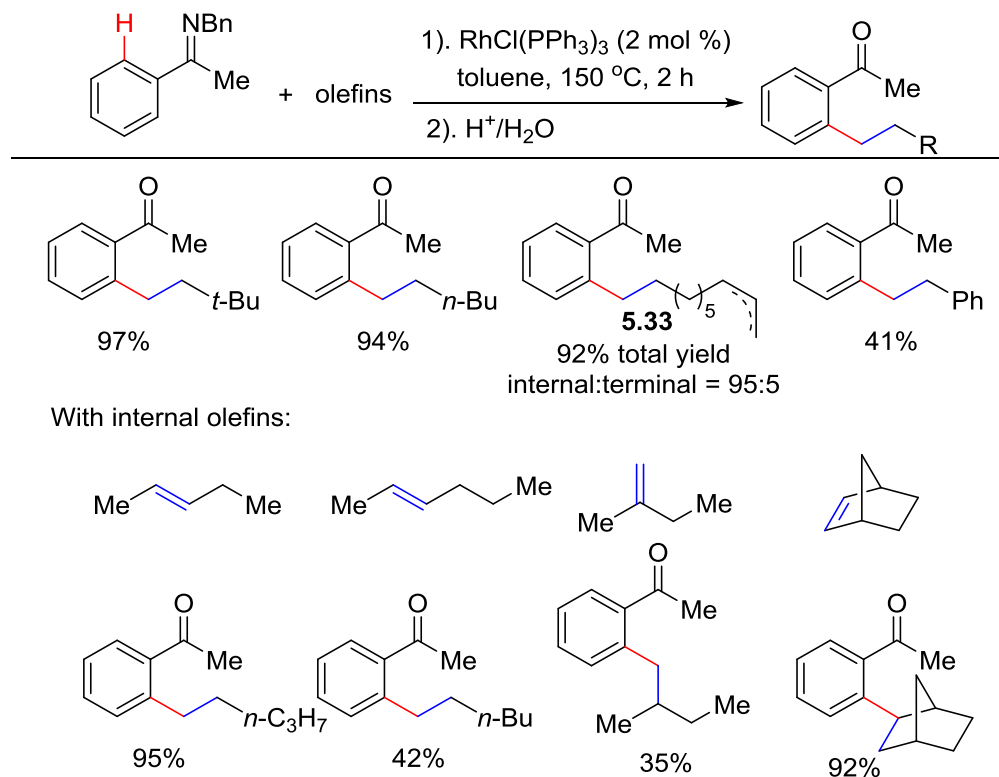


In 2000, Jun and coworkers developed a Rh-catalyzed dialkylation of benzaldehydes, in which both the *ipso*-position of the aldehyde and the *ortho*-position of the arene are alkylated with olefins (Scheme 5.41).⁵⁴ Through the examination of the reaction intermediates, the aldehyde C–H bond was proposed to be activated first. The resulting ketone can subsequently condense with benzylamine to give an imine intermediate, which should assist the *ortho*-alkylation.

Scheme 5.41. Rh-catalyzed *ipso*- and *ortho*-dialkylation of benzaldehydes.

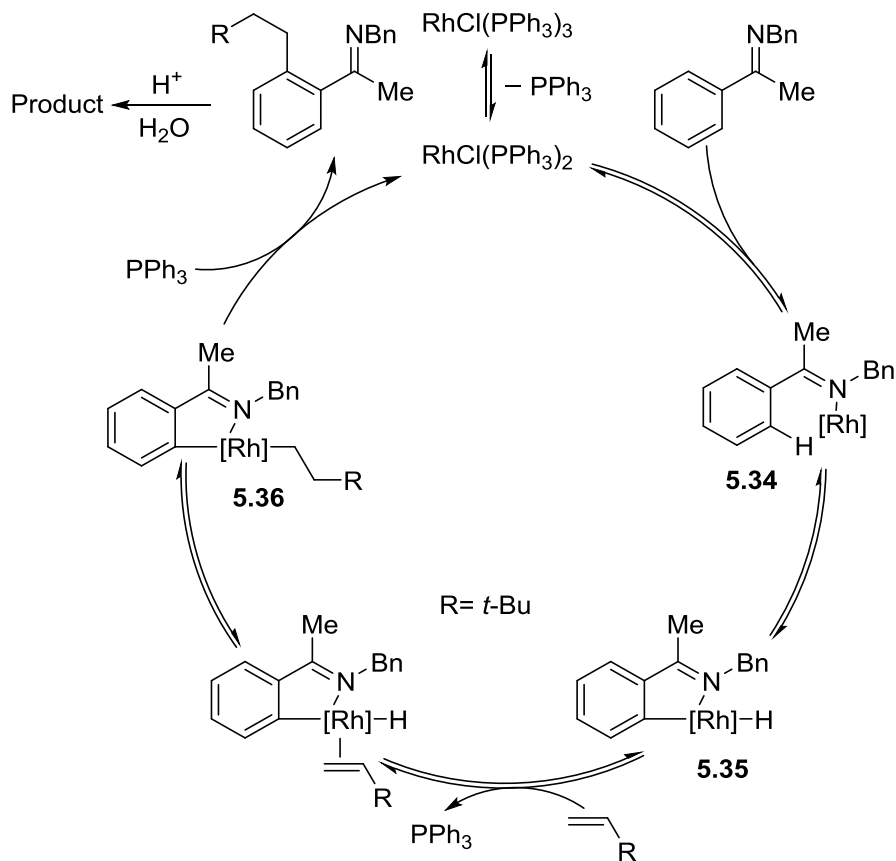


Scheme 5.42. Rh-catalyzed alkylation of aromatic ketimines with internal olefins.



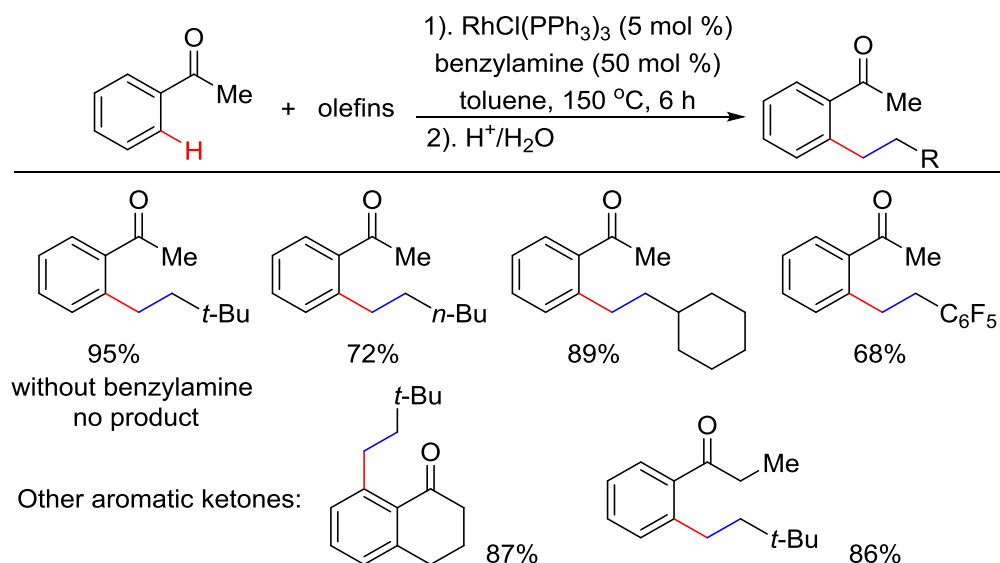
Later, in 2002, the Jun group developed a chelation-assisted alkylation of aromatic ketimines with olefins using Rh catalysis (Scheme 5.42).⁵⁵ Isomerizable 1-alkenes and α,ω -dienes (**5.33**) can afford the desired products in high yields, which were problematic in the previous Ru-based systems (Section 5.10). Notably, internal olefins also provided linear products, stemming from a facile isomerization of the alkene π -bond to the terminal position. In 2004, a microwave-assisted alkylation of aromatic imines was achieved by the same group.⁵⁶

Scheme 5.43. The proposed mechanism of Rh-catalyzed alkylation of aromatic ketimines.



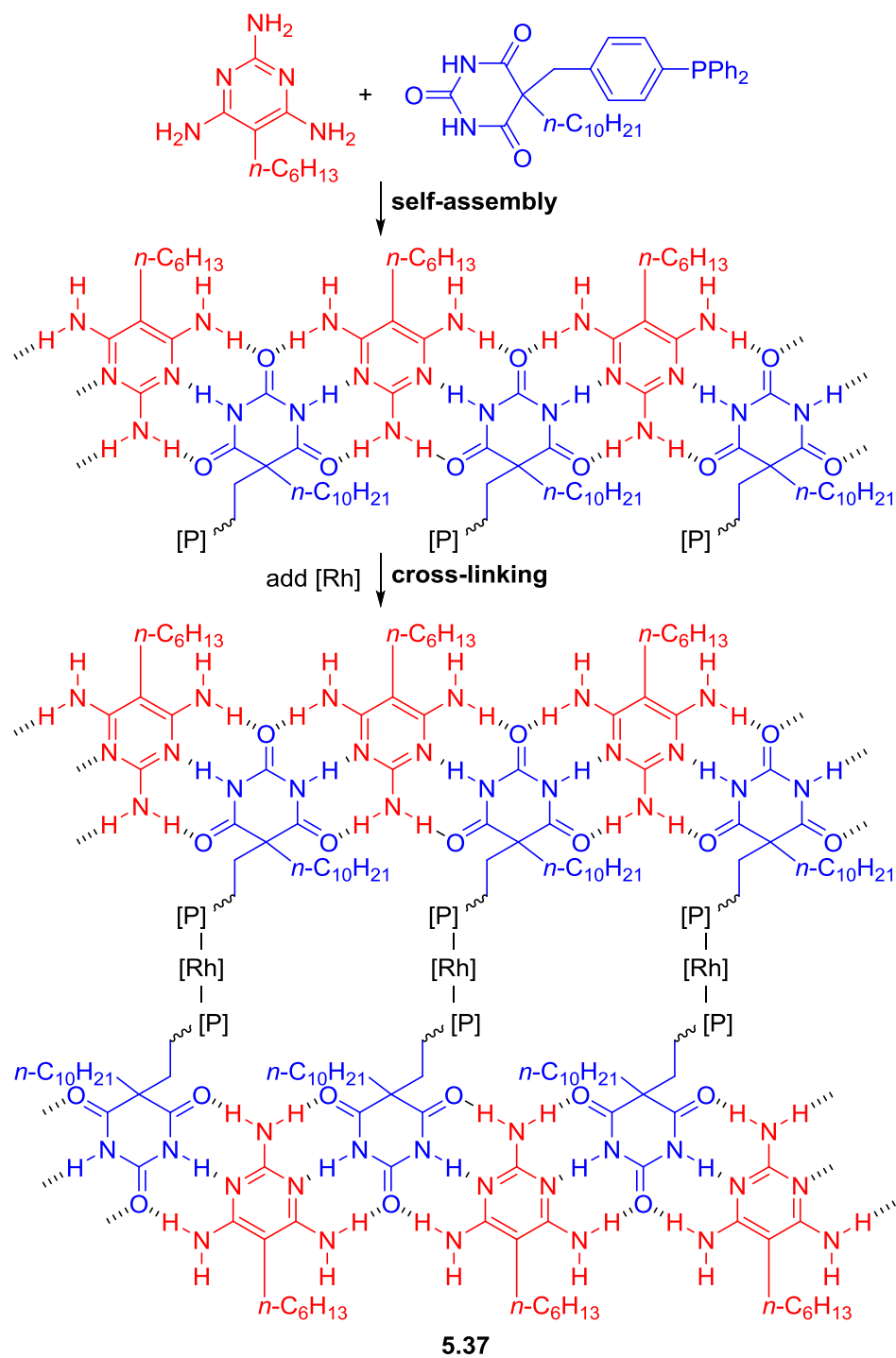
The catalytic cycle was proposed to begin with dissociation of PPh_3 and coordination with the nitrogen of the ketimine to give **5.34**. The subsequent oxidative addition of the C–H bond would give Rh-hydride intermediate **5.35**, which upon ligand exchange with an olefin, hydride migratory insertion, and reductive elimination affords the *ortho*-alkylated product (Scheme 5.43). Supported by H/D scrambling experiment, the reductive elimination was proposed as the rate-determining step.

Scheme 5.44. Rh-catalyzed alkylation of aromatic ketones with catalytic benzylamine.



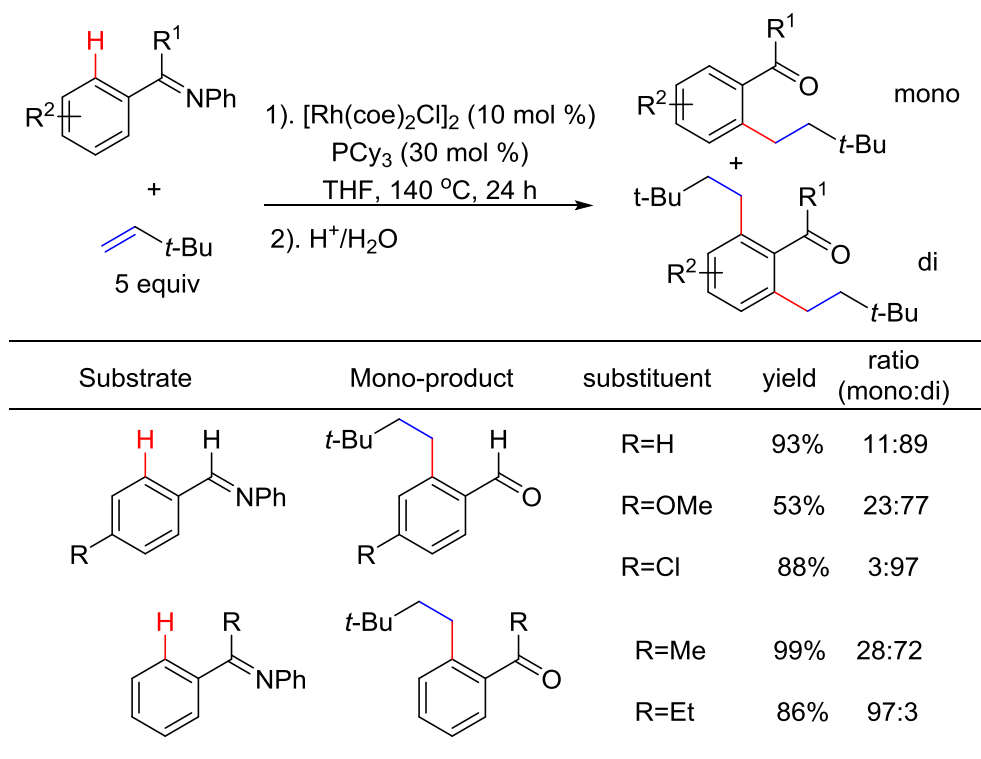
The imine moiety was found to play an important role in the *ortho* C–H alkylation reaction, likely due to its strong coordination ability. Given that imines can be reversibly formed from ketones and amines, a catalytic amount of amine, in principle, is needed to generate an imine intermediate in situ, which can ultimately enable a general *ortho* C–H alkylation of ketones. Indeed, Jun and coworkers found when 50 mol% of benzylamine was used, the aromatic ketones can be efficiently alkylated at the *ortho*-position (Scheme 5.44).

Scheme 5.45. Rh catalysis using recyclable self-assembly-supported (SAS) system.



In 2005, Jun and coworkers further developed a recyclable self-assembly-supported (SAS) system for the *ortho*-alkylation of aromatic imines.⁵⁷ The illustrative preparation of the SAS system is shown in Scheme 5.45. An interesting feature of this system is that it operates under homogeneous conditions at high temperature while it remained heterogeneous at room temperature. Such a property allowed the catalyst (**5.37**) to be easily recycled and reused for 8 cycles of the alkylation reaction without any loss of reactivity.

Scheme 5.46. Rh-catalyzed alkylation of aromatic aldimines and ketimines with olefins.

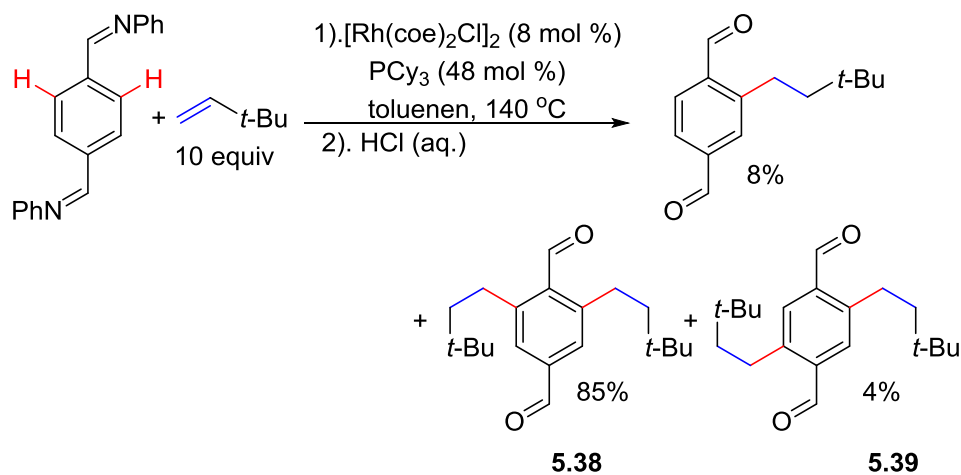


In 2001, Lim and coworkers reported a Rh-catalyzed alkylation of aromatic aldimines and ketimines with olefins.⁵⁸ Using electron-rich PCy₃ as the ligand, the bis-alkylation became the major reaction pathway. The reaction exhibits complete selectivity

for anti-Markovnikov addition. Using isomerizable alkenes as substrates gave lower yields (Scheme 5.46).

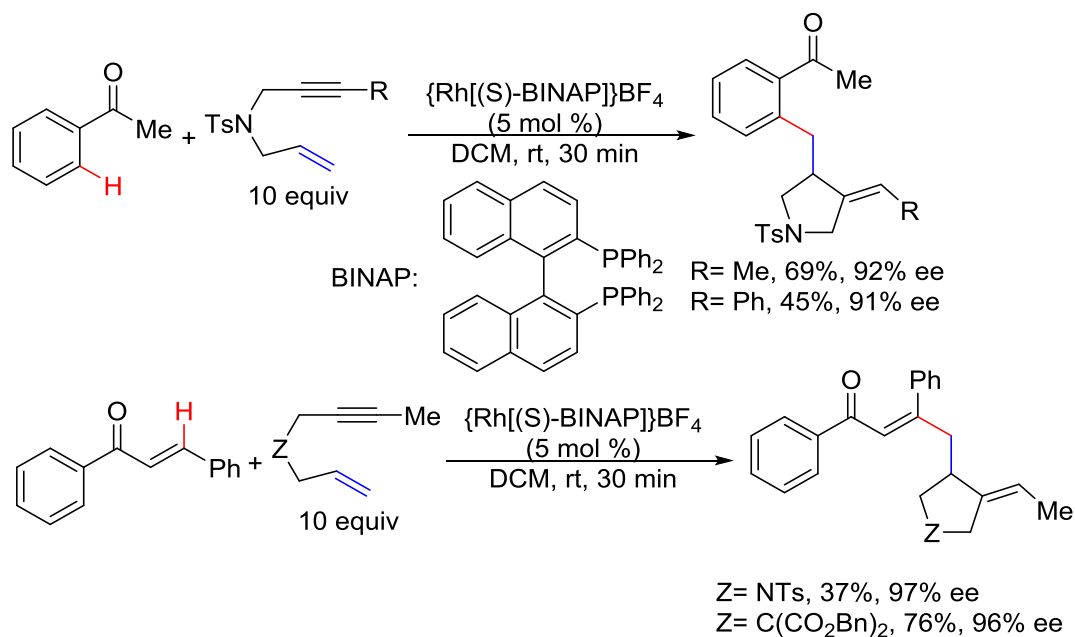
In 2005, Lim and coworkers further studied the Rh-catalyzed alkylation of terephthaldimine with olefins,⁵⁹ in which the 2,6-dialkylated product (**5.38**) was the major product instead of the 2,5-dialkylated isomer (**5.39**). When 2-alkylated substrate was used, the alkylation still occurred at the C6 position, which suggested the electron-donating alkyl substituent likely enhanced the coordination ability of the adjacent ketimine (Scheme 5.47).

Scheme 5.47. Rh-catalyzed alkylation of terephthaldimine with olefins.



In 2007, Shibata and coworkers investigated the Rh-catalyzed alkylation of aromatic ketones with diynes and enynes, in which a tandem transformation occurred resulting in a monocyclic product (Scheme 5.48).⁶⁰ When a chiral bidentate ligand (e.g. BINAP) was used, high enantioselectivity was obtained. A similar transformation was reported by Tanaka and coworkers in 2008 using (R)-H₈-BINAP as the chiral ligand.⁶¹

Scheme 5.48. Rh-catalyzed alkylation of aromatic ketones with diynes and enynes.



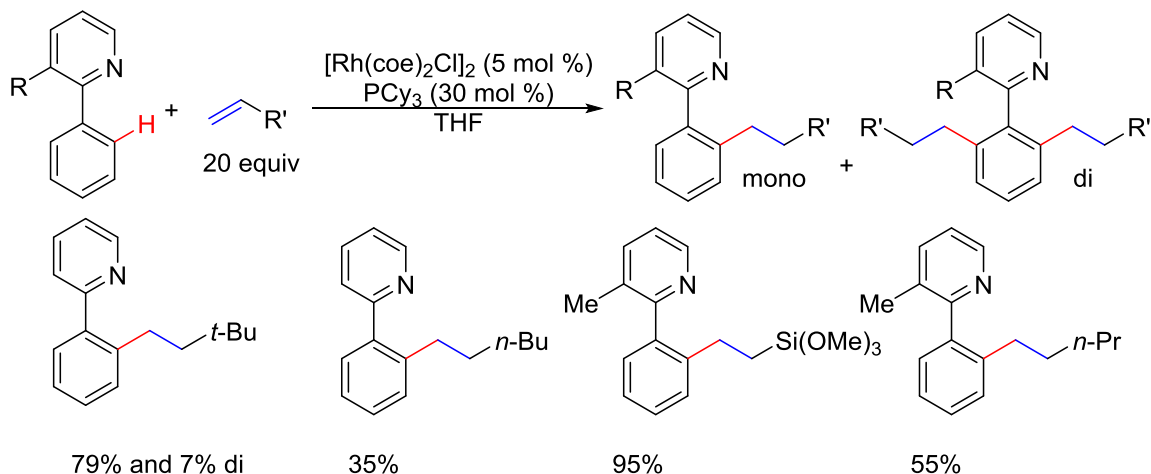
In 1994, Kim and coworkers described a Rh-catalyzed alkylation of 2-phenylpyridines with olefins (Scheme 5.49).⁶² The linear products were obtained as the major isomers, suggesting a Rh-hydride involved mechanism. Using isomerizable olefins as the alkylation reagents resulted in lower yields. By adding a methyl group at the 3-position of the pyridine ring, the mono-alkylated product was obtained exclusively.

Further investigations by the Kim group, showed that when styrene-type olefins were applied, the linear product was major; however, a minor branched product was also obtained due to the added stability of the 2-alkyl rhodium species at the benzylic position (Scheme 5.50).⁶³

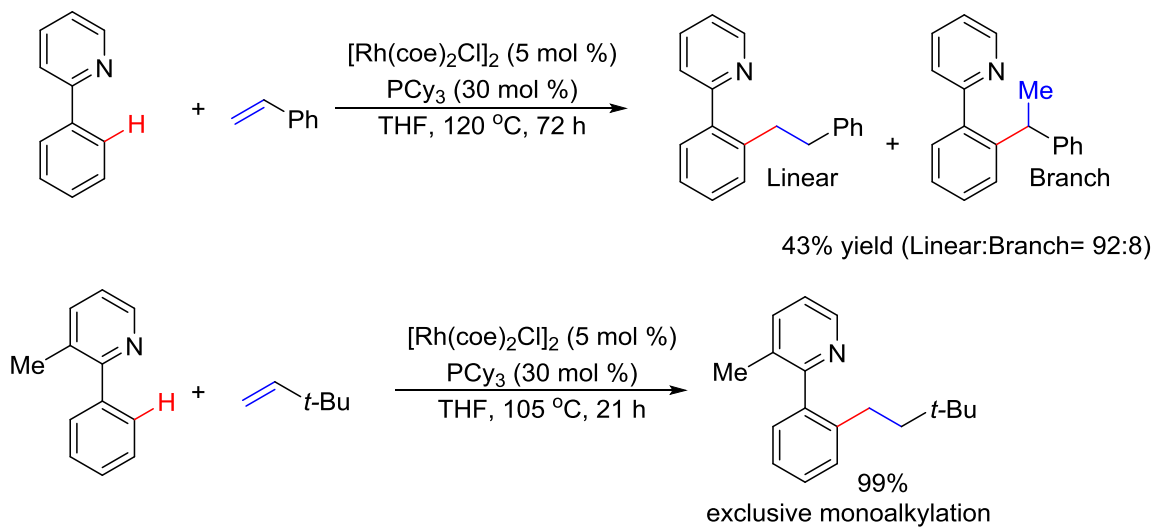
The ligand effects were also tested and found that phosphine ligands with a large cone angle such as PCy₃ gave higher reaction yields. The atroposelective alkylation reaction was reported in 2000 by Murai and coworkers.⁶⁴ The best result was obtained by

replacing PCy₃ with the chiral ligands, (R),(S)-PPFOMe, axial chirality was induced 49% ee, albeit in low yield (Scheme 5.51).

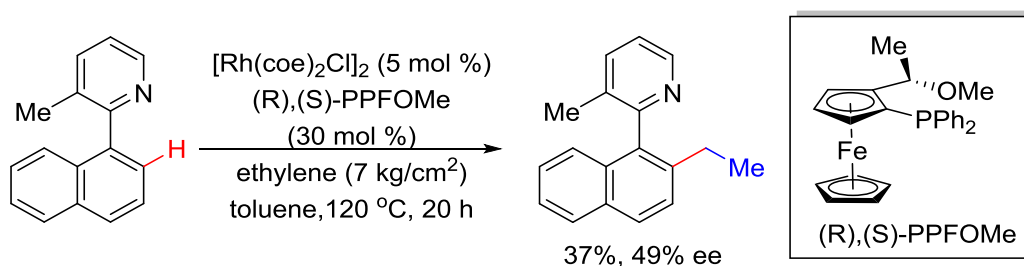
Scheme 5.49. Rh-catalyzed alkylation of 2-phenylpyridines with olefins.



Scheme 5.50. Rh-catalyzed alkylation of 2-phenylpyridines with styrene.

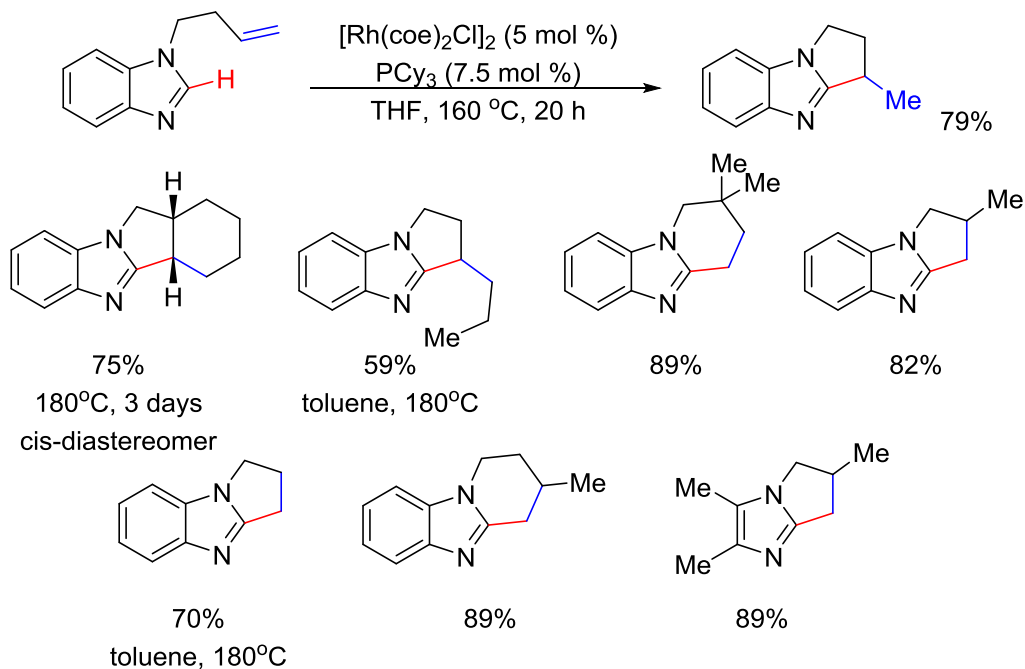


Scheme 5.51. Rh-catalyzed atroposelective alkylation with pyridine DG.

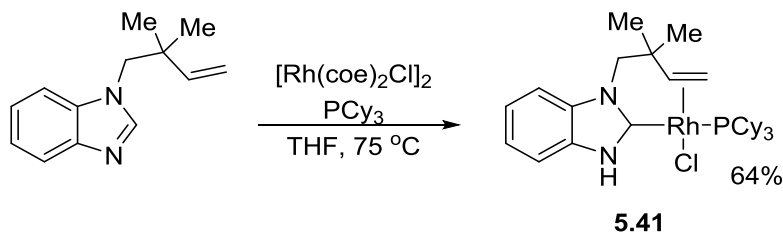


In 2001, Bergman, Ellman, and co-workers, reported an intramolecular C–H alkylation of heteroarenes, such as imidazoles and benzimidazoles.⁶⁵ PCy₃ proved to be an optimal ligand. The 2-position of the imidazole ring was selectively alkylated to form five- and six-membered rings (Scheme 5.52). In 2003, a microwave-assisted alkylation with an enhanced reaction rate was accomplished by the same team.⁶⁶

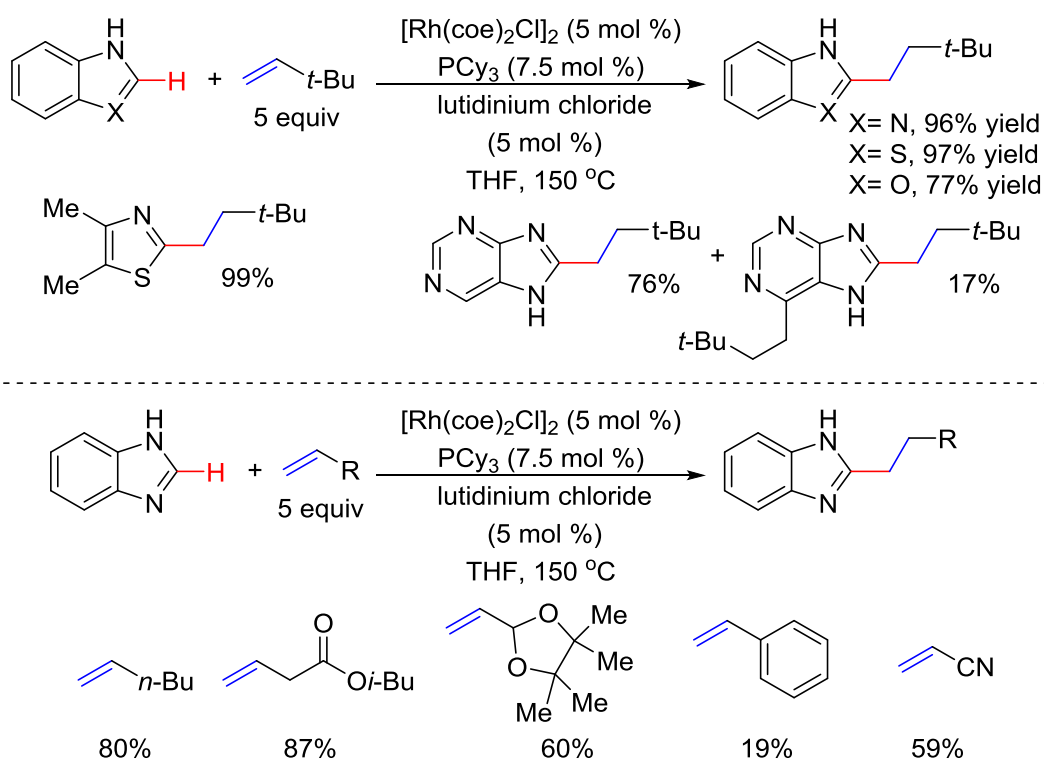
Scheme 5.52. Rh-catalyzed intramolecular C–H alkylation of heteroarenes.



Scheme 5.53. Mechanistic study of the intramolecular alkylation of heterocycles.



Scheme 5.54. Rh-catalyzed intermolecular C–H alkylation of heteroarenes.

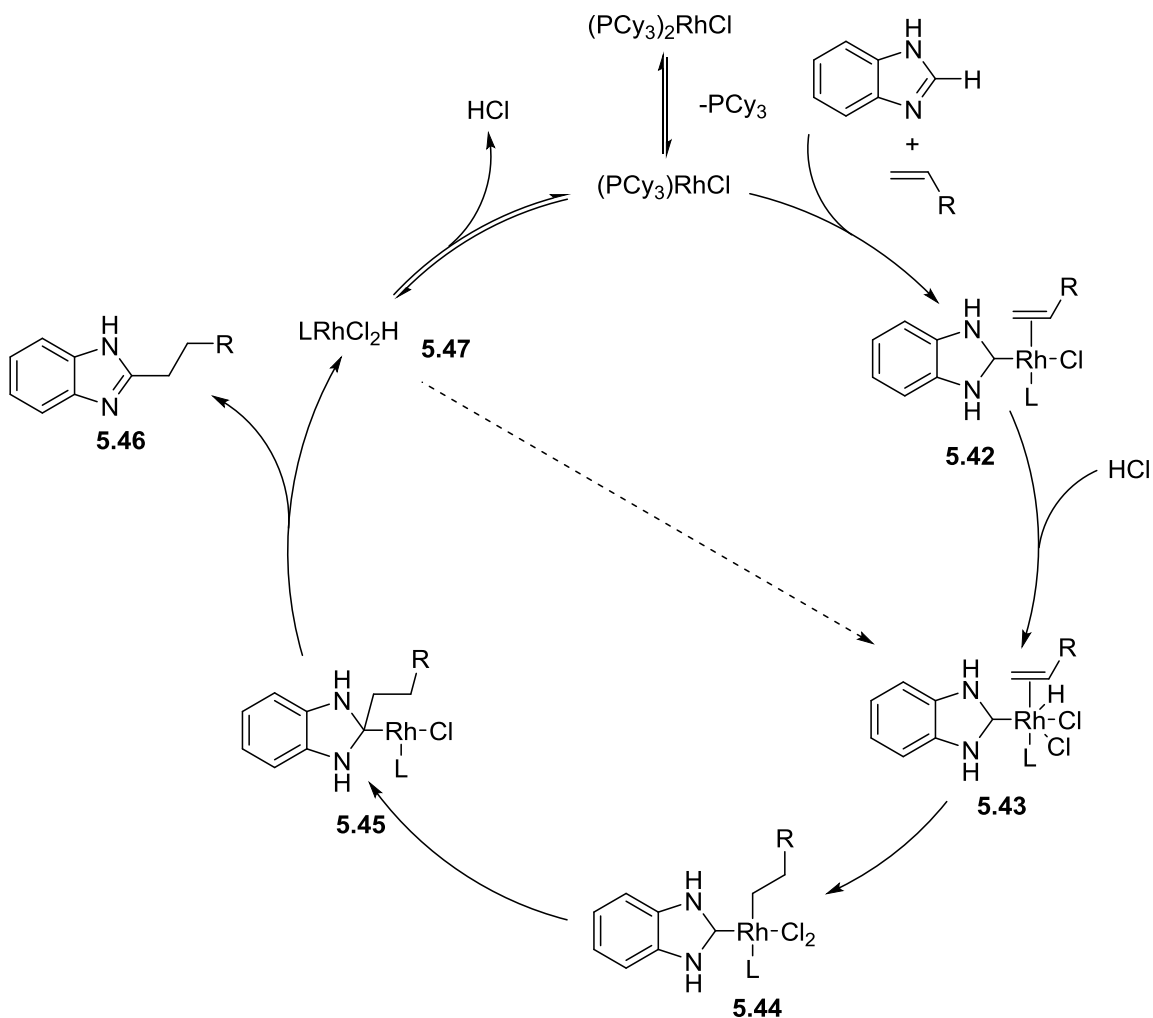


In 2002, Bergman, Ellman, and coworkers reported a mechanistic study of the previous intramolecular alkylation of heterocycles (Scheme 5.53).⁶⁷ The crystal structure of a carbene species **5.41** was obtained as strong evidence to support the proposed carbene insertion mechanism. The reaction goes through C–H activation to form a carbene then insertion into olefin and reductive elimination to give the final product.

According to the DFT calculation, the rate-determining step is the carbene insertion to the alkene.

In the same year, Bergman, Ellman, and coworker, realized an intermolecular alkylation of heterocycles with olefins (Scheme 5.54).⁶⁸ Lutidinium chloride was found to be an effective additive. On the other hand, using phosphonium salt, $\text{HClP}(t\text{-Bu})_2\text{Et}$, as a ligand without additives, the temperature for this reaction could drop to 75 °C.⁶⁹

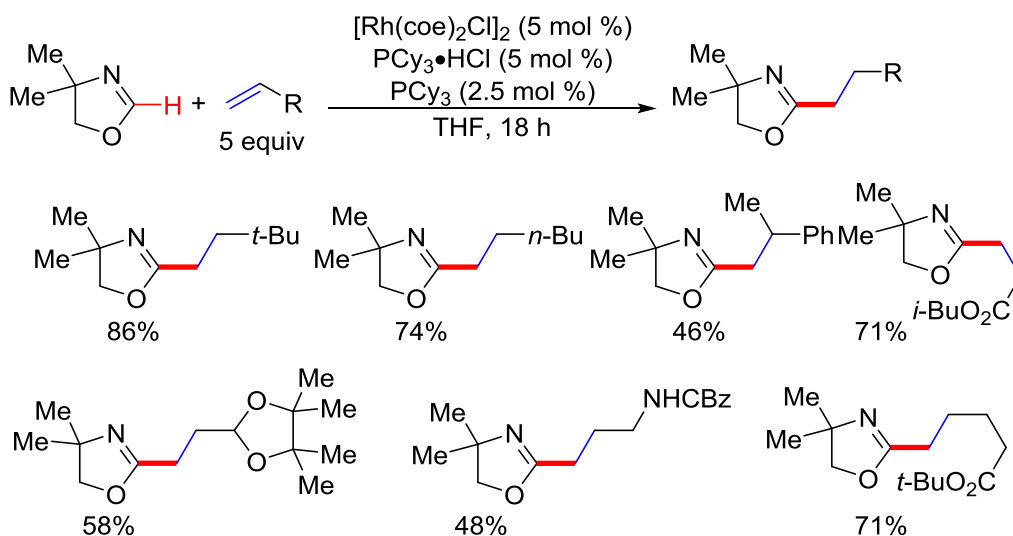
Scheme 5.55. Proposed mechanism for intermolecular alkylation of heterocycles.



The role of HClPCy_3 can be explained by the proposed mechanism shown in Scheme 5.55. After the C–H activation, intermediate **5.42** oxidatively adds into HCl to form a Rh(III) hydride **5.43**, which inserts into the olefin to give complex **5.44**. After alkyl migration and β -hydride elimination, the product **5.46** is released, and a potential catalyst **5.47** could react with substrates through proton transfer to form complex **5.43**.

In 2004, Bergman, Ellman, and coworker extended the Rh-catalyzed alkylation chemistry to 4,4-dimethyl-2-oxazolines (Scheme 5.56).⁷⁰ A broad range of alkenes can be coupled to give linear products in good to high yields. When only phosphine ligands were used in the reaction, no product formation was found, which suggested the $\text{PCy}_3 \cdot \text{HCl}$ salt was necessary. In some cases, the reaction temperature can be as low as 45 °C, and the isomerizable alkenes, such as 1-hexene, also worked well.

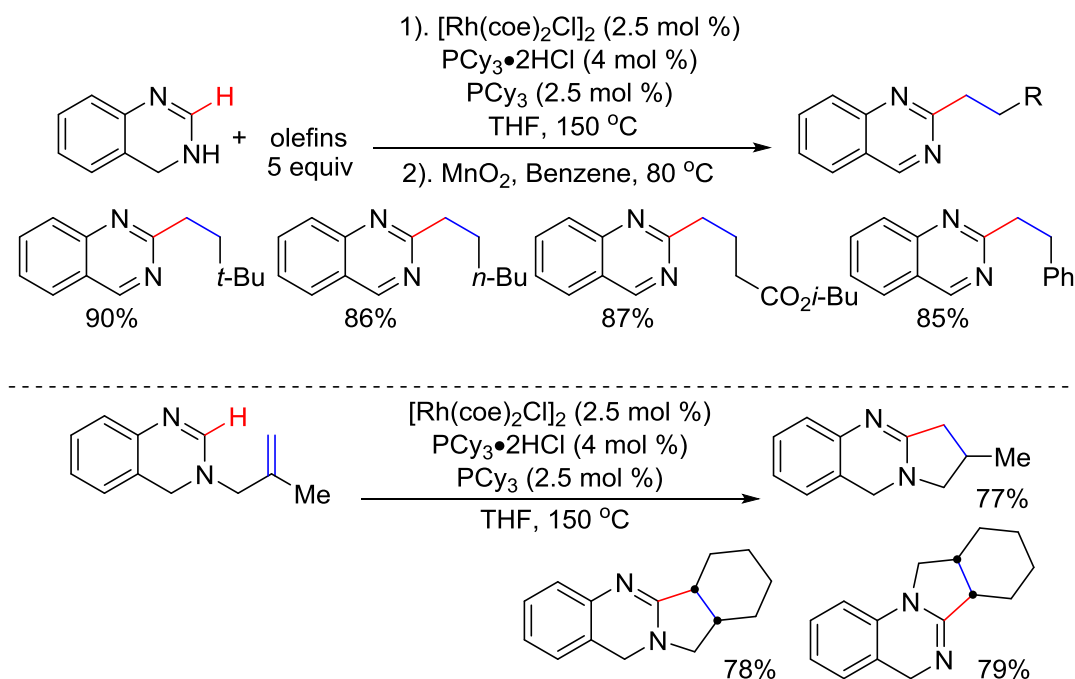
Scheme 5.56. Rh-catalyzed alkylation of 4,4-dimethyl-2-oxazolines with olefins.



In 2006, Bergman, Ellman, and co-workers extended the heteroarenes scope to 3,4-dihydroquinazoline (Scheme 5.57).⁷¹ Both the intermolecular and intramolecular C–

H alkylations with alkenes were demonstrated. For the intermolecular case, kinetic monitoring of the reaction revealed that the substrate first underwent C–H alkylation to give the alkylated 3,4-dihydroquinazoline, which was then converted to the corresponding quinazoline products through transfer hydrogenation. Thus, one equivalent of olefin was consumed as the oxidant. The intramolecular version can provide a fused five-membered ring, which fits the framework of some natural products, such as Vasicoline (see Scheme 5.67). In the same year, the experimental and computational studies on the mechanism were reported by the same groups.⁷¹

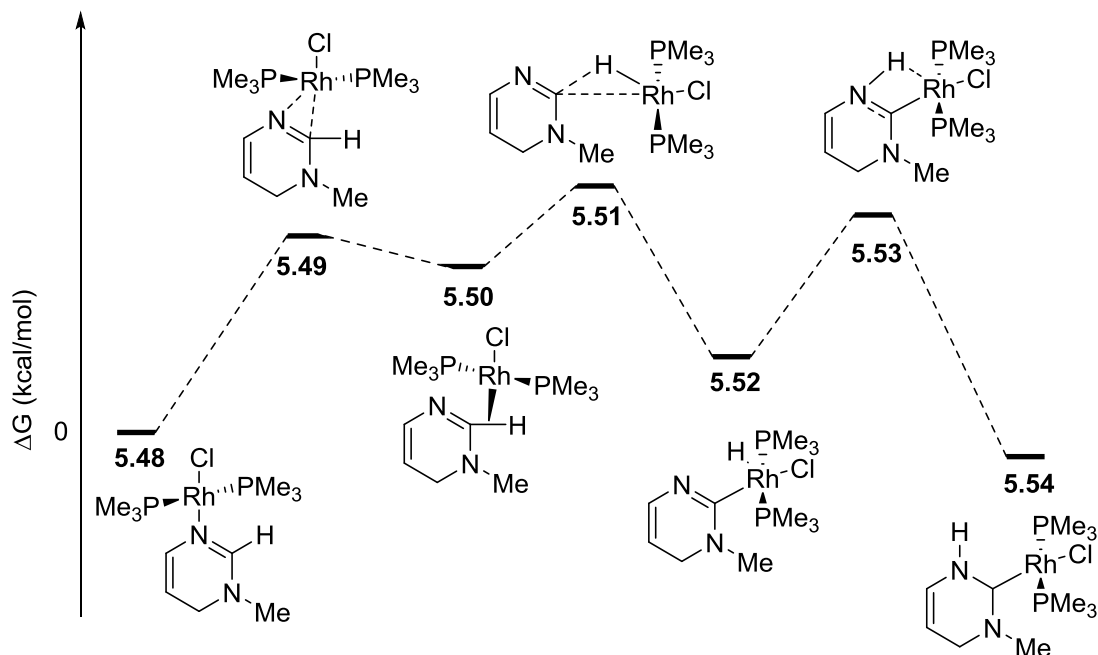
Scheme 5.57. Rh-catalyzed alkylation of 3,4-dihydroquinazoline with simple olefins.



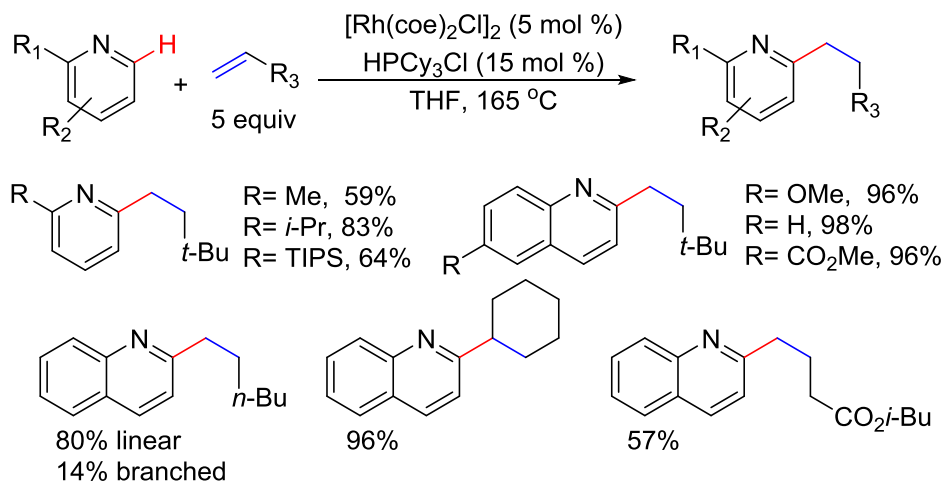
According to DFT calculations (Scheme 5.58), the C–H activation was initiated by coordination of the Rh catalyst with the sp^2 nitrogen on imidazoline **5.48**. Intermediate **5.48** can go through ligand exchange to give complex **5.50**, which can undergo oxidative addition to providing Rh-hydride species **5.52**. Upon migratory insertion into the C=N

double bond, an NHC-Rh complex **5.54** is formed, which can be isolated. This pathway is also supported by deuterium studies. Furthermore, the computational results were consistent with the experimental results obtained from kinetic studies.

Scheme 5.58. DFT calculations on Rh-catalyzed alkylation of 3,4-dihydroquinazoline.

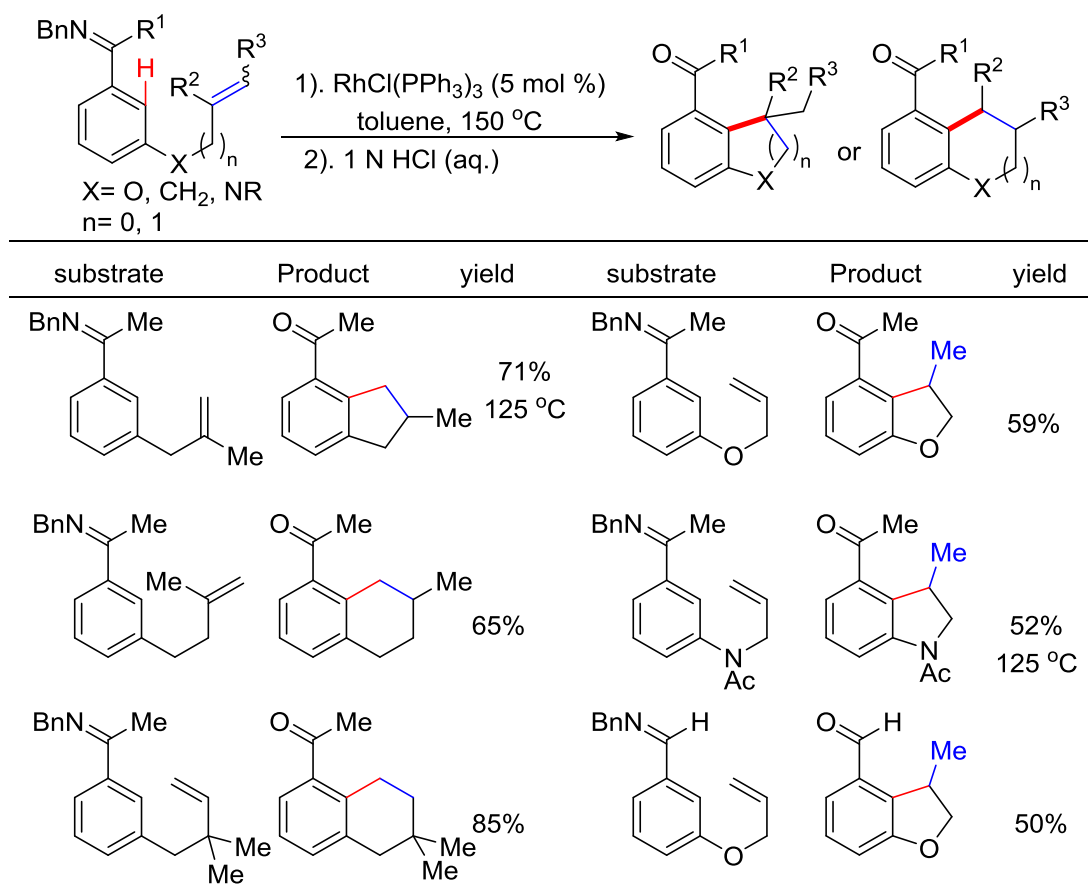


Scheme 5.59. Rh-catalyzed alkylation of quinolines and pyridines with olefins.



In 2007, Bergman, Ellman, and coworkers developed the Rh-catalyzed alkylation of quinolines and pyridines with olefins (Scheme 5.59).⁷² Mono-substitution at the C2 position of the pyridine proved to be critical. In most cases, the linear addition products were the exclusive product formed. Interestingly, when quinoline was used, both linear and branched products were observed in 80% and 14% yield respectively from alkylation with 1-hexene. The cyclic alkene was also found to be suitable coupling partner.

Scheme 5.60. Rh-catalyzed annulation of aromatic imines using Wilkinson's catalyst.

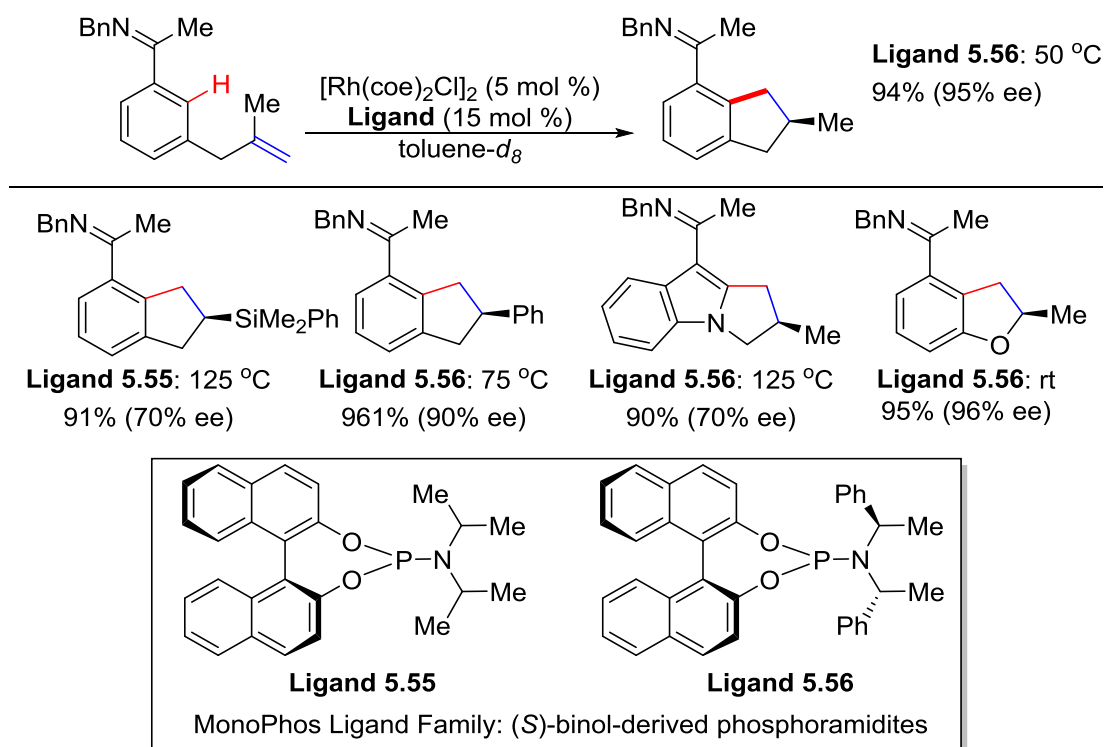


In 2001, Bergman, Ellman, and co-workers also developed a Rh-catalyzed annulation of aromatic imines via directed C–H activation with Wilkinson's catalyst (Scheme 5.60).⁷³ This method provides rapid access to functionalized heterocycles such

as indane, tetralane, dihydrobenzofuran, and dihydroindole derivatives. By changing the heteroatom and length of the tether, five- or six-membered rings can be prepared in good yield. The tethers containing heteroatoms are more effectively cyclized in an *exo*-fashion to provide five-membered rings while all-carbon tethers favored *endo*-cyclization.

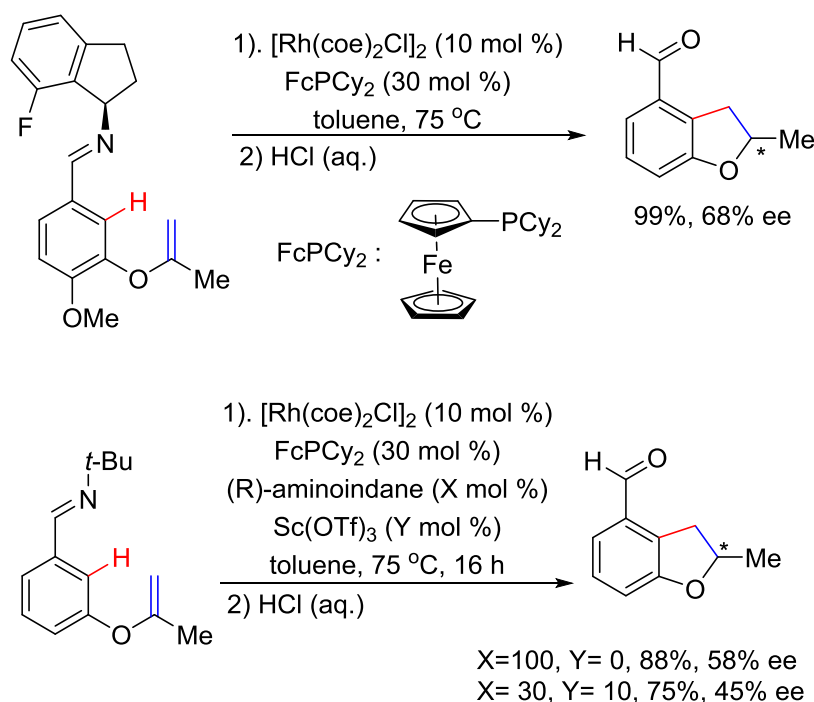
An enantioselective imine-directed alkylation was reported by the same team in 2004, using chiral phosphoramidites ligands (**5.55** and **5.56**, as shown in Scheme 5.61).⁷⁴ Lowering the reaction temperature helped the enantioselectivity. The enantioselective alkylation of aromatic imines with nitrogen-containing linkers or oxygen-containing linkers was also achieved.⁷⁵ These methods provide efficient access to many biologically active chiral indanes, dihydrobenzofurans, and dihydropyrrole indole. Application of this method in natural product synthesis will be mentioned in Scheme 5.68.

Scheme 5.61. Rh-catalyzed enantioselective alkylation using chiral ligands.



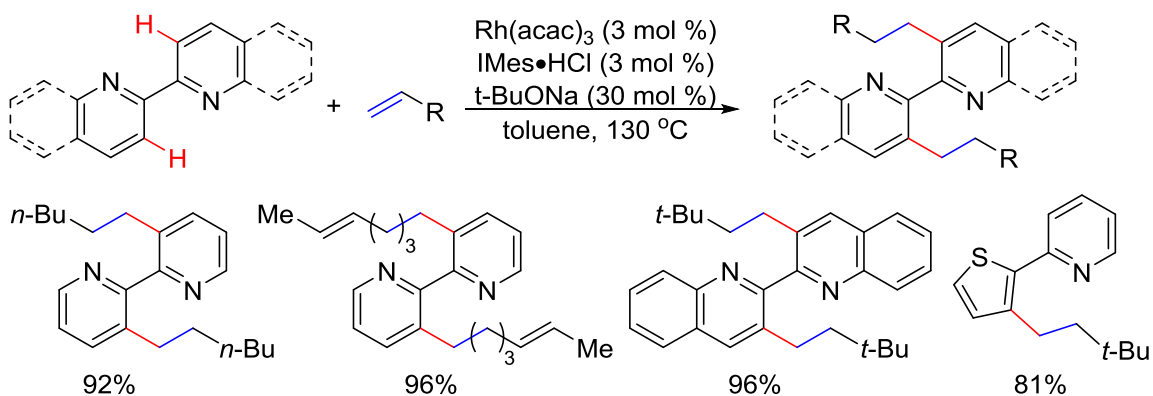
In 2007, Bergman, Ellman, and coworkers realized a Rh-catalyzed asymmetric alkylation using chiral aromatic imines (Scheme 5.62).⁷⁶ The C–H alkylation can take place in a diastereoselective fashion with a chiral primary amine group. Upon imine hydrolysis, enantioenriched aryl aldehydes can be obtained in moderate ee. The screening of the chiral amines revealed that 7-fluoro-aminoindane provided the highest selectivity. This regio- and the enantioselective reaction can also be achieved with a catalytic amount of chiral amines with precondensed achiral imines, in which the imine exchange reaction is accelerated by $\text{Sc}(\text{OTf})_3$.

Scheme 5.62. Rh-catalyzed asymmetric alkylation using chiral aromatic imines.

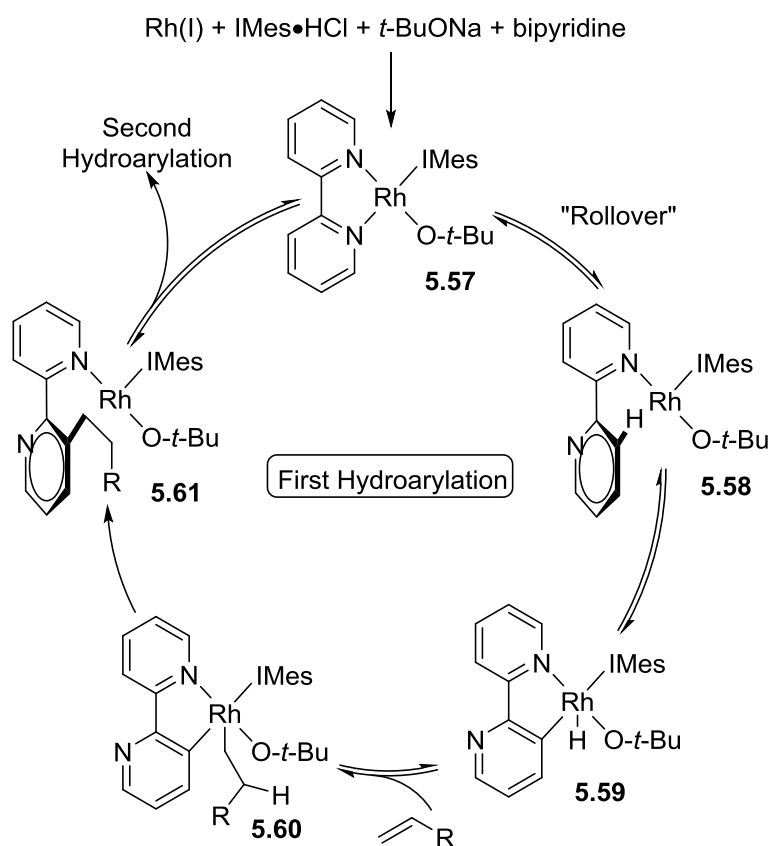


In 2012, Chang, Jung, and coworkers developed a Rh-catalyzed alkylation of 2,2'-bipyridines and 2,2'-bisquinolines with olefins.⁷⁷ A broad range of simple olefins was used as alkylation reagents to give the bis-alkylated products for 2,2'-bipyridine (Scheme 5.63). $\text{Rh}(\text{acac})_3$ was found to be the most suitable pre-catalyst in this reaction.

Scheme 5.63. Rh-catalyzed alkylation of 2,2'-bipyridines and 2,2'-bisquinolines.



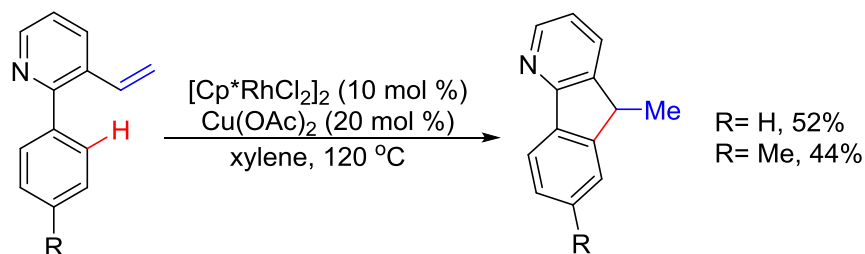
Scheme 5.64. The proposed mechanism of Rh-catalyzed alkylation of 2,2'-bipyridines.



According to the DFT studies, the proposed mechanism of the first hydroarylation cycle is shown in Scheme 5.64. The reductive elimination was proposed to be the rate-determining step, and the NHC ligand can help rollover of the bipyridine, due to the strong *trans*-effect. The catalytic cycle was initiated with formation of complex **5.57**, and dissociation of one pyridinyl group from the bipyridine to give **5.58**. The C–H activation occurred to give Rh-hydride **5.59**, which can undergo migratory insertion with the olefin and reductive elimination to give complex **5.61**. This intermediate can re-enter the catalytic cycle to give the bis-alkylated product.

In 2012, Shibata and coworker reported two examples of a Rh(III)-catalyzed intramolecular alkylation of 2-aryl-3-vinylpyridines to give the 9-methyl-4-azafluorenes in moderate yields (Scheme 5.65).⁷⁸ Neither $[\text{Cp}^*\text{RhCl}_2]_2$ nor $\text{Cu}(\text{OAc})_2$ was effective by itself, and the true catalyst was proposed to be a rhodium acetate. The role of the copper salt may be to provide acetate because other metal acetate salts can also produce the product. A **Type B** mechanism was proposed for this reaction.

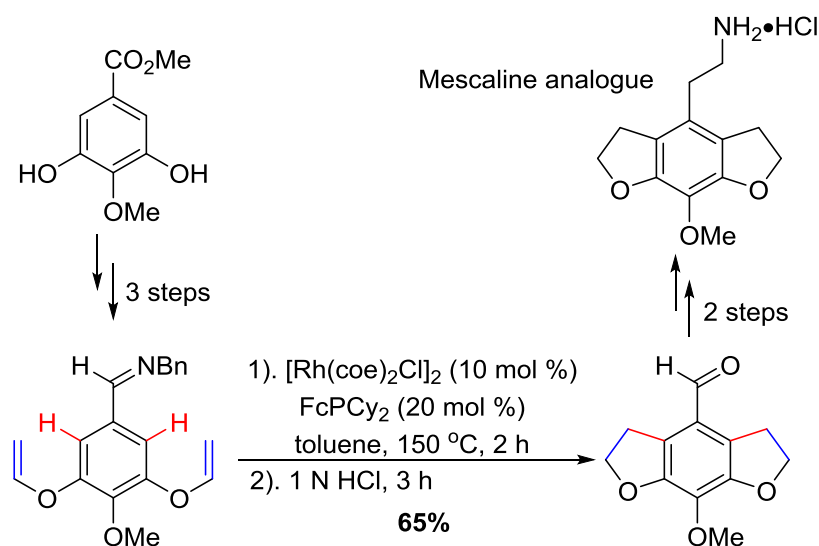
Scheme 5.65. Rh-catalyzed intramolecular alkylation of 2-aryl-3-vinylpyridines.



5.3.2.2 Application of Rhodium-Catalyzed Arene C–H Bond Alkylation

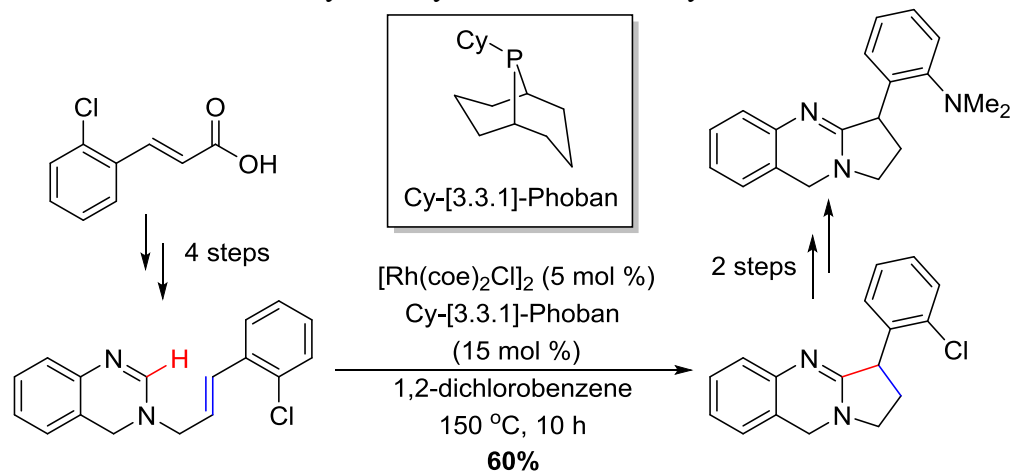
In 2003, Bergman, Ellman, and coworker disclosed the Rh-catalyzed synthesis of a tricyclic mescaline analog through an intramolecular alkylation.⁷⁹ Mescaline was discovered in 1896 and had been used as a prototypical compound for structure–activity relationship screening for treating central nervous system disorders. Utilizing the alkylation methodology, this drug was prepared in six steps with 38% overall yield (Scheme 5.66).

Scheme 5.66. Rh-catalyzed synthesis of a tricyclic mescaline analog.

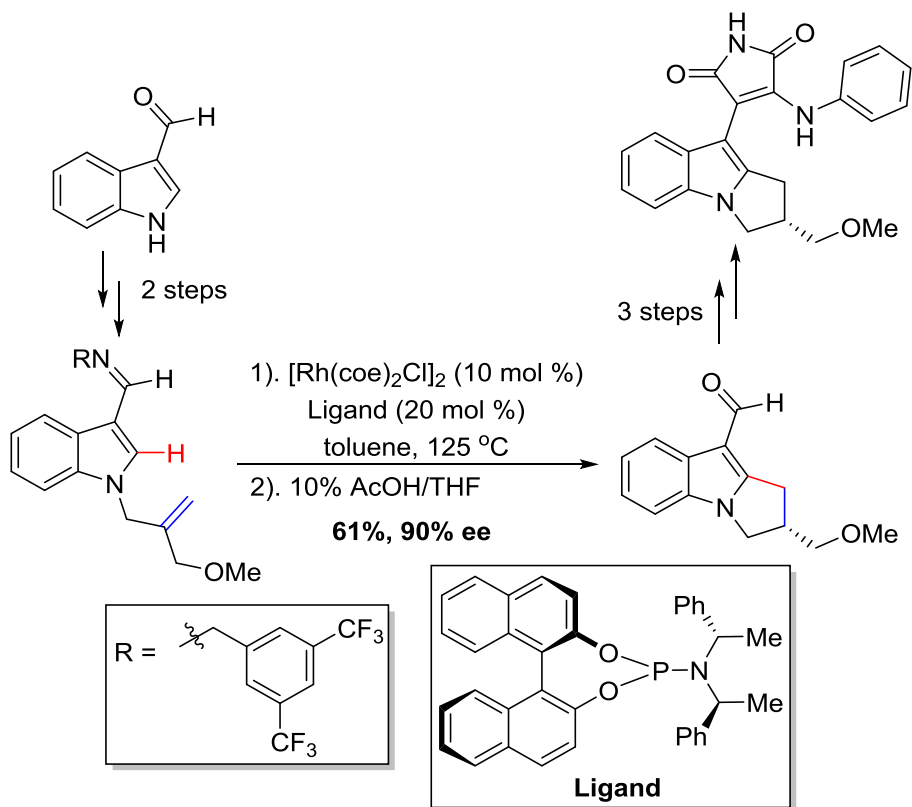


In 2006, the same team further extended the Rh-catalyzed alkylation method to the total synthesis of vasicoline.⁷¹ Vasicoline, a member of the quinazoline natural product family, has been isolated from various plants and microbial sources, which exhibits interesting antimalarial, anti-inflammatory, and antitumor activity. The natural product was synthesized in 7 linear steps with 10% overall yield from commercial materials. The key reaction involves an intramolecular C–H alkylation at the C2 position of the alkene-tethered 3,4-dihydroquinazoline (Scheme 5.67).

Scheme 5.67. Rh-catalyzed alkylation in the total synthesis of Vasicoline.

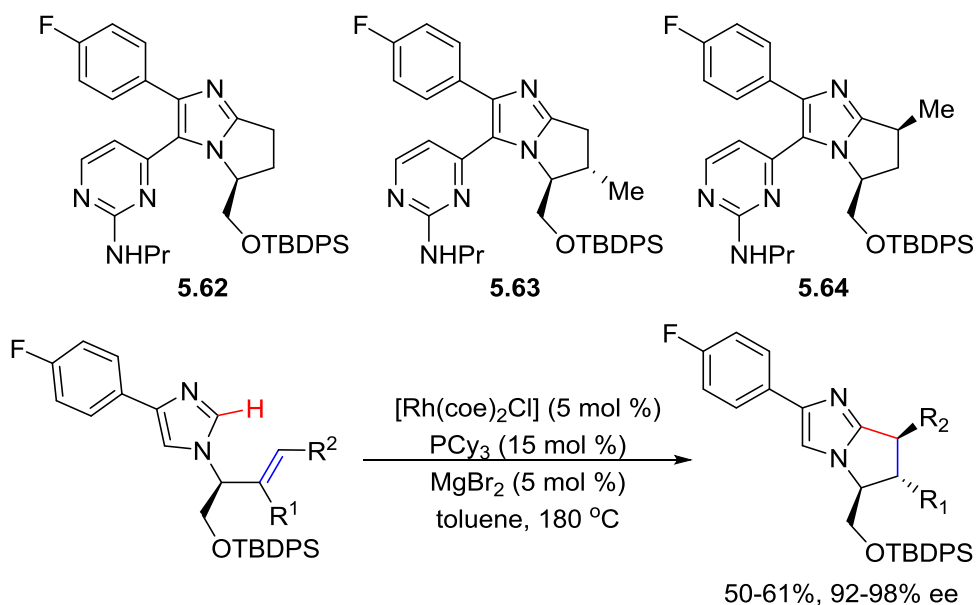


Scheme 5.68. Rh-catalyzed enantioselective synthesis of a protein kinase C inhibitor.



In the same year, the same team reported a Rh-catalyzed enantioselective synthesis of a protein kinase C inhibitor for isozyme β with a C–H bond alkylation strategy (Scheme 5.68).⁸⁰ The dihydropyrole indole core is a common motif found in biologically active compounds, which can be rapidly constructed using the imine-directed *ortho*-alkylation method. Good yield and high ee can be obtained using a phosphoramidite ligand.

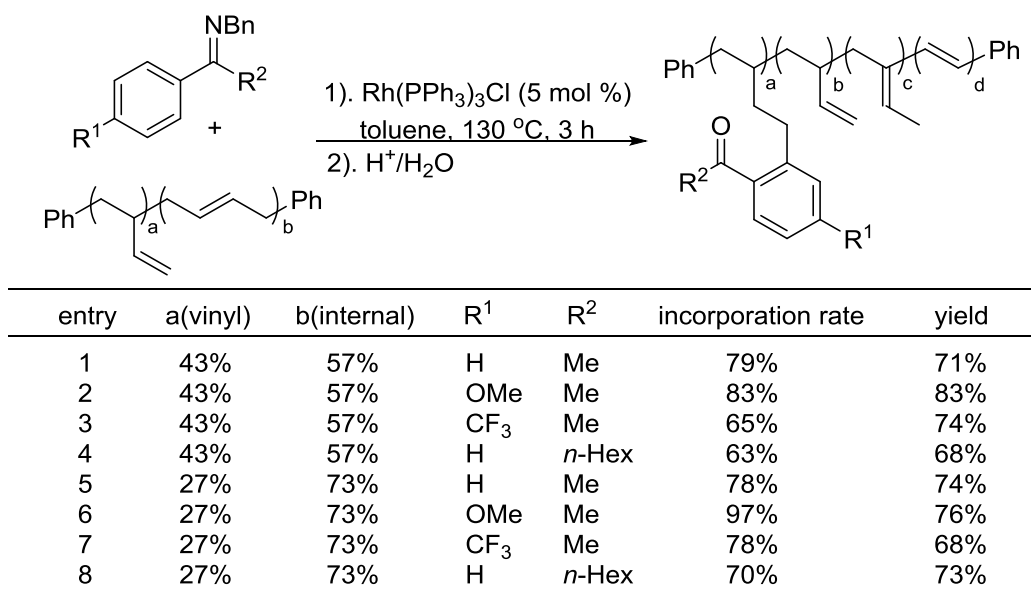
Scheme 5.69. Rh-catalyzed a concise synthesis of potent bicyclic bisaryl imidazoles.



In 2007, Bergman, Ellman, and coworkers developed a Rh-catalyzed concise synthesis of a number of potent bicyclic bisaryl imidazoles that serve as potent inhibitors of c-Jun *N*-terminal kinase (**5.62-5.64**), which can potentially treat neurodegenerative diseases (Scheme 5.69).⁸¹ The inhibitor **5.63** was prepared in 10 steps, in which the key step involved an intramolecular alkylation giving 50% yield and 90% ee. Notably, this methodology allows for diversification of these molecules and compound **5.64** was found to be the most potent inhibitor.

In 2007, Jun and coworkers reported a Rh-catalyzed alkylation of aromatic ketimines with a polybutadiene species.⁸² The modification of polybutadiene with a high ratio of vinyl-internal olefin groups exhibited a low conversion rate, due to steric congestion of the polymer substrate (Scheme 5.70). Isomerization of the backbone double bonds was observed.

Scheme 5.70. Rh-catalyzed alkylation of aromatic ketimines with polybutadiene.



Chapter 1 References

1. (a) Hartwig, J. F. *Acc. Chem. Res.* **2012**, *45*, (6), 864; (b) Baudoin, O. *Chem. Soc. Rev.* **2011**, *40*, (10), 4902; (c) Davies, H. M. L.; Denton, J. R. *Chem. Soc. Rev.* **2009**, *38*, (11), 3061; (d) Ackermann, L.; Vicente, R.; Kapdi, A. R. *Angew. Chem. Int. Ed.* **2009**, *48*, (52), 9792; (e) Labinger, J. A.; Bercaw, J. E. *Nature* **2002**, *417*, (6888), 507.
2. (a) Noisier, A. F. M.; Brimble, M. A. *Chem. Rev.* **2014**, *114*, (18), 8775; (b) Li, B. J.; Shi, Z. J. *Chem. Soc. Rev.* **2012**, *41*, (17), 5588; (c) Engle, K. M.; Mei, T. S.; Wasa, M.; Yu, J. Q. *Acc. Chem. Res.* **2012**, *45*, (6), 788; (d) Chen, X.; Engle, K. M.; Wang, D. H.; Yu, J. Q. *Angew. Chem. Int. Ed.* **2009**, *48*, (28), 5094.
3. (a) Daugulis, O.; Roane, J.; Tran, L. D. *Acc. Chem. Res.* **2015**, *48*, (4), 1053; (b) Rouquet, G.; Chatani, N. *Angew. Chem. Int. Ed.* **2013**, *52*, (45), 11726; (c) Neufeldt, S. R.; Sanford, M. S. *Acc. Chem. Res.* **2012**, *45*, (6), 936; (d) Lyons, T. W.; Sanford, M. S. *Chem. Rev.* **2010**, *110*, (2), 1147.
4. Rousseau, G.; Breit, B. *Angew. Chem. Int. Ed.* **2011**, *50*, (11), 2450.
5. Onoue, H.; Minami, K.; Nakagawa, K. *Bull. Chem. Soc. Jpn.* **1970**, *43*, (11), 3480.
6. Keuseman, K. J.; Smoliakova, I. P.; Dunina, V. V. *Organometallics* **2005**, *24*, (17), 4159.
7. Mawo, R. Y.; Mustakim, S.; Young, V. G., Jr.; Hoffmann, M. R.; Smoliakova, I. P. *Organometallics* **2007**, *26*, (7), 1801.
8. Zeni, G.; Larock, R. C. *Chem. Rev.* **2004**, *104*, (5), 2285.
9. Desai, L. V.; Hull, K. L.; Sanford, M. S. *J. Am. Chem. Soc.* **2004**, *126*, (31), 9542.
10. Neufeldt, S. R.; Sanford, M. S. *Org. Lett.* **2010**, *12*, (3), 532.
11. Stowers, K. J.; Kubota, A.; Sanford, M. S. *Chem. Sci.* **2012**, *3*, (11), 3192.
12. Thu, H.-Y.; Yu, W.-Y.; Che, C.-M. *J. Am. Chem. Soc.* **2006**, *128*, (28), 9048.
13. Peng, J.; Chen, C.; Xi, C. J. *Chem. Sci.* **2016**, *7*, (2), 1383.
14. Justicia, J.; Oltra, J. E.; Cuerva, J. M. *J. Org. Chem.* **2005**, *70*, (21), 8265.
15. Garcia-Granados, A.; Lopez, P. E.; Melguizo, E.; Parra, A.; Simeo, Y. *J. Org. Chem.* **2007**, *72*, (9), 3500.
16. Siler, D. A.; Mighion, J. D.; Sorensen, E. J. *Angew. Chem. Int. Ed.* **2014**, *53*, (21), 5332.
17. (a) Sharpe, R. J.; Johnson, J. S. *J. Am. Chem. Soc.* **2015**, *137*, (15), 4968; (b) Sharpe, R. J.; Johnson, J. S. *J. Org. Chem.* **2015**, *80*, (19), 9740.
18. (a) Trotta, A. H. *Org. Lett.* **2015**, *17*, (13), 3358; (b) Meng, Z.; Yu, H.; Li, L.; Tao, W.; Chen, H.; Wan, M.; Yang, P.; Edmonds, D. J.; Zhong, J.; Li, A. *Nat Commun* **2015**, *6*.
19. Desai, L. V.; Malik, H. A.; Sanford, M. S. *Org. Lett.* **2006**, *8*, (6), 1141.
20. Lennartz, P.; Raabe, G.; Bolm, C. *Adv. Synth. Catal.* **2012**, *354*, (17), 3237.
21. Liang, Y. F.; Wang, X. Y.; Yuan, Y. Z.; Liang, Y. J.; Li, X. Y.; Jiao, N. *Acs Catalysis* **2015**, *5*, (10), 6148.
22. Yu, W.-Y.; Sit, W. N.; Lai, K.-M.; Zhou, Z.; Chan, A. S. C. *J. Am. Chem. Soc.* **2008**, *130*, (11), 3304.

23. Sun, C. L.; Liu, N.; Li, B. J.; Yu, D. G.; Wang, Y.; Shi, Z. J. *Org. Lett.* **2010**, *12*, (1), 184.
24. Ren, Z.; Mo, F.; Dong, G. *J. Am. Chem. Soc.* **2012**, *134*, (41), 16991.
25. Xu, Y.; Yan, G.; Ren, Z.; Dong, G. *Nat Chem* **2015**, *7*, (10), 829.
26. Thompson, S. J.; Thach, D. Q.; Dong, G. B. *J. Am. Chem. Soc.* **2015**, *137*, (36), 11586.
27. Desai, L. V.; Stowers, K. J.; Sanford, M. S. *J. Am. Chem. Soc.* **2008**, *130*, (40), 13285.
28. Ren, Z.; Schulz, J. E.; Dong, G. *Org. Lett.* **2015**, *17*, (11), 2696.
29. K.; Chen, X. L.; Guan, M. Y.; Zhao, Y. S. *Org. Lett.* **2015**, *17*, (7), 1802.
30. Guo, K.; Chen, X. L.; Zhang, J. Y.; Zhao, Y. S. *Eur. Chem. J.* **2015**, *21*, (48), 17474.
31. Shi, B.-F.; Maugel, N.; Zhang, Y.-H.; Yu, J.-Q. *Angew. Chem. Int. Ed.* **2008**, *47*, (26), 4882.
32. Ohno, H.; Aso, A.; Kadoh, Y.; Fujii, N.; Tanaka, T. *Angew. Chem. Int. Ed.* **2007**, *46*, (33), 6325.
33. Liu, H.; Wang, L. M.; Tong, X. F. *Chem. Comm.* **2011**, *47*, (44), 12206.
34. Thirunavukkarasu, V. S.; Parthasarathy, K.; Cheng, C. H. *Angew. Chem. Int. Ed.* **2008**, *47*, (49), 9462.

Chapter 2 References

1. Labinger, J. A.; Bercaw, J. E. *Nature* **2002**, *417*, (6888), 507.
2. (a) Davies, H. M. L.; Du Bois, J.; Yu, J.-Q. *Chem. Soc. Rev.* **2011**, *40*, (4), 1855; (b) McMurray, L.; O'Hara, F.; Gaunt, M. J. *Chem. Soc. Rev.* **2011**, *40*, (4), 1885.
3. Davies, H. M. L.; Manning, J. R. *Nature* **2008**, *451*, (7177), 417.
4. Hartwig, J. F. *Acc. Chem. Res.* **2012**, *45*, (6), 864.
5. Neufeldt, S. R.; Sanford, M. S. *Acc. Chem. Res.* **2012**, *45*, (6), 936.
6. (a) Daugulis, O.; Do, H. Q.; Shabashov, D. *Acc. Chem. Res.* **2009**, *42*, (8), 1074; (b) Daugulis, O.; Roane, J.; Tran, L. D. *Acc. Chem. Res.* **2015**, *48*, (4), 1053.
7. Liang, Y. F.; Wang, X. Y.; Yuan, Y. Z.; Liang, Y. J.; Li, X. Y.; Jiao, N. *Acs Catalysis* **2015**, *5*, (10), 6148.
8. Engle, K. M.; Mei, T. S.; Wasa, M.; Yu, J. Q. *Acc. Chem. Res.* **2012**, *45*, (6), 788.
9. Desai, L. V.; Hull, K. L.; Sanford, M. S. *J. Am. Chem. Soc.* **2004**, *126*, (31), 9542.
10. (a) Gormisky, P. E.; White, M. C. *J. Am. Chem. Soc.* **2011**, *133*, (32), 12584; (b) Huang, C. H.; Ghavtadze, N.; Chattopadhyay, B.; Gevorgyan, V. *J. Am. Chem. Soc.* **2011**, *133*, (44), 17630.
11. Newhouse, T.; Baran, P. S. *Angew. Chem. Int. Ed.* **2011**, *50*, (15), 3362.
12. (a) Espino, C. G.; Du Bois, J. *Angew. Chem. Int. Ed.* **2001**, *40*, (3), 598; (b) Espino, C. G.; Wehn, P. M.; Chow, J.; Du Bois, J. *J. Am. Chem. Soc.* **2001**, *123*, (28), 6935.
13. Chen, K.; Richter, J. M.; Baran, P. S. *J. Am. Chem. Soc.* **2008**, *130*, (23), 7247.
14. Simmons, E. M.; Hartwig, J. F. *Nature* **2012**, *483*, (7387), 70.
15. Chen, K.; Baran, P. S. *Nature* **2009**, *459*, (7248), 824.
16. (a) Davies, H. M. L.; Morton, D. *Chem. Soc. Rev.* **2011**, *40*, (4), 1857; (b) Chen, M. S.; White, M. C. *Science* **2007**, *318*, (5851), 783.
17. Mawo, R. Y.; Mustakim, S.; Young, V. G., Jr.; Hoffmann, M. R.; Smoliakova, I. *P. Organometallics* **2007**, *26*, (7), 1801.
18. Keuseman, K. J.; Smoliakova, I. P.; Dunina, V. V. *Organometallics* **2005**, *24*, (17), 4159.
19. Giri, R.; Liang, J.; Lei, J. G.; Li, J. J.; Wang, D. H.; Chen, X.; Naggar, I. C.; Guo, C. Y.; Foxman, B. M.; Yu, J. Q. *Angew. Chem. Int. Ed.* **2005**, *44*, (45), 7420.
20. Dangel, B. D.; Godula, K.; Youn, S. W.; Sezen, B.; Sames, D. *J. Am. Chem. Soc.* **2002**, *124*, (40), 11856.
21. Martinez, A. G.; Vilar, E. T.; Fraile, A. G.; Cerero, S. D.; Ruiz, P. M. *Tetrahedron-Asymmetry* **1998**, *9*, (10), 1737.
22. Rousseaux, S.; Liegault, B.; Fagnou, K. *Chem. Sci.* **2012**, *3*, (1), 244.
23. Bigi, M. A.; Reed, S. A.; White, M. C. *J. Am. Chem. Soc.* **2012**, *134*, (23), 9721.
24. T. Gallagher, P.; C. A. Hunt, J.; P. Lightfoot, A.; J. Moody, C. *J. Chem. Soc., Perkin Trans. 1* **1997**, (17), 2633.
25. Kim, J. N.; Kim, K. M.; Ryu, E. K. *Synth. Commun.* **1992**, *22*, (10), 1427.
26. Harris, J. R.; Haynes, M. T.; Thomas, A. M.; Woerpel, K. A. *J. Org. Chem.* **2010**, *75*, (15), 5083.

27. Sakurada, I.; Yamasaki, S.; Göttlich, R.; Iida, T.; Kanai, M.; Shibasaki, M. *J. Am. Chem. Soc.* **2000**, *122*, (6), 1245.
28. Egri, G.; Baitz-Gács, E.; Poppe, L. *Tetrahedron: Asymmetry* **1996**, *7*, (5), 1437.

Chapter 3 References

1. (a) Engle, K. M.; Mei, T. S.; Wasa, M.; Yu, J. Q. *Acc. Chem. Res.* **2012**, *45*, (6), 788; (b) Neufeldt, S. R.; Sanford, M. S. *Acc. Chem. Res.* **2012**, *45*, (6), 936; (c) Daugulis, O.; Roane, J.; Tran, L. D. *Acc. Chem. Res.* **2015**, *48*, (4), 1053.
2. Desai, L. V.; Malik, H. A.; Sanford, M. S. *Org. Lett.* **2006**, *8*, (6), 1141.
3. Ren, Z.; Mo, F.; Dong, G. *J. Am. Chem. Soc.* **2012**, *134*, (41), 16991.
4. (a) Desai, L. V.; Hull, K. L.; Sanford, M. S. *J. Am. Chem. Soc.* **2004**, *126*, (31), 9542; (b) Neufeldt, S. R.; Sanford, M. S. *Org. Lett.* **2010**, *12*, (3), 532.
5. (a) Shao, Z.; Zhang, H. *Chem. Soc. Rev.* **2009**, *38*, (9), 2745; (b) Rousseau, G.; Breit, B. *Angew. Chem. Int. Ed.* **2011**, *50*, (11), 2450; (c) Zhang, F.; Spring, D. R. *Chem. Soc. Rev.* **2014**, *43*, (20), 6906; (d) Tan, K. L. *Acs Catal.* **2011**, *1*, (8), 877.
6. (a) Emorine, L. J.; Marullo, S.; Briend-Sutren, M.-M.; Patey, G.; Tate, K.; Delavier-Klutchko, C.; Strosberg, A. D. *Science* **1989**, *245*, (4922), 1118; (b) Edwards, M. J.; Flatman, R. H.; Mitchenall, L. A.; Stevenson, C. E. M.; Le, T. B. K.; Clarke, T. A.; McKay, A. R.; Fiedler, H.-P.; Buttner, M. J.; Lawson, D. M.; Maxwell, A. *Science* **2009**, *326*, (5958), 1415.
7. Wang, X.; Lu, Y.; Dai, H.-X.; Yu, J.-Q. *J. Am. Chem. Soc.* **2010**, *132*, (35), 12203.
8. Simmons, E. M.; Hartwig, J. F. *J. Am. Chem. Soc.* **2010**, *132*, (48), 17092.
9. Onoue, H.; Minami, K.; Nakagawa, K. *Bull. Chem. Soc. Jpn.* **1970**, *43*, (11), 3480.
10. Desai, L. V.; Stowers, K. J.; Sanford, M. S. *J. Am. Chem. Soc.* **2008**, *130*, (40), 13285.
11. Dangel, B. D.; Godula, K.; Youn, S. W.; Sezen, B.; Sames, D. *J. Am. Chem. Soc.* **2002**, *124*, (40), 11856.
12. Giri, R.; Liang, J.; Lei, J.-G.; Li, J.-J.; Wang, D.-H.; Chen, X.; Naggar, I. C.; Guo, C.; Foxman, B. M.; Yu, J.-Q. *Angew. Chem. Int. Ed.* **2005**, *44*, (45), 7420.
13. Hossain, M. D.; Kitamura, T. *Synthesis* **2005**, *2005*, (12), 1932.
14. Choong, I. C.; Ellman, J. A. *J. Org. Chem.* **1999**, *64*, (18), 6528.
15. Kang, T.; Kim, H.; Kim, J. G.; Chang, S. *Chem. Commun.* **2014**, *50*, (81), 12073.
16. Sharma, V.; Bachand, B.; Simard, M.; Wuest, J. D. *J. Org. Chem.* **1994**, *59*, (25), 7785.
17. Baraldi, P. G.; Barco, A.; Benetti, S.; Manfredini, S.; Simoni, D. *Synthesis* **1987**, *1987*, (3), 276.
18. Gaudiano, G.; Frigerio, M.; Bravo, P.; Koch, T. H. *J. Am. Chem. Soc.* **1990**, *112*, (18), 6704.
19. Soni, A.; Rehman, A.; Naik, K.; Dastidar, S.; Alam, M. S.; Ray, A.; Chaira, T.; Shah, V.; Palle, V. P.; Cliffe, I. A.; Sattigeri, V. J. *Bioorg. Med. Chem. Lett.* **2013**, *23*, (5), 1482.
20. Zhao, D.; Wu, N.; Zhang, S.; Xi, P.; Su, X.; Lan, J.; You, J. *Angew. Chem. Int. Ed.* **2009**, *48*, (46), 8729.

Chapter 4 References

1. (a) Baudoin, O. *Chem. Soc. Rev.* **2011**, 40, (10), 4902; (b) Li, B. J.; Shi, Z. J. *Chem. Soc. Rev.* **2012**, 41, (17), 5588; (c) Rouquet, G.; Chatani, N. *Angew. Chem. Int. Ed.* **2013**, 52, (45), 11726; (d) Noisier, A. F. M.; Brimble, M. A. *Chem. Rev.* **2014**, 114, (18), 8775; (e) Daugulis, O.; Roane, J.; Tran, L. D. *Acc. Chem. Res.* **2015**, 48, (4), 1053.
2. Labinger, J. A.; Bercaw, J. E. *Nature* **2002**, 417, (6888), 507.
3. (a) Chen, X.; Engle, K. M.; Wang, D. H.; Yu, J. Q. *Angew. Chem. Int. Ed.* **2009**, 48, (28), 5094; (b) Daugulis, O.; Do, H. Q.; Shabashov, D. *Acc. Chem. Res.* **2009**, 42, (8), 1074; (c) Lyons, T. W.; Sanford, M. S. *Chem. Rev.* **2010**, 110, (2), 1147; (d) Engle, K. M.; Mei, T. S.; Wasa, M.; Yu, J. Q. *Acc. Chem. Res.* **2012**, 45, (6), 788; (e) Neufeldt, S. R.; Sanford, M. S. *Acc. Chem. Res.* **2012**, 45, (6), 936.
4. (a) Guo, K.; Chen, X. L.; Zhang, J. Y.; Zhao, Y. S. *Chem. Eur. J.* **2015**, 21, (48), 17474; (b) Ren, Z.; Mo, F.; Dong, G. *J. Am. Chem. Soc.* **2012**, 134, (41), 16991; (c) Thompson, S. J.; Thach, D. Q.; Dong, G. B. *J. Am. Chem. Soc.* **2015**, 137, (36), 11586; (d) Xu, Y.; Yan, G.; Ren, Z.; Dong, G. *Nat Chem* **2015**, 7, (10); (e) K.; Chen, X. L.; Guan, M. Y.; Zhao, Y. S. *Org. Lett.* **2015**, 17, (7), 1802; (f) Ren, Z.; Schulz, J. E.; Dong, G. *Org. Lett.* **2015**, 17, (11), 2696; (g) Gao, P.; Guo, W.; Xue, J.; Zhao, Y.; Yuan, Y.; Xia, Y.; Shi, Z. *J. Am. Chem. Soc.* **2015**, 137, (38), 12231; (h) Kang, T.; Kim, Y.; Lee, D.; Wang, Z.; Chang, S. *J. Am. Chem. Soc.* **2014**, 136, (11), 4141.
5. Giri, R.; Shi, B. F.; Engle, K. M.; Maugel, N.; Yu, J. Q. *Chem. Soc. Rev.* **2009**, 38, (11), 3242.
6. (a) Parella, R.; Babu, S. A. *Synlett* **2014**, 25, (10), 1395; (b) Rousseaux, S.; Liegault, B.; Fagnou, K. *Chem. Sci.* **2012**, 3, (1), 244; (c) Hoshiya, N.; Kobayashi, T.; Arisawa, M.; Shuto, S. *Org. Lett.* **2013**, 15, (24), 6202; (d) Ladd, C. L.; Roman, D. S.; Charette, A. B. *Org. Lett.* **2013**, 15, (6), 1350; (e) Saget, T.; Perez, D.; Cramer, N. *Org. Lett.* **2013**, 15, (6), 1354; (f) Hoshiya, N.; Takenaka, K.; Shuto, S.; Uenishi, J. i. *Org. Lett.* **2016**, 18, (1), 48; (g) Cao, X.; Yang, W. D.; Liu, C.; Wei, F. L.; Wu, K.; Sun, W.; Song, J.; Xie, L. H.; Huang, W. *Org. Lett.* **2013**, 15, (12), 3102.
7. (a) Claire, P. P. K.; Jones, C. J.; McCleverty, J. A.; Coe, P. L.; Drew, M. G. B. *J. Organomet. Chem.* **1992**, 424, (1), 105; (b) Balegroune, F.; Grandjean, D.; Lakkis, D.; Matt, D. *J. Chem. Soc., Chem. Commun.* **1992**, (15), 1084; (c) Yoneda, A.; Newkome, G. R.; Morimoto, Y.; Higuchi, Y.; Yasuoka, N. *Acta Crystallogr. Sect. C* **1993**, 49, (3), 476; (d) Saxena, P.; Thirupathi, N.; Nethaji, M. *Organometallics* **2013**, 32, (24), 7580; (e) Saxena, P.; Thirupathi, N.; Nethaji, M. *Organometallics* **2014**, 33, (12), 3182.
8. Michael Büch, H.; Binger, P.; Benn, R.; Krüger, C.; Ruffinska, A. *Angew. Chem.* **1983**, 95, (10), 814.
9. (a) Lash, T. D. *Org. Lett.* **2011**, 13, (17), 4632; (b) Young, A. M.; Von Ruden, A. L.; Lash, T. D. *Org. Biomol. Chem.* **2011**, 9, (18), 6293; (c) Li, D.; Lash, T. D. *J. Org. Chem.* **2014**, 79, (15), 7112; (d) Lash, T. D. *Org. Biomol. Chem.* **2015**, 13, (29), 7846; (e) Musa, S.; Shpruhman, A.; Gelman, D. *J. Organomet. Chem.* **2012**, 699, 92; (f) Comanescu, C. C.; Iluc, V. M. *Organometallics* **2014**, 33, (21), 6059; (g) Cui, P.; Comanescu, C. C.; Iluc, V. M. *Chem. Commun.* **2015**, 51, (28), 6206.

10. Canty, A. J.; Denney, M. C.; Skelton, B. W.; White, A. H. *Organometallics* **2004**, 23, (5), 1122.

Chapter 5 References

1. (a) Brown, J. M.; Cooley, N. A. *Chem. Rev.* **1988**, 88, 1031. (7); (b) Li, C. J. *Chem. Rev.* **1993**, 93, (6), 2023.
2. Poulsen, T. B.; Jørgensen, K. A. *Chem. Rev.* **2008**, 108, (8), 2903.
3. (a) Arya, P.; Qin, H. *Tetrahedron* **2000**, 56, (7); (b) Dénès, F.; Pérez-Luna, A.; Chemla, F. *Chem. Rev.* **2010**, 110, (4), 2366.
4. (a) Trost, B. *Science* **1991**, 254, (5037), 1471; (b) Newhouse, T.; Baran, P. S.; Hoffmann, R. W. *Chem. Soc. Rev.* **2009**, 38, (11), 3010.
5. Ren, T.; Patel, M.; Blok, K. *Energy* **2006**, 31, (4), 425.
6. Wilger, D. J.; GrandjeanJean-Marc, M.; Lammert, T. R.; Nicewicz, D. A. *Nat. Chem.* **2014**, 6, (8), 720.
7. Colby, D. A.; Bergman, R. G.; Ellman, J. A. *Chem. Rev.* **2009**, 110, (2), 624.
8. Lewis, L. N.; Smith, J. F. *J. Am. Chem. Soc.* **1986**, 108, (10), 2728.
9. Murai, S.; Kakiuchi, F.; Sekine, S.; Tanaka, Y.; Kamatani, A.; Sonoda, M.; Chatani, N. *Nature* **1993**, 366, (6455), 529.
10. Matsumoto, T.; Taube, D. J.; Periana, R. A.; Taube, H.; Yoshida, H. *J. Am. Chem. Soc.* **2000**, 122, (30), 7414.
11. Lail, M.; Arrowood, B. N.; Gunnoe, T. B. *J. Am. Chem. Soc.* **2003**, 125, (25), 7506.
12. Andreatta, J. R.; McKeown, B. A.; Gunnoe, T. B. *J. Organomet. Chem.* **2011**, 696, (1), 305.
13. Kakiuchi, F.; Sekine, S.; Tanaka, Y.; Kamatani, A.; Sonoda, M.; Chatani, N.; Murai, S. *Bull. Chem. Soc. Jpn.* **1995**, 68, (1), 62.
14. Matsubara, T.; Koga, N.; Musaev, D. G.; Morokuma, K. *J. Am. Chem. Soc.* **1998**, 120, (48), 12692.
15. Matsubara, T.; Koga, N.; Musaev, D. G.; Morokuma, K. *Organometallics* **2000**, 19, (12), 2318.
16. Grigg, R.; Savic, V. *Tetrahedron Lett.* **1997**, 38, (32), 5737.
17. Du, H.; Liu, Q.; Shi, S.; Zhang, S. *J. Organomet. Chem.* **2001**, 627, (1), 127.
18. Kakiuchi, F.; Yamauchi, M.; Chatani, N.; Murai, S. *Chem. Lett.* **1996**, 25, (2), 111.
19. Kakiuchi, F.; Sato, T.; Tsujimoto, T.; Yamauchi, M.; Chatani, N.; Murai, S. *Chem. Lett.* **1998**, 27, (10), 1053.
20. Jazzar, R. F. R.; Mahon, M. F.; Whittlesey, M. K. *Organometallics* **2001**, 20, (17), 3745.
21. Busch, S.; Leitner, W. *Adv. Synth. Catal.* **2001**, 343, (2), 192.
22. Grellier, M.; Vendier, L.; Chaudret, B.; Albinati, A.; Rizzato, S.; Mason, S.; Sabo-Etienne, S. *J. Am. Chem. Soc.* **2005**, 127, (50), 17592.
23. Martinez, R.; Chevalier, R.; Darses, S.; Genet, J.-P. *Angew. Chem. Int. Ed.* **2006**, 45, (48), 8232.
24. Martinez, R.; Genet, J.-P.; Darses, S. *Chem. Commun.* **2008**, (33), 3855.

25. Martinez, R.; Simon, M.-O.; Chevalier, R.; Pautigny, C.; Genet, J.-P.; Darses, S. *J. Am. Chem. Soc.* **2009**, *131*, (22), 7887.
26. Simon, M.-O.; Martinez, R.; Genet, J.-P.; Darses, S. *J. Org. Chem.* **2009**, *75*, (1), 208.
27. Simon, M.-O.; Genet, J.-P.; Darses, S. *Org. Lett.* **2010**, *12*, (13), 3038.
28. Kakiuchi, F.; Kochi, T.; Mizushima, E.; Murai, S. *J. Am. Chem. Soc.* **2010**, *132*, (50), 17741.
29. Kakiuchi, F.; Sato, T.; Yamauchi, M.; Chatani, N.; Murai, S. *Chem. Lett.* **1999**, *28*, (1), 19.
30. Kakiuchi, F.; Sonoda, M.; Tsujimoto, T.; Chatani, N.; Murai, S. *Chem. Lett.* **1999**, *28*, (10), 1083.
31. Kakiuchi, F.; Tsujimoto, T.; Sonoda, M.; Chatani, N.; Murai, S. *Synlett* **2001**, *2001*, (Special Issue), 948.
32. Kakiuchi, F.; Ohtaki, H.; Sonoda, M.; Chatani, N.; Murai, S. *Chem. Lett.* **2001**, *30*, (9), 918.
33. Kakiuchi, F.; Sato, T.; Igi, K.; Chatani, N.; Murai, S. *Chem. Lett.* **2001**, *30*, (5), 386.
34. Kozhushkov, S. I.; Yufit, D. S.; Ackermann, L. *Org. Lett.* **2008**, *10*, (16), 3409.
35. Schinkel, M.; Marek, I.; Ackermann, L. *Angew. Chem. Int. Ed.* **2013**, *52*, (14), 3977.
36. Bartoszewicz, A.; Martín-Matute, B. *Org. Lett.* **2009**, *11*, (8), 1749.
37. Uchamaru, Y. *Chem. Commun.* **1999**, (12), 1133.
38. (a) Lail, M.; Bell, C. M.; Conner, D.; Cundari, T. R.; Gunnoe, T. B.; Petersen, J. L. *Organometallics* **2004**, *23*, (21), 11658; (b) Oxgaard, J.; Periana, R. A.; Goddard, W. A. *J. Am. Chem. Soc.* **2004**, *126*, (37), 11658.
39. Pittard, K. A.; Lee, J. P.; Cundari, T. R.; Gunnoe, T. B.; Petersen, J. L. *Organometallics* **2004**, *23*, (23), 5514.
40. Oxgaard, J.; Goddard, W. A. *J. Am. Chem. Soc.* **2003**, *126*, (2), 442.
41. DeYonker, N. J.; Foley, N. A.; Cundari, T. R.; Gunnoe, T. B.; Petersen, J. L. *Organometallics* **2007**, *26*, (26), 6604.
42. Foley, N. A.; Lail, M.; Lee, J. P.; Gunnoe, T. B.; Cundari, T. R.; Petersen, J. L. *J. Am. Chem. Soc.* **2007**, *129*, (21), 6765.
43. Foley, N. A.; Lee, J. P.; Ke, Z.; Gunnoe, T. B.; Cundari, T. R. *Acc. Chem. Res.* **2009**, *42*, (5), 585.
44. Burgess, S. A.; Joslin, E. E.; Gunnoe, T. B.; Cundari, T. R.; Sabat, M.; Myers, W. H. *Chem. Sci.* **2014**, *5*, (11), 4355.
45. Guo, H.; Tapsak, M. A.; Weber, W. P. *Macromolecules* **1995**, *28*, (13), 4714.
46. Lu, P.; Paulasaari, J.; Jin, K.; Bau, R.; Weber, W. P. *Organometallics* **1998**, *17*, (4), 584.
47. (a) Guo, H.; Wang, G.; Tapsak, M. A.; Weber, W. P. *Macromolecules* **1995**, *28*, (16), 5686; (b) Gupta, S. K.; Weber, W. P. *Macromolecules* **2000**, *33*, (1), 108.
48. Gupta, S. K.; Weber, W. P. *Macromolecules* **2002**, *35*, (9), 3369.

49. (a) Harris, P. W. R.; Woodgate, P. D. *J. Organomet. Chem.* **1996**, 506, (1–2), 339;
(b) Harris, P. W. R.; Woodgate, P. D. *J. Organomet. Chem.* **1997**, 530, (1–2), 211.
50. Brunet, J.-J.; Neibecker, D.; Philippot, K. *J. Chem. Soc., Chem. Commun.* **1992**, (17), 1215.
51. Oguma, K.; Miura, M.; Satoh, T.; Nomura, M. *J. Am. Chem. Soc.* **2000**, 122, (42), 10464.
52. Carrion, M. C.; Cole-Hamilton, D. J. *Chem. Commun.* **2006**, (43), 4527.
53. Lenges, C. P.; Brookhart, M. *J. Am. Chem. Soc.* **1999**, 121, (28), 6616.
54. Jun, C.-H.; Hong, J.-B.; Kim, Y.-H.; Chung, K.-Y. *Angew. Chem. Int. Ed.* **2000**, 39, (19), 3440.
55. Jun, C.-H.; Moon, C. W.; Hong, J.-B.; Lim, S.-G.; Chung, K.-Y.; Kim, Y.-H. *Chem. Eur. J.* **2002**, 8, (2), 485.
56. Vo-Thanh, G.; Lahrache, H.; Loupy, A.; Kim, I.-J.; Chang, D.-H.; Jun, C.-H. *Tetrahedron* **2004**, 60, (26), 5539.
57. Yoon, J. H.; Park, Y. J.; Lee, J. H.; Yoo, J.; Jun, C.-H. *Org. Lett.* **2005**, 7, (14), 2889.
58. Lim, Y.-G.; Han, J.-S.; Yang, S.-S.; Chun, J. H. *Tetrahedron Lett.* **2001**, 42, (29).
59. Lim, Y.-G.; Koo, B. T. *Tetrahedron Lett.* **2005**, 46, (46), 7997.
60. Tsuchikama, K.; Kuwata, Y.; Tahara, Y.-k.; Yoshinami, Y.; Shibata, T. *Org. Lett.* **2007**, 9, (16), 3097.
61. Tanaka, K.; Otake, Y.; Sagae, H.; Noguchi, K.; Hirano, M. *Angew. Chem. Int. Ed.* **2008**, 47, (7), 1312.
62. Lim, Y.-G.; Kim, Y. H.; Kang, J.-B. *J. Chem. Soc., Chem. Commun.* **1994**, (19), 2267.
63. Lim, Y.-G.; Kang, J.-B.; Kim, Y. H. *J. Chem. Soc., Perkin Trans. 1* **1996**, (17), 2201.
64. Kakiuchi, F.; Le Gendre, P.; Yamada, A.; Ohtaki, H.; Murai, S. *Tetrahedron: Asymmetry* **2000**, 11, (13), 2647.
65. Tan, K. L.; Bergman, R. G.; Ellman, J. A. *J. Am. Chem. Soc.* **2001**, 123, (11), 2685.
66. Tan, K. L.; Vasudevan, A.; Bergman, R. G.; Ellman, J. A.; Souers, A. J. *Org. Lett.* **2003**, 5, (12), 2131.
67. Tan, K. L.; Bergman, R. G.; Ellman, J. A. *J. Am. Chem. Soc.* **2002**, 124, (13), 3202.
68. Tan, K. L.; Bergman, R. G.; Ellman, J. A. *J. Am. Chem. Soc.* **2002**, 124, (47), 13964.
69. Tan, K. L.; Park, S.; Ellman, J. A.; Bergman, R. G. *J. Org. Chem.* **2004**, 69, (21), 7329.
70. Wiedemann, S. H.; Bergman, R. G.; Ellman, J. A. *Org. Lett.* **2004**, 6, (10), 1685.
71. Wiedemann, S. H.; Lewis, J. C.; Ellman, J. A.; Bergman, R. G. *J. Am. Chem. Soc.* **2006**, 128, (7), 2452.
72. Lewis, J. C.; Bergman, R. G.; Ellman, J. A. *J. Am. Chem. Soc.* **2007**, 129, (17), 5332.

73. Thalji, R. K.; Ahrendt, K. A.; Bergman, R. G.; Ellman, J. A. *J. Am. Chem. Soc.* **2001**, *123*, (39), 9692.
74. Thalji, R. K.; Ellman, J. A.; Bergman, R. G. *J. Am. Chem. Soc.* **2004**, *126*, (23), 7192.
75. (a) Thalji, R. K.; Ahrendt, K. A.; Bergman, R. G.; Ellman, J. A. *J. Org. Chem.* **2005**, *70*, (17), 6775; (b) Harada, H.; Thalji, R. K.; Bergman, R. G.; Ellman, J. A. *The J. Org. Chem.* **2008**, *73*, (17), 6772.
76. Watzke, A.; Wilson, R. M.; O'Malley, S. J.; Bergman, R. G.; Ellman, J. A. *Synlett* **2007**, *2007*, (15), 2383.
77. Kwak, J.; Ohk, Y.; Jung, Y.; Chang, S. *J. Am. Chem. Soc.* **2012**, *134*, (42), 17778.
78. Shibata, T.; Takayasu, S.; Yuzawa, S.; Otani, T. *Org. Lett.* **2012**, *14*, (19), 5106.
79. Ahrendt, K. A.; Bergman, R. G.; Ellman, J. A. *Org. Lett.* **2003**, *5*, (8), 1301.
80. Wilson, R. M.; Thalji, R. K.; Bergman, R. G.; Ellman, J. A. *Org. Lett.* **2006**, *8*, (8), 1745.
81. Rech, J. C.; Yato, M.; Duckett, D.; Ember, B.; LoGrasso, P. V.; Bergman, R. G.; Ellman, J. A. *J. Am. Chem. Soc.* **2007**, *129*, (3), 490.
82. Jo, E.-A.; Cho, E.-G.; Jun, C.-H. *Synlett* **2007**, *2007*, (7), 1059.